

Meta-Analysis of Genome-Wide Association Studies for Abdominal Aortic Aneurysm Identifies Four New Disease-Specific Risk Loci

Jones, G. T., Tromp, G., Kuivaniemi, H., Gretarsdottir, S., Baas, A. F., Giusti, B., ... Bown, M. J. (2016). Meta-Analysis of Genome-Wide Association Studies for Abdominal Aortic Aneurysm Identifies Four New Disease-Specific Risk Loci. *Circulation Research*. DOI: 10.1161/CIRCRESAHA.116.308765

Published in:
Circulation Research

Queen's University Belfast - Research Portal:
[Link to publication record in Queen's University Belfast Research Portal](#)

Publisher rights

© 2016 The Authors. This is an open access article published under a Creative Commons Attribution-NonCommercial-NoDerivs License (<https://creativecommons.org/licenses/by-nc-nd/4.0/>), which permits distribution and reproduction for non-commercial purposes, provided the author and source are cited.

General rights

Copyright for the publications made accessible via the Queen's University Belfast Research Portal is retained by the author(s) and / or other copyright owners and it is a condition of accessing these publications that users recognise and abide by the legal requirements associated with these rights.

Take down policy

The Research Portal is Queen's institutional repository that provides access to Queen's research output. Every effort has been made to ensure that content in the Research Portal does not infringe any person's rights, or applicable UK laws. If you discover content in the Research Portal that you believe breaches copyright or violates any law, please contact openaccess@qub.ac.uk.

CLINICAL TRACK

Meta-Analysis of Genome-Wide Association Studies for Abdominal Aortic Aneurysm Identifies Four New Disease-Specific Risk Loci

Gregory T. Jones¹, Gerard Tromp^{2,3}, Helena Kuivaniemi^{2,3}, Solveig Gretarsdottir⁴, Annette F. Baas⁵, Betti Giusti⁶, Ewa Strauss^{7,8}, Femke N.G. van 't Hof⁹, Thomas R. Webb^{10,11}, Robert Erdman², Marylyn D. Ritchie^{12,13}, James R. Elmore¹⁴, Anurag Verma¹², Sarah Pendergrass^{12,13}, Iftikhar J. Kullo¹⁵, Zi Ye¹⁵, Peggy L. Peissig¹⁶, Omri Gottesman¹⁷, Shefali S. Verma¹², Jennifer Malinowski¹⁸, Laura J. Rasmussen-Torvik¹⁹, Kenneth M. Borthwick², Diane T. Smelser², David R. Crosslin²⁰, Mariza de Andrade¹⁵, Evan J. Ryer¹⁴, Catherine A. McCarty²¹, Erwin P. Böttlinger¹⁷, Jennifer A. Pacheco¹⁹, Dana C. Crawford²², David S. Carrell²³, Glenn S. Gerhard²⁴, David P. Franklin²⁵, David J. Carey², Victoria L. Phillips¹, Michael J. A. Williams²⁶, Wenhua Wei¹, Ross Blair²⁷, Andrew A. Hill²⁸, Thodor M. Vasudevan²⁷, David R. Lewis²⁹, Ian Thomson¹, Jo Krysa¹, Geraldine B. Hill¹, Justin Roake²⁹, Tony R. Merriman³⁰, Grzegorz Oszkini⁸, Silvia Galora⁶, Claudia Saracini⁶, Rosanna Abbate⁶, Raffaele Pulli³¹, Carlo Pratesi³¹, The Cardiogenics Consortium, The International Consortium for Blood Pressure, Athanasios Saratzis^{10,11}, Ana R. Verissimo^{10,11}, Suzannah Bumpstead³², Stephen A. Badger³³, Rachel E. Clough³⁴, Gillian Cockerill³⁵, Hany Hafez³⁶, D. Julian A. Scott³⁷, T. Simon Futers³⁷, Simon P. R. Romaine^{10,37}, Katherine Bridge³⁷, Kathryn J. Griffin³⁷, Marc A Bailey³⁷, Alberto Smith³⁸, Matthew M. Thompson³⁵, Frank M. van Bockxmeer³⁹, Stefan E. Matthiasson⁴⁰, Gudmar Thorleifsson⁴, Unnur Thorsteinsdottir^{4,41}, Jan D. Blankensteijn⁴², Joep A. W. Teijink^{43,44}, Cisca Wijmenga⁴⁵, Jacqueline de Graaf⁴⁶, Lambertus A. Kiemeny⁴⁶, Jes S. Lindholt⁴⁷, Anne Hughes⁴⁸, Declan T. Bradley⁴⁹, Kathleen Stirrups^{50,51}, Jonathan Gollidge⁵², Paul E. Norman⁵³, Janet T. Powell⁵⁴, Steve E. Humphries⁵⁵, Stephen E. Hamby^{10,11}, Alison H. Goodall^{10,11}, Christopher P. Nelson^{10,11}, Natzli Sakalihan⁵⁶, Audrey Courtois⁶, Robert E. Ferrell⁵⁷, Per Eriksson⁵⁸, Lasse Folkersen^{58,59}, Anders Franco-Cereceda⁶⁰, John D. Eicher⁶¹, Andrew D. Johnson⁶¹, Christer Betsholtz^{62,63}, Arno Ruusalepp^{4,65,66}, Oscar Franzén^{66,67}, Eric E. Schadt⁶⁷, Johan L. M. Björkegren^{64,66,67,68}, Leonard Lipovich⁶⁹, Anne M. Drolet⁷⁰, E. L. Verhoeven⁷¹, C. J. Zeebregts⁷², R. H. Geelkerken⁷³, Marc R. van Sambeek⁴⁴, S. M. van Sterkenburg⁷⁵, J. P. de Vries⁷⁶, Kari Stefansson^{4,41}, John R. Thompson⁷⁷, Paul I. W. de Bakker^{5,78}, Panos Deloukas^{50,79}, Robert D. Sayers¹⁰, Seamus C. Harrison¹⁰, Andre van Rij¹, Nilesh J. Samani^{10,11}, Matthew J. Bown^{10,11}.

¹Surgery Department, University of Otago, Dunedin, New Zealand, ²The Sigfried and Janet Weis Center for Research, Geisinger Health System, Danville, PA, USA, ³Division of Molecular Biology and Human Genetics, Department of Biomedical Sciences, Faculty of Medicine and Health Sciences, Stellenbosch University, Tygerberg, South Africa, ⁴deCODE/Amgen, Reykjavik, Iceland, ⁵Department of Medical Genetics, University Medical Center Utrecht, Utrecht, The Netherlands, ⁶Atherothrombotic Disease Center, Department of Experimental and Clinical Medicine, University of Florence, Careggi Hospital, Florence, Italy, ⁷Institute of Human Genetics, Polish Academy of Sciences, Faculty of Nucleic Acid Function, Poznan, Poland, ⁸Department of General and Vascular Surgery, Poznan University of Medical Sciences, Poznan, Poland, ⁹Utrecht Stroke Center, Department of Neurology and Neurosurgery, Rudolf Magnus Institute of Neuroscience, University Medical Center Utrecht, Utrecht, The Netherlands, ¹⁰Department of Cardiovascular Sciences, University of Leicester, Leicester, UK, ¹¹NIHR Leicester Cardiovascular Biomedical Research Unit, Glenfield General Hospital, Leicester, UK, ¹²The Pennsylvania State University, University Park, PA, USA, ¹³Biomedical and Translational Informatics, Geisinger Health System, Danville, PA, USA, ¹⁴The Department of Vascular Surgery at Geisinger Medical Center, Danville, PA, USA, ¹⁵Mayo Clinic Rochester, Rochester, MN, USA, ¹⁶Marshfield Clinic Research Foundation, Marshfield, Wisconsin, USA, ¹⁷Icahn School of Medicine at Mount Sinai, New York, NY, USA, ¹⁸Vanderbilt University Nashville, Nashville, TN, USA, ¹⁹Northwestern University Feinberg School of Medicine, Chicago, IL, USA, ²⁰Department of Biomedical Informatics and Medical Education, University of Washington, Seattle, WA, USA, ²¹Research Division, Essentia Institute of Rural

Health, Duluth, MN, USA, ²²Case Western Reserve University, Cleveland, Ohio, USA, ²³Group Health Research Institute, Seattle, WA, USA, ²⁴Department of Medical Genetics and Molecular Biochemistry, Temple University School of Medicine, PA, USA, ²⁵Mission Clinic, Mission Health System, Asheville, North Carolina, USA, ²⁶Medicine Department, University of Otago, Dunedin, New Zealand, ²⁷Waikato Hospital, Hamilton, New Zealand, ²⁸Auckland City Hospital, Auckland, New Zealand, ²⁹Surgery Department, University of Otago, Christchurch, New Zealand, ³⁰Biochemistry Department, University of Otago, Dunedin, New Zealand, ³¹Vascular Surgery Unit, Department of Experimental and Clinical Medicine, University of Florence, Careggi Hospital, Florence, Italy, ³²Genetics of Complex Traits in Humans Group, Wellcome Trust Sanger Institute, Cambridge, UK, ³³School of Medicine, Queens University, Belfast, UK, ³⁴Department of Vascular Surgery, King's College London, London, UK, ³⁵Department of Vascular Surgery, St George's University of London, London, UK, ³⁶King Faisal Specialist Hospital and Research Centre, Jeddah, Saudi Arabia, ³⁷The Leeds Institute of Cardiovascular and Metabolic Medicine, University of Leeds, Leeds, UK, ³⁸Department of Vascular Surgery, Cardiovascular Division/BHF Centre of Research Excellence, King's College London, London, UK, ³⁹Department of Surgery, University of Western Australia, Crawley, Australia, ⁴⁰Laekning Medical Clinics, Reykjavik, Iceland, ⁴¹University of Iceland, Faculty of Medicine, Reykjavik, Iceland, ⁴²Department of Vascular Surgery, VU Medical Center, Amsterdam, The Netherlands, ⁴³CAPHRI Research School, University Maastricht, Eindhoven, The Netherlands, ⁴⁴Department of Vascular Surgery, Catharina Ziekenhuis, Eindhoven, The Netherlands, ⁴⁵Department of Genetics, UMC Groningen, Groningen, The Netherlands, ⁴⁶Radboud University Medical Centre, Radboud Institute for Health Sciences, Nijmegen, The Netherlands, ⁴⁷Elitary Research Centre of Individualized Medicine in Arterial Disease (CIMA), Department of Cardiothoracic and Vascular Surgery, Odense University Hospital, Odense, Denmark, ⁴⁸Independent researcher, 169 Ballylesson Rd, Belfast, UK, ⁴⁹Centre for Public Health, Queens University Belfast, Belfast, UK, ⁵⁰William Harvey Research Institute, Barts and The London School of Medicine and Dentistry, Queen Mary University of London, London, UK, ⁵¹Department of Haematology, University of Cambridge, Cambridge, UK, ⁵²Vascular Biology Unit, Queensland Research Centre for Peripheral Vascular Disease and the Department of Vascular and Endovascular Surgery, James Cook University and Townsville Hospital, Townsville, Australia, ⁵³Department of Surgery, University of Western Australia, Crawley, Australia, ⁵⁴Department of Surgery and Cancer, Imperial College London, London, UK, ⁵⁵Cardiovascular Genetics, Institute of Cardiovascular Science, University College London, London, UK, ⁵⁶Surgical Research Center GIGA-Cardiovascular Science Unit, University of Liège, Liège, Belgium, ⁵⁷Department of Human Genetics, University of Pittsburgh School of Public Health, Pittsburgh, Pennsylvania, USA, ⁵⁸Atherosclerosis Research Unit, Center for Molecular Medicine, Department of Medicine, Karolinska Institutet, Stockholm, Sweden, ⁵⁹Center for Biological Sequence Analysis, Technical University of Denmark, Copenhagen, Denmark, ⁶⁰Cardiothoracic Surgery Unit, Department of Molecular Medicine and Surgery, Karolinska Institutet, Stockholm, Sweden, ⁶¹Center for Population Studies, National Heart, Lung, and Blood Institute, The Framingham Heart Study, Framingham, Massachusetts, USA, ⁶²Department of Immunology, Genetics and Pathology, Rudbeck Laboratory, Uppsala University, Sweden, ⁶³Department of Medical Biochemistry and Biophysics, Vascular Biology Unit, Karolinska Institutet, Stockholm, Sweden, ⁶⁴Department of Physiology, Institute of Biomedicine and Translation Medicine, University of Tartu, Estonia, ⁶⁵Department of Cardiac Surgery, Tartu University Hospital, Tartu, Estonia, ⁶⁶Clinical Gene Networks AB, Stockholm, Sweden, ⁶⁷Department of Genetics & Genomic Sciences, Institute of Genomics and Multiscale Biology, Icahn School of Medicine at Mount Sinai, New York, NY, ⁶⁸Department of Medical Biochemistry and Biophysics, Karolinska Institutet, Stockholm, Sweden,

⁶⁹Department of Neurology, and ⁷⁰Center for Molecular Medicine and Genetics, Wayne State University, Detroit, Michigan, USA, ⁷¹Department of Vascular and Endovascular Surgery, Paracelsus Medical University Nuremberg, Nuremberg, Germany, ⁷²Department of Surgery (Division of Vascular Surgery), University Medical Center Groningen, University of Groningen, Groningen, The Netherlands, ⁷³Chirurgencoöperatie Oost Nederland, Enschede, The Netherlands, ⁷⁴Department of Surgery, TweeSteden Hospital, Tilburg, The Netherlands, ⁷⁵Department of Vascular Surgery, Rijnstate Ziekenhuis, Arnhem, The Netherlands, ⁷⁶Department of Vascular Surgery, St. Antonius Hospital, Nieuwegein, The Netherlands, ⁷⁷Department of Health Sciences, University of Leicester, UK, ⁷⁸Department of Epidemiology, Julius Center for Health Sciences and Primary Care, University Medical Center Utrecht, Utrecht, The Netherlands, ⁷⁹the Princess Al-Jawhara Al-Brahim Centre of Excellence in Research of Hereditary Disorders (PACER-HD), King Abdulaziz University, Jeddah, Saudi Arabia.

Running title: Meta-GWAS for Abdominal Aortic Aneurysm



Circulation Research

Subject Terms:

Aneurysm
Basic Science Research
Genetic, Association Studies
Genetics
Vascular Disease

ONLINE FIRST

Address correspondence to:

Dr. Matthew J. Bown
Cardiovascular Sciences, University of Leicester
Robert Kilpatrick Building
Leicester, LE2 7LX
United Kingdom
Tel: 0116 252 3190
Fax: 0116 252 3179
m.bown@le.ac.uk

Dr. Gregory T. Jones
Associate Professor
Surgery Department
University of Otago
Dunedin 9054
New Zealand
greg.jones@otago.ac.nz

In October 2016, the average time from submission to first decision for all original research papers submitted to *Circulation Research* was 15.7 days.

ABSTRACT

Rationale: Abdominal aortic aneurysm (AAA) is a complex disease with both genetic and environmental risk factors. Together, 6 previously identified risk loci only explain a small proportion of the heritability of AAA.

Objective: To identify additional AAA risk loci using data from all available genome-wide association studies (GWAS).

Methods and Results: Through a meta-analysis of 6 GWAS datasets and a validation study totalling 10,204 cases and 107,766 controls we identified 4 new AAA risk loci: 1q32.3 (*SMYD2*), 13q12.11 (*LINC00540*), 20q13.12 (near *PCIF1/MMP9/ZNF335*), and 21q22.2 (*ERG*). In various database searches we observed no new associations between the lead AAA SNPs and coronary artery disease, blood pressure, lipids or diabetes. Network analyses identified *ERG*, *IL6R* and *LDLR* as modifiers of *MMP9*, with a direct interaction between *ERG* and *MMP9*.

Conclusions: The 4 new risk loci for AAA appear to be specific for AAA compared with other cardiovascular diseases and related traits suggesting that traditional cardiovascular risk factor management may only have limited value in preventing the progression of aneurysmal disease.

Keywords:

Abdominal aortic aneurysm, genetics, meta-analysis, matrix metalloproteinases, genome-wide association studies, bioinformatics.

Nonstandard Abbreviations and Acronyms:

1000Genomes	a deep catalog of variation in the human genome based on DNA sequencing
AAA	abdominal aortic aneurysm
ANRIL	also known as CDKN2B-AS1, CDKN2B antisense RNA 1
ASAP	Advanced Study of Aortic Pathology
BCAR3	breast cancer anti-estrogen resistance 3
CAD	coronary artery disease
CARDIoGRAM	a consortium called Coronary ARtery DIsease Genome wide Replication and Meta-analysis
CELSR2	cadherin, EGF LAG seven-pass G-type receptor 2
ChIP	chromatin immunoprecipitation
CPDB	consensus pathway database
DAB2IP	DAB2 interacting protein
DEPICT	Data-driven Expression-Prioritized Integration for Complex Traits
DIAGRAM	a consortium called DIABetes Genetics Replication And Meta-analysis
eMERGE	electronic medical records and genomics
eQTL	expression quantitative trait locus
ELF1	E74 like ETS transcription factor 1
ERG	v-ets avian erythroblastosis virus E26 oncogene homolog
eSNP	expressed Single Nucleotide Polymorphism
ETS2	ETS proto-oncogene 2, transcription factor
FGF9	fibroblast growth factor 9
GRASP	The Genome-wide Repository of Associations between SNPs and Phenotypes
GTex	The Genotype-Tissue Expression
GWAS	genome-wide association study
GWAS3D	bioinformatics tool detecting human regulatory variants by integrative analysis of

GWAS	genome-wide associations, chromosome interactions and histone modifications.
HSP90	Central database providing integrative visualization of and access to GWAS data
ICD-9	heat shock protein 90
	9th edition of the International Statistical Classification of Diseases and Related Health Problems
IL6R	interleukin 6 receptor
IPA	Ingenuity Pathway Analysis
JAK	Janus kinase
JNK	c-Jun N-terminal kinase
LD	linkage disequilibrium
LDLR	low density lipoprotein receptor
LINC00540	long intergenic non-protein coding RNA 540
LRP1	low density lipoprotein receptor related protein 1
MAPK	mitogen activated kinase-like protein
METAL	a tool for meta-analysis of genome-wide association scans
MMP9	matrix metalloproteinase 9
NAB2	NGFI-A binding protein 2
NEURL2	neuralized E3 ubiquitin protein ligase 2
NFKB	nuclear factor of kappa light
NOTCH2	notch 2 member of type 1 transmembrane protein family
PCIF1	C-terminal inhibiting factor 1 of a protein called pancreatic and duodenal homeobox 1
PheWAS	phenome-wide association study
PIK3K	phosphatidylinositol-4,5-bisphosphate 3-kinase catalytic subunit alpha
PLTP	phospholipid transfer protein
PSRC1	proline and serine rich coiled-coil 1
RFX1	regulatory factor X1
RNA-Seq	whole genome RNA-sequence generated by high-throughput methods
ScanDB	SNP and CNV Annotation Database
SHESis	software platform for analyses of linkage disequilibrium, haplotype construction, and genetic association at polymorphism loci.
SMYD2	SET and MYND domain containing 2 (SET domain-containing proteins, such as catalyze lysine methylation)
	SET and MYND domain containing 2 (SET domain-containing proteins, such as catalyze lysine methylation)
SORT1	sortilin 1
STARNET	Stockholm-Tartu Atherosclerosis Reverse Network Engineering Task
STAT5	signal transducer and activator of transcription 5
TDRD10	tudor domain containing 10
TF	transcription factor
TGFβ	transforming growth factor beta
TNF	tumor necrosis factor
TYW1B	tRNA-yW synthesizing protein 1 homolog B
UBE2W	ubiquitin conjugating enzyme E2 W (putative)
UCSC	University of California Santa Cruz
WTCCC	Welcome Trust Case Control Consortium
VEGF	vascular endothelial growth factor
ZNF335	zinc finger protein 335



INTRODUCTION

Abdominal aortic aneurysms (AAAs; MIM100070) are a significant cause of mortality and morbidity in the western world. Although much less common than ischaemic heart disease or stroke, AAA is responsible for approximately 11,000 deaths/year in the USA, with no clinical treatment other than expensive, high-risk surgery¹. The US Preventative Services taskforce recommends AAA screening by ultrasound for all men aged 65 to 75 who have ever smoked². The UK NHS AAA Screening Programme screens all men at age 65 irrespective of smoking history yielding a prevalence of AAA (>29 mm) of 1.2%³.

AAA is an enigmatic complex disease. Whilst sharing risk factors for, and often co-existing with atherosclerosis, AAA can be considered to be a distinct entity from atherosclerosis. Smoking, a positive family history of AAA, and male sex have been consistently identified as the strongest risk factors for AAA. There is uncertainty over the influence of other traditional cardiovascular risk markers such as hypertension and hyperlipidemia. Furthermore, diabetes has been found to be negatively associated with AAA and is strongly protective against disease progression (AAA growth)¹.

Heritability of AAA is over 0.7,⁴ and individuals with a first-degree relative with AAA have a 2-fold higher risk of developing an AAA.⁵ Genome-wide association studies (GWAS) have identified 3 AAA risk loci on chromosomes 9 (*DAB2IP*⁶), 12 (*LRP1*⁷) and 19 (*LDLR*⁸). Further AAA risk loci on chromosomes 1 (*SORT1*⁹ and *IL6R*¹⁰) and 9 (*CDKN2BAS1/ANRIL*¹¹) were identified by candidate gene/locus approaches. Together, these explain only a small proportion of the heritability of AAA.

Overall, the high heritability estimates for AAA and the small number of loci identified suggest that there are further risk loci yet to be found. In the current study, we performed a meta-analysis of 6 available GWAS datasets for AAA on 4,972 cases and 99,858 controls, and confirmed the findings within validation data sets of 5,232 cases and 7,908 controls. This resulted in identification of 4 novel validated loci for AAA. We followed up positive results with extensive bioinformatics analyses and used data available from various databases to elucidate the potential biological significance of our findings to the pathobiology of AAA.

METHODS

An online supplement contains detailed methods and is available at <http://circres.ahajournals.org>.

Expanded aneurysm consortium.

All known studies with AAA genome-wide genotyping (Online Methods and Data; Online Table I) were invited to join the International Aneurysm Consortium. Additional samples (Online Methods and Data; Online Table II) were used for the validation study. All AAA cases had an infra-renal aortic diameter >30 mm. AAAs secondary to connective tissue diseases were excluded. The use of the samples in each study cohort was approved by local Ethics Committees or Institutional Review Boards.

Meta-analysis.

The discovery phase of the meta-GWAS was conducted using the METAL software package¹² on the 6 cohorts detailed in Online Table I, comprising 4,972 AAA cases and 99,858 controls. An effective sample number (N_{eff}) weighted analysis¹² was conducted due to case/control asymmetry within some of the contributing cohorts. Quality control included assessments for population stratification in each dataset and adjustment was performed if necessary. The analysis of each contributing GWAS had been performed independently and there was therefore no uniform analysis plan across all datasets. The individual GWAS datasets from Iceland and the Netherlands were adjusted for genomic inflation prior to inclusion in the meta-analysis. The overall meta-analysis was then adjusted for genomic inflation (λ) (Online Table I;

Online Figure I). An initial (λ -adjusted) discovery threshold of $P < 5 \times 10^{-6}$ was used to identify SNPs for subsequent validation genotyping. SNPs with high heterogeneity ($P_{\text{het}} < 0.005$ or $I^2 > 70\%$) were not taken forward for validation.

The lead SNPs [or their proxies in high linkage disequilibrium (LD)], identified in the discovery analyses, were then genotyped in a further 8 independent cohorts with 5,232 cases and 7,908 controls (Online Table II). Allele association analysis of each individual validation study cohort was carried out using the SHEsis web-based software package¹³. A combined (discovery-validation) fixed effect meta-analysis was performed using a Maentel–Haenzel method with the genome-wide P -value significance threshold being set at 5×10^{-8} . Random-effects (Han-Eskin method¹⁴) meta-analysis was also performed to determine if any results were sensitive to between-study heterogeneity.

SNP lookup in GWAS for other traits associated with AAA.

GWAS datasets for other traits were searched for associations with the AAA-associated SNPs to determine if the associations were unique to AAA or related to generalized cardiovascular disease. Results were obtained from meta-analyses of multiple primary GWAS datasets for each trait. Summary data for each AAA associated SNP (P -value and effect size) were extracted. P -values $< 5 \times 10^{-8}$ were considered to be significant. Results were available for type 2 diabetes¹⁵ (DIAGRAM consortium; <http://www.diagram-consortium.org/index.html>), coronary artery disease (CAD; CARDIoGRAM consortium¹⁶; www.CARDIOGRAMPLUSC4D.ORG), lipids (the Global Lipids Genetics Consortium¹⁷; <http://csg.sph.umich.edu/abecasis/public/lipids2013>) and blood pressure (the International Consortium for Blood Pressure¹⁸; http://www.ncbi.nlm.nih.gov/projects/gap/cgi-bin/study.cgi?study_id=phs000585.v1.p1).

Search for other associated traits and diseases using GWAS databases.

The Phenotype-Genotype Integrator¹⁹ (<http://www.ncbi.nlm.nih.gov/gap/phegeni#GenomeView>), the GWAS catalog (<http://www.gwascentral.org/index>), and the NHLBI GRASP catalog (GRASP v2.0; <http://grasp.nhlbi.nih.gov/Overview.aspx>)²⁰ were searched for diseases and traits associated with the lead SNPs at the AAA loci.

PheWAS analysis.

We performed a phenome-wide association study (PheWAS)^{21, 22} exploring associations between the 9 AAA-associated SNPs and an extensive group of diagnoses to identify novel associations and uncover potential pleiotropy. For the PheWAS we used data from the electronic Medical Records and Genomics (eMERGE) Network²³ with a total of 27,077 unrelated patients of European ancestry above 19 years of age. We divided these samples into 2 datasets by proportional sampling based on eMERGE site, sex, and genotyping platform (13,559 and 13,518 individuals in sets 1 and 2, respectively). We calculated associations between the 9 AAA-associated SNPs and case or control status based on the extensive set of ICD-9 diagnoses (2,408 and 2,385 in sets 1 and 2 respectively) where for a specific diagnosis, individuals with the diagnosis are considered cases. Associations were adjusted for sex, site, genotyping platform and the first 3 principal components to account for global ancestry.

Annotation of AAA associated SNPs using the UCSC genome browser, Pupasuite and GWAS3D.

Confirmed AAA-associated loci were manually annotated using the UCSC Genome Browser (<http://genome.ucsc.edu/cgi-bin/hgGateway>) on the hg19 human genome assembly. For the Pupasuite analyses SNPs in LD ($r^2 > 0.5$) and with lead SNPs at the novel AAA risk loci identified were extracted from the 1000 Genomes data and then entered into Pupasuite v3.1²⁴. In addition, all known (novel and previously identified) AAA-associated SNPs were entered into the GWAS3D²⁵ web-portal (<http://jjwanglab.org/gwas3d>) to identify functional SNPs.

Bioinformatic identification of candidate AAA genes and pathways using DEPICT.

An integrated gene function analysis was performed using the DEPICT tool (version 1.1)²⁶. Two separate runs were performed using either all independent SNPs with discovery metaGWAS $P < 5 \times 10^{-6}$ or just those 9 SNPs which reached $P < 5 \times 10^{-8}$ in the combined analysis. Both nominal P-values and false discovery rates (FDRs) were calculated.

Experimental evidence for functional variants at AAA loci.

SNPs at loci confirmed to be associated with AAA were examined for functional effects using multiple methods (Online methods). 1) To search for evidence of functional effects of SNPs at AAA associated loci 2 eQTL datasets based on publically available data, and a broad range of tissues with relatively large sample sizes were examined. Firstly, index and proxy SNPs were queried in a collected database of published expression SNP (eSNP) results. The collected eSNP results met criteria for statistical thresholds for association with gene transcript levels as described in the original publications. Secondly, additional eQTL data were integrated from online sources including ScanDB, the Broad Institute GTex browser, and the Pritchard Lab (eqtl.uchicago.edu). 2) To search for vascular tissue specific effects, eQTL data were also obtained from the Advanced Study of Aortic Pathology (ASAP) dataset²⁷ and RNA-seq data were from the Stockholm-Tartu Atherosclerosis Reverse Network Engineering Task (STARNET) database²⁸ (<http://www.mountsinai.org/profiles/johan-bjorkegren>). 3) Since some genes at AAA loci were associated with monocyte function and AAA is known to be an inflammatory disease²⁹, data from an eQTL analysis of peripheral blood monocytes were obtained from the Cardiogenics Consortium (<http://www.cardiogramplusc4d.org/>). 4) Lastly to search for effects in AAA tissue specifically, mRNA expression profiles of all the GWAS3D predicted distal targets, as well as SNP proximity implicated genes, were examined using a previously published genome-wide expression dataset on human aorta (GSE57691)³⁰, from which 49 AAA samples were compared with 10 organ donor control aortic samples. Transcription factor (TF) binding data were also obtained from a previous study³¹, which described chromatin-immunoprecipitation (ChIP)-chip for TFs ELF1, ETS2, RUNX1 and STAT5 using human aortic tissue in AAAs and healthy control aorta.

Network analysis.

We investigated whether most of the loci could be connected into a single network through intermediate nodes and interactions. A network integrating most of the loci would suggest mechanisms by which the loci could act in concert, whether synergistically or antagonistically, to affect the phenotype. The network(s) would also provide hypotheses for future investigation. Using the genes harboring AAA-associated SNPs as a starting set, we analysed potential interactions between the proteins and known intermediates (proteins, non-coding RNA and metabolites) using 2 independent analysis tools, Ingenuity Pathway Analysis® (IPA) tool version 9.0 (Qiagen's Ingenuity Systems, Redwood City, CA, USA; www.ingenuity.com) and Consensus PathDB (<http://cpdb.molgen.mpg.de/CPDB>)^{32,33}. The analyzed gene set had 14 genes since 2 of the 9 AAA loci included clusters of 3 genes and TNF was added due to recent literature demonstrating the strong effect of SMYD2 on IL6 and TNF production^{34,35} (see Online Table XIV for SNP annotations and online methods).

RESULTS

Meta-analysis of 6 GWAS datasets for AAA followed by a validation study reveals 4 new AAA susceptibility loci.

The meta-analysis of 6 GWAS datasets (4,972 AAA cases; 99,858 controls, Online Table I) revealed 19 loci of interest ($P < 1 \times 10^{-6}$, Online Tables III and IV, and Figure 1). Lead SNPs from these loci, including the 6 AAA risk loci reported previously, were analyzed in a validation study of 5,232 AAA cases and 7,908 controls (Online Tables II, V, VI and VII). Four new loci were independently significant ($P < 0.05$) in the validation cohort, had a direction of effect consistent with the discovery cohort and when combined with the discovery cohort had a P -value that surpassed a genome-wide significance (5×10^{-8}): 1q32.3 (*SMYD2*), 13q12.11 (*LINC00540*), 20q13.12 (near *PCIF1/MMP9/ZNF335*), and 21q22.2 (*ERG*) (Table 1, Online Tables V, VI and VII, and Figure 2). All previously reported associations with AAA were confirmed at genome-wide significance (Table 1, Online Table VII and Online Figure II) with the exception of 12q13.3 (*LRP1*), where the lead SNP identified in this meta-analysis and tested in our validation study only demonstrated a borderline association with AAA in the combined analysis ($P = 6.4 \times 10^{-7}$). There was evidence of significant heterogeneity in the results observed for rs1795061 (near *SMYD2*) and rs2836411 (*ERG*) (Online Table VII). A random effects model sensitivity analysis (Han-Eskin¹⁴ method) demonstrated minimal effect on the results for these two loci (Online Table VIII). The lead SNPs at two loci that were both below the threshold for genome-wide significance under the fixed-effects model (rs6516091, 20p12.3, near *FERMT1* and rs5954362, Xq27.2, *SPANXA1*), were significant in the random-effects model. However, since both demonstrated extreme heterogeneity ($I^2 \geq 0.7$) we did not consider these to be newly identified loci for AAA and these were excluded from further analysis.

New AAA loci appear to be specific for AAA.

To assess whether the loci identified in our meta-analysis were specific to AAA or, were also associated with diseases or risk factors known to be associated with AAA, we looked up results from GWAS of CAD⁶, hypertension³⁶ and lipid traits¹⁷. We also obtained results for diabetes¹⁵ to determine if there was a reverse effect at these loci since diabetes is a negative risk factor for AAA and negatively influences AAA growth¹. Other than the known associations at 1p13.3 (*SORT1*), and 9p21 (*CDKN2BAS1/ANRIL*) with CAD, 1p13.3 (*SORT1*) with HDL/LDL, and 19p13.2 (*LDLR*) with LDL, we observed no new associations between the lead SNPs at any of the AAA risk loci we had identified and these traits (Figure 3 and Online Table IX). In particular, no association was observed between diabetes and these SNPs. Literature searching revealed an association between rs4845625 at 1q21.3 (*IL6R*) and CAD but this was not in high LD with the lead SNP genotyped in our study at this locus ($R^2 = 0.54$)³⁷.

We also searched GWAS Central and Phenotype-Genotype Integrator, and carried out a GRASP³⁸ analysis for any associations of the lead AAA SNPs with traits other than those listed above. We identified additional genome-wide significant associations between 1q21.3/*IL6R* (rs4129267) and C-reactive protein/asthma, and nominal associations between 1p13.3/*SORT1* (rs602633), 21q22.2/*ERG* (rs2836411) and 19p13.2/*LDLR* (rs6511720) and height (Online Tables X, XI, and XII), a potential risk factor for AAA³⁹.

We also performed a PheWAS^{21,22} in the eMERGE data sets exploring the association between the 9 AAA-associated SNPs and an extensive group of diagnoses to identify novel associations and uncover potential pleiotropy. We considered identification of previously known associations, such as rs602633 associated with hyperglyceridemia and rs10757274 associated with CAD, to be indications that the PheWAS approach was robust. The PheWAS results demonstrated the known associations with CAD and lipid levels but did not identify any novel disease associations (Online Table XIII).

Annotation of SNPs at AAA loci.

Annotation did not identify any non-synonymous variants in high LD ($R^2 > 0.5$) with the lead SNPs at the AAA risk loci (Online Tables XIV and XV). Based on GWAS3D analysis, all 9 lead SNPs were associated with TF binding site affinity variants (Online Tables XVI and XVII). Eight SNPs had potential long range interactions with distal genomic regions (Figure 4). GWAS3D analysis also provided potential mechanistic insight for intergenic AAA variants such as rs9316871 (13q12.11) that had significant predicted regulatory variant interaction with *FGF9* (13q12.11). In addition, while the AAA association with rs599839 (1p13.3) showed strong long-range chromatin interaction with *SORT1* (as previously reported specifically in AAA⁹) it also had predicted distal interactions with other genes including *BCAR3* (1p22.1) and *NOTCH2* (1p12-p11).

DEPICT gene pathway prediction.

DEPICT identified 633 and 482 gene enrichment sets with nominal $P < 0.05$ using the discovery meta-GWAS SNP set ($P < 5 \times 10^{-6}$) and top 9 SNPs from the combined analysis, respectively. Only one of the gene sets (“decreased long bone epiphyseal plate size”) had an FDR < 0.2 . Gene set descriptions included multiple functional classes relevant to vascular biology, i.e. transforming growth factor beta (TGF- β) regulation, lipoprotein metabolism, inflammation induced extracellular matrix remodelling (RFX1), vascular smooth muscle cell function, vascular injury including haemorrhage, immune cell function (particularly T & B cells), acute phase response including IL6 secretion, apoptosis, hyperglycemia and the PI3K, JNK and MAPK cascades. In addition, there were multiple gene sets associated with long bone size and epiphyseal plate formation (Table 2, Online Table XVIII and Online Data File).

Functional effects of SNPs at AAA loci.

The lookup of SNPs at AAA loci in studies of functional effects included multi-tissue eQTL studies, vascular/monocyte specific eQTL and AAA-specific studies (mRNA expression and ChIP-chip). These analyses revealed several potential functional associations (Online Tables XI, XX, XXI and XXII, Online Figure III)^{27, 40}. Of most relevance to AAA, eQTLs were observed for rs3827066 (20q13.3) and *PLTP* expression in aortic tissue and for rs4129267 (1q21.3) and *IL6R* expression in mammary artery. RNA-Seq data also demonstrated independent eQTLs in mammary artery for 2 of the novel AAA associations we have identified: rs2836411 and *ERG* expression, and rs9316871 and *FGF9* expression. All eQTLs, with the exception of rs9316871 and *FGF9* were also seen in tissues other than arterial samples.

Several GWAS3D -predicted distal interacting genes had significantly different mRNA expression between AAA and control samples (Table 3, Online Table XXIII, and Online Figure IV)³⁰. For example, *BCAR3* had decreased mRNA expression in AAA tissue (as did *SORT1* itself). In addition, while the closest gene to rs9316871, a long intergenic non-coding RNA (*LINC00540*), was not part of the mRNA dataset, the predicted distal target *FGF9* had significantly increased mRNA expression in AAA tissue (Online Table XXIII).

ChIP-chip data from human AAA tissue³¹ revealed TF binding sites in 5 genes (*SMYD2*, *SORT1*, *CDKN2BAS1/ANRIL*, *ERG* and *DAB2IP*) which harbour AAA risk loci, but none of these binding sites included the lead SNP tested for association with AAA (Online Table XXIV).

Network analysis reveals a central role for matrix metalloproteinase 9.

Network analysis using both IPA and Consensus PathDB demonstrated similar results (Online Figures V and VI). Both analyses revealed a central role for MMP9 in AAA, with IPA identifying direct interactions (physical contact between two molecules such as binding or phosphorylation) between *ERG*,

IL6R and LDLR and MMP9, and Consensus PathDB identifying a direct interaction between ERG and MMP9 with secondary interactions (interactions without physical contact, such as signalling events) between both SMYD2 and LDLR, and MMP9. Upon removing TNF from the analysis (which had been added based on the strong effect of SMYD2 on IL6 and TNF production^{34, 35}) the genes at AAA loci each remained in independent sub-networks. Inclusion of TGFB1, implicated in thoracic aneurysms and Marfan syndrome, instead of TNF failed to coalesce the sub-networks. The long non-coding RNA ANRIL (*CDKN2BAS1*), our strongest hit in the genome (Figure 1), has been reported in numerous studies as a GWAS hotspot and a candidate gene for CAD, intracranial aneurysms, and diverse cardiometabolic disorders⁴¹, however this was not represented in either the IPA or Consensus PathDB networks.

DISCUSSION

The present study is the largest genetic association study of AAA performed to date, utilising 6 GWAS datasets for AAA with a total of 4,972 cases and 99,858 controls. Furthermore, we used an independent validation set of 5,232 AAA cases and 7,908 controls, and then carried out a pooled analysis of all 10,204 cases and 107,766 controls. We confirmed the association of 5 previously reported loci and identified 4 new loci associated with AAA at genome-wide levels of significance. In contrast to previously identified loci, lead SNPs at the newly identified loci did not demonstrate evidence of cross phenotype association with other cardio-metabolic phenotypes. In summary, the genetic evidence to date mirrors that seen in the epidemiological literature where it is clear that AAA and other forms of cardiovascular diseases are seen as distinct but overlapping phenotypes.

Previous genetic discoveries in AAA have pointed to inflammation and immune function (*IL6R* & *CDKN2BAS1/ANRIL*) and low-density lipoprotein metabolism (*SORT1* & *LDLR*) as important mediators of AAA development. The genes at the novel AAA loci identified here are relevant to aneurysm biology but their precise roles require further investigation. *MMP9* is within the 20q13.12 locus and matrix degradation via *MMP9* is known to play a key role in the development of AAA, evidenced by the observation of high levels of *MMP9* in end-stage disease specimens⁴². This is also an important finding given the development of novel pharmacotherapies that target inflammation and matrix degradation pathways such as tofacitinib (a novel JAK inhibitor). Although it is tempting to assume that *MMP9* is the causal association at this locus, there are, however, other candidate genes at this locus. Examination of the region and the association pattern with AAA (Figure 2) shows that the strongest signals are seen upstream of *MMP9* and are separated from *MMP9* by a recombination hotspot. Closer to the strongest association signal are *ZNF335* and *PCIF1*. There is no literature evidence for any potential link for *ZNF335* to AAA and the only identified genetic association of *ZNF335* is with celiac disease⁴³. Although rs181914932 is upstream and more proximal to *PCIF1*, it has been associated with the activity of *PLTP*⁴⁴, an adjacent gene in the same locus. Our eQTL analyses demonstrated an association between the lead SNP we assessed at this locus (rs3827066) and *PLTP* expression in aortic tissue (Online Tables XX and XXI). We have also shown that *PLTP* expression is significantly higher in aneurysmal aortic tissue compared to control aorta (Online Table XXIII and Online Figure IV). *PLTP* plays a role in cholesterol transport. These data strengthen the evidence, particularly when taken together with the *SORT1* and *LDLR* associations confirmed here, that aberrations of lipid metabolism play a key role in the development of AAA.

The other novel AAA loci identified here contain *LINC00540*, *ERG* and *SMYD2*. *LINC00540* is a long non-coding RNA with no currently known function, however, both our GWAS3D and eQTL analyses independently suggested an association with *FGF9*, which was also differentially expressed within AAA tissue. *ERG* encodes a transcription factor that is normally present in hematopoietic and endothelial cells. *ERG* has a role in VEGF/MAPK mediated vascular development⁴⁵, as well as regulating angiogenesis, which is known to play a role in the development of AAA^{46, 47}. *ERG* also plays a role in the embryonic

development of the aorta⁴⁵ and it has been hypothesized that *in utero* aortic development has a role in the later development of an AAA⁴⁸. In prostate cancer, ERG has been shown to regulate the expression of MMP9⁴⁹. Taken together this limited evidence points to several potential roles by which ERG may influence the development of AAA and, along with our significant eQTL observations, strongly suggest that further work in this area is warranted.

The role of SMYD2 in AAA is less clear. SMYD2 regulates *HSP90* methylation⁵⁰ and the inhibition of HSP90 has been shown to reduce AAA formation in murine models⁵¹, suggesting this as a possible link between SMYD2 and AAA. SMYD2 also plays a role in the differentiation of embryonic stem cells⁵², again suggesting a possible role for aberrations of *in utero* aortic development influencing the risk of aortic disease later in life.

The integrated gene function analysis tool DEPICT identified numerous pathways which are potentially relevant to aneurysm pathogenesis (Table 2). In particular, we note with interest that the strongest predicted set was associated with long bone epiphyseal plate formation, which is possibly consistent with previous studies reporting tall stature as a risk factor for AAA⁵³ and conversely short stature with occlusive coronary artery disease^{36,54}.

Our network analyses using 2 different bioinformatics tools also revealed a central role for MMP9 in AAA, with IPA identifying direct interactions between ERG, IL6R and LDLR, and MMP9, and Consensus PathDB identifying a direct interaction between ERG and MMP9 with secondary interactions between both SMYD2 and LDLR, and MMP9. These results suggest that the novel loci could act in concert, either synergistically or antagonistically, to affect the AAA phenotype, and provide hypotheses for future investigation using animal and cell culture models.

In this study we did not replicate the association previously identified between *LRP1* and AAA⁷. The samples from the original study that identified this association were included in this analysis, suggesting that this may have been a false positive association. However, there is evidence supporting LRP1 as a biologically plausible candidate pathway for AAA^{55, 56}. Variants at, or close to, LRP1 are also associated with other vascular/related phenotypes (aortic dissection⁵⁷, migraine⁵⁸ and lipid traits¹⁷). Since we observed a degree of heterogeneity at this locus in our analysis (Online Table VII) we consider that further investigation of this locus remains warranted despite our findings.

Our GWAS3D genome analysis predicted potential novel biological pathways in AAA pathogenesis. For example, *FGF9* was shown to have a possible distal interaction with the intergenic SNP rs9316871. *FGF9*, while not previously considered a strong candidate in AAA pathogenesis, was nevertheless at least partially validated by its increased mRNA expression in AAA tissue (Table 3). In AAA, both the medial and adventitial layers of the vessel wall are significantly more vascularised compared to non-aneurysmal tissue⁵⁹, and it is therefore interesting to note that *FGF9* has been shown to enhance angiogenesis and neovascularisation within mouse models of myocardial infarction⁶⁰.

The main strength of this study is the inclusion of all currently available worldwide GWAS datasets for AAA and formation of an expanded International Aneurysm Consortium. We acknowledge several limitations in our work. The overall numbers of samples included in our analysis are lower than for more common traits such as diabetes¹⁵ and CAD¹⁶. We also did not have an adequate number of females in our sample set to perform sex-specific analyses which may have been informative given the strong sexual dimorphism exhibited by AAA⁶¹. We recognise this limitation but the current focus of AAA screening programmes on men alone^{2,3} and the much reduced prevalence of AAA in women means that collecting adequate samples for such analyses is likely to be challenging. Some of the contributing GWAS studies such as the Aneurysm Consortium GWAS were derived from multi-centre sample collections which led to inter-cohort heterogeneity in clinical phenotyping of the case groups. Together with the limited covariate data available for the control groups in the GWAS studies that used population control samples, this led to

an inability to reliably adjust for clinical covariates in our overall analysis. Given these limitations, and in particular regarding the numbers of samples available for analysis in AAA, alternative approaches for investigating the genetic etiology of AAA need to be considered. The natural history of AAA with a long latent period (if detected early), during which patients are monitored by serial imaging studies offers the opportunity to study disease progression as a continuous trait, leveraging additional power over discrete trait approaches for the limited sample sizes available.³⁷

In conclusion, our meta-GWAS and the bioinformatics analyses, applying multiple techniques, has highlighted several potentially novel mechanisms of AAA pathobiology. These will require direct investigation in future studies to confirm their role in the development and progression of AAA.

ACKNOWLEDGMENTS

The AAA Consortium made use of the WTCCC data. The full list of investigators is available at www.wtccc.org.uk. Data on coronary artery disease/myocardial infarction were contributed by CARDIoGRAMplusC4D investigators and were downloaded from www.CARDIOGRAMPLUSC4D.ORG.

SOURCES OF FUNDING

The WTCCC project was funded by the Wellcome Trust (awards 076113 and 085475). The New Zealand project was funded by the Health Research Council of New Zealand (08-75, 14-155). Recruitment of AAA patients and controls in Belgium, Canada and Pittsburgh, USA was funded in part by the National Heart, Lung, and Blood Institute, NIH (HL064310, HL044682). The Geisinger sample collection was funded in part by the Pennsylvania Commonwealth Universal Research Enhancement program, the Geisinger Clinical Research Fund, the American Heart Association, and the Ben Franklin Technology Development Fund of Pennsylvania. The Barts Cardiovascular Biomedical Research Unit is funded by the National Institute for Health Research. The eMERGE Network is funded by NHGRI, with additional funding from NIGMS through the following grants: U01HG004438 to Johns Hopkins University; U01HG004424 to The Broad Institute; U01HG004438 to CIDR; U01HG004610 and U01HG006375 to Group Health Cooperative; U01HG004608 to Marshfield Clinic; U01HG006389 to Essentia Institute of Rural Health; U01HG04599 and U01HG006379 to Mayo Clinic; U01HG004609 and U01HG006388 to Northwestern University; U01HG04603 and U01HG006378 to Vanderbilt University; U01HG006385 to the Coordinating Center; U01HG006382 to Geisinger Health System; U01HG006380 to Icahn School of Medicine Mount Sinai. The generation and management of GWAS data for the Rotterdam Study (control samples for the Dutch GWAS) is supported by the Netherlands Organization of Scientific Research NWO Investments (175.010.2005.011, 911-03-012). This study is funded by the Research Institute for Diseases in the Elderly (014-93-015; RIDE2), the Netherlands Genomics Initiative (NGI)/NWO project nr. 050-060-810. The Italian sample collection were funded by grants from Ente Cassa di Risparmio di Firenze to Fiorgen Foundation, Florence, Italy, and from the Italian Ministry of Health. Sample collections from Poland were funded in part by the National Science Centre in Poland (6P05A03921, NN403250440). The Mayo Vascular Disease Biorepository was funded by a Marriot Award for Individualized Medicine and an Award from the Mayo Center of Individualized Medicine. The Vanderbilt dataset(s) were obtained from Vanderbilt University Medical Center's BioVU supported by institutional funding and by the National Center for Research Resources (UL1 RR024975-01, which is now at the National Center for Advancing Translational Sciences, UL1 TR000445-06). The ASAP study was supported by the Swedish Research Council, the Swedish Heart-Lung Foundation, the Leducq Foundation (MIBAVA), and a donation by Fredrik Lundberg. SEH holds a Chair funded by the British Heart Foundation, and is supported by the BHF (PG08/008) and by the National Institute for Health Research University College London Hospitals Biomedical Research Centre. The Cardiogenics project was supported by the European Union 6th Framework Programme (LSHM-CT-2006-037593). SCH is funded by a BHF clinical training fellowship (FS/11/16/28696). The STARNET biobank

and the generation of the RNASeq dataset was funded by Astra-Zeneca Translational Science Centre-Karolinska Institutet, the University of Tartu (SP1GVARENG), the Estonian Research Council (ETF 8853), the Torsten and Ragnar Söderberg Foundation, the Knut and Alice Wallenberg Foundation, the American Heart Association (A14SFRN20840000) and by the National Institute of Health (R01HL71207).

DISCLOSURES

Johan LM Björkegren is founder and major shareholder in Clinical Gene Networks AB (“CGN”) together with Arno Ruusalepp. Björkegren, Ruusalepp and Eric E Schadt are members of the board of directors. CGN has an invested interest in the STARNET biobank and dataset.

REFERENCES

1. Lederle FA. In the clinic. Abdominal aortic aneurysm. *Ann Intern Med.* 2009;150:ITC5-1-15.
2. Guirguis-Blake JM, Beil TL, Senger CA, Whitlock EP. Ultrasonography screening for abdominal aortic aneurysms: A systematic evidence review for the U.S. Preventive services task force. *Ann Intern Med.* 2014;160:321-329
3. Abdominal aortic aneurysm screening: 2014 to 2015 data. The NHS AAA Screening Programme. Available: <https://www.gov.uk/government/publications/abdominal-aortic-aneurysm-screening-2014-to-2015-data> Accessed 12th July 2016
4. Wahlgren CM, Larsson E, Magnusson PK, Hultgren R, Swedenborg J. Genetic and environmental contributions to abdominal aortic aneurysm development in a twin population. *J Vasc Surg.* 2010;51:3-7
5. Larsson E, Granath F, Swedenborg J, Hultgren R. A population-based case-control study of the familial risk of abdominal aortic aneurysm. *J Vasc Surg.* 2009;49:47-50
6. Gretarsdottir S, Baas AF, Thorleifsson G, et al. Genome-wide association study identifies a sequence variant within the *dab2ip* gene conferring susceptibility to abdominal aortic aneurysm. *Nat Genet.* 2010;42:692-U671
7. Bown MJ, Jones GT, Harrison SC, et al. Abdominal aortic aneurysm is associated with a variant in low-density lipoprotein receptor-related protein 1. *Am J Hum Genet.* 2011;89:619-627
8. Bradley DT, Hughes AE, Badger SA, et al. A variant in *LDLR* is associated with abdominal aortic aneurysm. *Circ Cardiovasc Genet.* 2013;6:498-504
9. Jones GT, Bown MJ, Gretarsdottir S, et al. A sequence variant associated with sortilin-1 (*SORT1*) on 1p13.3 is independently associated with abdominal aortic aneurysm. *Hum Mol Genet.* 2013;22(14):2941-7
10. Harrison SC, Smith AJ, Jones GT, et al. Interleukin-6 receptor pathways in abdominal aortic aneurysm. *Eur Heart J.* 2012 34(48):3707-16
11. Helgadottir A, Thorleifsson G, Magnusson KP, et al. The same sequence variant on 9p21 associates with myocardial infarction, abdominal aortic aneurysm and intracranial aneurysm. *Nat Genet.* 2008;40:217-224
12. Willer CJ, Li Y, Abecasis GR. Metal: Fast and efficient meta-analysis of genomewide association scans. *Bioinformatics.* 2010;26:2190-2191
13. Shi YY, He L. Shesis, a powerful software platform for analyses of linkage disequilibrium, haplotype construction, and genetic association at polymorphism loci. *Cell Res.* 2005;15:97-98
14. Han B, Eskin E. Random-effects model aimed at discovering associations in meta-analysis of genome-wide association studies. *Am J Hum Genet.* 2011;88:586-598
15. Morris AP, Voight BF, Teslovich TM, et al. Large-scale association analysis provides insights into the genetic architecture and pathophysiology of type 2 diabetes. *Nat Genet.* 2012;44:981-990
16. Schunkert H, König IR, Kathiresan S, et al. Large-scale association analysis identifies 13 new susceptibility loci for coronary artery disease. *Nat Genet.* 2011;43:333-338

17. Willer CJ, Schmidt EM, Sengupta S, et al. Discovery and refinement of loci associated with lipid levels. *Nat Genet.* 2013;45:1274-1283
18. Wain LV, Verwoert GC, O'Reilly PF, et al. Genome-wide association study identifies six new loci influencing pulse pressure and mean arterial pressure. *Nat Genet.* 2011;43:1005-1011
19. Ramos EM, Hoffman D, Junkins HA, Maglott D, Phan L, Sherry ST, Feolo M, Hindorff LA. Phenotype-genotype integrator (PheGenI): Synthesizing genome-wide association study (GWAS) data with existing genomic resources. *Eur J Hum Genet.* 2014;22:144-147
20. Leslie R, O'Donnell CJ, Johnson AD. Grasp: Analysis of genotype-phenotype results from 1390 genome-wide association studies and corresponding open access database. *Bioinformatics.* 2014;30:i185-194
21. Denny JC, Ritchie MD, Basford MA, Pulley JM, Bastarache L, Brown-Gentry K, Wang D, Masys DR, Roden DM, Crawford DC. Phewas: Demonstrating the feasibility of a phenome-wide scan to discover gene-disease associations. *Bioinformatics.* 2010;26:1205-1210
22. Pendergrass SA, Brown-Gentry K, Dudek S, et al. Phenome-wide association study (PheWAS) for detection of pleiotropy within the population architecture using genomics and epidemiology (PAGE) network. *PLoS Genet.* 2013;9:e1003087
23. Gottesman O, Kuivaniemi H, Tromp G, et al. The electronic medical records and genomics (eMERGE) network: Past, present, and future. *Genet Med.* 2013;15:761-771
24. Reumers J, Conde L, Medina I, Maurer-Stroh S, Van Durme J, Dopazo J, Rousseau F, Schymkowitz J. Joint annotation of coding and non-coding single nucleotide polymorphisms and mutations in the snpeffect and pupasuite databases. *Nucleic Acids Res.* 2008;36:D825-829
25. Li MJ, Wang LY, Xia Z, Sham PC, Wang J. Gwas3d: Detecting human regulatory variants by integrative analysis of genome-wide associations, chromosome interactions and histone modifications. *Nucleic Acids Res.* 2013;41:W150-158
26. Pers TH, Karjalainen JM, Chan Y, et al. Biological interpretation of genome-wide association studies using predicted gene functions. *Nat Commun.* 2015;6:5890
27. Folkersen L, van't Hooft F, Chernogubova E, Agardh HE, Hansson GK, Hedin U, Liska J, Syvanen AC, Paulsson-Berne G, Franco-Cereceda A, Hamsten A, Gabrielsen A, Eriksson P. Association of genetic risk variants with expression of proximal genes identifies novel susceptibility genes for cardiovascular disease. *Circ Cardiovasc Genet.* 2010;3:365-373
28. Björkegren JLM, Kovacic JC, Dudley JT, Schadt EE. Genome-wide significant loci: How important are they?: Systems genetics to understand heritability of coronary artery disease and other common complex disorders. *JACC.* 2015;65:830-845
29. Kuivaniemi H, Platsoucas CD, Tilson MD, 3rd. Aortic aneurysms: An immune disease with a strong genetic component. *Circulation.* 2008;117:242-252
30. Biros E, Gabel G, Moran CS, Schreurs C, Lindeman JH, Walker PJ, Nataatmadja M, West M, Holdt LM, Hinterseher I, Pilarsky C, Golledge J. Differential gene expression in human abdominal aortic aneurysm and aortic occlusive disease. *Oncotarget.* 2015;6:12984-12996
31. Pahl MC, Erdman R, Kuivaniemi H, Lillvis JH, Elmore JR, Tromp G. Transcriptional (ChIP-Chip) analysis of ELF1, ETS2, RUNX1 and STAT5 in human abdominal aortic aneurysm. *Int J Mol Sci.* 2015;16:11229-11258
32. Kamburov A, Stelzl U, Lehrach H, Herwig R. The ConsensusPathDB interaction database: 2013 update. *Nucleic Acids Res.* 2013;41:D793-800
33. Pentchev K, Ono K, Herwig R, Ideker T, Kamburov A. Evidence mining and novelty assessment of protein-protein interactions with the ConsensusPathDB plugin for cytoscape. *Bioinformatics.* 2010;26:2796-2797
34. Nguyen H, Allali-Hassani A, Antonysamy S, et al. LLY-507, a cell-active, potent, and selective inhibitor of protein-lysine methyltransferase smyd2. *J Biol Chem.* 2015;290:13641-13653
35. Xu G, Liu G, Xiong S, Liu H, Chen X, Zheng B. The histone methyltransferase SMYD2 is a negative regulator of macrophage activation by suppressing Interleukin 6 (IL-6) and Tumor Necrosis Factor alpha (TNF-alpha) production. *J Biol Chem.* 2015;290:5414-5423

36. Paajanen TA, Oksala NK, Kuukasjarvi P, Karhunen PJ. Short stature is associated with coronary heart disease: A systematic review of the literature and a meta-analysis. *Eur Heart J.* 2010;31:1802-1809
37. Deloukas P, Kanoni S, Willenborg C, et al. Large-scale association analysis identifies new risk loci for coronary artery disease. *Nat Genet.* 2013;45:25-33
38. Eicher JD, Landowski C, Stackhouse B, Sloan A, Chen W, Jensen N, Lien JP, Leslie R, Johnson AD. Grasp v2.0: An update on the genome-wide repository of associations between snps and phenotypes. *Nucleic Acids Res.* 2015;43:D799-804
39. Smelser DT, Tromp G, Elmore JR, Kuivaniemi H, Franklin DP, Kirchner HL, Carey DJ. Population risk factor estimates for abdominal aortic aneurysm from electronic medical records: A case control study. *BMC Cardiovasc Disord.* 2014;14:174
40. Zhang X, Gierman HJ, Levy D, Plump A, Dobrin R, Goring HH, Curran JE, Johnson MP, Blangero J, Kim SK, O'Donnell CJ, Emilsson V, Johnson AD. Synthesis of 53 tissue and cell line expression qtl datasets reveals master eqtls. *BMC Genomics.* 2014;15:532
41. Hannou SA, Wouters K, Paumelle R, Staels B. Functional genomics of the CDKN2a/b locus in cardiovascular and metabolic disease: What have we learned from GWASs? *Trends Endocrinol Metab.* 2015;26:176-184
42. Pearce WH, Shively VP. Abdominal aortic aneurysm as a complex multifactorial disease: Interactions of polymorphisms of inflammatory genes, features of autoimmunity, and current status of MMPs. *Ann NY Acad Sci.* 2006;1085:117-132
43. Coleman C, Quinn EM, Ryan AW, et al. Common polygenic variation in coeliac disease and confirmation of ZNF335 and NIFA as disease susceptibility loci. 2016;24:291-297
44. Kim DS, Burt AA, Ranchalis JE, Vuletic S, Vaisar T, Li WF, Rosenthal EA, Dong W, Eintracht JF, Motulsky AG, Brunzell JD, Albers JJ, Furlong CE, Jarvik GP. PLTP activity inversely correlates with CAAD: Effects of PON1 enzyme activity and genetic variants on PLTP activity. *J Lipid Res.* 2015;56:1351-1362
45. Wythe JD, Dang LT, Devine WP, Boudreau E, Artap ST, He D, Schachterle W, Stainier DY, Oettgen P, Black BL, Bruneau BG, Fish JE. ETS factors regulate VEGF-dependent arterial specification. *Developmental cell.* 2013;26:45-58
46. Choke E, Cockerill GW, Dawson J, Wilson RW, Jones A, Loftus IM, Thompson MM. Increased angiogenesis at the site of abdominal aortic aneurysm rupture. *Ann NY Acad Sci.* 2006;1085:315-319
47. Choke E, Thompson MM, Dawson J, Wilson WR, Sayed S, Loftus IM, Cockerill GW. Abdominal aortic aneurysm rupture is associated with increased medial neovascularization and overexpression of proangiogenic cytokines. *ATVB.* 2006;26:2077-2082
48. Norman PE, Powell JT. Site specificity of aneurysmal disease. *Circulation.* 2010;121:560-568
49. Tian TV, Tomavo N, Huot L, Flourens A, Bonnelye E, Flajollet S, Hot D, Leroy X, de Launoit Y, Duterque-Coquillaud M. Identification of novel TMPRSS2:ERG mechanisms in prostate cancer metastasis: Involvement of mmp9 and plxna2. *Oncogene.* 2014;33:2204-2214
50. Du SJ, Tan X, Zhang J. Smyd proteins: Key regulators in skeletal and cardiac muscle development and function. *Anatomical record (Hoboken, N.J. : 2007).* 2014;297:1650-1662
51. Qi J, Yang P, Yi B, Huo Y, Chen M, Zhang J, Sun J. Heat shock protein 90 inhibition by 17-DMAG attenuates abdominal aortic aneurysm formation in mice. *Am J Physiol.* 2015;308:H841-852
52. Sese B, Barrero MJ, Fabregat MC, Sander V, Izpisua Belmonte JC. SMYD2 is induced during cell differentiation and participates in early development. *Int J Dev Biol.* 2013;57:357-364
53. Reed D, Reed C, Stemmermann G, Hayashi T. Are aortic aneurysms caused by atherosclerosis? *Circulation.* 1992;85:205-211
54. Nelson CP, Hamby SE, Saleheen D, et al. Genetically determined height and coronary artery disease. *N Engl J Med.* 2015;372:1608-1618
55. Chan CY, Chan YC, Cheuk BL, Cheng SW. A pilot study on low-density lipoprotein receptor-related protein-1 in chinese patients with abdominal aortic aneurysm. *Eur J Vasc Endovasc Surg.* 2013;46:549-556

56. Muratoglu SC, Belgrave S, Hampton B, Migliorini M, Coksaygan T, Chen L, Mikhailenko I, Strickland DK. LRP1 protects the vasculature by regulating levels of connective tissue growth factor and HTRA1. *ATVB*. 2013;33:2137-2146
57. Guo DC, Grove ML, Prakash SK, et al. Genetic Variants in LRP1 and ULK4 Are Associated with Acute Aortic Dissections. *Am J Hum Genet*. 2016; 99: 762-9.
58. Chasman DI, Schurks M, Anttila V, et al. Genome-wide association study reveals three susceptibility loci for common migraine in the general population. *Nat Genet*. 2011; 43: 695-8.
59. Jones GT. Gregory T Jones (2011). *The Pathohistology of Abdominal Aortic Aneurysm, Diagnosis, Screening and Treatment of Abdominal, Thoracoabdominal and Thoracic Aortic Aneurysms*, Prof. Reinhart Grundmann (Ed.), ISBN: 978-953-307-466-5, InTech, Available from: <http://www.intechopen.com/books/diagnosis-screening-and-treatment-of-abdominal-thoracoabdominal-and-thoracic-aortic-aneurysms/the-pathohistology-of-abdominal-aortic-aneurysm>.
60. Singla D, Wang J. Fibroblast growth factor-9 activates C-KIT progenitor cells and enhances angiogenesis in the infarcted diabetic heart. *Oxid Med Cell Longev*. 2016;2016:5810908
61. Bloomer LD, Bown MJ, Tomaszewski M. Sexual dimorphism of abdominal aortic aneurysms: A striking example of "male disadvantage" in cardiovascular disease. *Atherosclerosis*. 2012;225:22-28



Circulation Research

ONLINE FIRST

FIGURE LEGENDS

Figure 1. Whole-genome association plot for the primary meta-analysis of genome-wide association studies of AAA. Data represent a meta-analysis of 4,972 AAA cases and 99,858 controls. The horizontal line indicates the P -value threshold of 5×10^{-6} used to select loci for validation studies. The 9 subsequently validated AAA loci are indicated along with the previously identified *LRP1* locus, which fell to $P=6.4 \times 10^{-7}$ in the combined discovery/ validation analysis. See Online Tables III and IV for details.

Figure 2. Regional association plots for four new AAA genome-wide significant loci at 1q32.3, 13q12.11, 20q13.12 and 21q22.2. New AAA genome-wide significant loci at 1q32.3 (near *SMYD2*), 13q12.11 (*LINC00540*), 20q13.12 (near *MMP9/ZNF335*), and 21q22.2 (*ERG*). $-\log_{10}(P_{\text{fixed}})$ values for SNPs from the AAA discovery meta-analysis of 4,972 cases and 99,858 controls were plotted against their genomic positions using LocusZoom (1000Genomes, EUR, Nov 2014). The peak SNP in each region is labelled (purple diamond), while the color indicates LD (r^2) with the peak.

Figure 3. Association between the lead SNPs at the AAA risk loci and association P -values for other cardiovascular risk factors/traits. See Online Table IX for details. CAD: Coronary Artery Disease; HDL: High-density Lipoprotein; LDL: Low-density Lipoprotein; TG: Triglyceride; DBP: Diastolic Blood Pressure; SBP: Systolic Blood Pressure.

Figure 4. Circle plot showing the lead SNP distal interaction regions based on the 9 replicated AAA GWAS SNPs. Top variants with highest regulatory signals and distal interaction regions are shown on the outer circle (significant regulatory variants are labelled with 'I_'). The inner circle shows genes and genomic loci, while the distal interactive signals are shown with red lines (width corresponds to intensity of interaction). Note the long-range interactions, such as that between variants associated with *IL6R* (rs4845620, 1q21.3) and *TYW1B* (7q11.23).

Research

ONLINE FIRST

NOVELTY AND SIGNIFICANCE

What Is Known?

- Abdominal aortic aneurysm (AAA) has a prevalence of approximately 1.5% in men over 65 years of age.
- Positive family history of AAA is a strong risk factor for AAA, however, only six robust and independently validated AAA genetic loci have been identified to date.

What New Information Does This Article Contribute?

- Four novel genetic loci associated with AAA were identified.
- Pathway analysis highlighted the potential importance of lipoprotein metabolism, inflammation and matrix metalloproteinases in AAA pathobiology.
- Potentially novel mechanisms, involving genes such as *ERG*, *PLTP* and *FGF9*, were implicated.

AAA is a significant health burden, particularly amongst elderly males. It has a strong heritable component, however, previously identified risk loci explain only a small proportion of this effect. No current effective medical therapies that slow AAA growth exist, highlighting the need to better understand factors influencing pathogenesis and disease progression. This study is the first meta-analysis of genome-wide association studies (GWAS) for AAA, (10,204 cases). Four novel loci were identified and five of the six previous AAA genetic associations were confirmed. The new loci showed no significant associations with other arterial disease phenotypes, potentially suggesting associations more specific to AAA than known loci (such as *CDKN2BAS1*, *SORT1* and *LDLR*). Associations were consistent with known AAA pathobiology, implicating lipoprotein metabolism, inflammation and matrix metalloproteinases, but also identified potentially novel mechanisms relating to genes such as *ERG* and *FGF9*. This study has identified novel, potentially disease specific, genetic associations with AAA. Further functional studies, investigating the translational potential of these observations, will be required.

Table 1: List of AAA associated loci surpassing a genome-wide significance threshold after combining GWAS data (4,972 cases and 99,858 controls) and validation data (5,232 cases and 7,908 controls). For all loci shown the direction of effect was consistent across all studies in the discovery phase. Full details are shown in Online Tables III, IV, V, VI and VII. Results shown for the Discovery, Validation and Combined analyses are all Maentel-Haenzel fixed effect meta-analysis method.

SNP	Ch	r	Position	Nearest gene(s)	Min_A II*	Maj_A II*	MAF	Discovery phase			Validation phase			Combined			
								OR	P-value	I ²	OR	P-value	I ²	OR	95% CI	P-value	I ²
Previously reported AAA risk loci:																	
rs602633	1		1098215	PSRC1-CELSR2-SORT1	T	G	0.199	0.845	3.12x10 ⁻²⁹	29.08	0.920	9.83x10 ⁻³	55.7	0.87	0.842–0.918	6.58x10⁻⁹	54.5
rs412926	1		1544262	IL6R	T	C	0.370	0.854	1.74x10 ⁻¹⁰	10	0.904	1.81x10 ⁻⁴	17.2	0.87	0.846–0.908	4.76x10⁻¹³	0.0
rs107572	9		2209605	CDKN2BAS1/ANRIL	A	G	0.462	0.832	2.71x10 ⁻¹³	13	0.774	1.02x10 ⁻²¹	64.2	0.80	0.778–0.834	1.54x10⁻³³	55.6
rs109853	9		1244252	DAB2IP	T	C	0.195	1.185	2.01x10 ⁻⁷	7	1.155	2.30x10 ⁻⁵	3.9	1.17	1.118–1.226	2.40x10⁻¹¹	9.2
rs651172	19		1120230	LDLR	T	G	0.096	0.743	8.60x10 ⁻¹³	13	0.868	6.02x10 ⁻⁴	68.2	0.80	0.759–0.851	7.90x10⁻¹⁴	61.0
Novel AAA risk loci:																	
rs179506	1		2144092	SMYD2	T	C	0.337	1.154	3.26x10 ⁻⁸	8	1.105	3.49x10 ⁻⁴	70.3	1.13	1.090–1.174	8.80x10⁻¹¹	61.9
rs931687	13		2286192	LINC00540	A	G	0.201	0.864	1.23x10 ⁻⁶	6	0.883	8.28x10 ⁻⁵	0.0	0.87	0.837–0.911	4.75x10⁻¹⁰	0.0
rs382706	20		4458602	PCIF1-ZNF335-MMP9	T	C	0.179	1.232	1.88x10 ⁻¹⁰	10	1.213	2.00x10 ⁻⁸	16.5	1.22	1.168–1.281	2.13x10⁻¹⁷	0.0
rs283641	21		3981983	ERG	T	C	0.369	1.149	2.51x10 ⁻⁸	8	1.072	1.13x10 ⁻²	28.3	1.11	1.074–1.154	5.80x10⁻⁹	42.2

* Effect allele indicated in bold

Table 2: DEPICT gene enrichment sets based on the top 10 validated loci. This table is a truncated version of the full list available as Online Table XVIII in the Supplement. Asterisk in the ID column indicates the gene sets that had a false discovery rate of <0.2

Original gene set ID	Original gene set description	DEPICT Nominal
MP:0006396*	Decreased long bone epiphyseal plate size	1.14x10 ⁻⁹
GO:0034381	Plasma lipoprotein particle clearance	5.22x10 ⁻⁷
ENSG00000132005	RFX1 PPI subnetwork	2.28x10 ⁻⁶
MP:0005595	Abnormal vascular smooth muscle physiology	1.55x10 ⁻³
ENSG00000122641	INHBA PPI subnetwork	1.79x10 ⁻³
MP:0002764	Short tibia	1.79x10 ⁻³
ENSG00000169047	IRS1 PPI subnetwork	2.21x10 ⁻³
GO:0050431	Transforming growth factor beta binding	2.47x ⁻¹⁰³
MP:0005590	Increased vasodilation	3.45x10 ⁻³
GO:0071813	Lipoprotein particle binding	3.51x10 ⁻³
GO:0005178	Integrin binding	4.08x10 ⁻³
ENSG00000133056	PIK3C2B PPI subnetwork	4.40x10 ⁻³
MP:0005095	Decreased T cell proliferation	4.84x10 ⁻³
ENSG00000149257	SERPINH1 PPI subnetwork	5.79x10 ⁻³
ENSG00000034152	MAP2K3 PPI subnetwork	6.58x10 ⁻³
ENSG00000017427	IGF1 PPI subnetwork	7.51x10 ⁻³
GO:0043406	Positive regulation of MAP kinase activity	7.65x10 ⁻³
MP:0000180	Abnormal circulating cholesterol level	7.71x10 ⁻³
MP:0001915	Intracranial hemorrhage	8.00x10 ⁻³
MP:0004883	Abnormal vascular wound healing	8.15x10 ⁻³
ENSG00000106992	AK1 PPI subnetwork	8.69x10 ⁻³
MP:0003419	Delayed endochondral bone ossification	8.98x10 ⁻³
MP:0000716	Abnormal immune system cell morphology	9.63x10 ⁻³
ENSG00000170581	STAT2 PPI subnetwork	9.79x10 ⁻³
GO:0043277	Apoptotic cell clearance	9.98x10 ⁻³
MP:0001828	Abnormal T cell activation	0.01
ENSG00000141506	PIK3R5 PPI subnetwork	0.01
GO:0000989	Transcription factor binding/transcription	0.01
GO:0007254	JNK cascade	0.01
GO:0014910	Regulation of smooth muscle cell migration	0.02
MP:0001552	Increased circulating triglyceride level	0.02
MP:0001559	Hyperglycemia	0.02
ENSG00000105851	PIK3CG PPI subnetwork	0.02
GO:0050900	Leukocyte migration	0.03
MP:0003957	Abnormal nitric oxide homeostasis	0.03
GO:0006953	Acute-phase response	0.03
ENSG00000206240	HLA-DRB1 PPI subnetwork	0.03
GO:0043123	Positive regulation of I-kappaB kinase/NF-	0.03
ENSG00000145431	PDGFC PPI subnetwork	0.04
MP:0008706	Decreased interleukin-6 secretion	0.04
MP:0008688	Decreased interleukin-2 secretion	0.04

Table 3: Genes predicted by GWAS3D analysis to be associated with putative AAA loci identified in the discovery study demonstrating significantly different mRNA expression in aneurysmal aortic wall samples from 49 patients with AAA compared to 10 organ donor control aortic samples. Non-significant results (30 genes) are shown in Online Table XXIII and box and whiskers plots on mRNA expression levels are presented in Online Figure IV.. See Figure 5 for results from the GWAS3D analysis.

GWAS 3D Gene selection	Gene	Locus	mRNA	AAA
Predicted distal interaction	BCAR3	1p22.1	1.8x10 ⁻⁴	decreased
SNP in proximity with lead	SORT1	1p13.3	1.1x10 ⁻⁴	decreased
Predicted distal interaction	NOTCH2	1p12	4.6x10 ⁻⁷	increased
Predicted distal interaction	TDRD10	1q21.3	0.006	increased
Predicted distal interaction	UBE2W	8q21.11	0.030	increased
SNP in proximity with lead	CDKN2BAS1/ANRIL	9p21.3	0.003	increased
SNP in proximity with lead	LRP1	12q13.3	0.008	decreased
SNP in proximity with lead	NAB2	12q13.3	1.1x10 ⁻⁵	decreased
Predicted distal interaction	FGF9	13q11	0.002	increased
SNP in proximity with lead	PLTP	20q13.12	0.011	increased

Circulation Research

ONLINE FIRST

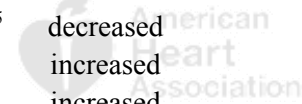
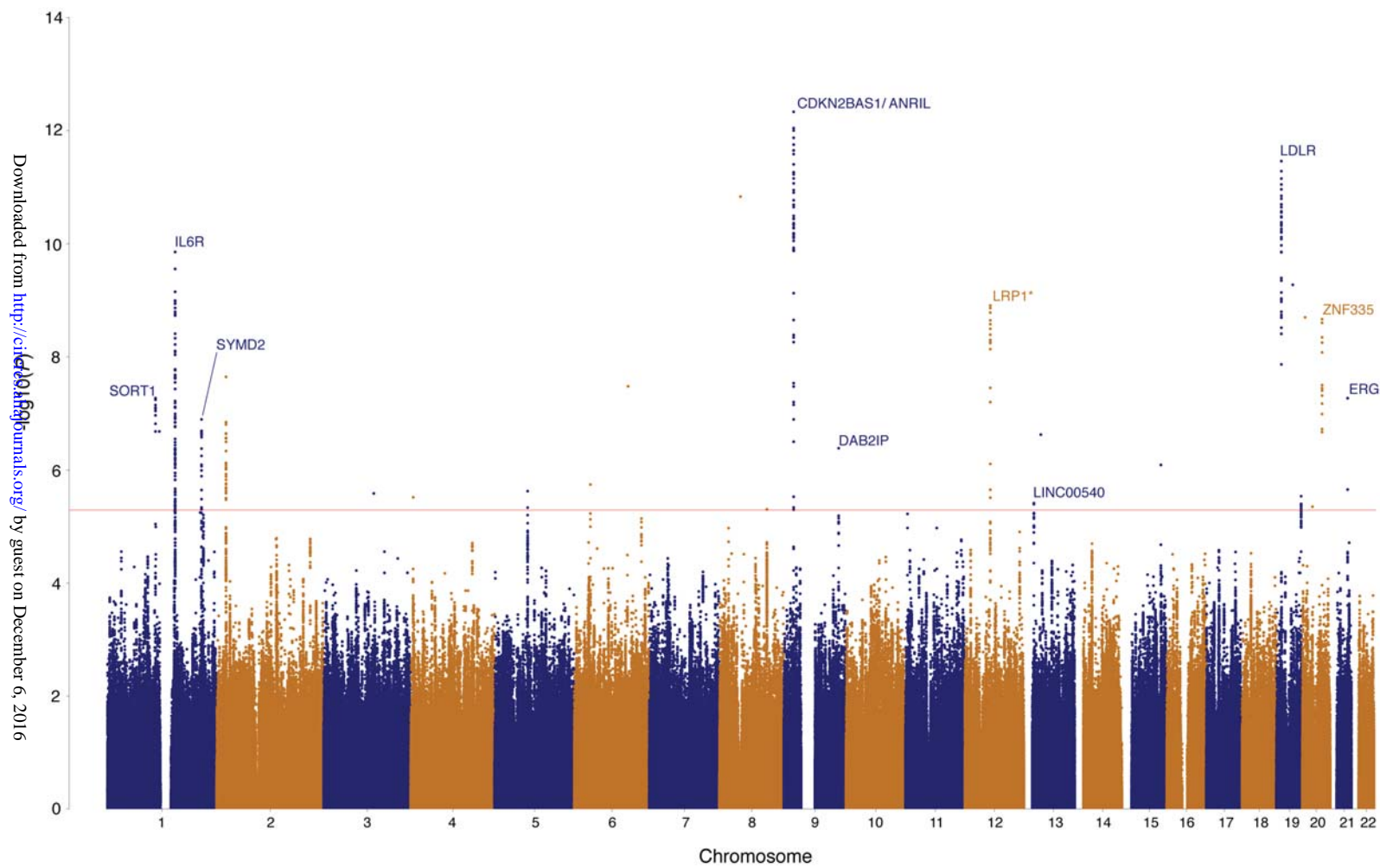


FIGURE 1



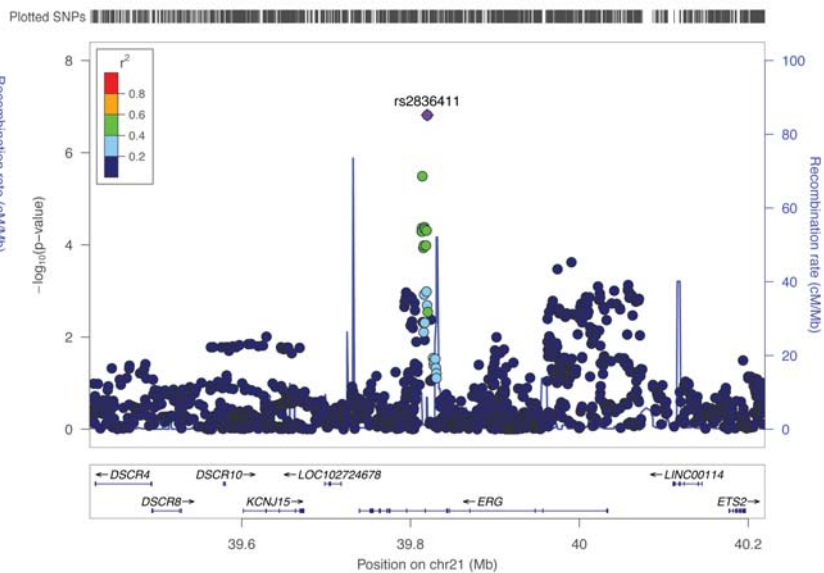
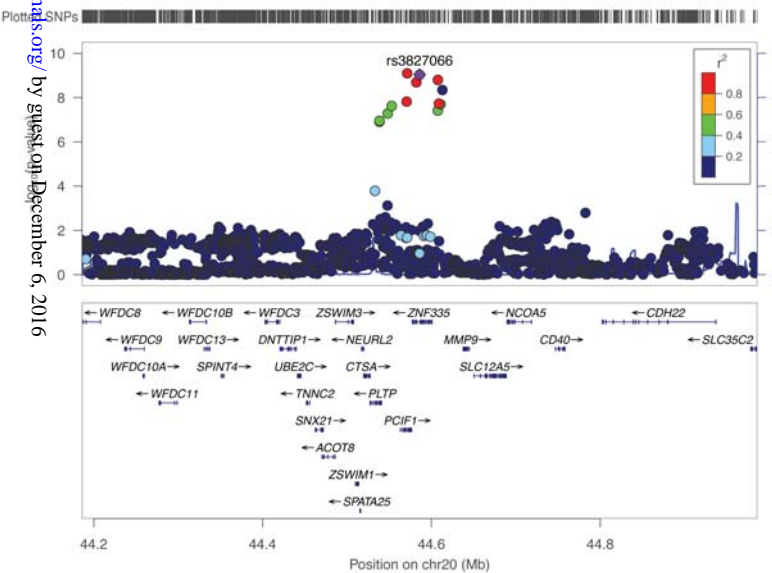
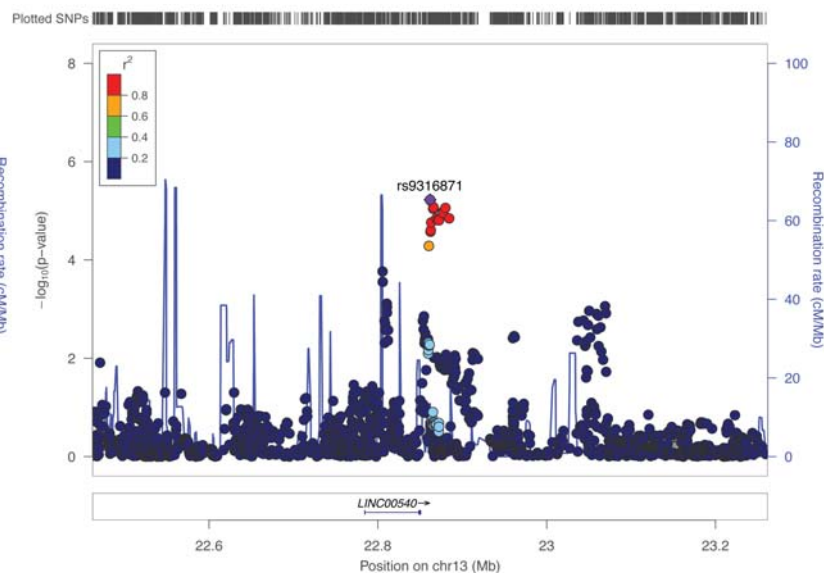
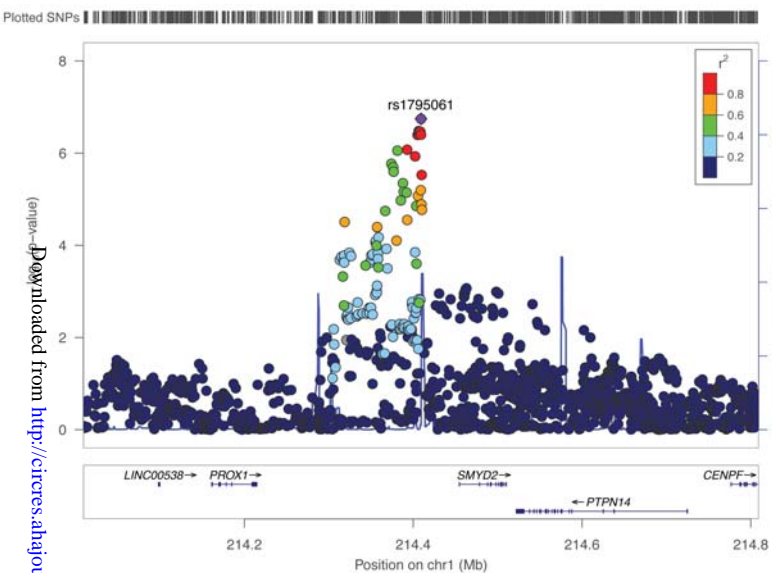
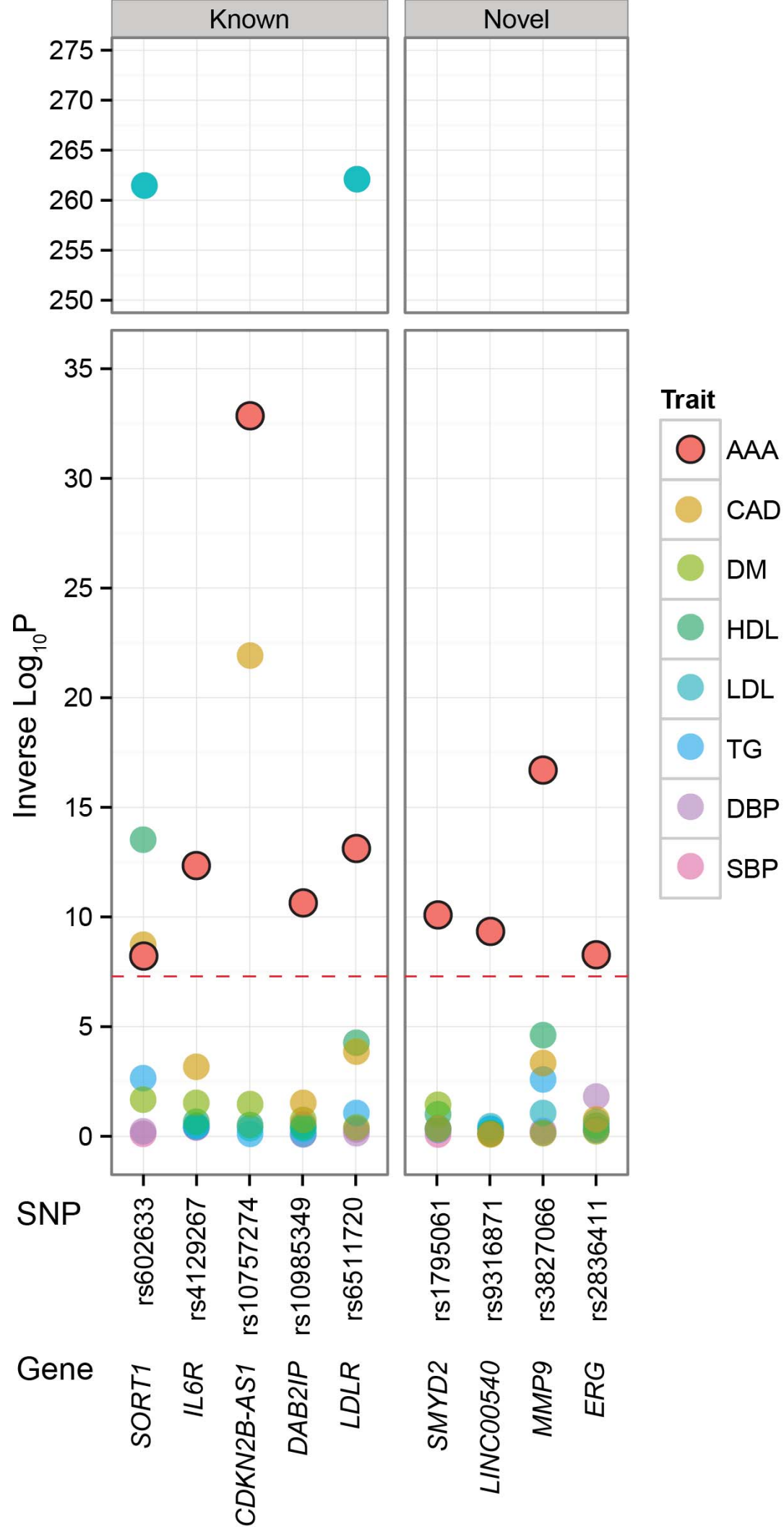


FIGURE 3



Meta-Analysis of Genome-Wide Association Studies for Abdominal Aortic Aneurysm Identifies Four New Disease-Specific Risk Loci

Gregory T Jones, Gerard Tromp, Helena Kuivaniemi, Solveig Gretarsdottir, Annette F Baas, Betti Giusti, Ewa Strauss, Femke N van 't Hof, Thomas Webb, Robert Erdman, Marylyn D Ritchie, James R Elmore, Anurag Verma, Sarah Pendergrass, Iftikhar J Kullo, Zi Ye, Peggy L Peissig, Omri Gottesman, Shefali S Verma, Jennifer Malinowski, Laura J Rasmussen-Torvik, Kenneth Borthwick, Diane T Smelser, David R Crosslin, Mariza de Andrade, Evan J Ryer, Catherine A McCarty, Erwin P Bottinger, Jennifer A Pacheco, Dana C Crawford, David S Carrell, Glenn S Gerhard, David P Franklin, David J Carey, Victoria L Phillips, Michael J Williams, Wenhua Wei, Ross Blair, Andrew A Hill, Thodur M Vasudevan, David R Lewis, Ian A Thomson, Jo Krysa, Geraldine B Hill, Justin Roake, Tony R Merriman, Grzegorz Oszkinis, Silvia Galora, Claudia Saracini, Rosanna Abbate, Raffaele Pulli, Carlo Pratesi, Athanasios Saratzis, Anna Verissimo, Suzannah J Bumpstead, Stephen A Badger, Rachel E Clough, Gillian W Cockerill, Hany Hafez, D J Scott, T S Futers, Simon P Romaine, Katherine Bridge, Kathryn J Griffin, Marc A Bailey, Alberto Smith, Matt M Thompson, Frank van Bockxmeer, Stefan E Matthiasson, Gudmar Thorleifsson, Unnur Thorsteinsdottir, Jan D Blankensteijn, Joep A Teijink, Cisca Wijmenga, Jacqueline de Graaf, Lambertus A Kiemeney, Jes S Lindholt, Anne E Hughes, Declan T Bradley, Kathleen Stirrups, Jonathan Golledge, Paul E Norman, Janet T Powell, Steve E Humphries, Stephen E Hamby, Alison H Goodall, Christopher P Nelson, Nazi Sakalihasan, Audrey Courtois, Robert E Ferrell, Per Eriksson, Lasse Folkersen, Anders Franco-Cereceda, John D Eicher, Andrew D Johnson, Christer Betsholtz, Arno Ruusalepp, Oscar Franzén, Eric Schadt, Johan L Björkegren, Leonard Lipovich, Anne M Drolet, Eric Verhoeven, Clark J Zeebregts, Robert H Geelkerken, Marc R van Sambeek, Steven M van Sterkenburg, Jean-Paul P de Vries, Kari Stefansson, John R Thompson, Paul I de Bakker, Panos Deloukas, Robert D Sayers, Seamus Harrison, Andre M van Rij, Nilesh J Samani and Matthew J Bown

Permissions: Requests for permissions to reproduce figures, tables, or portions of articles originally published in *Circulation Research* can be obtained via RightsLink, a service of the Copyright Clearance Center, not the Editorial Office. Once the online version of the published article for which permission is being requested is located, click Request Permissions in the middle column of the Web page under Services. Further information about this process is available in the [Permissions and Rights Question and Answer](#) document.

Reprints: Information about reprints can be found online at:
<http://www.lww.com/reprints>

Subscriptions: Information about subscribing to *Circulation Research* is online at:
<http://circres.ahajournals.org/subscriptions/>

Circ Res. published online November 29, 2016;
Circulation Research is published by the American Heart Association, 7272 Greenville Avenue, Dallas, TX 75231
Copyright © 2016 American Heart Association, Inc. All rights reserved.
Print ISSN: 0009-7330. Online ISSN: 1524-4571

The online version of this article, along with updated information and services, is located on the
World Wide Web at:

<http://circres.ahajournals.org/content/early/2016/12/02/CIRCRESAHA.116.308765>

Free via Open Access

Data Supplement (unedited) at:

<http://circres.ahajournals.org/content/suppl/2016/11/29/CIRCRESAHA.116.308765.DC1.html>

Permissions: Requests for permissions to reproduce figures, tables, or portions of articles originally published in *Circulation Research* can be obtained via RightsLink, a service of the Copyright Clearance Center, not the Editorial Office. Once the online version of the published article for which permission is being requested is located, click Request Permissions in the middle column of the Web page under Services. Further information about this process is available in the [Permissions and Rights Question and Answer](#) document.

Reprints: Information about reprints can be found online at:
<http://www.lww.com/reprints>

Subscriptions: Information about subscribing to *Circulation Research* is online at:
<http://circres.ahajournals.org/subscriptions/>

Original gene set ID

MP:0006396
GO:0034381
ENSG000000205250
ENSG000000132005
MP:0000708
ENSG000000167553
ENSG000000170421
MP:0003645
ENSG000000166866
REACTOME_APOPTOTIC_EXECUTION__PHASE
MP:0008182
GO:0008375
ENSG000000131941
ENSG000000169710
REACTOME_APOPTOTIC_CLEAVAGE_OF_CELLULAR_PROTEINS
ENSG00000013297
ENSG000000070159
ENSG000000091409
ENSG000000178209
REACTOME_P75_NTR_RECEPTOR:MEDIATED_SIGNALLING
GO:0001890
ENSG000000164344
MP:0002136
MP:0002655
ENSG000000143375
MP:0005595
ENSG000000122641
MP:0002764
MP:0003662
ENSG000000169047
ENSG000000125503
MP:0001179
GO:0043256
ENSG000000116809
GO:0050431
ENSG000000039560
ENSG000000164733
ENSG000000139567
MP:0005590
GO:0071813
GO:0071814
MP:0002082
GO:0071902
ENSG000000130147
GO:0005178
ENSG000000133056
ENSG000000172725
ENSG000000136286
ENSG000000078142

Original gene set description

decreased long bone epiphyseal plate size
plasma lipoprotein particle clearance
E2F4 PPI subnetwork
RFX1 PPI subnetwork
thymus hyperplasia
TUBA1C PPI subnetwork
KRT8 PPI subnetwork
increased pancreatic beta cell number
MYO1A PPI subnetwork
REACTOME_APOPTOTIC_EXECUTION__PHASE
decreased marginal zone B cell number
acetylglucosaminyltransferase activity
RHPN2 PPI subnetwork
FASN PPI subnetwork
REACTOME_APOPTOTIC_CLEAVAGE_OF_CELLULAR_PROTEINS
CLDN11 PPI subnetwork
PTPN3 PPI subnetwork
ITGA6 PPI subnetwork
PLEC PPI subnetwork
REACTOME_P75_NTR_RECEPTOR:MEDIATED_SIGNALLING
placenta development
KLKB1 PPI subnetwork
abnormal kidney physiology
abnormal keratinocyte morphology
CGN PPI subnetwork
abnormal vascular smooth muscle physiology
INHBA PPI subnetwork
short tibia
abnormal long bone epiphyseal plate proliferative zone
IRS1 PPI subnetwork
PPP1R12C PPI subnetwork
thick pulmonary interalveolar septum
laminin complex
ZBTB17 PPI subnetwork
transforming growth factor beta binding
RAI14 PPI subnetwork
CTSB PPI subnetwork
ACVRL1 PPI subnetwork
increased vasodilation
lipoprotein particle binding
protein-lipid complex binding
postnatal lethality
positive regulation of protein serine/threonine kinase activity
SH3BP4 PPI subnetwork
integrin binding
PIK3C2B PPI subnetwork
CORO1B PPI subnetwork
MYO1G PPI subnetwork
PIK3C3 PPI subnetwork

Nominal P value

1.14E-09
5.22E-07
1.27E-06
2.28E-06
6.32E-06
3.18E-05
9.59E-05
1.12E-04
2.32E-04
2.92E-04
3.06E-04
3.62E-04
3.75E-04
4.55E-04
5.46E-04
6.28E-04
6.56E-04
7.26E-04
8.57E-04
1.07E-03
1.08E-03
1.09E-03
1.17E-03
1.45E-03
1.48E-03
1.55E-03
1.79E-03
1.79E-03
2.01E-03
2.21E-03
2.23E-03
2.30E-03
2.33E-03
2.46E-03
2.47E-03
2.60E-03
2.64E-03
2.75E-03
3.45E-03
3.51E-03
3.51E-03
3.53E-03
3.87E-03
3.91E-03
4.08E-03
4.40E-03
4.45E-03
4.65E-03
4.72E-03

Original gene set ID

MP:0005095
ENSG00000145715
ENSG00000104725
KEGG_PATHWAYS_IN_CANCER
GO:0008194
ENSG00000078747
ENSG00000149257
ENSG00000114062
ENSG00000139144
ENSG00000143393
ENSG00000148498
ENSG00000196455
ENSG00000148660
ENSG00000034152
ENSG00000123124
MP:0008813
ENSG00000204175
GO:0001772
REACTOME_CASPASE:MEDIATED_CLEAVAGE_OF_CYTOSKELETAL_PROTEINS
ENSG00000017427
MP:0001954
GO:0016051
GO:0043406
REACTOME_CELL_DEATH_SIGNALLING_VIA_NRAGE_NRIF_AND_NADE
MP:0000180
ENSG00000170759
ENSG00000180530
ENSG00000138771
ENSG00000065882
ENSG00000138592
MP:0001915
ENSG00000131746
MP:0004883
ENSG00000091073
ENSG00000081189
ENSG00000154415
ENSG00000188313
MP:0004933
ENSG00000147065
ENSG00000165409
ENSG00000106992
GO:0007292
ENSG00000144061
MP:0003419
ENSG00000110880
ENSG00000197879
ENSG00000176476
ENSG00000176108
REACTOME_INTEGRIN_CELL_SURFACE_INTERACTIONS

Original gene set description

decreased T cell proliferation
RASA1 PPI subnetwork
ENSG00000104725 PPI subnetwork
KEGG_PATHWAYS_IN_CANCER
UDP-glycosyltransferase activity
ITCH PPI subnetwork
SERPINH1 PPI subnetwork
UBE3A PPI subnetwork
PIK3C2G PPI subnetwork
PI4KB PPI subnetwork
PARD3 PPI subnetwork
PIK3R4 PPI subnetwork
CAMK2G PPI subnetwork
MAP2K3 PPI subnetwork
WWP1 PPI subnetwork
decreased common myeloid progenitor cell number
GPRIN2 PPI subnetwork
immunological synapse
REACTOME_CASPASE:MEDIATED_CLEAVAGE_OF_CYTOSKELETAL_PROTEINS
IGF1 PPI subnetwork
respiratory distress
carbohydrate biosynthetic process
positive regulation of MAP kinase activity
REACTOME_CELL_DEATH_SIGNALLING_VIA_NRAGE_NRIF_AND_NADE
abnormal circulating cholesterol level
KIF5B PPI subnetwork
NRIP1 PPI subnetwork
SHROOM3 PPI subnetwork
TBC1D1 PPI subnetwork
USP8 PPI subnetwork
intracranial hemorrhage
TNS4 PPI subnetwork
abnormal vascular wound healing
ENSG00000091073 PPI subnetwork
MEF2C PPI subnetwork
PPP1R3A PPI subnetwork
PLSCR1 PPI subnetwork
abnormal epididymis epithelium morphology
MSN PPI subnetwork
TSHR PPI subnetwork
AK1 PPI subnetwork
female gamete generation
NPHP1 PPI subnetwork
delayed endochondral bone ossification
CORO1C PPI subnetwork
MYO1C PPI subnetwork
CCDC101 PPI subnetwork
CHMP6 PPI subnetwork
REACTOME_INTEGRIN_CELL_SURFACE_INTERACTIONS

Nominal P value

4.84E-03
4.96E-03
5.08E-03
5.17E-03
5.46E-03
5.48E-03
5.79E-03
5.85E-03
5.85E-03
5.87E-03
6.00E-03
6.19E-03
6.48E-03
6.58E-03
6.95E-03
7.37E-03
7.39E-03
7.40E-03
7.46E-03
7.51E-03
7.56E-03
7.65E-03
7.65E-03
7.67E-03
7.71E-03
7.79E-03
7.86E-03
7.89E-03
7.97E-03
7.99E-03
8.00E-03
8.01E-03
8.15E-03
8.22E-03
8.24E-03
8.33E-03
8.55E-03
8.61E-03
8.64E-03
8.64E-03
8.69E-03
8.93E-03
8.95E-03
8.98E-03
9.04E-03
9.22E-03
9.31E-03
9.44E-03
9.47E-03

Original gene set ID	Original gene set description	Nominal P value
GO:0030247	polysaccharide binding	0.02
ENSG00000126934	MAP2K2 PPI subnetwork	0.02
ENSG00000110395	CBL PPI subnetwork	0.02
ENSG00000179151	EDC3 PPI subnetwork	0.02
ENSG00000154162	CDH12 PPI subnetwork	0.02
ENSG00000184363	PKP3 PPI subnetwork	0.02
ENSG00000020577	SAMD4A PPI subnetwork	0.02
MP:0004139	abnormal gastric parietal cell morphology	0.02
ENSG00000168476	REEP4 PPI subnetwork	0.02
ENSG00000110651	CD81 PPI subnetwork	0.02
ENSG00000134184	GSTM1 PPI subnetwork	0.02
ENSG00000105376	ICAM5 PPI subnetwork	0.02
ENSG00000196954	CASP4 PPI subnetwork	0.02
MP:0003704	abnormal hair follicle development	0.02
ENSG00000050820	BCAR1 PPI subnetwork	0.02
ENSG00000151748	SAV1 PPI subnetwork	0.02
GO:0003714	transcription corepressor activity	0.02
ENSG00000115904	SOS1 PPI subnetwork	0.02
ENSG00000175793	SFN PPI subnetwork	0.02
ENSG00000100345	MYH9 PPI subnetwork	0.02
GO:0035091	phosphatidylinositol binding	0.02
ENSG00000149930	TAOK2 PPI subnetwork	0.02
GO:0042054	histone methyltransferase activity	0.02
MP:0000689	abnormal spleen morphology	0.02
GO:0001892	embryonic placenta development	0.02
ENSG00000130294	KIF1A PPI subnetwork	0.02
ENSG00000148965	SAA4 PPI subnetwork	0.02
GO:0034774	secretory granule lumen	0.02
ENSG00000166483	WEE1 PPI subnetwork	0.02
ENSG00000110237	ARHGEF17 PPI subnetwork	0.02
GO:0032608	interferon-beta production	0.02
ENSG00000152518	ZFP36L2 PPI subnetwork	0.02
MP:0010792	abnormal stomach mucosa morphology	0.02
ENSG00000189319	FAM53B PPI subnetwork	0.02
ENSG00000117461	PIK3R3 PPI subnetwork	0.02
GO:0034362	low-density lipoprotein particle	0.02
ENSG00000134072	CAMK1 PPI subnetwork	0.02
ENSG00000163362	C1orf106 PPI subnetwork	0.02
MP:0002816	colitis	0.02
GO:0050900	leukocyte migration	0.03
GO:0044304	main axon	0.03
ENSG00000071909	MYO3B PPI subnetwork	0.03
ENSG00000100714	MTHFD1 PPI subnetwork	0.03
ENSG00000198836	OPA1 PPI subnetwork	0.03
ENSG00000197442	MAP3K5 PPI subnetwork	0.03
ENSG00000206306	HLA-DRB1 PPI subnetwork	0.03
ENSG00000206240	HLA-DRB1 PPI subnetwork	0.03
GO:0031983	vesicle lumen	0.03
KEGG_REGULATION_OF_ACTIN_CYTOSKELETON	KEGG_REGULATION_OF_ACTIN_CYTOSKELETON	0.03

Original gene set ID	Original gene set description	Nominal P value
GO:0004713	protein tyrosine kinase activity	0.03
GO:0006953	acute-phase response	0.03
GO:0003712	transcription cofactor activity	0.03
MP:0000295	trabecula carnea hypoplasia	0.03
ENSG00000105647	PIK3R2 PPI subnetwork	0.03
GO:0060205	cytoplasmic membrane-bounded vesicle lumen	0.03
ENSG00000107566	ERLIN1 PPI subnetwork	0.03
ENSG00000114270	COL7A1 PPI subnetwork	0.03
ENSG00000135930	EIF4E2 PPI subnetwork	0.03
MP:0006413	increased T cell apoptosis	0.03
ENSG00000211949	ENSG00000211949 PPI subnetwork	0.03
ENSG00000125731	SH2D3A PPI subnetwork	0.03
MP:0000414	alopecia	0.03
ENSG00000160691	SHC1 PPI subnetwork	0.03
MP:0001282	short vibrissae	0.03
MP:0003996	clonic seizures	0.03
ENSG00000019991	HGF PPI subnetwork	0.03
MP:0010025	decreased total body fat amount	0.03
GO:0007568	aging	0.03
GO:0042809	vitamin D receptor binding	0.03
MP:0005331	insulin resistance	0.03
GO:0045682	regulation of epidermis development	0.03
MP:0001923	reduced female fertility	0.03
MP:0001219	thick epidermis	0.03
ENSG00000068615	REEP1 PPI subnetwork	0.03
ENSG00000171219	CDC42BPG PPI subnetwork	0.03
MP:0009583	increased keratinocyte proliferation	0.03
ENSG00000105810	CDK6 PPI subnetwork	0.03
ENSG00000105662	CRTC1 PPI subnetwork	0.03
MP:0003957	abnormal nitric oxide homeostasis	0.03
KEGG_SMALL_CELL_LUNG_CANCER	KEGG_SMALL_CELL_LUNG_CANCER	0.03
GO:0030669	clathrin-coated endocytic vesicle membrane	0.03
ENSG00000100030	MAPK1 PPI subnetwork	0.03
GO:0046328	regulation of JNK cascade	0.03
GO:0014070	response to organic cyclic compound	0.03
GO:0033500	carbohydrate homeostasis	0.03
GO:0042593	glucose homeostasis	0.03
REACTOME_PTM_GAMMA_CARBOXYLATION_HYPUSINE_FORMATION_AND_AF	REACTOME_PTM_GAMMA_CARBOXYLATION_HYPUSINE_FORMATION_AND_ARYLS	0.03
REACTOME_REGULATION_OF_SIGNALING_BY_CBL	REACTOME_REGULATION_OF_SIGNALING_BY_CBL	0.03
MP:0002418	increased susceptibility to viral infectior	0.03
MP:0003721	increased tumor growth/size	0.03
GO:0071845	cellular component disassembly at cellular leve	0.03
GO:0030518	intracellular steroid hormone receptor signaling pathway	0.03
ENSG00000116824	CD2 PPI subnetwork	0.03
MP:0003566	abnormal cell adhesion	0.03
GO:0034061	DNA polymerase activity	0.03
ENSG00000141968	VAV1 PPI subnetwork	0.03
GO:0001701	in utero embryonic development	0.03
MP:0000166	abnormal chondrocyte morphology	0.03

Original gene set ID**Original gene set description****Nominal P value**

MP:0008722	abnormal chemokine secretion	0.05
KEGG_CHRONIC_MYELOID_LEUKEMIA	KEGG_CHRONIC_MYELOID_LEUKEMIA	0.05
REACTOME_REGULATED_PROTEOLYSIS_OF_P75NTR	REACTOME_REGULATED_PROTEOLYSIS_OF_P75NTR	0.05
GO:0043588	skin development	0.05
GO:0010627	regulation of intracellular protein kinase cascade	0.05
GO:0044212	transcription regulatory region DNA binding	0.05
GO:0030027	lamellipodium	0.05
ENSG00000105976	MET PPI subnetwork	0.05
MP:0002792	abnormal retinal vasculature morphology	0.05
MP:0000069	kyphoscoliosis	0.05
GO:0034339	regulation of transcription from RNA polymerase II promoter by nuclear hormone receptor	0.05
ENSG00000141551	CSNK1D PPI subnetwork	0.05
MP:0005108	abnormal ulna morphology	0.05
MP:0002419	abnormal innate immunity	0.05
GO:0016757	transferase activity, transferring glycosyl groups	0.05
ENSG00000161800	RACGAP1 PPI subnetwork	0.05
MP:0006387	abnormal T cell number	0.05
GO:0005089	Rho guanyl-nucleotide exchange factor activity	0.05
ENSG00000117984	CTSD PPI subnetwork	0.05
ENSG00000105971	CAV2 PPI subnetwork	0.05
ENSG00000115085	ZAP70 PPI subnetwork	0.05
MP:0004609	vertebral fusion	0.05
ENSG00000135862	LAMC1 PPI subnetwork	0.05
MP:0003449	abnormal intestinal goblet cell morphology	0.05
MP:0002687	oligozoospermia	0.05
MP:0000714	increased thymocyte number	0.05
ENSG00000133030	MPRIP PPI subnetwork	0.05
ENSG00000079841	RIMS1 PPI subnetwork	0.05
ENSG00000130638	ATXN10 PPI subnetwork	0.05
MP:0002656	abnormal keratinocyte differentiation	0.05
ENSG00000129691	ASH2L PPI subnetwork	0.05
MP:0002650	abnormal ameloblast morphology	0.05
ENSG00000135503	ACVR1B PPI subnetwork	0.05
GO:0004715	non-membrane spanning protein tyrosine kinase activity	0.05
ENSG00000001497	LAS1L PPI subnetwork	0.05
GO:0018024	histone-lysine N-methyltransferase activity	0.05
GO:0000792	heterochromatin	0.05
ENSG00000111961	SASH1 PPI subnetwork	0.05
MP:0008840	abnormal spike wave discharge	0.05
ENSG00000139514	SLC7A1 PPI subnetwork	0.05
GO:0007249	I-kappaB kinase/NF-kappaB cascade	0.05
MP:0009886	failure of palatal shelf elevation	0.06
ENSG00000144668	ITGA9 PPI subnetwork	0.06
MP:0001798	impaired macrophage phagocytosis	0.06
MP:0004148	increased compact bone thickness	0.06
GO:0034637	cellular carbohydrate biosynthetic process	0.06
REACTOME_PLATELET_SENSITIZATION_BY_LDL	REACTOME_PLATELET_SENSITIZATION_BY_LDL	0.06
GO:0008170	N-methyltransferase activity	0.06
GO:0046890	regulation of lipid biosynthetic process	0.06

Original gene set ID	Original gene set description	Nominal P value
MP:0005439	decreased glycogen level	0.08
MP:0000493	rectal prolapse	0.08
REACTOME_CIRCADIAN_CLOCK	REACTOME_CIRCADIAN_CLOCK	0.08
ENSG00000182511	FES PPI subnetwork	0.08
ENSG00000065054	SLC9A3R2 PPI subnetwork	0.08
REACTOME_TRANSCRIPTIONAL_REGULATION_OF_WHITE_ADIPOCYTE_DIFFERENTIATION	REACTOME_TRANSCRIPTIONAL_REGULATION_OF_WHITE_ADIPOCYTE_DIFFERENTIATION	0.08
KEGG_DORSO_VENTRAL_AXIS_FORMATION	KEGG_DORSO_VENTRAL_AXIS_FORMATION	0.08
ENSG00000158402	CDC25C PPI subnetwork	0.08
ENSG00000107186	MPDZ PPI subnetwork	0.08
ENSG00000117395	EBNA1BP2 PPI subnetwork	0.08
GO:0032606	type I interferon production	0.08
ENSG00000101057	MYBL2 PPI subnetwork	0.08
ENSG00000163629	PTPN13 PPI subnetwork	0.08
REACTOME_METABOLISM_OF_WATER:SOLUBLE_VITAMINS_AND_COFACTORS	REACTOME_METABOLISM_OF_WATER:SOLUBLE_VITAMINS_AND_COFACTORS	0.08
REACTOME_METABOLISM_OF_VITAMINS_AND_COFACTORS	REACTOME_METABOLISM_OF_VITAMINS_AND_COFACTORS	0.08
ENSG00000133895	MEN1 PPI subnetwork	0.08
ENSG00000197451	HNRNPAB PPI subnetwork	0.08
GO:0043029	T cell homeostasis	0.08
GO:0031252	cell leading edge	0.08
GO:0009101	glycoprotein biosynthetic process	0.08
MP:0004616	lumbar vertebral transformation	0.08
MP:0003892	abnormal gastric gland morphology	0.08
MP:0002740	heart hypoplasia	0.08
MP:0000133	abnormal long bone metaphysis morphology	0.08
ENSG00000140009	ESR2 PPI subnetwork	0.08
KEGG_PANCREATIC_CANCER	KEGG_PANCREATIC_CANCER	0.08
MP:0001209	spontaneous skin ulceration	0.08
MP:0005017	decreased B cell number	0.08
ENSG00000107262	BAG1 PPI subnetwork	0.08
ENSG00000118260	CREB1 PPI subnetwork	0.08
ENSG00000169967	MAP3K2 PPI subnetwork	0.08
GO:0050840	extracellular matrix binding	0.08
ENSG00000198286	CARD11 PPI subnetwork	0.08
GO:0005085	guanyl-nucleotide exchange factor activity	0.08
ENSG00000126001	CEP250 PPI subnetwork	0.08
ENSG00000203879	GDI1 PPI subnetwork	0.08
GO:0046970	NAD-dependent histone deacetylase activity (H4-K16 specific)	0.08
GO:0034739	histone deacetylase activity (H4-K16 specific)	0.08
GO:0031078	histone deacetylase activity (H3-K14 specific)	0.08
GO:0032041	NAD-dependent histone deacetylase activity (H3-K14 specific)	0.08
REACTOME_INTERFERON_ALPHA_BETA_SIGNALING	REACTOME_INTERFERON_ALPHA_BETA_SIGNALING	0.08
MP:0000951	sporadic seizures	0.08
ENSG00000119401	TRIM32 PPI subnetwork	0.08
ENSG00000080815	PSEN1 PPI subnetwork	0.08
GO:0033674	positive regulation of kinase activity	0.08
ENSG00000102898	NUTF2 PPI subnetwork	0.08
GO:0008378	galactosyltransferase activity	0.08
MP:0000751	myopathy	0.08
ENSG00000119630	PGF PPI subnetwork	0.08

Original gene set ID	Original gene set description	Nominal P value
REACTOME_N:GLYCAN_TRIMMING_IN_THE_ER_AND_CALNEXINCALRETICULIN_CYC	REACTOME_N:GLYCAN_TRIMMING_IN_THE_ER_AND_CALNEXINCALRETICULIN_CYC	0.08
GO:0030728	ovulation	0.08
GO:0002577	regulation of antigen processing and presentation	0.08
GO:0031100	organ regeneration	0.08
ENSG00000063046	EIF4B PPI subnetwork	0.08
REACTOME_IMMUNOREGULATORY_INTERACTIONS_BETWEEN_A_LYMPHOID_AND_A_T_CELL	REACTOME_IMMUNOREGULATORY_INTERACTIONS_BETWEEN_A_LYMPHOID_AND_A_T_CELL	0.08
MP:0001745	increased circulating corticosterone level	0.08
MP:0003087	absent allantoin	0.08
ENSG00000198959	TGM2 PPI subnetwork	0.08
ENSG00000154380	ENAH PPI subnetwork	0.08
GO:0051347	positive regulation of transferase activity	0.08
ENSG00000099308	MAST3 PPI subnetwork	0.08
GO:0035250	UDP-galactosyltransferase activity	0.08
ENSG00000129682	FGF13 PPI subnetwork	0.08
MP:0008577	increased circulating interferon-gamma level	0.08
ENSG00000170579	DLGAP1 PPI subnetwork	0.08
GO:0005539	glycosaminoglycan binding	0.08
MP:0005090	increased double-negative T cell number	0.08
REACTOME_PEPTIDE_HORMONE_BIOSYNTHESIS	REACTOME_PEPTIDE_HORMONE_BIOSYNTHESIS	0.08
GO:0071900	regulation of protein serine/threonine kinase activity	0.09
GO:0045723	positive regulation of fatty acid biosynthetic process	0.09
GO:0016298	lipase activity	0.09
GO:0035770	ribonucleoprotein granule	0.09
ENSG00000085721	RRN3 PPI subnetwork	0.09
ENSG00000136250	AOAH PPI subnetwork	0.09
ENSG00000081237	PTPRC PPI subnetwork	0.09
ENSG00000143621	ILF2 PPI subnetwork	0.09
GO:0031098	stress-activated protein kinase signaling cascade	0.09
KEGG_STEROID_BIOSYNTHESIS	KEGG_STEROID_BIOSYNTHESIS	0.09
GO:0015936	coenzyme A metabolic process	0.09
ENSG00000212981	ENSG00000212981 PPI subnetwork	0.09
MP:0008750	abnormal interferon level	0.09
ENSG00000206297	TAP1 PPI subnetwork	0.09
ENSG00000206233	ENSG00000206233 PPI subnetwork	0.09
ENSG00000168394	TAP1 PPI subnetwork	0.09
GO:0031929	TOR signaling cascade	0.09
ENSG00000068305	MEF2A PPI subnetwork	0.09
ENSG00000090339	ICAM1 PPI subnetwork	0.09
ENSG00000049618	ARID1B PPI subnetwork	0.09
MP:0002665	decreased circulating corticosterone level	0.09
GO:0005796	Golgi lumen	0.09
REACTOME_INITIAL_TRIGGERING_OF_COMPLEMENT	REACTOME_INITIAL_TRIGGERING_OF_COMPLEMENT	0.09
GO:0006305	DNA alkylation	0.09
GO:0006306	DNA methylation	0.09
GO:0045061	thymic T cell selection	0.09
ENSG00000198734	F5 PPI subnetwork	0.09
ENSG00000130762	ARHGEF16 PPI subnetwork	0.09
ENSG00000166913	YWHAB PPI subnetwork	0.09
ENSG00000099917	MED15 PPI subnetwork	0.09

Original gene set ID	Original gene set description	Nominal P value
ENSG00000136169	SETDB2 PPI subnetwork	0.09
GO:0002260	lymphocyte homeostasis	0.09
MP:0003339	decreased pancreatic beta cell number	0.09
REACTOME_COMPLEMENT_CASCADE	REACTOME_COMPLEMENT_CASCADE	0.09
MP:0001792	impaired wound healing	0.09
GO:0008406	gonad development	0.09
ENSG00000171720	HDAC3 PPI subnetwork	0.09
GO:0004620	phospholipase activity	0.09
ENSG00000101266	CSNK2A1 PPI subnetwork	0.09
ENSG00000067191	CACNB1 PPI subnetwork	0.09
KEGG_FC_GAMMA_R_MEDIATED_PHAGOCYTOSIS	KEGG_FC_GAMMA_R_MEDIATED_PHAGOCYTOSIS	0.09
REACTOME_CHYLOMICRON:MEDIATED_LIPID_TRANSPORT	REACTOME_CHYLOMICRON:MEDIATED_LIPID_TRANSPORT	0.09
MP:0002780	decreased circulating testosterone leve	0.09
MP:0001216	abnormal epidermal layer morphology	0.09
GO:0045058	T cell selection	0.09
ENSG00000215440	NPEPL1 PPI subnetwork	0.09
GO:0007565	female pregnancy	0.09
GO:0010638	positive regulation of organelle organization	0.09
MP:0001147	small testis	0.1
ENSG00000101210	EEF1A2 PPI subnetwork	0.1
MP:0005294	abnormal heart ventricle morphology	0.1
GO:0030323	respiratory tube development	0.1
GO:0005542	folic acid binding	0.1
ENSG00000141646	SMAD4 PPI subnetwork	0.1
ENSG00000100888	CHD8 PPI subnetwork	0.1
ENSG00000072062	PRKACA PPI subnetwork	0.1
ENSG00000134853	PDGFRA PPI subnetwork	0.1
ENSG00000135069	PSAT1 PPI subnetwork	0.1
GO:0000118	histone deacetylase complex	0.1
GO:0071887	leukocyte apoptotic process	0.1
MP:0008271	abnormal bone ossification	0.1
GO:0008201	heparin binding	0.1
ENSG00000124222	STX16 PPI subnetwork	0.1
GO:0030299	intestinal cholesterol absorption	0.1
ENSG00000122194	PLG PPI subnetwork	0.1
MP:0001951	abnormal breathing pattern	0.1
ENSG00000105369	CD79A PPI subnetwork	0.1
ENSG00000170889	RPS9 PPI subnetwork	0.1
ENSG00000136149	ENSG00000136149 PPI subnetwork	0.1
GO:0043410	positive regulation of MAPK cascade	0.1
MP:0000642	enlarged adrenal glands	0.1
MP:0003795	abnormal bone structure	0.1
MP:0003648	abnormal radial glial cell morphology	0.1
MP:0004151	decreased circulating iron level	0.1
REACTOME_TRANSPORT_OF_INORGANIC_CATIONSANIONS_AND_AMINO_ACIDS	REACTOME_TRANSPORT_OF_INORGANIC_CATIONSANIONS_AND_AMINO_ACIDS	0.1
ENSG00000154727	GABPA PPI subnetwork	0.1
MP:0003427	parakeratosis	0.1
GO:0031300	intrinsic to organelle membrane	0.1
MP:0002098	abnormal vibrissa morphology	0.1

Original gene set ID	Original gene set description	Nominal P value
GO:0032607	interferon-alpha production	0.1
GO:0032647	regulation of interferon-alpha production	0.1
MP:0004358	bowed tibia	0.1
GO:0008544	epidermis development	0.1
ENSG00000101224	CDC25B PPI subnetwork	0.1
ENSG00000106144	CASP2 PPI subnetwork	0.1
MP:0001208	blistering	0.1
REACTOME_INTERLEUKIN:7_SIGNALING	REACTOME_INTERLEUKIN:7_SIGNALING	0.1
REACTOME_GAMMA:CARBOXYLATION_TRANSPORT_AND_AMINO:TERMINAL_C	REACTOME_GAMMA:CARBOXYLATION_TRANSPORT_AND_AMINO:TERMINAL_CLEA	0.1
ENSG00000107562	CXCL12 PPI subnetwork	0.1
GO:0005342	organic acid transmembrane transporter activity	0.1
GO:0005385	zinc ion transmembrane transporter activity	0.1
MP:0008883	abnormal enterocyte proliferation	0.1
GO:0048020	CCR chemokine receptor binding	0.1
ENSG00000172936	MYD88 PPI subnetwork	0.1
MP:0002375	abnormal thymus medulla morphology	0.1
GO:0003774	motor activity	0.1
GO:0071356	cellular response to tumor necrosis factor	0.11
MP:0003954	abnormal Reichert's membrane morphology	0.11
MP:0004592	small mandible	0.11
MP:0008111	abnormal granulocyte differentiation	0.11
GO:0030055	cell-substrate junction	0.11
MP:0000628	abnormal mammary gland development	0.11
ENSG00000158560	DYNC111 PPI subnetwork	0.11
GO:0019955	cytokine binding	0.11
GO:0034385	triglyceride-rich lipoprotein particle	0.11
GO:0034361	very-low-density lipoprotein particle	0.11
MP:0002759	abnormal caudal vertebrae morphology	0.11
GO:0055038	recycling endosome membrane	0.11
ENSG00000119139	TJP2 PPI subnetwork	0.11
REACTOME_PLATELET_DEGRANULATION	REACTOME_PLATELET_DEGRANULATION	0.11
GO:0007159	leukocyte cell-cell adhesion	0.11
ENSG00000096968	JAK2 PPI subnetwork	0.11
MP:0008050	decreased memory T cell number	0.11
GO:0006413	translational initiation	0.11
MP:0001393	ataxia	0.11
ENSG00000089009	RPL6 PPI subnetwork	0.11
REACTOME_NF:KB_IS_ACTIVATED_AND_SIGNALS_SURVIVAL	REACTOME_NF:KB_IS_ACTIVATED_AND_SIGNALS_SURVIVAL	0.11
ENSG00000089737	DDX24 PPI subnetwork	0.11
ENSG00000091831	ESR1 PPI subnetwork	0.11
GO:0034340	response to type I interferon	0.11
ENSG00000147507	ENSG00000147507 PPI subnetwork	0.11
MP:0004521	abnormal cochlear hair cell stereociliary bundle morphology	0.11
GO:0032354	response to follicle-stimulating hormone stimulus	0.11
ENSG00000108953	YWHAE PPI subnetwork	0.11
ENSG00000213923	CSNK1E PPI subnetwork	0.11
ENSG00000170017	ALCAM PPI subnetwork	0.11
GO:0016863	intramolecular oxidoreductase activity, transposing C=C bonds	0.11
ENSG00000146729	GBAS PPI subnetwork	0.11

Original gene set ID	Original gene set description	Nominal P value
ENSG00000181827	RFX7 PPI subnetwork	0.11
ENSG00000116285	ERRF1 PPI subnetwork	0.11
ENSG00000105193	RPS16 PPI subnetwork	0.11
ENSG00000093167	LRRFIP2 PPI subnetwork	0.11
KEGG_N_GLYCAN_BIOSYNTHESIS	KEGG_N_GLYCAN_BIOSYNTHESIS	0.11
ENSG00000113580	NR3C1 PPI subnetwork	0.11
ENSG00000058335	RASGRF1 PPI subnetwork	0.11
ENSG00000100815	TRIP11 PPI subnetwork	0.11
ENSG00000001630	CYP51A1 PPI subnetwork	0.11
ENSG00000166986	MARS PPI subnetwork	0.11
GO:0044403	symbiosis, encompassing mutualism through parasitism	0.11
MP:0008246	abnormal leukocyte morphology	0.12
MP:0003884	decreased macrophage cell number	0.12
REACTOME_DSCAM_INTERACTIONS	REACTOME_DSCAM_INTERACTIONS	0.12
ENSG00000126749	ENSG00000126749 PPI subnetwork	0.12
ENSG00000106665	CLIP2 PPI subnetwork	0.12
ENSG00000179776	CDH5 PPI subnetwork	0.12
ENSG00000142534	RPS11 PPI subnetwork	0.12
ENSG00000170677	SOCS6 PPI subnetwork	0.12
GO:0005272	sodium channel activity	0.12
MP:0008074	increased CD4-positive T cell number	0.12
ENSG00000077943	ITGA8 PPI subnetwork	0.12
GO:0016125	sterol metabolic process	0.12
GO:0071345	cellular response to cytokine stimulus	0.12
GO:0004004	ATP-dependent RNA helicase activity	0.12
MP:0005179	decreased circulating cholesterol level	0.12
GO:0031301	integral to organelle membrane	0.12
ENSG00000010610	CD4 PPI subnetwork	0.12
ENSG00000056345	ENSG00000056345 PPI subnetwork	0.12
ENSG00000100181	ENSG00000100181 PPI subnetwork	0.12
GO:0001078	RNA polymerase II core promoter proximal region sequence-specific DNA binding transcription factor activity	0.12
ENSG00000130402	ACTN4 PPI subnetwork	0.12
ENSG00000084207	GSTP1 PPI subnetwork	0.12
ENSG00000183305	MAGEA2B PPI subnetwork	0.12
ENSG00000034971	MYOC PPI subnetwork	0.12
MP:0004471	short nasal bone	0.12
MP:0003304	large intestinal inflammation	0.12
ENSG00000112078	KCTD20 PPI subnetwork	0.12
MP:0000565	oligodactyly	0.12
GO:0044419	interspecies interaction between organisms	0.12
MP:0001177	atelectasis	0.12
GO:0017136	NAD-dependent histone deacetylase activity	0.12
GO:0034979	NAD-dependent protein deacetylase activity	0.12
GO:0008585	female gonad development	0.12
ENSG00000105173	CCNE1 PPI subnetwork	0.12
ENSG00000105974	CAV1 PPI subnetwork	0.12
MP:0005296	abnormal humerus morphology	0.12
REACTOME_CHOLESTEROL_BIOSYNTHESIS	REACTOME_CHOLESTEROL_BIOSYNTHESIS	0.12
KEGG_GLYCOSPHINGOLIPID_BIOSYNTHESIS_LACTO_AND_NEOLACTO_SERIES	KEGG_GLYCOSPHINGOLIPID_BIOSYNTHESIS_LACTO_AND_NEOLACTO_SERIES	0.12

Original gene set ID**Original gene set description****Nominal P value**

GO:0007276	gamete generation	0.14
ENSG00000163519	TRAT1 PPI subnetwork	0.14
ENSG00000174748	RPL15 PPI subnetwork	0.14
MP:0006317	decreased urine sodium level	0.14
GO:0045104	intermediate filament cytoskeleton organizati	0.14
MP:0001284	absent vibrissae	0.14
ENSG00000185499	MUC1 PPI subnetwork	0.14
MP:0008127	decreased dendritic cell number	0.14
ENSG00000134242	PTPN22 PPI subnetwork	0.14
GO:0005044	scavenger receptor activity	0.14
ENSG00000087245	MMP2 PPI subnetwork	0.14
MP:0002727	decreased circulating insulin level	0.14
GO:0015012	heparan sulfate proteoglycan biosynthetic process	0.14
GO:0031965	nuclear membrane	0.14
GO:0005792	microsome	0.14
ENSG00000161835	GRASP PPI subnetwork	0.14
MP:0005089	decreased double-negative T cell number	0.14
REACTOME_CD28_DEPENDENT_PI3KAKT_SIGNALING	REACTOME_CD28_DEPENDENT_PI3KAKT_SIGNALING	0.14
GO:0051604	protein maturation	0.14
GO:0050691	regulation of defense response to virus by host	0.14
MP:0010465	aberrant origin of the right subclavian artery	0.14
REACTOME_REGULATION_OF_LIPID_METABOLISM_BY_PEROXISOME_PROLIFERATION	REACTOME_REGULATION_OF_LIPID_METABOLISM_BY_PEROXISOME_PROLIFERATION	0.14
REACTOME_P75NTR_RECRUITS_SIGNALLING_COMPLEXES	REACTOME_P75NTR_RECRUITS_SIGNALLING_COMPLEXES	0.14
REACTOME_NUCLEAR_RECEPTOR_TRANSCRIPTION_PATHWAY	REACTOME_NUCLEAR_RECEPTOR_TRANSCRIPTION_PATHWAY	0.14
ENSG00000139318	DUSP6 PPI subnetwork	0.14
MP:0003396	abnormal embryonic hematopoiesis	0.14
GO:0007346	regulation of mitotic cell cycle	0.14
GO:0045596	negative regulation of cell differentiation	0.14
GO:0007584	response to nutrient	0.14
GO:0048194	Golgi vesicle budding	0.14
REACTOME_METABOLISM_OF_PROTEINS	REACTOME_METABOLISM_OF_PROTEINS	0.14
MP:0003156	abnormal leukocyte migration	0.14
GO:0050654	chondroitin sulfate proteoglycan metabolic process	0.14
ENSG00000177731	FLII PPI subnetwork	0.14
GO:0071339	MLL1 complex	0.14
MP:0000598	abnormal liver morphology	0.14
GO:0002673	regulation of acute inflammatory response	0.14
ENSG00000130956	HABP4 PPI subnetwork	0.14
ENSG00000171490	RSL1D1 PPI subnetwork	0.14
ENSG00000169896	ITGAM PPI subnetwork	0.14
REACTOME_RESPONSE_TO_ELEVATED_PLATELET_CYTOSOLIC_CA2	REACTOME_RESPONSE_TO_ELEVATED_PLATELET_CYTOSOLIC_CA2	0.14
GO:0014911	positive regulation of smooth muscle cell migration	0.14
MP:0001953	respiratory failure	0.14
ENSG00000169398	PTK2 PPI subnetwork	0.14
ENSG00000182636	NDN PPI subnetwork	0.14
MP:0008209	decreased pre-B cell number	0.14
REACTOME_POST:TRANSLATIONAL_PROTEIN_MODIFICATION	REACTOME_POST:TRANSLATIONAL_PROTEIN_MODIFICATION	0.14
MP:0002113	abnormal skeleton development	0.14
ENSG00000171862	PTEN PPI subnetwork	0.14

Original gene set ID	Original gene set description	Nominal P value
GO:0003705	RNA polymerase II distal enhancer sequence-specific DNA binding transcription factor	0.15
GO:0001570	vasculogenesis	0.15
MP:0002731	megacolon	0.15
ENSG00000147403	RPL10 PPI subnetwork	0.15
ENSG00000175592	FOSL1 PPI subnetwork	0.15
ENSG00000174697	LEP PPI subnetwork	0.15
MP:0001919	abnormal reproductive system physiology	0.15
ENSG00000136574	GATA4 PPI subnetwork	0.15
ENSG00000162891	IL20 PPI subnetwork	0.15
MP:0000321	increased bone marrow cell number	0.15
GO:0046966	thyroid hormone receptor binding	0.15
GO:0019319	hexose biosynthetic process	0.15
GO:0032580	Golgi cisterna membrane	0.15
MP:0003638	abnormal response/metabolism to endogenous compounds	0.15
GO:0030947	regulation of vascular endothelial growth factor receptor signaling pathway	0.15
ENSG00000120948	TARDBP PPI subnetwork	0.15
ENSG00000166285	ENSG00000166285 PPI subnetwork	0.15
ENSG00000204359	CFB PPI subnetwork	0.15
GO:0008653	lipopolysaccharide metabolic process	0.15
GO:0042803	protein homodimerization activity	0.15
ENSG00000037241	RPL26L1 PPI subnetwork	0.15
GO:0048514	blood vessel morphogenesis	0.15
MP:0000416	sparse hair	0.15
ENSG00000128487	SPECC1 PPI subnetwork	0.15
REACTOME_GTP_HYDROLYSIS_AND_JOINING_OF_THE_60S_RIBOSOMAL_SUBUNIT	REACTOME_GTP_HYDROLYSIS_AND_JOINING_OF_THE_60S_RIBOSOMAL_SUBUNIT	0.15
ENSG00000189403	HMGB1 PPI subnetwork	0.15
ENSG00000148297	MED22 PPI subnetwork	0.15
GO:0006916	anti-apoptosis	0.15
ENSG00000117408	IPO13 PPI subnetwork	0.15
ENSG00000156273	BACH1 PPI subnetwork	0.16
MP:0000454	abnormal jaw morphology	0.16
ENSG00000213625	LEPROT PPI subnetwork	0.16
GO:0005313	L-glutamate transmembrane transporter activity	0.16
GO:0050650	chondroitin sulfate proteoglycan biosynthetic process	0.16
GO:0005179	hormone activity	0.16
MP:0002493	increased IgG level	0.16
GO:0004806	triglyceride lipase activity	0.16
GO:0015103	inorganic anion transmembrane transporter activity	0.16
GO:0070482	response to oxygen levels	0.16
ENSG00000196700	ZNF512B PPI subnetwork	0.16
ENSG00000134588	USP26 PPI subnetwork	0.16
GO:0001568	blood vessel development	0.16
GO:0016585	chromatin remodeling complex	0.16
REACTOME_RHO_GTPASE_CYCLE	REACTOME_RHO_GTPASE_CYCLE	0.16
REACTOME_SIGNALING_BY_RHO_GTPASES	REACTOME_SIGNALING_BY_RHO_GTPASES	0.16
GO:0043449	cellular alkene metabolic process	0.16
GO:0006691	leukotriene metabolic process	0.16
GO:0030098	lymphocyte differentiation	0.16
ENSG00000072195	SPEG PPI subnetwork	0.16

Original gene set ID	Original gene set description	Nominal P value
REACTOME_REGULATION_OF_PYRUVATE_DEHYDROGENASE_PDH_COMPLEX	REACTOME_REGULATION_OF_PYRUVATE_DEHYDROGENASE_PDH_COMPLEX	0.17
ENSG00000169136	ATF5 PPI subnetwork	0.17
MP:0006397	disorganized long bone epiphyseal plate	0.17
GO:0046546	development of primary male sexual characteristics	0.17
ENSG00000127318	IL22 PPI subnetwork	0.17
MP:0003998	decreased thermal nociceptive threshold	0.17
MP:0008782	increased B cell apoptosis	0.17
ENSG00000033327	GAB2 PPI subnetwork	0.17
GO:0015172	acidic amino acid transmembrane transporter activity	0.17
ENSG00000110492	MDK PPI subnetwork	0.17
GO:0010741	negative regulation of intracellular protein kinase cascade	0.17
GO:0005251	delayed rectifier potassium channel activity	0.17
GO:0042158	lipoprotein biosynthetic process	0.17
MP:0003140	dilated heart atrium	0.17
ENSG00000012660	ELOVL5 PPI subnetwork	0.17
REACTOME_HEMOSTASIS	REACTOME_HEMOSTASIS	0.17
ENSG00000127511	SIN3B PPI subnetwork	0.17
ENSG00000150281	CTF1 PPI subnetwork	0.17
ENSG00000125998	FAM83C PPI subnetwork	0.17
MP:0001190	reddish skin	0.17
GO:0043687	post-translational protein modification	0.17
GO:0006415	translational termination	0.18
GO:0032312	regulation of ARF GTPase activity	0.18
GO:0030198	extracellular matrix organization	0.18
GO:0043062	extracellular structure organization	0.18
GO:0046777	protein autophosphorylation	0.18
ENSG00000175221	MED16 PPI subnetwork	0.18
ENSG00000167721	TSR1 PPI subnetwork	0.18
GO:0019210	kinase inhibitor activity	0.18
GO:0022625	cytosolic large ribosomal subunit	0.18
MP:0001925	male infertility	0.18
ENSG00000129219	PLD2 PPI subnetwork	0.18
ENSG00000058729	RIOK2 PPI subnetwork	0.18
GO:0015450	P-P-bond-hydrolysis-driven protein transmembrane transporter activity	0.18
ENSG00000103742	IGDCC4 PPI subnetwork	0.18
MP:0002447	abnormal erythrocyte morphology	0.18
REACTOME_CELL_JUNCTION_ORGANIZATION	REACTOME_CELL_JUNCTION_ORGANIZATION	0.18
ENSG00000161970	RPL26 PPI subnetwork	0.18
ENSG00000147873	IFNA5 PPI subnetwork	0.18
ENSG00000186803	IFNA10 PPI subnetwork	0.18
ENSG00000120247	ENSG00000120247 PPI subnetwork	0.18
ENSG00000147877	ENSG00000147877 PPI subnetwork	0.18
ENSG00000188379	IFNA2 PPI subnetwork	0.18
ENSG00000186809	ENSG00000186809 PPI subnetwork	0.18
ENSG00000147885	IFNA16 PPI subnetwork	0.18
ENSG00000137080	IFNA21 PPI subnetwork	0.18
ENSG00000120242	IFNA8 PPI subnetwork	0.18
GO:0043967	histone H4 acetylation	0.18
MP:0002904	increased circulating parathyroid hormone leve	0.18

Original gene set ID	Original gene set description	Nominal P value
ENSG00000183311	TUBB PPI subnetwork	0.18
ENSG00000196230	TUBB PPI subnetwork	0.18
ENSG00000137379	ENSG00000137379 PPI subnetwork	0.18
GO:0004659	prenyltransferase activity	0.18
MP:0004229	abnormal embryonic erythropoiesis	0.18
MP:0000554	abnormal carpal bone morphology	0.18
ENSG00000133511	ENSG00000133511 PPI subnetwork	0.18
REACTOME_PLATELET_ACTIVATION_SIGNALING_AND_AGGREGATION	REACTOME_PLATELET_ACTIVATION_SIGNALING_AND_AGGREGATION	0.18
GO:0070085	glycosylation	0.18
ENSG00000133935	C14orf1 PPI subnetwork	0.18
REACTOME_NF:KB_ACTIVATION_THROUGH_FADDRIP:1_PATHWAY_MEDIATED_BY	REACTOME_NF:KB_ACTIVATION_THROUGH_FADDRIP:1_PATHWAY_MEDIATED_BY	0.18
MP:0002724	enhanced wound healing	0.18
ENSG00000110169	HPX PPI subnetwork	0.18
REACTOME_PLATELET_AGGREGATION_PLUG_FORMATION	REACTOME_PLATELET_AGGREGATION_PLUG_FORMATION	0.18
MP:0009743	preaxial polydactyly	0.18
ENSG00000188223	LIN37 PPI subnetwork	0.18
ENSG00000182774	RPS17L PPI subnetwork	0.18
ENSG00000184779	RPS17 PPI subnetwork	0.18
GO:0004675	transmembrane receptor protein serine/threonine kinase activity	0.18
MP:0009940	abnormal hippocampus pyramidal cell morphology	0.18
MP:0000928	incomplete cephalic closure	0.18
MP:0002666	increased circulating aldosterone leve	0.18
REACTOME_TERMINATION_OF_O:GLYCAN_BIOSYNTHESIS	REACTOME_TERMINATION_OF_O:GLYCAN_BIOSYNTHESIS	0.18
GO:0015924	mannosyl-oligosaccharide mannosidase activity	0.18
ENSG00000133805	AMPD3 PPI subnetwork	0.18
ENSG00000106125	FAM188B PPI subnetwork	0.18
ENSG00000157168	NRG1 PPI subnetwork	0.18
MP:0005025	abnormal response to infection	0.18
ENSG00000183405	ENSG00000183405 PPI subnetwork	0.18
ENSG00000182446	NPLOC4 PPI subnetwork	0.18
MP:0001819	abnormal immune cell physiology	0.18
MP:0003408	increased width of hypertrophic chondrocyte zone	0.18
MP:0009142	decreased prepulse inhibition	0.18
REACTOME_CYTOKINE_SIGNALING_IN_IMMUNE_SYSTEM	REACTOME_CYTOKINE_SIGNALING_IN_IMMUNE_SYSTEM	0.18
GO:0032680	regulation of tumor necrosis factor production	0.18
GO:0032640	tumor necrosis factor production	0.18
MP:0004808	abnormal hematopoietic stem cell morphology	0.18
GO:0043330	response to exogenous dsRNA	0.18
GO:0002922	positive regulation of humoral immune response	0.18
MP:0002432	abnormal CD4-positive T cell morphology	0.18
ENSG00000188529	SRSF10 PPI subnetwork	0.18
ENSG00000160213	CSTB PPI subnetwork	0.18
MP:0010067	increased red blood cell distribution width	0.18
ENSG00000111845	PAK1IP1 PPI subnetwork	0.18
ENSG00000198467	TPM2 PPI subnetwork	0.18
ENSG00000163513	TGFBR2 PPI subnetwork	0.18
ENSG00000075539	FRYL PPI subnetwork	0.18
MP:0006059	decreased susceptibility to ischemic brain injury	0.18
ENSG00000186468	RPS23 PPI subnetwork	0.18

Original gene set ID	Original gene set description	Nominal P value
GO:0031985	Golgi cisterna	0.19
ENSG00000118402	ELOVL4 PPI subnetwork	0.19
ENSG00000104969	SGTA PPI subnetwork	0.19
MP:0003984	embryonic growth retardation	0.19
KEGG_CELL_CYCLE	KEGG_CELL_CYCLE	0.19
ENSG00000145781	COMMD10 PPI subnetwork	0.19
GO:0043492	ATPase activity, coupled to movement of substances	0.19
ENSG00000169083	AR PPI subnetwork	0.19
ENSG00000115718	PROC PPI subnetwork	0.19
ENSG00000083845	RPS5 PPI subnetwork	0.19
ENSG00000197959	DNM3 PPI subnetwork	0.19
GO:0043401	steroid hormone mediated signaling pathway	0.19
MP:0003216	absence seizures	0.19
MP:0001289	persistence of hyaloid vascular system	0.19
ENSG00000064012	CASP8 PPI subnetwork	0.19
ENSG00000119408	NEK6 PPI subnetwork	0.19
MP:0001622	abnormal vasculogenesis	0.19
ENSG00000113520	IL4 PPI subnetwork	0.19
ENSG00000196656	ENSG00000196656 PPI subnetwork	0.19
ENSG00000197728	RPS26 PPI subnetwork	0.19
ENSG00000117410	ATP6V0B PPI subnetwork	0.19
REACTOME_METABOLISM_OF_STEROID_HORMONES_AND_VITAMINS_A_AND_D	REACTOME_METABOLISM_OF_STEROID_HORMONES_AND_VITAMINS_A_AND_D	0.19
ENSG00000164022	AIMP1 PPI subnetwork	0.19
MP:0001127	small ovary	0.19
MP:0000291	enlarged pericardium	0.19
ENSG00000163347	CLDN1 PPI subnetwork	0.19
ENSG00000112118	MCM3 PPI subnetwork	0.19
ENSG00000163050	ADCK3 PPI subnetwork	0.19
GO:0032480	negative regulation of type I interferon productior	0.19
GO:0090179	planar cell polarity pathway involved in neural tube closure	0.19
GO:0090178	regulation of establishment of planar polarity involved in neural tube closure	0.19
MP:0001601	abnormal myelopoiesis	0.19
ENSG00000106462	EZH2 PPI subnetwork	0.19
REACTOME_RNA_POLYMERASE_III_ABORTIVE_AND_RETRACTIVE_INITIATION	REACTOME_RNA_POLYMERASE_III_ABORTIVE_AND_RETRACTIVE_INITIATION	0.19
REACTOME_RNA_POLYMERASE_III_TRANSCRIPTION	REACTOME_RNA_POLYMERASE_III_TRANSCRIPTION	0.19
ENSG00000196365	LONP1 PPI subnetwork	0.19
MP:0002078	abnormal glucose homeostasis	0.19
ENSG00000006062	MAP3K14 PPI subnetwork	0.19
ENSG00000077150	NFKB2 PPI subnetwork	0.19
ENSG00000166197	NOLC1 PPI subnetwork	0.19
ENSG00000133101	CCNA1 PPI subnetwork	0.19
GO:0014706	striated muscle tissue development	0.19
MP:0010300	increased skin tumor incidence	0.19
GO:0009749	response to glucose stimulus	0.19
ENSG00000013441	CLK1 PPI subnetwork	0.19
ENSG00000120800	UTP20 PPI subnetwork	0.19
ENSG00000175387	SMAD2 PPI subnetwork	0.19
ENSG00000124006	OBSL1 PPI subnetwork	0.19
GO:0032494	response to peptidoglycan	0.19

Original gene set ID	Original gene set description	Nominal P value
GO:0004602	glutathione peroxidase activity	0.23
GO:0005765	lysosomal membrane	0.23
GO:0031018	endocrine pancreas development	0.23
ENSG00000163879	DNALI1 PPI subnetwork	0.23
GO:0002467	germinal center formation	0.23
ENSG00000111276	CDKN1B PPI subnetwork	0.23
ENSG00000088035	ALG6 PPI subnetwork	0.23
GO:0071222	cellular response to lipopolysaccharide	0.23
REACTOME_TAK1_ACTIVATES_NFKB_BY_PHOSPHORYLATION_AND_ACTIVATIO	REACTOME_TAK1_ACTIVATES_NFKB_BY_PHOSPHORYLATION_AND_ACTIVATION_O	0.23
GO:0019953	sexual reproduction	0.23
ENSG00000155868	MED7 PPI subnetwork	0.23
ENSG00000160307	S100B PPI subnetwork	0.23
ENSG00000070193	FGF10 PPI subnetwork	0.23
MP:0001106	abnormal Schwann cell morphology	0.23
MP:0001125	abnormal oocyte morphology	0.23
GO:0032870	cellular response to hormone stimulus	0.23
GO:0015711	organic anion transport	0.23
MP:0001829	increased activated T cell number	0.23
ENSG00000213023	SYT3 PPI subnetwork	0.23
GO:0005868	cytoplasmic dynein complex	0.23
GO:0070371	ERK1 and ERK2 cascade	0.23
GO:0035265	organ growth	0.23
MP:0004804	decreased susceptibility to autoimmune diabetes	0.23
MP:0008723	impaired eosinophil recruitment	0.23
ENSG00000111707	SUDS3 PPI subnetwork	0.23
GO:0060041	retina development in camera-type eye	0.23
MP:0003402	decreased liver weight	0.24
GO:0005811	lipid particle	0.24
REACTOME_FATTY_ACYL:COA_BIOSYNTHESIS	REACTOME_FATTY_ACYL:COA_BIOSYNTHESIS	0.24
ENSG00000108298	RPL19 PPI subnetwork	0.24
GO:0043009	chordate embryonic development	0.24
GO:0050866	negative regulation of cell activation	0.24
GO:0031114	regulation of microtubule depolymerization	0.24
ENSG00000101680	LAMA1 PPI subnetwork	0.24
KEGG_NITROGEN_METABOLISM	KEGG_NITROGEN_METABOLISM	0.24
MP:0003009	abnormal cytokine secretion	0.24
MP:0003755	abnormal palate morphology	0.24
REACTOME_INHIBITION_OF_REPLICATION_INITIATION_OF_DAMAGED_DNA_BY	REACTOME_INHIBITION_OF_REPLICATION_INITIATION_OF_DAMAGED_DNA_BY_RE	0.24
GO:0032259	methylation	0.24
ENSG00000186081	KRT5 PPI subnetwork	0.24
ENSG00000211614	ENSG00000211614 PPI subnetwork	0.24
ENSG00000141736	ERBB2 PPI subnetwork	0.24
ENSG00000165458	INPPL1 PPI subnetwork	0.24
MP:0008721	abnormal chemokine level	0.24
MP:0003071	decreased vascular permeability	0.24
MP:0005087	decreased acute inflammation	0.24
ENSG00000100294	MCAT PPI subnetwork	0.24
MP:0009789	decreased susceptibility to bacterial infection induced morbidity/mortality	0.24
MP:0008080	abnormal CD8-positive T cell differentiation	0.24

Original gene set ID	Original gene set description	Nominal P value
GO:0019203	carbohydrate phosphatase activity	0.24
GO:0030217	T cell differentiation	0.24
REACTOME_RIG:IMDA5_MEDIATED_INDUCION_OF_IFN:ALPHABETA_PATHWA	REACTOME_RIG:IMDA5_MEDIATED_INDUCION_OF_IFN:ALPHABETA_PATHWAYS	0.24
MP:0000162	lordosis	0.24
GO:0046649	lymphocyte activation	0.24
ENSG00000170248	PDCD61P PPI subnetwork	0.24
ENSG000000089597	GANAB PPI subnetwork	0.24
ENSG00000185630	PBX1 PPI subnetwork	0.24
GO:0002886	regulation of myeloid leukocyte mediated immunity	0.24
ENSG00000044524	EPHA3 PPI subnetwork	0.24
GO:0006497	protein lipidation	0.24
GO:0033017	sarcoplasmic reticulum membrane	0.24
REACTOME_TRAF6_MEDIATED_IRF7_ACTIVATION	REACTOME_TRAF6_MEDIATED_IRF7_ACTIVATION	0.24
ENSG00000164362	TERT PPI subnetwork	0.24
ENSG00000148082	SHC3 PPI subnetwork	0.24
GO:0044452	nucleolar part	0.24
GO:0005200	structural constituent of cytoskeleton	0.24
MP:0000784	forebrain hypoplasia	0.24
REACTOME_TRANSPORT_OF_VITAMINS_NUCLEOSIDES_AND_RELATED_MOLEC	REACTOME_TRANSPORT_OF_VITAMINS_NUCLEOSIDES_AND_RELATED_MOLECULE:	0.24
GO:0008138	protein tyrosine/serine/threonine phosphatase activity	0.24
ENSG00000173406	DAB1 PPI subnetwork	0.24
GO:0042056	chemoattractant activity	0.24
MP:0010825	abnormal lung saccule morphology	0.24
ENSG000000075388	FGF4 PPI subnetwork	0.24
ENSG00000008988	RPS20 PPI subnetwork	0.24
GO:0006270	DNA-dependent DNA replication initiation	0.24
ENSG00000122484	RPAP2 PPI subnetwork	0.24
GO:0048608	reproductive structure development	0.24
ENSG00000152556	PFKM PPI subnetwork	0.24
ENSG00000104267	CA2 PPI subnetwork	0.24
ENSG00000168028	RPSA PPI subnetwork	0.24
MP:0005508	abnormal skeleton morphology	0.24
GO:0003229	ventricular cardiac muscle tissue development	0.24
ENSG00000133703	KRAS PPI subnetwork	0.24
MP:0001304	cataracts	0.24
MP:0002765	short fibula	0.24
ENSG00000005844	ITGAL PPI subnetwork	0.24
MP:0003641	small lung	0.24
ENSG00000160741	CRTC2 PPI subnetwork	0.24
GO:0046474	glycerophospholipid biosynthetic process	0.24
GO:0006633	fatty acid biosynthetic process	0.24
ENSG00000169067	ACTBL2 PPI subnetwork	0.24
MP:0002416	abnormal proerythroblast morphology	0.24
ENSG00000158874	APOA2 PPI subnetwork	0.24
ENSG00000204843	DCTN1 PPI subnetwork	0.24
ENSG00000064601	CTSA PPI subnetwork	0.24
MP:0008135	small Peyer's patches	0.24
MP:0009655	abnormal secondary palate development	0.24
ENSG00000164251	F2RL1 PPI subnetwork	0.25

Original gene set ID	Original gene set description	Nominal P value
ENSG00000082146	STRADB PPI subnetwork	0.26
ENSG00000137713	PPP2R1B PPI subnetwork	0.26
ENSG00000117133	RPF1 PPI subnetwork	0.26
GO:0016581	NuRD complex	0.26
GO:0048705	skeletal system morphogenesis	0.26
REACTOME_SIGNALING_BY_NOTCH	REACTOME_SIGNALING_BY_NOTCH	0.26
ENSG00000116473	RAP1A PPI subnetwork	0.26
ENSG00000174791	RIN1 PPI subnetwork	0.26
GO:0045940	positive regulation of steroid metabolic process	0.26
MP:0002026	leukemia	0.26
GO:0048200	Golgi transport vesicle coating	0.26
GO:0035964	COPI-coated vesicle budding	0.26
GO:0048205	COPI coating of Golgi vesicle	0.26
MP:0008537	increased susceptibility to induced colitis	0.26
GO:0042157	lipoprotein metabolic process	0.26
MP:0000596	abnormal liver development	0.26
REACTOME_MITOCHONDRIAL_TRNA_AMINOACYLATION	REACTOME_MITOCHONDRIAL_TRNA_AMINOACYLATION	0.26
REACTOME_FATTY_ACID_TRIACYLGLYCEROL_AND_KETONE_BODY_METABOLISM	REACTOME_FATTY_ACID_TRIACYLGLYCEROL_AND_KETONE_BODY_METABOLISM	0.26
ENSG00000136383	ALPK3 PPI subnetwork	0.26
ENSG00000121274	PAPD5 PPI subnetwork	0.26
ENSG00000115170	ACVR1 PPI subnetwork	0.26
ENSG00000128731	HERC2 PPI subnetwork	0.26
MP:0011086	partial postnatal lethality	0.26
GO:0004725	protein tyrosine phosphatase activity	0.26
MP:0000091	short premaxilla	0.26
ENSG00000069399	BCL3 PPI subnetwork	0.26
MP:0002980	abnormal postural reflex	0.26
ENSG00000164404	GDF9 PPI subnetwork	0.26
GO:0008376	acetylgalactosaminyltransferase activity	0.26
GO:0005247	voltage-gated chloride channel activity	0.26
ENSG00000166025	AMOTL1 PPI subnetwork	0.26
ENSG00000108821	COL1A1 PPI subnetwork	0.26
ENSG00000078304	PPP2R5C PPI subnetwork	0.26
ENSG00000103502	CDIPT PPI subnetwork	0.26
GO:0045321	leukocyte activation	0.26
GO:0005614	interstitial matrix	0.26
ENSG00000196549	MME PPI subnetwork	0.26
ENSG00000124788	ATXN1 PPI subnetwork	0.26
ENSG00000166603	MC4R PPI subnetwork	0.26
REACTOME_ADAPTIVE_IMMUNE_SYSTEM	REACTOME_ADAPTIVE_IMMUNE_SYSTEM	0.26
ENSG00000120690	ELF1 PPI subnetwork	0.26
MP:0005036	diarrhea	0.26
ENSG00000198785	GRIN3A PPI subnetwork	0.26
ENSG00000162736	NCSTN PPI subnetwork	0.26
GO:0030173	integral to Golgi membrane	0.26
MP:0010402	ventricular septal defect	0.26
GO:0007229	integrin-mediated signaling pathway	0.26
GO:0006700	C21-steroid hormone biosynthetic process	0.26
ENSG00000106366	SERPINE1 PPI subnetwork	0.26

Original gene set ID	Original gene set description	Nominal P value
ENSG00000104517	UBR5 PPI subnetwork	0.27
GO:0022829	wide pore channel activity	0.27
ENSG00000092208	GEMIN2 PPI subnetwork	0.27
MP:0008597	decreased circulating interleukin-6 level	0.27
MP:0008395	abnormal osteoblast differentiation	0.27
ENSG00000140319	SRP14 PPI subnetwork	0.27
ENSG00000137818	RPLP1 PPI subnetwork	0.27
ENSG00000198034	RPS4X PPI subnetwork	0.27
REACTOME_NONSENSE_MEDIATED_DECAY_INDEPENDENT_OF_THE_EXON_JUNCTION	REACTOME_NONSENSE_MEDIATED_DECAY_INDEPENDENT_OF_THE_EXON_JUNCTION	0.27
MP:0004952	increased spleen weight	0.27
GO:0009161	ribonucleoside monophosphate metabolic process	0.27
GO:0006367	transcription initiation from RNA polymerase II promoter	0.27
REACTOME_TRAF6_MEDIATED_INDUCTION_OF_NFKB_AND_MAP_KINASES_UPON_ACTIVATION_OF_TOLL_LIKE_RECEPTOR_78_TLR78_CASCADE	REACTOME_TRAF6_MEDIATED_INDUCTION_OF_NFKB_AND_MAP_KINASES_UPON_ACTIVATION_OF_TOLL_LIKE_RECEPTOR_78_TLR78_CASCADE	0.27
REACTOME_MYD88_DEPENDENT_CASCADE_INITIATED_ON_ENDOSOME	REACTOME_MYD88_DEPENDENT_CASCADE_INITIATED_ON_ENDOSOME	0.27
GO:0019208	phosphatase regulator activity	0.27
MP:0003077	abnormal cell cycle	0.27
ENSG00000139626	ITGB7 PPI subnetwork	0.27
ENSG00000184787	UBE2G2 PPI subnetwork	0.27
GO:0030949	positive regulation of vascular endothelial growth factor receptor signaling pathway	0.27
MP:0001533	abnormal skeleton physiology	0.27
MP:0002075	abnormal coat/hair pigmentation	0.27
ENSG00000145912	NHP2 PPI subnetwork	0.27
GO:0055010	ventricular cardiac muscle tissue morphogenesis	0.27
GO:0006814	sodium ion transport	0.27
ENSG00000131368	MRPS25 PPI subnetwork	0.27
GO:0045120	pronucleus	0.27
MP:0005092	decreased double-positive T cell number	0.27
ENSG00000078808	SDF4 PPI subnetwork	0.27
ENSG00000198873	GRK5 PPI subnetwork	0.27
ENSG00000160584	SIK3 PPI subnetwork	0.27
KEGG_PYRUVATE_METABOLISM	KEGG_PYRUVATE_METABOLISM	0.27
MP:0003068	enlarged kidney	0.27
GO:0051591	response to cAMP	0.27
ENSG00000116030	SUMO1 PPI subnetwork	0.27
GO:0031012	extracellular matrix	0.27
ENSG00000150990	DHX37 PPI subnetwork	0.27
ENSG00000075618	FSCN1 PPI subnetwork	0.27
GO:0045814	negative regulation of gene expression, epigenetic	0.27
GO:0015893	drug transport	0.27
ENSG00000115705	TPO PPI subnetwork	0.27
ENSG00000185920	PTCH1 PPI subnetwork	0.27
ENSG00000115221	ITGB6 PPI subnetwork	0.28
GO:0007422	peripheral nervous system development	0.28
ENSG00000031698	SARS PPI subnetwork	0.28
MP:0003270	intestinal obstruction	0.28
GO:0048534	hemopoietic or lymphoid organ development	0.28
ENSG00000150760	DOCK1 PPI subnetwork	0.28
GO:0016741	transferase activity, transferring one-carbon groups	0.28

Original gene set ID	Original gene set description	Nominal P value
REACTOME_POST:TRANSLATIONAL_MODIFICATION_SYNTHESIS_OF_GPI:ANCHOR	REACTOME_POST:TRANSLATIONAL_MODIFICATION_SYNTHESIS_OF_GPI:ANCHOR	0.28
MP:0000267	abnormal heart development	0.28
ENSG000000205659	LIN52 PPI subnetwork	0.28
ENSG000000136352	NKX2-1 PPI subnetwork	0.28
ENSG000000108848	LUC7L3 PPI subnetwork	0.28
ENSG000000079335	CDC14A PPI subnetwork	0.28
MP:0003628	abnormal leukocyte adhesion	0.28
GO:0061008	hepaticobiliary system development	0.28
GO:0090287	regulation of cellular response to growth factor stimulus	0.28
MP:0006042	increased apoptosis	0.28
MP:0002144	abnormal B cell differentiation	0.28
ENSG000000107863	ARHGAP21 PPI subnetwork	0.28
ENSG000000196924	FLNA PPI subnetwork	0.28
ENSG000000160999	SH2B2 PPI subnetwork	0.28
GO:0051091	positive regulation of sequence-specific DNA binding transcription factor activity	0.28
ENSG000000132424	PNISR PPI subnetwork	0.28
GO:0017171	serine hydrolase activity	0.28
ENSG000000029534	ANK1 PPI subnetwork	0.28
REACTOME_SEMA4D_IN_SEMAPHORIN_SIGNALING	REACTOME_SEMA4D_IN_SEMAPHORIN_SIGNALING	0.28
ENSG000000160633	SAFB PPI subnetwork	0.28
GO:0050870	positive regulation of T cell activation	0.28
ENSG000000196498	NCOR2 PPI subnetwork	0.28
ENSG000000113460	BRX1 PPI subnetwork	0.28
GO:0002703	regulation of leukocyte mediated immunity	0.28
ENSG000000198625	MDM4 PPI subnetwork	0.28
ENSG000000178585	CTNNBIP1 PPI subnetwork	0.28
GO:0004435	phosphatidylinositol phospholipase C activity	0.28
KEGG_MAPK_SIGNALING_PATHWAY	KEGG_MAPK_SIGNALING_PATHWAY	0.28
GO:0002685	regulation of leukocyte migration	0.28
GO:0052548	regulation of endopeptidase activity	0.28
MP:0004200	decreased fetal size	0.28
GO:0045923	positive regulation of fatty acid metabolic process	0.28
MP:0004830	short incisors	0.28
MP:0002566	abnormal sexual interaction	0.28
GO:0015114	phosphate ion transmembrane transporter activity	0.28
GO:0050777	negative regulation of immune response	0.28
GO:0031589	cell-substrate adhesion	0.28
ENSG000000187778	MCRS1 PPI subnetwork	0.28
ENSG000000065154	OAT PPI subnetwork	0.28
ENSG000000182255	KCNA4 PPI subnetwork	0.28
GO:0005801	cis-Golgi network	0.28
ENSG000000109606	DHX15 PPI subnetwork	0.28
MP:0004773	abnormal bile composition	0.28
MP:0002417	abnormal megakaryocyte morphology	0.28
GO:0007129	synapsis	0.28
GO:0006544	glycine metabolic process	0.28
GO:0000785	chromatin	0.28
ENSG000000145907	G3BP1 PPI subnetwork	0.28
REACTOME_NEGATIVE_REGULATORS_OF_RIG:IMDA5_SIGNALING	REACTOME_NEGATIVE_REGULATORS_OF_RIG:IMDA5_SIGNALING	0.28

Original gene set ID**Original gene set description****Nominal P value**

MP:0002411	decreased susceptibility to bacterial infection	0.28
ENSG00000145414	NAF1 PPI subnetwork	0.28
GO:0014902	myotube differentiation	0.28
ENSG00000115207	GTF3C2 PPI subnetwork	0.28
ENSG00000138768	USO1 PPI subnetwork	0.28
ENSG00000162434	JAK1 PPI subnetwork	0.28
MP:0001672	abnormal embryogenesis/ development	0.28
ENSG00000113525	IL5 PPI subnetwork	0.28
GO:0048010	vascular endothelial growth factor receptor signaling pathway	0.28
ENSG00000125810	CD93 PPI subnetwork	0.28
GO:0017038	protein import	0.28
GO:0006638	neutral lipid metabolic process	0.28
ENSG00000101365	IDH3B PPI subnetwork	0.29
MP:0005441	increased urine calcium level	0.29
ENSG00000164985	PSIP1 PPI subnetwork	0.29
MP:0005423	abnormal somatic nervous system physiology	0.29
MP:0009435	abnormal miniature inhibitory postsynaptic currents	0.29
ENSG00000173545	ZNF622 PPI subnetwork	0.29
ENSG00000139921	TMX1 PPI subnetwork	0.29
GO:0042113	B cell activation	0.29
GO:0010675	regulation of cellular carbohydrate metabolic process	0.29
ENSG00000064547	LPAR2 PPI subnetwork	0.29
GO:0018393	internal peptidyl-lysine acetylation	0.29
GO:0033202	DNA helicase complex	0.29
GO:0031011	Ino80 complex	0.29
ENSG00000167004	PDIA3 PPI subnetwork	0.29
GO:0005097	Rab GTPase activator activity	0.29
REACTOME_TRANSPORT_TO_THE_GOLGI_AND_SUBSEQUENT_MODIFICATION	REACTOME_TRANSPORT_TO_THE_GOLGI_AND_SUBSEQUENT_MODIFICATION	0.29
MP:0004803	increased susceptibility to autoimmune diabetes	0.29
ENSG00000170365	SMAD1 PPI subnetwork	0.29
GO:0008239	dipeptidyl-peptidase activity	0.29
GO:0043574	peroxisomal transport	0.29
GO:0042035	regulation of cytokine biosynthetic process	0.29
GO:0044144	modulation of growth of symbiont involved in interaction with host	0.29
GO:0044126	regulation of growth of symbiont in host	0.29
GO:0044116	growth of symbiont involved in interaction with host	0.29
GO:0044117	growth of symbiont in host	0.29
GO:0044146	negative regulation of growth of symbiont involved in interaction with host	0.29
GO:0044130	negative regulation of growth of symbiont in host	0.29
GO:0044110	growth involved in symbiotic interaction	0.29
ENSG00000163399	ATP1A1 PPI subnetwork	0.29
ENSG00000186868	MAPT PPI subnetwork	0.29
ENSG00000198001	IRAK4 PPI subnetwork	0.29
GO:0070374	positive regulation of ERK1 and ERK2 cascade	0.29
KEGG_TYPE_II_DIABETES_MELLITUS	KEGG_TYPE_II_DIABETES_MELLITUS	0.29
MP:0008554	decreased circulating tumor necrosis factor level	0.29
GO:0005881	cytoplasmic microtubule	0.29
GO:0006954	inflammatory response	0.29
ENSG00000125740	FOSB PPI subnetwork	0.29

Original gene set ID	Original gene set description	Nominal P value
GO:0033280	response to vitamin D	0.29
REACTOME_RAP1_SIGNALLING	REACTOME_RAP1_SIGNALLING	0.29
GO:0005246	calcium channel regulator activity	0.29
MP:0004423	abnormal squamosal bone morphology	0.29
GO:0006399	tRNA metabolic process	0.29
GO:0019216	regulation of lipid metabolic process	0.29
REACTOME_NUCLEOTIDE:BINDING_DOMAIN_LEUCINE_RICH_REPEAT_CONTAINING	REACTOME_NUCLEOTIDE:BINDING_DOMAIN_LEUCINE_RICH_REPEAT_CONTAINING	0.29
ENSG00000131023	LATS1 PPI subnetwork	0.29
REACTOME_EFFECTS_OF_PIP2_HYDROLYSIS	REACTOME_EFFECTS_OF_PIP2_HYDROLYSIS	0.29
ENSG00000148606	POLR3A PPI subnetwork	0.29
MP:0001314	corneal opacity	0.29
GO:0035914	skeletal muscle cell differentiation	0.29
ENSG00000124383	MPHOSPH10 PPI subnetwork	0.29
GO:0045907	positive regulation of vasoconstriction	0.29
REACTOME_TRIGLYCERIDE_BIOSYNTHESIS	REACTOME_TRIGLYCERIDE_BIOSYNTHESIS	0.29
ENSG00000107882	SUFU PPI subnetwork	0.29
ENSG00000136982	DSCC1 PPI subnetwork	0.29
GO:0043966	histone H3 acetylation	0.29
ENSG00000082397	EPB41L3 PPI subnetwork	0.29
MP:0005013	increased lymphocyte cell number	0.29
GO:0051272	positive regulation of cellular component movement	0.29
GO:0015238	drug transmembrane transporter activity	0.29
ENSG00000206412	GNL1 PPI subnetwork	0.29
ENSG00000204590	GNL1 PPI subnetwork	0.29
ENSG00000206492	GNL1 PPI subnetwork	0.29
REACTOME_VITAMIN_B5_PANTOTHENATE_METABOLISM	REACTOME_VITAMIN_B5_PANTOTHENATE_METABOLISM	0.29
ENSG00000184922	FMNL1 PPI subnetwork	0.29
GO:0005070	SH3/SH2 adaptor activity	0.29
ENSG00000164930	FZD6 PPI subnetwork	0.29
ENSG00000111432	FZD10 PPI subnetwork	0.29
ENSG00000057593	F7 PPI subnetwork	0.29
ENSG00000155966	AFF2 PPI subnetwork	0.29
GO:0016820	hydrolase activity, acting on acid anhydrides, catalyzing transmembrane movement	0.29
GO:0006400	tRNA modification	0.29
GO:0001755	neural crest cell migration	0.29
ENSG00000113263	ITK PPI subnetwork	0.29
GO:0009746	response to hexose stimulus	0.29
GO:0000977	RNA polymerase II regulatory region sequence-specific DNA binding	0.29
GO:0000932	cytoplasmic mRNA processing body	0.29
ENSG00000120705	ETF1 PPI subnetwork	0.29
ENSG00000188536	HBA2 PPI subnetwork	0.29
ENSG00000206172	HBA1 PPI subnetwork	0.29
MP:0001806	decreased IgM level	0.29
MP:0001501	abnormal sleep pattern	0.29
GO:0045087	innate immune response	0.29
MP:0001325	abnormal retina morphology	0.29
ENSG00000145425	RPS3A PPI subnetwork	0.29
ENSG00000138018	EPT1 PPI subnetwork	0.29
ENSG00000166794	PPIB PPI subnetwork	0.29

Original gene set ID

ENSG00000074201
ENSG00000112242
REACTOME_MYD88_CASCADE_INITIATED_ON_PLASMA_MEMBRANE
REACTOME_TOLL_LIKE_RECEPTOR_10_TLR10_CASCADE
REACTOME_TOLL_LIKE_RECEPTOR_5_TLR5_CASCADE
GO:0004143
GO:0050852
GO:0051270
ENSG00000166908
MP:0002460
GO:0007507
GO:0007265
ENSG00000187391
ENSG00000178913
REACTOME_TRNA_AMINOACYLATION
MP:0005292
REACTOME_TOLL_LIKE_RECEPTOR_4_TLR4_CASCADE
GO:0045773
GO:0045637
ENSG00000132507
GO:0004521
MP:0008040
MP:0002463
GO:0032432
ENSG00000136936
REACTOME_TOLL_RECEPTOR_CASCADES
ENSG00000182718
KEGG_GLYCOSAMINOGLYCAN_BIOSYNTHESIS_HEPARAN_SULFATE
GO:0008320
GO:0022884
ENSG00000152147
GO:0055024
GO:0008637
ENSG00000108296
GO:0070227
GO:0002675
GO:0001104
ENSG00000196781
ENSG00000177105
GO:0006109
ENSG00000120071
ENSG00000106804
GO:0008373
ENSG00000187109
GO:0090329
ENSG00000198742
GO:0045646
GO:0032655
ENSG00000204319

Original gene set description

CLNS1A PPI subnetwork 0.3
E2F3 PPI subnetwork 0.3
REACTOME_MYD88_CASCADE_INITIATED_ON_PLASMA_MEMBRANE 0.3
REACTOME_TOLL_LIKE_RECEPTOR_10_TLR10_CASCADE 0.3
REACTOME_TOLL_LIKE_RECEPTOR_5_TLR5_CASCADE 0.3
diacylglycerol kinase activity 0.3
T cell receptor signaling pathway 0.3
regulation of cellular component movement 0.3
PIP4K2C PPI subnetwork 0.3
decreased immunoglobulin level 0.3
heart development 0.3
Ras protein signal transduction 0.3
MAGI2 PPI subnetwork 0.3
TAF7 PPI subnetwork 0.3
REACTOME_TRNA_AMINOACYLATION 0.3
improved glucose tolerance 0.3
REACTOME_TOLL_LIKE_RECEPTOR_4_TLR4_CASCADE 0.3
positive regulation of axon extension 0.3
regulation of myeloid cell differentiation 0.3
EIF5A PPI subnetwork 0.3
endoribonuclease activity 0.3
decreased NK T cell number 0.3
abnormal neutrophil physiology 0.3
actin filament bundle 0.3
XPA PPI subnetwork 0.3
REACTOME_TOLL_RECEPTOR_CASCADES 0.3
ANXA2 PPI subnetwork 0.3
KEGG_GLYCOSAMINOGLYCAN_BIOSYNTHESIS_HEPARAN_SULFATE 0.3
protein transmembrane transporter activity 0.3
macromolecule transmembrane transporter activity 0.3
GEMIN6 PPI subnetwork 0.3
regulation of cardiac muscle tissue development 0.3
apoptotic mitochondrial changes 0.3
CWC25 PPI subnetwork 0.3
lymphocyte apoptotic process 0.3
positive regulation of acute inflammatory response 0.3
RNA polymerase II transcription cofactor activity 0.3
TLE1 PPI subnetwork 0.3
RHOG PPI subnetwork 0.3
regulation of carbohydrate metabolic process 0.3
KIAA1267 PPI subnetwork 0.3
C5 PPI subnetwork 0.3
sialyltransferase activity 0.3
NAP1L1 PPI subnetwork 0.3
regulation of DNA-dependent DNA replication 0.3
SMURF1 PPI subnetwork 0.3
regulation of erythrocyte differentiatior 0.3
regulation of interleukin-12 production 0.3
ENSG00000204319 PPI subnetwork 0.3

Nominal P value

Original gene set ID	Original gene set description	Nominal P value
MP:0002945	abnormal inhibitory postsynaptic currents	0.3
ENSG00000161939	C17orf49 PPI subnetwork	0.3
MP:0009403	increased variability of skeletal muscle fiber size	0.3
GO:0005372	water transmembrane transporter activity	0.3
GO:0031099	regeneration	0.3
ENSG00000196405	EVL PPI subnetwork	0.3
ENSG00000105216	ENSG00000105216 PPI subnetwork	0.3
GO:0072332	signal transduction by p53 class mediator resulting in induction of apoptosis	0.3
ENSG00000086205	FOLH1 PPI subnetwork	0.3
REACTOME_SHC:MEDIATED_CASCADE	REACTOME_SHC:MEDIATED_CASCADE	0.31
GO:0033267	axon part	0.31
GO:0000123	histone acetyltransferase complex	0.31
GO:0031016	pancreas development	0.31
REACTOME_N:GLYCAN_ANTENNAE_ELONGATION_IN_THE_MEDIALTRANS:GOLGI	REACTOME_N:GLYCAN_ANTENNAE_ELONGATION_IN_THE_MEDIALTRANS:GOLGI	0.31
ENSG00000148296	SURF6 PPI subnetwork	0.31
GO:0051495	positive regulation of cytoskeleton organization	0.31
ENSG00000138448	ITGAV PPI subnetwork	0.31
ENSG00000137497	NUMA1 PPI subnetwork	0.31
GO:0004721	phosphoprotein phosphatase activity	0.31
MP:0002743	glomerulonephritis	0.31
MP:0010024	increased total body fat amount	0.31
ENSG00000135903	PAX3 PPI subnetwork	0.31
MP:0002625	heart left ventricle hypertrophy	0.31
MP:0003089	decreased skin tensile strength	0.31
ENSG00000196591	HDAC2 PPI subnetwork	0.31
GO:0043086	negative regulation of catalytic activity	0.31
ENSG00000127564	PKMYT1 PPI subnetwork	0.31
GO:0032313	regulation of Rab GTPase activity	0.31
GO:0032483	regulation of Rab protein signal transduction	0.31
GO:0016775	phosphotransferase activity, nitrogenous group as acceptor	0.31
ENSG00000138594	TMOD3 PPI subnetwork	0.31
ENSG00000132170	PPARG PPI subnetwork	0.31
MP:0002092	abnormal eye morphology	0.31
GO:0045060	negative thymic T cell selection	0.31
ENSG00000124641	MED20 PPI subnetwork	0.31
GO:0043038	amino acid activation	0.31
GO:0043039	tRNA aminoacylation	0.31
ENSG00000137275	RIPK1 PPI subnetwork	0.31
ENSG00000171681	ATF7IP PPI subnetwork	0.31
ENSG00000136238	RAC1 PPI subnetwork	0.31
GO:0017124	SH3 domain binding	0.31
GO:0003073	regulation of systemic arterial blood pressure	0.31
MP:0004157	interrupted aortic arch	0.31
ENSG00000181856	SLC2A4 PPI subnetwork	0.31
ENSG00000162702	ZNF281 PPI subnetwork	0.31
GO:0005732	small nucleolar ribonucleoprotein complex	0.31
MP:0005215	abnormal pancreatic islet morphology	0.31
ENSG00000063177	RPL18 PPI subnetwork	0.31
ENSG00000011260	UTP18 PPI subnetwork	0.31

Original gene set ID	Original gene set description	Nominal P value
GO:0006606	protein import into nucleus	0.31
MP:0002145	abnormal T cell differentiation	0.31
GO:0051427	hormone receptor binding	0.31
ENSG00000173369	C1QB PPI subnetwork	0.31
ENSG00000167193	CRK PPI subnetwork	0.31
GO:0017148	negative regulation of translation	0.31
GO:0030291	protein serine/threonine kinase inhibitor activity	0.31
ENSG00000141378	PTRH2 PPI subnetwork	0.31
GO:0031056	regulation of histone modification	0.31
REACTOME_CYCLIN_D_ASSOCIATED_EVENTS_IN_G1	REACTOME_CYCLIN_D_ASSOCIATED_EVENTS_IN_G1	0.31
REACTOME_G1_PHASE	REACTOME_G1_PHASE	0.31
GO:0043601	nuclear replisome	0.31
GO:0030894	replisome	0.31
ENSG00000163605	PPP4R2 PPI subnetwork	0.31
ENSG00000049323	LTBP1 PPI subnetwork	0.31
GO:0008285	negative regulation of cell proliferation	0.31
MP:0001146	abnormal testis morphology	0.31
ENSG00000147689	FAM83A PPI subnetwork	0.31
ENSG00000004660	CAMKK1 PPI subnetwork	0.31
REACTOME_BILE_SALT_AND_ORGANIC_ANION_SLC_TRANSPORTERS	REACTOME_BILE_SALT_AND_ORGANIC_ANION_SLC_TRANSPORTERS	0.31
GO:0021872	forebrain generation of neurons	0.31
ENSG00000112851	ERBB2IP PPI subnetwork	0.31
GO:0048520	positive regulation of behavior	0.31
REACTOME_TOLL LIKE RECEPTOR_2_TLR2_CASCADE	REACTOME_TOLL LIKE RECEPTOR_2_TLR2_CASCADE	0.31
REACTOME_TOLL LIKE RECEPTOR_TLR6TLR2_CASCADE	REACTOME_TOLL LIKE RECEPTOR_TLR6TLR2_CASCADE	0.31
REACTOME_MYD88MAL_CASCADE_INITIATED_ON_PLASMA_MEMBRANE	REACTOME_MYD88MAL_CASCADE_INITIATED_ON_PLASMA_MEMBRANE	0.31
REACTOME_TOLL LIKE RECEPTOR_TLR1TLR2_CASCADE	REACTOME_TOLL LIKE RECEPTOR_TLR1TLR2_CASCADE	0.31
GO:0030673	axolemma	0.31
GO:0030097	hemopoiesis	0.31
REACTOME_INTERLEUKIN:3_5_AND_GM:CSF_SIGNALING	REACTOME_INTERLEUKIN:3_5_AND_GM:CSF_SIGNALING	0.31
GO:0006312	mitotic recombination	0.31
ENSG000000085117	CD82 PPI subnetwork	0.31
GO:0048742	regulation of skeletal muscle fiber development	0.31
GO:0043303	mast cell degranulation	0.31
ENSG00000173281	PPP1R3B PPI subnetwork	0.31
REACTOME_SRP:DEPENDENT_COTRANSLATIONAL_PROTEIN_TARGETING_TO_M	REACTOME_SRP:DEPENDENT_COTRANSLATIONAL_PROTEIN_TARGETING_TO_MEM	0.31
ENSG00000161956	SEN3 PPI subnetwork	0.31
ENSG00000102753	KPNA3 PPI subnetwork	0.31
GO:0048641	regulation of skeletal muscle tissue development	0.31
GO:0005882	intermediate filament	0.31
ENSG00000164442	CITED2 PPI subnetwork	0.31
MP:0000239	absent common myeloid progenitor cells	0.31
ENSG00000212802	ENSG00000212802 PPI subnetwork	0.31
ENSG00000174766	ENSG00000174766 PPI subnetwork	0.31
MP:0002114	abnormal axial skeleton morphology	0.31
ENSG00000198933	TBKBP1 PPI subnetwork	0.31
ENSG00000129255	MPDU1 PPI subnetwork	0.31
GO:0006720	isoprenoid metabolic process	0.31
ENSG00000204271	SPIN3 PPI subnetwork	0.31

Original gene set ID**Original gene set description****Nominal P value**

Original gene set ID	Original gene set description	Nominal P value
ENSG00000186787	SPIN2B PPI subnetwork	0.31
MP:0004816	abnormal class switch recombination	0.31
MP:0002410	decreased susceptibility to viral infection	0.31
ENSG00000183093	ENSG00000183093 PPI subnetwork	0.31
ENSG00000077454	LRCH4 PPI subnetwork	0.31
ENSG00000205307	SAP25 PPI subnetwork	0.31
ENSG00000197263	OR8D2 PPI subnetwork	0.31
ENSG00000143514	TP53BP2 PPI subnetwork	0.31
MP:0004028	chromosome breakage	0.31
ENSG00000160208	RRP1B PPI subnetwork	0.31
ENSG00000089693	MLF2 PPI subnetwork	0.31
MP:0001429	dehydration	0.31
GO:0005667	transcription factor complex	0.31
REACTOME_PURINE_RIBONUCLEOSIDE_MONOPHOSPHATE_BIOSYNTHESIS	REACTOME_PURINE_RIBONUCLEOSIDE_MONOPHOSPHATE_BIOSYNTHESIS	0.31
GO:0002757	immune response-activating signal transduction	0.31
MP:0000284	double outlet heart right ventricle	0.31
GO:0007179	transforming growth factor beta receptor signaling pathway	0.31
ENSG00000112936	C7 PPI subnetwork	0.31
MP:0009254	disorganized pancreatic islets	0.31
GO:0001012	RNA polymerase II regulatory region DNA binding	0.31
MP:0004502	decreased incidence of chemically-induced tumors	0.31
GO:0034660	ncRNA metabolic process	0.31
ENSG00000164107	HAND2 PPI subnetwork	0.31
ENSG00000119616	FCF1 PPI subnetwork	0.31
GO:0080135	regulation of cellular response to stress	0.31
GO:0042393	histone binding	0.31
GO:0034284	response to monosaccharide stimulus	0.31
GO:0045095	keratin filament	0.31
ENSG00000104833	TUBB4A PPI subnetwork	0.31
ENSG00000162889	MAPKAPK2 PPI subnetwork	0.31
ENSG00000101665	SMAD7 PPI subnetwork	0.31
GO:0016272	prefoldin complex	0.31
ENSG00000128602	SMO PPI subnetwork	0.31
GO:0007051	spindle organization	0.31
ENSG00000070814	TCOF1 PPI subnetwork	0.31
REACTOME_SIGNAL_REGULATORY_PROTEIN_SIRP_FAMILY_INTERACTIONS	REACTOME_SIGNAL_REGULATORY_PROTEIN_SIRP_FAMILY_INTERACTIONS	0.31
MP:0008008	early cellular replicative senescence	0.31
GO:0060333	interferon-gamma-mediated signaling pathway	0.31
GO:0042249	establishment of planar polarity of embryonic epithelium	0.31
GO:0002822	regulation of adaptive immune response based on somatic recombination of immu	0.31
ENSG00000087088	BAX PPI subnetwork	0.31
ENSG00000172216	CEBPB PPI subnetwork	0.31
MP:0002108	abnormal muscle morphology	0.31
ENSG00000186416	NKRF PPI subnetwork	0.31
GO:0048863	stem cell differentiation	0.31
MP:0008875	abnormal xenobiotic pharmacokinetics	0.32
ENSG00000114767	RRP9 PPI subnetwork	0.32
MP:0004762	increased anti-double stranded DNA antibody leve	0.32
GO:0051321	meiotic cell cycle	0.32

Original gene set ID	Original gene set description	Nominal P value
MP:0004173	abnormal intervertebral disk morphology	0.32
ENSG00000125084	WNT1 PPI subnetwork	0.32
GO:0003215	cardiac right ventricle morphogenesis	0.32
ENSG00000149968	MMP3 PPI subnetwork	0.32
ENSG00000099389	ENSG00000099389 PPI subnetwork	0.32
ENSG00000118972	FGF23 PPI subnetwork	0.32
ENSG00000162521	RBBP4 PPI subnetwork	0.32
ENSG00000113916	BCL6 PPI subnetwork	0.32
ENSG00000037280	FLT4 PPI subnetwork	0.32
ENSG00000103653	CSK PPI subnetwork	0.32
ENSG00000111364	DDX55 PPI subnetwork	0.32
REACTOME_FRS2:MEDIATED_CASCADE	REACTOME_FRS2:MEDIATED_CASCADE	0.32
GO:0031228	intrinsic to Golgi membrane	0.32
MP:0006379	abnormal spermatocyte morphology	0.32
ENSG00000184678	HIST2H2BE PPI subnetwork	0.32
GO:0051240	positive regulation of multicellular organismal process	0.32
GO:0050321	tau-protein kinase activity	0.32
GO:0051635	bacterial cell surface binding	0.32
MP:0000364	abnormal vascular regression	0.32
ENSG00000104980	TIMM44 PPI subnetwork	0.32
GO:0042475	odontogenesis of dentin-containing tooth	0.32
REACTOME_PD:1_SIGNALING	REACTOME_PD:1_SIGNALING	0.32
GO:0006693	prostaglandin metabolic process	0.32
GO:0007259	JAK-STAT cascade	0.32
ENSG00000215301	DDX3X PPI subnetwork	0.32
GO:0016893	endonuclease activity, active with either ribo- or deoxyribonucleic acids and products	0.32
ENSG00000175390	EIF3F PPI subnetwork	0.32
GO:0008235	metalloexopeptidase activity	0.32
GO:0002764	immune response-regulating signaling pathway	0.32
MP:0002891	increased insulin sensitivity	0.32
GO:0051567	histone H3-K9 methylation	0.32
ENSG00000120158	RCL1 PPI subnetwork	0.32
KEGG_OTHER_GLYCAN_DEGRADATION	KEGG_OTHER_GLYCAN_DEGRADATION	0.32
GO:0051348	negative regulation of transferase activity	0.32
ENSG00000159348	CYB5R1 PPI subnetwork	0.32
GO:0002706	regulation of lymphocyte mediated immunity	0.32
ENSG00000196981	WDR5B PPI subnetwork	0.32
ENSG00000185736	ADARB2 PPI subnetwork	0.32
MP:0010254	nuclear cataracts	0.32
MP:0008078	increased CD8-positive T cell number	0.32
GO:0004629	phospholipase C activity	0.32
ENSG00000099194	SCD PPI subnetwork	0.32
ENSG00000112578	BYSL PPI subnetwork	0.32
ENSG00000164587	RPS14 PPI subnetwork	0.32
ENSG00000136271	DDX56 PPI subnetwork	0.32
REACTOME_ACTIVATION_OF_THE_MRNA_UPON_BINDING_OF_THE_CAP:BINDING	REACTOME_ACTIVATION_OF_THE_MRNA_UPON_BINDING_OF_THE_CAP:BINDING	0.32
GO:0046620	regulation of organ growth	0.32
GO:0070411	I-SMAD binding	0.32
ENSG00000176165	FOXP1 PPI subnetwork	0.32

Original gene set ID	Original gene set description	Nominal P value
ENSG00000181061	HIGD1A PPI subnetwork	0.33
GO:0005201	extracellular matrix structural constituent	0.33
ENSG00000140564	FURIN PPI subnetwork	0.33
REACTOME_METABOLISM_OF_CARBOHYDRATES	REACTOME_METABOLISM_OF_CARBOHYDRATES	0.33
MP:0005669	increased circulating leptin level	0.33
MP:0006126	abnormal outflow tract development	0.33
GO:0048565	digestive tract development	0.33
GO:0016577	histone demethylation	0.33
MP:0008826	abnormal splenic cell ratio	0.33
ENSG00000170345	FOS PPI subnetwork	0.33
ENSG00000127586	CHTF18 PPI subnetwork	0.33
GO:0002455	humoral immune response mediated by circulating immunoglobulin	0.33
ENSG00000057663	ATG5 PPI subnetwork	0.33
ENSG00000068024	HDAC4 PPI subnetwork	0.33
ENSG00000130772	MED18 PPI subnetwork	0.33
MP:0003932	abnormal molar crown morphology	0.33
GO:0051019	mitogen-activated protein kinase binding	0.33
ENSG00000163823	CCR1 PPI subnetwork	0.33
REACTOME_EXTRINSIC_PATHWAY_FOR_APOPTOSIS	REACTOME_EXTRINSIC_PATHWAY_FOR_APOPTOSIS	0.33
REACTOME_DEATH_RECEPTOR__SIGNALLING	REACTOME_DEATH_RECEPTOR__SIGNALLING	0.33
ENSG00000108773	KAT2A PPI subnetwork	0.33
GO:0048525	negative regulation of viral reproduction	0.33
GO:0045071	negative regulation of viral genome replication	0.33
GO:0007126	meiosis	0.33
GO:0051327	M phase of meiotic cell cycle	0.33
REACTOME_REMOVAL_OF_THE_FLAP_INTERMEDIATE	REACTOME_REMOVAL_OF_THE_FLAP_INTERMEDIATE	0.33
REACTOME_CLASS_C3_METABOTROPIC_Glutamatepheromone_receptors	REACTOME_CLASS_C3_METABOTROPIC_Glutamatepheromone_receptors	0.33
ENSG00000118503	TNFAIP3 PPI subnetwork	0.33
GO:0035336	long-chain fatty-acyl-CoA metabolic process	0.33
GO:0035338	long-chain fatty-acyl-CoA biosynthetic process	0.33
ENSG00000186340	THBS2 PPI subnetwork	0.33
GO:0016638	oxidoreductase activity, acting on the CH-NH2 group of donors	0.33
ENSG00000206211	ENSG00000206211 PPI subnetwork	0.33
ENSG00000204220	PFDN6 PPI subnetwork	0.33
ENSG00000206283	PFDN6 PPI subnetwork	0.33
ENSG00000171557	FGG PPI subnetwork	0.33
GO:0050792	regulation of viral reproduction	0.33
MP:0003743	abnormal facial morphology	0.33
MP:0005253	abnormal eye physiology	0.33
ENSG00000161980	POLR3K PPI subnetwork	0.33
GO:0008238	exopeptidase activity	0.33
MP:0003982	increased cholesterol level	0.33
MP:0000079	abnormal basioccipital bone morphology	0.33
GO:0005977	glycogen metabolic process	0.33
MP:0010418	perimembraneous ventricular septal defect	0.33
GO:0019827	stem cell maintenance	0.33
KEGG_CELL_ADHESION_MOLECULES_CAMS	KEGG_CELL_ADHESION_MOLECULES_CAMS	0.33
MP:0008284	abnormal hippocampus pyramidal cell layer	0.33
ENSG00000167674	ENSG00000167674 PPI subnetwork	0.33

Original gene set ID	Original gene set description	Nominal P value
MP:0002831	absent Peyer's patches	0.33
ENSG00000178568	ERBB4 PPI subnetwork	0.33
GO:0000272	polysaccharide catabolic process	0.33
GO:0034377	plasma lipoprotein particle assembly	0.33
GO:0065005	protein-lipid complex assembly	0.33
MP:0005358	abnormal incisor morphology	0.33
GO:0043296	apical junction complex	0.33
MP:0008438	abnormal cutaneous collagen fibril morphology	0.33
GO:0045597	positive regulation of cell differentiation	0.33
GO:0019717	synaptosome	0.33
ENSG00000102878	HSF4 PPI subnetwork	0.33
GO:0030427	site of polarized growth	0.33
KEGG_WNT_SIGNALING_PATHWAY	KEGG_WNT_SIGNALING_PATHWAY	0.33
ENSG00000078328	RBFOX1 PPI subnetwork	0.33
ENSG00000198231	DDX42 PPI subnetwork	0.33
GO:0007586	digestion	0.33
GO:0016558	protein import into peroxisome matrix	0.33
GO:0043022	ribosome binding	0.33
ENSG00000003402	CFLAR PPI subnetwork	0.33
MP:0001825	arrested T cell differentiation	0.33
ENSG00000174177	CTU2 PPI subnetwork	0.33
ENSG00000108592	FTSJ3 PPI subnetwork	0.33
GO:0071826	ribonucleoprotein complex subunit organization	0.33
GO:0002443	leukocyte mediated immunity	0.33
MP:0009395	increased nucleated erythrocyte cell number	0.33
ENSG00000181852	RNF41 PPI subnetwork	0.33
GO:0030879	mammary gland development	0.33
MP:0004901	decreased male germ cell number	0.33
ENSG00000170486	KRT72 PPI subnetwork	0.34
GO:0034504	protein localization to nucleus	0.34
ENSG00000164758	MED30 PPI subnetwork	0.34
REACTOME_NUCLEAR_SIGNALING_BY_ERBB4	REACTOME_NUCLEAR_SIGNALING_BY_ERBB4	0.34
ENSG00000175634	RPS6KB2 PPI subnetwork	0.34
ENSG00000146143	ENSG00000146143 PPI subnetwork	0.34
MP:0004948	abnormal neuronal precursor proliferation	0.34
MP:0008827	abnormal thymus cell ratio	0.34
MP:0002875	decreased erythrocyte cell number	0.34
GO:0005840	ribosome	0.34
MP:0009703	decreased birth body size	0.34
ENSG00000180138	CSNK1A1L PPI subnetwork	0.34
MP:0011083	complete lethality at weaning	0.34
ENSG00000139637	C12orf10 PPI subnetwork	0.34
GO:0071347	cellular response to interleukin-1	0.34
GO:0018904	organic ether metabolic process	0.34
ENSG00000143153	ATP1B1 PPI subnetwork	0.34
ENSG00000143622	RIT1 PPI subnetwork	0.34
ENSG00000188488	SERPINA5 PPI subnetwork	0.34
GO:0008146	sulfotransferase activity	0.34
GO:0016338	calcium-independent cell-cell adhesion	0.34

Original gene set ID	Original gene set description	Nominal P value
ENSG00000108559	NUP88 PPI subnetwork	0.34
GO:0006084	acetyl-CoA metabolic process	0.34
GO:0050920	regulation of chemotaxis	0.34
MP:0000333	decreased bone marrow cell number	0.34
GO:0003725	double-stranded RNA binding	0.34
MP:0010403	atrial septal defect	0.34
GO:0005921	gap junction	0.34
GO:0003013	circulatory system process	0.34
ENSG00000102871	TRADD PPI subnetwork	0.34
GO:0046134	pyrimidine nucleoside biosynthetic process	0.34
GO:0032103	positive regulation of response to external stimulus	0.34
GO:0045055	regulated secretory pathway	0.34
GO:0043189	H4/H2A histone acetyltransferase complex	0.34
ENSG00000156697	UTP14A PPI subnetwork	0.34
GO:0045182	translation regulator activity	0.34
ENSG00000080824	HSP90AA1 PPI subnetwork	0.34
GO:0002753	cytoplasmic pattern recognition receptor signaling pathway	0.34
GO:0070423	nucleotide-binding oligomerization domain containing signaling pathway	0.34
GO:0035872	nucleotide-binding domain, leucine rich repeat containing receptor signaling pathway	0.34
MP:0011093	complete embryonic lethality at implantation	0.34
GO:0015934	large ribosomal subunit	0.34
ENSG00000134376	CRB1 PPI subnetwork	0.34
ENSG00000131269	ABC7 PPI subnetwork	0.34
ENSG00000155438	MKI67IP PPI subnetwork	0.34
MP:0000217	abnormal leukocyte cell number	0.34
REACTOME_NOTCH:HLH_TRANSCRIPTION_PATHWAY	REACTOME_NOTCH:HLH_TRANSCRIPTION_PATHWAY	0.34
REACTOME_NICD_TRAFFICS_TO_NUCLEUS	REACTOME_NICD_TRAFFICS_TO_NUCLEUS	0.34
ENSG00000198918	RPL39 PPI subnetwork	0.34
MP:0000141	abnormal vertebral body morphology	0.34
GO:0050768	negative regulation of neurogenesis	0.34
GO:0046545	development of primary female sexual characteristics	0.34
GO:0007589	body fluid secretion	0.34
ENSG00000131462	TUBG1 PPI subnetwork	0.34
ENSG00000026508	CD44 PPI subnetwork	0.34
ENSG00000066926	FECH PPI subnetwork	0.34
MP:0000063	decreased bone mineral density	0.34
GO:0002684	positive regulation of immune system process	0.34
MP:0003052	omphalocele	0.34
GO:0009395	phospholipid catabolic process	0.34
ENSG00000064300	NGFR PPI subnetwork	0.34
ENSG00000185745	IFIT1 PPI subnetwork	0.34
ENSG00000171314	PGAM1 PPI subnetwork	0.34
GO:0045576	mast cell activation	0.34
GO:0015296	anion:cation symporter activity	0.34
ENSG00000125485	DDX31 PPI subnetwork	0.34
ENSG00000114978	MOB1A PPI subnetwork	0.34
ENSG00000197063	MAFG PPI subnetwork	0.35
ENSG00000076003	MCM6 PPI subnetwork	0.35
REACTOME_GLYCOGEN_BREAKDOWN_GLYCOGENOLYSIS	REACTOME_GLYCOGEN_BREAKDOWN_GLYCOGENOLYSIS	0.35

Original gene set ID	Original gene set description	Nominal P value
ENSG00000078579	FGF20 PPI subnetwork	0.35
MP:0004231	abnormal calcium ion homeostasis	0.35
ENSG00000142252	GEMIN7 PPI subnetwork	0.35
ENSG00000111450	STX2 PPI subnetwork	0.35
GO:0042277	peptide binding	0.35
GO:0042623	ATPase activity, coupled	0.35
GO:0016327	apicolateral plasma membrane	0.35
ENSG00000008710	PKD1 PPI subnetwork	0.35
MP:0006055	abnormal vascular endothelial cell morphology	0.35
ENSG00000196504	PRPF40A PPI subnetwork	0.35
MP:0008450	retinal photoreceptor degeneration	0.35
ENSG00000095015	MAP3K1 PPI subnetwork	0.35
MP:0000474	abnormal foregut morphology	0.35
GO:0008135	translation factor activity, nucleic acid binding	0.35
ENSG00000130726	TRIM28 PPI subnetwork	0.35
MP:0001914	hemorrhage	0.35
MP:0011348	abnormal renal glomerulus basement membrane morphology	0.35
ENSG00000147044	CASK PPI subnetwork	0.35
GO:0043627	response to estrogen stimulus	0.35
ENSG00000037042	TUBG2 PPI subnetwork	0.35
ENSG00000164692	COL1A2 PPI subnetwork	0.35
MP:0005348	increased T cell proliferation	0.35
ENSG00000100697	DICER1 PPI subnetwork	0.35
MP:0001326	retinal degeneration	0.35
ENSG00000047056	WDR37 PPI subnetwork	0.35
MP:0003997	tonic-clonic seizures	0.35
ENSG00000173889	PHC3 PPI subnetwork	0.35
MP:0000921	demyelination	0.35
GO:0045088	regulation of innate immune response	0.35
ENSG00000110245	APOC3 PPI subnetwork	0.35
ENSG00000215755	ENSG00000215755 PPI subnetwork	0.35
KEGG_NATURAL_KILLER_CELL_MEDIATED_CYTOTOXICITY	KEGG_NATURAL_KILLER_CELL_MEDIATED_CYTOTOXICITY	0.35
GO:0002429	immune response-activating cell surface receptor signaling pathway	0.35
GO:0004835	tubulin-tyrosine ligase activity	0.35
ENSG00000130520	LSM4 PPI subnetwork	0.35
REACTOME_FORMATION_OF_THE_TERNARY_COMPLEX_AND_SUBSEQUENTLY_	REACTOME_FORMATION_OF_THE_TERNARY_COMPLEX_AND_SUBSEQUENTLY_	0.35
GO:0045621	positive regulation of lymphocyte differentiator	0.35
REACTOME_ACTIVATED_TLR4_SIGNALLING	REACTOME_ACTIVATED_TLR4_SIGNALLING	0.35
ENSG00000086232	EIF2AK1 PPI subnetwork	0.35
REACTOME_TRANSLOCATION_OF_ZAP:70_TO_IMMUNOLOGICAL_SYNAPSE	REACTOME_TRANSLOCATION_OF_ZAP:70_TO_IMMUNOLOGICAL_SYNAPSE	0.35
MP:0001844	autoimmune response	0.35
GO:0030335	positive regulation of cell migration	0.35
ENSG00000114737	CISH PPI subnetwork	0.35
GO:0006820	anion transport	0.35
GO:0007088	regulation of mitosis	0.35
GO:0051783	regulation of nuclear division	0.35
MP:0008071	absent B cells	0.35
GO:0042098	T cell proliferation	0.35
REACTOME_GAP_JUNCTION_ASSEMBLY	REACTOME_GAP_JUNCTION_ASSEMBLY	0.35

Original gene set ID	Original gene set description	Nominal P value
GO:0042481	regulation of odontogenesis	0.35
GO:0008643	carbohydrate transport	0.35
ENSG00000099725	ENSG00000099725 PPI subnetwork	0.35
GO:0018410	C-terminal protein amino acid modification	0.35
ENSG00000157227	MMP14 PPI subnetwork	0.35
MP:0001158	abnormal prostate gland morphology	0.35
ENSG00000105085	MED26 PPI subnetwork	0.35
ENSG00000212908	ENSG00000212908 PPI subnetwork	0.35
ENSG00000213416	KRTAP4-12 PPI subnetwork	0.35
GO:0001782	B cell homeostasis	0.35
ENSG00000115946	PNO1 PPI subnetwork	0.35
GO:0071305	cellular response to vitamin D	0.35
GO:0006107	oxaloacetate metabolic process	0.35
GO:0070988	demethylation	0.35
GO:0018279	protein N-linked glycosylation via asparagine	0.35
GO:0018196	peptidyl-asparagine modification	0.35
ENSG00000118985	ELL2 PPI subnetwork	0.35
ENSG00000206212	ENSG00000206212 PPI subnetwork	0.35
ENSG00000182498	ENSG00000182498 PPI subnetwork	0.35
ENSG00000096150	RPS18 PPI subnetwork	0.35
GO:0046847	filopodium assembly	0.35
ENSG00000135387	CAPRIN1 PPI subnetwork	0.35
MP:0011090	partial perinatal lethality	0.35
GO:0032369	negative regulation of lipid transport	0.35
GO:0002821	positive regulation of adaptive immune response	0.35
ENSG00000111537	IFNG PPI subnetwork	0.35
ENSG00000135404	CD63 PPI subnetwork	0.35
GO:0009156	ribonucleoside monophosphate biosynthetic process	0.35
ENSG00000123091	RNF11 PPI subnetwork	0.35
GO:0051905	establishment of pigment granule localization	0.35
MP:0002357	abnormal spleen white pulp morphology	0.35
GO:0045582	positive regulation of T cell differentiation	0.35
GO:0051098	regulation of binding	0.35
GO:0005839	proteasome core complex	0.35
MP:0004704	short vertebral column	0.35
REACTOME_PHOSPHORYLATION_OF_CD3_AND_TCR_ZETA_CHAINS	REACTOME_PHOSPHORYLATION_OF_CD3_AND_TCR_ZETA_CHAINS	0.35
ENSG00000167552	TUBA1A PPI subnetwork	0.35
ENSG00000136931	NR5A1 PPI subnetwork	0.35
ENSG00000119953	SMNDC1 PPI subnetwork	0.35
GO:0017053	transcriptional repressor complex	0.35
ENSG00000130203	APOE PPI subnetwork	0.35
GO:0015662	ATPase activity, coupled to transmembrane movement of ions, phosphorylative me	0.35
ENSG00000145423	SFRP2 PPI subnetwork	0.35
GO:0071375	cellular response to peptide hormone stimulus	0.35
GO:0030318	melanocyte differentiation	0.35
GO:0030595	leukocyte chemotaxis	0.35
GO:0030036	actin cytoskeleton organization	0.35
ENSG00000139515	PDX1 PPI subnetwork	0.35
ENSG00000006075	CCL3 PPI subnetwork	0.35

Original gene set ID	Original gene set description	Nominal P value
MP:0001785	edema	0.35
GO:0006956	complement activation	0.35
REACTOME_L1CAM_INTERACTIONS	REACTOME_L1CAM_INTERACTIONS	0.35
REACTOME_GAP_JUNCTION_TRAFFICKING_AND_REGULATION	REACTOME_GAP_JUNCTION_TRAFFICKING_AND_REGULATION	0.35
ENSG00000142892	PIGK PPI subnetwork	0.35
KEGG_TOLL_LIKE_RECEPTOR_SIGNALING_PATHWAY	KEGG_TOLL_LIKE_RECEPTOR_SIGNALING_PATHWAY	0.35
ENSG00000088356	PDRG1 PPI subnetwork	0.35
MP:0004608	abnormal cervical axis morphology	0.36
MP:0006029	abnormal sclerotome morphology	0.36
ENSG00000077097	TOP2B PPI subnetwork	0.36
MP:0006303	abnormal retinal nerve fiber layer morphology	0.36
ENSG00000184083	FAM120C PPI subnetwork	0.36
MP:0002857	cochlear ganglion degeneration	0.36
ENSG00000004799	PDK4 PPI subnetwork	0.36
ENSG00000108826	MRPL27 PPI subnetwork	0.36
ENSG00000138346	DNA2 PPI subnetwork	0.36
ENSG00000178562	CD28 PPI subnetwork	0.36
ENSG00000143748	NVL PPI subnetwork	0.36
MP:0003051	curly tail	0.36
MP:0006279	abnormal limb development	0.36
REACTOME_MITOTIC_G2:G2M_PHASES	REACTOME_MITOTIC_G2:G2M_PHASES	0.36
ENSG00000136573	BLK PPI subnetwork	0.36
GO:0046928	regulation of neurotransmitter secretion	0.36
ENSG00000117091	CD48 PPI subnetwork	0.36
GO:0035257	nuclear hormone receptor binding	0.36
GO:0034142	toll-like receptor 4 signaling pathway	0.36
ENSG00000084674	APOB PPI subnetwork	0.36
GO:0006767	water-soluble vitamin metabolic process	0.36
REACTOME_DOWNSTREAM_TCR_SIGNALING	REACTOME_DOWNSTREAM_TCR_SIGNALING	0.36
ENSG00000104722	NEFM PPI subnetwork	0.36
MP:0001175	abnormal lung morphology	0.36
REACTOME_ACTIVATION_OF_THE_PRE:REPLICATIVE_COMPLEX	REACTOME_ACTIVATION_OF_THE_PRE:REPLICATIVE_COMPLEX	0.36
ENSG00000172845	SP3 PPI subnetwork	0.36
GO:0035085	cilium axoneme	0.36
MP:0011091	complete prenatal lethality	0.36
ENSG00000126247	CAPNS1 PPI subnetwork	0.36
MP:0008567	decreased interferon-gamma secretion	0.36
ENSG00000134954	ETS1 PPI subnetwork	0.36
GO:0043586	tongue development	0.36
ENSG00000085511	MAP3K4 PPI subnetwork	0.36
GO:0004175	endopeptidase activity	0.36
GO:0016605	PML body	0.36
ENSG00000093000	NUP50 PPI subnetwork	0.36
ENSG00000165637	VDAC2 PPI subnetwork	0.36
ENSG00000168918	INPP5D PPI subnetwork	0.36
ENSG00000120802	TMPO PPI subnetwork	0.36
REACTOME_TRIF_MEDIATED_TLR3_SIGNALING	REACTOME_TRIF_MEDIATED_TLR3_SIGNALING	0.36
REACTOME_TOLL_LIKE_RECEPTOR_3_TLR3_CASCADE	REACTOME_TOLL_LIKE_RECEPTOR_3_TLR3_CASCADE	0.36
REACTOME_RNA_POLYMERASE_I_RNA_POLYMERASE_III_AND_MITOCHONDRIAL_T	REACTOME_RNA_POLYMERASE_I_RNA_POLYMERASE_III_AND_MITOCHONDRIAL_T	0.36

Original gene set ID	Original gene set description	Nominal P value
MP:0001392	abnormal locomotor behavior	0.36
GO:0043218	compact myelin	0.36
KEGG_AMINOACYL_TRNA_BIOSYNTHESIS	KEGG_AMINOACYL_TRNA_BIOSYNTHESIS	0.36
ENSG00000168542	COL3A1 PPI subnetwork	0.36
ENSG00000163558	PRKCI PPI subnetwork	0.36
ENSG00000179295	PTPN11 PPI subnetwork	0.36
GO:0070192	chromosome organization involved in meiosis	0.36
ENSG00000117906	RCN2 PPI subnetwork	0.36
GO:0007606	sensory perception of chemical stimulus	0.36
GO:0048066	developmental pigmentation	0.36
MP:0005016	decreased lymphocyte cell number	0.36
MP:0005065	abnormal neutrophil morphology	0.36
ENSG00000158691	ZSCAN12 PPI subnetwork	0.36
ENSG00000124214	STAU1 PPI subnetwork	0.36
ENSG00000100413	POLR3H PPI subnetwork	0.36
GO:0006959	humoral immune response	0.36
GO:0071827	plasma lipoprotein particle organization	0.36
GO:0071825	protein-lipid complex subunit organization	0.36
ENSG00000075415	SLC25A3 PPI subnetwork	0.36
MP:0002962	increased urine protein level	0.36
ENSG00000111266	DUSP16 PPI subnetwork	0.36
REACTOME_INFLUENZA_VIRAL_RNA_TRANSCRIPTION_AND_REPLICATION	REACTOME_INFLUENZA_VIRAL_RNA_TRANSCRIPTION_AND_REPLICATION	0.36
GO:0019903	protein phosphatase binding	0.36
ENSG00000166484	MAPK7 PPI subnetwork	0.36
GO:0016891	endoribonuclease activity, producing 5'-phosphomonoesters	0.36
GO:0050727	regulation of inflammatory response	0.36
REACTOME_UNFOLDED_PROTEIN_RESPONSE	REACTOME_UNFOLDED_PROTEIN_RESPONSE	0.36
ENSG00000105939	ZC3HAV1 PPI subnetwork	0.36
MP:0004796	increased anti-histone antibody level	0.36
ENSG00000109072	SEBOX PPI subnetwork	0.36
ENSG00000132703	APCS PPI subnetwork	0.36
REACTOME_GLUCONEOGENESIS	REACTOME_GLUCONEOGENESIS	0.36
ENSG00000100316	RPL3 PPI subnetwork	0.36
ENSG00000154096	THY1 PPI subnetwork	0.36
ENSG00000129083	COPB1 PPI subnetwork	0.36
GO:0005096	GTPase activator activity	0.36
GO:0046965	retinoid X receptor binding	0.36
ENSG00000206506	HLA-G PPI subnetwork	0.36
ENSG00000206443	ENSG00000206443 PPI subnetwork	0.36
ENSG00000204632	HLA-G PPI subnetwork	0.36
MP:0001504	abnormal posture	0.36
ENSG00000168488	ATXN2L PPI subnetwork	0.36
REACTOME_ERKMAPK_TARGETS	REACTOME_ERKMAPK_TARGETS	0.36
ENSG00000062038	CDH3 PPI subnetwork	0.36
ENSG00000005007	UPF1 PPI subnetwork	0.36
ENSG00000115977	AAK1 PPI subnetwork	0.36
MP:0008279	arrest of spermiogenesis	0.36
ENSG00000105610	KLF1 PPI subnetwork	0.36
ENSG00000196943	C14orf21 PPI subnetwork	0.36

Original gene set ID	Original gene set description	Nominal P value
GO:0045672	positive regulation of osteoclast differentiation	0.36
GO:0005625	soluble fraction	0.36
GO:0006487	protein N-linked glycosylation	0.36
MP:0008582	short photoreceptor inner segment	0.36
ENSG00000147649	MTDH PPI subnetwork	0.36
GO:0046486	glycerolipid metabolic process	0.36
KEGG_GLYCOSPHINGOLIPID_BIOSYNTHESIS_GLOBO_SERIES	KEGG_GLYCOSPHINGOLIPID_BIOSYNTHESIS_GLOBO_SERIES	0.36
ENSG00000174175	SELP PPI subnetwork	0.36
GO:0005922	connexon complex	0.36
GO:0006493	protein O-linked glycosylation	0.36
ENSG00000162613	FUBP1 PPI subnetwork	0.36
ENSG00000162924	REL PPI subnetwork	0.36
GO:0090257	regulation of muscle system process	0.36
MP:0009937	abnormal neuron differentiation	0.36
MP:0000164	abnormal cartilage development	0.36
MP:0004982	abnormal osteoclast morphology	0.36
REACTOME_NFKB_AND_MAP_KINASES_ACTIVATION_MEDIATED_BY_TLR4_SIGI	REACTOME_NFKB_AND_MAP_KINASES_ACTIVATION_MEDIATED_BY_TLR4_SIGNALI	0.36
GO:0008656	cysteine-type endopeptidase activator activity involved in apoptotic proces:	0.36
GO:0018298	protein-chromophore linkage	0.36
ENSG00000112282	MED23 PPI subnetwork	0.36
ENSG00000114209	PDCD10 PPI subnetwork	0.36
GO:0061035	regulation of cartilage development	0.36
MP:0008641	increased circulating interleukin-1 beta leve	0.36
KEGG_GLYCEROPHOSPHOLIPID_METABOLISM	KEGG_GLYCEROPHOSPHOLIPID_METABOLISM	0.36
GO:0050931	pigment cell differentiation	0.36
GO:0009408	response to heat	0.36
REACTOME_ENDOGENOUS_STEROLS	REACTOME_ENDOGENOUS_STEROLS	0.36
GO:0001916	positive regulation of T cell mediated cytotoxicity	0.36
GO:0046949	fatty-acyl-CoA biosynthetic process	0.36
GO:0035337	fatty-acyl-CoA metabolic process	0.36
REACTOME_CONVERSION_FROM_APCCDC20_TO_APCCCDH1_IN_LATE_ANAPI	REACTOME_CONVERSION_FROM_APCCDC20_TO_APCCCDH1_IN_LATE_ANAPHASI	0.36
GO:0007141	male meiosis I	0.36
ENSG00000153395	LPCAT1 PPI subnetwork	0.36
MP:0008540	abnormal cerebrum morphology	0.36
REACTOME_MYD88:INDEPENDENT_CASCADE_INITIATED_ON_PLASMA_MEMBR	REACTOME_MYD88:INDEPENDENT_CASCADE_INITIATED_ON_PLASMA_MEMBRANI	0.37
GO:0070936	protein K48-linked ubiquitination	0.37
REACTOME_REGULATION_OF_INSULIN:LIKE_GROWTH_FACTOR_IGF_ACTIVITY_	REACTOME_REGULATION_OF_INSULIN:LIKE_GROWTH_FACTOR_IGF_ACTIVITY_BY_	0.37
MP:0003651	abnormal axon outgrowth	0.37
GO:0005923	tight junction	0.37
GO:0070160	occluding junction	0.37
GO:0008037	cell recognition	0.37
GO:0070193	synaptonemal complex organization	0.37
ENSG00000165630	PRPF18 PPI subnetwork	0.37
ENSG00000184110	EIF3C PPI subnetwork	0.37
ENSG00000149187	CEL1 PPI subnetwork	0.37
ENSG00000066336	SPI1 PPI subnetwork	0.37
GO:0005516	calmodulin binding	0.37
GO:0003016	respiratory system process	0.37
ENSG00000185236	RAB11B PPI subnetwork	0.37

Original gene set ID	Original gene set description	Nominal P value
GO:0048589	developmental growth	0.38
ENSG00000100347	SAMM50 PPI subnetwork	0.38
MP:0004751	increased length of allograft survival	0.38
GO:0042562	hormone binding	0.38
MP:0004618	thoracic vertebral transformation	0.38
MP:0005070	impaired NK cell cytotoxicity	0.38
ENSG00000169783	LINGO1 PPI subnetwork	0.38
ENSG00000171530	TBCA PPI subnetwork	0.38
ENSG00000164053	ATRIP PPI subnetwork	0.38
ENSG00000139083	ETV6 PPI subnetwork	0.38
REACTOME_SEMA4D_INDUCED_CELL_MIGRATION_AND_GROWTH: CONE_COLLAPSE	REACTOME_SEMA4D_INDUCED_CELL_MIGRATION_AND_GROWTH: CONE_COLLAPSE	0.38
GO:0042493	response to drug	0.38
ENSG00000101084	C20orf24 PPI subnetwork	0.38
REACTOME_INSULIN_RECEPTOR_SIGNALING_CASCADE	REACTOME_INSULIN_RECEPTOR_SIGNALING_CASCADE	0.38
GO:0043560	insulin receptor substrate binding	0.38
GO:0007339	binding of sperm to zona pellucida	0.38
MP:0008168	decreased B-1a cell number	0.38
ENSG00000137841	PLCB2 PPI subnetwork	0.38
ENSG00000150995	ITPR1 PPI subnetwork	0.38
GO:0050851	antigen receptor-mediated signaling pathway	0.38
REACTOME_CHAPERONIN_MEDIATED_PROTEIN_FOLDING	REACTOME_CHAPERONIN_MEDIATED_PROTEIN_FOLDING	0.38
GO:0034433	steroid esterification	0.38
GO:0034435	cholesterol esterification	0.38
GO:0034434	sterol esterification	0.38
GO:0009108	coenzyme biosynthetic process	0.38
MP:0005616	decreased susceptibility to type IV hypersensitivity reaction	0.38
GO:0031527	filopodium membrane	0.38
MP:0004007	abnormal lung vasculature morphology	0.38
ENSG00000205022	PABPN1L PPI subnetwork	0.38
ENSG00000138696	BMPR1B PPI subnetwork	0.38
ENSG00000142657	PGD PPI subnetwork	0.38
MP:0002451	abnormal macrophage physiology	0.38
GO:0042445	hormone metabolic process	0.38
MP:0008261	arrest of male meiosis	0.38
GO:0000146	microfilament motor activity	0.38
MP:0000564	syndactyly	0.38
MP:0002339	abnormal lymph node morphology	0.38
MP:0004919	abnormal positive T cell selection	0.38
ENSG00000196083	IL1RAP PPI subnetwork	0.38
ENSG00000142871	CYR61 PPI subnetwork	0.38
GO:0009988	cell-cell recognition	0.38
ENSG00000143466	IKBKE PPI subnetwork	0.38
ENSG00000148175	STOM PPI subnetwork	0.38
GO:0048864	stem cell development	0.38
ENSG00000143768	LEFTY2 PPI subnetwork	0.38
GO:0010564	regulation of cell cycle process	0.38
REACTOME_GLUCOSE_TRANSPORT	REACTOME_GLUCOSE_TRANSPORT	0.38
GO:0002279	mast cell activation involved in immune response	0.38
GO:0001667	ameboidal cell migration	0.38

Original gene set ID	Original gene set description	Nominal P value
REACTOME_GRB2SOS_PROVIDES_LINKAGE_TO_MAPK_SIGNALING_FOR_INTERGRIN	REACTOME_GRB2SOS_PROVIDES_LINKAGE_TO_MAPK_SIGNALING_FOR_INTERGRIN	0.39
GO:0007608	sensory perception of smell	0.39
MP:0000220	increased monocyte cell number	0.39
GO:0022604	regulation of cell morphogenesis	0.39
MP:0002407	abnormal double-negative T cell morphology	0.39
GO:0030834	regulation of actin filament depolymerization	0.39
GO:0033522	histone H2A ubiquitination	0.39
MP:0000039	abnormal otic capsule morphology	0.39
ENSG00000116213	WRAP73 PPI subnetwork	0.39
MP:0003123	paternal imprinting	0.39
MP:0006355	abnormal sixth branchial arch artery morphology	0.39
MP:0011104	partial embryonic lethality before implantation	0.39
GO:0032868	response to insulin stimulus	0.39
GO:0051303	establishment of chromosome localization	0.39
GO:0050000	chromosome localization	0.39
GO:0051875	pigment granule localization	0.39
GO:0007031	peroxisome organization	0.39
ENSG00000010803	SCMH1 PPI subnetwork	0.39
GO:0001750	photoreceptor outer segment	0.39
GO:0030674	protein binding, bridging	0.39
GO:0016628	oxidoreductase activity, acting on the CH-CH group of donors, NAD or NADP as acceptor	0.39
MP:0008584	photoreceptor outer segment degeneration	0.39
ENSG00000063322	MED29 PPI subnetwork	0.39
MP:0000495	abnormal colon morphology	0.39
ENSG00000015475	BID PPI subnetwork	0.39
MP:0000556	abnormal hindlimb morphology	0.39
ENSG000000174804	FZD4 PPI subnetwork	0.39
ENSG000000170653	ATF7 PPI subnetwork	0.39
REACTOME_INTRINSIC_PATHWAY_FOR_APOPTOSIS	REACTOME_INTRINSIC_PATHWAY_FOR_APOPTOSIS	0.39
GO:0045580	regulation of T cell differentiation	0.39
GO:0017046	peptide hormone binding	0.39
KEGG_STARCH_AND_SUCROSE_METABOLISM	KEGG_STARCH_AND_SUCROSE_METABOLISM	0.39
GO:0006501	C-terminal protein lipidation	0.39
ENSG000000162105	SHANK2 PPI subnetwork	0.39
ENSG000000084623	EIF3I PPI subnetwork	0.39
KEGG_MELANOGENESIS	KEGG_MELANOGENESIS	0.39
ENSG000000115947	ORC4 PPI subnetwork	0.39
ENSG000000110107	PRPF19 PPI subnetwork	0.39
MP:0002358	abnormal spleen periarteriolar lymphoid sheath morphology	0.39
ENSG000000105404	RABAC1 PPI subnetwork	0.39
GO:0016922	ligand-dependent nuclear receptor binding	0.39
ENSG000000131043	C20orf4 PPI subnetwork	0.39
MP:0002455	abnormal dendritic cell antigen presentation	0.39
GO:0002708	positive regulation of lymphocyte mediated immunity	0.39
GO:0002705	positive regulation of leukocyte mediated immunity	0.39
ENSG000000123349	PFDN5 PPI subnetwork	0.39
MP:0005657	abnormal neural plate morphology	0.39
GO:0030672	synaptic vesicle membrane	0.39
GO:0046822	regulation of nucleocytoplasmic transport	0.39

Original gene set ID	Original gene set description	Nominal P value
ENSG00000108797	CNTNAP1 PPI subnetwork	0.39
MP:0000743	muscle spasm	0.39
ENSG00000175216	CKAP5 PPI subnetwork	0.39
GO:0040017	positive regulation of locomotion	0.39
ENSG00000183943	PRKX PPI subnetwork	0.39
GO:0045880	positive regulation of smoothened signaling pathway	0.39
MP:0004567	decreased myocardial fiber number	0.39
MP:0002599	increased mean platelet volume	0.4
GO:0008305	integrin complex	0.4
ENSG00000174125	TLR1 PPI subnetwork	0.4
MP:0008596	increased circulating interleukin-6 level	0.4
MP:0002258	abnormal cricoid cartilage morphology	0.4
GO:0043304	regulation of mast cell degranulation	0.4
ENSG00000172795	DCP2 PPI subnetwork	0.4
ENSG00000105649	RAB3A PPI subnetwork	0.4
REACTOME_CENTROSOME_MATURATION	REACTOME_CENTROSOME_MATURATION	0.4
REACTOME_RECRUITMENT_OF_MITOTIC_CENTROSOME_PROTEINS_AND_COM	REACTOME_RECRUITMENT_OF_MITOTIC_CENTROSOME_PROTEINS_AND_COMPLE	0.4
GO:0030218	erythrocyte differentiation	0.4
MP:0000717	abnormal lymphocyte cell number	0.4
GO:0034138	toll-like receptor 3 signaling pathway	0.4
REACTOME_G2M_TRANSITION	REACTOME_G2M_TRANSITION	0.4
GO:0045787	positive regulation of cell cycle	0.4
GO:0030010	establishment of cell polarity	0.4
KEGG_VEGF_SIGNALING_PATHWAY	KEGG_VEGF_SIGNALING_PATHWAY	0.4
MP:0001385	pup cannibalization	0.4
GO:0033002	muscle cell proliferation	0.4
GO:0061061	muscle structure development	0.4
ENSG00000112306	RPS12 PPI subnetwork	0.4
GO:0007423	sensory organ development	0.4
GO:0009067	aspartate family amino acid biosynthetic process	0.4
GO:0005730	nucleolus	0.4
REACTOME_INFLUENZA_INFECTION	REACTOME_INFLUENZA_INFECTION	0.4
KEGG_BLADDER_CANCER	KEGG_BLADDER_CANCER	0.4
ENSG00000156508	EEF1A1 PPI subnetwork	0.4
ENSG00000004897	CDC27 PPI subnetwork	0.4
ENSG00000077080	ACTL6B PPI subnetwork	0.4
KEGG_METABOLISM_OF_XENOBIOTICS_BY_CYTOCHROME_P450	KEGG_METABOLISM_OF_XENOBIOTICS_BY_CYTOCHROME_P450	0.4
GO:0032587	ruffle membrane	0.4
ENSG00000115310	RTN4 PPI subnetwork	0.4
GO:0003208	cardiac ventricle morphogenesis	0.4
GO:0002697	regulation of immune effector process	0.4
ENSG00000141456	ENSG00000141456 PPI subnetwork	0.4
ENSG00000003400	CASP10 PPI subnetwork	0.4
GO:0048041	focal adhesion assembly	0.4
ENSG00000158373	HIST1H2BD PPI subnetwork	0.4
ENSG00000101246	ARFRP1 PPI subnetwork	0.4
MP:0008277	abnormal sternum ossification	0.4
ENSG00000136504	KAT7 PPI subnetwork	0.4
ENSG00000100767	PAPLN PPI subnetwork	0.4

Original gene set ID	Original gene set description	Nominal P value
GO:0042813	Wnt-activated receptor activity	0.4
REACTOME_MEIOTIC_SYNAPSIS	REACTOME_MEIOTIC_SYNAPSIS	0.4
GO:0002460	adaptive immune response based on somatic recombination of immune receptors b	0.4
ENSG00000147145	LPAR4 PPI subnetwork	0.4
GO:0032392	DNA geometric change	0.4
GO:0032508	DNA duplex unwinding	0.4
ENSG00000071462	WBSR22 PPI subnetwork	0.4
ENSG00000182899	RPL35A PPI subnetwork	0.4
MP:0000322	increased granulocyte number	0.4
ENSG00000183751	TBL3 PPI subnetwork	0.4
MP:0009890	cleft secondary palate	0.4
ENSG00000132646	PCNA PPI subnetwork	0.4
ENSG00000100325	ASCC2 PPI subnetwork	0.4
GO:0006662	glycerol ether metabolic process	0.4
ENSG00000116750	UCHL5 PPI subnetwork	0.4
GO:0007140	male meiosis	0.4
MP:0001751	increased circulating luteinizing hormone leve	0.4
ENSG00000168040	FADD PPI subnetwork	0.4
GO:0009214	cyclic nucleotide catabolic process	0.4
REACTOME_INTERLEUKIN:2_SIGNALING	REACTOME_INTERLEUKIN:2_SIGNALING	0.4
GO:0050865	regulation of cell activation	0.4
MP:0004769	abnormal synaptic vesicle morphology	0.4
ENSG00000133026	MYH10 PPI subnetwork	0.4
ENSG00000058600	POLR3E PPI subnetwork	0.4
ENSG00000137574	TGS1 PPI subnetwork	0.4
ENSG00000165806	CASP7 PPI subnetwork	0.4
MP:0006092	abnormal olfactory neuron morphology	0.4
MP:0008045	decreased NK cell number	0.4
ENSG00000163586	FABP1 PPI subnetwork	0.4
MP:0004042	decreased susceptibility to kidney reperfusion injur	0.4
GO:0043010	camera-type eye development	0.4
MP:0005014	increased B cell number	0.4
GO:0044441	cilium part	0.4
MP:0002260	abnormal thyroid cartilage morphology	0.4
GO:0003333	amino acid transmembrane transport	0.4
ENSG00000196136	SERPINA3 PPI subnetwork	0.4
GO:0015294	solute:cation symporter activity	0.4
ENSG00000109458	GAB1 PPI subnetwork	0.4
MP:0009146	abnormal pancreatic acinar cell morphology	0.4
ENSG00000067177	PHKA1 PPI subnetwork	0.4
MP:0000820	abnormal choroid plexus morphology	0.4
GO:0050853	B cell receptor signaling pathway	0.4
GO:0003407	neural retina development	0.4
ENSG00000116001	TIA1 PPI subnetwork	0.4
ENSG00000187790	FANCM PPI subnetwork	0.4
GO:0007435	salivary gland morphogenesis	0.4
ENSG00000065183	WDR3 PPI subnetwork	0.4
ENSG00000177600	RPLP2 PPI subnetwork	0.4
GO:0005242	inward rectifier potassium channel activity	0.4

Original gene set ID	Original gene set description	Nominal P value
ENSG00000204628	GNB2L1 PPI subnetwork	0.4
ENSG00000142156	COL6A1 PPI subnetwork	0.4
GO:0017022	myosin binding	0.4
ENSG00000141026	MED9 PPI subnetwork	0.4
GO:0016502	nucleotide receptor activity	0.4
GO:0001614	purinergic nucleotide receptor activity	0.4
ENSG00000117450	PRDX1 PPI subnetwork	0.4
MP:0002168	other aberrant phenotype	0.4
ENSG00000123358	NR4A1 PPI subnetwork	0.4
GO:0044247	cellular polysaccharide catabolic process	0.4
GO:0009251	glucan catabolic process	0.4
ENSG00000129282	MRM1 PPI subnetwork	0.4
ENSG00000196277	GRM7 PPI subnetwork	0.4
ENSG00000124762	CDKN1A PPI subnetwork	0.4
ENSG0000010671	BTK PPI subnetwork	0.4
ENSG00000159189	C1QC PPI subnetwork	0.4
GO:0030042	actin filament depolymerization	0.4
ENSG00000130312	MRPL34 PPI subnetwork	0.4
GO:0021799	cerebral cortex radially oriented cell migration	0.4
MP:0000531	right pulmonary isomerism	0.4
ENSG00000197283	SYNGAP1 PPI subnetwork	0.4
GO:0030496	midbody	0.4
ENSG00000140396	NCOA2 PPI subnetwork	0.4
GO:0017002	activin-activated receptor activity	0.4
MP:0002116	abnormal craniofacial bone morphology	0.4
GO:0002824	positive regulation of adaptive immune response based on somatic recombination c	0.4
GO:0032653	regulation of interleukin-10 production	0.4
MP:0001633	poor circulation	0.4
ENSG000000061676	NCKAP1 PPI subnetwork	0.4
ENSG00000100170	SLC5A1 PPI subnetwork	0.4
GO:0032401	establishment of melanosome localization	0.4
MP:0008586	disorganized photoreceptor outer segment	0.4
GO:0005099	Ras GTPase activator activity	0.4
ENSG00000162367	TAL1 PPI subnetwork	0.4
GO:0001540	beta-amyloid binding	0.4
GO:0032355	response to estradiol stimulus	0.4
MP:0003674	oxidative stress	0.4
ENSG00000118785	SPP1 PPI subnetwork	0.4
GO:0035254	glutamate receptor binding	0.4
GO:0006605	protein targeting	0.4
GO:0000795	synaptonemal complex	0.4
MP:0004617	sacral vertebral transformation	0.4
ENSG00000124635	HIST1H2BJ PPI subnetwork	0.4
ENSG00000067048	DDX3Y PPI subnetwork	0.4
ENSG00000152684	PELO PPI subnetwork	0.4
GO:0035383	thioester metabolic process	0.4
GO:0006637	acyl-CoA metabolic process	0.4
MP:0004837	abnormal neural fold formation	0.4
GO:0030057	desmosome	0.4

Original gene set ID	Original gene set description	Nominal P value
ENSG00000196470	SIAH1 PPI subnetwork	0.4
ENSG00000133961	NUMB PPI subnetwork	0.4
GO:0046873	metal ion transmembrane transporter activity	0.4
MP:0009888	palatal shelves fail to meet at midline	0.41
ENSG00000186951	PPARA PPI subnetwork	0.41
GO:0006509	membrane protein ectodomain proteolysis	0.41
ENSG00000114030	KPNA1 PPI subnetwork	0.41
ENSG00000184588	PDE4B PPI subnetwork	0.41
ENSG00000110330	BIRC2 PPI subnetwork	0.41
ENSG00000144891	AGTR1 PPI subnetwork	0.41
GO:0051216	cartilage development	0.41
ENSG00000101343	CRNKL1 PPI subnetwork	0.41
MP:0001861	lung inflammation	0.41
MP:0010766	abnormal NK cell physiology	0.41
MP:0009115	abnormal fat cell morphology	0.41
ENSG00000166128	RAB8B PPI subnetwork	0.41
ENSG00000149925	ALDOA PPI subnetwork	0.41
ENSG00000112249	ASCC3 PPI subnetwork	0.41
GO:0035267	NuA4 histone acetyltransferase complex	0.41
GO:0045745	positive regulation of G-protein coupled receptor protein signaling pathway	0.41
GO:0006476	protein deacetylation	0.41
ENSG00000111725	PRKAB1 PPI subnetwork	0.41
ENSG00000121031	ENSG00000121031 PPI subnetwork	0.41
ENSG00000204389	HSPA1A PPI subnetwork	0.41
ENSG00000204388	HSPA1B PPI subnetwork	0.41
ENSG00000212866	HSPA1B PPI subnetwork	0.41
ENSG00000215292	ENSG00000215292 PPI subnetwork	0.41
ENSG00000212860	ENSG00000212860 PPI subnetwork	0.41
GO:0048009	insulin-like growth factor receptor signaling pathway	0.41
REACTOME_BASIGIN_INTERACTIONS	REACTOME_BASIGIN_INTERACTIONS	0.41
GO:0005871	kinesin complex	0.41
MP:0006072	abnormal retinal apoptosis	0.41
ENSG00000131381	ZFYVE20 PPI subnetwork	0.41
ENSG00000102606	ARHGEF7 PPI subnetwork	0.41
MP:0004174	abnormal spine curvature	0.41
GO:0031231	intrinsic to peroxisomal membrane	0.41
GO:0005779	integral to peroxisomal membrane	0.41
GO:0008509	anion transmembrane transporter activity	0.41
GO:0003231	cardiac ventricle development	0.41
MP:0005282	decreased fatty acid level	0.41
ENSG00000134243	SORT1 PPI subnetwork	0.41
MP:0006410	abnormal common myeloid progenitor cell morphology	0.41
MP:0003886	abnormal embryonic epiblast morphology	0.41
GO:0000083	regulation of transcription involved in G1/S phase of mitotic cell cycle	0.41
MP:0004509	abnormal pelvic girdle bone morphology	0.41
ENSG00000131910	NROB2 PPI subnetwork	0.41
ENSG00000109971	HSPA8 PPI subnetwork	0.41
ENSG00000131236	CAP1 PPI subnetwork	0.41
REACTOME_AMINO_ACID_TRANSPORT_ACROSS_THE_PLASMA_MEMBRANE	REACTOME_AMINO_ACID_TRANSPORT_ACROSS_THE_PLASMA_MEMBRANE	0.41

Original gene set ID	Original gene set description	Nominal P value
MP:0005030	absent amnion	0.41
GO:0032098	regulation of appetite	0.41
ENSG000000183072	NKX2-5 PPI subnetwork	0.41
MP:0001469	abnormal contextual conditioning behavior	0.41
ENSG000000140285	FGF7 PPI subnetwork	0.41
GO:0005793	endoplasmic reticulum-Golgi intermediate compartment	0.41
ENSG000000196501	ENSG000000196501 PPI subnetwork	0.41
GO:0072376	protein activation cascade	0.41
GO:0032461	positive regulation of protein oligomerization	0.41
ENSG000000197597	ENSG000000197597 PPI subnetwork	0.41
MP:0004981	decreased neuronal precursor cell number	0.41
ENSG000000105229	PIAS4 PPI subnetwork	0.41
GO:0002756	MyD88-independent toll-like receptor signaling pathway	0.41
GO:0019867	outer membrane	0.41
GO:0043113	receptor clustering	0.41
MP:0000351	increased cell proliferation	0.41
GO:0050663	cytokine secretion	0.41
ENSG000000103351	CLUAP1 PPI subnetwork	0.41
ENSG000000113643	RARS PPI subnetwork	0.41
GO:0005768	endosome	0.41
GO:0019318	hexose metabolic process	0.41
MP:0008210	increased mature B cell number	0.41
GO:0071897	DNA biosynthetic process	0.41
GO:0016328	lateral plasma membrane	0.41
ENSG000000174197	MGA PPI subnetwork	0.41
ENSG000000170004	CHD3 PPI subnetwork	0.41
ENSG000000164045	CDC25A PPI subnetwork	0.41
ENSG000000206450	HLA-B PPI subnetwork	0.41
ENSG000000174227	PIGG PPI subnetwork	0.41
GO:0015758	glucose transport	0.41
GO:0008645	hexose transport	0.41
ENSG000000111640	GAPDH PPI subnetwork	0.41
ENSG000000154229	PRKCA PPI subnetwork	0.41
GO:0002761	regulation of myeloid leukocyte differentiation	0.41
ENSG000000072832	CRMP1 PPI subnetwork	0.41
MP:0002795	dilated cardiomyopathy	0.41
ENSG000000163466	ARPC2 PPI subnetwork	0.41
MP:0009746	enhanced behavioral response to xenobiotic	0.41
GO:0048771	tissue remodeling	0.41
ENSG000000135341	MAP3K7 PPI subnetwork	0.41
ENSG000000108094	CUL2 PPI subnetwork	0.41
GO:0009225	nucleotide-sugar metabolic process	0.41
ENSG000000198899	MT-ATP6 PPI subnetwork	0.41
ENSG000000070010	UFD1L PPI subnetwork	0.41
ENSG000000143878	RHOB PPI subnetwork	0.41
GO:0046930	pore complex	0.41
ENSG000000087111	PIGS PPI subnetwork	0.41
GO:0000082	G1/S transition of mitotic cell cycle	0.41
ENSG000000105401	CDC37 PPI subnetwork	0.41

Original gene set ID	Original gene set description	Nominal P value
ENSG00000117020	AKT3 PPI subnetwork	0.42
GO:0033344	cholesterol efflux	0.42
ENSG00000153006	SREK1IP1 PPI subnetwork	0.42
GO:0005774	vacuolar membrane	0.42
MP:0008617	increased circulating interleukin-12 level	0.42
ENSG00000156711	MAPK13 PPI subnetwork	0.42
MP:0003871	abnormal myelin sheath morphology	0.42
ENSG00000118965	WDR35 PPI subnetwork	0.42
GO:0005104	fibroblast growth factor receptor binding	0.42
MP:0001940	testis hypoplasia	0.42
ENSG00000138468	SENP7 PPI subnetwork	0.42
ENSG00000118640	VAMP8 PPI subnetwork	0.42
ENSG00000105663	ENSG00000105663 PPI subnetwork	0.42
MP:0000292	distended pericardium	0.42
MP:0001790	abnormal immune system physiology	0.42
MP:0001554	increased circulating free fatty acid leve	0.42
GO:0030099	myeloid cell differentiation	0.42
MP:0003633	abnormal nervous system physiology	0.42
GO:0016053	organic acid biosynthetic process	0.42
GO:0046394	carboxylic acid biosynthetic process	0.42
MP:0004696	abnormal thyroid follicle morphology	0.42
ENSG00000100353	EIF3D PPI subnetwork	0.42
GO:0051153	regulation of striated muscle cell differentiator	0.42
ENSG00000196611	MMP1 PPI subnetwork	0.42
ENSG00000213024	NUP62 PPI subnetwork	0.42
ENSG00000118007	STAG1 PPI subnetwork	0.42
ENSG00000106554	CHCHD3 PPI subnetwork	0.42
ENSG00000080608	KIAA0020 PPI subnetwork	0.42
GO:0031110	regulation of microtubule polymerization or depolymerizati	0.42
GO:0035384	thioester biosynthetic process	0.42
GO:0071616	acyl-CoA biosynthetic process	0.42
REACTOME_IRS:RELATED_EVENTS	REACTOME_IRS:RELATED_EVENTS	0.42
REACTOME_IRS:MEDIATED_SIGNALLING	REACTOME_IRS:MEDIATED_SIGNALLING	0.42
GO:0042559	pteridine-containing compound biosynthetic process	0.42
REACTOME_METABOLISM_OF_RNA	REACTOME_METABOLISM_OF_RNA	0.42
GO:0005529	GO:0005529	0.42
ENSG00000089902	RCOR1 PPI subnetwork	0.42
MP:0009404	centrally nucleated skeletal muscle fibers	0.42
REACTOME_ASSOCIATION_OF_TRICCCT_WITH_TARGET_PROTEINS_DURING_BI	REACTOME_ASSOCIATION_OF_TRICCCT_WITH_TARGET_PROTEINS_DURING_BIOSY	0.42
ENSG00000146587	RBAK PPI subnetwork	0.42
ENSG00000081248	CACNA1S PPI subnetwork	0.42
ENSG00000007402	CACNA2D2 PPI subnetwork	0.42
MP:0000822	abnormal brain ventricle morphology	0.42
GO:0045776	negative regulation of blood pressure	0.42
GO:0009266	response to temperature stimulus	0.42
GO:0006940	regulation of smooth muscle contraction	0.42
GO:0031111	negative regulation of microtubule polymerization or depolymerizati	0.42
MP:0002118	abnormal lipid homeostasis	0.42
ENSG00000177565	TBL1XR1 PPI subnetwork	0.42

Original gene set ID	Original gene set description	Nominal P value
MP:0000157	abnormal sternum morphology	0.43
ENSG00000173473	SMARCC1 PPI subnetwork	0.43
MP:0000837	abnormal hypothalamus morphology	0.43
MP:0011094	complete embryonic lethality before implantation	0.43
MP:0001614	abnormal blood vessel morphology	0.43
ENSG00000117385	LEPRE1 PPI subnetwork	0.43
MP:0003725	increased autoantibody level	0.43
ENSG00000109320	NFKB1 PPI subnetwork	0.43
GO:0002407	dendritic cell chemotaxis	0.43
ENSG00000105220	GPI PPI subnetwork	0.43
MP:0010872	increased trabecular bone mass	0.43
MP:0008682	decreased interleukin-17 secretion	0.43
MP:0005606	increased bleeding time	0.43
GO:0045839	negative regulation of mitosis	0.43
GO:0051784	negative regulation of nuclear division	0.43
MP:0000136	abnormal microglial cell morphology	0.43
GO:2000311	regulation of alpha-amino-3-hydroxy-5-methyl-4-isoxazole propionate selective glutamate transporter activity	0.43
MP:0001312	abnormal cornea morphology	0.43
ENSG00000113312	TTC1 PPI subnetwork	0.43
GO:0034329	cell junction assembly	0.43
GO:0070307	lens fiber cell development	0.43
ENSG00000099331	MYO9B PPI subnetwork	0.43
GO:0060076	excitatory synapse	0.43
ENSG00000181929	PRKAG1 PPI subnetwork	0.43
ENSG00000197961	ZNF121 PPI subnetwork	0.43
ENSG00000137876	RSL24D1 PPI subnetwork	0.43
GO:0016782	transferase activity, transferring sulfur-containing groups	0.43
MP:0002631	abnormal epididymis morphology	0.43
GO:0046006	regulation of activated T cell proliferation	0.43
MP:0004076	abnormal vitelline vascular remodeling	0.43
MP:0001800	abnormal humoral immune response	0.43
ENSG00000182367	ENSG00000182367 PPI subnetwork	0.43
MP:0003048	abnormal cervical vertebrae morphology	0.43
ENSG00000143498	TAF1A PPI subnetwork	0.43
MP:0000685	abnormal immune system morphology	0.43
MP:0005011	increased eosinophil cell number	0.43
GO:0009152	purine ribonucleotide biosynthetic process	0.43
GO:0007264	small GTPase mediated signal transduction	0.43
REACTOME_RNA_POLYMERASE_I_TRANSCRIPTION_TERMINATION	REACTOME_RNA_POLYMERASE_I_TRANSCRIPTION_TERMINATION	0.43
ENSG00000134255	CEPT1 PPI subnetwork	0.43
ENSG00000197616	MYH6 PPI subnetwork	0.43
ENSG00000139613	SMARCC2 PPI subnetwork	0.43
GO:0045028	G-protein coupled purinergic nucleotide receptor activity	0.43
GO:0001608	G-protein coupled nucleotide receptor activity	0.43
ENSG00000186153	WVVOX PPI subnetwork	0.43
ENSG00000155111	CDK19 PPI subnetwork	0.43
ENSG00000163635	ATXN7 PPI subnetwork	0.43
ENSG00000154767	XPC PPI subnetwork	0.43
MP:0010019	liver vascular congestion	0.43

Original gene set ID	Original gene set description	Nominal P value
GO:0050673	epithelial cell proliferation	0.43
MP:0002574	increased vertical activity	0.43
MP:0005421	loose skin	0.43
GO:0048638	regulation of developmental growth	0.43
GO:0009116	nucleoside metabolic process	0.43
GO:0032970	regulation of actin filament-based process	0.43
ENSG00000154764	WNT7A PPI subnetwork	0.43
ENSG00000105855	ITGB8 PPI subnetwork	0.43
ENSG00000070423	RNF126 PPI subnetwork	0.43
ENSG00000124588	NQO2 PPI subnetwork	0.43
GO:0005161	platelet-derived growth factor receptor binding	0.44
ENSG00000076604	TRAF4 PPI subnetwork	0.44
MP:0003718	maternal effect	0.44
ENSG00000065485	PDIA5 PPI subnetwork	0.44
ENSG00000065135	GNAI3 PPI subnetwork	0.44
ENSG00000100227	POLDIP3 PPI subnetwork	0.44
MP:0005353	abnormal patella morphology	0.44
MP:0008501	increased IgG2b level	0.44
MP:0004029	spontaneous chromosome breakage	0.44
GO:0032613	interleukin-10 production	0.44
MP:0000182	increased circulating LDL cholesterol level	0.44
MP:0004783	abnormal cardinal vein morphology	0.44
GO:0001518	voltage-gated sodium channel complex	0.44
ENSG00000165030	NFIL3 PPI subnetwork	0.44
KEGG_P53_SIGNALING_PATHWAY	KEGG_P53_SIGNALING_PATHWAY	0.44
MP:0005463	abnormal CD4-positive T cell physiology	0.44
GO:0048738	cardiac muscle tissue development	0.44
GO:0032869	cellular response to insulin stimulus	0.44
ENSG00000105695	MAG PPI subnetwork	0.44
GO:0048246	macrophage chemotaxis	0.44
GO:0040008	regulation of growth	0.44
ENSG00000171346	KRT15 PPI subnetwork	0.44
GO:0000070	mitotic sister chromatid segregation	0.44
GO:0042129	regulation of T cell proliferation	0.44
MP:0008593	increased circulating interleukin-10 level	0.44
GO:0002478	antigen processing and presentation of exogenous peptide antigen	0.44
ENSG00000204642	HLA-F PPI subnetwork	0.44
MP:0000030	abnormal tympanic ring morphology	0.44
ENSG00000104312	RIPK2 PPI subnetwork	0.44
ENSG00000035928	RFC1 PPI subnetwork	0.44
KEGG_GLYCOLYSIS_GLUCONEOGENESIS	KEGG_GLYCOLYSIS_GLUCONEOGENESIS	0.44
ENSG00000132432	SEC61G PPI subnetwork	0.44
GO:0043484	regulation of RNA splicing	0.44
ENSG00000002745	WNT16 PPI subnetwork	0.44
MP:0006043	decreased apoptosis	0.44
ENSG00000144580	RQCD1 PPI subnetwork	0.44
ENSG00000116251	RPL22 PPI subnetwork	0.44
MP:0003131	increased erythrocyte cell number	0.44
MP:0004703	abnormal vertebral column morphology	0.44

Original gene set ID	Original gene set description	Nominal P value
GO:0044283	small molecule biosynthetic process	0.44
GO:0003281	ventricular septum development	0.44
GO:0016407	acetyltransferase activity	0.44
MP:0004154	renal tubular necrosis	0.44
MP:0008522	abnormal lymph node germinal center morphology	0.44
ENSG000000093009	CDC45 PPI subnetwork	0.44
ENSG00000105963	ADAP1 PPI subnetwork	0.44
GO:0000096	sulfur amino acid metabolic process	0.44
GO:0046578	regulation of Ras protein signal transduction	0.44
GO:0005184	neuropeptide hormone activity	0.44
GO:0005086	ARF guanyl-nucleotide exchange factor activity	0.44
ENSG00000100297	MCM5 PPI subnetwork	0.44
GO:0000079	regulation of cyclin-dependent protein kinase activity	0.44
ENSG00000089234	BRAP PPI subnetwork	0.44
GO:0046660	female sex differentiation	0.44
REACTOME_VOLTAGE_GATED_POTASSIUM_CHANNELS	REACTOME_VOLTAGE_GATED_POTASSIUM_CHANNELS	0.44
GO:0007613	memory	0.44
GO:0042531	positive regulation of tyrosine phosphorylation of STAT proteir	0.44
ENSG00000158042	MRPL17 PPI subnetwork	0.44
GO:0050954	sensory perception of mechanical stimulus	0.44
MP:0004272	abnormal basement membrane morphology	0.44
GO:0005775	vacuolar lumen	0.44
GO:0008063	Toll signaling pathway	0.44
ENSG000000066379	ZNRD1 PPI subnetwork	0.44
ENSG00000206502	ZNRD1 PPI subnetwork	0.44
ENSG00000206429	ENSG00000206429 PPI subnetwork	0.44
ENSG00000106571	GLI3 PPI subnetwork	0.44
MP:0003179	decreased platelet cell number	0.44
REACTOME_NOD12_SIGNALING_PATHWAY	REACTOME_NOD12_SIGNALING_PATHWAY	0.44
ENSG000000096433	ITPR3 PPI subnetwork	0.44
MP:0001353	increased aggression towards mice	0.44
MP:0002736	abnormal nociception after inflammation	0.44
GO:0043383	negative T cell selection	0.44
ENSG000000050748	MAPK9 PPI subnetwork	0.44
ENSG00000126562	WNK4 PPI subnetwork	0.44
ENSG00000205572	SERF1B PPI subnetwork	0.44
ENSG00000172058	SERF1A PPI subnetwork	0.44
GO:0044437	vacuolar part	0.44
GO:0007183	SMAD protein complex assembly	0.44
GO:0035270	endocrine system development	0.44
KEGG_LYSOSOME	KEGG_LYSOSOME	0.44
GO:0004857	enzyme inhibitor activity	0.44
GO:0022616	DNA strand elongation	0.44
ENSG00000133103	COG6 PPI subnetwork	0.44
GO:0046460	neutral lipid biosynthetic process	0.44
GO:0046463	acylglycerol biosynthetic process	0.44
GO:2000242	negative regulation of reproductive process	0.44
GO:0030029	actin filament-based process	0.44
GO:0070888	E-box binding	0.44

Original gene set ID	Original gene set description	Nominal P value
KEGG_GLIOMA	KEGG_GLIOMA	0.44
GO:0048471	perinuclear region of cytoplasm	0.44
GO:0051494	negative regulation of cytoskeleton organization	0.44
GO:0070925	organelle assembly	0.44
ENSG00000137218	FRS3 PPI subnetwork	0.44
GO:0017069	snRNA binding	0.44
MP:0000688	lymphoid hyperplasia	0.44
ENSG00000171634	BPTF PPI subnetwork	0.44
GO:0017015	regulation of transforming growth factor beta receptor signaling pathway	0.44
GO:0004714	transmembrane receptor protein tyrosine kinase activity	0.44
ENSG00000120889	TNFRSF10B PPI subnetwork	0.44
ENSG00000196975	ANXA4 PPI subnetwork	0.44
ENSG00000121858	TNFSF10 PPI subnetwork	0.44
GO:0002449	lymphocyte mediated immunity	0.44
GO:0005212	structural constituent of eye lens	0.44
GO:0048745	smooth muscle tissue development	0.44
GO:0022613	ribonucleoprotein complex biogenesis	0.44
MP:0010373	myeloid hyperplasia	0.44
MP:0000036	absent semicircular canals	0.44
ENSG00000132485	ZRANB2 PPI subnetwork	0.44
ENSG00000106123	EPHB6 PPI subnetwork	0.44
GO:0042254	ribosome biogenesis	0.44
MP:0005102	abnormal iris pigmentation	0.44
ENSG00000206156	ENSG00000206156 PPI subnetwork	0.44
ENSG00000105372	RPS19 PPI subnetwork	0.44
MP:0005140	decreased cardiac muscle contractility	0.44
ENSG00000081019	RSBN1 PPI subnetwork	0.44
ENSG00000101439	CST3 PPI subnetwork	0.44
MP:0008186	increased pro-B cell number	0.44
GO:0032400	melanosome localization	0.44
ENSG00000154143	PANX3 PPI subnetwork	0.44
GO:0046902	regulation of mitochondrial membrane permeability	0.44
GO:0000159	protein phosphatase type 2A complex	0.44
MP:0005154	increased B cell proliferation	0.44
GO:0016705	oxidoreductase activity, acting on paired donors, with incorporation or reduction of	0.44
MP:0001384	abnormal pup retrieval	0.44
GO:0014047	glutamate secretion	0.44
MP:0001939	secondary sex reversal	0.44
GO:0016641	oxidoreductase activity, acting on the CH-NH2 group of donors, oxygen as acceptor	0.45
MP:0001273	decreased metastatic potential	0.45
ENSG00000071655	MBD3 PPI subnetwork	0.45
ENSG00000136854	STXBP1 PPI subnetwork	0.45
ENSG00000172071	EIF2AK3 PPI subnetwork	0.45
ENSG00000160563	MED27 PPI subnetwork	0.45
ENSG00000080802	CNOT4 PPI subnetwork	0.45
ENSG00000078018	MAP2 PPI subnetwork	0.45
GO:0007005	mitochondrion organization	0.45
ENSG00000100726	TELO2 PPI subnetwork	0.45
ENSG00000182541	LIMK2 PPI subnetwork	0.45

Original gene set ID	Original gene set description	Nominal P value
GO:0070412	R-SMAD binding	0.45
ENSG00000188739	RBM34 PPI subnetwork	0.45
GO:0035176	social behavior	0.45
ENSG00000144597	EAF1 PPI subnetwork	0.45
GO:0042987	amyloid precursor protein catabolic process	0.45
ENSG00000196226	HIST1H2BB PPI subnetwork	0.45
ENSG00000150907	FOXO1 PPI subnetwork	0.45
ENSG00000147536	GIN54 PPI subnetwork	0.45
REACTOME_ANTIGEN_PRESENTATION_FOLDING_ASSEMBLY_AND_PEPTIDE_LOADII	REACTOME_ANTIGEN_PRESENTATION_FOLDING_ASSEMBLY_AND_PEPTIDE_LOADII	0.45
ENSG00000117335	CD46 PPI subnetwork	0.45
ENSG00000135018	UBQLN1 PPI subnetwork	0.45
GO:0032956	regulation of actin cytoskeleton organization	0.45
MP:0001634	internal hemorrhage	0.45
ENSG00000124813	RUNX2 PPI subnetwork	0.45
GO:0043025	neuronal cell body	0.45
ENSG00000104332	SFRP1 PPI subnetwork	0.45
ENSG00000120057	SFRP5 PPI subnetwork	0.45
ENSG00000106483	SFRP4 PPI subnetwork	0.45
REACTOME_PHOSPHOLIPASE_C:MEDIATED_CASCADE	REACTOME_PHOSPHOLIPASE_C:MEDIATED_CASCADE	0.45
MP:0003360	abnormal depression-related behavior	0.45
GO:0060363	cranial suture morphogenesis	0.45
GO:0097094	craniofacial suture morphogenesis	0.45
GO:0043367	CD4-positive, alpha-beta T cell differentiation	0.45
GO:0000982	RNA polymerase II core promoter proximal region sequence-specific DNA binding tr	0.45
MP:0001719	absent vitelline blood vessels	0.45
GO:0016725	oxidoreductase activity, acting on CH or CH2 groups	0.45
ENSG00000145555	MYO10 PPI subnetwork	0.45
KEGG_ONE_CARBON_POOL_BY_FOLATE	KEGG_ONE_CARBON_POOL_BY_FOLATE	0.45
MP:0005410	abnormal fertilization	0.45
GO:0016746	transferase activity, transferring acyl groups	0.45
ENSG00000178982	EIF3K PPI subnetwork	0.45
GO:0016311	dephosphorylation	0.45
GO:0046112	nucleobase biosynthetic process	0.45
ENSG00000153187	HNRNPU PPI subnetwork	0.45
ENSG00000014138	POLA2 PPI subnetwork	0.45
ENSG00000112739	PRPF4B PPI subnetwork	0.45
ENSG00000132849	INADL PPI subnetwork	0.45
MP:0008560	increased tumor necrosis factor secretion	0.45
ENSG00000068976	PYGM PPI subnetwork	0.45
MP:0002928	abnormal bile duct morphology	0.45
GO:0031253	cell projection membrane	0.45
GO:0007163	establishment or maintenance of cell polarity	0.45
ENSG00000117528	ABCD3 PPI subnetwork	0.45
MP:0000603	pale liver	0.45
MP:0003944	abnormal T cell subpopulation ratio	0.45
MP:0002458	abnormal B cell number	0.45
ENSG00000214026	MRPL23 PPI subnetwork	0.45
ENSG00000156603	MED19 PPI subnetwork	0.45
GO:0007605	sensory perception of sound	0.45

Original gene set ID	Original gene set description	Nominal P value
ENSG00000178105	DDX10 PPI subnetwork	0.45
ENSG00000156931	VPS8 PPI subnetwork	0.45
ENSG00000141985	SH3GL1 PPI subnetwork	0.45
ENSG00000108819	ENSG00000108819 PPI subnetwork	0.45
GO:0070306	lens fiber cell differentiation	0.45
ENSG00000102144	PGK1 PPI subnetwork	0.45
GO:0006958	complement activation, classical pathway	0.45
REACTOME_LOSS_OF_PROTEINS_REQUIRED_FOR_INTERPHASE_MICROTUBULE	REACTOME_LOSS_OF_PROTEINS_REQUIRED_FOR_INTERPHASE_MICROTUBULE_OR	0.45
REACTOME_LOSS_OF_NLP_FROM_MITOTIC_CENTROSOMES	REACTOME_LOSS_OF_NLP_FROM_MITOTIC_CENTROSOMES	0.45
GO:0032663	regulation of interleukin-2 production	0.45
GO:0035258	steroid hormone receptor binding	0.45
GO:0030178	negative regulation of Wnt receptor signaling pathway	0.45
ENSG00000166710	B2M PPI subnetwork	0.45
GO:0042058	regulation of epidermal growth factor receptor signaling pathway	0.45
GO:0031968	organelle outer membrane	0.45
ENSG00000071051	NCK2 PPI subnetwork	0.45
ENSG00000163516	ANKZF1 PPI subnetwork	0.45
REACTOME_GAP_JUNCTION_TRAFFICKING	REACTOME_GAP_JUNCTION_TRAFFICKING	0.45
ENSG00000136044	APPL2 PPI subnetwork	0.45
ENSG00000125868	DSTN PPI subnetwork	0.45
ENSG00000095564	BTAF1 PPI subnetwork	0.45
ENSG00000196890	HIST3H2BB PPI subnetwork	0.45
GO:0000793	condensed chromosome	0.45
ENSG00000101442	ACTR5 PPI subnetwork	0.45
MP:0000753	paralysis	0.45
MP:0006020	decreased tympanic ring size	0.45
GO:0006760	folic acid-containing compound metabolic process	0.45
ENSG00000165632	TAF3 PPI subnetwork	0.45
GO:0048844	artery morphogenesis	0.45
ENSG00000128739	SNRPN PPI subnetwork	0.45
GO:0006664	glycolipid metabolic process	0.45
GO:0043209	myelin sheath	0.45
ENSG00000087191	PSMC5 PPI subnetwork	0.45
ENSG00000175536	LIPT2 PPI subnetwork	0.45
GO:0014704	intercalated disc	0.45
ENSG00000106682	EIF4H PPI subnetwork	0.45
GO:0002889	regulation of immunoglobulin mediated immune response	0.45
GO:0042104	positive regulation of activated T cell proliferator	0.45
ENSG00000148377	ID12 PPI subnetwork	0.45
GO:0043094	cellular metabolic compound salvage	0.45
ENSG00000196220	SRGAP3 PPI subnetwork	0.45
MP:0008518	retinal outer nuclear layer degeneration	0.45
ENSG00000116957	TBCE PPI subnetwork	0.45
MP:0000163	abnormal cartilage morphology	0.45
ENSG00000184009	ACTG1 PPI subnetwork	0.45
ENSG00000169032	MAP2K1 PPI subnetwork	0.45
GO:0008156	negative regulation of DNA replication	0.45
GO:0044433	cytoplasmic vesicle part	0.45
MP:0006058	decreased cerebral infarction size	0.45

Original gene set ID	Original gene set description	Nominal P value
ENSG00000172053	QARS PPI subnetwork	0.45
GO:0000959	mitochondrial RNA metabolic process	0.45
GO:0045598	regulation of fat cell differentiation	0.45
MP:0008474	absent spleen germinal center	0.45
MP:0008143	abnormal dendrite morphology	0.45
ENSG00000100784	RPS6KA5 PPI subnetwork	0.45
ENSG00000126005	ENSG00000126005 PPI subnetwork	0.45
ENSG00000069974	RAB27A PPI subnetwork	0.45
ENSG00000111669	TPI1 PPI subnetwork	0.45
KEGG_AMYOTROPHIC_LATERAL_SCLEROSIS_ALS	KEGG_AMYOTROPHIC_LATERAL_SCLEROSIS_ALS	0.45
MP:0009887	abnormal palatal shelf fusion at midline	0.45
GO:0001669	acrosomal vesicle	0.45
ENSG00000134460	IL2RA PPI subnetwork	0.45
ENSG00000166033	HTRA1 PPI subnetwork	0.45
REACTOME_CHROMOSOME_MAINTENANCE	REACTOME_CHROMOSOME_MAINTENANCE	0.46
ENSG00000099250	NRP1 PPI subnetwork	0.46
MP:0000926	absent floor plate	0.46
ENSG00000182866	LCK PPI subnetwork	0.46
ENSG00000155380	SLC16A1 PPI subnetwork	0.46
GO:0048524	positive regulation of viral reproduction	0.46
ENSG00000168066	SF1 PPI subnetwork	0.46
ENSG00000076864	RAP1GAP PPI subnetwork	0.46
MP:0001718	abnormal visceral yolk sac morphology	0.46
GO:0006363	termination of RNA polymerase I transcription	0.46
ENSG00000198612	COPS8 PPI subnetwork	0.46
MP:0001303	abnormal lens morphology	0.46
GO:0004497	monooxygenase activity	0.46
ENSG00000125484	GTF3C4 PPI subnetwork	0.46
ENSG00000197971	MBP PPI subnetwork	0.46
GO:0004519	endonuclease activity	0.46
ENSG00000105176	URI1 PPI subnetwork	0.46
GO:0004722	protein serine/threonine phosphatase activity	0.46
ENSG00000128833	MYO5C PPI subnetwork	0.46
GO:0005819	spindle	0.46
ENSG00000196540	ENSG00000196540 PPI subnetwork	0.46
GO:0017127	cholesterol transporter activity	0.46
GO:0035710	CD4-positive, alpha-beta T cell activation	0.46
GO:0042542	response to hydrogen peroxide	0.46
MP:0005438	abnormal glycogen homeostasis	0.46
ENSG00000150768	DLAT PPI subnetwork	0.46
GO:0002221	pattern recognition receptor signaling pathway	0.46
GO:0050911	detection of chemical stimulus involved in sensory perception of smell	0.46
GO:0070461	SAGA-type complex	0.46
GO:0034399	nuclear periphery	0.46
ENSG00000179071	CCDC89 PPI subnetwork	0.46
MP:0000746	weakness	0.46
ENSG00000135999	EPC2 PPI subnetwork	0.46
KEGG_PROSTATE_CANCER	KEGG_PROSTATE_CANCER	0.46
MP:0002576	abnormal enamel morphology	0.46

Original gene set ID	Original gene set description	Nominal P value
ENSG00000162735	PEX19 PPI subnetwork	0.46
ENSG00000009335	UBE3C PPI subnetwork	0.46
MP:0001675	abnormal ectoderm development	0.46
ENSG00000113558	SKP1 PPI subnetwork	0.46
ENSG00000042980	ADAM28 PPI subnetwork	0.46
MP:0001870	salivary gland inflammation	0.46
ENSG00000167461	RAB8A PPI subnetwork	0.46
ENSG00000163599	CTLA4 PPI subnetwork	0.46
GO:0060420	regulation of heart growth	0.46
MP:0002546	mydriasis	0.46
MP:0002495	increased IgA level	0.46
ENSG00000104613	INTS10 PPI subnetwork	0.46
MP:0000135	decreased compact bone thickness	0.46
ENSG00000132109	TRIM21 PPI subnetwork	0.46
GO:0034130	toll-like receptor 1 signaling pathway	0.46
ENSG00000099860	GADD45B PPI subnetwork	0.46
GO:0005769	early endosome	0.46
MP:0002184	abnormal innervation	0.46
GO:0070588	calcium ion transmembrane transport	0.46
MP:0003215	renal interstitial fibrosis	0.46
ENSG00000105048	TNNT1 PPI subnetwork	0.46
MP:0008828	abnormal lymph node cell ratio	0.46
GO:0051084	'de novo' posttranslational protein folding	0.46
GO:0008250	oligosaccharyltransferase complex	0.46
GO:0006271	DNA strand elongation involved in DNA replication	0.46
MP:0002884	abnormal branchial arch morphology	0.46
ENSG00000083520	DIS3 PPI subnetwork	0.46
ENSG00000164061	BSN PPI subnetwork	0.46
MP:0002080	prenatal lethality	0.46
MP:0000886	abnormal cerebellar granule layer	0.46
ENSG00000009790	TRAF3IP3 PPI subnetwork	0.46
ENSG00000211799	ENSG00000211799 PPI subnetwork	0.46
ENSG00000211810	ENSG00000211810 PPI subnetwork	0.46
ENSG00000211739	ENSG00000211739 PPI subnetwork	0.46
ENSG00000211735	ENSG00000211735 PPI subnetwork	0.46
GO:0043407	negative regulation of MAP kinase activity	0.46
GO:0045815	positive regulation of gene expression, epigenetic	0.46
ENSG00000175104	TRAF6 PPI subnetwork	0.46
ENSG00000139505	MTMR6 PPI subnetwork	0.46
ENSG00000133313	CNDP2 PPI subnetwork	0.46
REACTOME_INTERFERON_GAMMA_SIGNALING	REACTOME_INTERFERON_GAMMA_SIGNALING	0.46
GO:0046887	positive regulation of hormone secretion	0.46
KEGG_STEROID_HORMONE_BIOSYNTHESIS	KEGG_STEROID_HORMONE_BIOSYNTHESIS	0.46
GO:0050707	regulation of cytokine secretion	0.46
ENSG00000148053	NTRK2 PPI subnetwork	0.46
GO:0031109	microtubule polymerization or depolymerization	0.46
MP:0002421	abnormal cell-mediated immunity	0.46
MP:0004448	abnormal presphenoid bone morphology	0.46
MP:0002641	anisopoikilocytosis	0.46

Original gene set ID	Original gene set description	Nominal P value
GO:0051092	positive regulation of NF-kappaB transcription factor activity	0.46
GO:0015697	quaternary ammonium group transport	0.46
REACTOME_TETRAHYDROBIOPTERIN_BH4_SYNTHESIS_RECYCLING_SALVAGE_A	REACTOME_TETRAHYDROBIOPTERIN_BH4_SYNTHESIS_RECYCLING_SALVAGE_AND_	0.46
MP:0000065	abnormal bone marrow cavity morphology	0.46
GO:0002286	T cell activation involved in immune response	0.46
MP:0002672	abnormal branchial arch artery morphology	0.46
MP:0003990	decreased neurotransmitter release	0.46
GO:0019637	organophosphate metabolic process	0.46
REACTOME_NEUROTRANSMITTER_RELEASE_CYCLE	REACTOME_NEUROTRANSMITTER_RELEASE_CYCLE	0.46
GO:0008047	enzyme activator activity	0.46
REACTOME_FGFR2C_LIGAND_BINDING_AND_ACTIVATION	REACTOME_FGFR2C_LIGAND_BINDING_AND_ACTIVATION	0.46
GO:0003206	cardiac chamber morphogenesis	0.46
MP:0002275	abnormal type II pneumocyte morphology	0.46
ENSG00000196419	XRCC6 PPI subnetwork	0.46
MP:0008217	abnormal B cell activation	0.46
GO:0006096	glycolysis	0.46
GO:0005916	fascia adherens	0.46
GO:0005248	voltage-gated sodium channel activity	0.46
KEGG_LONG_TERM_DEPRESSION	KEGG_LONG_TERM_DEPRESSION	0.46
MP:0004418	small parietal bone	0.46
ENSG00000187079	TEAD1 PPI subnetwork	0.46
ENSG00000165156	ZHX1 PPI subnetwork	0.46
ENSG00000131788	PIAS3 PPI subnetwork	0.46
ENSG00000155229	MMS19 PPI subnetwork	0.46
GO:0060411	cardiac septum morphogenesis	0.46
GO:0000819	sister chromatid segregation	0.46
GO:0060412	ventricular septum morphogenesis	0.46
GO:0050909	sensory perception of taste	0.46
GO:0043584	nose development	0.46
GO:0006026	aminoglycan catabolic process	0.46
ENSG00000145692	BHMT PPI subnetwork	0.46
GO:0048665	neuron fate specification	0.46
GO:0031519	PcG protein complex	0.46
ENSG00000125249	RAP2A PPI subnetwork	0.46
GO:0048610	cellular process involved in reproduction	0.46
ENSG00000039319	ZFYVE16 PPI subnetwork	0.46
ENSG00000124207	CSE1L PPI subnetwork	0.46
ENSG00000147010	SH3KBP1 PPI subnetwork	0.46
ENSG00000143867	OSR1 PPI subnetwork	0.46
ENSG00000141447	OSBPL1A PPI subnetwork	0.46
ENSG00000154310	TNIK PPI subnetwork	0.46
GO:0060444	branching involved in mammary gland duct morphogenesis	0.46
ENSG00000180855	ZNF443 PPI subnetwork	0.46
ENSG00000077549	CAPZB PPI subnetwork	0.46
GO:0015108	chloride transmembrane transporter activity	0.46
MP:0011088	partial neonatal lethality	0.46
MP:0002702	decreased circulating free fatty acid leve	0.46
ENSG00000174307	PHLDA3 PPI subnetwork	0.47
ENSG00000130758	MAP3K10 PPI subnetwork	0.47

Original gene set ID	Original gene set description	Nominal P value
ENSG00000110799	VWF PPI subnetwork	0.47
REACTOME_PURINE_METABOLISM	REACTOME_PURINE_METABOLISM	0.47
ENSG00000126458	RRAS PPI subnetwork	0.47
MP:0001529	abnormal vocalization	0.47
MP:0000599	enlarged liver	0.47
MP:0003560	osteoarthritis	0.47
ENSG00000145817	YIPF5 PPI subnetwork	0.47
GO:0001502	cartilage condensation	0.47
ENSG00000164708	PGAM2 PPI subnetwork	0.47
ENSG00000089154	GCN1L1 PPI subnetwork	0.47
GO:0042059	negative regulation of epidermal growth factor receptor signaling pathway	0.47
ENSG00000105447	GRWD1 PPI subnetwork	0.47
MP:0001364	decreased anxiety-related response	0.47
REACTOME_RNA_POLYMERASE_III_TRANSCRIPTION_INITIATION_FROM_TYPE_1_P	REACTOME_RNA_POLYMERASE_III_TRANSCRIPTION_INITIATION_FROM_TYPE_1_P	0.47
ENSG00000183520	UTP11L PPI subnetwork	0.47
REACTOME_FGFR4_LIGAND_BINDING_AND_ACTIVATION	REACTOME_FGFR4_LIGAND_BINDING_AND_ACTIVATION	0.47
ENSG00000130561	SAG PPI subnetwork	0.47
ENSG00000173011	TADA2B PPI subnetwork	0.47
ENSG00000197892	KIF13B PPI subnetwork	0.47
ENSG00000198851	CD3E PPI subnetwork	0.47
ENSG00000135547	HEY2 PPI subnetwork	0.47
MP:0008212	absent mature B cells	0.47
GO:0015837	amine transport	0.47
GO:0006749	glutathione metabolic process	0.47
ENSG00000150455	TIRAP PPI subnetwork	0.47
ENSG00000183117	CSMD1 PPI subnetwork	0.47
ENSG00000069275	NUCKS1 PPI subnetwork	0.47
ENSG00000108515	ENO3 PPI subnetwork	0.47
GO:0060840	artery development	0.47
ENSG00000178028	DMAP1 PPI subnetwork	0.47
ENSG00000163602	RYBP PPI subnetwork	0.47
ENSG00000125991	ERGIC3 PPI subnetwork	0.47
ENSG00000144029	MRPS5 PPI subnetwork	0.47
REACTOME_FRS2:MEDIATED_ACTIVATION	REACTOME_FRS2:MEDIATED_ACTIVATION	0.47
MP:0000067	osteopetrosis	0.47
ENSG00000040199	PHLPP2 PPI subnetwork	0.47
ENSG00000135338	LCA5 PPI subnetwork	0.47
ENSG00000144566	RAB5A PPI subnetwork	0.47
KEGG_PATHOGENIC_ESCHERICHIA_COLI_INFECTION	KEGG_PATHOGENIC_ESCHERICHIA_COLI_INFECTION	0.47
ENSG00000072210	ALDH3A2 PPI subnetwork	0.47
GO:0032365	intracellular lipid transport	0.47
MP:0004024	aneuploidy	0.47
REACTOME_HORMONE:SENSITIVE_LIPASE_HSL:MEDIATED_TRIACYLGLYCEROL_HYD	REACTOME_HORMONE:SENSITIVE_LIPASE_HSL:MEDIATED_TRIACYLGLYCEROL_HYD	0.47
KEGG_SPHINGOLIPID_METABOLISM	KEGG_SPHINGOLIPID_METABOLISM	0.47
ENSG00000214265	SNURF PPI subnetwork	0.47
GO:0032269	negative regulation of cellular protein metabolic process	0.47
ENSG00000007237	GAS7 PPI subnetwork	0.47
MP:0002643	poikilocytosis	0.47
GO:0001783	B cell apoptotic process	0.47

Original gene set ID	Original gene set description	Nominal P value
ENSG00000073111	MCM2 PPI subnetwork	0.47
ENSG00000181191	PJA1 PPI subnetwork	0.47
ENSG00000169251	NMD3 PPI subnetwork	0.47
GO:0030259	lipid glycosylation	0.47
ENSG00000117000	RLF PPI subnetwork	0.47
ENSG00000204227	RING1 PPI subnetwork	0.47
ENSG00000206287	RING1 PPI subnetwork	0.47
ENSG00000206215	ENSG00000206215 PPI subnetwork	0.47
GO:0048017	inositol lipid-mediated signaling	0.47
GO:0048015	phosphatidylinositol-mediated signaling	0.47
GO:2000104	negative regulation of DNA-dependent DNA replication	0.47
REACTOME_NUCLEOTIDE:LIKE_PURINERGIC_RECEPTORS	REACTOME_NUCLEOTIDE:LIKE_PURINERGIC_RECEPTORS	0.47
ENSG00000211790	ENSG00000211790 PPI subnetwork	0.47
ENSG00000189162	ENSG00000189162 PPI subnetwork	0.47
ENSG00000181163	NPM1 PPI subnetwork	0.47
ENSG00000137413	TAF8 PPI subnetwork	0.47
REACTOME_AMINE:DERIVED_HORMONES	REACTOME_AMINE:DERIVED_HORMONES	0.47
GO:0034470	ncRNA processing	0.47
ENSG00000214021	TLL3 PPI subnetwork	0.47
ENSG00000092820	EZR PPI subnetwork	0.47
GO:0005244	voltage-gated ion channel activity	0.47
GO:0022832	voltage-gated channel activity	0.47
REACTOME_DNA_STRAND_ELONGATION	REACTOME_DNA_STRAND_ELONGATION	0.47
ENSG00000137709	POU2F3 PPI subnetwork	0.47
ENSG00000108179	PPIF PPI subnetwork	0.47
MP:0001053	abnormal neuromuscular synapse morphology	0.47
REACTOME_O:LINKED_GLYCOSYLATION_OF_MUCINS	REACTOME_O:LINKED_GLYCOSYLATION_OF_MUCINS	0.47
ENSG00000160654	CD3G PPI subnetwork	0.47
ENSG00000074266	EED PPI subnetwork	0.47
GO:0042976	activation of Janus kinase activity	0.47
GO:0002274	myeloid leukocyte activation	0.47
GO:0003205	cardiac chamber development	0.47
KEGG_PYRIMIDINE_METABOLISM	KEGG_PYRIMIDINE_METABOLISM	0.47
MP:0008657	increased interleukin-1 beta secretion	0.47
ENSG00000100664	EIF5 PPI subnetwork	0.47
ENSG00000015171	ZMYND11 PPI subnetwork	0.47
GO:0000151	ubiquitin ligase complex	0.47
GO:0005643	nuclear pore	0.47
MP:0001853	heart inflammation	0.47
GO:0010970	microtubule-based transport	0.47
ENSG00000148308	GTF3C5 PPI subnetwork	0.47
ENSG00000138081	FBXO11 PPI subnetwork	0.47
ENSG00000175324	LSM1 PPI subnetwork	0.47
ENSG00000100902	PSMA6 PPI subnetwork	0.47
GO:0050678	regulation of epithelial cell proliferation	0.47
MP:0008713	abnormal cytokine level	0.47
GO:0071774	response to fibroblast growth factor stimulus	0.47
GO:0044344	cellular response to fibroblast growth factor stimulus	0.47
GO:0022603	regulation of anatomical structure morphogenesis	0.47

Original gene set ID	Original gene set description	Nominal P value
MP:0000681	abnormal thyroid gland morphology	0.48
GO:0015929	hexosaminidase activity	0.48
ENSG000000125352	RNF113A PPI subnetwork	0.48
ENSG000000187840	EIF4EBP1 PPI subnetwork	0.48
ENSG000000115966	ATF2 PPI subnetwork	0.48
ENSG000000160844	GATS PPI subnetwork	0.48
GO:0060759	regulation of response to cytokine stimulus	0.48
ENSG000000140332	TLE3 PPI subnetwork	0.48
GO:0000075	cell cycle checkpoint	0.48
GO:0051101	regulation of DNA binding	0.48
ENSG000000108561	C1QBP PPI subnetwork	0.48
ENSG000000108424	KPNB1 PPI subnetwork	0.48
ENSG000000138032	PPM1B PPI subnetwork	0.48
ENSG000000135097	MSI1 PPI subnetwork	0.48
GO:0044297	cell body	0.48
GO:0000289	nuclear-transcribed mRNA poly(A) tail shortening	0.48
ENSG000000115274	INO80B PPI subnetwork	0.48
ENSG000000173207	CKS1B PPI subnetwork	0.48
GO:0003279	cardiac septum development	0.48
ENSG00000018236	CNTN1 PPI subnetwork	0.48
MP:0002359	abnormal spleen germinal center morphology	0.48
ENSG000000164889	SLC4A2 PPI subnetwork	0.48
ENSG000000044574	HSPA5 PPI subnetwork	0.48
ENSG000000179348	GATA2 PPI subnetwork	0.48
MP:0002391	abnormal Peyer's patch germinal center morphology	0.48
MP:0001404	no spontaneous movement	0.48
ENSG000000170876	TMEM43 PPI subnetwork	0.48
GO:0016079	synaptic vesicle exocytosis	0.48
ENSG000000105880	DLX5 PPI subnetwork	0.48
GO:0045851	pH reduction	0.48
ENSG000000135333	EPHA7 PPI subnetwork	0.48
ENSG000000114166	KAT2B PPI subnetwork	0.48
GO:0002712	regulation of B cell mediated immunity	0.48
REACTOME_FGFR2_LIGAND_BINDING_AND_ACTIVATION	REACTOME_FGFR2_LIGAND_BINDING_AND_ACTIVATION	0.48
GO:0001910	regulation of leukocyte mediated cytotoxicity	0.48
ENSG000000157349	DDX19B PPI subnetwork	0.48
MP:0004057	thin myocardium compact layer	0.48
GO:0031214	biomineral tissue development	0.48
MP:0003675	kidney cysts	0.48
GO:0001578	microtubule bundle formation	0.48
ENSG000000140400	MAN2C1 PPI subnetwork	0.48
ENSG000000102893	PHKB PPI subnetwork	0.48
GO:0006687	glycosphingolipid metabolic process	0.48
ENSG00000008056	SYN1 PPI subnetwork	0.48
MP:0000755	hindlimb paralysis	0.48
MP:0002362	abnormal spleen marginal zone morphology	0.48
GO:0032623	interleukin-2 production	0.48
ENSG000000143373	ZNF687 PPI subnetwork	0.48
MP:0001929	abnormal gametogenesis	0.48

Original gene set ID	Original gene set description	Nominal P value
MP:0002826	tonic seizures	0.48
ENSG00000047410	TPR PPI subnetwork	0.48
ENSG00000185130	HIST1H2BL PPI subnetwork	0.48
REACTOME_GO_AND_EARLY_G1	REACTOME_GO_AND_EARLY_G1	0.48
GO:0006644	phospholipid metabolic process	0.48
ENSG00000130589	RP4-697K14.7 PPI subnetwork	0.48
MP:0000274	enlarged heart	0.48
ENSG00000141582	CBX4 PPI subnetwork	0.48
ENSG00000050405	LIMA1 PPI subnetwork	0.48
ENSG00000108852	MPP2 PPI subnetwork	0.48
GO:0000287	magnesium ion binding	0.48
GO:0007283	spermatogenesis	0.48
GO:0048232	male gamete generation	0.48
MP:0004251	failure of heart looping	0.48
ENSG00000108100	CCNY PPI subnetwork	0.48
MP:0001730	embryonic growth arrest	0.48
MP:0000939	decreased motor neuron number	0.48
MP:0005312	pericardial effusion	0.48
ENSG00000007174	DNAH9 PPI subnetwork	0.48
ENSG00000180370	PAK2 PPI subnetwork	0.48
MP:0009866	abnormal aorta wall morphology	0.48
ENSG00000215021	PHB2 PPI subnetwork	0.48
ENSG00000117118	SDHB PPI subnetwork	0.48
GO:0007178	transmembrane receptor protein serine/threonine kinase signaling pathway	0.48
ENSG00000134046	MBD2 PPI subnetwork	0.48
MP:0005405	axon degeneration	0.48
MP:0000186	decreased circulating HDL cholesterol leve	0.48
MP:0000074	abnormal neurocranium morphology	0.48
GO:0032371	regulation of sterol transport	0.48
GO:0032374	regulation of cholesterol transport	0.48
ENSG00000111602	TIMELESS PPI subnetwork	0.49
REACTOME_COSTIMULATION_BY_THE_CD28_FAMILY	REACTOME_COSTIMULATION_BY_THE_CD28_FAMILY	0.49
REACTOME_DOWNSTREAM_SIGNAL_TRANSDUCTION	REACTOME_DOWNSTREAM_SIGNAL_TRANSDUCTION	0.49
GO:0032201	telomere maintenance via semi-conservative replication	0.49
GO:0007405	neuroblast proliferation	0.49
GO:0060026	convergent extension	0.49
ENSG00000113658	SMAD5 PPI subnetwork	0.49
ENSG00000160695	ENSG00000160695 PPI subnetwork	0.49
GO:0071705	nitrogen compound transport	0.49
ENSG00000130811	EIF3G PPI subnetwork	0.49
GO:0071843	cellular component biogenesis at cellular leve	0.49
GO:0030165	PDZ domain binding	0.49
ENSG00000009307	CSDE1 PPI subnetwork	0.49
ENSG00000132963	POMP PPI subnetwork	0.49
GO:0001974	blood vessel remodeling	0.49
ENSG00000167286	CD3D PPI subnetwork	0.49
MP:0000852	small cerebellum	0.49
GO:0016052	carbohydrate catabolic process	0.49
ENSG00000014216	CAPN1 PPI subnetwork	0.49

Original gene set ID	Original gene set description	Nominal P value
KEGG_GLYCEROLIPID_METABOLISM	KEGG_GLYCEROLIPID_METABOLISM	0.49
MP:0005010	abnormal CD8-positive T cell morphology	0.49
ENSG000000162236	STX5 PPI subnetwork	0.49
ENSG000000157500	APPL1 PPI subnetwork	0.49
MP:0002270	abnormal pulmonary alveolus morphology	0.49
GO:0048511	rhythmic process	0.49
GO:0050820	positive regulation of coagulation	0.49
GO:0016247	channel regulator activity	0.49
GO:0016853	isomerase activity	0.49
ENSG00000075624	ACTB PPI subnetwork	0.49
GO:0003014	renal system process	0.49
MP:0001882	abnormal lactation	0.49
GO:0043370	regulation of CD4-positive, alpha-beta T cell differentiator	0.49
GO:0061311	cell surface receptor signaling pathway involved in heart development	0.49
GO:0031418	L-ascorbic acid binding	0.49
ENSG000000171735	CAMTA1 PPI subnetwork	0.49
MP:0001721	absent visceral yolk sac blood islands	0.49
ENSG000000157152	ENSG000000157152 PPI subnetwork	0.49
ENSG000000177728	KIAA0195 PPI subnetwork	0.49
MP:0002856	abnormal vestibular ganglion morphology	0.49
GO:0033006	regulation of mast cell activation involved in immune response	0.49
GO:0046637	regulation of alpha-beta T cell differentiation	0.49
GO:0072594	establishment of protein localization to organelle	0.49
GO:0001654	eye development	0.49
GO:0002711	positive regulation of T cell mediated immunity	0.49
ENSG000000168497	SDPR PPI subnetwork	0.49
GO:0015248	sterol transporter activity	0.49
KEGG_ASCORBATE_AND_ALDARATE_METABOLISM	KEGG_ASCORBATE_AND_ALDARATE_METABOLISM	0.49
MP:0008809	increased spleen iron level	0.49
ENSG000000085733	CTTN PPI subnetwork	0.49
ENSG000000164346	NSA2 PPI subnetwork	0.49
MP:0000745	tremors	0.49
ENSG000000134769	DTNA PPI subnetwork	0.49
MP:0002912	abnormal excitatory postsynaptic potentia	0.49
ENSG000000198356	ASNA1 PPI subnetwork	0.49
ENSG000000104976	SNAPC2 PPI subnetwork	0.49
GO:0022037	metencephalon development	0.49
ENSG000000196262	PPIA PPI subnetwork	0.49
ENSG000000198618	ENSG000000198618 PPI subnetwork	0.49
GO:0032318	regulation of Ras GTPase activity	0.49
GO:0040012	regulation of locomotion	0.49
GO:0043542	endothelial cell migration	0.49
ENSG000000147168	IL2RG PPI subnetwork	0.49
MP:0010701	fusion of atlas and odontoid process	0.49
MP:0000336	decreased mast cell number	0.49
GO:0004003	ATP-dependent DNA helicase activity	0.49
GO:0009593	detection of chemical stimulus	0.49
REACTOME_REGULATION_OF_IFNG_SIGNALING	REACTOME_REGULATION_OF_IFNG_SIGNALING	0.49
MP:0001935	decreased litter size	0.49

Original gene set ID	Original gene set description	Nominal P value
ENSG00000125818	PSMF1 PPI subnetwork	0.49
GO:0045123	cellular extravasation	0.49
ENSG00000078967	UBE2D4 PPI subnetwork	0.49
ENSG00000129351	ILF3 PPI subnetwork	0.49
ENSG00000149131	SERPING1 PPI subnetwork	0.49
ENSG00000104408	EIF3E PPI subnetwork	0.49
ENSG00000152795	HNRPD L PPI subnetwork	0.49
GO:0033627	cell adhesion mediated by integrin	0.49
ENSG00000211889	ENSG00000211889 PPI subnetwork	0.49
ENSG00000137975	CLCA2 PPI subnetwork	0.49
ENSG00000157514	TSC22D3 PPI subnetwork	0.49
ENSG00000100284	TOM1 PPI subnetwork	0.49
ENSG00000124145	SDC4 PPI subnetwork	0.49
ENSG00000147082	CCNB3 PPI subnetwork	0.49
ENSG00000078699	CBFA2T2 PPI subnetwork	0.49
ENSG00000184216	IRAK1 PPI subnetwork	0.49
ENSG00000115942	ORC2 PPI subnetwork	0.49
ENSG00000168924	LETM1 PPI subnetwork	0.49
ENSG00000079246	XRCC5 PPI subnetwork	0.49
REACTOME_SIGNALING_BY_FGFR	REACTOME_SIGNALING_BY_FGFR	0.49
KEGG_PRION_DISEASES	KEGG_PRION_DISEASES	0.49
REACTOME_PYRUVATE_METABOLISM_AND_CITRIC_ACID_TCA_CYCLE	REACTOME_PYRUVATE_METABOLISM_AND_CITRIC_ACID_TCA_CYCLE	0.49
ENSG00000137309	HMGA1 PPI subnetwork	0.49
ENSG00000072803	FBXW11 PPI subnetwork	0.49
MP:0000920	abnormal myelination	0.49
MP:0009764	decreased sensitivity to induced morbidity/mortality	0.49
ENSG00000105989	WNT2 PPI subnetwork	0.49
ENSG00000075290	WNT8B PPI subnetwork	0.49
ENSG00000143816	WNT9A PPI subnetwork	0.49
ENSG00000169884	WNT10B PPI subnetwork	0.49
ENSG00000135925	WNT10A PPI subnetwork	0.49
ENSG00000158955	WNT9B PPI subnetwork	0.49
ENSG00000085741	WNT11 PPI subnetwork	0.49
ENSG00000061492	WNT8A PPI subnetwork	0.49
ENSG00000146109	ABT1 PPI subnetwork	0.49
ENSG00000175063	UBE2C PPI subnetwork	0.49
MP:0002774	small prostate gland	0.49
ENSG00000116560	SFPQ PPI subnetwork	0.49
GO:0022803	passive transmembrane transporter activity	0.49
GO:0015267	channel activity	0.49
GO:0061138	morphogenesis of a branching epithelium	0.49
ENSG00000100201	DDX17 PPI subnetwork	0.49
ENSG00000104814	MAP4K1 PPI subnetwork	0.49
ENSG00000166225	FRS2 PPI subnetwork	0.49
ENSG00000145901	TNIP1 PPI subnetwork	0.49
ENSG00000185245	GP1BA PPI subnetwork	0.5
MP:0001045	abnormal enteric ganglia morphology	0.5
ENSG00000158796	DEDD PPI subnetwork	0.5
MP:0000435	shortened head	0.5

Original gene set ID	Original gene set description	Nominal P value
KEGG_PANTOTHENATE_AND_COA_BIOSYNTHESIS	KEGG_PANTOTHENATE_AND_COA_BIOSYNTHESIS	0.5
ENSG00000106089	STX1A PPI subnetwork	0.5
GO:0051248	negative regulation of protein metabolic process	0.5
GO:0045639	positive regulation of myeloid cell differentiator	0.5
GO:0048029	monosaccharide binding	0.5
MP:0000438	abnormal cranium morphology	0.5
GO:0043235	receptor complex	0.5
REACTOME_RNA_POLYMERASE_III_TRANSCRIPTION_INITIATION	REACTOME_RNA_POLYMERASE_III_TRANSCRIPTION_INITIATION	0.5
REACTOME_IRAK2_MEDIATED_ACTIVATION_OF_TAK1_COMPLEX_UPON_TLR78	REACTOME_IRAK2_MEDIATED_ACTIVATION_OF_TAK1_COMPLEX_UPON_TLR78_OF	0.5
GO:0007131	reciprocal meiotic recombination	0.5
GO:0035825	reciprocal DNA recombination	0.5
GO:0006301	postreplication repair	0.5
GO:0046530	photoreceptor cell differentiation	0.5
ENSG00000139182	CLSTN3 PPI subnetwork	0.5
MP:0002027	lung adenocarcinoma	0.5
GO:0008081	phosphoric diester hydrolase activity	0.5
ENSG00000112651	MRPL2 PPI subnetwork	0.5
ENSG00000198216	CACNA1E PPI subnetwork	0.5
KEGG_PHOSPHATIDYLINOSITOL_SIGNALING_SYSTEM	KEGG_PHOSPHATIDYLINOSITOL_SIGNALING_SYSTEM	0.5
GO:0051004	regulation of lipoprotein lipase activity	0.5
MP:0004763	absent brainstem auditory evoked potentia	0.5
GO:0007062	sister chromatid cohesion	0.5
ENSG00000011465	DCN PPI subnetwork	0.5
ENSG00000182359	KBTBD3 PPI subnetwork	0.5
ENSG00000082516	GEMIN5 PPI subnetwork	0.5
GO:0008286	insulin receptor signaling pathway	0.5
GO:0032635	interleukin-6 production	0.5
GO:0032675	regulation of interleukin-6 production	0.5
ENSG00000119414	PPP6C PPI subnetwork	0.5
ENSG00000104064	GABPB1 PPI subnetwork	0.5
ENSG00000131828	PDHA1 PPI subnetwork	0.5
ENSG00000161920	MED11 PPI subnetwork	0.5
ENSG00000163811	WDR43 PPI subnetwork	0.5
MP:0004522	abnormal orientation of cochlear hair cell stereociliary bundles	0.5
REACTOME_CD28_CO:STIMULATION	REACTOME_CD28_CO:STIMULATION	0.5
ENSG00000137710	RDX PPI subnetwork	0.5
ENSG00000130041	ENSG00000130041 PPI subnetwork	0.5
ENSG00000177954	RPS27 PPI subnetwork	0.5
ENSG00000183814	LIN9 PPI subnetwork	0.5
REACTOME_SIGNALING_BY_WNT	REACTOME_SIGNALING_BY_WNT	0.5
REACTOME_DEGRADATION_OF_BETA:CATENIN_BY_THE_DESTRUCTION_COMPLEX	REACTOME_DEGRADATION_OF_BETA:CATENIN_BY_THE_DESTRUCTION_COMPLEX	0.5
ENSG00000204523	ENSG00000204523 PPI subnetwork	0.5
ENSG00000174405	LIG4 PPI subnetwork	0.5
GO:0051271	negative regulation of cellular component movement	0.5
GO:0032024	positive regulation of insulin secretior	0.5
MP:0005562	decreased mean corpuscular hemoglobin	0.5
GO:0033549	MAP kinase phosphatase activity	0.5
ENSG00000140451	PIF1 PPI subnetwork	0.5
GO:0003018	vascular process in circulatory system	0.5

Original gene set ID	Original gene set description	Nominal P value
GO:0031670	cellular response to nutrient	0.5
MP:0004726	abnormal nasal capsule morphology	0.5
ENSG000000055208	TAB2 PPI subnetwork	0.5
GO:0002573	myeloid leukocyte differentiation	0.5
ENSG00000196497	IPO4 PPI subnetwork	0.5
GO:0015081	sodium ion transmembrane transporter activity	0.5
ENSG00000130803	ZNF317 PPI subnetwork	0.5
MP:0005145	increased circulating VLDL cholesterol leve	0.5
ENSG00000148943	LIN7C PPI subnetwork	0.5
MP:0005630	increased lung weight	0.5
GO:0006754	ATP biosynthetic process	0.5
ENSG000000082014	SMARCD3 PPI subnetwork	0.5
MP:0002397	abnormal bone marrow morphology	0.5
ENSG000000090054	SPTLC1 PPI subnetwork	0.5
ENSG00000158186	MRAS PPI subnetwork	0.5
MP:0005659	decreased susceptibility to diet-induced obesity	0.5
GO:0030897	HOPS complex	0.5
GO:0042074	cell migration involved in gastrulation	0.5
GO:0010639	negative regulation of organelle organization	0.5
GO:0050880	regulation of blood vessel size	0.5
ENSG00000153107	ANAPC1 PPI subnetwork	0.5
ENSG00000166147	FBN1 PPI subnetwork	0.5
ENSG00000174233	ADCY6 PPI subnetwork	0.5
REACTOME_RAS_ACTIVATION_UOPN_CA2_INFUX_THROUGH_NMDA_RECEPTO	REACTOME_RAS_ACTIVATION_UOPN_CA2_INFUX_THROUGH_NMDA_RECEPTOR	0.5
GO:0035036	sperm-egg recognition	0.5
ENSG00000117500	TMED5 PPI subnetwork	0.5
ENSG00000127914	AKAP9 PPI subnetwork	0.51
GO:0050798	activated T cell proliferation	0.51
ENSG00000117360	PRPF3 PPI subnetwork	0.51
ENSG00000173372	C1QA PPI subnetwork	0.51
ENSG00000204301	NOTCH4 PPI subnetwork	0.51
REACTOME_MAP_KINASE_ACTIVATION_IN_TLR_CASCADE	REACTOME_MAP_KINASE_ACTIVATION_IN_TLR_CASCADE	0.51
GO:0043186	P granule	0.51
GO:0045495	pole plasm	0.51
GO:0060293	germ plasm	0.51
GO:0048016	inositol phosphate-mediated signaling	0.51
MP:0002024	T cell derived lymphoma	0.51
GO:0055037	recycling endosome	0.51
MP:0005172	reduced eye pigmentation	0.51
GO:0004866	endopeptidase inhibitor activity	0.51
MP:0003194	abnormal frequency of paradoxical sleep	0.51
MP:0005543	corneal thinning	0.51
ENSG00000071127	WDR1 PPI subnetwork	0.51
ENSG00000117322	CR2 PPI subnetwork	0.51
ENSG000000065675	PRKCQ PPI subnetwork	0.51
MP:0002747	abnormal aortic valve morphology	0.51
GO:0001948	glycoprotein binding	0.51
GO:0043473	pigmentation	0.51
GO:0050867	positive regulation of cell activation	0.51

Original gene set ID	Original gene set description	Nominal P value
ENSG00000165029	ABCA1 PPI subnetwork	0.51
GO:0009163	nucleoside biosynthetic process	0.51
MP:0005560	decreased circulating glucose level	0.51
REACTOME_SMOOTH_MUSCLE_CONTRACTION	REACTOME_SMOOTH_MUSCLE_CONTRACTION	0.51
GO:0006688	glycosphingolipid biosynthetic process	0.51
ENSG00000128829	EIF2AK4 PPI subnetwork	0.51
ENSG00000006715	VPS41 PPI subnetwork	0.51
ENSG00000105671	DDX49 PPI subnetwork	0.51
ENSG00000170632	ARMC10 PPI subnetwork	0.51
GO:0000976	transcription regulatory region sequence-specific DNA binding	0.51
GO:0019217	regulation of fatty acid metabolic process	0.51
GO:0043568	positive regulation of insulin-like growth factor receptor signaling pathway	0.51
MP:0001541	abnormal osteoclast physiology	0.51
ENSG00000127334	DYRK2 PPI subnetwork	0.51
ENSG00000183495	EP400 PPI subnetwork	0.51
ENSG00000174775	HRAS PPI subnetwork	0.51
ENSG00000133265	HSPBP1 PPI subnetwork	0.51
MP:0001081	abnormal cranial ganglia morphology	0.51
ENSG00000143933	CALM2 PPI subnetwork	0.51
ENSG00000160014	CALM3 PPI subnetwork	0.51
ENSG00000198668	CALM1 PPI subnetwork	0.51
ENSG00000013503	POLR3B PPI subnetwork	0.51
ENSG00000123066	MED13L PPI subnetwork	0.51
GO:0042737	drug catabolic process	0.51
GO:0030126	COPI vesicle coat	0.51
ENSG00000145391	SETD7 PPI subnetwork	0.51
ENSG00000061987	MON2 PPI subnetwork	0.51
GO:0045428	regulation of nitric oxide biosynthetic process	0.51
ENSG00000203814	HIST2H2BF PPI subnetwork	0.51
MP:0005094	abnormal T cell proliferation	0.51
GO:0009260	ribonucleotide biosynthetic process	0.51
GO:0070035	purine NTP-dependent helicase activity	0.51
GO:0008026	ATP-dependent helicase activity	0.51
GO:0043174	nucleoside salvage	0.51
ENSG00000120129	DUSP1 PPI subnetwork	0.51
GO:0051053	negative regulation of DNA metabolic process	0.51
ENSG00000113140	SPARC PPI subnetwork	0.51
ENSG00000135218	CD36 PPI subnetwork	0.51
ENSG00000185057	ENSG00000185057 PPI subnetwork	0.51
GO:0032715	negative regulation of interleukin-6 production	0.51
ENSG00000134686	PHC2 PPI subnetwork	0.51
GO:0015698	inorganic anion transport	0.51
ENSG00000064313	TAF2 PPI subnetwork	0.51
ENSG00000215328	HSPA1A PPI subnetwork	0.51
ENSG00000113494	PRLR PPI subnetwork	0.51
GO:0046504	glycerol ether biosynthetic process	0.51
GO:0008206	bile acid metabolic process	0.51
ENSG00000070018	LRP6 PPI subnetwork	0.51
ENSG00000139496	NUPL1 PPI subnetwork	0.51

Original gene set ID	Original gene set description	Nominal P value
GO:0006631	fatty acid metabolic process	0.51
GO:0048546	digestive tract morphogenesis	0.51
GO:0045444	fat cell differentiation	0.51
REACTOME_GLUTATHIONE_SYNTHESIS_AND_RECYCLING	REACTOME_GLUTATHIONE_SYNTHESIS_AND_RECYCLING	0.51
ENSG00000169375	SIN3A PPI subnetwork	0.51
ENSG00000147854	UHRF2 PPI subnetwork	0.51
ENSG00000173876	TUBB8 PPI subnetwork	0.51
MP:0000049	abnormal middle ear morphology	0.51
GO:0051222	positive regulation of protein transport	0.51
ENSG00000119917	IFIT3 PPI subnetwork	0.51
GO:0060113	inner ear receptor cell differentiation	0.51
GO:0060219	camera-type eye photoreceptor cell differentiator	0.51
GO:0035051	cardiac cell differentiation	0.51
ENSG00000115750	TAF1B PPI subnetwork	0.51
MP:0001516	abnormal motor coordination/ balance	0.51
GO:0019835	cytolysis	0.51
MP:0002273	abnormal pulmonary alveolus epithelial cell morphology	0.51
GO:0050864	regulation of B cell activation	0.51
MP:0003132	increased pre-B cell number	0.51
GO:0060828	regulation of canonical Wnt receptor signaling pathway	0.51
REACTOME_SEROTONIN_NEUROTRANSMITTER_RELEASE_CYCLE	REACTOME_SEROTONIN_NEUROTRANSMITTER_RELEASE_CYCLE	0.51
REACTOME_DOPAMINE_NEUROTRANSMITTER_RELEASE_CYCLE	REACTOME_DOPAMINE_NEUROTRANSMITTER_RELEASE_CYCLE	0.51
GO:0008629	induction of apoptosis by intracellular signals	0.51
ENSG00000167513	CDT1 PPI subnetwork	0.51
GO:0051251	positive regulation of lymphocyte activation	0.51
MP:0001092	abnormal trigeminal ganglion morphology	0.51
GO:0051147	regulation of muscle cell differentiation	0.51
REACTOME_RNA_POLYMERASE_III_TRANSCRIPTION_INITIATION_FROM_TYPE_2_PROMOTER	REACTOME_RNA_POLYMERASE_III_TRANSCRIPTION_INITIATION_FROM_TYPE_2_PROMOTER	0.51
ENSG00000131459	GFPT2 PPI subnetwork	0.51
ENSG00000008294	SPAG9 PPI subnetwork	0.51
GO:0040014	regulation of multicellular organism growth	0.51
KEGG_GLYCOPHINGOLIPID_BIOSYNTHESIS_GANGLIO_SERIES	KEGG_GLYCOPHINGOLIPID_BIOSYNTHESIS_GANGLIO_SERIES	0.51
GO:0030194	positive regulation of blood coagulation	0.51
MP:0006298	abnormal platelet activation	0.51
ENSG00000156313	RPGR PPI subnetwork	0.51
ENSG00000078399	HOXA9 PPI subnetwork	0.51
GO:0030837	negative regulation of actin filament polymerization	0.51
REACTOME_INTERACTIONS_OF_VPR_WITH_HOST_CELLULAR_PROTEINS	REACTOME_INTERACTIONS_OF_VPR_WITH_HOST_CELLULAR_PROTEINS	0.51
GO:0060021	palate development	0.51
GO:0008180	signalosome	0.51
REACTOME_CREB_PHOSPHORYLATION_THROUGH_THE_ACTIVATION_OF_RAS	REACTOME_CREB_PHOSPHORYLATION_THROUGH_THE_ACTIVATION_OF_RAS	0.51
ENSG00000153914	SREK1 PPI subnetwork	0.51
MP:0004098	abnormal cerebellar granule cell morphology	0.51
GO:0014031	mesenchymal cell development	0.52
GO:2000514	regulation of CD4-positive, alpha-beta T cell activation	0.52
ENSG00000139372	TDG PPI subnetwork	0.52
MP:0005362	abnormal Langerhans cell physiology	0.52
REACTOME_RNA_POLYMERASE_III_CHAIN_ELONGATION	REACTOME_RNA_POLYMERASE_III_CHAIN_ELONGATION	0.52
GO:0070201	regulation of establishment of protein localizer	0.52

Original gene set ID	Original gene set description	Nominal P value
GO:0005657	replication fork	0.52
ENSG00000081479	LRP2 PPI subnetwork	0.52
ENSG00000071243	ING3 PPI subnetwork	0.52
GO:0007043	cell-cell junction assembly	0.52
MP:0003938	abnormal ear development	0.52
ENSG00000100722	ZC3H14 PPI subnetwork	0.52
ENSG00000135679	MDM2 PPI subnetwork	0.52
ENSG00000116106	EPHA4 PPI subnetwork	0.52
REACTOME_HIGHLY_CALCIUM_PERMEABLE_POSTSYNAPTIC_NICOTINIC_ACETY	REACTOME_HIGHLY_CALCIUM_PERMEABLE_POSTSYNAPTIC_NICOTINIC_ACETYLCHI	0.52
GO:0006937	regulation of muscle contraction	0.52
ENSG00000165732	DDX21 PPI subnetwork	0.52
GO:0019438	aromatic compound biosynthetic process	0.52
ENSG00000175073	VCPIP1 PPI subnetwork	0.52
GO:0009113	purine base biosynthetic process	0.52
GO:0072655	establishment of protein localization in mitochondrion	0.52
GO:0044269	glycerol ether catabolic process	0.52
GO:0046464	acylglycerol catabolic process	0.52
GO:0046461	neutral lipid catabolic process	0.52
MP:0003627	abnormal leukocyte tethering or rolling	0.52
KEGG_TGF_BETA_SIGNALING_PATHWAY	KEGG_TGF_BETA_SIGNALING_PATHWAY	0.52
GO:0046148	pigment biosynthetic process	0.52
ENSG00000215754	ENSG00000215754 PPI subnetwork	0.52
ENSG00000156802	ATAD2 PPI subnetwork	0.52
REACTOME_SYNTHESIS_OF_GLYCOSYLPHOSPHATIDYLINOSITOL_GPI	REACTOME_SYNTHESIS_OF_GLYCOSYLPHOSPHATIDYLINOSITOL_GPI	0.52
ENSG00000185024	BRF1 PPI subnetwork	0.52
ENSG00000149970	CNKS2 PPI subnetwork	0.52
GO:0016579	protein deubiquitination	0.52
GO:0043021	ribonucleoprotein complex binding	0.52
MP:0006082	CNS inflammation	0.52
GO:0006362	transcription elongation from RNA polymerase I promoter	0.52
ENSG00000197238	HIST1H4J PPI subnetwork	0.52
ENSG00000183941	HIST2H4A PPI subnetwork	0.52
ENSG00000197914	HIST1H4K PPI subnetwork	0.52
ENSG00000198518	HIST1H4E PPI subnetwork	0.52
ENSG00000197837	HIST4H4 PPI subnetwork	0.52
ENSG00000182217	HIST2H4B PPI subnetwork	0.52
ENSG00000158406	HIST1H4H PPI subnetwork	0.52
ENSG00000198558	HIST1H4L PPI subnetwork	0.52
ENSG00000124529	HIST1H4B PPI subnetwork	0.52
ENSG00000197061	HIST1H4C PPI subnetwork	0.52
ENSG00000188987	HIST1H4D PPI subnetwork	0.52
ENSG00000198339	HIST1H4I PPI subnetwork	0.52
ENSG00000198327	HIST1H4F PPI subnetwork	0.52
ENSG00000196176	HIST1H4A PPI subnetwork	0.52
ENSG00000104738	MCM4 PPI subnetwork	0.52
GO:0005930	axoneme	0.52
ENSG00000168374	ARF4 PPI subnetwork	0.52
GO:0002696	positive regulation of leukocyte activation	0.52
MP:0006138	congestive heart failure	0.52

Original gene set ID	Original gene set description	Nominal P value
ENSG00000135269	TES PPI subnetwork	0.52
MP:0000102	abnormal nasal bone morphology	0.52
ENSG00000108679	LGALS3BP PPI subnetwork	0.52
ENSG00000111229	ARPC3 PPI subnetwork	0.52
GO:0031105	septin complex	0.52
GO:0032156	septin cytoskeleton	0.52
GO:0015297	antiporter activity	0.52
GO:0045665	negative regulation of neuron differentiation	0.52
ENSG00000166266	CUL5 PPI subnetwork	0.52
GO:0050860	negative regulation of T cell receptor signaling pathway	0.52
GO:0050858	negative regulation of antigen receptor-mediated signaling pathway	0.52
GO:0072378	blood coagulation, fibrin clot formation	0.52
GO:0070848	response to growth factor stimulus	0.52
ENSG00000145191	EIF2B5 PPI subnetwork	0.52
GO:0061134	peptidase regulator activity	0.52
GO:0020027	hemoglobin metabolic process	0.52
ENSG00000145782	ATG12 PPI subnetwork	0.52
MP:0000876	Purkinje cell degeneration	0.52
GO:0042612	MHC class I protein complex	0.52
ENSG00000171421	MRPL36 PPI subnetwork	0.52
ENSG00000104856	RELB PPI subnetwork	0.52
GO:0060341	regulation of cellular localization	0.52
MP:0009660	abnormal induced retinal neovascularization	0.52
GO:0030140	trans-Golgi network transport vesicle	0.52
ENSG00000135972	MRPS9 PPI subnetwork	0.52
ENSG00000100852	ARHGAP5 PPI subnetwork	0.52
GO:0005680	anaphase-promoting complex	0.52
ENSG00000171552	BCL2L1 PPI subnetwork	0.52
REACTOME_TELOMERE_C:STRAND_LAGGING_STRAND_SYNTHESIS	REACTOME_TELOMERE_C:STRAND_LAGGING_STRAND_SYNTHESIS	0.52
MP:0005671	abnormal response to transplant	0.52
GO:0060284	regulation of cell development	0.52
GO:0005243	gap junction channel activity	0.52
MP:0005598	decreased ventricle muscle contractility	0.52
GO:0007519	skeletal muscle tissue development	0.52
GO:0030155	regulation of cell adhesion	0.52
GO:0034707	chloride channel complex	0.52
GO:0016459	myosin complex	0.52
GO:0006144	purine base metabolic process	0.52
MP:0000208	decreased hematocrit	0.52
GO:0048729	tissue morphogenesis	0.52
ENSG00000100994	PYGB PPI subnetwork	0.52
ENSG00000070770	CSNK2A2 PPI subnetwork	0.52
GO:0007597	blood coagulation, intrinsic pathway	0.52
REACTOME_RECRUITMENT_OF_NUMA_TO_MITOTIC_CENTROSOMES	REACTOME_RECRUITMENT_OF_NUMA_TO_MITOTIC_CENTROSOMES	0.52
KEGG_ANTIGEN_PROCESSING_AND_PRESENTATION	KEGG_ANTIGEN_PROCESSING_AND_PRESENTATION	0.52
ENSG00000206234	ENSG00000206234 PPI subnetwork	0.52
ENSG00000204264	PSMB8 PPI subnetwork	0.52
ENSG00000206298	PSMB8 PPI subnetwork	0.52
GO:0009247	glycolipid biosynthetic process	0.52

Original gene set ID	Original gene set description	Nominal P value
GO:0051324	prophase	0.53
GO:0031498	chromatin disassembly	0.53
GO:0032986	protein-DNA complex disassembly	0.53
GO:0006337	nucleosome disassembly	0.53
MP:0001394	circling	0.53
MP:0004542	impaired acrosome reaction	0.53
ENSG00000077782	FGFR1 PPI subnetwork	0.53
ENSG00000006125	AP2B1 PPI subnetwork	0.53
MP:0002413	abnormal megakaryocyte progenitor cell morphology	0.53
MP:0001006	abnormal retinal cone cell morphology	0.53
ENSG00000015479	MATR3 PPI subnetwork	0.53
ENSG000000198130	HIBCH PPI subnetwork	0.53
GO:0031058	positive regulation of histone modification	0.53
GO:0016050	vesicle organization	0.53
MP:0000692	small spleen	0.53
ENSG000000144158	ENSG000000144158 PPI subnetwork	0.53
GO:0030529	ribonucleoprotein complex	0.53
ENSG00000069956	MAPK6 PPI subnetwork	0.53
REACTOME_PREFOLDIN_MEDIATED_TRANSFER_OF_SUBSTRATE_TO_CCTTRIC	REACTOME_PREFOLDIN_MEDIATED_TRANSFER_OF_SUBSTRATE_TO_CCTTRIC	0.53
REACTOME_COOPERATION_OF_PREFOLDIN_AND_TRICCT_IN_ACTIN_AND_TUBU	REACTOME_COOPERATION_OF_PREFOLDIN_AND_TRICCT_IN_ACTIN_AND_TUBU	0.53
ENSG000000169592	INO80E PPI subnetwork	0.53
ENSG000000162552	WNT4 PPI subnetwork	0.53
ENSG000000133027	PEMT PPI subnetwork	0.53
ENSG000000185627	PSMD13 PPI subnetwork	0.53
GO:0030424	axon	0.53
KEGG_FC_EPSILON_RI_SIGNALING_PATHWAY	KEGG_FC_EPSILON_RI_SIGNALING_PATHWAY	0.53
GO:0002755	MyD88-dependent toll-like receptor signaling pathway	0.53
ENSG00000081052	COL4A4 PPI subnetwork	0.53
ENSG000000067596	DHX8 PPI subnetwork	0.53
MP:0000248	macrocytosis	0.53
REACTOME_GABA_SYNTHESIS_RELEASE_REUPTAKE_AND_DEGRADATION	REACTOME_GABA_SYNTHESIS_RELEASE_REUPTAKE_AND_DEGRADATION	0.53
ENSG000000160712	IL6R PPI subnetwork	0.53
GO:0005852	eukaryotic translation initiation factor 3 complex	0.53
GO:0048598	embryonic morphogenesis	0.53
ENSG000000001626	CFTR PPI subnetwork	0.53
ENSG000000005175	RPAP3 PPI subnetwork	0.53
GO:0042461	photoreceptor cell development	0.53
GO:0007128	meiotic prophase I	0.53
GO:0031063	regulation of histone deacetylation	0.53
GO:0001085	RNA polymerase II transcription factor binding	0.53
ENSG000000149557	FEZ1 PPI subnetwork	0.53
ENSG000000049540	ELN PPI subnetwork	0.53
ENSG000000206279	DAXX PPI subnetwork	0.53
ENSG000000206206	DAXX PPI subnetwork	0.53
ENSG000000204209	DAXX PPI subnetwork	0.53
GO:0090175	regulation of establishment of planar polarity	0.53
GO:0060071	Wnt receptor signaling pathway, planar cell polarity pathway	0.53
GO:0001843	neural tube closure	0.53
ENSG000000163877	SNIP1 PPI subnetwork	0.53

Original gene set ID	Original gene set description	Nominal P value
GO:0051904	pigment granule transport	0.54
GO:0001649	osteoblast differentiation	0.54
ENSG00000094880	CDC23 PPI subnetwork	0.54
GO:0004540	ribonuclease activity	0.54
REACTOME_SYNTHESIS_SECRETION_AND_DEACYLATION_OF_GHRELIN	REACTOME_SYNTHESIS_SECRETION_AND_DEACYLATION_OF_GHRELIN	0.54
MP:0002786	abnormal Leydig cell morphology	0.54
MP:0000925	abnormal floor plate morphology	0.54
ENSG00000164494	PDSS2 PPI subnetwork	0.54
REACTOME_INTERLEUKIN_RECEPTOR_SHC_SIGNALING	REACTOME_INTERLEUKIN_RECEPTOR_SHC_SIGNALING	0.54
GO:0071173	spindle assembly checkpoint	0.54
REACTOME_ACTIVATION_OF_THE_AP:1_FAMILY_OF_TRANSCRIPTION_FACTORS	REACTOME_ACTIVATION_OF_THE_AP:1_FAMILY_OF_TRANSCRIPTION_FACTORS	0.54
MP:0002908	delayed wound healing	0.54
GO:0007269	neurotransmitter secretion	0.54
ENSG00000124802	EEF1E1 PPI subnetwork	0.54
GO:0045121	membrane raft	0.54
REACTOME_FGFR1_LIGAND_BINDING_AND_ACTIVATION	REACTOME_FGFR1_LIGAND_BINDING_AND_ACTIVATION	0.54
GO:0019433	triglyceride catabolic process	0.54
MP:0001302	eyelids open at birth	0.54
ENSG00000198062	POTEH PPI subnetwork	0.54
ENSG00000164609	SLU7 PPI subnetwork	0.54
GO:0045926	negative regulation of growth	0.54
REACTOME_METABOLISM_OF_NUCLEOTIDES	REACTOME_METABOLISM_OF_NUCLEOTIDES	0.54
ENSG00000079785	DDX1 PPI subnetwork	0.54
MP:0005465	abnormal T-helper 1 physiology	0.54
KEGG_ALPHA_LINOLENIC_ACID_METABOLISM	KEGG_ALPHA_LINOLENIC_ACID_METABOLISM	0.54
GO:0035150	regulation of tube size	0.54
KEGG_LINOLEIC_ACID_METABOLISM	KEGG_LINOLEIC_ACID_METABOLISM	0.54
ENSG00000099942	CRKL PPI subnetwork	0.54
MP:0006000	abnormal corneal epithelium morphology	0.54
ENSG00000101868	POLA1 PPI subnetwork	0.54
GO:0009112	nucleobase metabolic process	0.54
ENSG00000039650	PNKP PPI subnetwork	0.54
ENSG00000174827	PDZK1 PPI subnetwork	0.54
KEGG_LEISHMANIA_INFECTION	KEGG_LEISHMANIA_INFECTION	0.54
KEGG_OOCYTE_MEIOSIS	KEGG_OOCYTE_MEIOSIS	0.54
GO:0009968	negative regulation of signal transduction	0.54
ENSG00000120885	CLU PPI subnetwork	0.54
MP:0003634	abnormal glial cell morphology	0.54
ENSG00000165417	GTF2A1 PPI subnetwork	0.54
ENSG00000172115	CYCS PPI subnetwork	0.54
GO:0006891	intra-Golgi vesicle-mediated transport	0.54
MP:0002843	decreased systemic arterial blood pressure	0.54
MP:0001524	impaired limb coordination	0.54
MP:0005311	abnormal circulating amino acid level	0.54
ENSG00000075673	ATP12A PPI subnetwork	0.54
GO:0008543	fibroblast growth factor receptor signaling pathway	0.54
MP:0003936	abnormal reproductive system development	0.54
MP:0002465	abnormal eosinophil physiology	0.54
ENSG00000119535	CSF3R PPI subnetwork	0.54

Original gene set ID	Original gene set description	Nominal P value
ENSG00000139618	BRCA2 PPI subnetwork	0.54
ENSG00000100239	PPP6R2 PPI subnetwork	0.54
ENSG00000112159	MDN1 PPI subnetwork	0.54
ENSG00000100109	TFIP11 PPI subnetwork	0.54
ENSG00000187990	HIST1H2BG PPI subnetwork	0.54
ENSG00000168242	HIST1H2BI PPI subnetwork	0.54
ENSG00000180596	HIST1H2BC PPI subnetwork	0.54
ENSG00000197846	HIST1H2BF PPI subnetwork	0.54
ENSG00000126261	UBA2 PPI subnetwork	0.54
ENSG0000011485	PPP5C PPI subnetwork	0.54
ENSG00000101146	RAE1 PPI subnetwork	0.54
ENSG00000163810	TGM4 PPI subnetwork	0.54
ENSG00000142208	AKT1 PPI subnetwork	0.54
ENSG00000170312	CDK1 PPI subnetwork	0.54
KEGG_PORPHYRIN_AND_CHLOROPHYLL_METABOLISM	KEGG_PORPHYRIN_AND_CHLOROPHYLL_METABOLISM	0.54
GO:0010948	negative regulation of cell cycle process	0.54
GO:0070555	response to interleukin-1	0.54
GO:0009982	pseudouridine synthase activity	0.54
GO:0030934	anchoring collagen	0.54
GO:0005253	anion channel activity	0.54
GO:0019841	retinol binding	0.54
GO:0006885	regulation of pH	0.54
MP:0002887	decreased susceptibility to pharmacologically induced seizures	0.54
ENSG00000163069	SGCB PPI subnetwork	0.54
MP:0008807	increased liver iron level	0.54
GO:0043202	lysosomal lumen	0.54
ENSG00000197903	HIST1H2BK PPI subnetwork	0.54
ENSG00000164086	DUSP7 PPI subnetwork	0.54
GO:0008287	protein serine/threonine phosphatase complex	0.54
ENSG00000174989	FBXW8 PPI subnetwork	0.54
GO:0034483	heparan sulfate sulfotransferase activity	0.54
ENSG00000177879	AP3S1 PPI subnetwork	0.54
GO:0021549	cerebellum development	0.54
GO:0008175	tRNA methyltransferase activity	0.54
KEGG_GRAFT_VERSUS_HOST_DISEASE	KEGG_GRAFT_VERSUS_HOST_DISEASE	0.54
GO:0031577	spindle checkpoint	0.54
GO:0008366	axon ensheathment	0.54
GO:0007272	ensheathment of neurons	0.54
GO:0016339	calcium-dependent cell-cell adhesion	0.54
ENSG00000129993	CBFA2T3 PPI subnetwork	0.54
MP:0001363	increased anxiety-related response	0.54
ENSG00000126067	PSMB2 PPI subnetwork	0.54
ENSG00000066933	MYO9A PPI subnetwork	0.54
GO:0071855	neuropeptide receptor binding	0.54
REACTOME_SIGNAL_AMPLIFICATION	REACTOME_SIGNAL_AMPLIFICATION	0.54
ENSG0000006468	ETV1 PPI subnetwork	0.54
GO:0071295	cellular response to vitamin	0.54
ENSG00000111348	ARHGDI1 PPI subnetwork	0.54
ENSG00000143437	ARNT PPI subnetwork	0.54

Original gene set ID	Original gene set description	Nominal P value
ENSG00000160255	ITGB2 PPI subnetwork	0.54
GO:0071941	nitrogen cycle metabolic process	0.54
MP:0001270	distended abdomen	0.54
ENSG00000180185	FAHD1 PPI subnetwork	0.54
MP:0000460	mandible hypoplasia	0.54
KEGG_PROXIMAL_TUBULE_BICARBONATE_RECLAMATION	KEGG_PROXIMAL_TUBULE_BICARBONATE_RECLAMATION	0.54
ENSG00000184117	NIPSNAP1 PPI subnetwork	0.54
ENSG00000146232	NFKBIE PPI subnetwork	0.54
MP:0005104	abnormal tarsal bone morphology	0.54
GO:0050795	regulation of behavior	0.54
MP:0004753	abnormal miniature excitatory postsynaptic currents	0.54
ENSG00000113810	SMC4 PPI subnetwork	0.55
ENSG00000130706	ADRM1 PPI subnetwork	0.55
MP:0001489	decreased startle reflex	0.55
MP:0001762	polyuria	0.55
ENSG00000140600	SH3GL3 PPI subnetwork	0.55
GO:0045737	positive regulation of cyclin-dependent protein kinase activity	0.55
ENSG00000096063	SRPK1 PPI subnetwork	0.55
ENSG00000120087	HOXB7 PPI subnetwork	0.55
MP:0002123	abnormal hematopoiesis	0.55
ENSG00000177485	ZBTB33 PPI subnetwork	0.55
MP:0005466	abnormal T-helper 2 physiology	0.55
GO:0007130	synaptonemal complex assembly	0.55
GO:0010562	positive regulation of phosphorus metabolic process	0.55
GO:0045937	positive regulation of phosphate metabolic process	0.55
GO:0046634	regulation of alpha-beta T cell activation	0.55
GO:0044057	regulation of system process	0.55
GO:0061077	chaperone-mediated protein folding	0.55
GO:0005507	copper ion binding	0.55
ENSG00000175467	SART1 PPI subnetwork	0.55
GO:0008633	activation of pro-apoptotic gene products	0.55
GO:0019887	protein kinase regulator activity	0.55
GO:0030902	hindbrain development	0.55
GO:0005267	potassium channel activity	0.55
GO:0032535	regulation of cellular component size	0.55
MP:0009790	decreased susceptibility to viral infection induced morbidity/mortality	0.55
GO:0030867	rough endoplasmic reticulum membrane	0.55
GO:0043603	cellular amide metabolic process	0.55
GO:0046631	alpha-beta T cell activation	0.55
MP:0003606	kidney failure	0.55
MP:0001523	impaired righting response	0.55
GO:0032320	positive regulation of Ras GTPase activity	0.55
ENSG00000084234	APLP2 PPI subnetwork	0.55
GO:0007398	ectoderm development	0.55
ENSG00000125378	BMP4 PPI subnetwork	0.55
ENSG00000165059	PRKACG PPI subnetwork	0.55
GO:0045086	positive regulation of interleukin-2 biosynthetic process	0.55
MP:0003890	abnormal embryonic-extraembryonic boundary morphology	0.55
ENSG00000198791	CNOT7 PPI subnetwork	0.55

Original gene set ID	Original gene set description	Nominal P value
ENSG00000104419	NDRG1 PPI subnetwork	0.55
MP:0000245	abnormal erythropoiesis	0.55
ENSG00000117601	SERPINC1 PPI subnetwork	0.55
GO:0060485	mesenchyme development	0.55
GO:0042575	DNA polymerase complex	0.55
MP:0001120	abnormal uterus morphology	0.55
ENSG00000108055	SMC3 PPI subnetwork	0.55
ENSG00000102974	CTCF PPI subnetwork	0.55
MP:0004939	abnormal B cell morphology	0.55
GO:0005100	Rho GTPase activator activity	0.55
MP:0008528	polycystic kidney	0.55
MP:0009862	abnormal aorta elastic tissue morphology	0.55
MP:0004876	decreased mean systemic arterial blood pressure	0.55
GO:0007017	microtubule-based process	0.55
GO:0003007	heart morphogenesis	0.55
ENSG00000111262	KCNA1 PPI subnetwork	0.56
MP:0005159	azoospermia	0.56
ENSG00000180628	PCGF5 PPI subnetwork	0.56
ENSG00000177469	PTRF PPI subnetwork	0.56
ENSG00000122965	RBM19 PPI subnetwork	0.56
GO:0046658	anchored to plasma membrane	0.56
GO:0042625	ATPase activity, coupled to transmembrane movement of ions	0.56
ENSG00000162946	DISC1 PPI subnetwork	0.56
ENSG00000085231	TAF9 PPI subnetwork	0.56
ENSG00000069431	ABCC9 PPI subnetwork	0.56
GO:0006182	cGMP biosynthetic process	0.56
ENSG00000123374	CDK2 PPI subnetwork	0.56
REACTOME_CYTOSOLIC_TRNA_AMINOACYLATION	REACTOME_CYTOSOLIC_TRNA_AMINOACYLATION	0.56
REACTOME_SCF5K2:MEDIATED_DEGRADATION_OF_P27P21	REACTOME_SCF5K2:MEDIATED_DEGRADATION_OF_P27P21	0.56
MP:0011100	complete preweaning lethality	0.56
MP:0002176	increased brain weight	0.56
REACTOME_CGMP_EFFECTS	REACTOME_CGMP_EFFECTS	0.56
ENSG00000092203	TOX4 PPI subnetwork	0.56
ENSG00000165527	ARF6 PPI subnetwork	0.56
ENSG00000067704	IARS2 PPI subnetwork	0.56
GO:0090312	positive regulation of protein deacetylation	0.56
GO:2000027	regulation of organ morphogenesis	0.56
GO:0045177	apical part of cell	0.56
MP:0004779	abnormal production of surfactant	0.56
ENSG00000106976	DNM1 PPI subnetwork	0.56
ENSG00000106348	IMPDH1 PPI subnetwork	0.56
ENSG00000174446	SNAPC5 PPI subnetwork	0.56
ENSG00000167751	KLK2 PPI subnetwork	0.56
ENSG00000102572	STK24 PPI subnetwork	0.56
GO:0003950	NAD+ ADP-ribosyltransferase activity	0.56
ENSG00000159840	ZYX PPI subnetwork	0.56
ENSG00000105664	COMP PPI subnetwork	0.56
ENSG00000165684	SNAPC4 PPI subnetwork	0.56
GO:0061387	regulation of extent of cell growth	0.56

Original gene set ID	Original gene set description	Nominal P value
REACTOME_MITOTIC_SPINDLE_CHECKPOINT	REACTOME_MITOTIC_SPINDLE_CHECKPOINT	0.56
REACTOME_UNBLOCKING_OF_NMDA_RECEPTOR_Glutamate_Binding_And	REACTOME_UNBLOCKING_OF_NMDA_RECEPTOR_Glutamate_Binding_And_AC	0.56
MP:0002621	delayed neural tube closure	0.56
ENSG00000101558	VAPA PPI subnetwork	0.56
GO:0007040	lysosome organization	0.56
ENSG00000097046	CDC7 PPI subnetwork	0.56
MP:0008703	decreased interleukin-5 secretion	0.56
MP:0004486	decreased response of heart to induced stress	0.56
ENSG00000101189	C20orf20 PPI subnetwork	0.56
REACTOME_G1S:SPECIFIC_TRANSCRIPTION	REACTOME_G1S:SPECIFIC_TRANSCRIPTION	0.56
ENSG00000099341	PSMD8 PPI subnetwork	0.56
GO:0043534	blood vessel endothelial cell migration	0.56
ENSG00000106211	HSPB1 PPI subnetwork	0.56
ENSG00000198380	GFPT1 PPI subnetwork	0.56
GO:0005254	chloride channel activity	0.56
ENSG00000171867	PRNP PPI subnetwork	0.56
GO:0032368	regulation of lipid transport	0.56
ENSG00000206232	ENSG00000206232 PPI subnetwork	0.56
ENSG00000204261	ENSG00000204261 PPI subnetwork	0.56
ENSG00000206296	ENSG00000206296 PPI subnetwork	0.56
GO:0016776	phosphotransferase activity, phosphate group as acceptor	0.56
ENSG00000129559	NEDD8 PPI subnetwork	0.56
ENSG00000152661	GJA1 PPI subnetwork	0.56
GO:0016709	oxidoreductase activity, acting on paired donors, with incorporation or reduction of	0.56
GO:0035050	embryonic heart tube development	0.56
ENSG00000175084	DES PPI subnetwork	0.56
GO:0007588	excretion	0.56
GO:0050770	regulation of axonogenesis	0.56
ENSG00000114251	WNT5A PPI subnetwork	0.56
MP:0000111	cleft palate	0.56
ENSG00000155561	NUP205 PPI subnetwork	0.56
ENSG00000198018	ENTPD7 PPI subnetwork	0.56
REACTOME_P2Y_RECEPTORS	REACTOME_P2Y_RECEPTORS	0.56
GO:0043498	cell surface binding	0.56
MP:0008189	increased transitional stage B cell number	0.56
GO:0007059	chromosome segregation	0.56
GO:0008023	transcription elongation factor complex	0.56
MP:0005324	ascites	0.56
KEGG_FRUCTOSE_AND_MANNANOSE_METABOLISM	KEGG_FRUCTOSE_AND_MANNANOSE_METABOLISM	0.56
ENSG00000167930	ITFG3 PPI subnetwork	0.56
GO:0016514	SWI/SNF complex	0.56
GO:0016055	Wnt receptor signaling pathway	0.56
MP:0005334	abnormal fat pad morphology	0.56
ENSG00000108379	WNT3 PPI subnetwork	0.56
MP:0005464	abnormal platelet physiology	0.56
GO:0016064	immunoglobulin mediated immune response	0.56
GO:0032609	interferon-gamma production	0.56
GO:0035162	embryonic hemopoiesis	0.56
ENSG00000103168	TAF1C PPI subnetwork	0.56

Original gene set ID	Original gene set description	Nominal P value
MP:0006269	abnormal mammary gland growth during pregnancy	0.56
REACTOME_PHOSPHORYLATION_OF_THE_APCC	REACTOME_PHOSPHORYLATION_OF_THE_APCC	0.56
MP:0004090	abnormal sarcomere morphology	0.56
ENSG00000172794	RAB37 PPI subnetwork	0.56
GO:0042733	embryonic digit morphogenesis	0.56
REACTOME_DNA_REPLICATION_PRE:INITIATION	REACTOME_DNA_REPLICATION_PRE:INITIATION	0.56
REACTOME_MG1_TRANSITION	REACTOME_MG1_TRANSITION	0.56
ENSG00000134982	APC PPI subnetwork	0.56
GO:0045980	negative regulation of nucleotide metabolic process	0.56
GO:0008483	transaminase activity	0.56
MP:0001714	absent trophoblast giant cells	0.56
MP:0002950	abnormal neural crest cell migration	0.56
ENSG00000172116	CD8B PPI subnetwork	0.56
ENSG00000111186	WNT5B PPI subnetwork	0.56
GO:0015485	cholesterol binding	0.56
ENSG00000130414	NDUFA10 PPI subnetwork	0.56
GO:0003197	endocardial cushion development	0.56
GO:0008016	regulation of heart contraction	0.56
ENSG00000131238	PPT1 PPI subnetwork	0.56
MP:0009331	absent primitive node	0.56
GO:0032755	positive regulation of interleukin-6 production	0.56
ENSG00000198925	ATG9A PPI subnetwork	0.57
MP:0005326	abnormal podocyte morphology	0.57
GO:0005506	iron ion binding	0.57
ENSG00000123737	EXOSC9 PPI subnetwork	0.57
GO:0070646	protein modification by small protein removal	0.57
ENSG0000010030	ETV7 PPI subnetwork	0.57
ENSG00000197321	SVIL PPI subnetwork	0.57
ENSG00000197697	HIST1H2BE PPI subnetwork	0.57
ENSG00000138741	TRPC3 PPI subnetwork	0.57
GO:0001710	mesodermal cell fate commitment	0.57
ENSG00000124789	NUP153 PPI subnetwork	0.57
GO:0030100	regulation of endocytosis	0.57
GO:0051325	interphase	0.57
ENSG00000092964	DPYSL2 PPI subnetwork	0.57
GO:0015370	solute:sodium symporter activity	0.57
GO:0004576	oligosaccharyl transferase activity	0.57
REACTOME_VPU_MEDIATED_DEGRADATION_OF_CD4	REACTOME_VPU_MEDIATED_DEGRADATION_OF_CD4	0.57
KEGG_HOMOLOGOUS_RECOMBINATION	KEGG_HOMOLOGOUS_RECOMBINATION	0.57
GO:0016010	dystrophin-associated glycoprotein complex	0.57
REACTOME_CREB_PHOSPHORYLATION_THROUGH_THE_ACTIVATION_OF_CAM	REACTOME_CREB_PHOSPHORYLATION_THROUGH_THE_ACTIVATION_OF_CAMKII	0.57
GO:0042770	signal transduction in response to DNA damage	0.57
MP:0000913	abnormal brain development	0.57
ENSG00000136754	ABI1 PPI subnetwork	0.57
GO:0042692	muscle cell differentiation	0.57
REACTOME_KINESINS	REACTOME_KINESINS	0.57
ENSG00000178607	ERN1 PPI subnetwork	0.57
GO:0042805	actinin binding	0.57
GO:0006297	nucleotide-excision repair, DNA gap filling	0.57

Original gene set ID	Original gene set description	Nominal P value
ENSG00000122884	P4HA1 PPI subnetwork	0.57
GO:0003143	embryonic heart tube morphogenesis	0.57
ENSG00000153234	NR4A2 PPI subnetwork	0.57
ENSG00000135363	LMO2 PPI subnetwork	0.57
GO:0019894	kinesin binding	0.57
GO:0042440	pigment metabolic process	0.57
GO:0060538	skeletal muscle organ development	0.57
GO:0006275	regulation of DNA replication	0.57
ENSG00000100079	LGALS2 PPI subnetwork	0.57
REACTOME_ACTIVATION_OF_CHAPERONES_BY_ATF6:ALPHA	REACTOME_ACTIVATION_OF_CHAPERONES_BY_ATF6:ALPHA	0.57
GO:0016604	nuclear body	0.57
MP:0002199	abnormal brain commissure morphology	0.57
ENSG00000165996	PTPLA PPI subnetwork	0.57
GO:0004115	3',5'-cyclic-AMP phosphodiesterase activity	0.57
ENSG00000175792	RUVBL1 PPI subnetwork	0.57
ENSG00000111752	PHC1 PPI subnetwork	0.57
MP:0002085	abnormal embryonic tissue morphology	0.57
ENSG00000114982	KANSL3 PPI subnetwork	0.57
GO:0010745	negative regulation of macrophage derived foam cell differentiation	0.57
GO:0007094	mitotic cell cycle spindle assembly checkpoint	0.57
ENSG00000108823	SGCA PPI subnetwork	0.57
GO:0008395	steroid hydroxylase activity	0.57
GO:0001754	eye photoreceptor cell differentiation	0.57
GO:0032393	MHC class I receptor activity	0.57
REACTOME_CELL_CYCLE_MITOTIC	REACTOME_CELL_CYCLE_MITOTIC	0.57
GO:0030193	regulation of blood coagulation	0.57
GO:0019239	deaminase activity	0.57
MP:0005341	decreased susceptibility to atherosclerosis	0.57
ENSG00000102054	RBBP7 PPI subnetwork	0.57
MP:0001182	lung hemorrhage	0.57
GO:0021904	dorsal/ventral neural tube patterning	0.57
ENSG00000166478	ZNF143 PPI subnetwork	0.57
KEGG_BASAL_TRANSCRIPTION_FACTORS	KEGG_BASAL_TRANSCRIPTION_FACTORS	0.57
GO:0048566	embryonic digestive tract development	0.57
MP:0000788	abnormal cerebral cortex morphology	0.57
ENSG00000144285	SCN1A PPI subnetwork	0.57
MP:0000562	polydactyly	0.57
REACTOME_ION_TRANSPORT_BY_P:TYPE_ATPASES	REACTOME_ION_TRANSPORT_BY_P:TYPE_ATPASES	0.57
ENSG00000105287	PRKD2 PPI subnetwork	0.57
ENSG00000181610	MRPS23 PPI subnetwork	0.57
ENSG00000116478	HDAC1 PPI subnetwork	0.57
GO:0030901	midbrain development	0.57
ENSG00000158517	NCF1 PPI subnetwork	0.57
ENSG00000152818	UTRN PPI subnetwork	0.57
MP:0008076	abnormal CD4-positive T cell differentiation	0.57
KEGG_LYSINE_DEGRADATION	KEGG_LYSINE_DEGRADATION	0.57
MP:0011346	renal tubule atrophy	0.57
ENSG00000142599	RERE PPI subnetwork	0.57
REACTOME_METABOLISM_OF_NON:CODING_RNA	REACTOME_METABOLISM_OF_NON:CODING_RNA	0.57

Original gene set ID	Original gene set description	Nominal P value
REACTOME_SNRNP_ASSEMBLY	REACTOME_SNRNP_ASSEMBLY	0.57
ENSG00000159199	ATP5G1 PPI subnetwork	0.57
KEGG_CALCIIUM_SIGNALING_PATHWAY	KEGG_CALCIIUM_SIGNALING_PATHWAY	0.57
GO:0002039	p53 binding	0.57
ENSG00000148798	INA PPI subnetwork	0.57
GO:0030551	cyclic nucleotide binding	0.57
ENSG00000150347	ARID5B PPI subnetwork	0.57
GO:0032147	activation of protein kinase activity	0.57
ENSG00000188064	WNT7B PPI subnetwork	0.57
MP:0005307	head tossing	0.58
GO:0060047	heart contraction	0.58
ENSG00000163288	GABRB1 PPI subnetwork	0.58
GO:0051048	negative regulation of secretion	0.58
ENSG00000012223	LTF PPI subnetwork	0.58
GO:0045765	regulation of angiogenesis	0.58
ENSG00000089094	KDM2B PPI subnetwork	0.58
GO:0002504	antigen processing and presentation of peptide or polysaccharide antigen via MHC class II	0.58
ENSG00000186676	ENSG00000186676 PPI subnetwork	0.58
MP:0001876	decreased inflammatory response	0.58
GO:0046632	alpha-beta T cell differentiation	0.58
ENSG00000109339	MAPK10 PPI subnetwork	0.58
ENSG00000171564	FGB PPI subnetwork	0.58
GO:0010165	response to X-ray	0.58
ENSG00000135365	PHF21A PPI subnetwork	0.58
MP:0000633	abnormal pituitary gland morphology	0.58
MP:0000334	decreased granulocyte number	0.58
GO:0004984	olfactory receptor activity	0.58
GO:0034446	substrate adhesion-dependent cell spreading	0.58
ENSG00000136930	PSMB7 PPI subnetwork	0.58
ENSG00000139190	VAMP1 PPI subnetwork	0.58
ENSG00000075884	ARHGAP15 PPI subnetwork	0.58
REACTOME_BIOLOGICAL_OXIDATIONS	REACTOME_BIOLOGICAL_OXIDATIONS	0.58
ENSG00000115641	FHL2 PPI subnetwork	0.58
GO:0016409	palmitoyltransferase activity	0.58
MP:0002230	abnormal primitive streak formation	0.58
GO:0048306	calcium-dependent protein binding	0.58
GO:0001934	positive regulation of protein phosphorylation	0.58
ENSG00000115361	ACADL PPI subnetwork	0.58
REACTOME_VPR:MEDIATED_NUCLEAR_IMPORT_OF_PICS	REACTOME_VPR:MEDIATED_NUCLEAR_IMPORT_OF_PICS	0.58
GO:0030593	neutrophil chemotaxis	0.58
MP:0002651	abnormal sciatic nerve morphology	0.58
MP:0002233	abnormal nose morphology	0.58
ENSG00000075089	ACTR6 PPI subnetwork	0.58
ENSG00000107581	EIF3A PPI subnetwork	0.58
REACTOME_INTERACTIONS_OF_REV_WITH_HOST_CELLULAR_PROTEINS	REACTOME_INTERACTIONS_OF_REV_WITH_HOST_CELLULAR_PROTEINS	0.58
GO:0015116	sulfate transmembrane transporter activity	0.58
ENSG00000095794	CREM PPI subnetwork	0.58
GO:0010769	regulation of cell morphogenesis involved in differentiation	0.58
GO:0071363	cellular response to growth factor stimulus	0.58

Original gene set ID	Original gene set description	Nominal P value
MP:0004405	absent cochlear hair cells	0.58
GO:0043583	ear development	0.58
MP:0004261	abnormal embryonic neuroepithelium morphology	0.58
REACTOME_ANTIGEN_PROCESSING_UBIQUITINATION__PROTEASOME_DEGRAI	REACTOME_ANTIGEN_PROCESSING_UBIQUITINATION__PROTEASOME_DEGRADATI	0.58
GO:0031514	motile cilium	0.58
GO:0046415	urate metabolic process	0.58
ENSG00000114867	EIF4G1 PPI subnetwork	0.58
ENSG00000198677	TTC37 PPI subnetwork	0.58
ENSG00000116717	GADD45A PPI subnetwork	0.58
REACTOME_CLASS_I_MHC_MEDIATED_ANTIGEN_PROCESSING__PRESENTATIOI	REACTOME_CLASS_I_MHC_MEDIATED_ANTIGEN_PROCESSING__PRESENTATION	0.58
GO:0033119	negative regulation of RNA splicing	0.58
MP:0000914	exencephaly	0.58
GO:0048659	smooth muscle cell proliferation	0.58
GO:0060271	cilium morphogenesis	0.58
MP:0004774	abnormal bile salt level	0.58
MP:0001695	abnormal gastrulation	0.58
ENSG00000131504	DIAPH1 PPI subnetwork	0.58
GO:0048762	mesenchymal cell differentiation	0.58
REACTOME_ACTIVATION_OF_BH3:ONLY_PROTEINS	REACTOME_ACTIVATION_OF_BH3:ONLY_PROTEINS	0.58
ENSG00000073969	NSF PPI subnetwork	0.58
GO:0005548	phospholipid transporter activity	0.58
ENSG00000215120	ENSG00000215120 PPI subnetwork	0.58
ENSG00000134086	VHL PPI subnetwork	0.58
ENSG00000134058	CDK7 PPI subnetwork	0.58
MP:0004924	abnormal behavior	0.58
ENSG00000163531	NFASC PPI subnetwork	0.58
REACTOME_CYTOCHROME_P450_:ARRANGED_BY_SUBSTRATE_TYPE	REACTOME_CYTOCHROME_P450_:ARRANGED_BY_SUBSTRATE_TYPE	0.58
ENSG00000103051	COG4 PPI subnetwork	0.58
ENSG00000137345	MOG PPI subnetwork	0.58
ENSG00000206456	ENSG00000206456 PPI subnetwork	0.58
ENSG00000204655	MOG PPI subnetwork	0.58
GO:0019915	lipid storage	0.58
MP:0001654	hepatic necrosis	0.58
MP:0001328	disorganized retinal layers	0.58
GO:0000726	non-recombinational repair	0.58
ENSG00000185787	MORF4L1 PPI subnetwork	0.58
MP:0006011	abnormal endolymphatic duct morphology	0.58
REACTOME_ER:PHAGOSOME_PATHWAY	REACTOME_ER:PHAGOSOME_PATHWAY	0.58
ENSG00000123080	CDKN2C PPI subnetwork	0.58
REACTOME_SYNTHESIS_OF_DNA	REACTOME_SYNTHESIS_OF_DNA	0.58
GO:0035145	exon-exon junction complex	0.58
GO:0015079	potassium ion transmembrane transporter activity	0.58
GO:0050730	regulation of peptidyl-tyrosine phosphorylation	0.58
MP:0008388	hypochromic microcytic anemia	0.58
GO:0055008	cardiac muscle tissue morphogenesis	0.58
GO:0045664	regulation of neuron differentiation	0.58
ENSG00000168685	IL7R PPI subnetwork	0.58
KEGG_UBIQUITIN_MEDIATED_PROTEOLYSIS	KEGG_UBIQUITIN_MEDIATED_PROTEOLYSIS	0.58
ENSG00000044115	CTNNA1 PPI subnetwork	0.58

Original gene set ID	Original gene set description	Nominal P value
ENSG00000123338	NCKAP1L PPI subnetwork	0.58
GO:0042611	MHC protein complex	0.58
ENSG000000065613	SLK PPI subnetwork	0.58
ENSG00000133318	RTN3 PPI subnetwork	0.58
GO:0030818	negative regulation of cAMP biosynthetic process	0.58
GO:0030815	negative regulation of cAMP metabolic process	0.58
GO:0003015	heart process	0.58
GO:0032321	positive regulation of Rho GTPase activity	0.58
ENSG00000182533	CAV3 PPI subnetwork	0.58
ENSG00000143632	ACTA1 PPI subnetwork	0.58
ENSG00000008277	ADAM22 PPI subnetwork	0.58
REACTOME_EXPORT_OF_VIRAL_RIBONUCLEOPROTEINS_FROM_NUCLEUS	REACTOME_EXPORT_OF_VIRAL_RIBONUCLEOPROTEINS_FROM_NUCLEUS	0.58
GO:0045807	positive regulation of endocytosis	0.58
GO:0018212	peptidyl-tyrosine modification	0.58
GO:0034374	low-density lipoprotein particle remodeling	0.58
GO:0070851	growth factor receptor binding	0.58
GO:0006607	NLS-bearing substrate import into nucleus	0.59
ENSG00000131711	MAP1B PPI subnetwork	0.59
GO:0070585	protein localization in mitochondrion	0.59
REACTOME_MTOR_SIGNALLING	REACTOME_MTOR_SIGNALLING	0.59
MP:0010763	abnormal hematopoietic stem cell physiology	0.59
ENSG00000198087	CD2AP PPI subnetwork	0.59
REACTOME_MITOTIC_G1:G1S_PHASES	REACTOME_MITOTIC_G1:G1S_PHASES	0.59
GO:0031346	positive regulation of cell projection organization	0.59
ENSG00000023608	SNAPC1 PPI subnetwork	0.59
ENSG00000183735	TBK1 PPI subnetwork	0.59
ENSG00000112312	GMNN PPI subnetwork	0.59
GO:0016049	cell growth	0.59
GO:0001558	regulation of cell growth	0.59
GO:0046875	ephrin receptor binding	0.59
ENSG00000077238	IL4R PPI subnetwork	0.59
ENSG00000196305	IARS PPI subnetwork	0.59
ENSG00000136738	STAM PPI subnetwork	0.59
GO:0032649	regulation of interferon-gamma production	0.59
GO:0002294	CD4-positive, alpha-beta T cell differentiation involved in immune response	0.59
GO:0042093	T-helper cell differentiation	0.59
ENSG00000185359	HGS PPI subnetwork	0.59
GO:0030111	regulation of Wnt receptor signaling pathway	0.59
KEGG_INOSITOL_PHOSPHATE_METABOLISM	KEGG_INOSITOL_PHOSPHATE_METABOLISM	0.59
GO:0048538	thymus development	0.59
ENSG00000171566	PLRG1 PPI subnetwork	0.59
GO:0030120	vesicle coat	0.59
ENSG00000197459	HIST1H2BH PPI subnetwork	0.59
ENSG00000167645	YIF1B PPI subnetwork	0.59
MP:0002693	abnormal pancreas physiology	0.59
GO:0051259	protein oligomerization	0.59
GO:0000302	response to reactive oxygen species	0.59
ENSG00000170142	UBE2E1 PPI subnetwork	0.59
ENSG00000185619	PCGF3 PPI subnetwork	0.59

Original gene set ID	Original gene set description	Nominal P value
ENSG00000160007	ARHGAP35 PPI subnetwork	0.59
KEGG_PPAR_SIGNALING_PATHWAY	KEGG_PPAR_SIGNALING_PATHWAY	0.59
ENSG00000175602	CCDC85B PPI subnetwork	0.59
MP:0000233	abnormal blood flow velocity	0.59
MP:0006113	abnormal heart septum morphology	0.59
KEGG_PROPANOATE_METABOLISM	KEGG_PROPANOATE_METABOLISM	0.59
GO:0009743	response to carbohydrate stimulus	0.59
MP:0001263	weight loss	0.59
GO:0048660	regulation of smooth muscle cell proliferation	0.59
GO:0070830	tight junction assembly	0.59
GO:0018108	peptidyl-tyrosine phosphorylation	0.59
MP:0003733	abnormal retinal inner nuclear layer morphology	0.59
GO:0050818	regulation of coagulation	0.59
GO:0048934	peripheral nervous system neuron differentiation	0.59
GO:0048935	peripheral nervous system neuron development	0.59
ENSG00000086619	ERO1LB PPI subnetwork	0.59
ENSG00000198700	IPO9 PPI subnetwork	0.59
ENSG00000130208	APOC1 PPI subnetwork	0.59
ENSG00000067606	PRKCZ PPI subnetwork	0.59
GO:0003179	heart valve morphogenesis	0.59
REACTOME_CYCLIN_ACDK2:ASSOCIATED_EVENTS_AT_S_PHASE_ENTRY	REACTOME_CYCLIN_ACDK2:ASSOCIATED_EVENTS_AT_S_PHASE_ENTRY	0.59
GO:0005761	mitochondrial ribosome	0.59
GO:0000313	organellar ribosome	0.59
GO:0043198	dendritic shaft	0.59
ENSG00000151164	RAD9B PPI subnetwork	0.59
ENSG00000117594	HSD11B1 PPI subnetwork	0.59
ENSG00000157087	ATP2B2 PPI subnetwork	0.59
MP:0000848	abnormal pons morphology	0.59
GO:0042327	positive regulation of phosphorylation	0.59
ENSG00000113575	PPP2CA PPI subnetwork	0.59
MP:0005566	decreased blood urea nitrogen level	0.59
ENSG00000077522	ACTN2 PPI subnetwork	0.59
REACTOME_INHIBITION_OF_THE_PROTEOLYTIC_ACTIVITY_OF_APCC_REQUIRED_FC	REACTOME_INHIBITION_OF_THE_PROTEOLYTIC_ACTIVITY_OF_APCC_REQUIRED_FC	0.59
REACTOME_INACTIVATION_OF_APCC_VIA_DIRECT_INHIBITION_OF_THE_APCC_COI	REACTOME_INACTIVATION_OF_APCC_VIA_DIRECT_INHIBITION_OF_THE_APCC_COI	0.59
ENSG00000088833	NSFL1C PPI subnetwork	0.59
KEGG_AUTOIMMUNE_THYROID_DISEASE	KEGG_AUTOIMMUNE_THYROID_DISEASE	0.59
ENSG00000106829	TLE4 PPI subnetwork	0.59
GO:0019884	antigen processing and presentation of exogenous antigen	0.59
GO:0030135	coated vesicle	0.59
MP:0003644	thymus atrophy	0.59
ENSG00000173566	NUDT18 PPI subnetwork	0.59
GO:0015645	fatty acid ligase activity	0.59
ENSG00000099960	SLC7A4 PPI subnetwork	0.59
ENSG00000013293	SLC7A14 PPI subnetwork	0.59
ENSG00000173786	CNP PPI subnetwork	0.59
GO:0050679	positive regulation of epithelial cell proliferation	0.59
GO:0046427	positive regulation of JAK-STAT cascade	0.59
ENSG00000162692	VCAM1 PPI subnetwork	0.59
GO:0007350	blastoderm segmentation	0.59

Original gene set ID	Original gene set description	Nominal P value
KEGG_PROTEASOME	KEGG_PROTEASOME	0.59
ENSG00000197860	SGTB PPI subnetwork	0.59
REACTOME_LIGAND:GATED_ION_CHANNEL_TRANSPORT	REACTOME_LIGAND:GATED_ION_CHANNEL_TRANSPORT	0.59
REACTOME_RNA_POLYMERASE_I_TRANSCRIPTION_INITIATION	REACTOME_RNA_POLYMERASE_I_TRANSCRIPTION_INITIATION	0.59
GO:0015276	ligand-gated ion channel activity	0.59
GO:0022834	ligand-gated channel activity	0.59
ENSG00000172780	RAB43 PPI subnetwork	0.59
ENSG00000174547	MRPL11 PPI subnetwork	0.59
GO:0008652	cellular amino acid biosynthetic process	0.59
KEGG_PHENYLALANINE_METABOLISM	KEGG_PHENYLALANINE_METABOLISM	0.59
GO:0030863	cortical cytoskeleton	0.59
GO:0019842	vitamin binding	0.59
ENSG00000160867	FGFR4 PPI subnetwork	0.59
ENSG00000135597	REPS1 PPI subnetwork	0.59
MP:0003722	absent ureter	0.59
GO:0009411	response to UV	0.59
ENSG00000113240	CLK4 PPI subnetwork	0.59
ENSG00000168118	RAB4A PPI subnetwork	0.59
ENSG00000137462	TLR2 PPI subnetwork	0.59
ENSG00000134352	IL6ST PPI subnetwork	0.59
ENSG00000151532	VTI1A PPI subnetwork	0.59
GO:0048333	mesodermal cell differentiation	0.59
ENSG00000197956	S100A6 PPI subnetwork	0.59
GO:0032733	positive regulation of interleukin-10 production	0.59
ENSG00000125835	SNRNPB PPI subnetwork	0.59
MP:0002572	abnormal emotion/affect behavior	0.59
ENSG00000198056	PRIM1 PPI subnetwork	0.59
ENSG00000151148	UBE3B PPI subnetwork	0.59
ENSG00000054118	THRAP3 PPI subnetwork	0.59
ENSG00000120438	TCP1 PPI subnetwork	0.59
MP:0002335	decreased airway responsiveness	0.59
ENSG00000141027	NCOR1 PPI subnetwork	0.59
ENSG00000072952	MRVI1 PPI subnetwork	0.59
REACTOME_PI3KAKT_ACTIVATION	REACTOME_PI3KAKT_ACTIVATION	0.59
ENSG00000109846	CRYAB PPI subnetwork	0.59
REACTOME_REPAIR_SYNTHESIS_OF_PATCH_27:30_BASES_LONG_BY_DNA_PO	REACTOME_REPAIR_SYNTHESIS_OF_PATCH_27:30_BASES_LONG_BY_DNA_POLYM	0.59
REACTOME_REPAIR_SYNTHESIS_FOR_GAP:FILLING_BY_DNA_POLYMERASE_IN_	REACTOME_REPAIR_SYNTHESIS_FOR_GAP:FILLING_BY_DNA_POLYMERASE_IN_TC:R	0.59
REACTOME_SHC1_EVENTS_IN_ERBB4_SIGNALING	REACTOME_SHC1_EVENTS_IN_ERBB4_SIGNALING	0.59
GO:0030326	embryonic limb morphogenesis	0.59
GO:0035113	embryonic appendage morphogenesis	0.59
MP:0002628	hepatic steatosis	0.59
GO:0004653	polypeptide N-acetylgalactosaminyltransferase activity	0.6
GO:0072331	signal transduction by p53 class mediator	0.6
MP:0006069	abnormal retinal neuronal layer morphology	0.6
MP:0008699	increased interleukin-4 secretion	0.6
GO:0019724	B cell mediated immunity	0.6
KEGG_NON_HOMOLOGOUS_END_JOINING	KEGG_NON_HOMOLOGOUS_END_JOINING	0.6
REACTOME_PHASE_II_CONJUGATION	REACTOME_PHASE_II_CONJUGATION	0.6
ENSG00000120063	GNA13 PPI subnetwork	0.6

Original gene set ID	Original gene set description	Nominal P value
KEGG_PENTOSE_PHOSPHATE_PATHWAY	KEGG_PENTOSE_PHOSPHATE_PATHWAY	0.6
ENSG00000177426	TGIF1 PPI subnetwork	0.6
ENSG00000015153	YAF2 PPI subnetwork	0.6
REACTOME_XENOBIOTICS	REACTOME_XENOBIOTICS	0.6
ENSG00000137673	MMP7 PPI subnetwork	0.6
REACTOME_CDK:MEDIATED_PHOSPHORYLATION_AND_REMOVAL_OF_CDC6	REACTOME_CDK:MEDIATED_PHOSPHORYLATION_AND_REMOVAL_OF_CDC6	0.6
GO:0007631	feeding behavior	0.6
ENSG00000134287	ARF3 PPI subnetwork	0.6
GO:0043297	apical junction assembly	0.6
ENSG00000206274	ENSG00000206274 PPI subnetwork	0.6
ENSG00000206383	HSPA1L PPI subnetwork	0.6
ENSG00000124299	PEPD PPI subnetwork	0.6
ENSG00000162191	UBXN1 PPI subnetwork	0.6
ENSG00000139180	NDUFA9 PPI subnetwork	0.6
ENSG00000183049	CAMK1D PPI subnetwork	0.6
ENSG00000139549	DHH PPI subnetwork	0.6
GO:0042579	microbody	0.6
GO:0005777	peroxisome	0.6
REACTOME_SIGNALING_BY_INSULIN_RECEPTOR	REACTOME_SIGNALING_BY_INSULIN_RECEPTOR	0.6
ENSG00000155657	TTN PPI subnetwork	0.6
REACTOME_UBIQUITIN:DEPENDENT_DEGRADATION_OF_CYCLIN_D	REACTOME_UBIQUITIN:DEPENDENT_DEGRADATION_OF_CYCLIN_D	0.6
REACTOME_UBIQUITIN:DEPENDENT_DEGRADATION_OF_CYCLIN_D1	REACTOME_UBIQUITIN:DEPENDENT_DEGRADATION_OF_CYCLIN_D1	0.6
ENSG00000134759	ELP2 PPI subnetwork	0.6
GO:0030031	cell projection assembly	0.6
ENSG00000100867	DHRS2 PPI subnetwork	0.6
GO:0030433	ER-associated protein catabolic process	0.6
MP:0001491	unresponsive to tactile stimuli	0.6
ENSG00000106245	BUD31 PPI subnetwork	0.6
KEGG_SELENOAMINO_ACID_METABOLISM	KEGG_SELENOAMINO_ACID_METABOLISM	0.6
GO:0043535	regulation of blood vessel endothelial cell migration	0.6
GO:0015300	solute:solute antiporter activity	0.6
GO:0046364	monosaccharide biosynthetic process	0.6
GO:0050907	detection of chemical stimulus involved in sensory perceptior	0.6
KEGG_PURINE_METABOLISM	KEGG_PURINE_METABOLISM	0.6
MP:0001417	decreased exploration in new environment	0.6
ENSG00000114698	PLSCR4 PPI subnetwork	0.6
ENSG00000153922	CHD1 PPI subnetwork	0.6
MP:0000188	abnormal circulating glucose level	0.6
GO:0001763	morphogenesis of a branching structure	0.6
REACTOME_NEPNS2_INTERACTS_WITH_THE_CELLULAR_EXPORT_MACHINERY	REACTOME_NEPNS2_INTERACTS_WITH_THE_CELLULAR_EXPORT_MACHINERY	0.6
ENSG00000091428	RAPGEF4 PPI subnetwork	0.6
ENSG00000087460	GNAS PPI subnetwork	0.6
GO:0045214	sarcomere organization	0.6
MP:0001431	abnormal eating behavior	0.6
GO:0071174	mitotic cell cycle spindle checkpoint	0.6
ENSG00000196235	SUPT5H PPI subnetwork	0.6
GO:0031669	cellular response to nutrient levels	0.6
ENSG00000101856	PGRMC1 PPI subnetwork	0.6
ENSG00000173692	PSMD1 PPI subnetwork	0.6

Original gene set ID	Original gene set description	Nominal P value
MP:0000097	short maxilla	0.6
MP:0002064	seizures	0.6
MP:0000807	abnormal hippocampus morphology	0.6
GO:0018149	peptide cross-linking	0.6
ENSG00000120616	EPC1 PPI subnetwork	0.6
GO:0006303	double-strand break repair via nonhomologous end joining	0.6
GO:0030855	epithelial cell differentiation	0.6
GO:0005249	voltage-gated potassium channel activity	0.6
ENSG00000135100	HNF1A PPI subnetwork	0.6
ENSG00000163435	ELF3 PPI subnetwork	0.6
MP:0000880	decreased Purkinje cell number	0.6
ENSG00000082074	FYB PPI subnetwork	0.6
MP:0005221	abnormal rostral-caudal axis patterning	0.6
KEGG_NON_SMALL_CELL_LUNG_CANCER	KEGG_NON_SMALL_CELL_LUNG_CANCER	0.6
ENSG00000108443	RPS6KB1 PPI subnetwork	0.6
REACTOME_SIGNAL_TRANSDUCTION_BY_L1	REACTOME_SIGNAL_TRANSDUCTION_BY_L1	0.6
ENSG00000150991	UBC PPI subnetwork	0.6
REACTOME_REGULATION_OF_DNA_REPLICATION	REACTOME_REGULATION_OF_DNA_REPLICATION	0.6
ENSG00000133710	SPINK5 PPI subnetwork	0.6
GO:0033059	cellular pigmentation	0.6
MP:0008539	decreased susceptibility to induced colitis	0.6
ENSG00000166407	LMO1 PPI subnetwork	0.6
GO:0047485	protein N-terminus binding	0.6
KEGG_AXON_GUIDANCE	KEGG_AXON_GUIDANCE	0.6
ENSG00000086758	HUWE1 PPI subnetwork	0.6
ENSG00000092470	WDR76 PPI subnetwork	0.6
GO:0060606	tube closure	0.6
ENSG00000137561	TTPA PPI subnetwork	0.6
GO:0005496	steroid binding	0.6
GO:0071230	cellular response to amino acid stimulus	0.6
GO:0033365	protein localization to organelle	0.6
GO:0005798	Golgi-associated vesicle	0.6
REACTOME_NOREPINEPHRINE_NEUROTRANSMITTER_RELEASE_CYCLE	REACTOME_NOREPINEPHRINE_NEUROTRANSMITTER_RELEASE_CYCLE	0.6
GO:0004601	peroxidase activity	0.6
GO:0016684	oxidoreductase activity, acting on peroxide as acceptor	0.6
GO:0042274	ribosomal small subunit biogenesis	0.6
ENSG00000154473	BUB3 PPI subnetwork	0.6
GO:2000045	regulation of G1/S transition of mitotic cell cycle	0.6
GO:0008064	regulation of actin polymerization or depolymerization	0.6
GO:0048588	developmental cell growth	0.6
MP:0005668	decreased circulating leptin level	0.6
ENSG00000086827	ZW10 PPI subnetwork	0.6
GO:0002009	morphogenesis of an epithelium	0.6
GO:0020037	heme binding	0.6
MP:0001475	reduced long term depression	0.6
GO:0006164	purine nucleotide biosynthetic process	0.6
ENSG00000065978	YBX1 PPI subnetwork	0.6
ENSG00000130816	DNMT1 PPI subnetwork	0.6
ENSG00000168078	PBK PPI subnetwork	0.6

Original gene set ID	Original gene set description	Nominal P value
ENSG00000171824	EXOSC10 PPI subnetwork	0.6
GO:0009312	oligosaccharide biosynthetic process	0.6
MP:0002398	abnormal bone marrow cell morphology/development	0.61
GO:0006325	chromatin organization	0.61
GO:0006361	transcription initiation from RNA polymerase I promoter	0.61
GO:0006112	energy reserve metabolic process	0.61
KEGG_BUTANOATE_METABOLISM	KEGG_BUTANOATE_METABOLISM	0.61
REACTOME_ION_CHANNEL_TRANSPORT	REACTOME_ION_CHANNEL_TRANSPORT	0.61
GO:0021915	neural tube development	0.61
ENSG00000213658	LAT PPI subnetwork	0.61
KEGG_Cysteine_and_Methionine_Metabolism	KEGG_Cysteine_and_Methionine_Metabolism	0.61
ENSG00000099783	HNRNPM PPI subnetwork	0.61
MP:0003690	abnormal glial cell physiology	0.61
ENSG00000196331	HIST1H2BO PPI subnetwork	0.61
GO:0007498	mesoderm development	0.61
ENSG00000172680	MOS PPI subnetwork	0.61
ENSG00000110367	DDX6 PPI subnetwork	0.61
ENSG00000173175	ADCY5 PPI subnetwork	0.61
MP:0003209	abnormal pulmonary elastic fiber morphology	0.61
MP:0011427	mesangial cell hyperplasia	0.61
GO:0005262	calcium channel activity	0.61
MP:0008332	decreased lactotroph cell number	0.61
MP:0010103	small thoracic cage	0.61
ENSG00000095319	NUP188 PPI subnetwork	0.61
GO:0051289	protein homotetramerization	0.61
ENSG00000198722	UNC13B PPI subnetwork	0.61
GO:0048048	embryonic eye morphogenesis	0.61
ENSG00000113368	LMNB1 PPI subnetwork	0.61
MP:0008173	increased follicular B cell number	0.61
ENSG00000100346	CACNA1I PPI subnetwork	0.61
ENSG00000171311	EXOSC1 PPI subnetwork	0.61
ENSG00000095139	ARCN1 PPI subnetwork	0.61
ENSG00000101367	MAPRE1 PPI subnetwork	0.61
GO:0022600	digestive system process	0.61
ENSG00000008018	PSMB1 PPI subnetwork	0.61
GO:0032816	positive regulation of natural killer cell activator	0.61
ENSG00000156076	WIF1 PPI subnetwork	0.61
GO:0001959	regulation of cytokine-mediated signaling pathway	0.61
REACTOME_ADP_Signalling_Through_P2Y_Purinoceptor_1	REACTOME_ADP_Signalling_Through_P2Y_Purinoceptor_1	0.61
GO:0050434	positive regulation of viral transcription	0.61
ENSG00000100926	TM9SF1 PPI subnetwork	0.61
ENSG00000006634	DBF4 PPI subnetwork	0.61
GO:0042102	positive regulation of T cell proliferation	0.61
ENSG00000089048	ESF1 PPI subnetwork	0.61
ENSG00000110244	APOA4 PPI subnetwork	0.61
ENSG00000128908	INO80 PPI subnetwork	0.61
ENSG00000182872	RBM10 PPI subnetwork	0.61
MP:0009643	abnormal urine homeostasis	0.61
ENSG00000154342	WNT3A PPI subnetwork	0.61

Original gene set ID	Original gene set description	Nominal P value
ENSG00000163002	NUP35 PPI subnetwork	0.61
ENSG00000187266	EPOR PPI subnetwork	0.61
REACTOME_HOMOLOGOUS_RECOMBINATION_REPAIR	REACTOME_HOMOLOGOUS_RECOMBINATION_REPAIR	0.61
REACTOME_HOMOLOGOUS_RECOMBINATION_REPAIR_OF_REPLICATION:INDEP	REACTOME_HOMOLOGOUS_RECOMBINATION_REPAIR_OF_REPLICATION:INDEPEN	0.61
GO:0019200	carbohydrate kinase activity	0.61
ENSG00000085276	MECOM PPI subnetwork	0.61
ENSG00000187239	FNBP1 PPI subnetwork	0.61
GO:0006352	transcription initiation, DNA-dependent	0.61
ENSG00000109917	ZNF259 PPI subnetwork	0.61
MP:0002913	abnormal PNS synaptic transmission	0.61
ENSG00000113594	LIFR PPI subnetwork	0.61
MP:0000781	decreased corpus callosum size	0.61
GO:0006833	water transport	0.61
ENSG00000100285	NEFH PPI subnetwork	0.61
GO:0003746	translation elongation factor activity	0.61
ENSG00000125482	TTF1 PPI subnetwork	0.61
MP:0004799	increased susceptibility to experimental autoimmune encephalomyeliti	0.61
ENSG00000148468	FAM171A1 PPI subnetwork	0.61
ENSG00000112992	NNT PPI subnetwork	0.61
REACTOME_OLFACTORY_SIGNALING_PATHWAY	REACTOME_OLFACTORY_SIGNALING_PATHWAY	0.61
GO:0006821	chloride transport	0.61
MP:0003703	abnormal vestibulocochlear ganglion morphology	0.61
GO:0045076	regulation of interleukin-2 biosynthetic process	0.61
GO:0009069	serine family amino acid metabolic process	0.61
REACTOME_ORC1_REMOVAL_FROM_CHROMATIN	REACTOME_ORC1_REMOVAL_FROM_CHROMATIN	0.61
REACTOME_SWITCHING_OF_ORIGINS_TO_A_POST:REPLICATIVE_STATE	REACTOME_SWITCHING_OF_ORIGINS_TO_A_POST:REPLICATIVE_STATE	0.61
ENSG00000164742	ADCY1 PPI subnetwork	0.61
ENSG00000178409	BEND3 PPI subnetwork	0.61
REACTOME_CELL_CYCLE	REACTOME_CELL_CYCLE	0.61
ENSG00000198900	TOP1 PPI subnetwork	0.61
GO:2000146	negative regulation of cell motility	0.61
GO:0090066	regulation of anatomical structure size	0.61
ENSG00000170315	UBB PPI subnetwork	0.61
GO:0001673	male germ cell nucleus	0.61
REACTOME_REGULATION_OF_APOPTOSIS	REACTOME_REGULATION_OF_APOPTOSIS	0.61
MP:0001407	short stride length	0.61
ENSG00000119392	GLE1 PPI subnetwork	0.61
ENSG00000016402	IL20RA PPI subnetwork	0.61
MP:0011186	abnormal visceral endoderm morphology	0.61
MP:0000890	thin cerebellar molecular layer	0.61
GO:0000930	gamma-tubulin complex	0.61
ENSG00000110324	IL10RA PPI subnetwork	0.61
MP:0001340	abnormal eyelid morphology	0.61
ENSG00000173020	ADRBK1 PPI subnetwork	0.61
REACTOME_GAB1_SIGNALOSOME	REACTOME_GAB1_SIGNALOSOME	0.61
REACTOME_CYCLIN_AB1_ASSOCIATED_EVENTS_DURING_G2M_TRANSITION	REACTOME_CYCLIN_AB1_ASSOCIATED_EVENTS_DURING_G2M_TRANSITION	0.61
GO:0048008	platelet-derived growth factor receptor signaling pathway	0.61
ENSG00000167088	SNRPD1 PPI subnetwork	0.61
GO:0055013	cardiac muscle cell development	0.61

Original gene set ID	Original gene set description	Nominal P value
MP:0008705	increased interleukin-6 secretion	0.62
MP:0009434	paraparesis	0.62
ENSG00000076555	ACACB PPI subnetwork	0.62
KEGG_OLFACTORY_TRANSDUCTION	KEGG_OLFACTORY_TRANSDUCTION	0.62
ENSG00000112983	BRD8 PPI subnetwork	0.62
GO:0010883	regulation of lipid storage	0.62
ENSG00000175334	BANF1 PPI subnetwork	0.62
ENSG00000171560	FGA PPI subnetwork	0.62
MP:0002989	small kidney	0.62
ENSG00000138757	G3BP2 PPI subnetwork	0.62
MP:0008024	absent lymph nodes	0.62
MP:0002446	abnormal macrophage morphology	0.62
ENSG00000130725	UBE2M PPI subnetwork	0.62
REACTOME_NUCLEAR_IMPORT_OF_REV_PROTEIN	REACTOME_NUCLEAR_IMPORT_OF_REV_PROTEIN	0.62
MP:0001386	abnormal maternal nurturing	0.62
ENSG00000162594	IL23R PPI subnetwork	0.62
GO:0032272	negative regulation of protein polymerization	0.62
ENSG00000206281	TAPBP PPI subnetwork	0.62
ENSG00000112493	TAPBP PPI subnetwork	0.62
ENSG00000206208	TAPBP PPI subnetwork	0.62
ENSG00000186298	PPP1CC PPI subnetwork	0.62
MP:0000968	abnormal sensory neuron innervation pattern	0.62
REACTOME_AXON_GUIDANCE	REACTOME_AXON_GUIDANCE	0.62
GO:0048407	platelet-derived growth factor binding	0.62
REACTOME_PROLACTIN_RECEPTOR_SIGNALING	REACTOME_PROLACTIN_RECEPTOR_SIGNALING	0.62
MP:0004190	abnormal direction of embryo turning	0.62
ENSG00000023734	STRAP PPI subnetwork	0.62
GO:0031225	anchored to membrane	0.62
GO:0046906	tetrapyrrole binding	0.62
GO:0031272	regulation of pseudopodium assembly	0.62
MP:0001680	abnormal mesoderm development	0.62
MP:0000522	kidney cortex cysts	0.62
REACTOME_SPHINGOLIPID_DE_NOVO_BIOSYNTHESIS	REACTOME_SPHINGOLIPID_DE_NOVO_BIOSYNTHESIS	0.62
GO:0035567	non-canonical Wnt receptor signaling pathway	0.62
GO:0031513	nonmotile primary cilium	0.62
GO:0070603	SWI/SNF-type complex	0.62
ENSG00000140307	GTF2A2 PPI subnetwork	0.62
GO:0042462	eye photoreceptor cell development	0.62
REACTOME_POST_NMDA_RECEPTOR_ACTIVATION_EVENTS	REACTOME_POST_NMDA_RECEPTOR_ACTIVATION_EVENTS	0.62
GO:0000018	regulation of DNA recombination	0.62
GO:0072507	divalent inorganic cation homeostasis	0.62
MP:0000832	abnormal thalamus morphology	0.62
GO:0046782	regulation of viral transcription	0.62
MP:0008058	abnormal DNA repair	0.62
ENSG00000167414	GNG8 PPI subnetwork	0.62
ENSG00000092841	MYL6 PPI subnetwork	0.62
GO:0030425	dendrite	0.62
GO:0002063	chondrocyte development	0.62
GO:0048741	skeletal muscle fiber development	0.62

Original gene set ID	Original gene set description	Nominal P value
REACTOME_TRANSPORT_OF_GLUCCOSE_AND_OTHER_SUGARS_BILE_SALTS_ANI MP:0008533	REACTOME_TRANSPORT_OF_GLUCCOSE_AND_OTHER_SUGARS_BILE_SALTS_AND_O abnormal anterior visceral endoderm morphology	0.62
ENSG000000177542 MP:0003111	SLC25A22 PPI subnetwork abnormal cell nucleus morphology	0.62
MP:0004672	short ribs	0.62
ENSG000000116830 MP:0005545	TTF2 PPI subnetwork abnormal lens development	0.62
GO:0045622 MP:0000031	regulation of T-helper cell differentiatior abnormal cochlea morphology	0.62
GO:0032814	regulation of natural killer cell activation	0.62
MP:0004620	cervical vertebral fusion	0.62
GO:0044448	cell cortex part	0.62
GO:0030513	positive regulation of BMP signaling pathway	0.62
ENSG000000171453	POLR1C PPI subnetwork	0.62
REACTOME_RNA_POLYMERASE_III_TRANSCRIPTION_INITIATION_FROM_TYPE_3_Pf MP:0009814	REACTOME_RNA_POLYMERASE_III_TRANSCRIPTION_INITIATION_FROM_TYPE_3_Pf increased prostaglandin level	0.62
GO:0000084	S phase of mitotic cell cycle	0.62
GO:0047555	3',5'-cyclic-GMP phosphodiesterase activity	0.62
REACTOME_FACTORS_INVOLVED_IN_MEGAKARYOCYTE_DEVELOPMENT_AND_PLA GO:0002027	REACTOME_FACTORS_INVOLVED_IN_MEGAKARYOCYTE_DEVELOPMENT_AND_PLA regulation of heart rate	0.62
MP:0000430	absent maxillary shelf	0.62
GO:0006809	nitric oxide biosynthetic process	0.62
ENSG000000144908	ALDH1L1 PPI subnetwork	0.62
GO:0035136	forelimb morphogenesis	0.62
ENSG000000159023	EPB41 PPI subnetwork	0.62
ENSG000000169062	UPF3A PPI subnetwork	0.62
REACTOME_AUTODEGRADATION_OF_THE_E3_UBIQUITIN_LIGASE_COP1 ENSG000000083093	REACTOME_AUTODEGRADATION_OF_THE_E3_UBIQUITIN_LIGASE_COP1 PALB2 PPI subnetwork	0.63
ENSG000000120500	ARR3 PPI subnetwork	0.63
ENSG000000134001	EIF2S1 PPI subnetwork	0.63
REACTOME_DESTABILIZATION_OF_MRNA_BY_AUF1_HNRNP_D0 GO:0014032	REACTOME_DESTABILIZATION_OF_MRNA_BY_AUF1_HNRNP_D0 neural crest cell development	0.63
GO:0016591	DNA-directed RNA polymerase II, holoenzyme	0.63
GO:0071346	cellular response to interferon-gamma	0.63
GO:0014033	neural crest cell differentiation	0.63
MP:0004814	reduced linear vestibular evoked potentia	0.63
GO:0032722	positive regulation of chemokine production	0.63
ENSG000000139719	VPS33A PPI subnetwork	0.63
ENSG000000124334	IL9R PPI subnetwork	0.63
GO:0030330	DNA damage response, signal transduction by p53 class mediator	0.63
ENSG000000103152	MPG PPI subnetwork	0.63
ENSG000000126785	RHOJ PPI subnetwork	0.63
ENSG000000107263	RAPGEF1 PPI subnetwork	0.63
GO:0007091	mitotic metaphase/anaphase transition	0.63
GO:0003203	endocardial cushion morphogenesis	0.63
ENSG000000166900	STX3 PPI subnetwork	0.63
ENSG000000123562	MORF4L2 PPI subnetwork	0.63
MP:0001963	abnormal hearing physiology	0.63
MP:0004100	abnormal spinal cord interneuron morphology	0.63

Original gene set ID	Original gene set description	Nominal P value
ENSG00000158169	FANCC PPI subnetwork	0.63
MP:0004189	abnormal alveolar process morphology	0.63
KEGG_PENTOSE_AND_GLUCURONATE_INTERCONVERSIONS	KEGG_PENTOSE_AND_GLUCURONATE_INTERCONVERSIONS	0.63
ENSG00000005249	PRKAR2B PPI subnetwork	0.63
ENSG00000078369	GNB1 PPI subnetwork	0.63
ENSG00000088305	DNMT3B PPI subnetwork	0.63
ENSG00000176884	GRIN1 PPI subnetwork	0.63
GO:0006893	Golgi to plasma membrane transport	0.63
ENSG00000122966	CIT PPI subnetwork	0.63
ENSG00000137486	ARRB1 PPI subnetwork	0.63
REACTOME_REGULATION_OF_ACTIVATED_PAK:2P34_BY_PROTEASOME_MEDIATED	REACTOME_REGULATION_OF_ACTIVATED_PAK:2P34_BY_PROTEASOME_MEDIATED	0.63
GO:0031069	hair follicle morphogenesis	0.63
ENSG00000204390	HSPA1L PPI subnetwork	0.63
ENSG00000034713	GABARAPL2 PPI subnetwork	0.63
ENSG00000126351	THRA PPI subnetwork	0.63
GO:0051320	S phase	0.63
GO:0046849	bone remodeling	0.63
GO:0006376	mRNA splice site selection	0.63
GO:0016840	carbon-nitrogen lyase activity	0.63
ENSG00000106400	ZNHIT1 PPI subnetwork	0.63
ENSG00000167880	EVPL PPI subnetwork	0.63
GO:0015669	gas transport	0.63
GO:0044306	neuron projection terminus	0.63
GO:0060330	regulation of response to interferon-gamma	0.63
GO:0060334	regulation of interferon-gamma-mediated signaling pathway	0.63
GO:0070838	divalent metal ion transport	0.63
GO:0006302	double-strand break repair	0.63
ENSG00000113812	ACTR8 PPI subnetwork	0.63
REACTOME_REGULATION_OF_APCC_ACTIVATORS_BETWEEN_G1S_AND_EARLY	REACTOME_REGULATION_OF_APCC_ACTIVATORS_BETWEEN_G1S_AND_EARLY	0.63
MP:0008965	increased basal metabolism	0.63
MP:0001663	abnormal digestive system physiology	0.63
GO:0001539	ciliary or flagellar motility	0.63
ENSG00000025293	PHF20 PPI subnetwork	0.63
ENSG00000067900	ROCK1 PPI subnetwork	0.63
REACTOME_APC:CDC20_MEDIATED_DEGRADATION_OF_NEK2A	REACTOME_APC:CDC20_MEDIATED_DEGRADATION_OF_NEK2A	0.63
ENSG00000142684	ZNF593 PPI subnetwork	0.63
GO:0030336	negative regulation of cell migration	0.63
GO:0001947	heart looping	0.63
GO:0061371	determination of heart left/right asymmetry	0.63
MP:0002906	increased susceptibility to pharmacologically induced seizures	0.63
GO:0070979	protein K11-linked ubiquitination	0.63
ENSG00000103043	VAC14 PPI subnetwork	0.63
ENSG00000132002	DNAJB1 PPI subnetwork	0.63
GO:0048814	regulation of dendrite morphogenesis	0.63
ENSG00000172020	GAP43 PPI subnetwork	0.63
GO:0016209	antioxidant activity	0.63
ENSG00000113194	FAF2 PPI subnetwork	0.63
GO:0090103	cochlea morphogenesis	0.63
GO:0030101	natural killer cell activation	0.63

Original gene set ID

REACTOME_P53:DEPENDENT_G1S_DNA_DAMAGE_CHECKPOINT
 REACTOME_P53:DEPENDENT_G1_DNA_DAMAGE_RESPONSE
 REACTOME_PKB:MEDIATED_EVENTS
 ENSG00000077348
 ENSG00000152270
 GO:0034765
 MP:0002494
 ENSG00000100504
 ENSG00000130787
 REACTOME_SCF:BETA:TRCP_MEDIATED_DEGRADATION_OF_EMI1
 ENSG00000110448
 GO:0043623
 GO:0030137
 ENSG00000143771
 ENSG00000136108
 ENSG00000196084
 MP:0005269
 REACTOME_INTERLEUKIN:1_SIGNALING
 ENSG00000163918
 ENSG00000087258
 GO:0034220
 ENSG00000135945
 GO:0010950
 GO:0042267
 GO:0002228
 GO:0030125
 ENSG00000133706
 ENSG00000157916
 GO:0048754
 ENSG00000167085
 MP:0000885
 ENSG00000056558
 GO:0016861
 ENSG00000166851
 GO:0042734
 ENSG00000169139
 GO:0006575
 GO:0031970
 GO:0072503
 ENSG00000140694
 ENSG00000196510
 GO:0000049
 GO:0019751
 GO:0048871
 GO:0032660
 GO:0032620
 MP:0008027
 REACTOME_REGULATION_OF_GLUCOKINASE_BY_GLUCOKINASE_REGULATORY
 GO:0002699

Original gene set description

REACTOME_P53:DEPENDENT_G1S_DNA_DAMAGE_CHECKPOINT
 REACTOME_P53:DEPENDENT_G1_DNA_DAMAGE_RESPONSE
 REACTOME_PKB:MEDIATED_EVENTS
 EXOSC5 PPI subnetwork
 PDE3B PPI subnetwork
 regulation of ion transmembrane transport
 increased IgM level
 PYGL PPI subnetwork
 HIP1R PPI subnetwork
 REACTOME_SCF:BETA:TRCP_MEDIATED_DEGRADATION_OF_EMI1
 CD5 PPI subnetwork
 cellular protein complex assembly
 COPI-coated vesicle
 CNIH4 PPI subnetwork
 CKAP2 PPI subnetwork
 ENSG00000196084 PPI subnetwork
 abnormal occipital bone morphology
 REACTOME_INTERLEUKIN:1_SIGNALING
 RFC4 PPI subnetwork
 GNAO1 PPI subnetwork
 ion transmembrane transport
 REV1 PPI subnetwork
 positive regulation of endopeptidase activity
 natural killer cell mediated cytotoxicity
 natural killer cell mediated immunity
 clathrin vesicle coat
 LARS PPI subnetwork
 RER1 PPI subnetwork
 branching morphogenesis of a tube
 PHB PPI subnetwork
 ectopic Purkinje cell
 TRAF1 PPI subnetwork
 intramolecular oxidoreductase activity, interconverting aldoses and ketose:
 PLK1 PPI subnetwork
 presynaptic membrane
 UBE2V2 PPI subnetwork
 cellular modified amino acid metabolic process
 organelle envelope lumen
 cellular divalent inorganic cation homeostasis
 PARN PPI subnetwork
 ANAPC7 PPI subnetwork
 tRNA binding
 polyol metabolic process
 multicellular organismal homeostasis
 regulation of interleukin-17 production
 interleukin-17 production
 abnormal spinal cord white matter morphology
 REACTOME_REGULATION_OF_GLUCOKINASE_BY_GLUCOKINASE_REGULATORY_PR
 positive regulation of immune effector process

Nominal P value

0.63
 0.63
 0.63
 0.63
 0.63
 0.63
 0.63
 0.63
 0.63
 0.63
 0.63
 0.63
 0.63
 0.63
 0.63
 0.63
 0.63
 0.63
 0.63
 0.63
 0.63
 0.63
 0.63
 0.63
 0.63
 0.63
 0.63
 0.63
 0.63
 0.63
 0.63
 0.63
 0.63
 0.63
 0.63
 0.63
 0.63
 0.63
 0.63
 0.63
 0.63
 0.63
 0.63
 0.64
 0.64
 0.64
 0.64
 0.64
 0.64
 0.64
 0.64
 0.64
 0.64
 0.64
 0.64
 0.64
 0.64
 0.64
 0.64
 0.64
 0.64
 0.64
 0.64
 0.64
 0.64

Original gene set ID	Original gene set description	Nominal P value
GO:0016712	oxidoreductase activity, acting on paired donors, with incorporation or reduction of	0.64
ENSG00000214528	ENSG00000214528 PPI subnetwork	0.64
GO:0005758	mitochondrial intermembrane space	0.64
GO:0006900	membrane budding	0.64
GO:0010878	cholesterol storage	0.64
ENSG00000109103	UNC119 PPI subnetwork	0.64
GO:0019933	cAMP-mediated signaling	0.64
GO:0004889	acetylcholine-activated cation-selective channel activity	0.64
MP:0000371	diluted coat color	0.64
REACTOME_INTEGRATION_OF_ENERGY_METABOLISM	REACTOME_INTEGRATION_OF_ENERGY_METABOLISM	0.64
ENSG00000145623	OSMR PPI subnetwork	0.64
ENSG00000137070	IL11RA PPI subnetwork	0.64
GO:0016874	ligase activity	0.64
MP:0002102	abnormal ear morphology	0.64
GO:0090092	regulation of transmembrane receptor protein serine/threonine kinase signaling pat	0.64
KEGG_CHEMOKINE_SIGNALING_PATHWAY	KEGG_CHEMOKINE_SIGNALING_PATHWAY	0.64
GO:0042094	interleukin-2 biosynthetic process	0.64
GO:0009164	nucleoside catabolic process	0.64
GO:0021795	cerebral cortex cell migration	0.64
GO:0000780	condensed nuclear chromosome, centromeric region	0.64
GO:0045666	positive regulation of neuron differentiation	0.64
ENSG00000092853	CLSPN PPI subnetwork	0.64
ENSG00000129354	AP1M2 PPI subnetwork	0.64
ENSG00000141380	SS18 PPI subnetwork	0.64
GO:0002089	lens morphogenesis in camera-type eye	0.64
REACTOME_RNA_POLYMERASE_I_PROMOTER_ESCAPE	REACTOME_RNA_POLYMERASE_I_PROMOTER_ESCAPE	0.64
REACTOME_REGULATORY_RNA_PATHWAYS	REACTOME_REGULATORY_RNA_PATHWAYS	0.64
REACTOME_MICRORNA_MIRNA_BIOGENESIS	REACTOME_MICRORNA_MIRNA_BIOGENESIS	0.64
MP:0004765	decreased brainstem auditory evoked potentia	0.64
REACTOME_FORMATION_OF_TUBULIN_FOLDING_INTERMEDIATES_BY_CCTTRIC	REACTOME_FORMATION_OF_TUBULIN_FOLDING_INTERMEDIATES_BY_CCTTRIC	0.64
GO:0022890	inorganic cation transmembrane transporter activity	0.64
MP:0001297	microphthalmia	0.65
MP:0001183	overexpanded pulmonary alveoli	0.65
MP:0004046	abnormal mitosis	0.65
GO:0043204	perikaryon	0.65
ENSG00000143093	FAM40A PPI subnetwork	0.65
GO:0045667	regulation of osteoblast differentiation	0.65
GO:0001708	cell fate specification	0.65
GO:0007616	long-term memory	0.65
ENSG00000129465	RIPK3 PPI subnetwork	0.65
MP:0005558	decreased creatinine clearance	0.65
GO:0007501	mesodermal cell fate specification	0.65
ENSG00000007171	NOS2 PPI subnetwork	0.65
KEGG_VASCULAR_SMOOTH_MUSCLE_CONTRACTION	KEGG_VASCULAR_SMOOTH_MUSCLE_CONTRACTION	0.65
MP:0004324	vestibular hair cell degeneration	0.65
KEGG_ALLOGRAFT_REJECTION	KEGG_ALLOGRAFT_REJECTION	0.65
MP:0002023	B cell derived lymphoma	0.65
ENSG00000166592	RRAD PPI subnetwork	0.65
MP:0001783	decreased white adipose tissue amount	0.65

Original gene set ID	Original gene set description	Nominal P value
ENSG00000182520	ENSG00000182520 PPI subnetwork	0.65
MP:0000967	abnormal sensory neuron projections	0.66
GO:0051186	cofactor metabolic process	0.66
ENSG00000058668	ATP2B4 PPI subnetwork	0.66
ENSG00000161547	SRSF2 PPI subnetwork	0.66
MP:0004784	abnormal anterior cardinal vein morphology	0.66
ENSG00000096401	CDC5L PPI subnetwork	0.66
GO:0042026	protein refolding	0.66
ENSG00000163191	S100A11 PPI subnetwork	0.66
ENSG00000159113	ENSG00000159113 PPI subnetwork	0.66
REACTOME_APCCCDH1_MEDIATED_DEGRADATION_OF_CDC20_AND_OTHER_A	REACTOME_APCCCDH1_MEDIATED_DEGRADATION_OF_CDC20_AND_OTHER_APCC	0.66
ENSG00000139343	SNRPF PPI subnetwork	0.66
GO:0090102	cochlea development	0.66
GO:0008565	protein transporter activity	0.66
GO:0001664	G-protein coupled receptor binding	0.66
ENSG00000183691	NOG PPI subnetwork	0.66
GO:0019005	SCF ubiquitin ligase complex	0.66
GO:0042474	middle ear morphogenesis	0.66
ENSG000000004700	RECQL PPI subnetwork	0.66
REACTOME_PYRIMIDINE_METABOLISM	REACTOME_PYRIMIDINE_METABOLISM	0.66
MP:0003084	abnormal skeletal muscle fiber morphology	0.66
GO:0009952	anterior/posterior pattern specification	0.66
GO:0016072	rRNA metabolic process	0.66
GO:0031331	positive regulation of cellular catabolic process	0.66
ENSG00000127314	RAP1B PPI subnetwork	0.66
GO:0048839	inner ear development	0.66
GO:0050767	regulation of neurogenesis	0.66
ENSG00000125730	C3 PPI subnetwork	0.66
GO:0010035	response to inorganic substance	0.66
GO:0009615	response to virus	0.66
ENSG00000108883	EFTUD2 PPI subnetwork	0.66
GO:0018345	protein palmitoylation	0.66
MP:0002664	decreased circulating adrenocorticotropin level	0.66
ENSG00000112186	CAP2 PPI subnetwork	0.66
ENSG00000159459	UBR1 PPI subnetwork	0.66
ENSG00000131652	THOC6 PPI subnetwork	0.66
ENSG00000065548	ZC3H15 PPI subnetwork	0.66
GO:0009798	axis specification	0.66
ENSG00000027697	IFNGR1 PPI subnetwork	0.66
GO:0009314	response to radiation	0.66
GO:0000777	condensed chromosome kinetochore	0.66
MP:0002835	abnormal cranial suture morphology	0.66
MP:0005205	abnormal eye anterior chamber morphology	0.66
ENSG00000179950	PUF60 PPI subnetwork	0.66
GO:0071779	G1/S transition checkpoint	0.66
GO:0043087	regulation of GTPase activity	0.66
GO:0072372	primary cilium	0.66
GO:0001841	neural tube formation	0.66
ENSG00000169306	IL1RAPL1 PPI subnetwork	0.66

Original gene set ID	Original gene set description	Nominal P value
GO:0031072	heat shock protein binding	0.66
MP:0009456	impaired cued conditioning behavior	0.66
REACTOME_CRMP5_IN_SEMA3A_SIGNALING	REACTOME_CRMP5_IN_SEMA3A_SIGNALING	0.66
MP:0000154	rib fusion	0.66
GO:0007389	pattern specification process	0.66
MP:0008500	increased IgG2a level	0.66
ENSG00000165731	RET PPI subnetwork	0.66
GO:0010952	positive regulation of peptidase activity	0.66
GO:0021515	cell differentiation in spinal cord	0.66
GO:0002440	production of molecular mediator of immune response	0.66
ENSG00000136631	VPS45 PPI subnetwork	0.66
GO:0050873	brown fat cell differentiation	0.66
ENSG00000138190	EXOC6 PPI subnetwork	0.66
ENSG00000173744	AGFG1 PPI subnetwork	0.66
GO:0043073	germ cell nucleus	0.66
GO:0042552	myelination	0.66
ENSG00000069345	DNAJA2 PPI subnetwork	0.66
REACTOME_G_ALPHA_S_SIGNALLING_EVENTS	REACTOME_G_ALPHA_S_SIGNALLING_EVENTS	0.66
ENSG00000003436	TFPI PPI subnetwork	0.66
GO:0042044	fluid transport	0.66
ENSG00000138430	OLA1 PPI subnetwork	0.66
MP:0000194	hypercalcemia	0.66
GO:0000062	fatty-acyl-CoA binding	0.66
ENSG00000205220	PSMB10 PPI subnetwork	0.66
GO:0000038	very long-chain fatty acid metabolic process	0.66
GO:0018208	peptidyl-proline modification	0.66
GO:0032981	mitochondrial respiratory chain complex I assembly	0.66
GO:0097031	mitochondrial respiratory chain complex I biogenesis	0.66
GO:0010257	NADH dehydrogenase complex assembly	0.66
ENSG00000115561	CHMP3 PPI subnetwork	0.66
MP:0004022	abnormal cone electrophysiology	0.66
ENSG00000092199	HNRNPC PPI subnetwork	0.66
ENSG00000106070	GRB10 PPI subnetwork	0.66
GO:0007093	mitotic cell cycle checkpoint	0.66
ENSG00000072958	AP1M1 PPI subnetwork	0.66
ENSG00000142677	IL22RA1 PPI subnetwork	0.66
ENSG00000132361	KIAA0664 PPI subnetwork	0.66
MP:0011501	increased glomerular capsule space	0.66
ENSG00000103342	GSPT1 PPI subnetwork	0.66
GO:0030983	mismatched DNA binding	0.66
REACTOME_CELL:CELL_JUNCTION_ORGANIZATION	REACTOME_CELL:CELL_JUNCTION_ORGANIZATION	0.66
GO:0010171	body morphogenesis	0.66
MP:0006358	absent pinna reflex	0.66
ENSG00000088247	KHSRP PPI subnetwork	0.66
ENSG00000134871	COL4A2 PPI subnetwork	0.66
MP:0001463	abnormal spatial learning	0.66
GO:0031432	titin binding	0.66
GO:0008021	synaptic vesicle	0.66
GO:0015464	acetylcholine receptor activity	0.66

Original gene set ID	Original gene set description	Nominal P value
MP:0002703	abnormal renal tubule morphology	0.66
GO:0002062	chondrocyte differentiation	0.67
ENSG000000100644	HIF1A PPI subnetwork	0.67
GO:0051258	protein polymerization	0.67
ENSG000000114745	GORASP1 PPI subnetwork	0.67
ENSG000000144381	HSPD1 PPI subnetwork	0.67
GO:0009124	nucleoside monophosphate biosynthetic process	0.67
ENSG000000159128	IFNGR2 PPI subnetwork	0.67
GO:0000216	M/G1 transition of mitotic cell cycle	0.67
ENSG000000154277	UCHL1 PPI subnetwork	0.67
ENSG000000170624	SGCD PPI subnetwork	0.67
GO:0033151	V(D)J recombination	0.67
GO:0016254	preassembly of GPI anchor in ER membrane	0.67
ENSG000000151693	ASAP2 PPI subnetwork	0.67
GO:0030216	keratinocyte differentiation	0.67
MP:0002823	abnormal rib development	0.67
ENSG000000095261	PSMD5 PPI subnetwork	0.67
GO:0030041	actin filament polymerization	0.67
GO:0021903	rostrocaudal neural tube patterning	0.67
ENSG000000070831	CDC42 PPI subnetwork	0.67
ENSG000000165912	PACSIN3 PPI subnetwork	0.67
ENSG000000187741	FANCA PPI subnetwork	0.67
GO:0006766	vitamin metabolic process	0.67
GO:0070167	regulation of biomineral tissue development	0.67
GO:0051597	response to methylmercury	0.67
KEGG_TASTE_TRANSDUCTION	KEGG_TASTE_TRANSDUCTION	0.67
ENSG000000175582	RAB6A PPI subnetwork	0.67
KEGG_TYROSINE_METABOLISM	KEGG_TYROSINE_METABOLISM	0.67
GO:0048736	appendage development	0.67
GO:0060173	limb development	0.67
ENSG000000100380	ST13 PPI subnetwork	0.67
GO:0030663	COPI coated vesicle membrane	0.67
REACTOME_CDC20PHOSPHO:APCC_MEDIATED_DEGRADATION_OF_CYCLIN_A	REACTOME_CDC20PHOSPHO:APCC_MEDIATED_DEGRADATION_OF_CYCLIN_A	0.67
GO:0055074	calcium ion homeostasis	0.67
GO:0042471	ear morphogenesis	0.67
GO:0007067	mitosis	0.67
GO:0000280	nuclear division	0.67
ENSG000000186051	TAL2 PPI subnetwork	0.67
GO:0009066	aspartate family amino acid metabolic process	0.67
GO:0009950	dorsal/ventral axis specification	0.67
ENSG000000074800	ENO1 PPI subnetwork	0.67
GO:0016811	hydrolase activity, acting on carbon-nitrogen (but not peptide) bonds, in linear amid	0.67
MP:0000733	abnormal muscle development	0.67
GO:0007595	lactation	0.67
KEGG_AMINO_SUGAR_AND_NUCLEOTIDE_SUGAR_METABOLISM	KEGG_AMINO_SUGAR_AND_NUCLEOTIDE_SUGAR_METABOLISM	0.67
ENSG000000074211	PPP2R2C PPI subnetwork	0.67
ENSG000000147889	CDKN2A PPI subnetwork	0.67
MP:0001944	abnormal pancreas morphology	0.67
ENSG000000147684	NDUFB9 PPI subnetwork	0.67

Original gene set ID	Original gene set description	Nominal P value
ENSG00000068654	POLR1A PPI subnetwork	0.67
REACTOME_METABOLISM_OF_POLYAMINES	REACTOME_METABOLISM_OF_POLYAMINES	0.67
GO:0000087	M phase of mitotic cell cycle	0.67
GO:0007158	neuron cell-cell adhesion	0.67
GO:0032452	histone demethylase activity	0.67
GO:0046519	sphingoid metabolic process	0.67
MP:0002591	decreased mean corpuscular volume	0.67
ENSG00000120149	MSX2 PPI subnetwork	0.67
MP:0004772	abnormal bile secretion	0.67
GO:0032844	regulation of homeostatic process	0.67
MP:0002916	increased synaptic depression	0.67
MP:0004321	short sternum	0.67
ENSG00000172137	CALB2 PPI subnetwork	0.67
ENSG00000101400	SNTA1 PPI subnetwork	0.67
GO:0016597	amino acid binding	0.67
ENSG00000069248	NUP133 PPI subnetwork	0.67
REACTOME_G:PROTEIN_BETAGAMMA_SIGNALLING	REACTOME_G:PROTEIN_BETAGAMMA_SIGNALLING	0.67
GO:0005778	peroxisomal membrane	0.67
GO:0031903	microbody membrane	0.67
GO:0004950	chemokine receptor activity	0.67
GO:0001637	G-protein coupled chemoattractant receptor activity	0.67
ENSG00000137936	BCAR3 PPI subnetwork	0.67
GO:0051890	regulation of cardioblast differentiation	0.67
ENSG00000057608	GDI2 PPI subnetwork	0.67
GO:0035326	enhancer binding	0.67
GO:0060627	regulation of vesicle-mediated transport	0.67
MP:0003604	single kidney	0.67
REACTOME_SIGNALING_BY_EGFR_IN_CANCER	REACTOME_SIGNALING_BY_EGFR_IN_CANCER	0.67
GO:0001659	temperature homeostasis	0.67
ENSG00000076924	XAB2 PPI subnetwork	0.67
MP:0005344	increased circulating bilirubin level	0.67
ENSG00000082458	DLG3 PPI subnetwork	0.67
ENSG00000169016	E2F6 PPI subnetwork	0.67
GO:0005164	tumor necrosis factor receptor binding	0.67
GO:0000407	pre-autophagosomal structure	0.67
MP:0001176	abnormal lung development	0.67
GO:0000041	transition metal ion transport	0.67
GO:0007194	negative regulation of adenylate cyclase activity	0.67
GO:0031280	negative regulation of cyclase activity	0.67
ENSG00000055163	CYFIP2 PPI subnetwork	0.67
GO:0001707	mesoderm formation	0.67
GO:0030832	regulation of actin filament length	0.67
ENSG00000114942	EEF1B2 PPI subnetwork	0.67
ENSG00000094914	AAAS PPI subnetwork	0.67
GO:0002717	positive regulation of natural killer cell mediated immunity	0.67
GO:0045954	positive regulation of natural killer cell mediated cytotoxicity	0.67
ENSG00000123496	IL13RA2 PPI subnetwork	0.67
ENSG00000164485	IL22RA2 PPI subnetwork	0.67
ENSG00000103522	IL21R PPI subnetwork	0.67

Original gene set ID	Original gene set description	Nominal P value
ENSG00000076944	STXBP2 PPI subnetwork	0.67
MP:0008392	decreased primordial germ cell number	0.67
MP:0003921	abnormal heart left ventricle morphology	0.67
MP:0003446	renal hypoplasia	0.67
ENSG00000136603	SKIL PPI subnetwork	0.67
ENSG00000147162	OGT PPI subnetwork	0.67
GO:0048286	lung alveolus development	0.67
GO:0033003	regulation of mast cell activation	0.67
GO:0055007	cardiac muscle cell differentiation	0.67
REACTOME_STABILIZATION_OF_P53	REACTOME_STABILIZATION_OF_P53	0.67
MP:0003797	abnormal compact bone morphology	0.67
ENSG00000105204	DYRK1B PPI subnetwork	0.67
GO:0071214	cellular response to abiotic stimulus	0.67
REACTOME_NITRIC_OXIDE_STIMULATES_GUANYLATE_CYCLASE	REACTOME_NITRIC_OXIDE_STIMULATES_GUANYLATE_CYCLASE	0.67
REACTOME_POSTSYNAPTIC_NICOTINIC_ACETYLCHOLINE_RECEPTORS	REACTOME_POSTSYNAPTIC_NICOTINIC_ACETYLCHOLINE_RECEPTORS	0.67
REACTOME_ACETYLCHOLINE_BINDING_AND_DOWNSTREAM_EVENTS	REACTOME_ACETYLCHOLINE_BINDING_AND_DOWNSTREAM_EVENTS	0.67
REACTOME_ACTIVATION_OF_NICOTINIC_ACETYLCHOLINE_RECEPTORS	REACTOME_ACTIVATION_OF_NICOTINIC_ACETYLCHOLINE_RECEPTORS	0.67
GO:0003170	heart valve development	0.67
GO:0010817	regulation of hormone levels	0.67
REACTOME_REGULATION_OF_MRNA_STABILITY_BY_PROTEINS_THAT_BIND_AU	REACTOME_REGULATION_OF_MRNA_STABILITY_BY_PROTEINS_THAT_BIND_AU:RIK	0.67
ENSG00000104325	DECR1 PPI subnetwork	0.67
GO:0033124	regulation of GTP catabolic process	0.67
GO:0051350	negative regulation of lyase activity	0.67
KEGG_RENIN_ANGIOTENSIN_SYSTEM	KEGG_RENIN_ANGIOTENSIN_SYSTEM	0.67
GO:0010038	response to metal ion	0.67
ENSG00000163631	ALB PPI subnetwork	0.67
ENSG00000104897	SF3A2 PPI subnetwork	0.67
ENSG00000163806	SPDYA PPI subnetwork	0.67
MP:0004404	cochlear outer hair cell degeneration	0.67
REACTOME_PLATELET_ADHESION_TO_EXPOSED_COLLAGEN	REACTOME_PLATELET_ADHESION_TO_EXPOSED_COLLAGEN	0.67
GO:0030530	heterogeneous nuclear ribonucleoprotein complex	0.67
ENSG00000066117	SMARCD1 PPI subnetwork	0.67
GO:0008094	DNA-dependent ATPase activity	0.67
GO:0006013	mannose metabolic process	0.67
GO:0043200	response to amino acid stimulus	0.67
MP:0005553	increased circulating creatinine level	0.67
ENSG00000011052	NME2 PPI subnetwork	0.67
ENSG00000179051	RCC2 PPI subnetwork	0.68
MP:0001077	abnormal spinal nerve morphology	0.68
GO:0035107	appendage morphogenesis	0.68
GO:0035108	limb morphogenesis	0.68
GO:0005942	phosphatidylinositol 3-kinase complex	0.68
GO:0072384	organelle transport along microtubule	0.68
GO:0006520	cellular amino acid metabolic process	0.68
GO:0090068	positive regulation of cell cycle process	0.68
MP:0008498	decreased IgG3 level	0.68
ENSG00000182979	MTA1 PPI subnetwork	0.68
GO:0048285	organelle fission	0.68
ENSG00000101161	PRPF6 PPI subnetwork	0.68

Original gene set ID

REACTOME_PLATELET_HOMEOSTASIS

MP:0000752

GO:0045165

ENSG00000184486

GO:0008514

GO:0015672

GO:0045766

MP:0006359

ENSG00000150672

ENSG00000137076

ENSG00000153147

GO:0015804

ENSG00000173867

MP:0003059

GO:0007006

GO:0002763

ENSG00000072849

ENSG00000179036

GO:0016830

ENSG00000053900

GO:0072522

ENSG00000101199

ENSG00000171533

MP:0009766

ENSG00000136045

GO:0055001

ENSG00000143761

GO:0017144

MP:0000043

REACTOME_APCCDC20_MEDIATED_DEGRADATION_OF_SECURIN

ENSG00000197822

ENSG00000134852

GO:0001573

ENSG00000039537

ENSG00000213585

ENSG00000025770

ENSG00000146007

GO:0005741

GO:0006874

MP:0008410

MP:0002642

GO:0021543

REACTOME_EARLY_PHASE_OF_HIV_LIFE_CYCLE

REACTOME_CYCLIN_E_ASSOCIATED_EVENTS_DURING_G1S_TRANSITION

GO:0019320

REACTOME_LAGGING_STRAND_SYNTHESIS

REACTOME_DESTABILIZATION_OF_MRNA_BY_TRISTETRAPROLIN_TTP

ENSG00000167815

MP:0008535

Original gene set description

REACTOME_PLATELET_HOMEOSTASIS

dystrophic muscle

cell fate commitment

POU3F2 PPI subnetwork

organic anion transmembrane transporter activity

monovalent inorganic cation transport

positive regulation of angiogenesis

absent startle reflex

DLG2 PPI subnetwork

TLN1 PPI subnetwork

SMARCA5 PPI subnetwork

neutral amino acid transport

ENSG00000173867 PPI subnetwork

decreased insulin secretion

mitochondrial membrane organization

positive regulation of myeloid leukocyte differentiator

DERL2 PPI subnetwork

ENSG00000179036 PPI subnetwork

carbon-carbon lyase activity

ANAPC4 PPI subnetwork

purine-containing compound biosynthetic process

ARFGAP1 PPI subnetwork

MAP6 PPI subnetwork

increased sensitivity to xenobiotic induced morbidity/mortality

PWP1 PPI subnetwork

muscle cell development

ARF1 PPI subnetwork

drug metabolic process

organ of Corti degeneration

REACTOME_APCCDC20_MEDIATED_DEGRADATION_OF_SECURIN

OCLN PPI subnetwork

CLOCK PPI subnetwork

ganglioside metabolic process

C6 PPI subnetwork

VDAC1 PPI subnetwork

NCAPH2 PPI subnetwork

ZMAT2 PPI subnetwork

mitochondrial outer membrane

cellular calcium ion homeostasis

increased cellular sensitivity to ultraviolet irradiation

anisocytosis

pallium development

REACTOME_EARLY_PHASE_OF_HIV_LIFE_CYCLE

REACTOME_CYCLIN_E_ASSOCIATED_EVENTS_DURING_G1S_TRANSITION

hexose catabolic process

REACTOME_LAGGING_STRAND_SYNTHESIS

REACTOME_DESTABILIZATION_OF_MRNA_BY_TRISTETRAPROLIN_TTP

PRDX2 PPI subnetwork

enlarged lateral ventricles

Nominal P value

0.68

0.68

0.68

0.68

0.68

0.68

0.68

0.68

0.68

0.68

0.68

0.68

0.68

0.68

0.68

0.68

0.68

0.68

0.68

0.68

0.68

0.68

0.68

0.68

0.68

0.68

0.68

0.68

0.68

0.68

0.68

0.68

0.68

0.68

0.68

0.68

0.68

0.68

0.68

0.68

0.68

0.68

0.68

0.68

0.68

0.68

0.68

0.68

0.68

Original gene set ID	Original gene set description	Nominal P value
GO:0043648	dicarboxylic acid metabolic process	0.68
ENSG00000140795	MYLK3 PPI subnetwork	0.68
GO:0030512	negative regulation of transforming growth factor beta receptor signaling pathway	0.68
ENSG00000133243	BTBD2 PPI subnetwork	0.68
GO:0015077	monovalent inorganic cation transmembrane transporter activity	0.68
GO:0003151	outflow tract morphogenesis	0.68
ENSG000000085840	ORC1 PPI subnetwork	0.68
GO:0009123	nucleoside monophosphate metabolic process	0.68
ENSG00000130204	TOMM40 PPI subnetwork	0.68
ENSG00000120708	TGFBI PPI subnetwork	0.68
ENSG00000165392	WRN PPI subnetwork	0.68
ENSG00000081985	IL12RB2 PPI subnetwork	0.68
ENSG00000175029	CTBP2 PPI subnetwork	0.68
MP:0002813	microcytosis	0.68
GO:0019898	extrinsic to membrane	0.68
ENSG00000206267	ENSG00000206267 PPI subnetwork	0.68
ENSG00000204351	SKIV2L PPI subnetwork	0.68
ENSG00000076242	MLH1 PPI subnetwork	0.68
ENSG00000076554	TPD52 PPI subnetwork	0.68
ENSG00000006451	RALA PPI subnetwork	0.68
GO:0007076	mitotic chromosome condensation	0.68
GO:0033762	response to glucagon stimulus	0.68
ENSG00000173805	HAP1 PPI subnetwork	0.68
ENSG00000206495	TRIM39 PPI subnetwork	0.68
ENSG00000206419	ENSG00000206419 PPI subnetwork	0.68
ENSG00000204599	TRIM39 PPI subnetwork	0.68
GO:0019905	syntaxin binding	0.68
GO:0061351	neural precursor cell proliferation	0.68
ENSG00000079950	STX7 PPI subnetwork	0.68
MP:0000242	impaired fertilization	0.68
REACTOME_GABA_RECEPTOR_ACTIVATION	REACTOME_GABA_RECEPTOR_ACTIVATION	0.68
ENSG00000206407	ENSG00000206407 PPI subnetwork	0.68
ENSG00000204569	PPP1R10 PPI subnetwork	0.68
ENSG00000206489	PPP1R10 PPI subnetwork	0.68
GO:0006266	DNA ligation	0.68
GO:2000179	positive regulation of neural precursor cell proliferati	0.68
GO:0044439	peroxisomal part	0.69
GO:0044438	microbody part	0.69
MP:0002626	increased heart rate	0.69
ENSG00000007392	LUC7L PPI subnetwork	0.69
GO:0060562	epithelial tube morphogenesis	0.69
ENSG00000101811	CSTF2 PPI subnetwork	0.69
ENSG00000121741	ZMYM2 PPI subnetwork	0.69
GO:0009896	positive regulation of catabolic process	0.69
GO:0031341	regulation of cell killing	0.69
GO:0005759	mitochondrial matrix	0.69
GO:0030659	cytoplasmic vesicle membrane	0.69
ENSG00000131724	IL13RA1 PPI subnetwork	0.69
KEGG_GLUTATHIONE_METABOLISM	KEGG_GLUTATHIONE_METABOLISM	0.69

Original gene set ID	Original gene set description	Nominal P value
MP:0008663	increased interleukin-12 secretion	0.69
ENSG00000173418	NAA20 PPI subnetwork	0.69
GO:0010573	vascular endothelial growth factor production	0.69
GO:0010574	regulation of vascular endothelial growth factor productior	0.69
ENSG00000206353	SKIV2L PPI subnetwork	0.69
ENSG00000138814	PPP3CA PPI subnetwork	0.69
MP:0004096	abnormal midbrain-hindbrain boundary development	0.69
GO:0009880	embryonic pattern specification	0.69
ENSG00000127616	SMARCA4 PPI subnetwork	0.69
ENSG00000153046	CDYL PPI subnetwork	0.69
MP:0006036	abnormal mitochondrial physiology	0.69
GO:0007214	gamma-aminobutyric acid signaling pathway	0.69
GO:0021987	cerebral cortex development	0.69
MP:0005608	cardiac interstitial fibrosis	0.69
MP:0004532	abnormal inner hair cell stereociliary bundle morphology	0.69
ENSG00000079102	RUNX1T1 PPI subnetwork	0.69
GO:0042490	mechanoreceptor differentiation	0.69
GO:0016045	detection of bacterium	0.69
GO:0015985	energy coupled proton transport, down electrochemical gradient	0.69
GO:0015986	ATP synthesis coupled proton transport	0.69
MP:0002797	increased thigmotaxis	0.69
GO:0055003	cardiac myofibril assembly	0.69
KEGG_O_GLYCAN_BIOSYNTHESIS	KEGG_O_GLYCAN_BIOSYNTHESIS	0.69
ENSG00000011304	PTBP1 PPI subnetwork	0.69
ENSG00000130177	CDC16 PPI subnetwork	0.69
GO:0051247	positive regulation of protein metabolic proces	0.69
GO:0048596	embryonic camera-type eye morphogenesis	0.69
MP:0005318	decreased triglyceride level	0.69
ENSG000000091129	NRCAM PPI subnetwork	0.69
ENSG00000112062	MAPK14 PPI subnetwork	0.69
ENSG00000156374	PCGF6 PPI subnetwork	0.69
ENSG00000142192	APP PPI subnetwork	0.69
ENSG00000116754	SRSF11 PPI subnetwork	0.69
ENSG00000173598	NUDT4 PPI subnetwork	0.69
GO:0030833	regulation of actin filament polymerization	0.69
GO:0060560	developmental growth involved in morphogenesis	0.69
ENSG000000005156	LIG3 PPI subnetwork	0.69
ENSG00000124422	USP22 PPI subnetwork	0.69
MP:0005403	abnormal nerve conduction	0.69
ENSG00000178896	EXOSC4 PPI subnetwork	0.69
ENSG00000132535	DLG4 PPI subnetwork	0.69
GO:0045649	regulation of macrophage differentiation	0.69
GO:0090307	spindle assembly involved in mitosis	0.69
GO:0043279	response to alkaloid	0.69
MP:0000432	abnormal head morphology	0.69
REACTOME_AUTODEGRADATION_OF_CDH1_BY_CDH1APCC	REACTOME_AUTODEGRADATION_OF_CDH1_BY_CDH1APCC	0.69
ENSG00000172943	PHF8 PPI subnetwork	0.69
GO:0031674	I band	0.69
ENSG00000139436	GIT2 PPI subnetwork	0.69

Original gene set ID	Original gene set description	Nominal P value
ENSG00000029363	BCLAF1 PPI subnetwork	0.69
GO:0010575	positive regulation vascular endothelial growth factor productior	0.69
ENSG000000130382	MLLT1 PPI subnetwork	0.69
ENSG000000177733	HNRNPA0 PPI subnetwork	0.69
ENSG000000111802	TDP2 PPI subnetwork	0.69
ENSG000000157601	MX1 PPI subnetwork	0.69
ENSG000000141959	PFKL PPI subnetwork	0.69
GO:0030018	Z disc	0.69
MP:0006264	decreased systemic arterial systolic blood pressure	0.69
GO:0021885	forebrain cell migration	0.69
ENSG000000139842	CUL4A PPI subnetwork	0.69
GO:0006898	receptor-mediated endocytosis	0.69
MP:0005026	decreased susceptibility to parasitic infectior	0.69
ENSG000000164418	GRIK2 PPI subnetwork	0.69
ENSG000000094631	HDAC6 PPI subnetwork	0.69
GO:0005892	acetylcholine-gated channel complex	0.69
GO:0044440	endosomal part	0.69
ENSG000000117748	RPA2 PPI subnetwork	0.69
ENSG000000164611	PTTG1 PPI subnetwork	0.69
GO:0035064	methylated histone residue binding	0.69
MP:0002914	abnormal endplate potential	0.69
ENSG000000138795	LEF1 PPI subnetwork	0.69
GO:0010810	regulation of cell-substrate adhesion	0.69
MP:0000748	progressive muscle weakness	0.69
MP:0002929	abnormal bile duct development	0.69
GO:0048485	sympathetic nervous system development	0.69
GO:0034703	cation channel complex	0.69
ENSG000000067225	PKM2 PPI subnetwork	0.69
ENSG000000142453	CARM1 PPI subnetwork	0.69
REACTOME_PIP3_ACTIVATES_AKT_SIGNALING	REACTOME_PIP3_ACTIVATES_AKT_SIGNALING	0.69
GO:0045921	positive regulation of exocytosis	0.69
GO:0016747	transferase activity, transferring acyl groups other than amino-acyl group:	0.69
MP:0000279	ventricular hypoplasia	0.69
MP:0005298	abnormal clavicle morphology	0.69
ENSG000000108344	PSMD3 PPI subnetwork	0.69
GO:0061041	regulation of wound healing	0.69
MP:0004355	short radius	0.69
MP:0005166	decreased susceptibility to injury	0.69
GO:0046320	regulation of fatty acid oxidation	0.69
MP:0008687	increased interleukin-2 secretion	0.69
MP:0003632	abnormal nervous system morphology	0.69
GO:0051480	cytosolic calcium ion homeostasis	0.69
KEGG_MISMATCH_REPAIR	KEGG_MISMATCH_REPAIR	0.69
ENSG000000185345	PARK2 PPI subnetwork	0.69
GO:0045686	negative regulation of glial cell differentiator	0.69
REACTOME_TRANSPORT_OF_RIBONUCLEOPROTEINS_INTO_THE_HOST_NUCLEI	REACTOME_TRANSPORT_OF_RIBONUCLEOPROTEINS_INTO_THE_HOST_NUCLEUS	0.69
ENSG000000117318	ID3 PPI subnetwork	0.69
GO:0046651	lymphocyte proliferation	0.69
ENSG000000166206	GABRB3 PPI subnetwork	0.7

Original gene set ID	Original gene set description	Nominal P value
GO:0006919	activation of cysteine-type endopeptidase activity involved in apoptotic proces:	0.7
GO:0002052	positive regulation of neuroblast proliferati	0.7
GO:0046635	positive regulation of alpha-beta T cell activation	0.7
GO:0030278	regulation of ossification	0.7
ENSG00000080503	SMARCA2 PPI subnetwork	0.7
ENSG00000175203	DCTN2 PPI subnetwork	0.7
ENSG00000118495	PLAGL1 PPI subnetwork	0.7
GO:0050830	defense response to Gram-positive bacterium	0.7
GO:0032570	response to progesterone stimulus	0.7
GO:0042451	purine nucleoside biosynthetic process	0.7
GO:0042455	ribonucleoside biosynthetic process	0.7
GO:0046129	purine ribonucleoside biosynthetic process	0.7
ENSG00000173465	SSSCA1 PPI subnetwork	0.7
GO:0022836	gated channel activity	0.7
ENSG00000168005	C11orf84 PPI subnetwork	0.7
GO:0015459	potassium channel regulator activity	0.7
ENSG00000039068	CDH1 PPI subnetwork	0.7
GO:0002495	antigen processing and presentation of peptide antigen via MHC class I	0.7
REACTOME_DAG_AND_IP3_SIGNALING	REACTOME_DAG_AND_IP3_SIGNALING	0.7
ENSG00000136026	CKAP4 PPI subnetwork	0.7
ENSG00000112640	PPP2R5D PPI subnetwork	0.7
ENSG00000145332	KLHL8 PPI subnetwork	0.7
GO:0051146	striated muscle cell differentiation	0.7
ENSG00000142945	KIF2C PPI subnetwork	0.7
ENSG00000148180	GSN PPI subnetwork	0.7
ENSG00000107295	SH3GL2 PPI subnetwork	0.7
ENSG00000059378	PARP12 PPI subnetwork	0.7
GO:0048488	synaptic vesicle endocytosis	0.7
ENSG00000163440	PDCL2 PPI subnetwork	0.7
MP:0005542	corneal vascularization	0.7
ENSG00000173702	MUC13 PPI subnetwork	0.7
ENSG00000186879	ENSG00000186879 PPI subnetwork	0.7
GO:0050829	defense response to Gram-negative bacterium	0.7
GO:2000736	regulation of stem cell differentiation	0.7
GO:0030516	regulation of axon extension	0.7
GO:0051301	cell division	0.7
GO:0006942	regulation of striated muscle contraction	0.7
GO:0004112	cyclic-nucleotide phosphodiesterase activity	0.7
MP:0005333	decreased heart rate	0.7
GO:0022029	telencephalon cell migration	0.7
MP:0001924	infertility	0.7
MP:0011228	abnormal vitamin D level	0.7
ENSG00000147130	ZMYM3 PPI subnetwork	0.7
ENSG00000082258	CCNT2 PPI subnetwork	0.7
GO:0009416	response to light stimulus	0.7
REACTOME_AQUAPORIN:MEDIATED_TRANSPORT	REACTOME_AQUAPORIN:MEDIATED_TRANSPORT	0.7
MP:0004113	abnormal aortic arch morphology	0.7
MP:0004398	cochlear inner hair cell degeneration	0.7
MP:0004505	decreased renal glomerulus number	0.7

Original gene set ID	Original gene set description	Nominal P value
GO:0007187	G-protein coupled receptor signaling pathway, coupled to cyclic nucleotide second r	0.7
GO:0032039	integrator complex	0.7
ENSG000000128340	RAC2 PPI subnetwork	0.7
GO:0003001	generation of a signal involved in cell-cell signaling	0.7
GO:0023061	signal release	0.7
MP:0008502	increased IgG3 level	0.7
GO:0000421	autophagic vacuole membrane	0.7
GO:0014014	negative regulation of gliogenesis	0.7
MP:0002492	decreased IgE level	0.7
ENSG000000132182	NUP210 PPI subnetwork	0.7
MP:0002663	failure to form blastocele	0.7
GO:0031575	mitotic cell cycle G1/S transition checkpoint	0.7
GO:0046488	phosphatidylinositol metabolic process	0.7
ENSG000000196911	KPNA5 PPI subnetwork	0.7
MP:0001426	polydipsia	0.7
ENSG000000148229	POLE3 PPI subnetwork	0.7
ENSG000000183684	ALYREF PPI subnetwork	0.7
KEGG_BASE_EXCISION_REPAIR	KEGG_BASE_EXCISION_REPAIR	0.7
GO:0051960	regulation of nervous system development	0.7
REACTOME_ASSOCIATION_OF_LICENSING_FACTORS_WITH_THE_PRE:REPLICAT	REACTOME_ASSOCIATION_OF_LICENSING_FACTORS_WITH_THE_PRE:REPLICATIVE_	0.7
MP:0006030	abnormal otic vesicle development	0.7
ENSG000000166971	AKTIP PPI subnetwork	0.7
REACTOME_SIGNALING_BY_PDGF	REACTOME_SIGNALING_BY_PDGF	0.7
MP:0008181	increased marginal zone B cell number	0.7
GO:0010874	regulation of cholesterol efflux	0.7
ENSG000000085063	CD59 PPI subnetwork	0.7
GO:0008076	voltage-gated potassium channel complex	0.7
GO:0034705	potassium channel complex	0.7
GO:0035137	hindlimb morphogenesis	0.7
GO:0014048	regulation of glutamate secretion	0.7
ENSG000000163875	MEAF6 PPI subnetwork	0.7
ENSG000000156299	TIAM1 PPI subnetwork	0.7
ENSG000000188229	TUBB4B PPI subnetwork	0.7
GO:0060415	muscle tissue morphogenesis	0.7
ENSG000000100368	CSF2RB PPI subnetwork	0.7
ENSG000000134717	BTF3L4 PPI subnetwork	0.7
KEGG_DILATED_CARDIOMYOPATHY	KEGG_DILATED_CARDIOMYOPATHY	0.7
GO:0008234	cysteine-type peptidase activity	0.7
GO:0045216	cell-cell junction organization	0.7
MP:0008734	decreased susceptibility to endotoxin shock	0.7
ENSG000000103343	ZNF174 PPI subnetwork	0.7
ENSG000000120875	DUSP4 PPI subnetwork	0.7
MP:0002941	increased circulating alanine transaminase leve	0.7
GO:0009791	post-embryonic development	0.7
GO:0050804	regulation of synaptic transmission	0.7
GO:0030136	clathrin-coated vesicle	0.7
GO:0050994	regulation of lipid catabolic process	0.7
ENSG000000013561	RNF14 PPI subnetwork	0.7
GO:0030808	regulation of nucleotide biosynthetic process	0.7

Original gene set ID	Original gene set description	Nominal P value
GO:0030802	regulation of cyclic nucleotide biosynthetic process	0.7
MP:0000480	increased rib number	0.7
ENSG000000127588	GNG13 PPI subnetwork	0.7
GO:0033116	endoplasmic reticulum-Golgi intermediate compartment membrane	0.7
ENSG000000126226	PCID2 PPI subnetwork	0.7
GO:0032642	regulation of chemokine production	0.7
REACTOME_SIGNALING_BY_EGFR	REACTOME_SIGNALING_BY_EGFR	0.7
GO:0032943	mononuclear cell proliferation	0.7
GO:0030162	regulation of proteolysis	0.7
GO:0008154	actin polymerization or depolymerization	0.7
REACTOME_DCC_MEDIATED_ATTRACTIVE_SIGNALING	REACTOME_DCC_MEDIATED_ATTRACTIVE_SIGNALING	0.71
REACTOME_RNA_POLYMERASE_I_TRANSCRIPTION	REACTOME_RNA_POLYMERASE_I_TRANSCRIPTION	0.71
MP:0000520	absent kidney	0.71
REACTOME_POTASSIUM_CHANNELS	REACTOME_POTASSIUM_CHANNELS	0.71
GO:0048486	parasympathetic nervous system development	0.71
GO:0005884	actin filament	0.71
ENSG000000173120	KDM2A PPI subnetwork	0.71
REACTOME_G1S_TRANSITION	REACTOME_G1S_TRANSITION	0.71
GO:0006007	glucose catabolic process	0.71
MP:0002608	increased hematocrit	0.71
GO:0010720	positive regulation of cell development	0.71
GO:0030521	androgen receptor signaling pathway	0.71
GO:0072531	pyrimidine-containing compound transmembrane transport	0.71
KEGG_B_CELL_RECEPTOR_SIGNALING_PATHWAY	KEGG_B_CELL_RECEPTOR_SIGNALING_PATHWAY	0.71
MP:0000823	abnormal lateral ventricle morphology	0.71
MP:0002910	abnormal excitatory postsynaptic currents	0.71
REACTOME_GAP:FILLING_DNA_REPAIR_SYNTHESIS_AND_LIGATION_IN_TC:NER	REACTOME_GAP:FILLING_DNA_REPAIR_SYNTHESIS_AND_LIGATION_IN_TC:NER	0.71
REACTOME_GAP:FILLING_DNA_REPAIR_SYNTHESIS_AND_LIGATION_IN_GG:NEF	REACTOME_GAP:FILLING_DNA_REPAIR_SYNTHESIS_AND_LIGATION_IN_GG:NER	0.71
ENSG000000104164	PLDN PPI subnetwork	0.71
ENSG000000102312	PORCN PPI subnetwork	0.71
MP:0005176	eyelids fail to open	0.71
ENSG000000122585	NPY PPI subnetwork	0.71
REACTOME_TAT:MEDIATED_HIV:1_ELONGATION_ARREST_AND_RECOVERY	REACTOME_TAT:MEDIATED_HIV:1_ELONGATION_ARREST_AND_RECOVERY	0.71
REACTOME_PAUSING_AND_RECOVERY_OF_TAT:MEDIATED_HIV:1_ELONGATIO	REACTOME_PAUSING_AND_RECOVERY_OF_TAT:MEDIATED_HIV:1_ELONGATION	0.71
GO:0000776	kinetochore	0.71
ENSG000000111664	GNB3 PPI subnetwork	0.71
MP:0008034	enhanced lipolysis	0.71
GO:0002237	response to molecule of bacterial origin	0.71
GO:0004536	deoxyribonuclease activity	0.71
ENSG000000163017	ACTG2 PPI subnetwork	0.71
GO:0060048	cardiac muscle contraction	0.71
GO:0009410	response to xenobiotic stimulus	0.71
GO:0071466	cellular response to xenobiotic stimulus	0.71
ENSG000000164105	SAP30 PPI subnetwork	0.71
GO:0016042	lipid catabolic process	0.71
GO:0032496	response to lipopolysaccharide	0.71
GO:0012506	vesicle membrane	0.71
ENSG000000152413	HOMER1 PPI subnetwork	0.71
REACTOME_G_ALPHA_Q_SIGNALLING_EVENTS	REACTOME_G_ALPHA_Q_SIGNALLING_EVENTS	0.71

Original gene set ID	Original gene set description	Nominal P value
GO:0045777	positive regulation of blood pressure	0.72
REACTOME_PRESYNAPTIC_NICOTINIC_ACETYLCHOLINE_RECEPTORS	REACTOME_PRESYNAPTIC_NICOTINIC_ACETYLCHOLINE_RECEPTORS	0.72
ENSG00000137403	HLA-F PPI subnetwork	0.72
ENSG00000213066	FGFR1OP PPI subnetwork	0.72
ENSG00000157766	ACAN PPI subnetwork	0.72
GO:0032451	demethylase activity	0.72
REACTOME_CROSS:PRESENTATION_OF_SOLUBLE_EXOGENOUS_ANTIGENS_ENDOSOMAL_PATHWAY	REACTOME_CROSS:PRESENTATION_OF_SOLUBLE_EXOGENOUS_ANTIGENS_ENDOSOMAL_PATHWAY	0.72
ENSG00000120837	NFYB PPI subnetwork	0.72
GO:0000226	microtubule cytoskeleton organization	0.72
GO:0051145	smooth muscle cell differentiation	0.72
ENSG00000111052	LIN7A PPI subnetwork	0.72
ENSG00000151247	EIF4E PPI subnetwork	0.72
ENSG00000130640	TUBGCP2 PPI subnetwork	0.72
GO:0010001	glial cell differentiation	0.72
MP:0005587	abnormal Meckel's cartilage morphology	0.72
GO:0015074	DNA integration	0.72
GO:0048715	negative regulation of oligodendrocyte differentiation	0.72
ENSG00000164975	SNAPC3 PPI subnetwork	0.72
ENSG00000158290	CUL4B PPI subnetwork	0.72
ENSG00000125743	SNRPD2 PPI subnetwork	0.72
ENSG00000138685	FGF2 PPI subnetwork	0.72
GO:0006364	rRNA processing	0.72
GO:0042092	type 2 immune response	0.72
REACTOME_RNA_POLYMERASE_I_PROMOTER_OPENING	REACTOME_RNA_POLYMERASE_I_PROMOTER_OPENING	0.72
GO:0033180	proton-transporting V-type ATPase, V1 domain	0.72
GO:0030509	BMP signaling pathway	0.72
GO:0035115	embryonic forelimb morphogenesis	0.72
ENSG00000115594	IL1R1 PPI subnetwork	0.72
GO:0048747	muscle fiber development	0.72
GO:0010744	positive regulation of macrophage derived foam cell differentiation	0.72
MP:0002196	absent corpus callosum	0.72
REACTOME_SYNTHESIS_SECRETION_AND_INACTIVATION_OF_GLUCAGON:LIKE_PEP_TIDES	REACTOME_SYNTHESIS_SECRETION_AND_INACTIVATION_OF_GLUCAGON:LIKE_PEP_TIDES	0.72
REACTOME_INCRETIN_SYNTHESIS_SECRETION_AND_INACTIVATION	REACTOME_INCRETIN_SYNTHESIS_SECRETION_AND_INACTIVATION	0.72
GO:0006643	membrane lipid metabolic process	0.72
MP:0001921	reduced fertility	0.72
GO:0010463	mesenchymal cell proliferation	0.72
MP:0001685	abnormal endoderm development	0.72
ENSG00000104388	RAB2A PPI subnetwork	0.72
MP:0001065	abnormal trigeminal nerve morphology	0.72
ENSG00000104320	NBN PPI subnetwork	0.72
MP:0005656	decreased aggression	0.72
ENSG00000215902	ENSG00000215902 PPI subnetwork	0.72
REACTOME_G:PROTEIN_MEDIATED_EVENTS	REACTOME_G:PROTEIN_MEDIATED_EVENTS	0.72
ENSG00000137672	TRPC6 PPI subnetwork	0.72
GO:0009190	cyclic nucleotide biosynthetic process	0.72
GO:0010833	telomere maintenance via telomere lengthening	0.72
MP:0001701	incomplete embryo turning	0.72
GO:0046365	monosaccharide catabolic process	0.72
ENSG00000149782	PLCB3 PPI subnetwork	0.72

Original gene set ID	Original gene set description	Nominal P value
GO:0008080	N-acetyltransferase activity	0.72
MP:0003354	astrocytosis	0.72
GO:0007041	lysosomal transport	0.72
ENSG00000082898	XPO1 PPI subnetwork	0.72
GO:0030119	AP-type membrane coat adaptor complex	0.72
GO:0090277	positive regulation of peptide hormone secretior	0.72
ENSG00000106399	RPA3 PPI subnetwork	0.72
ENSG00000164867	NOS3 PPI subnetwork	0.72
ENSG00000177700	POLR2L PPI subnetwork	0.72
ENSG00000079805	DNM2 PPI subnetwork	0.72
ENSG00000113196	HAND1 PPI subnetwork	0.72
ENSG00000104879	CKM PPI subnetwork	0.72
GO:0007492	endoderm development	0.72
ENSG00000110148	CCKBR PPI subnetwork	0.72
ENSG00000033050	ABCF2 PPI subnetwork	0.72
GO:0072132	mesenchyme morphogenesis	0.72
MP:0002020	increased tumor incidence	0.72
REACTOME_PROCESSIVE_SYNTHESIS_ON_THE_C:STRAND_OF_THE_TELOMERE	REACTOME_PROCESSIVE_SYNTHESIS_ON_THE_C:STRAND_OF_THE_TELOMERE	0.72
GO:0031406	carboxylic acid binding	0.72
GO:0031901	early endosome membrane	0.72
ENSG00000153767	GTF2E1 PPI subnetwork	0.72
ENSG00000118491	C6orf94 PPI subnetwork	0.72
ENSG00000181789	COPG PPI subnetwork	0.72
GO:0004549	tRNA-specific ribonuclease activity	0.72
ENSG00000024048	UBR2 PPI subnetwork	0.72
GO:0021532	neural tube patterning	0.72
MP:0003070	increased vascular permeability	0.72
GO:0008589	regulation of smoothened signaling pathway	0.72
ENSG00000100836	PABPN1 PPI subnetwork	0.72
GO:0030199	collagen fibril organization	0.72
REACTOME_RNA_POLYMERASE_I_PROMOTER_CLEARANCE	REACTOME_RNA_POLYMERASE_I_PROMOTER_CLEARANCE	0.72
GO:0032602	chemokine production	0.72
MP:0005165	increased susceptibility to injury	0.72
ENSG00000104626	ERI1 PPI subnetwork	0.72
MP:0001566	hyperphosphatemia	0.73
GO:0043679	axon terminus	0.73
GO:2000677	regulation of transcription regulatory region DNA binding	0.73
GO:0032319	regulation of Rho GTPase activity	0.73
ENSG00000204086	RPA4 PPI subnetwork	0.73
ENSG00000113318	MSH3 PPI subnetwork	0.73
ENSG00000103994	ZFP106 PPI subnetwork	0.73
GO:0006805	xenobiotic metabolic process	0.73
MP:0010769	abnormal survival	0.73
ENSG00000215727	ENSG00000215727 PPI subnetwork	0.73
ENSG00000065518	NDUFB4 PPI subnetwork	0.73
MP:0004543	abnormal sperm physiology	0.73
GO:0004693	cyclin-dependent protein kinase activity	0.73
ENSG00000186184	POLR1D PPI subnetwork	0.73
REACTOME_ACTIVATION_OF_NMDA_RECEPTOR_UPON_Glutamate_BINDING	REACTOME_ACTIVATION_OF_NMDA_RECEPTOR_UPON_Glutamate_BINDING_AN	0.73

Original gene set ID	Original gene set description	Nominal P value
MP:0001807	decreased IgA level	0.74
GO:0009145	purine nucleoside triphosphate biosynthetic process	0.74
ENSG000000134480	CCNH PPI subnetwork	0.74
REACTOME_DNA_REPLICATION	REACTOME_DNA_REPLICATION	0.74
ENSG000000151067	CACNA1C PPI subnetwork	0.74
ENSG000000169429	IL8 PPI subnetwork	0.74
GO:0007286	spermatid development	0.74
MP:0001402	hypoactivity	0.74
GO:0050808	synapse organization	0.74
ENSG000000166930	MS4A5 PPI subnetwork	0.74
ENSG000000077312	SNRPA PPI subnetwork	0.75
GO:0019002	GMP binding	0.75
ENSG000000065526	SPEN PPI subnetwork	0.75
ENSG000000184672	RALYL PPI subnetwork	0.75
ENSG000000136560	TANK PPI subnetwork	0.75
MP:0004947	skin inflammation	0.75
GO:0004690	cyclic nucleotide-dependent protein kinase activity	0.75
ENSG000000198569	SLC34A3 PPI subnetwork	0.75
ENSG000000123268	ATF1 PPI subnetwork	0.75
GO:0006184	GTP catabolic process	0.75
GO:0051385	response to mineralocorticoid stimulus	0.75
ENSG000000106628	POLD2 PPI subnetwork	0.75
GO:0055065	metal ion homeostasis	0.75
MP:0000538	abnormal urinary bladder morphology	0.75
REACTOME_BIOSYNTHESIS_OF_THE_N:GLYCAN_PRECURSOR_DOLICHOL_LIPID	REACTOME_BIOSYNTHESIS_OF_THE_N:GLYCAN_PRECURSOR_DOLICHOL_LIPID:LINK	0.75
GO:0050714	positive regulation of protein secretion	0.75
ENSG000000215320	ENSG000000215320 PPI subnetwork	0.75
ENSG000000143977	SNRPG PPI subnetwork	0.75
MP:0004986	abnormal osteoblast morphology	0.75
ENSG000000163453	IGFBP7 PPI subnetwork	0.75
MP:0011290	decreased nephron number	0.75
ENSG000000141552	ANAPC11 PPI subnetwork	0.75
GO:0006672	ceramide metabolic process	0.75
GO:0004386	helicase activity	0.75
ENSG00000014641	MDH1 PPI subnetwork	0.75
MP:0000150	abnormal rib morphology	0.75
ENSG000000102001	CACNA1F PPI subnetwork	0.75
ENSG000000162290	ENSG000000162290 PPI subnetwork	0.75
GO:0043547	positive regulation of GTPase activity	0.75
MP:0002972	abnormal cardiac muscle contractility	0.75
GO:0006040	amino sugar metabolic process	0.75
ENSG000000116062	MSH6 PPI subnetwork	0.75
ENSG000000126821	SGPP1 PPI subnetwork	0.75
MP:0000230	abnormal systemic arterial blood pressure	0.75
ENSG000000048052	HDAC9 PPI subnetwork	0.75
GO:0051588	regulation of neurotransmitter transport	0.75
GO:0001676	long-chain fatty acid metabolic process	0.75
ENSG000000187514	PTMA PPI subnetwork	0.75
ENSG00000030066	NUP160 PPI subnetwork	0.75

Original gene set ID	Original gene set description	Nominal P value
GO:0040013	negative regulation of locomotion	0.75
ENSG00000099800	TIMM13 PPI subnetwork	0.75
ENSG00000155897	ADCY8 PPI subnetwork	0.75
ENSG00000111716	LDHB PPI subnetwork	0.75
GO:0046883	regulation of hormone secretion	0.75
ENSG00000106305	AIMP2 PPI subnetwork	0.75
ENSG00000108518	PFN1 PPI subnetwork	0.75
ENSG00000087586	AURKA PPI subnetwork	0.75
GO:0040036	regulation of fibroblast growth factor receptor signaling pathway	0.75
MP:0000005	increased brown adipose tissue amount	0.75
GO:0030072	peptide hormone secretion	0.75
ENSG00000178999	AURKB PPI subnetwork	0.75
GO:0042176	regulation of protein catabolic process	0.75
GO:0003230	cardiac atrium development	0.75
MP:0003235	abnormal alisphenoid bone morphology	0.75
ENSG00000172613	RAD9A PPI subnetwork	0.75
ENSG00000165629	ATP5C1 PPI subnetwork	0.75
MP:0000455	abnormal maxilla morphology	0.75
MP:0005297	spina bifida occulta	0.75
MP:0001410	head bobbing	0.75
ENSG00000160789	LMNA PPI subnetwork	0.75
ENSG00000126602	TRAP1 PPI subnetwork	0.75
GO:0019439	aromatic compound catabolic process	0.75
GO:0002312	B cell activation involved in immune response	0.75
ENSG00000079819	EPB41L2 PPI subnetwork	0.75
GO:0007050	cell cycle arrest	0.75
GO:0044349	DNA excision	0.75
GO:0000718	nucleotide-excision repair, DNA damage removal	0.75
ENSG00000141404	GNAL PPI subnetwork	0.75
GO:0030799	regulation of cyclic nucleotide metabolic process	0.75
GO:0010742	macrophage derived foam cell differentiation	0.75
GO:0090077	foam cell differentiation	0.75
ENSG00000100142	POLR2F PPI subnetwork	0.75
GO:0008237	metallopeptidase activity	0.75
ENSG00000127337	YEATS4 PPI subnetwork	0.75
GO:0032543	mitochondrial translation	0.75
GO:0016624	oxidoreductase activity, acting on the aldehyde or oxo group of donors, disulfide as	0.75
MP:0002878	abnormal corticospinal tract morphology	0.75
ENSG00000145649	GZMA PPI subnetwork	0.75
GO:0033293	monocarboxylic acid binding	0.75
ENSG00000125970	RALY PPI subnetwork	0.75
ENSG00000168412	MTNR1A PPI subnetwork	0.75
ENSG00000070061	IKBKAP PPI subnetwork	0.75
MP:0005461	abnormal dendritic cell morphology	0.75
GO:0046209	nitric oxide metabolic process	0.75
MP:0002639	micrognathia	0.75
GO:0071496	cellular response to external stimulus	0.75
ENSG00000169031	COL4A3 PPI subnetwork	0.75
GO:0006283	transcription-coupled nucleotide-excision repair	0.75

Original gene set ID	Original gene set description	Nominal P value
ENSG00000171403	KRT9 PPI subnetwork	0.75
GO:0055002	striated muscle cell development	0.75
GO:0001158	enhancer sequence-specific DNA binding	0.75
ENSG00000128266	GNAZ PPI subnetwork	0.75
GO:0006725	cellular aromatic compound metabolic process	0.75
REACTOME_PLCG1_EVENTS_IN_ERBB2_SIGNALING	REACTOME_PLCG1_EVENTS_IN_ERBB2_SIGNALING	0.75
REACTOME_THROMBOXANE_SIGNALING_THROUGH_TP_RECEPTOR	REACTOME_THROMBOXANE_SIGNALING_THROUGH_TP_RECEPTOR	0.75
ENSG00000101150	TPD52L2 PPI subnetwork	0.75
KEGG_HYPERTROPHIC_CARDIOMYOPATHY_HCM	KEGG_HYPERTROPHIC_CARDIOMYOPATHY_HCM	0.75
ENSG00000147669	POLR2K PPI subnetwork	0.75
MP:0008023	abnormal styloid process morphology	0.75
GO:0014069	postsynaptic density	0.75
GO:0044327	dendritic spine head	0.75
GO:0006310	DNA recombination	0.75
REACTOME_P53:INDEPENDENT_G1S_DNA_DAMAGE_CHECKPOINT	REACTOME_P53:INDEPENDENT_G1S_DNA_DAMAGE_CHECKPOINT	0.75
REACTOME_P53:INDEPENDENT_DNA_DAMAGE_RESPONSE	REACTOME_P53:INDEPENDENT_DNA_DAMAGE_RESPONSE	0.75
REACTOME_UBIQUITIN_MEDIATED_DEGRADATION_OF_PHOSPHORYLATED_CD	REACTOME_UBIQUITIN_MEDIATED_DEGRADATION_OF_PHOSPHORYLATED_CDC25	0.75
ENSG00000149016	TUT1 PPI subnetwork	0.75
ENSG00000126767	ELK1 PPI subnetwork	0.75
ENSG00000108854	SMURF2 PPI subnetwork	0.75
ENSG00000126267	COX6B1 PPI subnetwork	0.75
ENSG00000092054	MYH7 PPI subnetwork	0.75
MP:0004131	abnormal embryonic cilium morphology	0.75
GO:0030071	regulation of mitotic metaphase/anaphase transition	0.75
GO:0004437	inositol or phosphatidylinositol phosphatase activity	0.75
MP:0003345	decreased rib number	0.75
GO:0051340	regulation of ligase activity	0.75
ENSG00000146535	GNA12 PPI subnetwork	0.75
ENSG00000105373	GLTSCR2 PPI subnetwork	0.75
REACTOME_EICOSANOID_LIGAND:BINDING_RECEPTORS	REACTOME_EICOSANOID_LIGAND:BINDING_RECEPTORS	0.76
ENSG00000170348	TMED10 PPI subnetwork	0.76
ENSG00000187953	ENSG00000187953 PPI subnetwork	0.76
ENSG00000122512	PMS2 PPI subnetwork	0.76
ENSG00000169249	ZRSR2 PPI subnetwork	0.76
ENSG00000136824	SMC2 PPI subnetwork	0.76
GO:0043567	regulation of insulin-like growth factor receptor signaling pathway	0.76
ENSG00000145736	GTF2H2 PPI subnetwork	0.76
GO:0032271	regulation of protein polymerization	0.76
ENSG00000116584	ARHGEF2 PPI subnetwork	0.76
ENSG00000168438	CDC40 PPI subnetwork	0.76
ENSG00000130024	PHF10 PPI subnetwork	0.76
GO:0060393	regulation of pathway-restricted SMAD protein phosphorylation	0.76
GO:0016866	intramolecular transferase activity	0.76
GO:0003002	regionalization	0.76
ENSG00000100028	SNRPD3 PPI subnetwork	0.76
ENSG00000169057	MECP2 PPI subnetwork	0.76
ENSG00000119335	SET PPI subnetwork	0.76
MP:0001052	abnormal muscle innervation	0.76
MP:0002206	abnormal CNS synaptic transmission	0.76

Original gene set ID	Original gene set description	Nominal P value
MP:0004021	abnormal rod electrophysiology	0.76
ENSG00000075711	DLG1 PPI subnetwork	0.76
ENSG00000197170	PSMD12 PPI subnetwork	0.76
GO:0030553	cGMP binding	0.76
ENSG00000119138	KLF9 PPI subnetwork	0.76
REACTOME_NETRIN:1_SIGNALING	REACTOME_NETRIN:1_SIGNALING	0.76
ENSG00000154429	C1orf96 PPI subnetwork	0.76
ENSG00000131149	KIAA0182 PPI subnetwork	0.76
MP:0008898	abnormal acrosome morphology	0.76
ENSG00000175895	PLEKHF2 PPI subnetwork	0.76
MP:0002752	abnormal somatic nervous system morphology	0.76
ENSG00000151065	DCP1B PPI subnetwork	0.76
GO:0005791	rough endoplasmic reticulum	0.76
ENSG00000112081	SRSF3 PPI subnetwork	0.76
GO:0045263	proton-transporting ATP synthase complex, coupling factor F(o)	0.76
GO:0006939	smooth muscle contraction	0.76
ENSG00000134574	DDB2 PPI subnetwork	0.76
ENSG00000125676	THOC2 PPI subnetwork	0.76
ENSG00000197780	TAF13 PPI subnetwork	0.76
GO:0010827	regulation of glucose transport	0.76
GO:0004385	guanylate kinase activity	0.76
MP:0010386	abnormal urinary bladder physiology	0.76
GO:0000076	DNA replication checkpoint	0.76
GO:0060441	epithelial tube branching involved in lung morphogenesis	0.76
ENSG00000113555	PCDH12 PPI subnetwork	0.76
ENSG00000111087	GLI1 PPI subnetwork	0.76
GO:0030814	regulation of cAMP metabolic process	0.76
ENSG00000137054	POLR1E PPI subnetwork	0.76
ENSG00000159461	AMFR PPI subnetwork	0.76
GO:0030817	regulation of cAMP biosynthetic process	0.76
ENSG00000177951	BET1L PPI subnetwork	0.76
ENSG00000198846	TOX PPI subnetwork	0.76
ENSG00000124097	ENSG00000124097 PPI subnetwork	0.76
ENSG00000103460	TOX3 PPI subnetwork	0.76
MP:0002882	abnormal neuron morphology	0.76
ENSG00000007168	PAFAH1B1 PPI subnetwork	0.76
GO:0050686	negative regulation of mRNA processing	0.76
GO:0006875	cellular metal ion homeostasis	0.76
ENSG00000168477	TNXB PPI subnetwork	0.76
GO:0042787	protein ubiquitination involved in ubiquitin-dependent protein catabolic process	0.76
MP:0001688	abnormal somite development	0.76
GO:0072528	pyrimidine-containing compound biosynthetic process	0.76
MP:0003233	prolonged QT interval	0.76
REACTOME_SULFUR_AMINO_ACID_METABOLISM	REACTOME_SULFUR_AMINO_ACID_METABOLISM	0.76
GO:0002377	immunoglobulin production	0.76
GO:0006665	sphingolipid metabolic process	0.76
ENSG00000115241	PPM1G PPI subnetwork	0.76
ENSG000000064961	HMG20B PPI subnetwork	0.76
GO:0016616	oxidoreductase activity, acting on the CH-OH group of donors, NAD or NADP as acceptor	0.76

Original gene set ID	Original gene set description	Nominal P value
ENSG00000041357	PSMA4 PPI subnetwork	0.76
ENSG00000198910	L1CAM PPI subnetwork	0.76
GO:0015833	peptide transport	0.76
ENSG00000103671	TRIP4 PPI subnetwork	0.76
KEGG_NOD_LIKE_RECEPTOR_SIGNALING_PATHWAY	KEGG_NOD_LIKE_RECEPTOR_SIGNALING_PATHWAY	0.76
GO:0051384	response to glucocorticoid stimulus	0.76
ENSG00000153044	CENPH PPI subnetwork	0.76
ENSG00000160916	ENSG00000160916 PPI subnetwork	0.76
GO:0005743	mitochondrial inner membrane	0.76
GO:0005770	late endosome	0.76
GO:0051428	peptide hormone receptor binding	0.76
GO:0002790	peptide secretion	0.76
GO:0043161	proteasomal ubiquitin-dependent protein catabolic process	0.76
ENSG00000072682	P4HA2 PPI subnetwork	0.76
GO:0030279	negative regulation of ossification	0.76
GO:0002792	negative regulation of peptide secretion	0.76
ENSG00000110436	SLC1A2 PPI subnetwork	0.76
MP:0005517	decreased liver regeneration	0.76
ENSG00000121931	LRIF1 PPI subnetwork	0.76
ENSG00000198576	ARC PPI subnetwork	0.76
ENSG00000174231	PRPF8 PPI subnetwork	0.76
MP:0010404	ostium primum atrial septal defect	0.76
GO:0007204	elevation of cytosolic calcium ion concentrati	0.76
ENSG00000128708	HAT1 PPI subnetwork	0.76
MP:0002135	abnormal kidney morphology	0.76
GO:0010576	metalloenzyme regulator activity	0.76
GO:0001510	RNA methylation	0.76
ENSG00000076053	RBM7 PPI subnetwork	0.76
GO:0031329	regulation of cellular catabolic process	0.76
ENSG00000106541	AGR2 PPI subnetwork	0.76
ENSG00000136875	PRPF4 PPI subnetwork	0.76
GO:0021782	glial cell development	0.76
GO:0051047	positive regulation of secretion	0.76
GO:0008144	drug binding	0.76
GO:0008227	G-protein coupled amine receptor activity	0.76
GO:0043392	negative regulation of DNA binding	0.76
GO:0021602	cranial nerve morphogenesis	0.76
GO:0090090	negative regulation of canonical Wnt receptor signaling pathway	0.77
GO:0006298	mismatch repair	0.77
ENSG00000133083	DCLK1 PPI subnetwork	0.77
GO:0010332	response to gamma radiation	0.77
GO:0009142	nucleoside triphosphate biosynthetic proces	0.77
ENSG00000135486	HNRNPA1 PPI subnetwork	0.77
GO:0007369	gastrulation	0.77
REACTOME_M_PHASE	REACTOME_M_PHASE	0.77
ENSG00000174021	GNG5 PPI subnetwork	0.77
ENSG00000063244	U2AF2 PPI subnetwork	0.77
ENSG00000103194	USP10 PPI subnetwork	0.77
GO:0032412	regulation of ion transmembrane transporter activity	0.77

Original gene set ID	Original gene set description	Nominal P value
ENSG00000149554	CHEK1 PPI subnetwork	0.77
REACTOME_GPCR_LIGAND_BINDING	REACTOME_GPCR_LIGAND_BINDING	0.77
MP:0002812	spherocytosis	0.77
GO:0045191	regulation of isotype switching	0.77
MP:0003148	decreased cochlear coiling	0.77
MP:0010903	abnormal pulmonary alveolus wall morphology	0.77
ENSG00000115694	STK25 PPI subnetwork	0.77
ENSG00000164244	PRRC1 PPI subnetwork	0.77
ENSG00000146731	CCT6A PPI subnetwork	0.77
ENSG00000135336	ORC3 PPI subnetwork	0.77
ENSG00000122122	SASH3 PPI subnetwork	0.77
ENSG00000174718	C12orf35 PPI subnetwork	0.77
GO:0044309	neuron spine	0.77
GO:0043197	dendritic spine	0.77
MP:0008482	decreased spleen germinal center number	0.77
ENSG00000114315	HES1 PPI subnetwork	0.77
GO:0060216	definitive hemopoiesis	0.77
MP:0005202	lethargy	0.77
GO:0046933	hydrogen ion transporting ATP synthase activity, rotational mechanism	0.77
GO:0044456	synapse part	0.77
ENSG00000140350	ANP32A PPI subnetwork	0.77
GO:0050661	NADP binding	0.77
GO:0005109	frizzled binding	0.77
ENSG00000101843	PSMD10 PPI subnetwork	0.77
GO:0021761	limbic system development	0.77
ENSG00000109332	UBE2D3 PPI subnetwork	0.77
REACTOME_NEURONAL_SYSTEM	REACTOME_NEURONAL_SYSTEM	0.77
ENSG00000183763	TRAIIP PPI subnetwork	0.77
REACTOME_PI3K_EVENTS_IN_ERBB4_SIGNALING	REACTOME_PI3K_EVENTS_IN_ERBB4_SIGNALING	0.77
GO:0006171	cAMP biosynthetic process	0.77
GO:0046879	hormone secretion	0.77
GO:0016471	vacuolar proton-transporting V-type ATPase complex	0.77
MP:0002919	enhanced paired-pulse facilitation	0.77
GO:0045335	phagocytic vesicle	0.77
MP:0000521	abnormal kidney cortex morphology	0.77
ENSG00000147439	BIN3 PPI subnetwork	0.77
MP:0001890	anencephaly	0.77
GO:0009894	regulation of catabolic process	0.77
REACTOME_TELOMERE_MAINTENANCE	REACTOME_TELOMERE_MAINTENANCE	0.77
ENSG00000143379	SETDB1 PPI subnetwork	0.77
GO:0007368	determination of left/right symmetry	0.77
GO:0060992	response to fungicide	0.77
ENSG00000163960	UBXN7 PPI subnetwork	0.77
REACTOME_FANCONI_ANEMIA_PATHWAY	REACTOME_FANCONI_ANEMIA_PATHWAY	0.77
MP:0000644	dextrocardia	0.77
MP:0001044	abnormal enteric nervous system morphology	0.77
GO:0032589	neuron projection membrane	0.77
ENSG00000180209	MYLPF PPI subnetwork	0.77
ENSG00000087274	ADD1 PPI subnetwork	0.77

Original gene set ID	Original gene set description	Nominal P value
MP:0003702	abnormal chromosome morphology	0.77
REACTOME_CLASS_A1_RHODOPSIN:LIKE_RECEPTORS	REACTOME_CLASS_A1_RHODOPSIN:LIKE_RECEPTORS	0.77
ENSG000000116459	ATP5F1 PPI subnetwork	0.77
GO:0001533	cornified envelope	0.77
MP:0002998	abnormal bone remodeling	0.77
MP:0002682	decreased mature ovarian follicle number	0.77
ENSG00000205937	RNPS1 PPI subnetwork	0.77
ENSG000000101444	AHCY PPI subnetwork	0.77
GO:0030017	sarcomere	0.77
ENSG00000164109	MAD2L1 PPI subnetwork	0.77
GO:0010389	regulation of G2/M transition of mitotic cell cycle	0.77
ENSG00000108528	SLC25A11 PPI subnetwork	0.77
ENSG00000196284	SUPT3H PPI subnetwork	0.77
REACTOME_TANDEM_PORE_DOMAIN_POTASSIUM_CHANNELS	REACTOME_TANDEM_PORE_DOMAIN_POTASSIUM_CHANNELS	0.77
GO:0017091	AU-rich element binding	0.77
ENSG00000127928	GNGT1 PPI subnetwork	0.77
ENSG00000011007	TCEB3 PPI subnetwork	0.77
ENSG00000128609	NDUFA5 PPI subnetwork	0.77
ENSG00000182180	MRPS16 PPI subnetwork	0.77
GO:0006699	bile acid biosynthetic process	0.77
GO:0009954	proximal/distal pattern formation	0.77
REACTOME_PI3K_EVENTS_IN_ERBB2_SIGNALING	REACTOME_PI3K_EVENTS_IN_ERBB2_SIGNALING	0.77
ENSG00000136273	HUS1 PPI subnetwork	0.77
ENSG00000042832	TG PPI subnetwork	0.77
REACTOME_POLYMERASE_SWITCHING_ON_THE_C:STRAND_OF_THE_TELOMER	REACTOME_POLYMERASE_SWITCHING_ON_THE_C:STRAND_OF_THE_TELOMERE	0.77
REACTOME_LEADING_STRAND_SYNTHESIS	REACTOME_LEADING_STRAND_SYNTHESIS	0.77
REACTOME_POLYMERASE_SWITCHING	REACTOME_POLYMERASE_SWITCHING	0.77
MP:0010856	dilated respiratory conducting tubes	0.77
KEGG_EPITHELIAL_CELL_SIGNALING_IN_HELICOBACTER_PYLORI_INFECTION	KEGG_EPITHELIAL_CELL_SIGNALING_IN_HELICOBACTER_PYLORI_INFECTION	0.77
GO:0008278	cohesin complex	0.77
ENSG00000213611	ENSG00000213611 PPI subnetwork	0.77
ENSG00000177889	UBE2N PPI subnetwork	0.77
REACTOME_PLC_BETA_MEDIATED_EVENTS	REACTOME_PLC_BETA_MEDIATED_EVENTS	0.77
MP:0002016	ovary cysts	0.77
ENSG00000147869	CER1 PPI subnetwork	0.77
ENSG00000108294	PSMB3 PPI subnetwork	0.77
GO:0042742	defense response to bacterium	0.77
GO:0008093	cytoskeletal adaptor activity	0.77
REACTOME_DUAL_INCISION_REACTION_IN_GG:NER	REACTOME_DUAL_INCISION_REACTION_IN_GG:NER	0.77
REACTOME_FORMATION_OF_INCISION_COMPLEX_IN_GG:NER	REACTOME_FORMATION_OF_INCISION_COMPLEX_IN_GG:NER	0.77
MP:0000757	herniated abdominal wall	0.77
ENSG00000164270	HTR4 PPI subnetwork	0.77
GO:0002293	alpha-beta T cell differentiation involved in immune response	0.77
GO:0002287	alpha-beta T cell activation involved in immune response	0.77
ENSG00000170558	CDH2 PPI subnetwork	0.77
ENSG00000117592	PRDX6 PPI subnetwork	0.77
ENSG00000197818	SLC9A8 PPI subnetwork	0.77
MP:0001636	irregular heartbeat	0.78
ENSG00000163082	SGPP2 PPI subnetwork	0.78

Original gene set ID	Original gene set description	Nominal P value
MP:0001071	abnormal facial nerve morphology	0.78
ENSG00000002016	RAD52 PPI subnetwork	0.78
ENSG000000120253	NUP43 PPI subnetwork	0.78
GO:0051899	membrane depolarization	0.78
GO:0021766	hippocampus development	0.78
GO:0006836	neurotransmitter transport	0.78
GO:0042384	cilium assembly	0.78
ENSG000000179915	NRXN1 PPI subnetwork	0.78
GO:0010743	regulation of macrophage derived foam cell differentiation	0.78
MP:0005431	decreased oocyte number	0.78
ENSG000000115233	PSMD14 PPI subnetwork	0.78
ENSG000000108272	DHRS11 PPI subnetwork	0.78
MP:0003896	prolonged PR interval	0.78
ENSG000000104852	SNRNP70 PPI subnetwork	0.78
ENSG000000067334	DNTTIP2 PPI subnetwork	0.78
MP:0000534	abnormal ureter morphology	0.78
MP:0008146	asymmetric rib-sternum attachment	0.78
MP:0000729	abnormal myogenesis	0.78
GO:0048167	regulation of synaptic plasticity	0.78
ENSG000000183023	SLC8A1 PPI subnetwork	0.78
ENSG000000153162	BMP6 PPI subnetwork	0.78
GO:0046039	GTP metabolic process	0.78
GO:0005504	fatty acid binding	0.78
ENSG000000156970	BUB1B PPI subnetwork	0.78
GO:0031966	mitochondrial membrane	0.78
ENSG000000111358	GTF2H3 PPI subnetwork	0.78
GO:0003207	cardiac chamber formation	0.78
GO:0000077	DNA damage checkpoint	0.78
ENSG000000114026	OGG1 PPI subnetwork	0.78
REACTOME_INHIBITION_OF_VOLTAGE_GATED_CA2_CHANNELS_VIA_GBETAG	REACTOME_INHIBITION_OF_VOLTAGE_GATED_CA2_CHANNELS_VIA_GBETAG	0.78
REACTOME_ACTIVATION_OF_G_PROTEIN_GATED_POTASSIUM_CHANNELS	REACTOME_ACTIVATION_OF_G_PROTEIN_GATED_POTASSIUM_CHANNELS	0.78
REACTOME_G_PROTEIN_GATED_POTASSIUM_CHANNELS	REACTOME_G_PROTEIN_GATED_POTASSIUM_CHANNELS	0.78
ENSG000000186852	ENSG000000186852 PPI subnetwork	0.78
GO:0007409	axonogenesis	0.78
GO:0019003	GDP binding	0.78
REACTOME_SEROTONIN_RECEPTORS	REACTOME_SEROTONIN_RECEPTORS	0.78
MP:0001093	small trigeminal ganglion	0.78
ENSG000000131876	SNRPA1 PPI subnetwork	0.78
MP:0008267	abnormal hippocampus CA3 region morphology	0.78
GO:0006595	polyamine metabolic process	0.78
GO:0007173	epidermal growth factor receptor signaling pathway	0.78
ENSG000000112559	MDF1 PPI subnetwork	0.78
MP:0003657	abnormal erythrocyte osmotic lysis	0.78
GO:0090278	negative regulation of peptide hormone secretion	0.78
ENSG000000067369	TP53BP1 PPI subnetwork	0.78
MP:0002286	cryptorchism	0.78
ENSG000000181218	HIST3H2A PPI subnetwork	0.78
ENSG000000212868	ENSG000000212868 PPI subnetwork	0.78
ENSG000000198727	MT-CYB PPI subnetwork	0.78

Original gene set ID	Original gene set description	Nominal P value
ENSG00000166508	MCM7 PPI subnetwork	0.78
ENSG00000100412	ACO2 PPI subnetwork	0.78
GO:0045202	synapse	0.78
REACTOME_JNK_C:JUN_KINASES_PHOSPHORYLATION_AND_ACTIVATION_MEDIATED_BY_JNK	REACTOME_JNK_C:JUN_KINASES_PHOSPHORYLATION_AND_ACTIVATION_MEDIATED_BY_JNK	0.78
KEGG_NICOTINATE_AND_NICOTINAMIDE_METABOLISM	KEGG_NICOTINATE_AND_NICOTINAMIDE_METABOLISM	0.78
ENSG00000075651	PLD1 PPI subnetwork	0.78
ENSG00000171848	RRM2 PPI subnetwork	0.78
GO:0030501	positive regulation of bone mineralization	0.78
MP:0006301	abnormal mesenchyme morphology	0.78
GO:0006684	sphingomyelin metabolic process	0.78
ENSG00000135823	STX6 PPI subnetwork	0.78
GO:0022898	regulation of transmembrane transporter activity	0.78
GO:0006397	mRNA processing	0.78
MP:0001096	abnormal glossopharyngeal ganglion morphology	0.78
ENSG00000168243	GNG4 PPI subnetwork	0.78
REACTOME_G2M_CHECKPOINTS	REACTOME_G2M_CHECKPOINTS	0.78
MP:0005637	abnormal iron homeostasis	0.78
ENSG00000141446	ESCO1 PPI subnetwork	0.78
ENSG00000183454	GRIN2A PPI subnetwork	0.78
GO:0019228	regulation of action potential in neuron	0.78
ENSG00000059769	DNAJC25 PPI subnetwork	0.78
ENSG00000162419	GMEB1 PPI subnetwork	0.78
GO:0009295	nucleoid	0.78
MP:0002229	neurodegeneration	0.78
ENSG00000132872	SYT4 PPI subnetwork	0.78
MP:0001525	impaired balance	0.78
REACTOME_PROTEOLYTIC_CLEAVAGE_OF_SNARE_COMPLEX_PROTEINS	REACTOME_PROTEOLYTIC_CLEAVAGE_OF_SNARE_COMPLEX_PROTEINS	0.78
REACTOME_REGULATION_OF_INSULIN_SECRETION_BY_ACETYLCHOLINE	REACTOME_REGULATION_OF_INSULIN_SECRETION_BY_ACETYLCHOLINE	0.78
REACTOME_SIGNALING_BY_ERBB2	REACTOME_SIGNALING_BY_ERBB2	0.78
ENSG00000213639	PPP1CB PPI subnetwork	0.78
ENSG00000117399	CDC20 PPI subnetwork	0.78
ENSG00000047315	POLR2B PPI subnetwork	0.78
KEGG_TYPE_I_DIABETES_MELLITUS	KEGG_TYPE_I_DIABETES_MELLITUS	0.78
ENSG00000005194	CIAPIN1 PPI subnetwork	0.78
MP:0004158	right aortic arch	0.78
MP:0003635	abnormal synaptic transmission	0.78
ENSG00000198788	MUC2 PPI subnetwork	0.78
ENSG00000198932	GPRASP1 PPI subnetwork	0.78
GO:0002292	T cell differentiation involved in immune response	0.78
ENSG00000125845	BMP2 PPI subnetwork	0.78
ENSG00000136807	CDK9 PPI subnetwork	0.78
MP:0006074	abnormal retinal rod bipolar cell morphology	0.78
REACTOME_ORGANIC_CATIONANIONZWITTERION_TRANSPORT	REACTOME_ORGANIC_CATIONANIONZWITTERION_TRANSPORT	0.78
GO:0005326	neurotransmitter transporter activity	0.78
GO:0010092	specification of organ identity	0.79
ENSG00000152822	GRM1 PPI subnetwork	0.79
ENSG00000071894	CPSF1 PPI subnetwork	0.79
MP:0000269	abnormal heart looping	0.79
REACTOME_BETA_DEFENSINS	REACTOME_BETA_DEFENSINS	0.79

Original gene set ID**Original gene set description****Nominal P value**

GO:0070301	cellular response to hydrogen peroxide	0.79
ENSG00000213465	ARL2 PPI subnetwork	0.79
ENSG00000212874	ENSG00000212874 PPI subnetwork	0.79
ENSG00000198712	MT-CO2 PPI subnetwork	0.79
MP:0005329	abnormal myocardium layer morphology	0.79
ENSG00000196092	PAX5 PPI subnetwork	0.79
MP:0003232	abnormal forebrain development	0.79
GO:0019321	pentose metabolic process	0.79
MP:0001596	hypotension	0.79
ENSG00000182621	PLCB1 PPI subnetwork	0.79
GO:0030195	negative regulation of blood coagulation	0.79
ENSG00000173575	CHD2 PPI subnetwork	0.79
ENSG00000162704	ARPC5 PPI subnetwork	0.79
MP:0008788	abnormal fetal cardiomyocyte morphology	0.79
GO:0055080	cation homeostasis	0.79
ENSG00000164330	EBF1 PPI subnetwork	0.79
ENSG00000058272	PPP1R12A PPI subnetwork	0.79
ENSG00000142655	PEX14 PPI subnetwork	0.79
GO:0031576	G2/M transition checkpoint	0.79
GO:0008173	RNA methyltransferase activity	0.79
GO:0016849	phosphorus-oxygen lyase activity	0.79
GO:0016831	carboxy-lyase activity	0.79
ENSG00000100911	PSME2 PPI subnetwork	0.79
ENSG00000167863	ATP5H PPI subnetwork	0.79
MP:0001522	impaired swimming	0.79
GO:0001653	peptide receptor activity	0.79
MP:0000955	abnormal spinal cord morphology	0.79
GO:0031163	metallo-sulfur cluster assembly	0.79
GO:0016226	iron-sulfur cluster assembly	0.79
MP:0004252	abnormal direction of heart looping	0.79
ENSG00000181090	EHMT1 PPI subnetwork	0.79
REACTOME_ASSEMBLY_OF_THE_PRE:REPLICATIVE_COMPLEX	REACTOME_ASSEMBLY_OF_THE_PRE:REPLICATIVE_COMPLEX	0.79
REACTOME_APCCDC20_MEDIATED_DEGRADATION_OF_MITOTIC_PROTEINS	REACTOME_APCCDC20_MEDIATED_DEGRADATION_OF_MITOTIC_PROTEINS	0.79
GO:0016769	transferase activity, transferring nitrogenous groups	0.79
GO:0001935	endothelial cell proliferation	0.79
MP:0002988	decreased urine osmolality	0.79
ENSG00000100764	PSMC1 PPI subnetwork	0.79
ENSG00000165525	NEMF PPI subnetwork	0.79
MP:0005584	abnormal enzyme/coenzyme activity	0.79
MP:0001958	emphysema	0.79
GO:0009060	aerobic respiration	0.79
GO:0051707	response to other organism	0.79
GO:0051969	regulation of transmission of nerve impulse	0.79
ENSG00000177189	RPS6KA3 PPI subnetwork	0.79
MP:0003222	increased cardiomyocyte apoptosis	0.79
GO:0004518	nuclease activity	0.79
ENSG00000100567	PSMA3 PPI subnetwork	0.79
GO:0046164	alcohol catabolic process	0.79
REACTOME_DEPOLARIZATION_OF_THE_PRESYNAPTIC_TERMINAL_TRIGGERS_T	REACTOME_DEPOLARIZATION_OF_THE_PRESYNAPTIC_TERMINAL_TRIGGERS_THE_I	0.79

Original gene set ID	Original gene set description	Nominal P value
ENSG00000069329	VPS35 PPI subnetwork	0.79
MP:0000937	abnormal motor neuron morphology	0.79
REACTOME_ACTIVATED_AMPK_STIMULATES_FATTY:ACID_OXIDATION_IN_MUSCLE	REACTOME_ACTIVATED_AMPK_STIMULATES_FATTY:ACID_OXIDATION_IN_MUSCLE	0.79
ENSG00000124535	WRNIP1 PPI subnetwork	0.79
ENSG00000134371	CDC73 PPI subnetwork	0.79
ENSG00000085872	CHERP PPI subnetwork	0.79
GO:0046580	negative regulation of Ras protein signal transduction	0.79
MP:0001380	reduced male mating frequency	0.79
ENSG00000124333	VAMP7 PPI subnetwork	0.79
MP:0003313	abnormal locomotor activation	0.79
MP:0002183	gliosis	0.79
ENSG00000168522	FNTA PPI subnetwork	0.79
GO:0045669	positive regulation of osteoblast differentiation	0.79
GO:0010498	proteasomal protein catabolic process	0.79
KEGG_FATTY_ACID_METABOLISM	KEGG_FATTY_ACID_METABOLISM	0.79
REACTOME_LYSOSOME_VESICLE_BIOGENESIS	REACTOME_LYSOSOME_VESICLE_BIOGENESIS	0.79
GO:0009084	glutamine family amino acid biosynthetic process	0.79
ENSG00000117758	STX12 PPI subnetwork	0.79
GO:0021510	spinal cord development	0.79
ENSG00000178950	GAK PPI subnetwork	0.79
ENSG00000104835	FBXO17 PPI subnetwork	0.79
GO:0004745	retinol dehydrogenase activity	0.79
GO:0051537	2 iron, 2 sulfur cluster binding	0.79
ENSG00000125450	NUP85 PPI subnetwork	0.79
GO:0009201	ribonucleoside triphosphate biosynthetic process	0.79
ENSG00000104884	ERCC2 PPI subnetwork	0.79
ENSG00000003756	RBM5 PPI subnetwork	0.79
ENSG00000127922	SHFM1 PPI subnetwork	0.79
ENSG00000134899	ERCC5 PPI subnetwork	0.79
MP:0000297	abnormal atrioventricular cushion morphology	0.79
GO:0016607	nuclear speck	0.79
MP:0008221	abnormal hippocampal commissure morphology	0.79
ENSG00000173163	COMMD1 PPI subnetwork	0.79
ENSG00000139970	RTN1 PPI subnetwork	0.79
ENSG00000189283	FHIT PPI subnetwork	0.79
GO:0010578	regulation of adenylate cyclase activity involved in G-protein coupled receptor signaling pathway	0.79
GO:0007189	adenylate cyclase-activating G-protein coupled receptor signaling pathway	0.79
GO:0010579	positive regulation of adenylate cyclase activity involved in G-protein coupled receptor signaling pathway	0.79
GO:0007156	homophilic cell adhesion	0.79
ENSG00000101158	TH1L PPI subnetwork	0.79
GO:0030003	cellular cation homeostasis	0.79
ENSG00000143870	PDIAG PPI subnetwork	0.79
REACTOME_SIGNALING_BY_BMP	REACTOME_SIGNALING_BY_BMP	0.79
GO:0090087	regulation of peptide transport	0.79
GO:0002791	regulation of peptide secretion	0.79
ENSG00000035862	TIMP2 PPI subnetwork	0.79
GO:0007224	smoothed signaling pathway	0.79
GO:0042133	neurotransmitter metabolic process	0.79
GO:0000460	maturation of 5.8S rRNA	0.79

Original gene set ID	Original gene set description	Nominal P value
ENSG00000183207	RUVBL2 PPI subnetwork	0.79
MP:0005404	abnormal axon morphology	0.79
ENSG00000068323	TFE3 PPI subnetwork	0.79
GO:0051438	regulation of ubiquitin-protein ligase activity	0.79
ENSG00000117533	VAMP4 PPI subnetwork	0.79
GO:0005681	spliceosomal complex	0.79
ENSG00000140829	DHX38 PPI subnetwork	0.79
GO:0051052	regulation of DNA metabolic process	0.8
GO:0008277	regulation of G-protein coupled receptor protein signaling pathway	0.8
MP:0004966	abnormal inner cell mass proliferation	0.8
MP:0003008	enhanced long term potentiation	0.8
ENSG00000175054	ATR PPI subnetwork	0.8
ENSG00000114107	CEP70 PPI subnetwork	0.8
GO:0008430	selenium binding	0.8
ENSG00000113522	RAD50 PPI subnetwork	0.8
ENSG00000168061	SAC3D1 PPI subnetwork	0.8
ENSG00000128534	NAA38 PPI subnetwork	0.8
ENSG00000168067	MAP4K2 PPI subnetwork	0.8
GO:0031649	heat generation	0.8
ENSG00000075188	NUP37 PPI subnetwork	0.8
GO:0005865	striated muscle thin filament	0.8
ENSG00000111788	ENSG00000111788 PPI subnetwork	0.8
ENSG00000214826	ENSG00000214826 PPI subnetwork	0.8
ENSG00000137834	SMAD6 PPI subnetwork	0.8
ENSG00000172175	MALT1 PPI subnetwork	0.8
MP:0002675	asthenozoospermia	0.8
REACTOME_MITOTIC_M:MG1_PHASES	REACTOME_MITOTIC_M:MG1_PHASES	0.8
REACTOME_ACTIVATION_OF_APCC_AND_APCCDC20_MEDIATED_DEGRADATION_OF_P53	REACTOME_ACTIVATION_OF_APCC_AND_APCCDC20_MEDIATED_DEGRADATION_OF_P53	0.8
ENSG00000159720	ATP6V0D1 PPI subnetwork	0.8
REACTOME_NEF:MEDIATES_DOWN_MODULATION_OF_CELL_SURFACE_RECEPTOR_FUNCTION	REACTOME_NEF:MEDIATES_DOWN_MODULATION_OF_CELL_SURFACE_RECEPTOR_FUNCTION	0.8
GO:0000956	nuclear-transcribed mRNA catabolic process	0.8
MP:0006316	increased urine sodium level	0.8
ENSG00000140262	TCF12 PPI subnetwork	0.8
GO:0004691	cAMP-dependent protein kinase activity	0.8
GO:0031396	regulation of protein ubiquitination	0.8
ENSG00000189091	SF3B3 PPI subnetwork	0.8
REACTOME_GRB2_EVENTS_IN_ERBB2_SIGNALING	REACTOME_GRB2_EVENTS_IN_ERBB2_SIGNALING	0.8
MP:0000029	abnormal malleus morphology	0.8
GO:0044106	cellular amine metabolic process	0.8
ENSG00000151461	UPF2 PPI subnetwork	0.8
GO:0032561	guanyl ribonucleotide binding	0.8
GO:0019001	guanyl nucleotide binding	0.8
GO:0006977	DNA damage response, signal transduction by p53 class mediator resulting in cell cycle arrest	0.8
GO:0072401	signal transduction involved in DNA integrity checkpoint	0.8
GO:0072431	signal transduction involved in mitotic cell cycle G1/S transition DNA damage checkpoint	0.8
GO:0072413	signal transduction involved in mitotic cell cycle checkpoint	0.8
GO:0072422	signal transduction involved in DNA damage checkpoint	0.8
GO:0072474	signal transduction involved in mitotic cell cycle G1/S checkpoint	0.8
ENSG00000183558	HIST2H2AA3 PPI subnetwork	0.8

Original gene set ID	Original gene set description	Nominal P value
ENSG00000203812	HIST2H2AA4 PPI subnetwork	0.8
ENSG00000128692	ENSG00000128692 PPI subnetwork	0.8
GO:0007411	axon guidance	0.8
ENSG00000072415	MPP5 PPI subnetwork	0.8
MP:0000936	small telencephalic vesicles	0.8
MP:0000611	jaundice	0.8
GO:0043254	regulation of protein complex assembly	0.8
ENSG00000213246	SUPT4H1 PPI subnetwork	0.8
ENSG00000100056	DGCR14 PPI subnetwork	0.8
GO:0031672	A band	0.8
MP:0000286	abnormal mitral valve morphology	0.8
GO:0002700	regulation of production of molecular mediator of immune response	0.8
GO:0007274	neuromuscular synaptic transmission	0.8
KEGG_SPLICEOSOME	KEGG_SPLICEOSOME	0.8
GO:0016667	oxidoreductase activity, acting on a sulfur group of donors	0.8
MP:0006380	abnormal spermatid morphology	0.8
MP:0003141	cardiac fibrosis	0.8
GO:0048846	axon extension involved in axon guidance	0.8
ENSG00000136813	KIAA0368 PPI subnetwork	0.8
MP:0002777	absent ovarian follicles	0.8
GO:0030510	regulation of BMP signaling pathway	0.8
GO:0008536	Ran GTPase binding	0.8
ENSG00000130779	CLIP1 PPI subnetwork	0.8
GO:0071377	cellular response to glucagon stimulus	0.8
ENSG00000135916	ITM2C PPI subnetwork	0.8
ENSG00000215476	ENSG00000215476 PPI subnetwork	0.8
ENSG00000206476	ENSG00000206476 PPI subnetwork	0.8
ENSG00000213780	GTF2H4 PPI subnetwork	0.8
ENSG00000122218	COPA PPI subnetwork	0.8
MP:0001932	abnormal spermiogenesis	0.8
MP:0009757	impaired behavioral response to morphine	0.8
ENSG00000157483	MYO1E PPI subnetwork	0.8
GO:0070169	positive regulation of biomineral tissue development	0.8
GO:0007623	circadian rhythm	0.8
GO:0032331	negative regulation of chondrocyte differentiation	0.8
MP:0000278	abnormal myocardial fiber morphology	0.8
ENSG00000137992	DBT PPI subnetwork	0.8
GO:0044062	regulation of excretion	0.8
GO:0050664	oxidoreductase activity, acting on NADH or NADPH, oxygen as acceptor	0.8
GO:0060324	face development	0.8
ENSG00000172315	TP53RK PPI subnetwork	0.8
GO:0033178	proton-transporting two-sector ATPase complex, catalytic domain	0.8
ENSG00000109107	ALDOC PPI subnetwork	0.8
GO:0006353	transcription termination, DNA-dependent	0.8
GO:0060479	lung cell differentiation	0.8
MP:0010090	increased circulating creatine kinase level	0.8
GO:0015036	disulfide oxidoreductase activity	0.8
GO:0060795	cell fate commitment involved in formation of primary germ layer	0.8
REACTOME_PEPTIDE_LIGAND:BINDING_RECEPTORS	REACTOME_PEPTIDE_LIGAND:BINDING_RECEPTORS	0.8

Original gene set ID	Original gene set description	Nominal P value
GO:0046633	alpha-beta T cell proliferation	0.8
GO:0008556	potassium-transporting ATPase activity	0.8
GO:0070663	regulation of leukocyte proliferation	0.8
ENSG00000152208	GRID2 PPI subnetwork	0.8
GO:0002053	positive regulation of mesenchymal cell proliferation	0.8
ENSG00000065609	SNAP91 PPI subnetwork	0.8
GO:0046676	negative regulation of insulin secretion	0.8
ENSG00000143228	NUF2 PPI subnetwork	0.8
ENSG00000170606	HSPA4 PPI subnetwork	0.8
ENSG00000108175	ZMIZ1 PPI subnetwork	0.8
ENSG00000172201	ID4 PPI subnetwork	0.8
GO:0051953	negative regulation of amine transport	0.8
GO:0042147	retrograde transport, endosome to Golgi	0.81
ENSG00000172572	PDE3A PPI subnetwork	0.81
ENSG00000198478	SH3BGRL2 PPI subnetwork	0.81
GO:0050819	negative regulation of coagulation	0.81
MP:0003862	decreased aggression towards males	0.81
ENSG00000102981	PARD6A PPI subnetwork	0.81
MP:0010264	increased hepatoma incidence	0.81
GO:0003211	cardiac ventricle formation	0.81
ENSG00000095002	MSH2 PPI subnetwork	0.81
REACTOME_TRANSMISSION_ACROSS_CHEMICAL_SYNAPSES	REACTOME_TRANSMISSION_ACROSS_CHEMICAL_SYNAPSES	0.81
ENSG00000170296	GABARAP PPI subnetwork	0.81
GO:0008528	G-protein coupled peptide receptor activity	0.81
GO:0006913	nucleocytoplasmic transport	0.81
GO:0031644	regulation of neurological system process	0.81
ENSG00000174243	DDX23 PPI subnetwork	0.81
GO:0032467	positive regulation of cytokinesis	0.81
ENSG00000169621	APLF PPI subnetwork	0.81
GO:0030816	positive regulation of cAMP metabolic process	0.81
GO:0030819	positive regulation of cAMP biosynthetic process	0.81
ENSG00000166579	NDEL1 PPI subnetwork	0.81
REACTOME_NCAM1_INTERACTIONS	REACTOME_NCAM1_INTERACTIONS	0.81
GO:0051046	regulation of secretion	0.81
ENSG00000106299	WASL PPI subnetwork	0.81
ENSG00000206505	HLA-A PPI subnetwork	0.81
GO:0097061	dendritic spine organization	0.81
GO:0060997	dendritic spine morphogenesis	0.81
ENSG00000129514	FOXA1 PPI subnetwork	0.81
ENSG00000211895	ENSG00000211895 PPI subnetwork	0.81
ENSG00000180353	HCLS1 PPI subnetwork	0.81
ENSG00000144231	POLR2D PPI subnetwork	0.81
MP:0001433	polyphagia	0.81
MP:0002106	abnormal muscle physiology	0.81
GO:0070717	poly-purine tract binding	0.81
ENSG00000099995	SF3A1 PPI subnetwork	0.81
ENSG00000163132	MSX1 PPI subnetwork	0.81
ENSG00000060069	CTDP1 PPI subnetwork	0.81
GO:0044243	multicellular organismal catabolic process	0.81

Original gene set ID	Original gene set description	Nominal P value
ENSG00000075856	SART3 PPI subnetwork	0.81
MP:0000953	abnormal oligodendrocyte morphology	0.81
MP:0003920	abnormal heart right ventricle morphology	0.81
ENSG00000166501	PRKCB PPI subnetwork	0.82
GO:0030670	phagocytic vesicle membrane	0.82
ENSG00000162923	WDR26 PPI subnetwork	0.82
ENSG00000138293	NCOA4 PPI subnetwork	0.82
KEGG_GLYCINE_SERINE_AND_THREONINE_METABOLISM	KEGG_GLYCINE_SERINE_AND_THREONINE_METABOLISM	0.82
GO:0006826	iron ion transport	0.82
GO:0022010	central nervous system myelination	0.82
GO:0032291	axon ensheathment in central nervous system	0.82
MP:0005620	abnormal muscle contractility	0.82
GO:0002042	cell migration involved in sprouting angiogenesis	0.82
GO:0005048	signal sequence binding	0.82
GO:0071248	cellular response to metal ion	0.82
ENSG00000078668	VDAC3 PPI subnetwork	0.82
ENSG00000108691	CCL2 PPI subnetwork	0.82
ENSG00000104177	MYEF2 PPI subnetwork	0.82
ENSG00000186810	CXCR3 PPI subnetwork	0.82
MP:0000153	rib bifurcation	0.82
ENSG00000155959	VBP1 PPI subnetwork	0.82
ENSG00000102683	SGCG PPI subnetwork	0.82
ENSG00000121552	CSTA PPI subnetwork	0.82
ENSG00000126215	XRCC3 PPI subnetwork	0.82
ENSG00000145494	NDUFS6 PPI subnetwork	0.82
MP:0006032	abnormal ureteric bud morphology	0.82
ENSG00000104915	STX10 PPI subnetwork	0.82
MP:0005599	increased cardiac muscle contractility	0.82
ENSG00000206328	ENSG00000206328 PPI subnetwork	0.82
ENSG00000204490	TNF PPI subnetwork	0.82
ENSG00000206439	TNF PPI subnetwork	0.82
GO:0007610	behavior	0.82
REACTOME_RNA_POLYMERASE_II_PRE:TRANSCRIPTION_EVENTS	REACTOME_RNA_POLYMERASE_II_PRE:TRANSCRIPTION_EVENTS	0.82
REACTOME_MITOTIC_PROMETAPHASE	REACTOME_MITOTIC_PROMETAPHASE	0.82
MP:0003161	absent lateral semicircular canal	0.82
GO:0032391	photoreceptor connecting cilium	0.82
ENSG00000137815	RTF1 PPI subnetwork	0.82
ENSG00000154174	TOMM70A PPI subnetwork	0.82
ENSG00000170260	ZNF212 PPI subnetwork	0.82
GO:0006406	mRNA export from nucleus	0.82
GO:0015802	basic amino acid transport	0.82
GO:0045761	regulation of adenylate cyclase activity	0.82
GO:0060198	clathrin sculpted vesicle	0.82
GO:0050755	chemokine metabolic process	0.82
ENSG00000115685	PPP1R7 PPI subnetwork	0.82
ENSG00000083312	TNPO1 PPI subnetwork	0.82
GO:0032964	collagen biosynthetic process	0.82
GO:0033205	cell cycle cytokinesis	0.82
GO:0009914	hormone transport	0.82

Original gene set ID	Original gene set description	Nominal P value
ENSG00000129170	CSRP3 PPI subnetwork	0.82
GO:0042776	mitochondrial ATP synthesis coupled proton transport	0.82
MP:0001968	abnormal touch/ nociception	0.82
KEGG_GAP_JUNCTION	KEGG_GAP_JUNCTION	0.82
REACTOME_FORMATION_OF_RNA_POL_II_ELONGATION_COMPLEX	REACTOME_FORMATION_OF_RNA_POL_II_ELONGATION_COMPLEX	0.82
REACTOME_RNA_POLYMERASE_II_TRANSCRIPTION_ELONGATION	REACTOME_RNA_POLYMERASE_II_TRANSCRIPTION_ELONGATION	0.82
REACTOME_FORMATION_OF_HIV:1_ELONGATION_COMPLEX_IN_THE_ABSENC	REACTOME_FORMATION_OF_HIV:1_ELONGATION_COMPLEX_IN_THE_ABSENCE_O	0.82
MP:0008661	decreased interleukin-10 secretion	0.82
ENSG00000143702	CEP170 PPI subnetwork	0.82
GO:0046961	proton-transporting ATPase activity, rotational mechanism	0.82
MP:0005449	abnormal food intake	0.82
ENSG00000090273	NUDC PPI subnetwork	0.82
GO:0045259	proton-transporting ATP synthase complex	0.82
GO:0021511	spinal cord patterning	0.82
ENSG00000111361	EIF2B1 PPI subnetwork	0.82
GO:0051932	synaptic transmission, GABAergic	0.82
GO:0009306	protein secretion	0.82
GO:0042744	hydrogen peroxide catabolic process	0.82
ENSG00000136152	COG3 PPI subnetwork	0.82
ENSG00000196961	AP2A1 PPI subnetwork	0.82
ENSG00000102096	PIM2 PPI subnetwork	0.82
ENSG00000169439	SDC2 PPI subnetwork	0.82
GO:0048645	organ formation	0.82
ENSG00000185624	P4HB PPI subnetwork	0.82
ENSG00000080986	NDC80 PPI subnetwork	0.82
GO:0097060	synaptic membrane	0.82
GO:0007632	visual behavior	0.82
MP:0004462	small basisphenoid bone	0.82
GO:0003785	actin monomer binding	0.82
REACTOME_GLUCAGON_SIGNALING_IN_METABOLIC_REGULATION	REACTOME_GLUCAGON_SIGNALING_IN_METABOLIC_REGULATION	0.82
GO:0050432	catecholamine secretion	0.82
GO:0031267	small GTPase binding	0.82
MP:0005352	small cranium	0.82
MP:0009712	impaired conditioned place preference behavior	0.82
ENSG00000175115	PACS1 PPI subnetwork	0.82
ENSG00000091651	ORC6 PPI subnetwork	0.82
GO:0005525	GTP binding	0.82
ENSG00000089280	FUS PPI subnetwork	0.82
GO:0034704	calcium channel complex	0.82
ENSG00000214122	ENSG00000214122 PPI subnetwork	0.82
ENSG00000145241	CENPC1 PPI subnetwork	0.82
ENSG00000117713	ARID1A PPI subnetwork	0.82
ENSG00000139546	TARBP2 PPI subnetwork	0.82
ENSG00000213672	NCKIPSD PPI subnetwork	0.82
ENSG00000170927	PKHD1 PPI subnetwork	0.82
ENSG00000080345	RIF1 PPI subnetwork	0.82
GO:0001660	fever generation	0.82
ENSG00000131795	RBM8A PPI subnetwork	0.82
ENSG00000015285	WAS PPI subnetwork	0.82

Original gene set ID	Original gene set description	Nominal P value
GO:0006103	2-oxoglutarate metabolic process	0.82
ENSG00000116350	SRSF4 PPI subnetwork	0.83
GO:0030073	insulin secretion	0.83
GO:0007602	phototransduction	0.83
GO:0032281	alpha-amino-3-hydroxy-5-methyl-4-isoxazolepropionic acid selective glutamate rece	0.83
GO:0032153	cell division site	0.83
GO:0032155	cell division site part	0.83
MP:0005027	increased susceptibility to parasitic infectior	0.83
ENSG00000125651	GTF2F1 PPI subnetwork	0.83
REACTOME_TAT:MEDIATED_ELONGATION_OF_THE_HIV:1_TRANSCRIPT	REACTOME_TAT:MEDIATED_ELONGATION_OF_THE_HIV:1_TRANSCRIPT	0.83
REACTOME_HIV:1_TRANSCRIPTION_ELONGATION	REACTOME_HIV:1_TRANSCRIPTION_ELONGATION	0.83
REACTOME_FORMATION_OF_HIV:1_ELONGATION_COMPLEX_CONTAINING_HI	REACTOME_FORMATION_OF_HIV:1_ELONGATION_COMPLEX_CONTAINING_HIV:1_	0.83
ENSG00000163541	SUCLG1 PPI subnetwork	0.83
MP:0010053	decreased grip strength	0.83
ENSG00000077420	APBB1P PPI subnetwork	0.83
GO:0051168	nuclear export	0.83
GO:0006997	nucleus organization	0.83
ENSG00000167110	GOLGA2 PPI subnetwork	0.83
GO:0009581	detection of external stimulus	0.83
ENSG00000159131	GART PPI subnetwork	0.83
ENSG00000168148	HIST3H3 PPI subnetwork	0.83
ENSG00000165916	PSMC3 PPI subnetwork	0.83
ENSG00000073792	IGF2BP2 PPI subnetwork	0.83
ENSG00000072315	TRPC5 PPI subnetwork	0.83
GO:0030574	collagen catabolic process	0.83
ENSG00000158869	FCER1G PPI subnetwork	0.83
MP:0003861	abnormal nervous system development	0.83
ENSG00000013573	DDX11 PPI subnetwork	0.83
GO:0001508	regulation of action potential	0.83
MP:0003924	herniated diaphragm	0.83
GO:0031076	embryonic camera-type eye development	0.83
ENSG00000122126	OCRL PPI subnetwork	0.83
ENSG00000168291	PDHB PPI subnetwork	0.83
ENSG00000183395	PMCH PPI subnetwork	0.83
ENSG00000182054	IDH2 PPI subnetwork	0.83
REACTOME_GLOBAL_GENOMIC_NER_GG:NER	REACTOME_GLOBAL_GENOMIC_NER_GG:NER	0.83
MP:0005107	abnormal stapes morphology	0.83
GO:0005484	SNAP receptor activity	0.83
MP:0003992	increased mortality induced by ionizing radiatior	0.83
GO:0019829	cation-transporting ATPase activity	0.83
ENSG00000167283	ATP5L PPI subnetwork	0.83
GO:0042730	fibrinolysis	0.83
GO:0034654	nucleobase-containing compound biosynthetic process	0.83
REACTOME_HIV:1_TRANSCRIPTION_INITIATION	REACTOME_HIV:1_TRANSCRIPTION_INITIATION	0.83
REACTOME_RNA_POLYMERASE_II_TRANSCRIPTION_PRE:INITIATION_AND_PRO	REACTOME_RNA_POLYMERASE_II_TRANSCRIPTION_PRE:INITIATION_AND_PROMO	0.83
REACTOME_RNA_POLYMERASE_II_TRANSCRIPTION_INITIATION	REACTOME_RNA_POLYMERASE_II_TRANSCRIPTION_INITIATION	0.83
REACTOME_RNA_POLYMERASE_II_HIV:1_PROMOTER_ESCAPE	REACTOME_RNA_POLYMERASE_II_HIV:1_PROMOTER_ESCAPE	0.83
REACTOME_RNA_POLYMERASE_II_TRANSCRIPTION_INITIATION_AND_PROMOT	REACTOME_RNA_POLYMERASE_II_TRANSCRIPTION_INITIATION_AND_PROMOTER_	0.83
REACTOME_RNA_POLYMERASE_II_PROMOTER_ESCAPE	REACTOME_RNA_POLYMERASE_II_PROMOTER_ESCAPE	0.83

Original gene set ID	Original gene set description	Nominal P value
GO:0051437	positive regulation of ubiquitin-protein ligase activity involved in mitotic cell cycle	0.83
ENSG00000185532	PRKG1 PPI subnetwork	0.83
ENSG00000089169	RPH3A PPI subnetwork	0.83
GO:0015980	energy derivation by oxidation of organic compounds	0.83
ENSG00000160062	ZBTB8A PPI subnetwork	0.83
MP:0000933	abnormal rhombomere morphology	0.83
ENSG00000178952	TUFM PPI subnetwork	0.83
GO:0033044	regulation of chromosome organization	0.83
GO:0016701	oxidoreductase activity, acting on single donors with incorporation of molecular oxy	0.83
ENSG00000160803	UBQLN4 PPI subnetwork	0.83
ENSG00000100519	PSMC6 PPI subnetwork	0.83
ENSG00000073050	XRCC1 PPI subnetwork	0.83
GO:0018130	heterocycle biosynthetic process	0.83
ENSG00000078140	UBE2K PPI subnetwork	0.83
ENSG00000171475	WIPF2 PPI subnetwork	0.83
MP:0001666	abnormal intestinal absorption	0.83
ENSG00000146047	HIST1H2BA PPI subnetwork	0.83
GO:0016445	somatic diversification of immunoglobulins	0.83
ENSG00000150753	CCT5 PPI subnetwork	0.83
GO:0009074	aromatic amino acid family catabolic process	0.83
ENSG00000171195	MUC7 PPI subnetwork	0.83
GO:0006901	vesicle coating	0.83
KEGG_RETINOL_METABOLISM	KEGG_RETINOL_METABOLISM	0.83
GO:0007271	synaptic transmission, cholinergic	0.83
GO:0006278	RNA-dependent DNA replication	0.83
MP:0004756	abnormal proximal convoluted tubule morphology	0.83
REACTOME_THE_ROLE_OF_NEF_IN_HIV:1_REPLICATION_AND_DISEASE_PATHC	REACTOME_THE_ROLE_OF_NEF_IN_HIV:1_REPLICATION_AND_DISEASE_PATHOGEN	0.83
ENSG00000129152	MYOD1 PPI subnetwork	0.83
MP:0001693	failure of primitive streak formation	0.83
GO:0000209	protein polyubiquitination	0.83
ENSG00000198211	TUBB3 PPI subnetwork	0.83
ENSG00000176788	BASP1 PPI subnetwork	0.83
ENSG00000094804	CDC6 PPI subnetwork	0.83
ENSG00000068796	KIF2A PPI subnetwork	0.83
MP:0010868	increased bone trabecula number	0.83
GO:0016675	oxidoreductase activity, acting on a heme group of donors	0.83
GO:0051339	regulation of lyase activity	0.83
ENSG00000176248	ANAPC2 PPI subnetwork	0.83
ENSG00000156467	UQCRB PPI subnetwork	0.83
GO:0005813	centrosome	0.83
ENSG00000135213	POM121C PPI subnetwork	0.83
ENSG00000119383	PPP2R4 PPI subnetwork	0.83
ENSG00000184381	PLA2G6 PPI subnetwork	0.83
ENSG00000138778	CENPE PPI subnetwork	0.83
ENSG00000167549	CORO6 PPI subnetwork	0.83
GO:0005126	cytokine receptor binding	0.83
ENSG00000188170	ENSG00000188170 PPI subnetwork	0.83
REACTOME_FORMATION_OF_ATP_BY_CHEMIOSMOTIC_COUPLING	REACTOME_FORMATION_OF_ATP_BY_CHEMIOSMOTIC_COUPLING	0.83
REACTOME_EGFR_DOWNREGULATION	REACTOME_EGFR_DOWNREGULATION	0.83

Original gene set ID	Original gene set description	Nominal P value
ENSG00000130340	SNX9 PPI subnetwork	0.83
GO:0005849	mRNA cleavage factor complex	0.83
GO:0048305	immunoglobulin secretion	0.83
REACTOME_PKA_ACTIVATION	REACTOME_PKA_ACTIVATION	0.83
REACTOME_PROCESSING_OF_CAPPED_INTRON:CONTAINING_PRE:MRNA	REACTOME_PROCESSING_OF_CAPPED_INTRON:CONTAINING_PRE:MRNA	0.83
ENSG00000177084	POLE PPI subnetwork	0.83
ENSG00000163161	ERCC3 PPI subnetwork	0.83
ENSG00000133116	KL PPI subnetwork	0.83
ENSG00000141034	C17orf39 PPI subnetwork	0.83
ENSG00000110801	PSMD9 PPI subnetwork	0.83
ENSG00000150086	GRIN2B PPI subnetwork	0.83
ENSG00000159164	SV2A PPI subnetwork	0.83
GO:0050670	regulation of lymphocyte proliferation	0.83
GO:0051169	nuclear transport	0.84
ENSG00000091181	IL5RA PPI subnetwork	0.84
GO:0009070	serine family amino acid biosynthetic process	0.84
MP:0003311	aminoaciduria	0.84
REACTOME_MRNA_SPLICING_:MINOR_PATHWAY	REACTOME_MRNA_SPLICING_:MINOR_PATHWAY	0.84
ENSG00000112379	KIAA1244 PPI subnetwork	0.84
MP:0001415	increased exploration in new environment	0.84
GO:0006260	DNA replication	0.84
GO:0009584	detection of visible light	0.84
ENSG00000100292	HMOX1 PPI subnetwork	0.84
ENSG00000178741	COX5A PPI subnetwork	0.84
GO:0090101	negative regulation of transmembrane receptor protein serine/threonine kinase signaling	0.84
GO:0031279	regulation of cyclase activity	0.84
MP:0006108	abnormal hindbrain development	0.84
GO:0031401	positive regulation of protein modification process	0.84
MP:0002753	dilated heart left ventricle	0.84
GO:0008188	neuropeptide receptor activity	0.84
ENSG00000132464	ENAM PPI subnetwork	0.84
ENSG00000075785	RAB7A PPI subnetwork	0.84
GO:0006206	pyrimidine base metabolic process	0.84
GO:0016879	ligase activity, forming carbon-nitrogen bonds	0.84
ENSG00000133226	SRRM1 PPI subnetwork	0.84
GO:0016918	retinal binding	0.84
ENSG00000111786	SRSF9 PPI subnetwork	0.84
GO:0004222	metalloendopeptidase activity	0.84
GO:0048037	cofactor binding	0.84
REACTOME_DEADENYLATION:DEPENDENT_MRNA_DECAY	REACTOME_DEADENYLATION:DEPENDENT_MRNA_DECAY	0.84
GO:0006091	generation of precursor metabolites and energy	0.84
GO:0009607	response to biotic stimulus	0.84
ENSG00000204356	RDBP PPI subnetwork	0.84
ENSG00000206268	RDBP PPI subnetwork	0.84
ENSG00000206357	RDBP PPI subnetwork	0.84
ENSG00000183625	CCR3 PPI subnetwork	0.84
ENSG00000160201	U2AF1 PPI subnetwork	0.84
ENSG00000100650	SRSF5 PPI subnetwork	0.84
ENSG00000156261	CCT8 PPI subnetwork	0.84

Original gene set ID	Original gene set description	Nominal P value
ENSG00000122180	MYOG PPI subnetwork	0.84
ENSG00000144642	RBMS3 PPI subnetwork	0.84
GO:0005125	cytokine activity	0.84
ENSG00000180190	C8orf42 PPI subnetwork	0.84
ENSG00000151224	MAT1A PPI subnetwork	0.84
GO:0032633	interleukin-4 production	0.84
ENSG00000164815	ORC5 PPI subnetwork	0.84
ENSG00000101413	RPRD1B PPI subnetwork	0.84
ENSG00000156049	GNA14 PPI subnetwork	0.84
ENSG00000125351	UPF3B PPI subnetwork	0.84
GO:0051054	positive regulation of DNA metabolic process	0.84
MP:0000877	abnormal Purkinje cell morphology	0.84
MP:0003730	abnormal photoreceptor inner segment morphology	0.84
GO:0032784	regulation of transcription elongation, DNA-dependent	0.84
GO:0002474	antigen processing and presentation of peptide antigen via MHC class	0.84
ENSG00000149311	ATM PPI subnetwork	0.84
GO:0060512	prostate gland morphogenesis	0.84
MP:0000929	open neural tube	0.84
GO:0042613	MHC class II protein complex	0.84
GO:0000375	RNA splicing, via transesterification reactions	0.84
REACTOME_E2F_MEDIATED_REGULATION_OF_DNA_REPLICATION	REACTOME_E2F_MEDIATED_REGULATION_OF_DNA_REPLICATION	0.84
ENSG00000134602	ENSG00000134602 PPI subnetwork	0.84
ENSG00000085662	AKR1B1 PPI subnetwork	0.84
GO:0009635	response to herbicide	0.84
GO:0008353	RNA polymerase II carboxy-terminal domain kinase activity	0.84
REACTOME_MUSCLE_CONTRACTION	REACTOME_MUSCLE_CONTRACTION	0.84
GO:0006220	pyrimidine nucleotide metabolic process	0.84
GO:0043395	heparan sulfate proteoglycan binding	0.84
GO:0007033	vacuole organization	0.84
MP:0004073	caudal body truncation	0.84
REACTOME_PROCESSING_OF_INTRONLESS_PRE:MRNAS	REACTOME_PROCESSING_OF_INTRONLESS_PRE:MRNAS	0.84
REACTOME_MRNA_PROCESSING	REACTOME_MRNA_PROCESSING	0.84
GO:0006511	ubiquitin-dependent protein catabolic process	0.84
GO:0000152	nuclear ubiquitin ligase complex	0.85
GO:0004993	serotonin receptor activity	0.85
ENSG00000138385	SSB PPI subnetwork	0.85
ENSG00000172409	CLP1 PPI subnetwork	0.85
GO:0009165	nucleotide biosynthetic process	0.85
ENSG00000163737	PF4 PPI subnetwork	0.85
REACTOME_DNA_REPAIR	REACTOME_DNA_REPAIR	0.85
ENSG00000169020	ATP5I PPI subnetwork	0.85
GO:0006813	potassium ion transport	0.85
REACTOME_TRANSCRIPTION_OF_THE_HIV_GENOME	REACTOME_TRANSCRIPTION_OF_THE_HIV_GENOME	0.85
GO:0030312	external encapsulating structure	0.85
GO:0006140	regulation of nucleotide metabolic process	0.85
ENSG00000100804	PSMB5 PPI subnetwork	0.85
MP:0005650	abnormal limb bud morphology	0.85
MP:0002718	abnormal inner cell mass morphology	0.85
REACTOME_MYOGENESIS	REACTOME_MYOGENESIS	0.85

Original gene set ID	Original gene set description	Nominal P value
REACTOME_CDO_IN_MYOGENESIS	REACTOME_CDO_IN_MYOGENESIS	0.85
GO:0048813	dendrite morphogenesis	0.85
MP:0009336	increased splenocyte proliferation	0.85
ENSG00000060339	CCAR1 PPI subnetwork	0.85
GO:0030838	positive regulation of actin filament polymerization	0.85
GO:0050807	regulation of synapse organization	0.85
MP:0003290	intestinal hypoperistalsis	0.85
REACTOME_TRANSPORT_OF_MATURE_MRNA_DERIVED_FROM_AN_INTRONLESS_TRANSCRIPT	REACTOME_TRANSPORT_OF_MATURE_MRNA_DERIVED_FROM_AN_INTRONLESS_TRANSCRIPT	0.85
GO:0009799	specification of symmetry	0.85
ENSG00000115145	STAM2 PPI subnetwork	0.85
GO:0032944	regulation of mononuclear cell proliferation	0.85
MP:0000272	abnormal aorta morphology	0.85
GO:0015812	gamma-aminobutyric acid transport	0.85
ENSG00000115875	SRSF7 PPI subnetwork	0.85
GO:0042220	response to cocaine	0.85
GO:0014073	response to tropane	0.85
ENSG00000171724	VAT1L PPI subnetwork	0.85
MP:0002575	increased circulating ketone body level	0.85
GO:0004842	ubiquitin-protein ligase activity	0.85
ENSG00000109111	SUPT6H PPI subnetwork	0.85
ENSG00000144028	SNRNP200 PPI subnetwork	0.85
MP:0000266	abnormal heart morphology	0.85
ENSG00000142039	CCDC97 PPI subnetwork	0.85
GO:0005815	microtubule organizing center	0.85
GO:0048701	embryonic cranial skeleton morphogenesis	0.85
ENSG00000198523	PLN PPI subnetwork	0.85
GO:0051443	positive regulation of ubiquitin-protein ligase activity	0.85
ENSG00000136450	SRSF1 PPI subnetwork	0.85
GO:0042743	hydrogen peroxide metabolic process	0.85
REACTOME_SIGNALLING_TO_P38_VIA_RIT_AND_RIN	REACTOME_SIGNALLING_TO_P38_VIA_RIT_AND_RIN	0.85
ENSG00000205531	NAP1L4 PPI subnetwork	0.85
ENSG00000088256	GNA11 PPI subnetwork	0.85
ENSG00000157020	SEC13 PPI subnetwork	0.85
REACTOME_PKA_ACTIVATION_IN_GLUCAGON_SIGNALLING	REACTOME_PKA_ACTIVATION_IN_GLUCAGON_SIGNALLING	0.85
REACTOME_CALCITONIN-LIKE_LIGAND_RECEPTORS	REACTOME_CALCITONIN-LIKE_LIGAND_RECEPTORS	0.85
ENSG00000110717	NDUFS8 PPI subnetwork	0.85
ENSG00000102387	TAF7L PPI subnetwork	0.85
ENSG00000129084	PSMA1 PPI subnetwork	0.85
ENSG00000100280	AP1B1 PPI subnetwork	0.85
GO:0006360	transcription from RNA polymerase I promoter	0.85
GO:0051536	iron-sulfur cluster binding	0.85
GO:0051540	metal cluster binding	0.85
ENSG00000134444	KIAA1468 PPI subnetwork	0.85
GO:0016032	viral reproduction	0.85
ENSG00000141232	TOB1 PPI subnetwork	0.85
GO:0030239	myofibril assembly	0.85
MP:0006089	abnormal vestibular sacculi morphology	0.85
ENSG00000105705	SUGP1 PPI subnetwork	0.85
MP:0003149	abnormal tectorial membrane morphology	0.85

Original gene set ID	Original gene set description	Nominal P value
GO:0003382	epithelial cell morphogenesis	0.86
GO:0008608	attachment of spindle microtubules to kinetochore	0.86
GO:0042354	L-fucose metabolic process	0.86
ENSG00000133812	SBF2 PPI subnetwork	0.86
ENSG00000124507	PACSIN1 PPI subnetwork	0.86
MP:0004738	abnormal brainstem auditory evoked potentia	0.86
REACTOME_PROSTACYCLIN_SIGNALLING_THROUGH_PROSTACYCLIN_RECEPTOR	REACTOME_PROSTACYCLIN_SIGNALLING_THROUGH_PROSTACYCLIN_RECEPTOR	0.86
ENSG00000143079	CTTNBP2NL PPI subnetwork	0.86
GO:0006887	exocytosis	0.86
ENSG00000152056	AP1S3 PPI subnetwork	0.86
REACTOME_CAM_PATHWAY	REACTOME_CAM_PATHWAY	0.86
REACTOME_CALMODULIN_INDUCED_EVENTS	REACTOME_CALMODULIN_INDUCED_EVENTS	0.86
GO:0000781	chromosome, telomeric region	0.86
REACTOME_AMINE_LIGAND_BINDING_RECEPTORS	REACTOME_AMINE_LIGAND_BINDING_RECEPTORS	0.86
ENSG00000107371	EXOSC3 PPI subnetwork	0.86
REACTOME_SIGNALING_BY_ROBO_RECEPTOR	REACTOME_SIGNALING_BY_ROBO_RECEPTOR	0.86
ENSG00000188986	COBRA1 PPI subnetwork	0.86
REACTOME_ADHERENS_JUNCTIONS_INTERACTIONS	REACTOME_ADHERENS_JUNCTIONS_INTERACTIONS	0.86
ENSG00000122566	HNRNPA2B1 PPI subnetwork	0.86
MP:0000359	abnormal mast cell morphology	0.86
MP:0004722	abnormal platelet dense granule number	0.86
ENSG00000188342	GTF2F2 PPI subnetwork	0.86
GO:0001774	microglial cell activation	0.86
ENSG00000127920	GNG11 PPI subnetwork	0.86
ENSG00000112079	STK38 PPI subnetwork	0.86
GO:0009953	dorsal/ventral pattern formation	0.86
GO:0031032	actomyosin structure organization	0.86
GO:0050912	detection of chemical stimulus involved in sensory perception of taste	0.86
ENSG00000132383	RPA1 PPI subnetwork	0.86
ENSG00000086102	NFX1 PPI subnetwork	0.86
ENSG00000182185	RAD51B PPI subnetwork	0.86
ENSG00000183856	IQGAP3 PPI subnetwork	0.86
GO:0048483	autonomic nervous system development	0.86
GO:0023021	termination of signal transduction	0.86
ENSG00000169813	HNRNPF PPI subnetwork	0.86
ENSG00000100503	NIN PPI subnetwork	0.86
ENSG00000159377	PSMB4 PPI subnetwork	0.86
GO:0016702	oxidoreductase activity, acting on single donors with incorporation of molecular oxy	0.86
GO:0009582	detection of abiotic stimulus	0.86
MP:0009760	abnormal mitotic spindle morphology	0.86
MP:0004568	fusion of glossopharyngeal and vagus nerve	0.86
MP:0008148	abnormal rib-sternum attachment	0.86
ENSG00000160199	PKNOX1 PPI subnetwork	0.86
MP:0004970	kidney atrophy	0.86
ENSG00000077063	CTTNBP2 PPI subnetwork	0.86
ENSG00000124193	SRSF6 PPI subnetwork	0.86
MP:0004163	abnormal adenohypophysis morphology	0.86
GO:0034622	cellular macromolecular complex assembly	0.86
ENSG00000145321	GC PPI subnetwork	0.86

Original gene set ID	Original gene set description	Nominal P value
MP:0002920	decreased paired-pulse facilitation	0.87
MP:0008272	abnormal endochondral bone ossification	0.87
MP:0002066	abnormal motor capabilities/coordination/movement	0.87
MP:0009133	decreased white fat cell size	0.87
ENSG00000120254	MTHFD1L PPI subnetwork	0.87
GO:0005328	neurotransmitter:sodium symporter activity	0.87
GO:0033108	mitochondrial respiratory chain complex assembly	0.87
ENSG00000206503	HLA-A PPI subnetwork	0.87
ENSG00000013583	HEBP1 PPI subnetwork	0.87
MP:0005171	absent coat pigmentation	0.87
ENSG00000170310	STX8 PPI subnetwork	0.87
REACTOME_CLATHRIN_DERIVED_VESICLE_BUDDING	REACTOME_CLATHRIN_DERIVED_VESICLE_BUDDING	0.87
REACTOME_TRANS:GOLGI_NETWORK_VESICLE_BUDDING	REACTOME_TRANS:GOLGI_NETWORK_VESICLE_BUDDING	0.87
GO:0016790	thiolester hydrolase activity	0.87
ENSG00000151923	TIAL1 PPI subnetwork	0.87
MP:0005193	abnormal anterior eye segment morphology	0.87
ENSG00000137259	HIST1H2AB PPI subnetwork	0.87
ENSG00000168274	HIST1H2AE PPI subnetwork	0.87
REACTOME_NEUROTRANSMITTER_RECEPTOR_BINDING_AND_DOWNSTREAM_TRANSDUCTION	REACTOME_NEUROTRANSMITTER_RECEPTOR_BINDING_AND_DOWNSTREAM_TRANSDUCTION	0.87
GO:0050803	regulation of synapse structure and activity	0.87
ENSG00000163159	VPS72 PPI subnetwork	0.87
ENSG00000111245	MYL2 PPI subnetwork	0.87
ENSG00000155130	MARCKS PPI subnetwork	0.87
GO:0021953	central nervous system neuron differentiation	0.87
GO:0006213	pyrimidine nucleoside metabolic process	0.87
ENSG00000125354	SEPT6 PPI subnetwork	0.87
GO:0043632	modification-dependent macromolecule catabolic process	0.87
ENSG00000090060	PAPOLA PPI subnetwork	0.87
REACTOME_ADP_SIGNALLING_THROUGH_P2Y_PURINOCEPTOR_12	REACTOME_ADP_SIGNALLING_THROUGH_P2Y_PURINOCEPTOR_12	0.87
MP:0002633	persistent truncus arteriosus	0.87
ENSG00000134690	CDCA8 PPI subnetwork	0.87
ENSG00000116329	OPRD1 PPI subnetwork	0.87
GO:0051028	mRNA transport	0.87
MP:0002332	abnormal exercise endurance	0.87
GO:0019787	small conjugating protein ligase activity	0.87
GO:0051966	regulation of synaptic transmission, glutamatergic	0.87
ENSG00000167977	KCTD5 PPI subnetwork	0.87
ENSG00000168298	HIST1H1E PPI subnetwork	0.87
ENSG00000173636	ENSG00000173636 PPI subnetwork	0.87
ENSG00000166477	LEO1 PPI subnetwork	0.87
ENSG00000069424	KCNAB2 PPI subnetwork	0.87
ENSG00000085365	ENSG00000085365 PPI subnetwork	0.87
MP:0010107	abnormal renal reabsorption	0.87
ENSG00000089053	ANAPC5 PPI subnetwork	0.87
MP:0005445	abnormal neurotransmitter secretion	0.87
GO:0019363	pyridine nucleotide biosynthetic process	0.87
GO:0072525	pyridine-containing compound biosynthetic process	0.87
GO:0009064	glutamine family amino acid metabolic process	0.87
GO:0007190	activation of adenylate cyclase activity	0.87

Original gene set ID	Original gene set description	Nominal P value
ENSG00000165494	PCF11 PPI subnetwork	0.87
ENSG00000083857	FAT1 PPI subnetwork	0.87
ENSG00000070961	ATP2B1 PPI subnetwork	0.87
ENSG00000138668	HNRNPD PPI subnetwork	0.87
ENSG00000068878	PSME4 PPI subnetwork	0.87
MP:0003864	abnormal midbrain development	0.87
MP:0005191	head tilt	0.87
MP:0000189	hypoglycemia	0.87
ENSG00000171497	PPID PPI subnetwork	0.87
ENSG00000125266	EFNB2 PPI subnetwork	0.87
GO:0070403	NAD+ binding	0.87
ENSG00000149532	CPSF7 PPI subnetwork	0.87
GO:0021527	spinal cord association neuron differentiator	0.87
GO:0032813	tumor necrosis factor receptor superfamily binding	0.88
ENSG00000174851	YIF1A PPI subnetwork	0.88
GO:0060487	lung epithelial cell differentiation	0.88
ENSG00000141503	MINK1 PPI subnetwork	0.88
ENSG00000080603	SRCAP PPI subnetwork	0.88
ENSG00000099622	CIRBP PPI subnetwork	0.88
GO:0051213	dioxygenase activity	0.88
REACTOME_REGULATION_OF_INSULIN_SECRETION_BY_GLU	REACTOME_REGULATION_OF_INSULIN_SECRETION_BY_GLU	0.88
ENSG00000105011	ASF1B PPI subnetwork	0.88
MP:0004819	decreased skeletal muscle mass	0.88
REACTOME_AMYLOIDS	REACTOME_AMYLOIDS	0.88
MP:0005075	abnormal melanosome morphology	0.88
KEGG_TRYPTOPHAN_METABOLISM	KEGG_TRYPTOPHAN_METABOLISM	0.88
ENSG00000031691	CENPQ PPI subnetwork	0.88
GO:2000516	positive regulation of CD4-positive, alpha-beta T cell activator	0.88
GO:0043372	positive regulation of CD4-positive, alpha-beta T cell differentiator	0.88
ENSG00000120334	CENPL PPI subnetwork	0.88
ENSG00000116095	PLEKHA3 PPI subnetwork	0.88
GO:0045762	positive regulation of adenylate cyclase activity	0.88
GO:0031281	positive regulation of cyclase activity	0.88
ENSG00000089685	BIRC5 PPI subnetwork	0.88
GO:0021781	glial cell fate commitment	0.88
ENSG00000120699	EXOSC8 PPI subnetwork	0.88
ENSG00000103363	TCEB2 PPI subnetwork	0.88
MP:0010984	abnormal metanephric mesenchyme morphology	0.88
ENSG00000169213	RAB3B PPI subnetwork	0.88
ENSG00000179899	ENSG00000179899 PPI subnetwork	0.88
ENSG00000196531	NACA PPI subnetwork	0.88
GO:0072080	nephron tubule development	0.88
MP:0004066	abnormal primitive node morphology	0.88
GO:0051439	regulation of ubiquitin-protein ligase activity involved in mitotic cell cycle	0.88
ENSG00000148835	TAF5 PPI subnetwork	0.88
ENSG00000095585	BLNK PPI subnetwork	0.88
GO:0001838	embryonic epithelial tube formation	0.88
ENSG00000184408	KCND2 PPI subnetwork	0.88
ENSG00000171793	CTPS PPI subnetwork	0.88

Original gene set ID	Original gene set description	Nominal P value
ENSG00000197905	TEAD4 PPI subnetwork	0.88
ENSG00000140379	BCL2A1 PPI subnetwork	0.88
MP:0002058	neonatal lethality	0.88
GO:0032934	sterol binding	0.88
MP:0005157	holoprosencephaly	0.88
GO:0048002	antigen processing and presentation of peptide antigen	0.88
GO:0051058	negative regulation of small GTPase mediated signal transduction	0.88
MP:0004599	abnormal vertebral arch morphology	0.88
GO:0051349	positive regulation of lyase activity	0.88
GO:0031145	anaphase-promoting complex-dependent proteasomal ubiquitin-dependent protein	0.88
GO:0007223	Wnt receptor signaling pathway, calcium modulating pathway	0.88
GO:0007218	neuropeptide signaling pathway	0.88
GO:0032835	glomerulus development	0.88
GO:0000236	mitotic prometaphase	0.88
REACTOME_AMINO_ACID_SYNTHESIS_AND_INTERCONVERSION_TRANSAMINATION	REACTOME_AMINO_ACID_SYNTHESIS_AND_INTERCONVERSION_TRANSAMINATION	0.88
GO:0035249	synaptic transmission, glutamatergic	0.88
GO:0005753	mitochondrial proton-transporting ATP synthase complex	0.88
ENSG00000184575	XPOT PPI subnetwork	0.88
ENSG00000137947	GTF2B PPI subnetwork	0.88
GO:0010972	negative regulation of G2/M transition of mitotic cell cycle	0.88
ENSG00000110768	GTF2H1 PPI subnetwork	0.88
ENSG00000117153	KLHL12 PPI subnetwork	0.88
ENSG00000168002	POLR2G PPI subnetwork	0.88
ENSG00000138663	COPS4 PPI subnetwork	0.88
MP:0003120	abnormal tracheal cartilage morphology	0.88
ENSG00000172660	TAF15 PPI subnetwork	0.88
ENSG00000119203	CPSF3 PPI subnetwork	0.88
ENSG00000164076	CAMKV PPI subnetwork	0.88
MP:0000783	abnormal forebrain morphology	0.88
ENSG00000132334	PTPRE PPI subnetwork	0.88
MP:0002841	impaired skeletal muscle contractility	0.88
ENSG00000132692	BCAN PPI subnetwork	0.88
ENSG00000095380	NANS PPI subnetwork	0.88
MP:0000270	abnormal heart tube morphology	0.88
GO:0003009	skeletal muscle contraction	0.88
GO:0034614	cellular response to reactive oxygen species	0.88
GO:0060590	ATPase regulator activity	0.88
REACTOME_MEMBRANE_TRAFFICKING	REACTOME_MEMBRANE_TRAFFICKING	0.88
ENSG00000102384	CENPI PPI subnetwork	0.88
GO:0032465	regulation of cytokinesis	0.88
GO:0006284	base-excision repair	0.88
ENSG00000137642	SORL1 PPI subnetwork	0.88
ENSG00000106100	NOD1 PPI subnetwork	0.88
GO:0045981	positive regulation of nucleotide metabolic process	0.88
ENSG00000197111	PCBP2 PPI subnetwork	0.88
ENSG00000177302	TOP3A PPI subnetwork	0.88
ENSG00000165934	CPSF2 PPI subnetwork	0.88
GO:0042088	T-helper 1 type immune response	0.88
GO:0047496	vesicle transport along microtubule	0.88

Original gene set ID	Original gene set description	Nominal P value
ENSG00000100554	ATP6V1D PPI subnetwork	0.88
GO:0051539	4 iron, 4 sulfur cluster binding	0.88
MP:0000966	decreased sensory neuron number	0.88
GO:0009409	response to cold	0.88
ENSG00000137055	PLAA PPI subnetwork	0.88
GO:0016567	protein ubiquitination	0.88
GO:0016903	oxidoreductase activity, acting on the aldehyde or oxo group of donor:	0.88
GO:0019674	NAD metabolic process	0.88
ENSG00000206258	TNXB PPI subnetwork	0.88
ENSG00000198692	EIF1AY PPI subnetwork	0.88
ENSG00000197558	ENSG00000197558 PPI subnetwork	0.88
ENSG00000127388	ENSG00000127388 PPI subnetwork	0.88
ENSG00000161888	SPC24 PPI subnetwork	0.88
ENSG00000181790	BAI1 PPI subnetwork	0.88
ENSG00000166451	CENPN PPI subnetwork	0.88
ENSG00000020922	MRE11A PPI subnetwork	0.89
GO:0046641	positive regulation of alpha-beta T cell proliferation	0.89
GO:0042391	regulation of membrane potential	0.89
GO:0017157	regulation of exocytosis	0.89
GO:0006405	RNA export from nucleus	0.89
ENSG00000100151	PICK1 PPI subnetwork	0.89
GO:0032729	positive regulation of interferon-gamma production	0.89
ENSG00000114812	VIPR1 PPI subnetwork	0.89
GO:0006403	RNA localization	0.89
GO:0030684	preribosome	0.89
ENSG00000169976	SF3B5 PPI subnetwork	0.89
ENSG00000105323	HNRNPUL1 PPI subnetwork	0.89
GO:0045624	positive regulation of T-helper cell differentiation	0.89
ENSG00000127481	UBR4 PPI subnetwork	0.89
MP:0001793	altered susceptibility to infection	0.89
ENSG00000129757	CDKN1C PPI subnetwork	0.89
ENSG00000118194	TNNT2 PPI subnetwork	0.89
GO:0021675	nerve development	0.89
GO:0046356	acetyl-CoA catabolic process	0.89
GO:0048193	Golgi vesicle transport	0.89
GO:0044449	contractile fiber part	0.89
ENSG00000113456	RAD1 PPI subnetwork	0.89
ENSG00000157404	KIT PPI subnetwork	0.89
GO:0030801	positive regulation of cyclic nucleotide metabolic process	0.89
MP:0000774	decreased brain size	0.89
ENSG00000111275	ALDH2 PPI subnetwork	0.89
ENSG00000146963	LUC7L2 PPI subnetwork	0.89
MP:0000137	abnormal vertebrae morphology	0.89
ENSG00000204133	ENSG00000204133 PPI subnetwork	0.89
GO:0051313	attachment of spindle microtubules to chromosome	0.89
MP:0009907	decreased tongue size	0.89
GO:0005003	ephrin receptor activity	0.89
ENSG00000163527	STT3B PPI subnetwork	0.89
GO:0051023	regulation of immunoglobulin secretion	0.89

Original gene set ID	Original gene set description	Nominal P value
ENSG00000196747	HIST1H2AI PPI subnetwork	0.89
ENSG00000196787	HIST1H2AG PPI subnetwork	0.89
ENSG00000196866	HIST1H2AD PPI subnetwork	0.89
ENSG00000184348	HIST1H2AK PPI subnetwork	0.89
ENSG00000198374	HIST1H2AL PPI subnetwork	0.89
ENSG00000198728	LDB1 PPI subnetwork	0.89
GO:0000910	cytokinesis	0.89
ENSG00000103496	STX4 PPI subnetwork	0.89
REACTOME_PLATELET_CALCIIUM_HOMEOSTASIS	REACTOME_PLATELET_CALCIIUM_HOMEOSTASIS	0.89
MP:0005478	decreased circulating thyroxine level	0.89
MP:0003172	abnormal lysosome physiology	0.89
GO:0016620	oxidoreductase activity, acting on the aldehyde or oxo group of donors, NAD or NAC	0.89
ENSG00000184886	PIGW PPI subnetwork	0.89
ENSG00000159251	ACTC1 PPI subnetwork	0.89
ENSG00000169564	PCBP1 PPI subnetwork	0.89
REACTOME_TRANSPORT_OF_MATURE_MRNA_DERIVED_FROM_AN_INTRON:CONT	REACTOME_TRANSPORT_OF_MATURE_MRNA_DERIVED_FROM_AN_INTRON:CONT	0.89
GO:0050671	positive regulation of lymphocyte proliferation	0.89
ENSG00000100162	CENPM PPI subnetwork	0.89
ENSG00000198938	MT-CO3 PPI subnetwork	0.89
GO:0008374	O-acyltransferase activity	0.89
MP:0000940	abnormal motor neuron innervation	0.89
GO:0046605	regulation of centrosome cycle	0.89
MP:0001422	abnormal drinking behavior	0.89
GO:0021889	olfactory bulb interneuron differentiator	0.89
REACTOME_FORMATION_OF_THE_HIV:1_EARLY_ELONGATION_COMPLEX	REACTOME_FORMATION_OF_THE_HIV:1_EARLY_ELONGATION_COMPLEX	0.89
REACTOME_FORMATION_OF_THE_EARLY_ELONGATION_COMPLEX	REACTOME_FORMATION_OF_THE_EARLY_ELONGATION_COMPLEX	0.89
ENSG00000156052	GNAQ PPI subnetwork	0.89
GO:0030016	myofibril	0.89
ENSG00000152253	SPC25 PPI subnetwork	0.89
GO:0003156	regulation of organ formation	0.89
ENSG00000087250	MT3 PPI subnetwork	0.89
ENSG00000188312	CENPP PPI subnetwork	0.89
GO:0060428	lung epithelium development	0.89
MP:0002231	abnormal primitive streak morphology	0.89
ENSG00000165119	HNRNPK PPI subnetwork	0.89
REACTOME_ENDOSOMAL_SORTING_COMPLEX_REQUIRED_FOR_TRANSPORT_ESCR	REACTOME_ENDOSOMAL_SORTING_COMPLEX_REQUIRED_FOR_TRANSPORT_ESCR	0.89
GO:0008542	visual learning	0.89
ENSG00000114503	NCBP2 PPI subnetwork	0.89
ENSG00000115163	CENPA PPI subnetwork	0.89
MP:0003324	increased liver adenoma incidence	0.89
GO:0000149	SNARE binding	0.89
REACTOME_CDC6_ASSOCIATION_WITH_THE_ORCORIGIN_COMPLEX	REACTOME_CDC6_ASSOCIATION_WITH_THE_ORCORIGIN_COMPLEX	0.89
ENSG00000110955	ATP5B PPI subnetwork	0.89
GO:0005891	voltage-gated calcium channel complex	0.89
ENSG00000105669	COPE PPI subnetwork	0.89
GO:0001936	regulation of endothelial cell proliferati	0.89
KEGG_PEROXISOME	KEGG_PEROXISOME	0.89
ENSG00000013455	ENSG00000013455 PPI subnetwork	0.89
GO:0050997	quaternary ammonium group binding	0.89

Original gene set ID	Original gene set description	Nominal P value
MP:0004084	abnormal cardiac muscle relaxation	0.89
ENSG00000155974	GRIP1 PPI subnetwork	0.89
GO:0016331	morphogenesis of embryonic epithelium	0.89
ENSG00000115953	ENSG00000115953 PPI subnetwork	0.89
MP:0005192	increased motor neuron number	0.89
MP:0001286	abnormal eye development	0.89
MP:0005106	abnormal incus morphology	0.89
ENSG00000115252	PDE1A PPI subnetwork	0.89
GO:0005834	heterotrimeric G-protein complex	0.89
GO:0006000	fructose metabolic process	0.89
MP:0003271	abnormal duodenum morphology	0.89
GO:0045333	cellular respiration	0.89
ENSG00000136709	WDR33 PPI subnetwork	0.89
KEGG_SNARE_INTERACTIONS_IN_VESICULAR_TRANSPORT	KEGG_SNARE_INTERACTIONS_IN_VESICULAR_TRANSPORT	0.89
GO:0006873	cellular ion homeostasis	0.89
GO:0002208	somatic diversification of immunoglobulins involved in immune response	0.89
GO:0045190	isotype switching	0.89
GO:0002204	somatic recombination of immunoglobulin genes involved in immune response	0.89
GO:0021513	spinal cord dorsal/ventral patterning	0.89
REACTOME_TRANSPORT_OF_MATURE_MRNAS_DERIVED_FROM_INTRONLESS	REACTOME_TRANSPORT_OF_MATURE_MRNAS_DERIVED_FROM_INTRONLESS_TRA	0.89
REACTOME_THROMBIN_SIGNALLING_THROUGH_PROTEINASE_ACTIVATED_RECE	REACTOME_THROMBIN_SIGNALLING_THROUGH_PROTEINASE_ACTIVATED_RECE	0.89
KEGG_ARGININE_AND_PROLINE_METABOLISM	KEGG_ARGININE_AND_PROLINE_METABOLISM	0.9
ENSG00000108828	VAT1 PPI subnetwork	0.9
GO:0051082	unfolded protein binding	0.9
GO:0007215	glutamate receptor signaling pathway	0.9
MP:0002766	situs inversus	0.9
GO:0050806	positive regulation of synaptic transmission	0.9
GO:0042288	MHC class I protein binding	0.9
ENSG00000138674	SEC31A PPI subnetwork	0.9
ENSG00000105379	ETFB PPI subnetwork	0.9
ENSG00000187735	TCEA1 PPI subnetwork	0.9
MP:0002696	decreased circulating glucagon level	0.9
MP:0004566	myocardial fiber degeneration	0.9
GO:0007200	phospholipase C-activating G-protein coupled receptor signaling pathway	0.9
MP:0002279	abnormal diaphragm morphology	0.9
GO:0032880	regulation of protein localization	0.9
ENSG00000130066	SAT1 PPI subnetwork	0.9
MP:0005317	increased triglyceride level	0.9
GO:0022904	respiratory electron transport chain	0.9
GO:0006308	DNA catabolic process	0.9
ENSG00000112526	ENSG00000112526 PPI subnetwork	0.9
ENSG00000204256	BRD2 PPI subnetwork	0.9
ENSG00000215077	BRD2 PPI subnetwork	0.9
ENSG00000126698	DNAJC8 PPI subnetwork	0.9
ENSG00000002834	LASP1 PPI subnetwork	0.9
GO:0045063	T-helper 1 cell differentiation	0.9
ENSG00000169371	SNUPN PPI subnetwork	0.9
GO:0048710	regulation of astrocyte differentiation	0.9
GO:0060191	regulation of lipase activity	0.9

Original gene set ID	Original gene set description	Nominal P value
GO:0010243	response to organic nitrogen	0.9
GO:0017085	response to insecticide	0.9
ENSG000000134109	EDEM1 PPI subnetwork	0.9
GO:0046467	membrane lipid biosynthetic process	0.9
ENSG000000114573	ATP6V1A PPI subnetwork	0.9
GO:0072593	reactive oxygen species metabolic process	0.9
KEGG_SULFUR_METABOLISM	KEGG_SULFUR_METABOLISM	0.9
GO:0050881	musculoskeletal movement	0.9
GO:0050879	multicellular organismal movement	0.9
GO:0050953	sensory perception of light stimulus	0.9
ENSG000000169045	HNRNPH1 PPI subnetwork	0.9
ENSG000000096717	SIRT1 PPI subnetwork	0.9
GO:0007601	visual perception	0.9
GO:0005814	centriole	0.9
ENSG000000090989	EXOC1 PPI subnetwork	0.9
GO:0030163	protein catabolic process	0.9
ENSG000000181029	TRAPPC5 PPI subnetwork	0.9
GO:0032993	protein-DNA complex	0.9
ENSG000000184983	NDUFA6 PPI subnetwork	0.9
ENSG000000185658	BRWD1 PPI subnetwork	0.9
REACTOME_TRANSCRIPTION:COUPLED_NER_TC:NER	REACTOME_TRANSCRIPTION:COUPLED_NER_TC:NER	0.9
KEGG_CITRATE_CYCLE_TCA_CYCLE	KEGG_CITRATE_CYCLE_TCA_CYCLE	0.9
ENSG000000057468	MSH4 PPI subnetwork	0.9
ENSG000000147443	DOK2 PPI subnetwork	0.9
GO:0050690	regulation of defense response to virus by virus	0.9
ENSG000000105656	ELL PPI subnetwork	0.9
GO:0051983	regulation of chromosome segregation	0.9
GO:0034440	lipid oxidation	0.9
ENSG000000157344	ENSG000000157344 PPI subnetwork	0.9
ENSG000000105289	TJP3 PPI subnetwork	0.9
ENSG000000198648	STK39 PPI subnetwork	0.9
ENSG000000028137	TNFRSF1B PPI subnetwork	0.9
GO:0015949	nucleobase-containing small molecule interconversion	0.9
REACTOME_G:PROTEIN_ACTIVATION	REACTOME_G:PROTEIN_ACTIVATION	0.9
ENSG000000165023	DIRAS2 PPI subnetwork	0.9
ENSG000000092201	SUPT16H PPI subnetwork	0.9
GO:0051018	protein kinase A binding	0.9
MP:0003463	abnormal single cell response	0.9
ENSG000000128524	ATP6V1F PPI subnetwork	0.9
MP:0000841	abnormal hindbrain morphology	0.9
GO:0033013	tetrapyrrole metabolic process	0.9
GO:0006778	porphyrin-containing compound metabolic process	0.9
KEGG_NUCLEOTIDE_EXCISION_REPAIR	KEGG_NUCLEOTIDE_EXCISION_REPAIR	0.9
ENSG000000213619	NDUFS3 PPI subnetwork	0.91
KEGG_GLYCOSAMINOGLYCAN_BIOSYNTHESIS KERATAN_SULFATE	KEGG_GLYCOSAMINOGLYCAN_BIOSYNTHESIS KERATAN_SULFATE	0.91
GO:0048713	regulation of oligodendrocyte differentiation	0.91
GO:0060425	lung morphogenesis	0.91
GO:0015030	Cajal body	0.91
ENSG000000138092	CENPO PPI subnetwork	0.91

Original gene set ID	Original gene set description	Nominal P value
GO:0006613	cotranslational protein targeting to membrane	0.92
ENSG00000126945	HNRNPH2 PPI subnetwork	0.92
ENSG00000171747	LGALS4 PPI subnetwork	0.92
GO:0002828	regulation of type 2 immune response	0.92
ENSG00000004487	KDM1A PPI subnetwork	0.92
ENSG00000158022	TRIM63 PPI subnetwork	0.92
REACTOME_ABORTIVE_ELONGATION_OF_HIV:1_TRANSCRIPT_IN_THE_ABSENC	REACTOME_ABORTIVE_ELONGATION_OF_HIV:1_TRANSCRIPT_IN_THE_ABSENCE_O	0.92
GO:0051436	negative regulation of ubiquitin-protein ligase activity involved in mitotic cell cycl	0.92
GO:0030317	sperm motility	0.92
ENSG00000198824	CHAMP1 PPI subnetwork	0.92
GO:0048013	ephrin receptor signaling pathway	0.92
GO:0001706	endoderm formation	0.92
ENSG00000100241	SBF1 PPI subnetwork	0.92
GO:0048708	astrocyte differentiation	0.92
ENSG00000184432	COPB2 PPI subnetwork	0.92
GO:0016594	glycine binding	0.92
ENSG00000070182	SPTB PPI subnetwork	0.92
GO:0050657	nucleic acid transport	0.92
GO:0051236	establishment of RNA localization	0.92
GO:0050658	RNA transport	0.92
ENSG00000010818	HIVEP2 PPI subnetwork	0.92
GO:0071158	positive regulation of cell cycle arrest	0.92
ENSG00000122705	CLTA PPI subnetwork	0.92
ENSG00000105258	POLR2I PPI subnetwork	0.92
GO:0042588	zymogen granule	0.92
GO:0070665	positive regulation of leukocyte proliferation	0.92
GO:0005932	microtubule basal body	0.92
GO:0031594	neuromuscular junction	0.92
GO:0016862	intramolecular oxidoreductase activity, interconverting keto- and enol-group:	0.92
GO:0006370	mRNA capping	0.92
ENSG00000132639	SNAP25 PPI subnetwork	0.92
GO:0030900	forebrain development	0.92
GO:0070972	protein localization in endoplasmic reticulum	0.92
ENSG00000115128	ENSG00000115128 PPI subnetwork	0.92
GO:0060079	regulation of excitatory postsynaptic membrane potentia	0.92
GO:0070647	protein modification by small protein conjugation or remova	0.92
KEGG_VIBRIO_CHOLERAЕ_INFECTION	KEGG_VIBRIO_CHOLERAЕ_INFECTION	0.92
GO:0016676	oxidoreductase activity, acting on a heme group of donors, oxygen as accepto	0.92
GO:0015002	heme-copper terminal oxidase activity	0.92
GO:0004129	cytochrome-c oxidase activity	0.92
ENSG00000154710	RABGEF1 PPI subnetwork	0.92
GO:0044257	cellular protein catabolic process	0.92
GO:0016917	GABA receptor activity	0.92
ENSG00000048828	FAM120A PPI subnetwork	0.92
ENSG00000166226	CCT2 PPI subnetwork	0.92
GO:0009264	deoxyribonucleotide catabolic process	0.92
GO:0030313	cell envelope	0.92
GO:0044462	external encapsulating structure part	0.92
ENSG00000154723	ATP5J PPI subnetwork	0.92

Original gene set ID	Original gene set description	Nominal P value
ENSG00000137825	ITPKA PPI subnetwork	0.92
MP:0009838	abnormal sperm axoneme morphology	0.92
ENSG00000164402	SEPT8 PPI subnetwork	0.92
GO:0002637	regulation of immunoglobulin production	0.92
GO:0031334	positive regulation of protein complex assembly	0.92
REACTOME_ACTIVATION_OF_KAINATE_RECEPTORS_UPON_Glutamate_BINDING	REACTOME_ACTIVATION_OF_KAINATE_RECEPTORS_UPON_Glutamate_BINDING	0.92
GO:0001759	organ induction	0.92
ENSG00000109519	GRPEL1 PPI subnetwork	0.92
ENSG00000147099	HDAC8 PPI subnetwork	0.92
ENSG00000100410	PHF5A PPI subnetwork	0.92
ENSG00000160783	PMF1 PPI subnetwork	0.92
ENSG00000142856	ITGB3BP PPI subnetwork	0.92
GO:0072210	metanephric nephron development	0.92
GO:0050433	regulation of catecholamine secretion	0.92
ENSG00000065150	IPO5 PPI subnetwork	0.92
GO:0010959	regulation of metal ion transport	0.92
REACTOME_AMINE_COMPOUND_SLC_TRANSPORTERS	REACTOME_AMINE_COMPOUND_SLC_TRANSPORTERS	0.92
ENSG00000102109	PCSK1N PPI subnetwork	0.92
ENSG00000122952	ZWINT PPI subnetwork	0.92
GO:0043034	costamere	0.92
REACTOME_TRAFFICKING_OF_AMPA_RECEPTORS	REACTOME_TRAFFICKING_OF_AMPA_RECEPTORS	0.92
REACTOME_Glutamate_BINDING_ACTIVATION_OF_AMPA_RECEPTORS_AND_SYN	REACTOME_Glutamate_BINDING_ACTIVATION_OF_AMPA_RECEPTORS_AND_SYN	0.92
GO:0019395	fatty acid oxidation	0.92
GO:0042436	indole-containing compound catabolic process	0.92
GO:0046218	indolalkylamine catabolic process	0.92
GO:0006569	tryptophan catabolic process	0.92
ENSG00000188386	PPP3R2 PPI subnetwork	0.92
MP:0004615	cervical vertebral transformation	0.92
ENSG00000121621	KIF18A PPI subnetwork	0.92
ENSG00000119318	RAD23B PPI subnetwork	0.92
ENSG00000115254	ENSG00000115254 PPI subnetwork	0.92
ENSG00000167136	ENDOG PPI subnetwork	0.92
GO:0016197	endosomal transport	0.92
GO:0016469	proton-transporting two-sector ATPase complex	0.92
ENSG00000060558	GNA15 PPI subnetwork	0.92
MP:0001905	abnormal dopamine level	0.92
ENSG00000129473	BCL2L2 PPI subnetwork	0.92
ENSG00000168496	FEN1 PPI subnetwork	0.92
ENSG00000167083	GNGT2 PPI subnetwork	0.92
REACTOME_Glucagon:TYPE_Ligand_Receptors	REACTOME_Glucagon:TYPE_Ligand_Receptors	0.92
ENSG00000118680	MYL12B PPI subnetwork	0.92
GO:0046503	glycerolipid catabolic process	0.92
ENSG00000124610	HIST1H1A PPI subnetwork	0.92
REACTOME_INSULIN_RECEPTOR_RECYCLING	REACTOME_INSULIN_RECEPTOR_RECYCLING	0.92
GO:0006281	DNA repair	0.92
REACTOME_STRIATED_MUSCLE_CONTRACTION	REACTOME_STRIATED_MUSCLE_CONTRACTION	0.92
GO:0030148	sphingolipid biosynthetic process	0.92
GO:0016054	organic acid catabolic process	0.92
GO:0046395	carboxylic acid catabolic process	0.92

Original gene set ID	Original gene set description	Nominal P value
REACTOME_DARPP:32_EVENTS	REACTOME_DARPP:32_EVENTS	0.92
GO:0006521	regulation of cellular amino acid metabolic process	0.92
MP:0004101	abnormal brain interneuron morphology	0.93
ENSG00000129990	SYT5 PPI subnetwork	0.93
ENSG00000184702	SEPT5 PPI subnetwork	0.93
ENSG00000183474	GTF2H2C PPI subnetwork	0.93
ENSG00000124795	DEK PPI subnetwork	0.93
ENSG00000112290	WASF1 PPI subnetwork	0.93
GO:0009583	detection of light stimulus	0.93
GO:0072073	kidney epithelium development	0.93
GO:0016236	macroautophagy	0.93
MP:0003672	abnormal ureter development	0.93
ENSG00000159259	CHAF1B PPI subnetwork	0.93
ENSG00000143368	SF3B4 PPI subnetwork	0.93
GO:0006721	terpenoid metabolic process	0.93
REACTOME_IRON_UPTAKE_AND_TRANSPORT	REACTOME_IRON_UPTAKE_AND_TRANSPORT	0.93
ENSG00000153207	AHCTF1 PPI subnetwork	0.93
GO:0032446	protein modification by small protein conjugation	0.93
GO:0044447	axoneme part	0.93
GO:0007626	locomotory behavior	0.93
GO:0042033	chemokine biosynthetic process	0.93
GO:0005245	voltage-gated calcium channel activity	0.93
REACTOME_INHIBITION_OF_INSULIN_SECRETION_BY_ADRENALINENORADRENALIN	REACTOME_INHIBITION_OF_INSULIN_SECRETION_BY_ADRENALINENORADRENALIN	0.93
ENSG00000124172	ATP5E PPI subnetwork	0.93
ENSG00000025800	KPNA6 PPI subnetwork	0.93
REACTOME_TRYPTOPHAN_CATABOLISM	REACTOME_TRYPTOPHAN_CATABOLISM	0.93
ENSG00000184357	HIST1H1B PPI subnetwork	0.93
GO:0050905	neuromuscular process	0.93
ENSG00000138071	ACTR2 PPI subnetwork	0.93
REACTOME_ENERGY_DEPENDENT_REGULATION_OF_MTOR_BY_LKB1:AMPK	REACTOME_ENERGY_DEPENDENT_REGULATION_OF_MTOR_BY_LKB1:AMPK	0.93
MP:0001898	abnormal long term depression	0.93
KEGG_GLYOXYLATE_AND_DICARBOXYLATE_METABOLISM	KEGG_GLYOXYLATE_AND_DICARBOXYLATE_METABOLISM	0.93
GO:0006289	nucleotide-excision repair	0.93
ENSG00000163636	PSMD6 PPI subnetwork	0.93
ENSG00000168556	ING2 PPI subnetwork	0.93
GO:0030594	neurotransmitter receptor activity	0.93
GO:0000775	chromosome, centromeric region	0.93
ENSG00000166337	TAF10 PPI subnetwork	0.93
REACTOME_SYNTHESIS_AND_INTERCONVERSION_OF_NUCLEOTIDE_DI:_AND_T	REACTOME_SYNTHESIS_AND_INTERCONVERSION_OF_NUCLEOTIDE_DI:_AND_TRIP	0.93
GO:0007413	axonal fasciculation	0.93
ENSG00000143850	PLEKHA6 PPI subnetwork	0.93
REACTOME_INSULIN_SYNTHESIS_AND_PROCESSING	REACTOME_INSULIN_SYNTHESIS_AND_PROCESSING	0.93
GO:0032838	cell projection cytoplasm	0.93
ENSG00000106588	PSMA2 PPI subnetwork	0.93
MP:0000750	abnormal muscle regeneration	0.93
ENSG00000198947	DMD PPI subnetwork	0.93
GO:0034453	microtubule anchoring	0.93
GO:0042573	retinoic acid metabolic process	0.93
ENSG00000133059	DSTYK PPI subnetwork	0.93

Original gene set ID	Original gene set description	Nominal P value
GO:0031023	microtubule organizing center organization	0.94
GO:0030968	endoplasmic reticulum unfolded protein response	0.94
GO:0034620	cellular response to unfolded protein	0.94
ENSG00000120265	PCMT1 PPI subnetwork	0.94
ENSG00000169217	CD2BP2 PPI subnetwork	0.94
GO:0055093	response to hyperoxia	0.94
ENSG00000197299	BLM PPI subnetwork	0.94
REACTOME_METABOLISM_OF_PORPHYRINS	REACTOME_METABOLISM_OF_PORPHYRINS	0.94
GO:0001655	urogenital system development	0.94
ENSG00000107554	DNMBP PPI subnetwork	0.94
GO:0021954	central nervous system neuron development	0.94
ENSG00000125870	SNRPB2 PPI subnetwork	0.94
ENSG00000105509	HAS1 PPI subnetwork	0.94
REACTOME_HIV_INFECTION	REACTOME_HIV_INFECTION	0.94
REACTOME_REGULATION_OF_AMPK_ACTIVITY_VIA_LKB1	REACTOME_REGULATION_OF_AMPK_ACTIVITY_VIA_LKB1	0.94
REACTOME_ACTIVATION_OF_GENES_BY_ATF4	REACTOME_ACTIVATION_OF_GENES_BY_ATF4	0.94
MP:0000830	abnormal diencephalon morphology	0.94
ENSG00000181555	SETD2 PPI subnetwork	0.94
GO:0048168	regulation of neuronal synaptic plasticity	0.94
ENSG00000066248	NGEF PPI subnetwork	0.94
GO:0048557	embryonic digestive tract morphogenesis	0.94
ENSG00000172732	MUS81 PPI subnetwork	0.94
ENSG00000072864	NDE1 PPI subnetwork	0.94
GO:0031646	positive regulation of neurological system proces:	0.94
ENSG00000188486	H2AFX PPI subnetwork	0.94
GO:0009310	amine catabolic process	0.94
GO:0008066	glutamate receptor activity	0.94
GO:0001822	kidney development	0.94
ENSG00000065833	ME1 PPI subnetwork	0.94
ENSG00000164687	FABP5 PPI subnetwork	0.94
GO:0051297	centrosome organization	0.94
MP:0005533	increased body temperature	0.94
ENSG00000161057	PSMC2 PPI subnetwork	0.94
ENSG00000115808	STRN PPI subnetwork	0.94
GO:0060193	positive regulation of lipase activity	0.94
ENSG00000205726	ITSN1 PPI subnetwork	0.94
KEGG_NEUROACTIVE_LIGAND_RECEPTOR_INTERACTION	KEGG_NEUROACTIVE_LIGAND_RECEPTOR_INTERACTION	0.94
GO:0045295	gamma-catenin binding	0.94
ENSG00000115760	BIRC6 PPI subnetwork	0.94
MP:0003384	abnormal ventral body wall morphology	0.94
REACTOME_PACKAGING_OF_TELOMERE_ENDS	REACTOME_PACKAGING_OF_TELOMERE_ENDS	0.94
ENSG00000183091	NEB PPI subnetwork	0.94
GO:0072001	renal system development	0.94
ENSG00000107611	CUBN PPI subnetwork	0.94
MP:0008789	abnormal olfactory epithelium morphology	0.94
GO:0055072	iron ion homeostasis	0.94
MP:0001787	pericardial edema	0.94
MP:0001777	abnormal body temperature homeostasis	0.94
MP:0003063	increased coping response	0.94

Original gene set ID	Original gene set description	Nominal P value
GO:0015931	nucleobase-containing compound transport	0.94
ENSG00000138413	IDH1 PPI subnetwork	0.94
ENSG00000152455	SUV39H2 PPI subnetwork	0.94
GO:0010470	regulation of gastrulation	0.94
GO:0007617	mating behavior	0.95
GO:0000786	nucleosome	0.95
GO:0009072	aromatic amino acid family metabolic process	0.95
GO:0033176	proton-transporting V-type ATPase complex	0.95
GO:0008328	ionotropic glutamate receptor complex	0.95
ENSG00000131558	EXOC4 PPI subnetwork	0.95
GO:0051653	spindle localization	0.95
GO:0051293	establishment of spindle localization	0.95
MP:0011448	decreased dopaminergic neuron number	0.95
ENSG00000162928	PEX13 PPI subnetwork	0.95
ENSG00000107819	SFXN3 PPI subnetwork	0.95
GO:0005234	extracellular-glutamate-gated ion channel activity	0.95
ENSG00000058262	SEC61A1 PPI subnetwork	0.95
MP:0001526	abnormal placing response	0.95
ENSG00000092108	SCFD1 PPI subnetwork	0.95
GO:0043523	regulation of neuron apoptotic process	0.95
ENSG00000108387	SEPT4 PPI subnetwork	0.95
ENSG00000100146	SOX10 PPI subnetwork	0.95
GO:0048019	receptor antagonist activity	0.95
GO:0030547	receptor inhibitor activity	0.95
REACTOME_CDT1_ASSOCIATION_WITH_THE_CDC6ORCORIGIN_COMPLEX	REACTOME_CDT1_ASSOCIATION_WITH_THE_CDC6ORCORIGIN_COMPLEX	0.95
GO:0008306	associative learning	0.95
REACTOME_NACL:_DEPENDENT_NEUROTRANSMITTER_TRANSPORTERS	REACTOME_NACL:_DEPENDENT_NEUROTRANSMITTER_TRANSPORTERS	0.95
GO:0051402	neuron apoptotic process	0.95
ENSG00000170734	POLH PPI subnetwork	0.95
ENSG00000025772	TOMM34 PPI subnetwork	0.95
GO:0050871	positive regulation of B cell activation	0.95
ENSG00000126457	PRMT1 PPI subnetwork	0.95
GO:0043178	alcohol binding	0.95
GO:0060601	lateral sprouting from an epithelium	0.95
GO:0009434	microtubule-based flagellum	0.95
GO:0048704	embryonic skeletal system morphogenesis	0.95
ENSG00000167641	PPP1R14A PPI subnetwork	0.95
GO:0005231	excitatory extracellular ligand-gated ion channel activity	0.95
GO:0016651	oxidoreductase activity, acting on NADH or NADPH	0.95
GO:0022408	negative regulation of cell-cell adhesion	0.95
GO:0031080	Nup107-160 complex	0.95
ENSG00000105402	NAPA PPI subnetwork	0.95
GO:0048368	lateral mesoderm development	0.95
GO:0070528	protein kinase C signaling cascade	0.95
ENSG00000184752	NDUFA12 PPI subnetwork	0.95
KEGG_HUNTINGTONS_DISEASE	KEGG_HUNTINGTONS_DISEASE	0.95
MP:0002842	increased systemic arterial blood pressure	0.95
ENSG00000085832	EPS15 PPI subnetwork	0.95
ENSG00000030304	MUSK PPI subnetwork	0.95

Original gene set ID	Original gene set description	Nominal P value
ENSG00000189043	NDUFA4 PPI subnetwork	0.95
ENSG00000180817	PPA1 PPI subnetwork	0.95
GO:0003678	DNA helicase activity	0.95
GO:0006775	fat-soluble vitamin metabolic process	0.95
ENSG00000088320	REM1 PPI subnetwork	0.95
ENSG00000022355	GABRA1 PPI subnetwork	0.95
ENSG00000167491	GATAD2A PPI subnetwork	0.95
GO:0014075	response to amine stimulus	0.95
ENSG00000183765	CHEK2 PPI subnetwork	0.95
ENSG00000169189	NSMCE1 PPI subnetwork	0.95
MP:0004736	abnormal distortion product otoacoustic emission	0.95
GO:0010518	positive regulation of phospholipase activity	0.95
ENSG00000149136	SSRP1 PPI subnetwork	0.95
ENSG00000169925	BRD3 PPI subnetwork	0.95
GO:0072087	renal vesicle development	0.95
REACTOME_SYNTHESIS_SECRETION_AND_INACTIVATION_OF_GLU	REACTOME_SYNTHESIS_SECRETION_AND_INACTIVATION_OF_GLU	0.95
GO:0031234	extrinsic to internal side of plasma membrane	0.95
GO:0032982	myosin filament	0.95
GO:0060249	anatomical structure homeostasis	0.95
ENSG00000182473	EXOC7 PPI subnetwork	0.95
ENSG00000179091	CYC1 PPI subnetwork	0.95
GO:0031123	RNA 3'-end processing	0.95
GO:0021772	olfactory bulb development	0.95
GO:0021988	olfactory lobe development	0.95
GO:0006099	tricarboxylic acid cycle	0.95
ENSG00000173660	UQCRH PPI subnetwork	0.95
GO:0048024	regulation of nuclear mRNA splicing, via spliceosome	0.95
ENSG00000172757	CFL1 PPI subnetwork	0.95
GO:0050890	cognition	0.95
GO:0070997	neuron death	0.95
GO:0014013	regulation of gliogenesis	0.95
GO:0016411	acylglycerol O-acyltransferase activity	0.95
MP:0006007	abnormal basal ganglion morphology	0.95
ENSG00000090372	STRN4 PPI subnetwork	0.95
GO:0017137	Rab GTPase binding	0.95
REACTOME_POST:ELONGATION_PROCESSING_OF_INTRON:CONTAINING_PRE:M	REACTOME_POST:ELONGATION_PROCESSING_OF_INTRON:CONTAINING_PRE:MRN	0.95
REACTOME_MRNA_3:END_PROCESSING	REACTOME_MRNA_3:END_PROCESSING	0.95
GO:0072088	nephron epithelium morphogenesis	0.95
REACTOME_G_ALPHA_Z_SIGNALLING_EVENTS	REACTOME_G_ALPHA_Z_SIGNALLING_EVENTS	0.95
REACTOME_DUAL_INCISION_REACTION_IN_TC:NER	REACTOME_DUAL_INCISION_REACTION_IN_TC:NER	0.95
REACTOME_FORMATION_OF_TRANSCRIPTION:COUPLED_NER_TC:NER_REPAIR	REACTOME_FORMATION_OF_TRANSCRIPTION:COUPLED_NER_TC:NER_REPAIR_CO	0.95
ENSG00000087302	C14orf166 PPI subnetwork	0.95
GO:0001975	response to amphetamine	0.95
GO:0045454	cell redox homeostasis	0.95
GO:0072329	monocarboxylic acid catabolic process	0.95
ENSG00000130479	MAP1S PPI subnetwork	0.95
MP:0002938	white spotting	0.95
ENSG00000049245	VAMP3 PPI subnetwork	0.96
GO:0042168	heme metabolic process	0.96

Original gene set ID	Original gene set description	Nominal P value
REACTOME_TRANSFERRIN_ENDOCYTOSIS_AND_RECYCLING	REACTOME_TRANSFERRIN_ENDOCYTOSIS_AND_RECYCLING	0.96
MP:0004624	abnormal thoracic cage morphology	0.96
ENSG000000101182	PSMA7 PPI subnetwork	0.96
GO:0007270	neuron-neuron synaptic transmission	0.96
MP:0006054	spinal hemorrhage	0.96
GO:0051937	catecholamine transport	0.96
ENSG000000141543	EIF4A3 PPI subnetwork	0.96
ENSG000000134057	CCNB1 PPI subnetwork	0.96
GO:0019861	flagellum	0.96
REACTOME_RNA_POL_II_CTD_PHOSPHORYLATION_AND_INTERACTION_WITH_C	REACTOME_RNA_POL_II_CTD_PHOSPHORYLATION_AND_INTERACTION_WITH_C	0.96
GO:0030288	outer membrane-bounded periplasmic space	0.96
GO:0042597	periplasmic space	0.96
GO:0072077	renal vesicle morphogenesis	0.96
REACTOME_NEF_MEDIATED_DOWNREGULATION_OF_MHC_CLASS_I_COMPLEX	REACTOME_NEF_MEDIATED_DOWNREGULATION_OF_MHC_CLASS_I_COMPLEX	0.96
ENSG000000163464	CXCR1 PPI subnetwork	0.96
GO:0042379	chemokine receptor binding	0.96
ENSG000000065057	NTHL1 PPI subnetwork	0.96
ENSG000000169021	UQCRFS1 PPI subnetwork	0.96
KEGG_VALINE_LEUCINE_AND_ISOLEUCINE_DEGRADATION	KEGG_VALINE_LEUCINE_AND_ISOLEUCINE_DEGRADATION	0.96
GO:0022900	electron transport chain	0.96
GO:0016358	dendrite development	0.96
GO:0072006	nephron development	0.96
ENSG000000166411	IDH3A PPI subnetwork	0.96
ENSG000000125356	NDUFA1 PPI subnetwork	0.96
GO:0072028	nephron morphogenesis	0.96
MP:0002804	abnormal motor learning	0.96
ENSG000000144848	ATG3 PPI subnetwork	0.96
ENSG000000125944	HNRNPR PPI subnetwork	0.96
KEGG_PARKINSONS_DISEASE	KEGG_PARKINSONS_DISEASE	0.96
GO:0014003	oligodendrocyte development	0.96
GO:0043269	regulation of ion transport	0.96
ENSG000000111445	RFC5 PPI subnetwork	0.96
GO:0031907	microbody lumen	0.96
GO:0005782	peroxisomal matrix	0.96
ENSG000000147133	TAF1 PPI subnetwork	0.96
GO:0031625	ubiquitin protein ligase binding	0.96
ENSG000000164683	HEY1 PPI subnetwork	0.96
GO:0042572	retinol metabolic process	0.96
ENSG000000145864	GABRB2 PPI subnetwork	0.96
ENSG000000170906	NDUFA3 PPI subnetwork	0.96
MP:0003964	abnormal noradrenaline level	0.96
GO:0048475	coated membrane	0.96
GO:0030117	membrane coat	0.96
MP:0000061	fragile skeleton	0.96
REACTOME_PROCESSING_OF_CAPPED_INTRONLESS_PRE:MRNA	REACTOME_PROCESSING_OF_CAPPED_INTRONLESS_PRE:MRNA	0.96
REACTOME_POST:ELONGATION_PROCESSING_OF_INTRONLESS_PRE:MRNA	REACTOME_POST:ELONGATION_PROCESSING_OF_INTRONLESS_PRE:MRNA	0.96
ENSG000000184270	HIST2H2AB PPI subnetwork	0.96
ENSG000000071564	TCF3 PPI subnetwork	0.96
GO:0045685	regulation of glial cell differentiation	0.96

Original gene set ID	Original gene set description	Nominal P value
GO:0008343	adult feeding behavior	0.96
GO:0051971	positive regulation of transmission of nerve impulse	0.96
GO:0022406	membrane docking	0.96
MP:0006090	abnormal utricle morphology	0.96
MP:0009453	enhanced contextual conditioning behavior	0.96
ENSG00000090266	NDUFB2 PPI subnetwork	0.96
ENSG00000115590	IL1R2 PPI subnetwork	0.96
GO:0090130	tissue migration	0.96
GO:0044450	microtubule organizing center part	0.96
GO:0034976	response to endoplasmic reticulum stress	0.96
ENSG00000112685	EXOC2 PPI subnetwork	0.96
GO:0048806	genitalia development	0.96
GO:0001756	somitogenesis	0.96
ENSG00000184445	KNTC1 PPI subnetwork	0.96
REACTOME_CITRIC_ACID_CYCLE_TCA_CYCLE	REACTOME_CITRIC_ACID_CYCLE_TCA_CYCLE	0.96
MP:0000285	abnormal heart valve morphology	0.96
GO:0007585	respiratory gaseous exchange	0.96
GO:0031124	mRNA 3'-end processing	0.96
MP:0001982	decreased chemically-elicited antinociception	0.96
GO:0033555	multicellular organismal response to stress	0.96
GO:0034599	cellular response to oxidative stress	0.96
GO:0006888	ER to Golgi vesicle-mediated transport	0.96
GO:0072075	metanephric mesenchyme development	0.96
GO:0010453	regulation of cell fate commitment	0.96
GO:0042775	mitochondrial ATP synthesis coupled electron transport	0.96
GO:0042773	ATP synthesis coupled electron transport	0.96
GO:0006733	oxidoreduction coenzyme metabolic process	0.96
ENSG00000107758	PPP3CB PPI subnetwork	0.96
GO:0031424	keratinization	0.96
GO:0004532	exoribonuclease activity	0.96
GO:0006936	muscle contraction	0.96
GO:0042162	telomeric DNA binding	0.96
GO:0072273	metanephric nephron morphogenesis	0.96
MP:0003425	abnormal optic vesicle formation	0.96
REACTOME_VIRAL_MESSENGER_RNA_SYNTHESIS	REACTOME_VIRAL_MESSENGER_RNA_SYNTHESIS	0.96
GO:0001657	ureteric bud development	0.96
GO:0003338	metanephros morphogenesis	0.96
GO:0009612	response to mechanical stimulus	0.96
ENSG00000169242	EFNA1 PPI subnetwork	0.96
GO:0030048	actin filament-based movement	0.96
ENSG00000103479	RBL2 PPI subnetwork	0.96
REACTOME_THE_CITRIC_ACID_TCA_CYCLE_AND_RESPIRATORY_ELECTRON_TRANSPORT	REACTOME_THE_CITRIC_ACID_TCA_CYCLE_AND_RESPIRATORY_ELECTRON_TRANSPORT	0.96
GO:0060688	regulation of morphogenesis of a branching structure	0.96
GO:0072524	pyridine-containing compound metabolic process	0.96
GO:0019362	pyridine nucleotide metabolic process	0.96
GO:0004970	ionotropic glutamate receptor activity	0.96
GO:0016646	oxidoreductase activity, acting on the CH-NH group of donors, NAD or NADP as acceptor	0.96
GO:0005859	muscle myosin complex	0.96
ENSG00000165288	BRWD3 PPI subnetwork	0.96

Original gene set ID	Original gene set description	Nominal P value
GO:0002825	regulation of T-helper 1 type immune response	0.98
MP:0002953	thick ventricular wall	0.98
ENSG000000204120	GIGYF2 PPI subnetwork	0.98
ENSG000000167792	NDUFV1 PPI subnetwork	0.98
REACTOME_DEPOSITION_OF_NEW_CENPA:CONTAINING_NUCLEOSOMES_AT_T	REACTOME_DEPOSITION_OF_NEW_CENPA:CONTAINING_NUCLEOSOMES_AT_THE_	0.98
REACTOME_NUCLEOSOME_ASSEMBLY	REACTOME_NUCLEOSOME_ASSEMBLY	0.98
ENSG000000164919	COX6C PPI subnetwork	0.98
GO:0040001	establishment of mitotic spindle localizati	0.98
GO:0003401	axis elongation	0.98
GO:0043524	negative regulation of neuron apoptotic process	0.98
GO:0043176	amine binding	0.98
GO:0009062	fatty acid catabolic process	0.98
ENSG000000136888	ATP6V1G1 PPI subnetwork	0.98
ENSG00000010244	ZNF207 PPI subnetwork	0.98
GO:0016835	carbon-oxygen lyase activity	0.98
KEGG_CARDIAC_MUSCLE_CONTRACTION	KEGG_CARDIAC_MUSCLE_CONTRACTION	0.98
ENSG000000140416	TPM1 PPI subnetwork	0.98
GO:0060572	morphogenesis of an epithelial bud	0.98
ENSG000000065534	MYLK PPI subnetwork	0.98
ENSG000000167306	MYO5B PPI subnetwork	0.98
GO:0031593	polyubiquitin binding	0.98
MP:0004725	decreased platelet serotonin level	0.98
GO:0072527	pyrimidine-containing compound metabolic process	0.98
MP:0006065	abnormal heart position or orientation	0.98
ENSG000000164258	NDUFS4 PPI subnetwork	0.98
MP:0009232	abnormal sperm nucleus morphology	0.98
GO:0010632	regulation of epithelial cell migration	0.98
GO:0051924	regulation of calcium ion transport	0.98
MP:0004215	abnormal myocardial fiber physiology	0.98
ENSG000000186230	ZNF749 PPI subnetwork	0.98
GO:0010824	regulation of centrosome duplication	0.98
ENSG000000187555	USP7 PPI subnetwork	0.98
ENSG000000215697	ENSG000000215697 PPI subnetwork	0.98
ENSG000000168397	ATG4B PPI subnetwork	0.98
GO:0071241	cellular response to inorganic substance	0.98
GO:0015939	pantothenate metabolic process	0.98
MP:0008412	increased cellular sensitivity to oxidative stress	0.98
ENSG000000173894	CBX2 PPI subnetwork	0.98
GO:0060675	ureteric bud morphogenesis	0.98
REACTOME_CLEAVAGE_OF_GROWING_TRANSCRIPT_IN_THE_TERMINATION_RI	REACTOME_CLEAVAGE_OF_GROWING_TRANSCRIPT_IN_THE_TERMINATION_REGIC	0.98
REACTOME_RNA_POLYMERASE_II_TRANSCRIPTION_TERMINATION	REACTOME_RNA_POLYMERASE_II_TRANSCRIPTION_TERMINATION	0.98
REACTOME_POST:ELONGATION_PROCESSING_OF_THE_TRANSCRIPT	REACTOME_POST:ELONGATION_PROCESSING_OF_THE_TRANSCRIPT	0.98
ENSG000000032514	ENSG000000032514 PPI subnetwork	0.98
ENSG000000119013	NDUFB3 PPI subnetwork	0.98
ENSG000000120251	GRIA2 PPI subnetwork	0.98
GO:0006119	oxidative phosphorylation	0.98
ENSG000000099246	RAB18 PPI subnetwork	0.98
GO:0061053	somite development	0.98
GO:0033275	actin-myosin filament sliding	0.98

Original gene set ID	Original gene set description	Nominal P value
GO:0030049	muscle filament sliding	0.98
MP:0000433	microcephaly	0.98
ENSG000000167258	CDK12 PPI subnetwork	0.98
GO:0016634	oxidoreductase activity, acting on the CH-CH group of donors, oxygen as acceptor	0.98
GO:0021952	central nervous system projection neuron axonogenesis	0.98
ENSG000000124164	VAPB PPI subnetwork	0.98
GO:0009109	coenzyme catabolic process	0.98
MP:0004087	abnormal muscle fiber morphology	0.98
ENSG000000182117	NOP10 PPI subnetwork	0.98
GO:0051187	cofactor catabolic process	0.98
REACTOME_RESOLUTION_OF_AP_SITES_VIA_THE_MULTIPLE_NUCLEOTIDE_PATCH	REACTOME_RESOLUTION_OF_AP_SITES_VIA_THE_MULTIPLE_NUCLEOTIDE_PATCH	0.98
REACTOME_REMOVAL_OF_DNA_PATCH_CONTAINING_ABASIC_RESIDUE	REACTOME_REMOVAL_OF_DNA_PATCH_CONTAINING_ABASIC_RESIDUE	0.98
GO:0090183	regulation of kidney development	0.98
ENSG000000003096	KLHL13 PPI subnetwork	0.98
ENSG000000170515	PA2G4 PPI subnetwork	0.98
ENSG000000125447	GGA3 PPI subnetwork	0.98
ENSG000000077721	UBE2A PPI subnetwork	0.98
MP:0002674	abnormal sperm motility	0.98
MP:0001706	abnormal left-right axis patterning	0.98
MP:0004132	absent embryonic cilia	0.98
GO:0001658	branching involved in ureteric bud morphogenesis	0.98
GO:0008009	chemokine activity	0.98
GO:0060134	prepulse inhibition	0.98
ENSG000000163535	SGOL2 PPI subnetwork	0.98
GO:0006369	termination of RNA polymerase II transcription	0.98
GO:0009898	internal side of plasma membrane	0.98
ENSG000000105968	H2AFV PPI subnetwork	0.98
GO:0007098	centrosome cycle	0.98
ENSG000000092531	SNAP23 PPI subnetwork	0.98
GO:0006488	dolichol-linked oligosaccharide biosynthetic process	0.99
GO:0016101	diterpenoid metabolic process	0.99
ENSG000000171132	PRKCE PPI subnetwork	0.99
GO:0006513	protein monoubiquitination	0.99
GO:0042312	regulation of vasodilation	0.99
ENSG000000160194	NDUFV3 PPI subnetwork	0.99
GO:0009068	aspartate family amino acid catabolic process	0.99
GO:0006904	vesicle docking involved in exocytosis	0.99
ENSG00000010256	UQCRC1 PPI subnetwork	0.99
GO:0044236	multicellular organismal metabolic process	0.99
GO:0008045	motor axon guidance	0.99
REACTOME_TRAFFICKING_OF_GLUR2:CONTAINING_AMPA_RECEPTORS	REACTOME_TRAFFICKING_OF_GLUR2:CONTAINING_AMPA_RECEPTORS	0.99
ENSG000000139197	PEX5 PPI subnetwork	0.99
GO:0001523	retinoid metabolic process	0.99
MP:0002954	abnormal aerobic energy metabolism	0.99
MP:0011386	increased metanephric mesenchyme apoptosis	0.99
GO:0072163	mesonephric epithelium development	0.99
GO:0072164	mesonephric tubule development	0.99
ENSG000000180104	EXOC3 PPI subnetwork	0.99
ENSG000000212872	ENSG000000212872 PPI subnetwork	0.99

Original gene set ID	Original gene set description	Nominal P value
GO:0042537	benzene-containing compound metabolic process	0.99
ENSG00000197579	TOPORS PPI subnetwork	0.99
ENSG00000054116	TRAPPC3 PPI subnetwork	0.99
GO:0071824	protein-DNA complex subunit organization	0.99
ENSG00000143614	GATAD2B PPI subnetwork	0.99
GO:0070252	actin-mediated cell contraction	0.99
GO:0021955	central nervous system neuron axonogenesis	0.99
GO:0046513	ceramide biosynthetic process	0.99
GO:0004843	ubiquitin-specific protease activity	0.99
ENSG00000213496	ENSG00000213496 PPI subnetwork	0.99
ENSG00000197265	GTF2E2 PPI subnetwork	0.99
GO:0005747	mitochondrial respiratory chain complex I	0.99
GO:0045271	respiratory chain complex I	0.99
GO:0030964	NADH dehydrogenase complex	0.99
GO:0045652	regulation of megakaryocyte differentiation	0.99
GO:0007099	centriole replication	0.99
MP:0001899	absent long term depression	0.99
ENSG00000197548	ATG7 PPI subnetwork	0.99
MP:0000819	abnormal olfactory bulb morphology	0.99
GO:0060174	limb bud formation	0.99
GO:0031055	chromatin remodeling at centromere	0.99
ENSG00000125798	FOXA2 PPI subnetwork	0.99
ENSG00000188459	ENSG00000188459 PPI subnetwork	0.99
ENSG00000197930	ERO1L PPI subnetwork	0.99
GO:0015872	dopamine transport	0.99
GO:0032963	collagen metabolic process	0.99
ENSG00000119048	UBE2B PPI subnetwork	0.99
ENSG00000168393	DTYMK PPI subnetwork	0.99
ENSG00000215694	ENSG00000215694 PPI subnetwork	0.99
GO:0043486	histone exchange	0.99
GO:0034502	protein localization to chromosome	0.99
GO:0005230	extracellular ligand-gated ion channel activity	0.99
ENSG00000147853	AK3 PPI subnetwork	0.99
GO:0009081	branched chain family amino acid metabolic process	0.99
GO:0007618	mating	0.99
GO:0030534	adult behavior	0.99
GO:0008137	NADH dehydrogenase (ubiquinone) activity	0.99
GO:0050136	NADH dehydrogenase (quinone) activity	0.99
GO:0003954	NADH dehydrogenase activity	0.99
ENSG00000163032	VSNL1 PPI subnetwork	0.99
GO:0004953	icosanoid receptor activity	0.99
GO:0004954	prostanoid receptor activity	0.99
GO:0033572	transferrin transport	0.99
GO:0015682	ferric iron transport	0.99
ENSG00000130176	CNN1 PPI subnetwork	0.99
ENSG00000183648	NDUFB1 PPI subnetwork	0.99
ENSG00000127184	COX7C PPI subnetwork	0.99
GO:0001964	startle response	0.99
REACTOME_MITOCHONDRIAL_FATTY_ACID_BETA:OXIDATION	REACTOME_MITOCHONDRIAL_FATTY_ACID_BETA:OXIDATION	0.99

Original gene set ID	Original gene set description	Nominal P value
GO:0007494	midgut development	0.99
ENSG00000124702	KLHDC3 PPI subnetwork	0.99
ENSG00000178127	NDUFV2 PPI subnetwork	0.99
ENSG00000212870	ENSG00000212870 PPI subnetwork	0.99
ENSG00000198786	MT-ND5 PPI subnetwork	0.99
GO:0042596	fear response	0.99
MP:0002243	abnormal vomeronasal organ morphology	0.99
GO:0072529	pyrimidine-containing compound catabolic process	0.99
ENSG00000147123	NDUFB11 PPI subnetwork	0.99
MP:0000747	muscle weakness	0.99
GO:0071103	DNA conformation change	0.99
ENSG00000185513	L3MBTL1 PPI subnetwork	0.99
GO:0050684	regulation of mRNA processing	1
GO:0006739	NADP metabolic process	1
GO:0044259	multicellular organismal macromolecule metabolic process	1
ENSG00000138029	HADHB PPI subnetwork	1
GO:0006740	NADPH regeneration	1
ENSG00000108587	GOSR1 PPI subnetwork	1
ENSG00000109390	NDUFC1 PPI subnetwork	1
ENSG00000172301	C17orf79 PPI subnetwork	1
GO:0002209	behavioral defense response	1
KEGG_PROTEIN_EXPORT	KEGG_PROTEIN_EXPORT	1
GO:0046520	sphingoid biosynthetic process	1
GO:0016655	oxidoreductase activity, acting on NADH or NADPH, quinone or similar compound as	1
ENSG00000112357	PEX7 PPI subnetwork	1
ENSG00000111875	ASF1A PPI subnetwork	1
ENSG00000185214	ENSG00000185214 PPI subnetwork	1
GO:0009262	deoxyribonucleotide metabolic process	1
ENSG00000155511	GRIA1 PPI subnetwork	1
GO:0065004	protein-DNA complex assembly	1
GO:0051952	regulation of amine transport	1
GO:0003924	GTPase activity	1
ENSG00000151366	NDUFC2 PPI subnetwork	1
ENSG00000147416	ATP6V1B2 PPI subnetwork	1
GO:0004869	cysteine-type endopeptidase inhibitor activity	1
MP:0010454	abnormal truncus arteriosus septation	1
GO:0034728	nucleosome organization	1
ENSG00000166963	MAP1A PPI subnetwork	1
ENSG00000115738	ID2 PPI subnetwork	1
ENSG00000187837	HIST1H1C PPI subnetwork	1
GO:0034080	CenH3-containing nucleosome assembly at centromere	1
GO:0006336	DNA replication-independent nucleosome assembly	1
GO:0034724	DNA replication-independent nucleosome organization	1
ENSG00000185621	LMLN PPI subnetwork	1
GO:0003995	acyl-CoA dehydrogenase activity	1
MP:0008531	increased chemical nociceptive threshold	1
ENSG00000121390	PSPC1 PPI subnetwork	1
GO:0021871	forebrain regionalization	1
ENSG00000206440	NFKBIL1 PPI subnetwork	1

Original gene set ID	Original gene set description	Nominal P value
ENSG00000168593	ENSG00000168593 PPI subnetwork	1
MP:0005480	increased circulating triiodothyronine leve	1
GO:0006098	pentose-phosphate shunt	1
GO:0042401	cellular biogenic amine biosynthetic process	1
GO:0000178	exosome (RNase complex)	1
ENSG00000198888	MT-ND1 PPI subnetwork	1
GO:0042136	neurotransmitter biosynthetic process	1
ENSG00000131747	TOP2A PPI subnetwork	1
ENSG00000131495	NDUFA2 PPI subnetwork	1
REACTOME_MRNA_DECAY_BY_3_TO_5_EXORIBONUCLEASE	REACTOME_MRNA_DECAY_BY_3_TO_5_EXORIBONUCLEASE	1
ENSG00000165264	NDUFB6 PPI subnetwork	1
MP:0002007	increased cellular sensitivity to gamma-irradiation	1
ENSG00000092330	TINF2 PPI subnetwork	1
ENSG00000212876	ENSG00000212876 PPI subnetwork	1
ENSG00000198763	MT-ND2 PPI subnetwork	1
GO:0006333	chromatin assembly or disassembly	1
GO:0031497	chromatin assembly	1
GO:0007628	adult walking behavior	1
GO:0016780	phosphotransferase activity, for other substituted phosphate group:	1
GO:0033540	fatty acid beta-oxidation using acyl-CoA oxidase	1
ENSG00000083896	YTHDC1 PPI subnetwork	1
GO:0032204	regulation of telomere maintenance	1
ENSG00000108671	PSMD11 PPI subnetwork	1
GO:0001504	neurotransmitter uptake	1
ENSG00000108468	CBX1 PPI subnetwork	1
ENSG00000079462	PFAFH1B3 PPI subnetwork	1
GO:0015992	proton transport	1
GO:0009378	four-way junction helicase activity	1
ENSG00000116288	PARK7 PPI subnetwork	1
REACTOME_RESPIRATORY_ELECTRON_TRANSPORT	REACTOME_RESPIRATORY_ELECTRON_TRANSPORT	1
GO:0021536	diencephalon development	1
REACTOME_RESPIRATORY_ELECTRON_TRANSPORT_ATP_SYNTHESIS_BY_CHEM	REACTOME_RESPIRATORY_ELECTRON_TRANSPORT_ATP_SYNTHESIS_BY_CHEMIOSM	1
ENSG00000013275	PSMC4 PPI subnetwork	1
GO:0006818	hydrogen transport	1
ENSG00000167774	NDUFA7 PPI subnetwork	1
GO:0006282	regulation of DNA repair	1
GO:0006323	DNA packaging	1
GO:0050922	negative regulation of chemotaxis	1
GO:0015991	ATP hydrolysis coupled proton transport	1
GO:0015988	energy coupled proton transport, against electrochemical gradien	1
GO:0015078	hydrogen ion transmembrane transporter activity	1
ENSG00000111880	RNGTT PPI subnetwork	1
KEGG_OXIDATIVE_PHOSPHORYLATION	KEGG_OXIDATIVE_PHOSPHORYLATION	1
GO:0008344	adult locomotory behavior	1
GO:0031290	retinal ganglion cell axon guidance	1
ENSG00000140990	NDUFB10 PPI subnetwork	1
ENSG00000153140	CETN3 PPI subnetwork	1
ENSG00000120696	KBTBD7 PPI subnetwork	1
GO:0006334	nucleosome assembly	1

Original gene set ID	Original gene set description	Nominal P value
GO:0006586	indolalkylamine metabolic process	1
GO:0042430	indole-containing compound metabolic process	1
GO:0018958	phenol-containing compound metabolic process	1
GO:0000381	regulation of alternative nuclear mRNA splicing, via spliceosome	1
ENSG00000108433	GOSR2 PPI subnetwork	1
GO:0001963	synaptic transmission, dopaminergic	1
REACTOME_E2F:ENABLED_INHIBITION_OF_PRE:REPLICATION_COMPLEX_FORM	REACTOME_E2F:ENABLED_INHIBITION_OF_PRE:REPLICATION_COMPLEX_FORMATI	1
GO:0006635	fatty acid beta-oxidation	1
ENSG00000203813	HIST1H3H PPI subnetwork	1
ENSG00000203852	HIST2H3A PPI subnetwork	1
ENSG00000131143	COX4I1 PPI subnetwork	1
ENSG00000166848	TERF2IP PPI subnetwork	1
MP:0000761	thin diaphragm muscle	1
GO:0021983	pituitary gland development	1
ENSG00000115677	HDLBP PPI subnetwork	1
ENSG00000113327	GABRG2 PPI subnetwork	1
GO:0006879	cellular iron ion homeostasis	1
GO:0021756	striatum development	1
GO:2001020	regulation of response to DNA damage stimulus	1
GO:0043044	ATP-dependent chromatin remodeling	1
GO:0006576	cellular biogenic amine metabolic process	1
GO:0009636	response to toxin	1
GO:0032200	telomere organization	1
GO:0009083	branched chain family amino acid catabolic process	1
REACTOME_BRANCHED:CHAIN_AMINO_ACID_CATABOLISM	REACTOME_BRANCHED:CHAIN_AMINO_ACID_CATABOLISM	1
REACTOME_PEROXISOMAL_LIPID_METABOLISM	REACTOME_PEROXISOMAL_LIPID_METABOLISM	1
ENSG00000179841	AKAP5 PPI subnetwork	1
GO:0000723	telomere maintenance	1
ENSG00000196532	HIST1H3C PPI subnetwork	1
ENSG00000198366	HIST1H3A PPI subnetwork	1
ENSG00000197153	HIST1H3J PPI subnetwork	1
ENSG00000197409	HIST1H3D PPI subnetwork	1
ENSG00000178458	ENSG00000178458 PPI subnetwork	1
ENSG00000112727	ENSG00000112727 PPI subnetwork	1
ENSG00000124693	HIST1H3B PPI subnetwork	1
ENSG00000196966	HIST1H3E PPI subnetwork	1
ENSG00000182572	HIST1H3I PPI subnetwork	1
ENSG00000180198	RCC1 PPI subnetwork	1
KEGG_ALZHEIMERS_DISEASE	KEGG_ALZHEIMERS_DISEASE	1
GO:0000380	alternative nuclear mRNA splicing, via spliceosome	1
GO:0017156	calcium ion-dependent exocytosis	1

SUPPLEMENTAL MATERIAL

Jones et al.: Meta-analysis of genome-wide association studies for abdominal aortic aneurysm identifies four new disease specific risk loci

ONLINE METHODS AND DATA*

	Page
Discovery and validation cohort descriptions	2
Meta-analysis	9
SNP lookup in GWAS for traits associated with AAA	30
Search for other associated traits and diseases using GWAS databases	32
PheWAS analysis	37
Annotation of AAA associated SNPs using the UCSC Genome Browser	38
Pupasuite analysis	41
GWAS3D analysis	44
DEPICT analysis	49
Functional effects of SNPs at AAA loci	60
Validation of GWAS3D results using mRNA expression data	67
Look-up for transcription factor binding sites	70
Network analysis	72
Consortia contributing data	76
References	79

*for clarity and ease of use each section contains methods, results, figures and tables relevant to that section.

INDIVIDUAL GWAS STUDIES

All known studies with AAA genome-wide genotyping data were invited to join the International Aneurysm Consortium effort. All studies agreed to participate in the meta-GWAS, with cohort case control descriptions and inclusion/exclusion criteria having been previously reported¹⁻³ (**Online Table I**). All AAA cases shared a common definition of infra-renal aortic diameter ≥ 30 mm. Patients with connective tissue disease associated AAAs (e.g. Marfan, Ehlers-Danlos, Loeys-Dietz) were excluded from the study. Each GWAS was based on a case-control analysis of AAA modelled as a discrete trait. The statistical analysis of the Aneurysm Consortium and New Zealand GWAS datasets was repeated specifically for this study and therefore was harmonized using identical imputation and analysis methods. Data from the remaining cohorts consisted of summary data obtained from previously performed analyses.

The use of the samples in each study cohort was approved by the local Ethics Committees or Institutional Review Boards.

DISCOVERY AND VALIDATION COHORT DESCRIPTIONS (Online Tables I and II)

a) Discovery Cohorts

Aneurysm Consortium (AC) AAA GWAS dataset: The Aneurysm Consortium recruited cases of AAA from centres across the United Kingdom and Western Australia. Cases were defined as an infra-renal aortic diameter ≥ 30 mm proven on ultrasound or computerized tomography (CT) scan. Controls were taken from the WTCCC2 common control group^{1,4} and were therefore unscreened for AAA.

Data were from 1,866 cases with AAA and 5,435 unscreened controls from the Wellcome Trust Case Control Consortium 2 (WTCCC2) study consisting of samples from the 1958 British Birth Cohort and from the UK National Blood Service. DNA samples were processed at the Wellcome Trust Sanger Institute (WTSI). Genomic DNA was quantified by PicoGreen assay, and quality control (QC) assured by both agarose gel electrophoresis and Sequenom iPLEX genotyping of 29 SNPs and 4 sex-specific markers. Genotyping for the discovery study was performed using Illumina 1.2M (controls) or 670K (AAA) BeadChips. Raw intensity data were normalized using BeadStudio and genotypes were called concurrently from the combined case-control data set using the Illuminus algorithm⁵.

As part of the original Aneurysm Consortium GWAS individual sample QC had been performed as follows. QC was first performed by exclusion of SNPs with call rates < 0.98 and those that demonstrated significant deviation from Hardy-Weinberg equilibrium in the control group ($P < 5 \times 10^{-4}$). Duplicate samples and those that failed genotyping (sample call rates < 0.98) were also excluded from further analysis. Genotyping cluster plots for all SNPs with $P < 1 \times 10^{-4}$ were visually inspected to exclude from further analysis positive associations generated by erroneous genotyping or calling. Checks for population stratification were performed by PLINK⁶ identical by state clustering and extreme outliers were removed from the analysis.

Imputation was performed using IMPUTE 2.2 run on the BCISNPmax database platform (version 3.5, BCI Platforms, Espoo, Finland). The reference haplotypes were based on the 1000 Genomes June 2011 release. Imputed calls were filtered by quality score (excluding those < 0.9) to restrict to higher quality imputed SNPs.

Following imputation further QC filtering was performed, excluding SNPs with call rates < 0.98 and those that demonstrated significant deviation from Hardy-Weinberg equilibrium in the control group ($P < 5 \times 10^{-4}$). Duplicate samples and those that failed genotyping (sample call rate < 0.98) were also excluded from further analysis. Association testing was carried out in PLINK⁶.

New Zealand (NZ) Vascular Genetics Study AAA GWAS dataset: The Vascular Research Consortium of New Zealand recruited New Zealand men and women with a proven history of AAA (infra-renal aortic diameter ≥ 30 mm proven on ultrasound or CT scan). Approximately 80% had undergone surgical AAA repair (typically AAA's > 50 - 55 mm in diameter). The vast majority of cases ($>97\%$) were of Anglo-European ancestry. The control group underwent an abdominal ultrasound scan to exclude (>25 mm) concurrent AAA and Anglo-European ancestry was required for inclusion. Controls were also screened for peripheral artery disease (PAD; using ankle brachial index), carotid artery disease (ultrasound) and other cardiovascular risk factors.

Two separate GWAS were performed using New Zealand samples. NZ GWAS 1 consisted of 608 AAA patients (474 male) and 612 elderly controls (450 male), genotyped using the Affymetrix SNP 6 GeneChip array. All samples had call rates >0.95 (mean 0.992). NZ GWAS 2 consisted of 397 AAA patients (332 male) and 384 elderly controls (308 male), genotyped using the Illumina Infinium Omni2.5 BeadChip array. All samples had call rates >0.95 (mean 0.990). All NZ genomic DNA samples exceeded manufacturer's quality and quantity requirements having undergone pre-assessment by Nanophotometer (Implen GmbH, München, Germany) and agarose gel electrophoresis.

Imputation was conducted separately on NZ GWAS 1 and 2 data sets using the same methods as used for the Aneurysm Consortium datasets. IMPUTE 2.2 was run on the BCISNPmax database platform (version 3.5, BCI Platforms, Espoo, Finland). The reference haplotypes were based on the 1000 Genomes June 2011 release. Imputed calls were filtered by quality score (excluding those <0.9) to restrict to higher quality imputed SNPs. The genomic inflation factors (λ) were 1.07 and 1.05, respectively (MAF >0.05).

Both NZ GWAS 1 and 2 data sets underwent QC filtering, excluding SNPs with call rates < 0.98 and those that demonstrated significant deviation from Hardy-Weinberg equilibrium in the control group ($P < 5 \times 10^{-4}$). Duplicate samples and those that failed genotyping (sample call rate < 0.98) were also excluded from further analysis. Association testing was carried out in PLINK⁶.

US (PA) GWAS dataset: AAA patients were enrolled through the Department of Vascular Surgery at Geisinger Medical Center, Danville, Pennsylvania, USA as previously reported^{2,7}. To identify cases and controls from the electronic medical records, an ePhenotyping algorithm was developed⁸. Briefly, Structured Query Language (SQL) was used to script the algorithm utilizing "Current Procedural Terminology" (CPT) and "International Classification of Diseases" (ICD-9) codes as well as demographic and encounter data to classify individuals as case, control, or excluded. AAA cases were defined as having an AAA repair procedure (case Type 1), or at least one appropriate specialty encounter (vascular clinic) with a ruptured AAA (case Type 2), or at least two specialty encounters with an unruptured AAA (case Type 3). Controls were neither cases nor those excluded, had an encounter within the past 5 years, and had never been assigned an ICD9 code of 441.*, where * is a 1 or 2 digit code. Individuals were excluded if 1) they had a thoracic aortic aneurysm or a rare heritable disease with aortic manifestation; 2) they were younger than 40 or older than 89 years, 3) they had a single encounter with a code without mention of rupture (441.4), or 4) they had not had an encounter within the past 5 years. Rare heritable diseases were excluded because the goal of the current study was to identify non-syndromic AAA. Controls under 40 years might yet manifest an AAA, while cases under 40 years of age and without rare syndromic forms of aortic aneurysms are likely due to trauma. The AAA algorithm can be downloaded from www.PheKb.org. The algorithm was validated on a subset of individuals by manual chart review, and implemented at eMERGE network sites. The algorithm was implemented as a workflow in the Konstanz Information Miner (KNIME) (<http://www.knime.org/>).

AAA cases had infrarenal aortic diameter ≥ 30 mm as revealed by abdominal imaging. Approximately 20% of individuals with AAA had a family history of AAA. A control group was obtained through the Geisinger MyCode[®] Project, a cohort of Geisinger Clinic patients recruited for genomic studies. The MyCode[®] controls were matched for age distribution and sex to the Geisinger Vascular Clinic AAA cases. Based on electronic medical records, controls had no ICD-9 codes for AAA in their records, but they were not screened by ultrasonography for AAA. Both cases and controls from the Geisinger Clinic were of European descent.

The Geisinger cohort used for this study was a subset of a larger cohort comprising 3,264 samples from 3,149 individuals with three phenotypes: 922 putative AAA cases, 981 obesity cases and 1,246 controls. Samples were genotyped on the Illumina HumanOmniExpress-12v1.0 genotyping platform at the University of Pittsburgh Genomics and Proteomics Core Laboratories. Genotypes were called using the Illumina GenomeStudio v2010.3 software. QC consisted of a number of steps: identification of cross-contamination and removal of specimens, call rate of samples (> 0.98 SNPs called), sex consistency between annotated sex and genotyped sex, SNP discordance between replicate sample pairs, SNP call rate (> 0.95 calls in all specimens), SNP minor allele frequency (> 0.01), SNP Hardy-Weinberg equilibrium ($P > 1 \times 10^{-4}$), and selection of replicates to retain based on sex-specific Mahalanobis distance (< 4.1) and Illumina P10.GC (> 0.71). Cross-contamination of samples was detected by excess heterozygosity and excess relatedness (related to more than half of other samples at $\text{Pi-hat} > 0.0625$); four samples were removed prior to other QC steps. After the QC steps above, related individuals (pairwise $\text{Pi-hat} > 0.15$) were removed, retaining the individual and specimen with the highest call rate. A second round of QC was applied using the above SNP and sample criteria to ensure consistency after removal of SNPs and individuals. In addition, the SNP criteria were analyzed per chromosome to ensure that there were no systematic differences (no differences detected). Lastly, principle component analysis (PCA) was used to determine if there were any batch effects during genotyping (no evidence for batch effects). Of the 3,264 samples, 153 were removed for one or more of the QC reasons above. Of the 731,306 SNPs, 95,369 were removed; 2,012 were discordant, 13,107 had a low call rate, 78,086 had a MAF < 0.01 , and 14,056 had a HWE $P < 1 \times 10^{-4}$ (9,047 SNPs were removed for more than one reason).

The final meta-analysis cohort comprised only those individuals who were identified as definitive AAA cases or controls using the rigorous ePhenotyping algorithm described above.

Imputation was performed as previously described⁹. Briefly: SNPs were re-mapped to the Genome Reference Consortium Human build 37 (GRCh37) and the program liftOver run to ensure mapping consistency. Subsequently all SNPs were mapped from the Illumina TOP notation to the plus (+) strand. Strand was checked using SHAPEIT2 (version r2.644)¹⁰. Next the data were phased using SHAPEIT2. Imputation was performed using IMPUTE2 (version 2.3.0)¹¹. Chromosomes were divided into 6 MB segments with 250 kbp overlap between segments. A total of 5,719,283 SNPs with an info score of ≥ 0.9 were used for analysis.

Association analysis without adjustment was performed using PLINK (v1.09)⁶ and the imputed SNPs.

The eMERGE Network Imputed GWAS for 41 Phenotypes (the dbGaP eMERGE Phase 1 and 2 Merged data Submission) accession number is: phs000888.v1.p1 which includes the Geisinger AAA data.

Iceland, deCODE Genetics AAA GWAS dataset: Icelandic individuals with AAA (defined as infra-renal aortic diameter ≥ 30 mm) were recruited from a registry of individuals who were admitted at Landspítali University Hospital, in Reykjavik, Iceland, 1980 – 2006. AAA patients were either followed up or treated by intervention for emergency repair of symptomatic or ruptured AAA or for an elective repair by surgery or endovascular intervention. In total, whole genome data from 557 subjects with AAA, enrolled as part of the cardiovascular disease (CVD) genetics program at deCODE,

were included in the metaGWAS. The Icelandic controls used (n=89,235) were selected from individuals who have participated in various GWA studies and who were recruited as part of genetic programs at deCODE. Individuals with known CVD were excluded as controls² but controls were unscreened for AAA.

The Icelandic case and control samples were assayed with the Illumina HumanHap300, HumanHapCNV370 or HumanHap610 bead chips (Illumina, SanDiego, CA, USA). Only SNPs present on all chips were included in the analysis and SNPs were excluded if they had (a) call rates < 95% in cases or controls, (b) MAF<0.01 in the controls, or (c) showed significant deviation from HWE in the controls ($P < 1 \times 10^{-4}$). These criteria were applied separately to genotype data from each of the chip types used and SNPs that showed significant deviation ($P < 0.0001$ in an ANOVA test) in frequency between the chips were excluded from the analysis. Any samples with a call rate < 0.98 were excluded from the analysis. The final analysis included 293,677 SNPs present on all three chips.

For case-control association analysis, we used a standard likelihood ratio statistic, implemented in the NEMO software¹², to calculate two-sided P values and ORs for each individual allele, assuming a multiplicative model for risk¹³.

Familial imputation: For the Icelandic data set, we extended the classical case-control association analysis to include *in silico* genotypes of affected individuals who were not genotyped but who had genotyped relatives¹⁴ among the 40,000 Icelanders (about 13% of all living Icelanders) genotyped with the Illumina SNP chips at deCODE Genetics. For every ungenotyped affected individual, we calculated the probability distribution of the genotypes of his or her relatives, given his or her four possible phased genotypes. In practice, we included only genotypes of the affected individual's parents, children, siblings, half-siblings (and the half-sibling's parents), grandparents, grandchildren (and the grandchildren's parents) and spouses. The contribution of the ungenotyped affected individuals through this familial imputation to the effective sample size of the affected individuals, $n_{a,eff}$, was estimated using the Fisher information.

Genomic control: Some of the individuals in the Icelandic case-control groups are related to each other, causing the χ^2 test statistic to have a mean >1 and median >0.455. We estimated the genome-wide inflation factor λ_g as the average of the 293,677 χ^2 statistics to adjust for both relatedness and potential population stratification¹⁴.

The Netherlands AAA GWAS dataset: The AAA sample set from Utrecht was recruited in 2007-2009 from 8 centres in The Netherlands², mainly when individuals visited their vascular surgeon in the clinic or, in rare cases, during hospital admission for elective or emergency AAA surgery. An AAA was defined as an infrarenal aorta ≥ 30 mm. The sample set comprised 89.9% males, with a mean AAA diameter of 58.4 mm, 61.7% had been operated on, of which 8.1 % were after rupture. The Dutch controls used in the AAA GWAS were recruited as part of the Nijmegen Biomedical Study and the Nijmegen Bladder Cancer Study (see <http://dceg.cancer.gov/icbc/membership.html>).

Genotyping was performed on Illumina HumanHap610 chips.² As controls, we included 2,791 Dutch subjects who were recruited as part of the Nijmegen Biomedical Study (n=1,832) and the Nijmegen Bladder Cancer Study (n=1,278)^{15, 16} These controls were genotyped on Illumina CNV370 Duo BeadChips.

QC: We performed QC using PLINK version 1.07⁶. After removal of SNPs with A/T or C/G alleles and SNPs that were not called in any individual, we performed sample QC and SNP QC.

Sample QC was performed after merging cases and controls, using a subset of common, high-quality SNPs (as defined by SNPs without deviation from HWE ($P > 0.001$), with high MA) (>0.2) and with low rate of missing genotypes (<0.01)). Linkage disequilibrium (LD) pruning ($r^2 > 0.5$) was performed. Subjects were removed based on the following three criteria: missing genotypes (subjects with call

rates < 0.95 were removed), heterozygosity (subjects were excluded if the inbreeding coefficient deviated more than 3 standard deviations from the mean) and cryptic relatedness (by calculating identity-by-descent (IBD) for each pair of individuals). In each pair with an IBD proportion of >20%, a subject was excluded, if it exhibited distant relatedness with more than one individual. For case-control pairs, we removed the control subject. In the case-case or control-control pairs, the subject with the lowest call rate was excluded.

Using these common, high-quality SNPs, we performed PCA using EIGENSTRAT on the remaining study subjects and HapMap-CEU subjects. We excluded SNPs from three regions with known long-distance LD: the major histocompatibility (MHC) region (chr6: 25.8-36 Mbp), the chromosome 8 inversion (chr8: 6-16 Mbp) and a chromosome 17 region (chr17: 40-45 Mbp). We created PC plots with the first four PCs, using R version 2.11.¹⁷ Based on visual inspection of these plots, we excluded subjects that appeared to be outliers with respect to the CEU or the study population. After outlier removal, we recomputed PCs for them to be included as covariates in the logistic regression models.

After sample QC, we excluded SNPs with more than 2% missing genotypes, MAF < 0.01, missing genotype rate higher than MAF, and HWE deviation ($P < 0.001$). Because cases and controls had been genotyped separately, we performed these QC steps in each study cohort separately and again after merging cases and controls. We also removed SNPs with a differential degree of missing genotypes between cases and controls ($P < 1 \times 10^{-5}$; chi-squared test).

Imputation: We performed genotype imputation using the pre-phasing/imputation stepwise approach implemented in IMPUTE2 and SHAPEIT (chunk size of 3 Mb and default parameters)^{10, 18}. The imputation reference set consisted of 2,184 phased haplotypes from the full 1000 Genomes Project data set (February 2012; 40,318,253 variants). All genomic locations are given in NCBI Build 37/UCSC hg19 coordinates. After imputation, SNPs with an imputation accuracy score < 0.6 or MAF < 0.005 were excluded.

Association testing: Association testing was carried out in PLINK⁶ using imputed SNP dosages. We included as covariates the first four PCs. We calculated genomic inflation factors (λ_{GC}), defined as the ratio of the median of the empirically observed distribution of the test statistic to the expected median¹⁹.

b) Validation Cohorts

Aneurysm Consortium (AC) validation cohort: The same inclusion/exclusion criteria and recruitment sites were used as for the Aneurysm Consortium AAA GWAS. The lead SNPs (or their high LD proxies), identified in the discovery analysis, were genotyped at The Wellcome Trust Sanger Institute, Cambridge, UK using Sequenom iPLEX platform. Allele frequency summary results (odds ratio and 95% confidence interval) were generated using Chi-squared tests as implemented in the SHEsis web-based software package²⁰ (available: <http://analysis.bio-x.cn/SHEsisMain.htm>). Deviation from HWE was estimated and results are shown in **Online Table VI**.

New Zealand (NZ) Validation cohort: NZ validation cohort participants were recruited from the same sites as those in the GWAS. Case and control inclusion/exclusion criteria were identical to that of the NZ AAA GWAS, with all controls having been screened by ultrasound.

The lead SNPs (or their high LD proxies), identified in the discovery analysis, were genotyped at the Vascular Research Group, University of Otago using the TaqMan (LifeTechnologies) platform. Allele frequency summary results (odds ratio and 95% confidence interval) were generated using Chi-squared tests as implemented in the SHEsis web-based software package²⁰. Deviation from HWE was estimated and results are shown in **Online Table VI**.

Belgium and Canada validation cohorts: These sample-sets, in which all individuals were of European descent, included individuals with AAA who were admitted either for emergency repair of ruptured AAA or for an elective surgery to the University Hospital of Liege (Liege, Belgium) and to Dalhousie University Hospital (Halifax, Canada). AAA was defined as an infrarenal aortic diameter \geq 30 mm. Details of these case-control sets have been reported previously^{21, 22}. Approximately 40% of individuals with AAA had a family history of AAA. Control samples (51% males) were obtained from spouses of individuals with AAA or from individuals admitted to the same hospitals for reasons other than AAA. Controls had no known AAA, but they were not screened by ultrasonography for AAA.

The lead SNPs (or their high LD proxies), identified in the discovery analysis, were genotyped in the Tromp-Kuivaniemi Laboratory at Geisinger Health System using TaqMan (LifeTechnologies) platform. Allele frequency summary results (odds ratio and 95% confidence interval) were generated using Chi-squared tests as implemented in the SHESis web-based software package²⁰. Deviation from HWE was estimated and results are shown in **Online Table VI**.

eMERGE phase II (US) validation cohort: This cohort consisted of 338 AAA cases and 1,696 controls with GWAS data⁹ available from Mayo Clinic, Marshfield Clinic, Mount Sinai School of Medicine, Vanderbilt University, Northwestern University and Group Health Research Institute. The cases and controls were ascertained from the electronic medical records²³ using an ePhenotyping algorithm⁸ as described above. The samples had been genotyped in various GWAS and then imputed (see above). Allele frequency summary results (odds ratio and 95% confidence interval) were generated using Chi-squared tests as implemented in the SHESis web-based software package²⁰. Deviation from HWE was estimated and results are shown in **Online Table VI**. The eMERGE Network Imputed GWAS for 41 Phenotypes (the dbGaP eMERGE Phase 1 and 2 Merged data Submission) accession number is: phs000888.v1.p1 which includes these data.

US Validation 2 cohort: A second US case/control validation cohort was derived from the Mayo Vascular Disease Biorepository²⁴ (Mayo VDB; <http://www.mayo.edu/research/labs/cardiovascular-biomarkers/vascular-diseases-biorepository>), the Presbyterian University Hospital in Pittsburgh²⁵, Vanderbilt University (BioVU[®])²⁶, Marshfield Clinic (Personalized Medicine Research Project[®])²⁷, Mount Sinai School of Medicine (BioMe[®])²⁸, and Northwestern University (NUgene[®])²⁹. The cases and controls at Mayo Clinic, Vanderbilt University, Marshfield Clinic, Mount Sinai School of Medicine, and Northwestern University were phenotypically ascertained using the same ePhenotyping algorithm⁸ described above, whereas the AAA cases from the Presbyterian University Hospital in Pittsburgh were patients who had undergone elective or emergency surgery for AAA²⁵.

The lead SNPs (or their high LD proxies), identified in the discovery analysis, were genotyped in the Tromp-Kuivaniemi Laboratory at Geisinger Health System using TaqMan (LifeTechnologies) platform. Allele frequency summary results (odds ratio and 95% confidence interval) were generated using Chi-squared tests as implemented in the SHESis web-based software package²⁰. Deviation from HWE was estimated and results are shown in **Online Table VI**.

Italy validation cohort: This group consisted of 761 AAA cases and 520 controls. AAA cases were individuals referred to the Vascular Surgery Unit of the University of Florence. Familial and inflammatory AAAs were excluded from the study. All control subjects (n=520) had a negative personal and family history of AAA and were of comparable age and sex distribution to that of the AAA patients. A more detailed description of the study populations has been previously published³⁰.

The lead SNPs (or their high LD proxies), identified in the discovery analysis, were genotyped in the Giusti Laboratory at University of Florence using TaqMan (LifeTechnologies) platform. Allele frequency summary results (odds ratio and 95% confidence interval) were generated using Chi-squared tests as implemented in the SHEsis web-based software package²⁰. Deviation from HWE was estimated and results are shown in **Online Table VI**.

Poland validation cohort: This group consisted of 481 AAA cases scheduled for surgery at the Department of General and Vascular Surgery of the Poznan University of Medical Sciences in the years 1999–2011. The control group, consisting of 487 subjects matched for age (± 5 years) and sex to the AAA patients, was selected during the same time from the Poznan district³¹. The collection of samples was approved by the Bioethics Committee of the Poznan University of Medical Sciences. The diagnosis of AAA was evaluated by computed tomography angiography or magnetic resonance angiography. Based on physical examination supplemented with ultrasound duplex color scanning, the coexistence of PAD was recognized in 60.3% of the AAA patients. All patients were treated pharmacologically with statins, antiplatelet drugs and other drugs (antihypertensive or antidiabetic), depending on their clinical condition. The exclusion criteria for the controls included known aneurysms and PAD.

The lead SNPs (or their high LD proxies), identified in the discovery analysis, were genotyped in the Tromp-Kuivaniemi Laboratory at Geisinger Health System using TaqMan (LifeTechnologies) platform. Allele frequency summary results (odds ratio and 95% confidence interval) were generated using Chi-squared tests as implemented in the SHEsis web-based software package²⁰. Deviation from HWE was estimated and results are shown in **Online Table VI**.

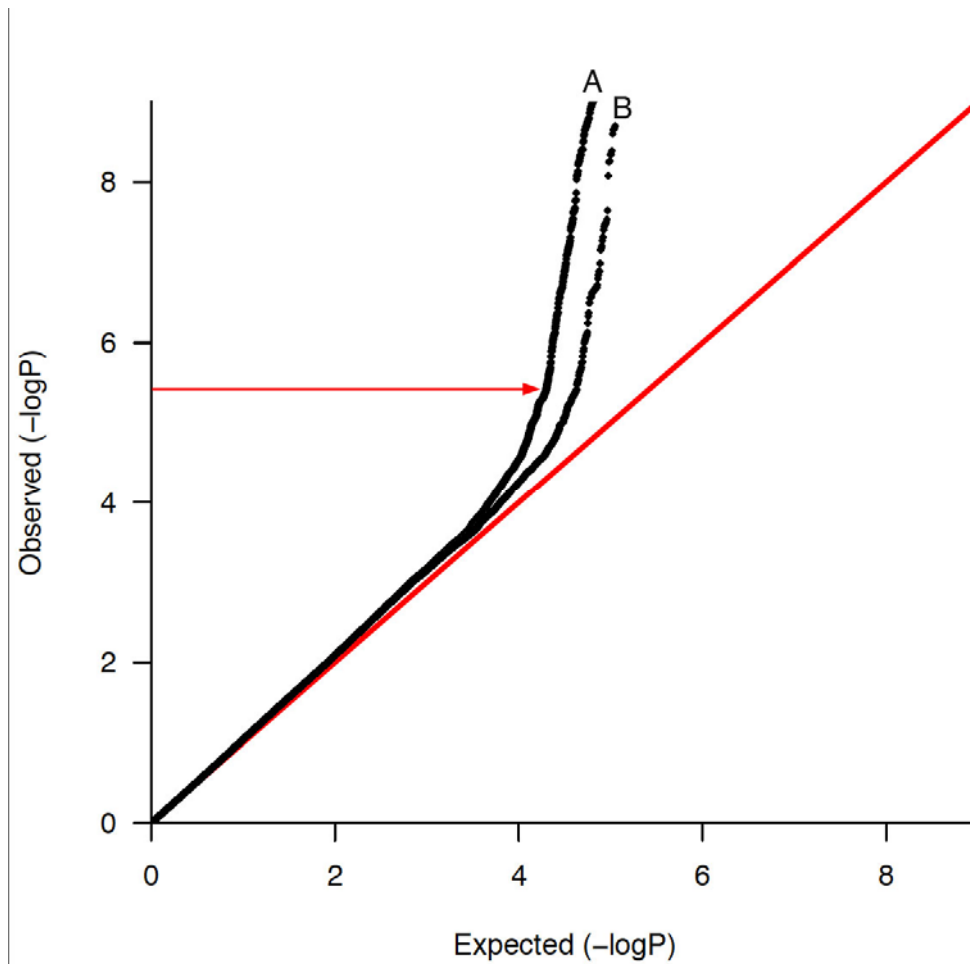
META-ANALYSIS of GWAS datasets

The discovery analysis consisted of the six cohorts with GWAS data detailed above, comprising 4,972 AAA cases and 99,858 controls, that were genotyped with a variety of genome-wide SNP arrays (**Online Table I**). All cohorts underwent QC filtering using the manufacturers' array-specific guidelines but with consistently applied inclusion criteria of SNP or sample call rates >95% and HWE $P > 5 \times 10^{-5}$ in controls^{1-3,7}. Each cohort then underwent imputation (⁹see above). Following imputation SNPs were quality controlled by quality score ($Q > 0.9$) and $MAF > 0.05$ in controls filtering, resulting in a common set of 5,363,770 SNPs across all discovery phase participants.

To obtain data for combination in the meta-analysis each case-control cohort was first analysed individually. Logistic regression models were used with AAA as a binary outcome in each cohort. Summary data [sample size, P-value, effect size (or log odds ratio), and the effect allele], unadjusted for covariates, for each SNP were combined in the meta-analysis.

The metaGWAS analysis was conducted using the METAL software package³² on the BCISNPmax database platform (version 3.5, BCI Platforms, Espoo, Finland). METAL was implemented using the sample size scheme with weighting based on the effective sample size [$N_{\text{eff}} = 4 / (1/N_{\text{cases}} + 1/N_{\text{controls}})$]. This approach was preferred over an inverse-variance weighted meta-analysis due to the disproportionate number of controls in some of the contributing cohorts and the fact that effect standard errors were not available in the data provided from Iceland and the United States (Geisinger) (**Online Table I**). The GWAS datasets from Iceland and the Netherlands were adjusted for genomic inflation prior to inclusion in the meta-analysis. The overall meta-GWAS analysis was adjusted for genomic inflation (λ) in each cohort (**Online Table I; Online Figure I**). An initial (λ -adjusted) discovery threshold of $P < 5 \times 10^{-6}$ was used to identify SNPs for subsequent validation genotyping.

The lead SNPs (or their high LD proxies), identified in the discovery analysis, were then genotyped in a further 8 independent cohorts (**Online Table II**). Each cohort's allele frequency summary results (odds ratio and 95% confidence interval) were generated using Chi-squared tests as implemented in the SHEsis web-based software package. Combined (discovery+validation) fixed effect meta-analysis was performed using a Maentel–Haenzel method with the genome-wide P -value significance threshold being set at 5×10^{-8} . The Maentel-Haenzel method was chosen since SNPs from the discovery and validation studies that were being combined demonstrated effects in the same direction and with low/medium heterogeneity. A sensitivity analyses of the combined (discovery+validation) study data were also performed using a random-effects model³³. The results from the discovery phase are presented in **Table 1; Online Tables III and IV; Figures 1 and 2; and Online Figures I and II**. The validation results are presented in **Table 1 and Online Tables V and VI**. Results from the combined analyses are presented in **Table 1 and Online Table VII**. Results from the sensitivity analysis are shown in **Online Table VIII**.



Online Figure I. Q-Q plot for the AAA meta-GWAS, showing (A) all 5.3 M SNPs with MAF>0.05 and (B) excluding the six previously identified loci (all SNPs within 100 kb of the peak variant associated with *SORT1*, *IL6R*, *CDKN2BAS1*, *DAB2IP*, *LDLR*, *LRP1*), generated from a comparison of 4,972 cases and 99,858 controls from 6 separate GWAS. The red arrow indicates the (λ -adjusted) $P < 5 \times 10^{-6}$ discovery threshold (362 SNPs in plot A).

Online Table I. Genome-wide association study (GWAS) cohort details. Individual level data were not available to calculate overall median age.

GWAS cohorts	Cases			Controls			GWAS Case weight (%)	Total* Case weight (%)	N _{effective}	Genotyping platform	Genomic inflation (λ) factor	Prior Adjustments
	Nn	%Male	Median Age (years)	N	% Male	Median Age (years)						
NZ 1	608	78	75	612	74	69	12.2	6.0	1,220	Affymetrix SNP6	1.07	None
NZ 2	397	84	77	384	80	67	8.0	3.9	781	Illumina Omni2.5	1.05	None
Aneurysm Consortium	1,846	98	72	5,605	49	52	37.1	18.1	5,555	Illumina 670	1.15	None
Netherlands	840	90	68	2,791	60	51	16.9	8.2	2,583	Illumina 300/370/610	1.11	Lambda
US (PA)	724	99	77	1,231	68	68	14.6	7.1	1,824	Illumina OmniExpress	1.06	None
Iceland deCODE	557	77	72	89,235	44	60	11.2	5.5	2,214	Illumina 300/370/610	0.70	Lambda
Total	4,972		N/A	99,858		N/A		48.7%	14,176			

Online Table II. Independent validation cohort details

Validation cohorts	Cases			Controls			Validation Case weight (%)	Total* Case weight (%)	N _{effective}	Genotyping platform
	N	% Male	Median Age (years)	N	% Male	Median Age (years)				
Aneurysm Consortium validation (AC)	1,236	84	72	2,196	93	68	23.6	12.1	3,163	Sequenom
NZ validation	753	81	77	1,237	67	68	14.4	7.4	1,872	Taqman
Italy validation	761	79	73	520	78	72	14.5	7.5	1,236	Taqman
Poland validation	481	86	69	487	72	59	9.2	4.7	968	Taqman
eMERGE US validation 1	338	80	82	1696	80	82	6.5	3.3	1127	Imputed data from various GWAS platforms
US validation 2	1,176	82	73	1,371	64	68	22.5	11.5	2,532	Taqman
Belgium validation	339	91	N/A	265	68	N/A	6.5	3.3	595	Taqman
Canada validation	148	75	N/A	136	79	N/A	2.8	1.5	283	Taqman
Total	5,232		N/A	7,908		N/A		51.3%		

*Combined (GWAS + Validation) analysis consisted of 10,204 AAA cases and 107,766 controls.

Online Table III: Summary of results for the lead SNPs at 19 putative AAA associated loci ($P < 5 \times 10^{-6}$) in the meta-analysis of 6 primary AAA GWAS datasets with a total of 4,972 AAA cases and 99,858 controls (see **Online Table I** for details on these cohorts). The results were based on an $N_{\text{effective}}$ weighted METAL analysis. The order of cohorts in the direction column is the same as that in **Online Table I** [NZ 1, NZ 2, Aneurysm Consortium, Netherlands, US (PA), Iceland (deCODE)]. See **Online Table IV** for MAF values for cases and controls separately.

Chr	SNP	Position	Gene	Risk allele	Other allele	Direction	$N_{\text{effective}}$ weighted analysis		
							P	Phet	I^2
1	rs602633	109821511	Near <i>PSRC1 CELSR2 SORT1</i>	T	G	-----	1.72×10^{-07}	0.097	46.3
1	rs12133641	154428283	<i>IL6R</i>	A	G	+++++	1.67×10^{-10}	0.903	0.0
1	<i>rs4129267 proxySNP</i>	154426264	<i>IL6R</i>	T	C	-----	9.26×10^{-10}	0.886	0.0
1	rs1795061	214409280	near <i>SMYD2</i>	T	C	+++++	1.80×10^{-07}	0.069	51.2
2	rs13382862	20882449	near <i>C2orf43</i> and <i>GDF7</i>	A	G	-----	3.03×10^{-08}	0.878	0.0
4	rs10029392	5616048	<i>EVC2</i>	T	G	+++++	4.60×10^{-06}	0.147	38.8
5	rs12659791	74757758	<i>COL4A3BP</i>	T	C	-----+	2.28×10^{-06}	0.105	45.1
6	rs3176334	36648364	<i>CDKN1A</i>	C	T	-----	1.45×10^{-06}	0.627	0.0
6	<i>rs733590 proxySNP</i>	36645203	<i>CDKN1A</i>	T	C	-----	8.74×10^{-06}	0.584	0.0
8	rs3110425	107649626	<i>OXR1</i>	T	C	-----	3.25×10^{-06}	0.895	0.0
9	rs10757274	22096055	<i>CDKN2BAS1/ANRIL</i>	A	G	-----	2.32×10^{-13}	0.520	0.0
9	rs10985349	124425243	<i>DAB2IP</i>	T	C	+++++	8.98×10^{-07}	0.181	34.0
12	rs1385526	57532749	<i>LRP1</i>	C	G	-----	1.31×10^{-09}	0.597	0.0
13	rs9316871	22861921	<i>LINC00540</i>	A	G	+++++	5.95×10^{-06}	0.143	39.4
15	rs17189674	89040591	<i>DET1</i>	A	G	+++++	1.05×10^{-06}	0.663	0.0
19	rs6511720	11202306	<i>LDLR</i>	T	G	-----	5.71×10^{-12}	0.679	0.0
19	rs12980543	56096197	<i>ZNF579</i>	A	G	+++++	2.30×10^{-06}	0.301	17.4
19	<i>rs11084402 proxySNP</i>	56093365	<i>ZNF579</i>	T	C	+++++	4.33×10^{-06}	0.218	29.0
20	rs6516091	6050622	near <i>FERMT1</i>	A	G	+++++	3.82×10^{-09}	0.027	60.5
20	rs58749629	44571317	near <i>PCIF1 ZNF335 MMP9</i>	A	G	+++++	7.97×10^{-10}	0.473	0.0
20	<i>rs3827066 proxySNP</i>	44586023	near <i>PCIF1 ZNF335 MMP9</i>	T	C	+++++	9.18×10^{-10}	0.729	0.0
21	rs2836411	39819830	<i>ERG</i>	T	C	+++++	1.53×10^{-07}	0.103	45.5
X	rs5954362	140673423	<i>SPANXA1</i>	G	C	---	2.73×10^{-07}	0.271	23.2

Online Table IV: Individual cohort data from the 6 primary AAA GWAS studies, combined using the Maentel–Haenzel fixed effect method, for the lead SNPs at the 19 putative AAA loci identified in the meta-analysis of GWAS. See **Online Table I** for details on these cohorts. This table spans this and the following 6 pages.

CHR	SNP	POSITION	Region	Cohort	OR (95% CI)	P	Case/ Control	MAF _{AAA}	MAF _{Control}	
1	rs602633	109821511	Near <i>PSRC1 CELSR2 SORT1</i>	NZ GWAS 1	0.653 (0.535 - 0.797)	2.59E-05	608/ 612	0.1743	0.2442	
				NZ GWAS 2	0.874 (0.680 - 1.125)	0.2952	397/ 384	0.1870	0.2083	
				Aneurysm Consortium GWAS	0.864 (0.785 - 0.950)	0.002639	1846/ 5605	0.1942	0.2181	
				Netherlands GWAS	0.899 (0.778 - 1.038)	0.1458	840/ 2791	0.2151	0.2336	
				US (PA) GWAS	0.793 (0.680 - 0.925)	0.003166	724/ 1231	0.1843	0.2217	
				Iceland deCODE GWAS	0.916 (0.783 - 1.073)	0.2768	557/ 89235	0.1944	0.2085	
									OR (95% CI)	Z-score
Combined					0.845 (0.796 - 0.897)	-5.534	3.1E-08	5	29.4	0.215
1	rs12133641 rs4129267 proxy	154428283 154426264	<i>IL6R</i>	NZ GWAS 1	0.841 (0.715 - 0.989)	0.03596	608/ 612	0.3881	0.43	
				NZ GWAS 2	0.838 (0.683 - 1.027)	0.08904	397/ 384	0.3687	0.4108	
				Aneurysm Consortium GWAS	0.878 (0.813 - 0.948)	8.50E-04	1846/ 5605	0.3762	0.4072	
				Netherlands GWAS	0.818 (0.723 - 0.924)	0.001291	840/ 2791	0.3475	0.3936	
				US (PA) GWAS	0.817 (0.720 - 0.927)	0.001744	724/ 1231	0.3455	0.3925	
				Iceland deCODE GWAS	0.879 (0.775 - 0.997)	0.04487	557/ 89235	0.3857	0.4169	
									OR (95% CI)	Z-score
Combined					0.854 (0.813 - 0.896)	-6.382	1.7E-10	5	0	0.945
1	rs1795061	214409280	near <i>SMYD2</i>	NZ GWAS 1	1.033 (0.868 - 1.229)	0.716	608/ 612	0.3224	0.3153	
				NZ GWAS 2	1.364 (1.087 - 1.713)	0.007383	397/ 384	0.3456	0.2791	
				Aneurysm Consortium GWAS	1.135 (1.048 - 1.229)	0.001908	1846/ 5605	0.3342	0.3067	
				Netherlands GWAS	1.075 (0.943 - 1.225)	0.2806	840/ 2791	0.2952	0.2784	
				US (PA) GWAS	1.324 (1.163 - 1.507)	2.16E-05	724/ 1231	0.3517	0.2907	
				Iceland deCODE GWAS	1.133 (0.997 - 1.287)	0.0559	557/ 89235	0.4247	0.3954	
									OR (95% CI)	Z-score
Combined					1.154(1.097 - 1.214)	5.527	3.3E-07	5	47.9	0.087

CHR	SNP	POSITION	Region	Cohort	OR (95% CI)	P	Case/ Control	MAF _{AAA}	MAF _{Control}
2	rs13382862	20882449	<i>C2orf43</i> and <i>GDF7</i>	NZ GWAS 1	0.886 (0.742 - 1.057)	0.1787	608/ 612	0.3424	0.3701
				NZ GWAS 2	0.766 (0.618 - 0.948)	0.01432	397/ 384	0.3307	0.3922
				Aneurysm Consortium GWAS	0.865 (0.799 - 0.937)	3.78E-04	1846/ 5605	0.3359	0.3689
				Netherlands GWAS	0.862 (0.763 - 0.974)	0.0176	840/ 2791	0.3430	0.3761
				US (PA) GWAS	0.855 (0.750 - 0.974)	0.01851	724/ 1231	0.3255	0.3609
				Iceland deCODE GWAS	0.892 (0.782 - 1.016)	0.08629	557/ 89235	0.3420	0.3683
				OR (95% CI)	Z-score	P-value	df (Q)	HetI²	HetPval
Combined	0.863 (0.820 - 0.907)	-5.75	8.8E-09	5	0	0.942			
4	rs10029392	5616048	<i>EVC2</i>	NZ GWAS 1	2.071 (1.444 - 2.968)	5.47E-05	608/ 612	0.0801	0.0404
				NZ GWAS 2	1.199 (0.733 - 1.961)	0.4692	397/ 384	0.0467	0.0393
				Aneurysm Consortium GWAS	1.306 (1.081 - 1.578)	0.005588	1846/ 5605	0.0436	0.0338
				Netherlands GWAS	1.180 (0.869 - 1.601)	0.2894	840/ 2791	0.0396	0.0358
				US (PA) GWAS	1.166 (0.882 - 1.542)	0.28	724/ 1231	0.0517	0.0447
				Iceland deCODE GWAS	1.402 (1.033 - 1.904)	0.03019	557/ 89235	0.0587	0.0445
				OR (95% CI)	Z-score	P-value	df (Q)	HetI²	HetPval
Combined	1.331 (1.1851 - 1.495)	4.825	1.4E-06	5	32.1	0.195			
5	rs12659791	74757758	<i>COL4A3BP</i>	NZ GWAS 1	1.284 (0.837 - 1.970)	0.2512	608/ 612	0.1763	0.1429
				NZ GWAS 2	1.067 (0.808 - 1.409)	0.6466	397/ 384	0.1549	0.1466
				Aneurysm Consortium GWAS	1.304 (1.181 - 1.440)	1.59E-07	1846/ 5605	0.1785	0.1428
				Netherlands GWAS	1.216 (1.040 - 1.421)	0.01392	840/ 2791	0.1710	0.1480
				US (PA) GWAS	1.077 (0.909 - 1.278)	0.3911	724/ 1231	0.1510	0.1417
				Iceland deCODE GWAS	0.986 (0.819 - 1.188)	0.8844	557/ 89235	0.1264	0.1279
				OR (95% CI)	Z-score	P-value	df (Q)	HetI²	HetPval
Combined	1.192 (1.115 - 1.274)	5.151	2.6E-07	5	45.5	0.102			

CHR	SNP	POSITION	Region	Cohort	OR (95% CI)	P	Case/ Control	MAF _{AAA}	MAF _{Control}
6	rs733590 proxy	36648364	CDKN1A	NZ GWAS 1	1.027 (0.870 - 1.213)	0.7498	608/ 612	0.3550	0.3489
				NZ GWAS 2	1.108 (0.896 - 1.371)	0.3434	397/ 384	0.3405	0.3178
				Aneurysm Consortium GWAS	1.128 (1.040 - 1.224)	0.003699	1846/ 5605	0.3612	0.3339
				Netherlands GWAS	1.228 (1.085 - 1.391)	0.001181	840/ 2791	0.4027	0.3552
				US (PA) GWAS	1.160 (1.024 - 1.315)	0.01962	724/ 1231	0.4052	0.3699
				Iceland deCODE GWAS	1.056 (0.925 - 1.206)	0.42	557/ 89235	0.3449	0.3329
				Combined	OR (95% CI)	Z-score	P-value	df (Q)	HetI²
	1.127 (1.072 - 1.186)	4.665	3.1E-06	5	0	0.546			
8	rs3110425	107649626	OXR1	NZ GWAS 1	0.909 (0.769 - 1.075)	0.2639	608/ 612	0.3460	0.3679
				NZ GWAS 2	0.852 (0.692 - 1.048)	0.1284	397/ 384	0.3469	0.3842
				Aneurysm Consortium GWAS	0.883 (0.816 - 0.955)	0.001861	1846/ 5605	0.3310	0.3613
				Netherlands GWAS	0.865 (0.764 - 0.980)	0.02225	840/ 2791	0.3340	0.3680
				US (PA) GWAS	0.954 (0.840 - 1.085)	4.68E-01	724/ 1231	0.3650	0.3760
				Iceland deCODE GWAS	0.849 (0.752 - 0.959)	0.012	557/ 89235	0.3480	0.3870
				Combined	OR (95% CI)	Z-score	P-value	df (Q)	HetI²
	0.885 (0.843 - 0.93)	-4.873	1.1E-06	5	0	0.784			
9	rs10757274	22096055	ANRIL/ CDKN2B-AS1	NZ GWAS 1	0.814 (0.694 - 0.955)	0.01152	608/ 612	0.4553	0.5066
				NZ GWAS 2	0.922 (0.755 - 1.125)	0.4232	397/ 384	0.4484	0.4686
				Aneurysm Consortium GWAS	0.842 (0.781 - 0.908)	7.91E-06	1846/ 5605	0.4707	0.5137
				Netherlands GWAS	0.742 (0.660 - 0.834)	6.31E-07	840/ 2791	0.4746	0.5465
				US (PA) GWAS	0.883 (0.782 - 0.997)	0.04425	724/ 1231	0.4793	0.5104
				Iceland deCODE GWAS	0.838 (0.739 - 0.949)	0.005418	557/ 89235	0.5111	0.555
				Combined	OR (95% CI)	Z-score	P-value	df (Q)	HetI²
	0.832 (0.793 - 0.872)	-7.612	2.7E-14	5	9.9	0.352			

CHR	SNP	POSITION	Region	Cohort	OR (95% CI)	P	Case/ Control	MAF _{AAA}	MAF _{Control}
9	rs10985349	124425243	DAB2IP	NZ GWAS 1	1.326 (1.078 - 1.630)	0.007382	608/ 612	0.2053	0.1631
				NZ GWAS 2	1.443 (1.112 - 1.872)	0.005649	397/ 384	0.2091	0.1549
				Aneurysm Consortium GWAS	1.159 (1.038 - 1.294)	0.008684	1846/ 5605	0.1666	0.1471
				Netherlands GWAS	1.036 (0.890 - 1.206)	0.6491	840/ 2791	0.2192	0.2110
				US (PA) GWAS	1.223 (1.050 - 1.425)	0.009782	724/ 1231	0.2055	0.1746
				Iceland deCODE GWAS	1.212 (1.027 - 1.429)	0.02253	557/ 89235	0.2427	0.2130
				Combined	OR (95% CI)	Z-score	P-value	df (Q)	HetI²
	1.185 (1.112 - 1.264)	5.198	2.0E-07	5	18.1	0.296			
12	rs1385526	57532749	LRP1	NZ GWAS 1	0.863 (0.728 - 1.024)	0.09069	608/ 612	0.3165	0.3491
				NZ GWAS 2	0.820 (0.659 - 1.021)	0.07616	397/ 384	0.3043	0.3478
				Aneurysm Consortium GWAS	0.798 (0.737 - 0.865)	3.19E-08	1846/ 5605	0.3125	0.3629
				Netherlands GWAS	0.893 (0.788 - 1.011)	0.07384	840/ 2791	0.3182	0.3452
				US (PA) GWAS	0.902 (0.790 - 1.030)	0.1277	724/ 1231	0.3047	0.3269
				Iceland deCODE GWAS	0.904 (0.796 - 1.028)	0.1233	557/ 89235	0.3945	0.4186
				Combined	OR (95% CI)	Z-score	P-value	df (Q)	HetI²
	0.851 (0.809 - 0.895)	-6.295	3.1E-10	5	0	0.613			
13	rs9316871	22861921	LINC00540	NZ GWAS 1	0.979 (0.804 - 1.190)	0.8279	608/ 612	0.2048	0.2083
				NZ GWAS 2	0.678 (0.530 - 0.869)	0.002047	397/ 384	0.1755	0.2388
				Aneurysm Consortium GWAS	0.823 (0.750 - 0.903)	3.92E-05	1846/ 5605	0.1923	0.2244
				Netherlands GWAS	0.891 (0.770 - 1.030)	0.1191	840/ 2791	0.1931	0.2104
				US (PA) GWAS	0.880 (0.760 - 1.020)	0.08905	724/ 1231	0.2103	0.2324
				Iceland deCODE GWAS	0.969 (0.821 - 1.143)	0.7052	557/ 89235	0.1763	0.1809
				Combined	OR (95% CI)	Z-score	P-value	df (Q)	HetI²
	0.864 (0.815 - 0.917)	-4.850	1.23E-06	5	33.2	0.187			

CHR	SNP	POSITION	Region	Cohort	OR (95% CI)	P	Case/ Control	MAF _{AAA}	MAF _{Control}
15	rs17189674	89040591	DET1	NZ GWAS 1	1.227 (0.966 - 1.559)	0.09398	608/ 612	0.1410	0.1180
				NZ GWAS 2	1.595 (1.140 - 2.230)	0.006056	397/ 384	0.1273	0.0838
				Aneurysm Consortium GWAS	1.241 (1.096 - 1.406)	6.51E-04	1846/ 5605	0.1123	0.0925
				Netherlands GWAS	1.194 (0.991 - 1.438)	0.06165	840/ 2791	0.1314	0.1148
				US (PA) GWAS	1.109 (0.916 - 1.344)	0.2889	724/ 1231	0.1167	0.1064
				Iceland deCODE GWAS	1.181 (0.983 - 1.418)	0.07515	557/ 89235	0.1645	0.1448
				OR (95% CI)	Z-score	P-value	df (Q)	HetI²	HetPval
Combined	1.216 (1.128 - 1.311)	5.091	3.6E-07	5	0	0.742			
19	rs6511720	11202306	LDLR	NZ GWAS 1	0.611 (0.403 - 0.927)	0.01942	608/ 612	0.04043	0.06452
				NZ GWAS 2	0.717 (0.514 - 1.001)	0.05007	397/ 384	0.08564	0.11550
				Aneurysm Consortium GWAS	0.764 (0.676 - 0.863)	1.48E-05	1846/ 5605	0.09778	0.12430
				Netherlands GWAS	0.650 (0.529 - 0.797)	3.74E-05	840/ 2791	0.08240	0.12150
				US (PA) GWAS	0.742 (0.608 - 0.905)	0.003207	724/ 1231	0.09655	0.12590
				Iceland deCODE GWAS	0.855 (0.684 - 1.068)	0.1668	557/ 89235	0.07480	0.08720
				OR (95% CI)	Z-score	P-value	df (Q)	HetI²	HetPval
Combined	0.743 (0.685 - 0.806)	-7.151	8.6E-13	5	0	0.829			
19	rs12980543 rs11084402 proxy	56096197 56093365	ZNF579	NZ GWAS 1	1.011 (0.832 - 1.227)	0.9147	608/ 612	0.2170	0.2152
				NZ GWAS 2	1.280 (1.006 - 1.628)	0.04423	397/ 384	0.2418	0.1995
				Aneurysm Consortium GWAS	1.077 (0.984 - 1.180)	0.1091	1846/ 5605	0.2153	0.2030
				Netherlands GWAS	1.217 (1.051 - 1.409)	0.00854	840/ 2791	0.2159	0.1824
				US (PA) GWAS	1.273 (1.094 - 1.481)	0.001733	724/ 1231	0.2131	0.1754
				Iceland deCODE GWAS	1.281 (1.059 - 1.549)	0.01071	557/ 89235	0.1734	0.1430
				OR (95% CI)	Z-score	P-value	df (Q)	HetI²	HetPval
Combined	1.152 (1.086 - 1.223)	4.669	3.0E-06	5	33.2	0.187			

CHR	SNP	POSITION	Region	Cohort	OR (95% CI)	P	Case/ Control	MAF _{AAA}	MAF _{Control}	
20	rs6516091	6050622	near <i>FERMT1</i>	NZ GWAS 1	1.263 (0.991 - 1.609)	0.05848	608/ 612	0.1381	0.1126	
				NZ GWAS 2	1.271 (0.931 - 1.734)	0.13	397/ 384	0.1297	0.1050	
				Aneurysm Consortium GWAS	1.399 (1.261 - 1.551)	1.73E-10	1846/ 5605	0.1655	0.1242	
				Netherlands GWAS	1.187 (0.994 - 1.416)	0.05749	840/ 2791	0.1298	0.1150	
				US (PA) GWAS	1.186 (0.987 - 1.426)	0.06916	724/ 1231	0.1290	0.1110	
				Iceland deCODE GWAS	0.968 (0.783 - 1.197)	0.7619	557/ 89235	0.0938	0.0966	
									OR (95% CI)	Z-score
Combined					1.262 (1.177 - 1.354)	6.525	6.8E-11	5	56.2	0.044
20	rs58749629 rs3827066 proxy	44571317 44586023	Near <i>MMP9/ZNF335</i>	NZ GWAS 1	1.062 (0.846 - 1.333)	0.6044	608/ 612	0.1503	0.1427	
				NZ GWAS 2	1.101 (0.847 - 1.430)	0.4723	397/ 384	0.1827	0.1688	
				Aneurysm Consortium GWAS	1.237 (1.119 - 1.368)	2.97E-05	1846/ 5605	0.1743	0.1457	
				Netherlands GWAS	1.287 (1.099 - 1.506)	0.001752	840/ 2791	0.1761	0.1414	
				US (PA) GWAS	1.246 (1.067 - 1.456)	0.005513	724/ 1231	0.1972	0.1647	
				Iceland deCODE GWAS	1.325 (1.094 - 1.606)	0.003994	557/ 89235	0.1492	0.1193	
									OR (95% CI)	Z-score
Combined					1.233 (1.156 - 1.314)	6.371	1.9E-10	5	0	0.444
21	rs2836411	39819830	<i>ERG</i>	NZ GWAS 1	1.313 (1.113 - 1.548)	0.001228	608/ 612	0.3980	0.3350	
				NZ GWAS 2	1.076 (0.876 - 1.321)	0.4862	397/ 384	0.3823	0.3652	
				Aneurysm Consortium GWAS	1.132 (1.048 - 1.223)	0.00155	1846/ 5605	0.3814	0.3525	
				Netherlands GWAS	1.204 (1.065 - 1.361)	0.002983	840/ 2791	0.4016	0.3611	
				US (PA) GWAS	1.232 (1.086 - 1.397)	0.001164	724/ 1231	0.3821	0.3342	
				Iceland deCODE GWAS	1.000 (0.878 - 1.139)	0.9964	557/ 89235	0.3330	0.3331	
									OR (95% CI)	Z-score
Combined					1.149 (1.095 - 1.207)	5.573	2.5E-08	5	30.1	0.209

CHR	SNP	POSITION	Region	Cohort	OR (95% CI)	P	Case/ Control	MAF _{AAA}	MAF _{Control}	
X	RS5954362	140673423	SPANXA1	NZ GWAS 1	0.750 (0.556 - 1.007)	0.05496	474/ 450	0.2372	0.2930	
				NZ GWAS 2	0.862 (0.586 - 1.269)	0.4522	332/ 308	0.2310	0.2584	
				Aneurysm Consortium GWAS	0.584 (0.499 - 0.685)	1.81E-11	1815/ 2736	0.1894	0.2856	
					OR (95% CI)	Z-score	P-value	df (Q)	HetI ²	HetPval
Combined					0.642 (0.563 - 0.732)	-6.105	1.0E-09	2	3.91	0.142

Online Table V: Summary of results for the combined (using the Maentel–Haenzel fixed effect method) validation study cohorts for the lead SNPs at putative AAA associated loci. The SNPs with $P < 5 \times 10^{-6}$ in the meta-analysis of 6 primary AAA GWAS datasets were genotyped in 8 different validation cohorts for a total of 5,232 AAA cases and 7,908 controls (see **Online Table II** for details on these cohorts). Results including MAFs for cases and controls in each individual cohort are shown in **Online Table VI**. Where a proxy SNP was typed the original lead SNP from the discovery study is shown above the proxy SNP typed in the validation study.

Chr	SNP	Position	Gene	Risk allele	Other allele	P	Direction	Phet	I^2
1	rs602633	109821511	Near <i>PSRC1 CELSR2 SORT1</i>	T	G	0.01	----+--	0.027	55.8
1	rs12133641	154428283	<i>IL6R</i>	A	G				
	<i>rs4129267 proxySNP</i>	154426264	<i>IL6R</i>	T	C	1.81×10^{-4}	+-----	0.294	17.2
1	rs1795061	214409280	near <i>SMYD2</i>	T	C	3.49×10^{-4}	+++++++	0	70.3
2	rs13382862	20882449	near <i>C2orf43</i> and <i>GDF7</i>	A	G	0.360	-----+	0.278	19.2
4	rs10029392	5616048	<i>EVC2</i>	T	G	0.267	++---++	0.195	29.2
5	rs12659791	74757758	<i>COL4A3BP</i>	T	C	0.966	-+-----	0.749	0.0
6	rs3176334	36648364	<i>CDKN1A</i>	C	T				
	<i>rs733590 proxySNP</i>	36645203	<i>CDKN1A</i>	T	C	0.789	+++++--	0.754	0.0
8	rs3110425	107649626	<i>OXR1</i>	T	C	0.261	+-----+	0.268	20.4
9	rs10757274	22096055	<i>CDKN2BAS1/ANRIL</i>	A	G	1.02×10^{-21}	-----	0.001	64.2
9	rs10985349	124425243	<i>DAB2IP</i>	T	C	2.30×10^{-5}	+++++++	0.4	3.9
12	rs1385526	57532749	<i>LRP1</i>	C	G	0.622	+++++++	0.33	12.8
13	rs9316871	22861921	<i>LINC00540</i>	A	G	8.28×10^{-5}	-----+	0.795	0.0
15	rs17189674	89040591	<i>DET1</i>	A	G	0.744	--++++-	0.102	41.5
19	rs6511720	11202306	<i>LDLR</i>	T	G	6.02×10^{-4}	-----+	0.003	68.2
19	rs12980543	56096197	<i>ZNF579</i>	A	G				
	<i>rs11084402 proxySNP</i>	56093365	<i>ZNF579</i>	T	C	0.364	+-----	0.12	38.9
20	rs6516091	6050622	near <i>FERMT1</i>	A	G	0.867	+-----	0.104	41.1
20	rs58749629	44571317	near <i>PCIF1 ZNF335 MMP9</i>	A	G				
	<i>rs3827066 proxySNP</i>	44586023	near <i>PCIF1 ZNF335 MMP9</i>	T	C	2.00×10^{-8}	+++++++	0.3	16.5
21	rs2836411	39819830	<i>ERG</i>	T	C	0.011	+++++++	0.203	28.3
X	rs5954362	140673423	<i>SPANXA1</i>	G	C	0.172	-+---	0.005	73.2

Online Table VI: Results of validation for the lead SNPs (combined using the Maentel–Haenzel fixed effect method) at putative AAA loci identified in the meta-analysis of GWAS. The SNPs with $P < 5 \times 10^{-6}$ in the meta-analysis of 6 primary AAA GWAS datasets were genotyped in 8 different validation cohorts for a total of up to 5,232 AAA cases and 7,908 controls (see **Online Table II** for details on these cohorts). This table spans this and the following 5 pages. Where a proxy SNP is indicated the results are for that proxy SNP.

Chromosome	SNP	POSITION	Region	Cohort	OR (95% CI)	Case/control	MAFAAA	MAFControl	HWEControl	HWEAAA				
1	rs602633	109821511	Near PSRC1 CELSR2 SORT1	AC	0.885 (0.781-1.002)	1236/2196	0.191	0.211	0.079	0.799				
				US2	0.864 (0.757-0.987)	1157/1374	0.211	0.236	0.724	0.248				
				NZ	0.933 (0.794-1.095)	753/1237	0.201	0.213	0.473	0.183				
				Italy	1.201 (0.995-1.449)	718/636	0.220	0.190	0.200	0.210				
				Poland	1.133 (0.904-1.421)	443/474	0.218	0.197	0.652	0.995				
				eMERGE	0.784 (0.639-0.963)	330/1648	0.203	0.245	0.005	0.248				
				Belgium	0.8 (0.591-1.082)	302/216	0.192	0.229	0.198	0.959				
				Canada	0.803 (0.533-1.211)	126/118	0.230	0.271	0.881	0.870				
									OR (95% CI)	Z-score	P-value	df (Q)	HetPVal	I-squared
				Combined:					0.92 (0.863-0.98)	-2.582	0.010	7	0.027	55.770
1	rs12133641 rs4129267 proxy	154428283 154426264	IL6R	AC	1.001 (0.904-1.108)	1236/2196	0.386	0.386	0.706	0.293				
				US2	0.879 (0.783-0.986)	1137/1324	0.369	0.400	0.798	0.689				
				NZ	0.835 (0.732-0.954)	753/1237	0.377	0.420	0.155	0.022				
				Italy	0.897 (0.765-1.052)	714/585	0.364	0.390	0.286	0.179				
				Poland	0.925 (0.768-1.114)	480/481	0.353	0.371	0.731	0.000				
				eMERGE	0.927 (0.781-1.099)	345/1724	0.354	0.371	0.137	0.840				
				Belgium	0.767 (0.606-0.971)	334/256	0.361	0.424	0.440	0.410				
				Canada	0.761 (0.541-1.072)	139/133	0.381	0.447	0.025	0.427				
									OR (95% CI)	Z-score	P-value	df (Q)	HetPVal	I-squared
				Combined:					0.904 (0.857-0.953)	-3.743	1.81E-04	7	0.294	17.200
1	rs1795061	214409280	Near SMYD2	AC	1.171 (1.053-1.302)	1236/2196	0.332	0.298	0.869	0.360				
				US2	0.91 (0.808-1.024)	1172/1386	0.301	0.321	0.469	0.892				
				NZ	1.077 (0.939-1.236)	753/1237	0.336	0.319	0.060	0.026				
				Italy	1.434 (1.21-1.698)	761/558	0.340	0.264	0.226	0.071				
				Poland	1.025 (0.848-1.239)	470/487	0.332	0.326	0.823	0.025				
				eMERGE	1.088 (0.915-1.294)	340/1679	0.347	0.328	0.216	0.991				
				Belgium	1.28 (0.996-1.646)	335/260	0.327	0.275	0.605	0.583				
				Canada	1.32 (0.916-1.905)	132/132	0.352	0.292	0.075	0.364				
									OR (95% CI)	Z-score	P-value	df (Q)	HetPVal	I-squared
				Combined:					1.105 (1.046-1.168)	3.576	3.49E-04	7	0.000	70.300

Chromosome	SNP	POSITION	Region	Cohort	OR (95% CI)	Case/control	MAFAAA	MAFControl	HWEControl	HWEAAA				
2	rs13382862	20882449	near C2orf43 and GDF7	AC	0.942 (0.85-1.045)	1236/2196	0.358	0.372	0.224	0.156				
				US2	0.94 (0.836-1.057)	1109/1386	0.346	0.360	0.103	0.291				
				NZ	0.87 (0.759-0.997)	753/1237	0.335	0.366	0.140	0.741				
				Italy	1.109 (0.931-1.321)	727/558	0.287	0.266	0.158	0.345				
				Poland	1.099 (0.906-1.332)	450/452	0.366	0.344	0.465	0.098				
				eMERGE	1.083 (0.913-1.285)	335/1645	0.388	0.369	0.970	0.918				
				Belgium	1.024 (0.794-1.319)	310/256	0.310	0.305	0.821	0.209				
				Canada	0.998 (0.705-1.413)	142/131	0.370	0.370	0.720	0.021				
									OR (95% CI)	Z-score	P-value	df (Q)	HetPVal	I-squared
				Combined:					0.975 (0.923-1.029)	-0.915	0.360	7	0.278	19.156
4	rs10029392	5616048	EVC2	AC	1.014 (0.814-1.263)	1698/2209	0.044	0.043	0.655	0.110				
				US2*	0.876 (0.678-1.132)	1169/1387	0.046	0.052	0.217	0.088				
				NZ*	1.233 (0.92-1.651)	753/1237	0.057	0.047	0.809	0.106				
				Italy	0.767 (0.588-0.999)	678/556	0.088	0.112	0.423	0.709				
				Poland*	0.809 (0.6-1.092)	472/481	0.091	0.110	0.074	0.963				
				eMERGE	0.921 (0.642-1.321)	343/1707	0.054	0.058	0.998	0.006				
				Belgium*	1.09 (0.545-2.18)	335/225	0.030	0.027	0.652	0.573				
				Canada*	2.2 (0.754-6.422)	133/130	0.041	0.019	0.823	0.091				
									OR (95% CI)	Z-score	P-value	df (Q)	HetPVal	I-squared
				Combined:					0.94 (0.843-1.049)	-1.111	0.267	7	0.195	29.200
5	rs12659791	74757758	COL4A3BP	AC	0.963 (0.839-1.105)	1236/2196	0.149	0.154	0.071	0.307				
				US2	1.063 (0.91-1.242)	1151/1371	0.153	0.145	0.398	0.663				
				NZ	0.959 (0.802-1.148)	753/1237	0.152	0.158	0.149	0.581				
				Italy	1.051 (0.83-1.332)	732/439	0.151	0.145	0.484	0.177				
				Poland	0.976 (0.771-1.236)	486/488	0.169	0.172	0.002	0.553				
				eMERGE	0.979 (0.773-1.241)	345/1723	0.138	0.140	0.818	0.807				
				Belgium	0.91 (0.669-1.237)	339/266	0.156	0.169	0.298	0.126				
				Canada	1.62 (0.898-2.921)	105/91	0.167	0.110	0.239	0.953				
									OR (95% CI)	Z-score	P-value	df (Q)	HetPVal	I-squared
				Combined:					0.998 (0.929-1.073)	-0.043	0.966	7	0.749	0.000

Chromosome	SNP	POSITION	Region	Cohort	OR (95% CI)	Case/control	MAFAAA	MAFControl	HWEControl	HWEAAA				
6	rs3176334 rs733590 proxy	36648364 36645203	CDKN1A	AC	1.042 (0.94-1.156)	1236/2196	0.356	0.347	0.523	0.412				
				US2	1.006 (0.897-1.127)	1157/1374	0.379	0.378	0.871	0.072				
				NZ	1.026 (0.894-1.178)	753/1237	0.333	0.327	0.268	0.428				
				Italy	0.978 (0.831-1.149)	733/546	0.371	0.376	0.163	0.992				
				Poland	1.021 (0.846-1.232)	455/453	0.398	0.393	0.702	0.557				
				eMERGE	0.893 (0.748-1.066)	318/1599	0.357	0.383	0.525	0.391				
				Belgium	1.127 (0.888-1.43)	331/254	0.394	0.366	0.776	0.917				
				Canada	0.84 (0.585-1.205)	142/132	0.296	0.333	0.361	0.150				
									OR (95% CI)	Z-score	P-value	df (Q)	HetPVal	I-squared
				Combined:					1.007 (0.955-1.063)	0.2678	0.789	7	0.754	0.000
8	rs3110425	107649626	OXR1	AC	1.079 (0.974-1.196)	1225/2167	0.374	0.356	0.111	0.315				
				US2	0.933 (0.826-1.053)	987/1323	0.355	0.371	0.568	0.248				
				NZ	1.088 (0.949-1.247)	704/1174	0.382	0.361	0.107	0.279				
				Italy	1.058 (0.878-1.275)	532/445	0.359	0.346	0.883	0.226				
				Poland	1.214 (0.999-1.475)	449/457	0.363	0.319	0.770	0.164				
				eMERGE	0.942 (0.794-1.118)	342/1711	0.360	0.373	0.971	0.448				
				Belgium	0.910 (0.713-1.163)	313/246	0.356	0.378	0.558	0.672				
				Canada	1.036 (0.725-1.481)	126/118	0.230	0.271	0.881	0.870				
									OR (95% CI)	Z-score	P-value	df (Q)	HetPVal	I-squared
				Combined:					1.032 (0.977-1.090)	1.124	0.261	7	0.268	20.420
9	rs10757274	22096055	ANRIL CDKN2BAS1/	AC	0.831 (0.752-0.917)	1236/2196	0.456	0.502	0.273	0.163				
				US	0.748 (0.67-0.836)	1162/1382	0.451	0.523	0.099	0.622				
				NZ	0.885 (0.777-1.007)	753/1237	0.466	0.497	0.561	0.038				
				Italy	0.63 (0.527-0.753)	540/464	0.371	0.484	0.236	0.052				
				Poland	0.679 (0.565-0.816)	451/468	0.463	0.560	0.616	0.551				
				eMERGE	0.68 (0.576-0.804)	336/1696	0.435	0.530	0.333	0.922				
				Belgium	0.959 (0.757-1.214)	313/248	0.455	0.466	0.333	0.977				
				Canada	0.674 (0.468-0.97)	117/117	0.427	0.526	0.535	0.320				
									OR (95% CI)	Z-score	P-value	df (Q)	HetPVal	I-squared
				Combined:					0.774 (0.735-0.816)	-9.575	1.02E-21	7	0.001	64.200

Chromosome	SNP	POSITION	Region	Cohort	OR (95% CI)	Case/control	MAFAAA	MAFControl	HWEControl	HWEAAA				
9	rs10985349	124425243	DAB2IP	AC	0.998 (0.876-1.135)	1236/2196	0.179	0.179	0.878	0.696				
				US2	1.208 (1.051-1.387)	1171/1385	0.211	0.181	0.625	0.165				
				NZ	1.266 (1.072-1.495)	753/1237	0.199	0.164	0.865	0.720				
				Italy	1.227 (0.975-1.544)	729/620	0.138	0.115	0.061	0.327				
				Poland	1.182 (0.947-1.476)	485/488	0.215	0.189	0.322	0.228				
				eMERGE	1.215 (0.969-1.523)	299/1544	0.189	0.161	0.346	0.381				
				Belgium	1.139 (0.848-1.53)	338/266	0.192	0.173	0.682	0.220				
				Canada	1.304 (0.861-1.975)	149/134	0.221	0.179	0.177	0.116				
									OR (95% CI)	Z-score	P-value	df (Q)	HetPVal	I-squared
				Combined:					1.155 (1.081-1.235)	4.233	2.30E-05	7	0.400	3.900
12	rs1385526	57532749	LRP1	AC	0.983 (0.886-1.092)	1236/2196	0.339	0.343	0.293	0.297				
				US2	0.905 (0.804-1.019)	1161/1382	0.306	0.328	0.668	0.221				
				NZ	0.918 (0.801-1.052)	753/1237	0.333	0.352	0.160	0.840				
				Italy	1.135 (0.942-1.366)	509/493	0.351	0.323	0.072	0.392				
				Poland	1.058 (0.875-1.28)	453/480	0.359	0.346	0.083	0.580				
				eMERGE	1.124 (0.944-1.339)	342/1695	0.336	0.311	0.695	0.170				
				Belgium	0.966 (0.749-1.244)	324/246	0.306	0.313	0.744	0.647				
				Canada	1.031 (0.706-1.506)	132/120	0.311	0.304	0.181	0.607				
									OR (95% CI)	Z-score	P-value	df (Q)	HetPVal	I-squared
				Combined:					0.986 (0.933-1.042)	-0.493	0.622	7	0.330	12.800
13	rs9316871	22861921	LINC00540	AC	0.905 (0.801-1.023)	1236/2196	0.199	0.216	0.094	0.193				
				US2	0.845 (0.738-0.966)	1176/1384	0.202	0.231	0.624	0.052				
				NZ	0.834 (0.711-0.978)	753/1237	0.195	0.225	0.210	0.727				
				Italy	0.925 (0.776-1.102)	621/646	0.262	0.278	0.178	0.107				
				Poland	0.884 (0.721-1.085)	469/483	0.251	0.274	0.222	0.038				
				eMERGE	1.008 (0.828-1.226)	345/1724	0.223	0.222	0.049	0.954				
				Belgium	0.79 (0.592-1.053)	330/251	0.185	0.223	0.854	0.920				
				Canada	0.798 (0.515-1.235)	133/125	0.177	0.212	0.004	0.271				
									OR (95% CI)	Z-score	P-value	df (Q)	HetPVal	I-squared
				Combined:					0.883 (0.83-0.94)	-3.936	8.28E-05	7	0.795	0.000

Chromosome	SNP	POSITION	Region	Cohort	OR (95% CI)	Case/control	MAFAAA	MAFControl	HWEControl	HWEAAA			
15	rs17189674	89040591	DET1	AC	0.889 (0.763-1.036)	1236/2196	0.115	0.128	0.264	0.949			
				US2	0.934 (0.781-1.116)	1170/1381	0.104	0.110	0.000	0.846			
				NZ	1.301 (1.065-1.588)	753/1237	0.130	0.103	0.499	0.429			
				Italy	1.115 (0.862-1.441)	616/872	0.127	0.116	0.113	0.276			
				Poland	0.912 (0.686-1.212)	488/489	0.105	0.113	0.559	0.260			
				eMERGE	1.072 (0.815-1.411)	320/1649	0.108	0.101	0.553	0.114			
				Belgium	1.214 (0.849-1.737)	340/266	0.125	0.105	0.973	0.403			
				Canada	0.927 (0.557-1.542)	201/137	0.113	0.120	0.105	0.944			
								OR (95% CI)	Z-score	P-value	df (Q)	HetPVal	I-squared
				Combined:	1.014 (0.935-1.099)	0.327	0.744	7	0.102	41.500			
19	rs6511720	11202306	LDLR	AC	0.969 (0.826-1.136)	1236/2196	0.107	0.110	0.144	0.384			
				US2	0.93 (0.792-1.092)	1166/1383	0.132	0.141	0.000	0.000			
				NZ	0.849 (0.69-1.045)	753/1237	0.103	0.119	0.737	0.454			
				Italy	0.566 (0.436-0.736)	667/567	0.079	0.132	0.736	0.242			
				Poland	0.607 (0.454-0.812)	477/479	0.087	0.136	0.944	0.132			
				eMERGE	0.933 (0.709-1.227)	320/1639	0.108	0.101	0.553	0.114			
				Belgium	1.162 (0.817-1.653)	336/260	0.129	0.113	0.102	0.079			
				Canada	1.025 (0.63-1.67)	141/133	0.138	0.135	0.676	0.231			
								OR (95% CI)	Z-score	P-value	df (Q)	HetPVal	I-squared
				Combined:	0.868 (0.801-0.941)	-3.431	6.02E-04	7	0.003	68.200			
19	rs12980543 rs11084402 proxy	56096197 56093365	near ZNF579 near ZNF579	AC	1.033 (0.913-1.169)	1217/2169	0.205	0.199	0.239	0.604			
				US2	0.889 (0.771-1.025)	1164/1386	0.176	0.193	0.216	0.988			
				NZ	1.113 (0.953-1.3)	737/1217	0.230	0.212	0.665	0.832			
				Italy	1.075 (0.871-1.326)	648/503	0.196	0.185	0.124	0.203			
				Poland	1.014 (0.802-1.281)	474/485	0.177	0.176	0.737	0.780			
				eMERGE	1.145 (0.935-1.402)	344/1723	0.209	0.188	0.967	0.200			
				Belgium	1.293 (0.97-1.722)	337/262	0.223	0.181	0.068	0.140			
				Canada	0.73 (0.486-1.096)	135/125	0.207	0.264	0.130	0.142			
								OR (95% CI)	Z-score	P-value	df (Q)	HetPVal	I-squared
				Combined:	1.03 (0.966-1.099)	0.908	0.364	7.000	0.120	38.900			

Chromosome	SNP	POSITION	Region	Cohort	OR (95% CI)	Case/control	MAFAAA	MAFControl	HWEControl	HWEAAA				
20	rs6516091	6050622	near FERMT1	AC	1.112 (0.961-1.287)	1236/2196	0.136	0.124	0.911	0.431				
				US2	0.901 (0.768-1.057)	1173/1384	0.132	0.144	0.625	0.149				
				NZ	1.094 (0.9-1.33)	753/1237	0.131	0.121	0.682	0.424				
				Italy	0.834 (0.667-1.043)	715/589	0.137	0.160	0.357	0.152				
				Poland	0.824 (0.619-1.096)	485/488	0.100	0.119	0.363	0.002				
				eMERGE	0.94 (0.741-1.192)	343/1716	0.137	0.145	0.047	0.511				
				Belgium	1.355 (0.947-1.939)	339/266	0.133	0.102	0.065	0.153				
				Canada	1.089 (0.671-1.768)	149/137	0.138	0.128	0.857	0.415				
									OR (95% CI)	Z-score	P-value	df (Q)	HetPVal	I-squared
				Combined:					0.994 (0.921-1.072)	-0.167	0.867	7	0.104	41.100
20	rs58749629 rs3827066 proxy	44571317 44586023	near PCIF1 ZNF335 MMP9 near PCIF1 ZNF335 MMP9	AC	1.076 (0.94-1.233)	1236/2196	0.160	0.151	0.688	0.617				
				US2	1.197 (1.035-1.385)	1171/1384	0.185	0.160	0.510	0.814				
				NZ	1.372 (1.153-1.632)	753/1237	0.185	0.142	0.132	0.899				
				Italy	1.263 (1.05-1.518)	709/579	0.256	0.214	0.380	0.275				
				Poland	1.373 (1.092-1.728)	487/486	0.210	0.163	0.958	0.907				
				eMERGE	1.077 (0.86-1.348)	345/1713	0.159	0.150	0.160	0.926				
				Belgium	1.291 (0.956-1.743)	340/265	0.196	0.158	0.280	0.733				
				Canada	1.469 (0.983-2.197)	146/132	0.260	0.193	0.023	0.028				
									OR (95% CI)	Z-score	P-value	df (Q)	HetPVal	I-squared
				Combined:					1.213 (1.134-1.298)	5.616	2.00E-08	7	0.300	16.500
21	rs2836411	39819830	ERG	AC	1.05 (0.947-1.164)	1236/2196	0.367	0.355	0.409	0.483				
				US2	1.085 (0.966-1.218)	1171/1382	0.350	0.331	0.073	0.877				
				NZ	1.171 (1.023-1.339)	753/1237	0.387	0.351	0.733	0.258				
				Italy	0.898 (0.757-1.065)	706/625	0.263	0.285	0.088	0.332				
				Poland	1.125 (0.935-1.354)	482/484	0.380	0.352	0.990	0.769				
				eMERGE	1.045 (0.88-1.241)	345/1724	0.349	0.339	0.485	0.797				
				Belgium	1.01 (0.797-1.281)	339/264	0.358	0.356	0.224	0.715				
				Canada	1.457 (1.04-2.041)	150/137	0.440	0.350	0.422	0.314				
									OR (95% CI)	Z-score	P-value	df (Q)	HetPVal	I-squared
				Combined:					1.072 (1.016-1.131)	2.533	0.011	7	0.203	28.300
X	rs5954362	140673423	SPANXA1	Males only										
				NZ	0.816 (0.636-1.047)	585/762	0.248	0.288						
				Belgium	1.301 (0.972-1.741)	319/183	0.310	0.257						
				Canada	0.536 (0.294-0.978)	155/32	0.272	0.411						
				eMERGE	1.189 (1.044-1.353)	1145/1134	0.311	0.276						
				Poland	0.948 (0.759-1.186)	426/355	0.286	0.297						
					OR (95% CI)	Z-score	P-value	df (Q)	HetPVal	I-squared				
Combined:					1.069 (0.972-1.175)	1.366	0.172	4	0.005	73.200				

Online Table VII: Combined results from GWAS meta-analysis and validation studies. Shaded rows indicate validated AAA risk loci that are also shown in Table 1 in the main text. A fixed effect meta-analysis was performed using a Maentel–Haenzel method with the genome-wide *P*-value significance threshold being set at 5×10^{-8} .

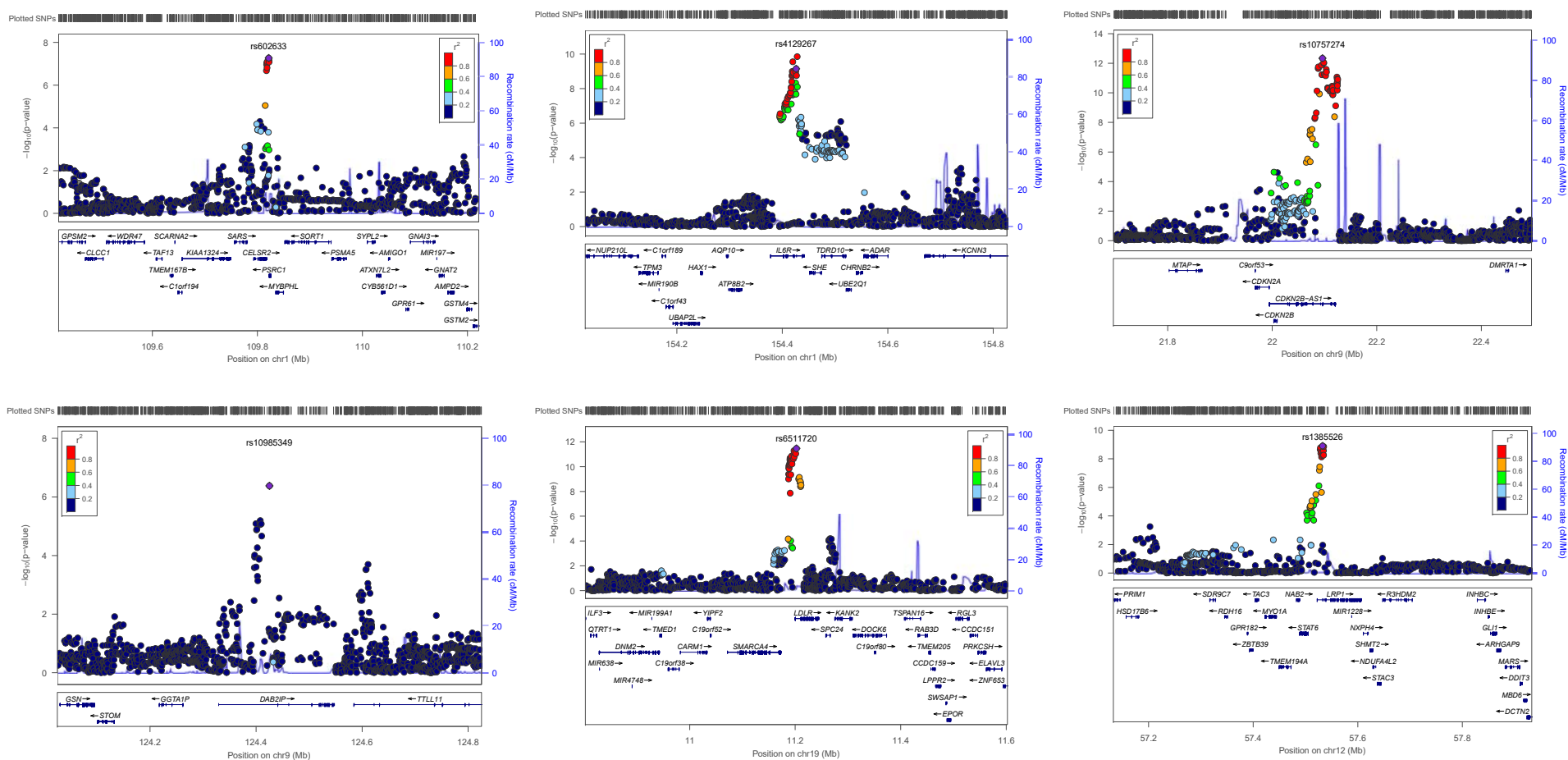
Chr	SNP	Position	Gene	Minor allele	Other allele	Meta-GWAS (lambda adjusted)				Combined validation studies					Combined meta-analysis and validation							
						MAF	P-value	Direction	HetPVal	OR	L95	U95	Z-score	P-value	OR	L95	U95	Z-score	P-value	df	HetPVal	
1*	rs602633	109821511	Near <i>PSRC1</i> <i>CELSR2</i> <i>SORT1</i>	T	G	0.199	1.72×10^{-07}	-----	0.097	0.920	0.863	0.980	-2.582	9.83×10^{-03}	0.879	0.842	0.918	-5.801	6.58×10^{-09}	13	7.60×10^{-03}	
1*	rs12133641	154428283	<i>IL6R</i>	A	G		1.67×10^{-10}	+++++	0.903													
1	rs4129267 (proxy)	154426264	<i>IL6R</i>	T	C	0.370	9.26×10^{-10}	-----	0.886	0.904	0.857	0.953	-3.743	1.81×10^{-04}	0.876	0.846	0.908	-7.232	4.76×10^{-13}	13	0.478	
1	rs1795061	214409280	near <i>SMYD2</i>	T	C	0.336	1.79×10^{-07}	+++++	0.069	1.105	1.046	1.168	3.576	3.49×10^{-04}	1.131	1.090	1.174	6.486	8.80×10^{-11}	13	1.14×10^{-03}	
2	rs13382862	20882449	near <i>C2orf43</i> and <i>GDF7</i>	A	G	0.341	3.03×10^{-08}	-----	0.878	0.975	0.923	1.029	-0.915	3.60×10^{-01}	0.913	0.880	0.947	-4.845	1.3×10^{-06}	13	8.01×10^{-02}	
4	rs10029392	5616048	<i>EVC2</i>	T	G	0.052	4.60×10^{-06}	+++++	0.147	0.940	0.843	1.049	-1.111	2.67×10^{-01}	1.107	1.022	1.198	2.496	1.25×10^{-02}	13	6.51×10^{-04}	
5	rs12659791	74757758	<i>COL4A3BP</i>	T	C	0.159	2.28×10^{-06}	--+--	0.105	0.998	0.929	1.073	-0.043	9.66×10^{-01}	1.098	1.046	1.153	3.752	1.8×10^{-04}	13	1.69×10^{-02}	
6	rs3176334	36648364	<i>CDKN1A</i>	T	C		1.50×10^{-06}	-----	0.627													
6	rs733590 (proxy)	36645203	<i>CDKN1A</i>	T	C	0.367	8.74×10^{-06}	-----	0.584	1.007	0.955	1.063	0.2678	7.89×10^{-01}	1.070	1.031	1.110	3.588	3.33×10^{-04}	13	0.183	
9*	rs10757274	22096055	<i>CDKN2BAS1/ANRIL</i>	A	G	0.351	2.32×10^{-13}	-----	0.520	0.774	0.735	0.816	-9.575	1.02×10^{-21}	0.806	0.778	0.834	-12.069	1.54×10^{-33}	13	5.94×10^{-03}	
9*	rs10985349	124425243	<i>DAB2IP</i>	T	C	0.462	8.98×10^{-07}	+++++	0.181	1.155	1.081	1.235	4.233	2.30×10^{-05}	1.171	1.118	1.226	6.682	2.4×10^{-11}	13	3.52×10^{-01}	
12*	rs1385526	57532749	<i>LRP1</i>	C	G	0.195	1.31×10^{-09}	-----	0.597	0.986	0.933	1.042	-0.493	6.22×10^{-01}	0.910	0.877	0.944	-4.980	6.4×10^{-07}	13	9.38×10^{-03}	
13	rs9316871	22861921	<i>LINC00540</i>	A	G	0.328	5.95×10^{-06}	+++++	0.143	0.883	0.830	0.940	-3.936	8.28×10^{-05}	0.873	0.837	0.911	-6.227	4.8×10^{-10}	13	0.488	
15	rs17189674	89040591	<i>DET1</i>	A	G	0.201	1.05×10^{-06}	+++++	0.663	1.014	0.935	1.099	0.327	7.44×10^{-01}	1.118	1.058	1.181	3.957	7.59×10^{-05}	13	1.71×10^{-02}	
19*	rs6511720	11202306	<i>LDLR</i>	T	G	0.122	5.71×10^{-12}	-----	0.679	0.868	0.801	0.941	-3.431	6.02×10^{-04}	0.804	0.759	0.851	-7.472	7.9×10^{-14}	13	1.53×10^{-03}	
19	rs12980543	56096197	near <i>ZNF579</i>	A	G		2.30×10^{-06}	+++++	0.301													
19	rs11084402 proxy	56093365	near <i>ZNF579</i>	T	C	0.206	4.33×10^{-06}	+++++	0.218	1.030	0.966	1.099	0.908	3.64×10^{-01}	1.095	1.048	1.144	4.050	5.1×10^{-05}	13	0.019	
20	rs6516091	6050622	near <i>FERMT1</i>	A	G	0.135	3.82×10^{-09}	+++++	0.027	0.994	0.921	1.072	-0.167	8.67×10^{-01}	1.131	1.074	1.190	4.680	2.9×10^{-06}	13	4.01×10^{-05}	
20	rs58749629	44571317	near <i>PCIF1</i> <i>ZNF335</i> <i>MMP9</i>	A	G		7.97×10^{-10}	+++++	0.760													
20	rs3827066 proxy	44586023	near <i>PCIF1</i> <i>ZNF335</i> <i>MMP9</i>	T	C	0.179	9.18×10^{-10}	+++++	0.729	1.213	1.134	1.298	5.616	2.00×10^{-08}	1.223	1.168	1.281	8.486	2.1×10^{-17}	13	0.552	
21	rs2836411	39819830	<i>ERG</i>	T	C	0.369	1.53×10^{-07}	+++++	0.103	1.072	1.016	1.131	2.533	1.13×10^{-02}	1.113	1.074	1.154	5.823	5.8×10^{-09}	13	4.83×10^{-02}	
X	rs5954362	140673423	<i>SPANXA1</i>	C	G	0.241	1.0310^{-09}	---	0.142	1.069	0.972	1.175	1.366	1.72×10^{-01}	0.896	0.829	0.967	-2.807	5.0×10^{-03}	7	4.18×10^{-10}	

*Loci previously identified as associated with AAA.

Online Table VIII: Sensitivity analysis comparing results from the combined GWAS meta-analysis and validation studies using a fixed effects model with a random-effects model. Results for loci surpassing the threshold for genome-wide significance are shown in bold. *Loci previously identified as associated with AAA

Chr	SNP	Position	Gene	Minor allele	Other allele	MAF	df	HetPVal	I ²	Fixed effects model		Random effects model	
										OR (95% CI)	P-value	OR (95% CI)	P-value
1*	rs602633	109821511	Near <i>PSRC1 CELSR2 SORT1</i>	T	G	0.199	13	7.60x10 ⁻⁰³	54.5	0.879 (0.842 - 0.918)	6.58x10⁻⁰⁹	0.881 (0.822 - 0.943)	3.18x10⁻⁹
1*	rs12133641	154428283	<i>IL6R</i>	A	G								
1	rs4129267 (proxy)	154426264	<i>IL6R</i>	T	C	0.370	13	0.478	0.0	0.876 (0.846 - 0.908)	4.76x10⁻¹³	0.876 (0.846 - 0.908)	1.03x10⁻¹²
1	rs1795061	214409280	near <i>SMYD2</i>	T	C	0.336	13	1.14x10 ⁻⁰³	61.9	1.131 (1.090 - 1.174)	8.80x10⁻¹¹	1.142 (1.07 - 1.218)	3.47x10⁻¹²
2	rs13382862	20882449	near <i>C2orf43</i> and <i>GDF7</i>	A	G	0.341	13	8.01x10 ⁻⁰²	37.1	0.913 (0.880 - 0.947)	1.3x10 ⁻⁰⁶	0.921 (0.877 - 0.968)	2.05x10 ⁻⁶
4	rs10029392	5616048	<i>EVC2</i>	T	G	0.052	13	6.51x10 ⁻⁰⁴	63.6	1.107 (1.022 - 1.198)	1.25x10 ⁻⁰²	1.120 (0.973 - 1.289)	1.88x10 ⁻⁴
5	rs12659791	74757758	<i>COL4A3BP</i>	T	C	0.159	13	1.69x10 ⁻⁰²	50.1	1.098 (1.046 - 1.153)	1.8x10 ⁻⁰⁴	1.071 (0.993 - 1.156)	8.18x10 ⁻⁶
6	rs3176334	36648364	<i>CDKN1A</i>	T	C								
6	rs733590 (proxy)	36645203	<i>CDKN1A</i>	T	C	0.367	13	0.183	25.2	1.070 (1.031 - 1.11)	3.33x10 ⁻⁰⁴	1.064 (1.017 - 1.112)	5.06x10 ⁻⁴
9*	rs10757274	22096055	<i>CDKN2BAS1/ANRIL</i>	A	G	0.351	13	5.94x10 ⁻⁰³	55.6	0.806 (0.778 - 0.834)	1.54x10⁻³³	0.797 (0.753 - 0.843)	1.21x10⁻³³
9*	rs10985349	124425243	<i>DAB2IP</i>	T	C	0.462	13	3.52x10 ⁻⁰¹	9.2	1.171 (1.118 - 1.226)	2.4x10⁻¹¹	1.174 (1.117 - 1.233)	4.47x10⁻¹¹
12*	rs1385526	57532749	<i>LRP1</i>	C	G	0.195	13	9.38x10 ⁻⁰³	53.4	0.910 (0.877 - 0.944)	6.4x10 ⁻⁰⁷	0.930 (0.877 - 0.986)	6.541x10 ⁻⁸
13	rs9316871	22861921	<i>LINC00540</i>	A	G	0.328	13	0.488	0.0	0.873 (0.837 - 0.911)	4.8x10⁻¹⁰	0.873 (0.837 - 0.911)	9.98x10⁻¹⁰
15	rs17189674	89040591	<i>DET1</i>	A	G	0.201	13	1.71x10 ⁻⁰²	50.0	1.118 (1.058 - 1.181)	7.59x10 ⁻⁰⁵	1.120 (1.031 - 1.217)	1.26x10 ⁻⁵
19*	rs6511720	11202306	<i>LDLR</i>	T	G	0.122	13	1.53x10 ⁻⁰³	61.0	0.804 (0.759 - 0.851)	7.9x10⁻¹⁴	0.795 (0.72 - 0.878)	7.19x10⁻¹⁵
19	rs12980543	56096197	near <i>ZNF579</i>	A	G								
19	rs11084402 (proxy)	56093365	near <i>ZNF579</i>	T	C	0.206	13	0.019	49.4	1.095 (1.048 - 1.144)	5.1x10 ⁻⁰⁵	1.101 (1.031 - 1.176)	2.51x10 ⁻⁵
20	rs6516091	6050622	near <i>FERMT1</i>	A	G	0.135	13	4.01x10 ⁻⁰⁵	70.0	1.131 (1.074 - 1.19)	2.9x10 ⁻⁰⁶	1.088 (0.983 - 1.203)	6.58x10⁻¹⁰
20	rs58749629	44571317	near <i>PCIF1 ZNF335 MMP9</i>	A	G								
20	rs3827066 (proxy)	44586023	near <i>PCIF1 ZNF335 MMP9</i>	T	C	0.179	13	0.552	0.0	1.223 (1.168 - 1.281)	2.1x10⁻¹⁷	1.223 (1.168 - 1.281)	6.12x10⁻¹⁷
21	rs2836411	39819830	<i>ERG</i>	T	C	0.369	13	4.83x10 ⁻⁰²	42.2	1.113 (1.074 - 1.154)	5.8x10⁻⁰⁹	1.112 (1.057 - 1.17)	7.07x10⁻⁹
X	rs5954362	140673423	<i>SPANXA1</i>	C	G	0.241	7	4.18x10 ⁻¹⁰	87.9	0.896 (0.829 - 0.967)	5.0x10 ⁻⁰³	0.857 (0.672 - 1.092)	3.08x10⁻¹¹

Online Figure II: Regional association plots for previously reported AAA risk loci.



Five of the 6 previously identified AAA loci at 1p13.3 (*SORT1*), 1q21.3 (*IL6R*), 9p21 (*CDKN2BAS1/ANRIL*), 9q33 (*DAB2IP*) and 19p13.2 (*LDLR*) were replicated in this meta-GWAS and validation analysis. Although the previously reported¹ 12q13 (*LRP1*) locus (lower right panel) reached the discovery threshold ($P=1.1 \times 10^{-9}$), it fell below the genome-wide threshold when combined with the validation cohorts (combined $P=6.4 \times 10^{-7}$).

SNP LOOKUP IN GWAS FOR OTHER TRAITS ASSOCIATED WITH AAA

Data for AAA associated SNPs (those passing the genome-wide association threshold after combination of the results of the meta-analysis and validation studies) were obtained from GWAS datasets for other traits associated with AAA to determine if the associations were unique to AAA or related to generalized CVD (**Online Table IX and Figure 3**). All results were from meta-analyses of multiple primary GWAS datasets for each trait. Summary results for each AAA associated SNP (P-value and effect size) were extracted. Results for type 2 diabetes³⁴ were obtained from the DIAGRAM consortium (<http://www.diagram-consortium.org/index.html>), CAD data from the CARDIoGRAM consortium³⁵ (www.CARDIOGRAMPLUSC4D.ORG), lipid trait data from the Global Lipids Genetics Consortium³⁶ (<http://csg.sph.umich.edu/abecasis/public/lipids2013>) and blood pressure data from the International Consortium for Blood Pressure³⁷ (http://www.ncbi.nlm.nih.gov/projects/gap/cgi-bin/study.cgi?study_id=phs000585.v1.p1).

Online Table IX: Results of lookup of AAA associated SNPs in GWAS of other cardiovascular traits (See also below). CAD: Coronary Artery Disease; HDL: High-density Lipoprotein; LDL: Low-density Lipoprotein; TG: Triglyceride; DBP: Diastolic Blood Pressure; SBP: Systolic Blood Pressure.

	Chr	Position	SNP	Locus	Gene(s)	AAA risk allele	OR (95%CI)			P					
							n cases	n controls							
Type 2 Diabetes	1	109821511	rs602633	1p13.3	CELSR2/SORT1	T	1.05 (1.01 - 1.1)	9580	53810	0.025					
	1	154426264	rs4129267	1q21.3	IL6R	T	0.96 (0.93 - 1.00)	12171	56862	0.037					
	9	22096055	rs10757274	9p21	ANRIL	A	0.96 (0.94 - 1.00)	12171	56862	0.041					
	9	124425243	rs10985349	9q33.2	DAB2IP	T	1.03 (0.98 - 1.07)	12171	56862	0.210					
	19	11202306	rs6511720	19p13.2	LDLR	T	1.02 (0.96 - 1.10)	8558	52735	0.480					
CAD	1	109821511	rs602633	1p13.3	CELSR2/SORT1	T	0.90 (0.87 - 0.93)	20375	61324	2.16x10 ⁻⁹					
	1	154426264	rs4129267	1q21.3	IL6R	T	0.95 (0.93 - 0.98)	20784	58718	0.001					
	9	22096055	rs10757274	9p21	ANRIL	A	0.78 (0.74 - 0.82)	21932	62260	1.44x10 ⁻²²					
	9	124425243	rs10985349	9q33.2	DAB2IP	T	1.04 (1.00 - 1.09)	14133	36016	0.036					
	19	11202306	rs6511720	19p13.2	LDLR	T	0.88 (0.83 - 0.94)	8948	47471	1.61x10 ⁻⁰⁴					
Lipid traits	1	109821511	rs602633	1p13.3	CELSR2/SORT1	T	HDL beta (SE)	n	P	LDL beta (SE)	n	P	TG beta (SE)	n	P
	1	154426264	rs4129267	1q21.3	IL6R	T	0.0073 (0.0051)	94311	0.077	-0.0066 (0.0057)	89888	0.230	-0.0129 (0.005)	91013	0.032
	9	22096055	rs10757274	9p21	ANRIL	A	0.0328 (0.0041)	185599	3.50x10 ⁻¹⁴	-0.1591 (0.0044)	171593	1.50x10 ⁻²⁶¹	-0.0121 (0.004)	176361	0.003
	9	124425243	rs10985349	9q33.2	DAB2IP	T	-0.0047 (0.0048)	92706	0.371	0.0036 (0.0051)	83064	0.524	0.0012 (0.0047)	86702	0.907
	19	11202306	rs6511720	19p13.2	LDLR	T	-0.006 (0.0068)	86409	0.435	0.0067 (0.0075)	82099	0.557	-0.0039 (0.0066)	83111	0.944
Blood Pressure	1	109821511	rs602633	1p13.3	CELSR2/SORT1	T	DBP beta (SE)	n	P	SBP beta (SE)	n	P			
	1	154426264	rs4129267	1q21.3	IL6R	T	0.0704 (0.0665)	66347	0.289	-0.0568 (0.1044)	66352	0.586			
	9	22096055	rs10757274	9p21	ANRIL	A	0.0257 (0.0748)	66774	0.731	0.0100 (0.1180)	66781	0.932			
	9	124425243	rs10985349	9q33.2	DAB2IP	T	NA	NA	NA	NA	NA				
	19	11202306	rs6511720	19p13.2	LDLR	T	-0.0020 (0.0807)	58126	0.980	0.1229 (0.1283)	58171	0.338			
Type 2 Diabetes	1	214409280	rs1795061	1q32.3	near SMYD2	T	OR (95%CI)	n cases	n controls	P					
	13	22861921	rs9316871	13q12.11	LINC00540	G	1.04 (1.00 - 1.08)	9580	53810	0.044					
	20	44586023	rs3827066	20q13.12	Near MMP9/ZNF335	T	1 (0.96 - 1.04)	11902	53152	0.940					
	21	39819830	rs2836411	21q22.2	ERG	T	1.00 (0.95 - 1.06)	9580	53810	0.890					
	21	39819830	rs2836411	21q22.2	ERG	T	1.01 (0.97 - 1.04)	12171	56862	0.720					
CAD	1	214409280	rs1795061	1q32.3	near SMYD2	T	OR	n cases	n controls	P					
	13	22861921	rs9316871	13q12.11	LINC00540	G	0.99 (0.96 - 1.02)	20441	61399	0.533					
	20	44586023	rs3827066	20q13.12	Near MMP9/ZNF335	T	1.00 (0.97 - 1.03)	21588	59365	0.974					
	21	39819830	rs2836411	21q22.2	ERG	T	1.07 (1.03 - 1.12)	19108	59177	5.48x10 ⁻⁰⁴					
	21	39819830	rs2836411	21q22.2	ERG	T	1.02 (0.99 - 1.05)	21424	59122	0.205					
Lipid traits	1	214409280	rs1795061	1q32.3	near SMYD2	T	HDL beta (SE)	n	P	LDL beta (SE)	n	P	TG beta (SE)	n	P
	13	22861921	rs9316871	13q12.11	LINC00540	G	0.0075 (0.0054)	94311	0.119	0.0023 (0.0059)	89888	0.572	-0.0047 (0.0052)	91013	0.501
	20	44586023	rs3827066	20q13.12	Near MMP9/ZNF335	T	-0.0013 (0.0058)	90317	0.883	0.006 (0.0063)	85936	0.417	0.0018 (0.0058)	86976	0.563
	21	39819830	rs2836411	21q22.2	ERG	T	0.0208 (0.0048)	185539	2.96x10 ⁻⁰⁵	-0.0092 (0.0052)	171507	0.103	-0.0156 (0.0047)	176203	0.003
	21	39819830	rs2836411	21q22.2	ERG	T	-0.0047 (0.005)	92801	0.402	-0.0082 (0.0055)	88414	0.269	0.0054 (0.0049)	89466	0.566
Blood pressure	1	214409280	rs1795061	1q32.3	near SMYD2	T	DBP beta (SE)	n	P	SBP beta (SE)	n	P			
	13	22861921	rs9316871	13q12.11	LINC00540	G	0.0320 (0.0691)	63232	0.643	0.0047 (0.1084)	63243	0.965			
	20	44586023	rs3827066	20q13.12	Near MMP9/ZNF335	T	0.0429 (0.0734)	69617	0.559	-0.0201 (0.1163)	69623	0.863			
	21	39819830	rs2836411	21q22.2	ERG	T	-0.0397 (0.0878)	59823	0.651	-0.0276 (0.1380)	59806	0.842			
	21	39819830	rs2836411	21q22.2	ERG	T	0.1536 (0.0650)	67634	0.018	0.0487 (0.1024)	67631	0.635			

SEARCH FOR OTHER ASSOCIATED TRAITS AND DISEASES USING GWAS DATABASES

The Phenotype-Genotype Integrator³⁸ (<http://www.ncbi.nlm.nih.gov/gap/phegeni#GenomeView>) and the GWAS catalog (<http://www.gwascentral.org/index>) were searched for diseases and traits associated with the lead SNPs at the AAA loci. In addition, we searched NHLBI GRASP catalog (GRASP v2.0; <http://grasp.nhlbi.nih.gov/Overview.aspx>)^{39, 40} to find any further associations. The results obtained using the Phenotype-Genotype Integrator are shown in **Online Table X**, the search results from the GWAS catalog are presented in **Online Table XI**, and those using GRASP in **Online Table XII**.

PheGenI includes results from the NHGRI/EBI catalog. GRASP (Genome-Wide Repository of Associations Between SNPs and Phenotypes) is the largest GWAS results database in terms of coverage. It includes all available genetic association results from papers, their supplements and web-based content meeting the following guidelines:

- All associations with $P < 0.05$ from GWAS defined as $\geq 25,000$ markers tested for 1 or more traits.
- Study exclusion criteria: CNV-only studies, replication/follow-up studies testing $< 25K$ markers, non-human only studies, article not in English, gene-environment or gene-gene GWAS where single SNP main effects are not given, linkage only studies, aCGH/LOH only studies, heterozygosity/homozygosity (genome-wide or long run) studies, studies only presenting gene-based or pathway-based results, simulation-only studies, studies which we judge as redundant with prior studies since they do not provide significant inclusion of new samples or exposure of new results (e.g., many methodological papers on the WTCCC and FHS GWAS).

Online Table X: Results from the GWAS database search using the tool called Phenotype-Genotype Integrator (<http://www.ncbi.nlm.nih.gov/gap/phegeni#GenomeView>). All lead SNPs at the AAA loci were used for the search, but only two of the SNPs (rs4129267 and rs6511720) had hits.

Chr	Location	SNP	Gene	Trait	Location in gene	P-Value	Source	PubMed ID
1	154426264	rs4129267	IL6R	Receptors, Interleukin-6	intron	2.00×10^{-57}	NHGRI	18464913
				C-Reactive Protein	intron	2.00×10^{-48}	NHGRI	21300955
				Asthma	intron	2.00×10^{-08}	NHGRI	21907864
				Maximal Midexpiratory Flow Rate	intron	7.00×10^{-06}	NHGRI	17903307
19	11202306	rs6511720	LDLR	Cholesterol, LDL	intron	4.00×10^{-117}	NHGRI	20686565
				Cholesterol	intron	7.00×10^{-97}	NHGRI	20686565
				Cholesterol, LDL	intron	2.00×10^{-51}	NHGRI	18193044
				Cholesterol, LDL	intron	2.00×10^{-26}	NHGRI	19060906
				Cholesterol, LDL	intron	4.00×10^{-26}	NHGRI	18193043
				1-Alkyl-2-acetylglycerophosphocholine Esterase	intron	3.00×10^{-11}	NHGRI	22003152
				Cholesterol, LDL	intron	5.00×10^{-11}	NHGRI	21943158
Atherosclerosis	intron	1.00×10^{-07}	NHGRI	21909108				

Online Table XI: Results of the dbGAP SNP lookup using the GWAS Catalog available at <http://www.gwascentral.org/index>. The total number of results in the GWAS Catalog (“n results in dbGAP”) and the number of associations with $P < 1 \times 10^{-3}$ (column labelled “n $P < 1 \times 10^{-3}$ ”) are shown. Details on the associations with $P < 1 \times 10^{-3}$ for each SNP are described.

SNP	Chromosome	Position	Gene(s)	n results in dbGAP	n $P < 1 \times 10^{-3}$	P-value	Phenotype	Study
rs602633	1	109821511	<i>PSRC1-CELSR2-SORT1</i>	16	3	4.80×10^{-14}	LDL cholesterol levels	Meta-analysis of plasma lipid concentrations (HGVST214)
						5.70×10^{-14}	Serum LDL cholesterol levels	GWAS of LDL-cholesterol concentrations (HGVST227)
						0.0001862	Height	GWAS of height (HGVST634)
rs4129267	1	154426264	<i>IL6R</i>	77	6	2.00×10^{-37}	Protein quantitative trait loci	GWAS of protein quantitative trait loci (HGVST264)
						2.00×10^{-48}	C-reactive protein level	GWAS of C-reactive protein levels (HGVST728)
						2.00×10^{-68}	Asthma	Unspecified analysis (HGVRS1753)
						7.39×10^{-66}	Percent predicted forced expiratory flow	GWAS of pulmonary function phenotypes in the Framingham Heart Study (HGVST212)
						1.92×10^{-65}	Asthma; Total asthma sample fixed effects (HGVRS1509)	GWAS of asthma (HGVST631)
0.00014411	Asthma; Total asthma sample random effects (HGVRS1257)	GWAS of asthma (HGVST631)						
rs1795061	1	214409280	<i>SMYD2</i>	19	0			
rs10757274	9	22096055	<i>ANRIL</i>	6	2	8.00×10^{-45}	Coronary heart disease	GWAS of Coronary heart disease (HGVST1380)
						3.70×10^{-56}	Coronary heart disease	GWAS of Coronary heart disease (HGVST57)
rs10985349	9	124425243	<i>DAB2IP</i>	19	0			
rs9316871	13	22861921	<i>LINC00540</i>	101	2	0.0007248	Schizophrenia	GWAS of schizophrenia (HGVST903)
						0.00084	Crohn's disease	GWAS of Crohn's disease (HGVST680)
rs6511720	19	11202306	<i>LDLR</i>	57	14	2×10^{-51}	LDL cholesterol	Meta-analysis of lipid concentrations (HGVST203)
						4.2×10^{-26}	LDL cholesterol levels	Meta-analysis of plasma lipid concentrations (HGVST214)
						2×10^{-25}	LDL cholesterol	GWAS of HDL cholesterol, triglycerides and LDL cholesterol (HGVST235)
						0.00026672	Serum cholesterol	GWAS of serum cholesterol levels in a British population (HGVST312)
						0.0005127	Height	GWAS of height (HGVST634)
						0.0000001	Carotid intima media thickness, plaque	GWAS of carotid intima media thickness (HGVST923)
						3×10^{-11}	Lipoprotein-associated phospholipase A2 activity and mass (Activity concentrations)	GWAS of lipoprotein-associated phospholipase A2 activity and mass (HGVST931)
						5×10^{-11}	Cardiovascular disease risk factors (LDL)	GWAS of cardiovascular disease risk factors (HGVST956)
						0.000000004	Metabolite levels	GWAS of Metabolite levels (HGVST1409)
rs3827066	20	44586023	<i>PCIF1-ZNF335-MMP9</i>	15	0	2×10^{-31}	Lipid metabolism phenotypes (LDL-C.assay, whole)	GWAS of Lipid metabolism phenotypes (HGVST1667)
						3×10^{-18}	Lipid metabolism phenotypes (APOB.assay, fasting)	GWAS of Lipid metabolism phenotypes (HGVST1667)
						1×10^{-25}	Lipid metabolism phenotypes (LDL-C.assay, fasting)	GWAS of Lipid metabolism phenotypes (HGVST1667)
						5×10^{-25}	Lipid metabolism phenotypes (APOB.assay, whole)	GWAS of Lipid metabolism phenotypes (HGVST1667)
rs2836411	21	39819830	<i>ERG</i>	94	1	0.0009289	Height	GWAS of height (HGVST634)

Online Table XII: Previously reported associations of the lead SNPs from AAA loci identified from an analysis of GRASP v2.0 (<http://grasp.nhlbi.nih.gov/Overview.aspx>). The Phenotypes, P values and sample sizes are those reported in the original publication that is referenced under 'Phenotype' in the table. The SNP, chromosome, position and genes are those from this analysis that were entered into GRASP v2.0 as a query. This table spans 3 pages.

SNP	CHR	Position	Gene	Phenotype	P value	Ancestry	Total	Total Replication	Total				
rs602633	1	109821511	<i>PSRC1-CELSR2-SORT1</i>	LDL cholesterol ⁴¹	4.80x10 ⁻¹⁴	European	8656	11399	20055				
				LDL cholesterol in serum ⁴²	5.70x10 ⁻¹⁴	European	11685	5036	16721				
				LDL cholesterol ⁴³	7.60x10 ⁻⁴¹	European	19840	20623	40463				
				LDL cholesterol ⁴⁴	3.10x10 ⁻⁰⁸	European	5059	0	5059				
				APOB (apolipoprotein B) ⁴⁴	2.20x10 ⁻⁰⁷	European	5059	0	5059				
				Coronary artery disease (CAD) ⁴⁵	9.00x10 ⁻⁰⁸	Unspecified	8319	10707	19026				
				LDL cholesterol change with statins ⁴⁶	8.40x10 ⁻⁰⁸	European	3928	0	3928				
				LDL cholesterol ⁴⁶	8.40x10 ⁻⁰⁸	European	3928	0	3928				
				Total cholesterol change with statins ⁴⁶	5.50x10 ⁻⁰⁶	European	3928	0	3928				
				Total cholesterol ⁴⁶	5.50x10 ⁻⁰⁶	European	3928	0	3928				
				LDL cholesterol ⁴⁷	4.90x10 ⁻¹⁶	Mixed	100184	39875	140059				
				Total cholesterol ⁴⁷	3.90x10 ⁻¹⁷	Mixed	100184	39875	140059				
				HDL cholesterol ⁴⁷	5.20x10 ⁻⁰⁷	Mixed	100184	39875	140059				
				Height ⁴⁸	1.90x10 ⁻⁰⁴	European	133653	50074	183727				
				LDL cholesterol ⁴⁹	2.90x10 ⁻⁰⁶	African	8090	8849	16939				
				LDL cholesterol ⁵⁰	1.20x10 ⁻²²	European	11683	0	11683				
				LDL cholesterol (baseline) ⁵¹	5.00x10 ⁻⁰⁸	European	5244	0	5244				
				Lp-PLA2 activity ⁵²	1.40x10 ⁻¹⁶	European	13664	0	13664				
				Total cholesterol ⁵³	5.90x10 ⁻⁶⁵	European	66240	25282	91522				
				LDL cholesterol ⁵³	6.90x10 ⁻⁶⁵	European	66240	25282	91522				
				HDL cholesterol ⁵³	1.30x10 ⁻⁰⁷	European	66240	25282	91522				
				Coronary artery disease (CAD) ⁵⁴	4.70x10 ⁻²⁶	Mixed	194427	15613	210040				
				Coronary artery disease (CAD) age <=50 ⁵⁴	2.80x10 ⁻²⁰	Mixed	194427	15613	210040				
				Coronary artery disease (CAD) (males) ⁵⁴	1.30x10 ⁻¹⁸	Mixed	194427	15613	210040				
				Coronary artery disease (CAD) with myocardial infarction (MI) ⁵⁴	2.20x10 ⁻¹⁶	Mixed	194427	15613	210040				
				Coronary artery disease (CAD) age >50 ⁵⁴	5.00x10 ⁻⁰⁸	Mixed	194427	15613	210040				
				Coronary artery disease (CAD) (females) ⁵⁴	3.40x10 ⁻⁰⁵	Mixed	194427	15613	210040				
				rs4129267	1	154426264	<i>IL6R</i>	Lung function, predicted forced expiratory flow (FEF) ⁵⁵	7.40x10 ⁻⁰⁶	European	1222	0	1222
								Plasma C-reactive protein (female) ⁵⁶	2.00x10 ⁻⁰⁸	European	6345	0	6345
								Soluble IL6R (sIL6R) ⁵⁷	2.50x10 ⁻⁷⁶	European	1200	0	1200
C-reactive protein [log (mg/l)] ⁵⁸	4.40x10 ⁻⁰⁴	European	4763					0	4763				
Plasma fibrinogen (females) ⁵⁹	1.80x10 ⁻¹¹	European	17686					0	17686				
Asthma ⁶⁰	1.90x10 ⁻⁰⁵	European	26475					0	26475				
Fibrinogen ⁶¹	8.40x10 ⁻⁰⁷	Mixed	30291					0	30291				
C-reactive protein (CRP) ⁶²	2.10x10 ⁻⁴⁸	European	66185					16540	82725				
Asthma ⁶⁰	2.40x10 ⁻⁰⁸	European	7197					57800	64997				
Interleukin-6 (IL-6) levels ⁶³	2.40x10 ⁻⁰⁸	European	4694					1392	6086				
C-reactive protein (CRP) ⁶⁴	1.80x10 ⁻⁰⁵	Mixed	11828					11991	23819				
Coronary artery disease (CAD) ⁵⁴	1.70x10 ⁻⁰⁸	Mixed	194427					15613	210040				
Interleukin-6 (IL-6) levels ⁶⁵	1.60x10 ⁻²¹	European	8356					0	8356				
C-reactive protein (CRP) ⁶⁵	8.80x10 ⁻¹²	European	8356					0	8356				
rs1795061	1	214409280	<i>SMYD2</i>					None					
rs10757274	9	22096055	<i>ANRIL</i>	Coronary heart disease (CHD) ⁶⁶	3.70x10 ⁻⁰⁶	Mixed	634	28047	28681				
				Coronary artery disease (CAD) ⁴⁵	7.00x10 ⁻¹¹	Unspecified	8319	10707	19026				
				Coronary artery disease (CAD) ⁶⁷	7.60x10 ⁻⁴⁵	Asian	6534	26932	33466				
				Coronary artery calcification (CAC) ⁶⁸	8.00x10 ⁻¹⁰	European	4518	0	4518				

SNP	CHR	Position	Gene	Phenotype	P value	Ancestry	Total	Total Replication	Total
				Coronary artery calcification (CAC) ⁶⁹	6.80x10 ⁻⁸⁸	Mixed	1509	3344	4853
rs10985349	9	124425243	DAB2IP	None					
rs9316871	13	22861921	LINC00540	Body mass index (BMI) ⁷⁰	6.90x10 ⁻⁰⁴	European	5217	0	5217
				Schizophrenia ⁷¹	9.40x10 ⁻⁰⁵	European	16161	31375	47536
				HDL cholesterol change with statins ⁴⁶	7.70x10 ⁻⁰⁴	European	3928	0	3928
rs6511720	19	11202306	LDLR	LDL cholesterol ⁴¹	4.20x10 ⁻²⁶	European	8656	11399	20055
				LDL cholesterol ⁷²	2.00x10 ⁻⁵¹	Mixed	2758	22803	25561
				LDL cholesterol ⁴³	5.20x10 ⁻³⁰	European	19840	20623	40463
				LDL cholesterol exam 1 values ⁴³	3.00x10 ⁻⁰⁴	European	19840	20623	40463
				Total cholesterol (exam 1) ⁴³	3.40x10 ⁻⁰⁴	European	19840	20623	40463
				LDL cholesterol (mmol/l) ³⁸	1.50x10 ⁻⁰⁹	European	4763	0	4763
				Total cholesterol ⁷³	6.80x10 ⁻¹⁸	European	22562	0	22562
				APOB (apolipoprotein B) ⁷⁴	7.00x10 ⁻¹⁸	European	6382	970	7352
				LDL cholesterol ⁷⁴	5.20x10 ⁻¹⁵	European	6382	970	7352
				LDL cholesterol ⁴⁴	7.30x10 ⁻²⁴	European	5059	0	5059
				APOB (apolipoprotein B) ⁴⁴	6.80x10 ⁻¹⁵	European	5059	0	5059
				LDL cholesterol lipoprotein fraction concentration ⁷⁵	2.30x10 ⁻³¹	European/Unspecified	17296	9472	26768
				LDL cholesterol lipoprotein fraction concentration in fasting sample ⁷⁵	1.50x10 ⁻²⁵	European/Unspecified	17296	9472	26768
				APOB assay lipoprotein fraction concentration ⁷⁵	4.80x10 ⁻²⁵	European/Unspecified	17296	9472	26768
				APOB assay lipoprotein fraction concentration in fasting sample ⁷⁵	2.80x10 ⁻¹⁸	European/Unspecified	17296	9472	26768
				LDL cholesterol large lipoprotein fraction concentration ⁷⁵	4.30x10 ⁻¹⁵	European/Unspecified	17296	9472	26768
				LDL cholesterol total lipoprotein fraction concentration ⁷⁵	1.90x10 ⁻¹³	European/Unspecified	17296	9472	26768
				LDL cholesterol large lipoprotein fraction concentration in fasting sample ⁷⁵	3.00x10 ⁻¹²	European/Unspecified	17296	9472	26768
				VLDL cholesterol small lipoprotein fraction concentration ⁷⁵	1.60x10 ⁻¹⁰	European/Unspecified	17296	9472	26768
				LDL cholesterol total lipoprotein fraction concentration in fasting sample ⁷⁵	2.10x10 ⁻⁰⁹	European/Unspecified	17296	9472	26768
				VLDL cholesterol small lipoprotein fraction concentration in fasting sample ⁷⁵	1.90x10 ⁻⁰⁸	European/Unspecified	17296	9472	26768
				LDL cholesterol change with statins ⁴⁶	2.80x10 ⁻⁰⁵	European	3928	0	3928
				LDL cholesterol ⁴⁶	2.80x10 ⁻⁰⁵	European	3928	0	3928
				LDL cholesterol ⁴⁷	8.60x10 ⁻¹²	Mixed	100184	39875	140059
				Total cholesterol ⁴⁷	1.70x10 ⁻¹⁰	Mixed	100184	39875	140059
				Coronary artery disease (CAD) ⁴⁷	5.00x10 ⁻⁰⁹	Mixed	100184	39875	140059
				Height ⁴⁸	5.10x10 ⁻⁰⁴	European	133653	50074	183727
				LDL cholesterol ⁴⁹	2.00x10 ⁻⁵¹	African	8090	8849	16939
				Presence of carotid artery plaque ⁷⁶	8.20x10 ⁻⁰⁸	European	31211	11273	42484
				Carotid artery plaque ⁷⁶	1.00x10 ⁻⁰⁷	European	31211	11273	42484
				Coronary artery disease (CAD) ⁷⁶	2.00x10 ⁻⁰⁴	European	31211	11273	42484
				LDL cholesterol ⁵⁰	5.00x10 ⁻¹¹	European	11683	0	11683
				Coronary artery disease (CAD) ⁷⁷	1.10x10 ⁻⁰⁸	Mixed	50587	57594	108181
				LDL cholesterol (baseline) ⁵¹	5.20x10 ⁻¹⁵	European	5244	0	5244
				Lp-PLA2 activity ⁵²	2.60x10 ⁻¹¹	European	13664	0	13664
				Lp-PLA2 mass ⁵²	5.50x10 ⁻⁰⁵	European	13664	0	13664
				Metabolic syndrome domains (Atherogenic Dyslipidemia - PC1) ⁷⁸	5.20x10 ⁻³⁰	Mixed	25755	0	25755
				Metabolic syndrome domains (Multivariate analysis) ⁷⁸	8.30x10 ⁻²⁸	Mixed	25755	0	25755
				LDL cholesterol ⁷⁹	1.40x10 ⁻⁴⁹	Mixed	44957	0	44957
				LDL cholesterol (female) ⁷⁹	7.50x10 ⁻²⁹	Mixed	44957	0	44957
				LDL cholesterol (male) ⁷⁹	3.10x10 ⁻²⁵	Mixed	44957	0	44957
				LDL cholesterol ⁵³	1.30x10 ⁻⁷⁹	European	66240	25282	91522
				Total cholesterol ⁵³	1.70x10 ⁻⁷¹	European	66240	25282	91522
				APOB (apolipoprotein B) ⁸⁰	4.10x10 ⁻²⁷	European	3895	14810	18705
				LDL cholesterol ⁸⁰	3.80x10 ⁻²⁵	European	3895	14810	18705
				APOB (apolipoprotein B) response after 40mg daily simvastatin treatment ⁸⁰	1.40x10 ⁻⁰⁷	European	3895	14810	18705
				LDL cholesterol response after 40mg daily simvastatin treatment ⁸⁰	4.30x10 ⁻⁰⁷	European	3895	14810	18705
				LDL cholesterol ⁸¹	2.60x10 ⁻¹⁷	Mixed	9813	7000	16813
				Total cholesterol ⁸¹	1.80x10 ⁻¹⁶	Mixed	9813	7000	16813

SNP	CHR	Position	Gene	Phenotype	P value	Ancestry	Total	Total Replication	Total
				Total cholesterol ⁵²	4.40x10 ⁻⁵⁴	Hispanic	2240	2121	4361
rs3827066	20	44586023	<i>PCIF1-ZNF335-MMP9</i>	Coronary artery disease (CAD) ⁵⁴	1.40x10 ⁻⁰⁵	Mixed	194427	15613	210040
rs2836411	21	39819830	<i>ERG</i>	None					

PheWAS ANALYSIS

We performed a phenome-wide association study (PheWAS)^{83, 84} exploring the association between the 9 AAA-associated SNPs and an extensive group of diagnoses to identify novel associations and uncover potential pleiotropy. For the PheWAS we used data from the electronic Medical Records and Genomics (eMERGE) Network²³ derived from 7 adult sites with a total of 27,077 unrelated patients of European ancestry above 19 years of age. We divided these samples into two datasets by proportional sampling based on eMERGE site, sex, and genotyping platform (13,559 and 13,518 individuals in sets 1 and 2, respectively). We calculated associations between the 9 AAA-associated SNPs and case or control status based on the extensive set of ICD-9 diagnoses, where for a specific diagnosis, individuals with the diagnosis are considered cases. Associations were adjusted for sex, site, genotyping platform and the first 3 principal components to account for global ancestry. We considered the identification of previously known associations, such as rs602633 associated with hyperglyceridemia and rs10757274 associated with CAD, to be indications that the PheWAS approach was robust. The PheWAS results are presented in **Online Table XIII**.

Online Table XIII: PheWAS Results

Chr	Position	SNP	Locus	Gene(s)	PheWAS associations	ICD-9 Description	PheWAS dataset 1			PheWAS dataset 2		
							n cases/controls	Beta(SE)	P	n cases/controls	Beta(SE)	P
1	214409280	rs1795061	1q32.3	near <i>SMYD2</i>	None							
1	154426264	rs4129267	1q21.3	<i>IL6R</i>	None							
1	109821511	rs602633	1p13.3	<i>CELSR2/SORT1</i>	6	Other and unspecified hyperlipidemia	5467/5722	-0.187 (0.035)	7.86171x10 ⁻⁰⁸	5539/5645	-0.151 (0.035)	1.54x10 ⁻⁰⁵
						Other and unspecified hyperlipidemia	5467/5722	-0.187 (0.0345)	7.86171x10 ⁻⁰⁸	2506/8687	-0.114 (0.042)	0.006402
						Pure hypercholesterolemia	2436/8780	-0.116 (0.042)	0.0055185	5539/5645	-0.151 (0.035)	1.54x10 ⁻⁰⁵
						Pure hypercholesterolemia	2436/8780	-0.116 (0.042)	0.0055185	2506/8687	-0.114 (0.042)	0.006402
						Mixed hyperlipidemia	1310/11032	-0.141 (0.054)	0.0083104	5539/5645	-0.151 (0.035)	1.54x10 ⁻⁰⁵
						Mixed hyperlipidemia	1310/11032	-0.141 (0.054)	0.0083104	2506/8687	-0.114 (0.042)	0.006402
9	22096055	rs10757274	9p21	<i>ANRIL</i>	2	Coronary atherosclerosis of native coronary artery	2332/9886	0.210 (0.034)	3.70081x10 ⁻¹⁰	2141/9972	0.158 (0.035)	6.9x10 ⁻⁰⁶
						Coronary atherosclerosis of unspecified type of vessel, native or graft	2167/10004	0.202 (0.035)	4.61186x10 ⁻⁰⁹	2141/9972	0.158 (0.035)	6.9x10 ⁻⁰⁶
9	124425243	rs10985349	9q33.2	<i>DAB2IP</i>	None							
13	22861921	rs9316871	13q12.11	<i>LINC00540</i>	None							
19	11202306	rs6511720	19p13.2	<i>LDLR</i>	4	Other and unspecified hyperlipidemia	5638/5878	-0.201 (0.046)	1.05931x10 ⁻⁰⁵	2583/8928	-0.218 (0.055)	4.95x10 ⁻⁰⁵
						Other and unspecified hyperlipidemia	5638/5878	-0.201 (0.046)	1.05931x10 ⁻⁰⁵	5697/5803	-0.173 (0.045)	9.53x10 ⁻⁰⁵
						Pure hypercholesterolemia	2502/9017	-0.183 (0.056)	0.000948352	2583/8928	-0.218 (0.055)	4.95x10 ⁻⁰⁵
						Pure hypercholesterolemia	2502/9017	-0.183 (0.056)	0.000948352	5697/5803	-0.173 (0.045)	9.53x10 ⁻⁰⁵
20	44586023	rs3827066	20q13.12	Near <i>PCIF1/MMP9/ZNF335</i>	None							
21	39819830	rs2836411	21q22.2	<i>ERG</i>	None							

ANNOTATION OF AAA ASSOCIATED SNPs USING THE UCSC GENOME BROWSER

The 9 AAA-associated loci were manually annotated using the UCSC Genome Browser (<http://genome.ucsc.edu/cgi-bin/hgGateway>) on the hg19 human genome assembly. To annotate a gene, the SNP identification number (rs ID) was typed into the browser, and the genomic region centered on the SNP was examined. We noted genomic elements within 10 kbp of the SNP and on either side of the SNP. Within the browser, there were eleven main tracks that were used to annotate the SNP, which displayed gene locations, related literature, full-length public transcriptome data (mRNAs and ESTs), regulation, conservation, and repetitive elements. The results of this annotation are presented in **Online Table XIV**.

Gene Location

We used several UCSC Genome Browser tracks to determine whether a locus was exonic, intronic, or intergenic, as well as the identity and classification of the gene, if any, at the locus. One of the tracks used was the UCSC Known Genes track. This track displays information on genes and their location, including both protein-coding and non-coding RNA genes⁸⁵. Within this track, NCBI Reference Sequence (RefSeq) genes and GenBank genes were aligned to the genome (by the UCSC Genome Bioinformatics team) using the BLAST-like alignment tool (BLAT)⁸⁶⁻⁸⁸. In order to be included, genes needed a 98% alignment. The track also included gene models from the Consensus CDS (CCDS) project. Predicted genes from tRNA and mouse genes from Rfam with synteny to the human genome are also included in the track^{89, 90}. The track also reports whether the gene is coding or non-coding. In addition to using the NCBI RefSeq to search proteins, UniProt proteins are also reported⁹¹.

Another UCSC track that describes the location of coding and non-coding genes is the NCBI RefSeq track. This displays genes that were aligned to genome with at least a 96% match⁸⁸. We also used ENCODE Consortium's Gencode human gene catalog (v19)⁹². The track combines automatic annotations with manual and experimentally validated entries. Another track used to examine gene location is the Broad Institute lincRNA track. The long intergenic non-coding RNA (lincRNA) data were collected by RNA sequencing (RNA-seq)⁹³. In addition to lincRNAs, the track also displays transcripts of uncertain coding potential (TUCP). For each of these gene types, expression was displayed across 22 different cell and tissue types⁹⁴.

Related Literature

The loci were also annotated according to their relationship to other SNPs. The National Human Genome Research Institute (NHGRI) has a UCSC track of manually curated loci from published Genome-Wide Association Studies (GWAS)⁹⁵ with $P < 1.0 \times 10^{-5}$. This track was used to check independent previously reported disease or phenotype association of each SNP, and to see if the locus of interest fell within a "SNP cloud", which is an area with several SNPs all significantly associated with complementary or biologically similar quantitative traits.

mRNAs and ESTs

In addition to looking at genes, mRNAs and expressed sequence tags (ESTs) were examined. One track used was the human mRNA track. This is comprised of human mRNAs from GenBank aligned to the genome using BLAT^{86, 87}. The Human ESTs track was compiled in the same manner, and included both spliced and un-spliced ESTs. Both of these tracks contain raw full-length public transcriptome data

captured through transcript-to-genome alignments and were used to confirm the presence of genes, to interrogate gene expression profiles, to derive comprehensive information on gene structures (promoters, splice junctions, 3'ends), and novel transcriptional units absent from gene databases.

Regulation

There were also several UCSC Browser tracks used to examine epigenetic and post-transcriptional regulation in the vicinity of a SNP. One track is the TS miRNA track. This shows 3' untranslated region (UTR) microRNA (miRNA) binding sites predicted using TargetScanHuman version 5.1. First, the UTRs were scanned for miRNA sites⁹⁶. After all the matches were found, they were ranked⁹⁷. Another track that displayed regulatory information was the ENCODE Regulation supertrack, which consists of 7 sub-tracks. All of the tracks were used in annotating the locus. The first of these sub-tracks is the transcription track, which displays ENCODE RNA-seq results from cells representing 9 different tissues⁹⁸.

Three of the sub-tracks show information on histone modifications. This was collected by ENCODE using chromatin immunoprecipitation sequencing (ChIP-seq) on cells representing seven different tissues⁹⁹. One histone modification is the monomethylation of lysine 4 in the histone 3 protein, referred to as H3K4Me1. Another modification is the acetylation of lysine 27 in the same histone protein, referred to as H3K27Ac. The presence of either modification suggests an activating regulatory element, and the co-occurrence of the two modifications indicates a putative enhancer region. The third histone modification examined is a trimethylation of lysine 4 in the same histone protein, referred to as H3K4Me3. This signal indicates the presence of a promoter.

Another sub-track we used is the DNase hypersensitivity track version 3, which shows areas of open chromosome accessibility in 125 different cell lines¹⁰⁰. The final two sub-tracks display transcription factor binding sites (TFBSs). Both were created using ChIP-Seq and have information for 161 different transcription factors in 91 different cell types¹⁰¹. The differentiating factor between the two tracks is that one includes information from Factorbook, which displays consensus motifs in binding sites¹⁰².

Conservation

To examine the evolutionary conservation of a locus, the PhyloP Conservation track is used. This displays conservation across 100 different species in a human-centric multispecies alignment¹⁰³.

Repetitive Elements

The final track used is RepeatMaster, which searches the genome for 10 different forms of repeating elements, including long interspersed nuclear elements (LINE), short interspersed nuclear element (SINE), and retrotransposons. This track uses information from the Genetic Information Research Institute's (GIRI) Repbase Update library¹⁰⁴ and makes it possible to determine whether a SNP resides within a genomic repetitive element.

Online Table XIV. Annotation of AAA-Associated SNPs using the UCSC Genome Browser
(<http://genome.ucsc.edu/cgi-bin/hgGateway>)

SNP rs#	Information Available in UCSC Genome Browser
rs1795061	Intron of one mRNA (AY343912), but no ESTs ~550 bp downstream of CEBP beta binding site with consensus motif
rs4129267	In a LINE repeat NHGRI: associated with CAD, asthma, C-protein levels, and protein quantitative traits. Intron of <i>IL6R</i> (involved in immune responses), H3K4Me1 expression In a DNase hypersensitivity cluster (83/125) and 7 TFBSs, including one with a consensus site (MYC). Low expression level. Two ESTs are near the hypersensitivity site, but are not related to any gene/mRNAs.
rs602633	NHGRI: associated with stroke 850 bp downstream of 3' end of <i>PSRC1</i> (involved in mitosis) 900 bp downstream of large H3K4Me1 peak; high transcription levels Associated with a DNase site (9/125) and 3 TFBSs, including a consensus site in <i>EGR1</i> . Approximately 1 kb upstream of a DNase hypersensitivity region (125/125, 100% of cell types) with a large H3K4Me1 peak and mild H3K27Ac levels. There are 36 TFBSs, 6 with consensus motifs. 3 kb downstream of <i>CELSR2</i> (brain expressed cadherin like protein). This region also has high H3K4Me1 expression and moderate H3K27Ac levels, indicating an enhancer region. There are also high transcription levels. There is a DNase hypersensitivity region (62/125) that correlates with 50 TFBSs, 18 with consensus motifs. 5 kbp downstream of another DNase hypersensitivity site (20/125) with 6 TFBSs, 4 of which have consensus motifs. SNP cloud with 9 other SNPs, which have been associated with cholesterol and lipid levels, as well as stroke, and CAD
rs10757274	NHGRI: associated with CAD In a LINE and intron of <i>ANRIL</i> 1.6 kb upstream from high H3K4Me1 and moderate H3K27Ac DNase hypersensitivity site (61) and 15 TFBSs (2 consensus motifs) 7 kbp upstream from a putative enhancer region (high H3K4Me1 and H3K27Ac), associated with DNase hypersensitivity (88) and over 50 TFBSs
rs10985349	Intron of <i>DAB2IP</i> In a DNase hypersensitivity cluster (22) and H3K4Me1 peak
rs9316871	Intergenic
rs6511720	NHGRI: associated with CAD and aneurysm, as well as with lipid and cholesterol levels Intronic to <i>LDLR</i> Moderate transcription levels High levels of H3K4Me1, H3K4Me3, and H3K27Ac (indicating an enhancer/promoter region) In a DNase hypersensitivity cluster of 105/125 with approximately 40 TFBSs (9 consensus motifs)
rs3827066	Intron of <i>ZNF335</i> Moderate transcription levels
rs2836411	Intron of <i>ERG</i> High H3K4Me1 levels, mild H3K27Ac levels Inside a DNase hypersensitivity cluster (11)

PUPASUITE ANALYSIS

The lead SNPs at the 4 novel AAA risk loci (**Table 1**) were identified in the 1000 Genomes phase 3 CEU panel. SNPs in LD ($r^2 > 0.5$) and the lead SNPs were extracted from the 1000 Genomes data and entered into Pupasuite v3.1¹⁰⁵ (**Online Table XV**). No non-synonymous, transcript structure, transcript processing, transcription factor (TF) binding site (Transfac/Jaspar/Oreganno), miRNA sequence, miRNA target, splice site or other functional results were identified.

Online Table XV: Pupasuite 3.1 output for SNPs in LD ($r^2 > 0.5$) with lead SNPs at novel AAA loci.

*Transcript IDs are shown without the full Ensembl Transcript ID (ENST number) for display purposes.

This table spans 2 pages.

Lead SNP	Chr	Position	Nearest gene(s)	LD SNPs	r^2	Location relative to transcript	Gene	Transcript(s)*
rs1795061	1	214409280	SMYD2	rs1795065	1	INTERGENIC		
				rs1660364	1	INTERGENIC		
				rs1660365	1	INTERGENIC		
				rs1795064	1	INTERGENIC		
				rs1795063	1	INTERGENIC		
				rs1795062	1	INTERGENIC		
				rs1660368	1	INTERGENIC		
				rs199679227	1	INTERGENIC		
				rs1660371	1	INTERGENIC		
				rs1795060	1	INTERGENIC		
				rs201675223	0.978	INTERGENIC		
				rs1147673	0.912	INTERGENIC		
				rs12745411	0.724	INTERGENIC		
				rs11585945	0.724	INTERGENIC		
				rs61819142	0.724	INTERGENIC		
				rs12754343	0.724	INTERGENIC		
rs17784245	0.628	INTERGENIC						
rs1021639	0.609	INTERGENIC						
rs9316871	13	22861921	LINC00540	rs9506822	0.85	INTERGENIC		
				rs9510086	0.763	INTERGENIC		
				rs12863716	0.763	INTERGENIC		
				rs7336555	0.763	INTERGENIC		
				rs12857403	0.763	INTERGENIC		
				rs12866004	0.763	INTERGENIC		
				rs11618858	0.763	INTERGENIC		
				rs7994761	0.763	INTERGENIC		
				rs9506820	0.696	INTERGENIC		
				rs3827066	20	44586023	PCIF1-ZNF335-MMP9	rs73128528
		INTRONIC	ZNF335					322927
		INTRONIC	ZNF335					426788
rs17448653	0.629	DOWNSTREAM	ZNF335					494955
		INTRONIC	ZNF335					243961
		INTRONIC	ZNF335					322927
		INTRONIC	ZNF335					426788
		UPSTREAM	ZNF335					475002
		WITHIN_NON_CODING_GENE	ZNF335					476822
rs2836411	21	39819830	ERG					rs2836399
						WITHIN_NON_CODING_GENE	ERG	468474, 473107, 481609, 492833
				rs2298336	0.53	INTRONIC	ERG	288319, 357391, 398897, 398899, 398905, 398907, 398910, 398911, 398916, 398919, 415743, 417133, 429727, 442448, 451178, 453032
						WITHIN_NON_CODING_GENE	ERG	468474, 473107, 481609, 492833
				rs2836402	0.53	INTRONIC	ERG	288319, 357391, 398897,

					398899, 398905, 398907, 398910, 398911, 398916, 398919, 415743, 417133, 429727, 442448, 451178, 453032
				WITHIN_NON_CODING_GENE	ERG 468474, 473107, 481609, 492833
rs2836400	0.519	INTRONIC		ERG	288319, 357391, 398897, 398899, 398905, 398907, 398910, 398911, 398916, 398919, 415743, 417133, 429727, 442448, 451178, 453032
				WITHIN_NON_CODING_GENE	ERG 468474, 473107, 481609, 492833
rs2836407	0.519	INTRONIC		ERG	288319, 357391, 398897, 398899, 398905, 398907, 398910, 398911, 398916, 398919, 415743, 417133, 429727, 442448, 451178, 453032
				UPSTREAM	ERG 492833
				WITHIN_NON_CODING_GENE	ERG 468474, 473107, 481609
rs2836409	0.519	INTRONIC		ERG	288319, 398897, 398899, 398905, 398907, 398910, 398911, 398916, 398919, 417133, 442448, 451178, 453032
				UPSTREAM	ERG 357391, 415743, 429727, 492833
				WITHIN_NON_CODING_GENE	ERG 468474, 473107, 481609

GWAS3D ANALYSIS

The 9 AAA GWAS SNPs (LeadSNP) were entered into the GWAS3D¹⁰⁶ web-portal (<http://jjwanglab.org/gwas3d>), using the following settings: 1. SNP dataset: 1000 Genomes pilot 1, 2. Population: EUR, 3. LD threshold: $R^2 > 0.8$, 4. Cell type: All; and 5. all ENCODE TF Family Motifs (binding site P-value 0.02).

The predicted lead functional SNP (Fn_SNPID) associations for the 9 AAA SNPs are shown in **Figure 4 and Online Table XVI**. For example, the AAA GWAS SNP rs602633 is in high LD with rs599839, which has previously been associated with AAA³. GWAS3D predicted the rs599839 variant to alter STAT, Ets, p300 and RFX5 binding affinities.

The extended list of potential functional variant associations within each locus is shown in **Online Table XVII**. All AAA SNPs were predicted to be associated with transcription factor binding site affinity variants and eight map to interactions with distal regions.

Online Table XVI: Lead functional associations for each of the 9 replicated AAA SNPs.

Fn_SNPID	Chr:Position	Locus	Combined P	LeadSNP	GWAS P	R ²	Status
rs4977575	9:22124744	9p21.3	1.70x10 ⁻³⁵	rs10757274	1.5x10 ⁻³³	0.87	█
rs73128528	20:44582187	ZNF335	3.72x10 ⁻¹⁹	rs3827066	2.1x10 ⁻¹⁷	0.83	█
rs73015013	19:11190873	19p13.2	2.58x10 ⁻¹⁶	rs6511720	7.9x10 ⁻¹⁴	0.94	█
rs4845620	1:154406656	IL6R	9.92x10 ⁻¹⁵	rs4129267	4.8x10 ⁻¹³	0.87	█
rs1660368	1:214407335	1q32.3	4.64x10 ⁻¹⁴	rs1795061	8.8x10 ⁻¹¹	0.97	█
rs599839	1:109822166	1p13.3	3.07x10 ⁻¹³	rs602633	6.6x10 ⁻⁹	0.92	█
rs9510086	13:22862440	13q12.11	8.33x10 ⁻¹²	rs9316871	4.8x10 ⁻¹⁰	0.82	█
rs10985349	9:124425243	DAB2IP	7.46x10 ⁻¹¹	rs10985349	2.4x10 ⁻¹¹	1	█
rs2836411	21:39819830	ERG	4.72x10 ⁻⁹	rs2836411	5.8x10 ⁻⁹	1	█

█	Leading variant		
█	Significant TFBS		
█	Mapping on distal interaction		
█	Mapping on putative enhancer region		
█	Mapping on GERP++ conservation element		

Online Table XVII: Significant regulatory variants detected by the GWAS3D algorithm. Status: distal interaction (td), transcription factor binding affinity (bda), chromatin modification state (chromhmm), sites under evolutionary constraint (gerp). This table spans 4 pages.

SNPID	CHRPOS	GENOTYPE	LOCUS	FINALP	LeadSNP	LEADSNP_P	RSQUARE	STATUS
rs4977575	9:22124744	C G	9p21.3	1.70x10 ⁻³⁵	rs10757274	1.54x10 ⁻³³	0.87	td,bda,enhancer,gerp
rs1333049	9:22125503	G C	9p21.3	3.13x10 ⁻³⁵	rs10757274	1.54x10 ⁻³³	0.88	td,bda,enhancer
rs1333046	9:22124123	T A	9p21.3	6.47x10 ⁻³⁵	rs10757274	1.54x10 ⁻³³	0.93	td,bda,enhancer
rs10738610	9:22123766	A C	9p21.3	4.51x10 ⁻³⁴	rs10757274	1.54x10 ⁻³³	0.93	td,bda,enhancer
rs7857118	9:22124140	A T	9p21.3	4.85x10 ⁻³⁴	rs10757274	1.54x10 ⁻³³	0.92	td,bda,enhancer
rs7859362	9:22105927	T C	ANRIL	7.83x10 ⁻³⁴	rs10757274	1.54x10 ⁻³³	0.93	td,bda,enhancer
rs10217586	9:22121349	A T	9p21.3	9.21x10 ⁻³⁴	rs10757274	1.54x10 ⁻³³	0.81	td,bda,enhancer
rs7859727	9:22102165	C T	ANRIL	1.12x10 ⁻³³	rs10757274	1.54x10 ⁻³³	0.97	td,bda,enhancer
rs10811656	9:22124472	C T	9p21.3	1.19x10 ⁻³³	rs10757274	1.54x10 ⁻³³	0.85	td,bda,enhancer
rs1333043	9:22106731	T A	ANRIL	2.16x10 ⁻³³	rs10757274	1.54x10 ⁻³³	0.93	td,bda,enhancer
rs2891168	9:22098619	A G	ANRIL	2.44x10 ⁻³³	rs10757274	1.54x10 ⁻³³	0.99	td,bda,enhancer
rs10738608	9:22094796	A C	ANRIL	2.72x10 ⁻³³	rs10757274	1.54x10 ⁻³³	0.95	td,bda,enhancer
rs10738607	9:22088094	A G	ANRIL	2.72x10 ⁻³³	rs10757274	1.54x10 ⁻³³	0.95	td,bda,enhancer
rs6475609	9:22106271	A G	ANRIL	4.57x10 ⁻³³	rs10757274	1.54x10 ⁻³³	0.93	td,bda,enhancer
rs2383207	9:22115959	A G	ANRIL	4.60x10 ⁻³³	rs10757274	1.54x10 ⁻³³	0.90	td,bda,enhancer
rs1537370	9:22084310	C T	ANRIL	1.19x10 ⁻³²	rs10757274	1.54x10 ⁻³³	0.84	td,bda,enhancer
rs10511701	9:22112599	T C	ANRIL	1.39x10 ⁻³²	rs10757274	1.54x10 ⁻³³	0.90	td,bda,enhancer
rs1333047	9:22124504	A T	9p21.3	1.53x10 ⁻³²	rs10757274	1.54x10 ⁻³³	0.87	td,bda,enhancer
rs10757275	9:22106225	G A	ANRIL	1.67x10 ⁻³²	rs10757274	1.54x10 ⁻³³	0.94	td,bda,enhancer
rs1333048	9:22125347	A C	9p21.3	1.67x10 ⁻³²	rs10757274	1.54x10 ⁻³³	0.94	td,bda,enhancer
rs4977574	9:22098574	A G	ANRIL	2.01x10 ⁻³²	rs10757274	1.54x10 ⁻³³	0.99	td,bda,enhancer
rs10757278	9:22124477	A G	9p21.3	2.25x10 ⁻³²	rs10757274	1.54x10 ⁻³³	0.88	td,bda,enhancer
rs1537374	9:22116046	A G	ANRIL	2.27x10 ⁻³²	rs10757274	1.54x10 ⁻³³	0.90	td,bda,enhancer
rs1537375	9:22116071	T C	ANRIL	2.66x10 ⁻³²	rs10757274	1.54x10 ⁻³³	0.91	td,bda,enhancer
rs7341791	9:22112427	A G	ANRIL	2.69x10 ⁻³²	rs10757274	1.54x10 ⁻³³	0.89	td,bda,enhancer
rs10757279	9:22124630	A G	9p21.3	3.05x10 ⁻³²	rs10757274	1.54x10 ⁻³³	0.88	td,bda,enhancer
rs2383206	9:22115026	A G	ANRIL	3.05x10 ⁻³²	rs10757274	1.54x10 ⁻³³	0.90	td,bda,enhancer
rs7341786	9:22112241	A C	ANRIL	3.35x10 ⁻³²	rs10757274	1.54x10 ⁻³³	0.89	td,bda,enhancer
rs10757272	9:22088260	C T	ANRIL	3.38x10 ⁻³²	rs10757274	1.54x10 ⁻³³	0.96	td,bda,enhancer
rs1537376	9:22116220	T C	ANRIL	3.95x10 ⁻³²	rs10757274	1.54x10 ⁻³³	0.90	td,bda,enhancer
rs1537373	9:22103341	T G	ANRIL	5.37x10 ⁻³²	rs10757274	1.54x10 ⁻³³	0.96	td,bda,enhancer
rs10757274	9:22096055	A G	ANRIL	6.09x10 ⁻³²	rs10757274	1.54x10 ⁻³³	1.00	td,bda,enhancer,self
rs2210538	9:22092257	G A	ANRIL	6.51x10 ⁻³²	rs10757274	1.54x10 ⁻³³	0.85	td,bda,enhancer
rs1537371	9:22099568	C A	ANRIL	6.84x10 ⁻³²	rs10757274	1.54x10 ⁻³³	0.96	td,bda,enhancer
rs10757277	9:22124450	A G	9p21.3	6.93x10 ⁻³²	rs10757274	1.54x10 ⁻³³	0.88	td,bda,enhancer
rs10733376	9:22114469	G C	ANRIL	7.49x10 ⁻³²	rs10757274	1.54x10 ⁻³³	0.90	td,bda,enhancer

SNPID	CHRPOS	GENOTYPE	LOCUS	FINALP	LeadSNP	LEADSNP_P	RSQUARE	STATUS
rs10738606	9:22088090	A T	ANRIL	9.11x10 ⁻³²	rs10757274	1.54x10 ⁻³³	0.95	td,bda,enhancer
rs4977757	9:22094330	A G	ANRIL	9.23x10 ⁻³²	rs10757274	1.54x10 ⁻³³	0.91	td,bda,enhancer
rs1004638	9:22115589	A T	ANRIL	9.85x10 ⁻³²	rs10757274	1.54x10 ⁻³³	0.90	td,bda,enhancer
rs10738609	9:22114495	A C,G,T	ANRIL	1.05x10 ⁻³¹	rs10757274	1.54x10 ⁻³³	0.91	td,bda,enhancer
rs9644860	9:22090603	C T	ANRIL	1.08x10 ⁻³¹	rs10757274	1.54x10 ⁻³³	0.81	td,bda,enhancer
rs944797	9:22115286	T C	ANRIL	1.14x10 ⁻³¹	rs10757274	1.54x10 ⁻³³	0.90	td,bda,enhancer
rs1556516	9:22100176	G C	ANRIL	1.37x10 ⁻³¹	rs10757274	1.54x10 ⁻³³	0.96	td,bda,enhancer
rs10116277	9:22081397	G T	ANRIL	1.58x10 ⁻³¹	rs10757274	1.54x10 ⁻³³	0.85	td,bda,enhancer
rs1412834	9:22110131	T C	ANRIL	1.59x10 ⁻³¹	rs10757274	1.54x10 ⁻³³	0.91	td,bda,enhancer
rs1333042	9:22103813	A G	ANRIL	1.84x10 ⁻³¹	rs10757274	1.54x10 ⁻³³	0.95	td,bda,enhancer
rs6475606	9:22081850	C T	ANRIL	2.11x10 ⁻³¹	rs10757274	1.54x10 ⁻³³	0.85	td,bda,enhancer
rs1970112	9:22085598	T C	ANRIL	2.49x10 ⁻³¹	rs10757274	1.54x10 ⁻³³	0.86	td,bda,enhancer
rs73128528	20:44582187	A T	ZNF335	3.72x10 ⁻¹⁹	rs3827066	2.10x10 ⁻¹⁷	0.83	bda,enhancer
rs7267295	20:44570683	C T	PCIF1	4.78x10 ⁻¹⁸	rs3827066	2.10x10 ⁻¹⁷	0.84	td,bda,enhancer
rs58749629	20:44571317	G A	PCIF1	1.84x10 ⁻¹⁶	rs3827066	2.10x10 ⁻¹⁷	0.91	td,bda,enhancer
rs73015013	19:11190873	C T	19p13.2	2.58x10 ⁻¹⁶	rs6511720	7.90x10 ⁻¹⁴	0.94	td,bda,enhancer
rs8124182	20:44608901	G A	20q13.12	2.86x10 ⁻¹⁶	rs3827066	2.10x10 ⁻¹⁷	0.84	td,bda,enhancer
rs7270354	20:44607661	G A	20q13.12	4.86x10 ⁻¹⁶	rs3827066	2.10x10 ⁻¹⁷	0.91	td,bda,enhancer
chr19:11190074	19:11190074	G A	19p13.2	1.41x10 ⁻¹⁵	rs6511720	7.90x10 ⁻¹⁴	0.96	td,bda,enhancer
chr19:11189272	19:11189272	T C	19p13.2	1.65x10 ⁻¹⁵	rs6511720	7.90x10 ⁻¹⁴	0.94	td,bda,enhancer
chr19:11189937	19:11189937	T A	19p13.2	1.81x10 ⁻¹⁵	rs6511720	7.90x10 ⁻¹⁴	0.96	td,bda,enhancer
rs6511720	19:11202306	G T	LDLR	2.06x10 ⁻¹⁵	rs6511720	7.90x10 ⁻¹⁴	1	bda,enhancer,chromhmm,self
rs56289821	19:11188247	G A	19p13.2	3.84x10 ⁻¹⁵	rs6511720	7.90x10 ⁻¹⁴	0.92	td,bda,enhancer
rs8106503	19:11196886	T C	19p13.2	6.27x10 ⁻¹⁵	rs6511720	7.90x10 ⁻¹⁴	0.94	td,bda,enhancer,chromhmm
rs4845620	1:154406656	A G	IL6R	9.92x10 ⁻¹⁵	rs4129267	4.76x10 ⁻¹³	0.87	td,bda,enhancer
rs17248720	19:11198187	C T	LDLR	1.87x10 ⁻¹⁴	rs6511720	7.90x10 ⁻¹⁴	0.91	td,bda,enhancer,chromhmm
rs1660368	1:214407335	C T	1q32.3	4.64x10 ⁻¹⁴	rs1795061	8.80x10 ⁻¹¹	0.97	td,bda,enhancer,gerp
rs4537545	1:154418879	C T	IL6R	4.72x10 ⁻¹⁴	rs4129267	4.76x10 ⁻¹³	0.87	td,bda,enhancer
chr19:11187358	19:11187358	T G	19p13.2	5.55x10 ⁻¹⁴	rs6511720	7.90x10 ⁻¹⁴	0.92	td,bda,enhancer
rs56383622	1:154405024	A G	IL6R	5.67x10 ⁻¹⁴	rs4129267	4.76x10 ⁻¹³	0.87	td,bda,enhancer
chr19:11191197	19:11191197	G A	19p13.2	7.26x10 ⁻¹⁴	rs6511720	7.90x10 ⁻¹⁴	0.94	td,bda,enhancer
rs57217136	19:11201124	T C	LDLR	8.82x10 ⁻¹⁴	rs6511720	7.90x10 ⁻¹⁴	1	bda,enhancer,chromhmm
rs4129267	1:154426264	C T	IL6R	9.12x10 ⁻¹⁴	rs4129267	4.76x10 ⁻¹³	1	bda,enhancer,self
rs12151108	19:11197261	G A	19p13.2	1.10x10 ⁻¹³	rs6511720	7.90x10 ⁻¹⁴	0.93	td,bda,enhancer
rs17248727	19:11198502	T C	LDLR	1.31x10 ⁻¹³	rs6511720	7.90x10 ⁻¹⁴	0.92	td,bda,enhancer,chromhmm
rs2228145	1:154426970	A C,T	IL6R	1.39x10 ⁻¹³	rs4129267	4.76x10 ⁻¹³	0.99	bda,enhancer
chr19:11189205	19:11189205	C G	19p13.2	1.54x10 ⁻¹³	rs6511720	7.90x10 ⁻¹⁴	0.94	td,bda,enhancer
chr19:11189980	19:11189980	C A	19p13.2	1.73x10 ⁻¹³	rs6511720	7.90x10 ⁻¹⁴	0.96	td,bda,enhancer
chr19:11188899	19:11188899	C T	19p13.2	1.74x10 ⁻¹³	rs6511720	7.90x10 ⁻¹⁴	0.94	td,bda,enhancer
rs73015021	19:11192915	A G	19p13.2	1.91x10 ⁻¹³	rs6511720	7.90x10 ⁻¹⁴	0.96	td,bda,enhancer

SNPID	CHRPOS	GENOTYPE	LOCUS	FINALP	LeadSNP	LEADSNP_P	RSQUARE	STATUS
chr19:11190544	19:11190544	C T	19p13.2	2.15x10 ⁻¹³	rs6511720	7.90x10 ⁻¹⁴	0.88	td,bda,enhancer
rs6684439	1:154395839	C T	<i>IL6R</i>	2.51x10 ⁻¹³	rs4129267	4.76x10 ⁻¹³	0.83	td,bda,enhancer
chr19:11191729	19:11191729	C T	19p13.2	2.95x10 ⁻¹³	rs6511720	7.90x10 ⁻¹⁴	0.94	td,bda,enhancer
rs599839	1:109822166	G A	1p13.3	3.07x10 ⁻¹³	rs602633	6.58x10 ⁻⁰⁹	0.92	td,bda,enhancer,gerp
chr19:11190481	19:11190481	G T	19p13.2	3.15x10 ⁻¹³	rs6511720	7.90x10 ⁻¹⁴	0.96	td,bda,enhancer
rs10412048	19:11193949	A G	19p13.2	3.58x10 ⁻¹³	rs6511720	7.90x10 ⁻¹⁴	0.93	td,bda,enhancer
rs73015011	19:11189764	T C	19p13.2	3.78x10 ⁻¹³	rs6511720	7.90x10 ⁻¹⁴	0.94	td,bda,enhancer
rs4845373	1:154417829	C T	<i>IL6R</i>	4.52x10 ⁻¹³	rs4129267	4.76x10 ⁻¹³	0.87	td,bda,enhancer
rs55997232	19:11188117	C T	19p13.2	4.98x10 ⁻¹³	rs6511720	7.90x10 ⁻¹⁴	0.94	td,bda,enhancer
rs56125973	19:11188164	T C	19p13.2	5.03x10 ⁻¹³	rs6511720	7.90x10 ⁻¹⁴	0.91	td,bda,enhancer
chr19:11188850	19:11188850	T C	19p13.2	6.17x10 ⁻¹³	rs6511720	7.90x10 ⁻¹⁴	0.93	td,bda,enhancer
rs12126142	1:154425456	G A	<i>IL6R</i>	6.17x10 ⁻¹³	rs4129267	4.76x10 ⁻¹³	1	bda,enhancer
chr19:11187422	19:11187422	T C	19p13.2	6.25x10 ⁻¹³	rs6511720	7.90x10 ⁻¹⁴	0.93	td,bda,enhancer
chr19:11190556	19:11190556	T C	19p13.2	6.99x10 ⁻¹³	rs6511720	7.90x10 ⁻¹⁴	0.93	td,bda,enhancer
rs10402112	19:11191677	T A	19p13.2	7.26x10 ⁻¹³	rs6511720	7.90x10 ⁻¹⁴	0.94	td,bda,enhancer
rs11265613	1:154418415	T C	<i>IL6R</i>	7.93x10 ⁻¹³	rs4129267	4.76x10 ⁻¹³	0.88	td,bda,enhancer
chr19:11187324	19:11187324	C G	19p13.2	8.25x10 ⁻¹³	rs6511720	7.90x10 ⁻¹⁴	0.93	td,bda,enhancer
rs55791371	19:11188153	A C	19p13.2	8.67x10 ⁻¹³	rs6511720	7.90x10 ⁻¹⁴	0.93	td,bda,enhancer
rs1147673	1:214402313	A G	1q32.3	9.07x10 ⁻¹³	rs1795061	8.80x10 ⁻¹¹	0.93	td,bda,enhancer
rs61194703	19:11192193	A T	19p13.2	9.20x10 ⁻¹³	rs6511720	7.90x10 ⁻¹⁴	0.94	td,bda,enhancer
chr19:11190292	19:11190292	T C	19p13.2	1.03x10 ⁻¹²	rs6511720	7.90x10 ⁻¹⁴	0.94	td,bda,enhancer
rs4845622	1:154411419	A C	<i>IL6R</i>	1.13x10 ⁻¹²	rs4129267	4.76x10 ⁻¹³	0.87	td,bda,enhancer
rs73015024	19:11197598	G T	19p13.2	1.13x10 ⁻¹²	rs6511720	7.90x10 ⁻¹⁴	0.94	td,bda,enhancer
rs12133641	1:154428283	A G	<i>IL6R</i>	1.32x10 ⁻¹²	rs4129267	4.76x10 ⁻¹³	0.97	bda,enhancer
chr19:11190534	19:11190534	G A	19p13.2	1.36x10 ⁻¹²	rs6511720	7.90x10 ⁻¹⁴	0.93	td,bda,enhancer
chr19:11190110	19:11190110	A G	19p13.2	1.44x10 ⁻¹²	rs6511720	7.90x10 ⁻¹⁴	0.96	td,bda,enhancer
chr19:11190549	19:11190549	G A	19p13.2	1.50x10 ⁻¹²	rs6511720	7.90x10 ⁻¹⁴	0.93	td,bda,enhancer
rs73015016	19:11191300	G A	19p13.2	1.56x10 ⁻¹²	rs6511720	7.90x10 ⁻¹⁴	0.94	td,bda,enhancer
rs12730935	1:154419892	G A	<i>IL6R</i>	1.60x10 ⁻¹²	rs4129267	4.76x10 ⁻¹³	0.86	td,bda
chr19:11192831	19:11192831	A G	19p13.2	1.88x10 ⁻¹²	rs6511720	7.90x10 ⁻¹⁴	0.94	td,bda,enhancer
rs73015020	19:11192550	G A	19p13.2	1.98x10 ⁻¹²	rs6511720	7.90x10 ⁻¹⁴	0.93	td,bda,enhancer
rs4576655	1:154418749	C T	<i>IL6R</i>	2.56x10 ⁻¹²	rs4129267	4.76x10 ⁻¹³	0.88	td,bda,enhancer
rs4845621	1:154409730	G A	<i>IL6R</i>	2.95x10 ⁻¹²	rs4129267	4.76x10 ⁻¹³	0.87	td,bda
rs4393147	1:154414037	C T	<i>IL6R</i>	3.16x10 ⁻¹²	rs4129267	4.76x10 ⁻¹³	0.87	td,bda,enhancer
rs12753254	1:154416935	G A	<i>IL6R</i>	3.49x10 ⁻¹²	rs4129267	4.76x10 ⁻¹³	0.87	td,bda,enhancer
rs4845372	1:154415396	C A	<i>IL6R</i>	4.58x10 ⁻¹²	rs4129267	4.76x10 ⁻¹³	0.83	td,bda,enhancer
rs6664201	1:154414296	C T	<i>IL6R</i>	5.08x10 ⁻¹²	rs4129267	4.76x10 ⁻¹³	0.87	td,bda,enhancer
rs4845623	1:154415777	A G	<i>IL6R</i>	5.10x10 ⁻¹²	rs4129267	4.76x10 ⁻¹³	0.83	td,bda,enhancer
rs7521458	1:154407713	T C	<i>IL6R</i>	5.55x10 ⁻¹²	rs4129267	4.76x10 ⁻¹³	0.87	td,bda
rs12730036	1:154416969	C T	<i>IL6R</i>	6.86x10 ⁻¹²	rs4129267	4.76x10 ⁻¹³	0.87	td,bda,enhancer

SNPID	CHRPOS	GENOTYPE	LOCUS	FINALP	LeadSNP	LEADSNP_P	RSQUARE	STATUS
rs9510086	13:22862440	G C	13q12.11	8.33x10 ⁻¹²	rs9316871	4.80x10 ⁻¹⁰	0.81	td,bda,enhancer
rs7518199	1:154407419	A C	<i>IL6R</i>	8.49x10 ⁻¹²	rs4129267	4.76x10 ⁻¹³	0.87	td,bda,enhancer
rs4453032	1:154414086	A G	<i>IL6R</i>	8.54x10 ⁻¹²	rs4129267	4.76x10 ⁻¹³	0.87	td,bda,enhancer
rs1795065	1:214405194	G A	1q32.3	1.75x10 ⁻¹¹	rs1795061	8.80x10 ⁻¹¹	0.97	td,bda,enhancer
rs1795060	1:214410021	C T	1q32.3	1.90x10 ⁻¹¹	rs1795061	8.80x10 ⁻¹¹	1	bda,enhancer
rs12740374	1:109817590	G T	<i>CELSR2</i>	2.07x10 ⁻¹¹	rs602633	6.58x10 ⁻⁰⁹	0.90	td,bda,enhancer,chromhmm,gerp
rs904320	1:214408457	A T	1q32.3	4.93x10 ⁻¹¹	rs1795061	8.80x10 ⁻¹¹	0.98	td,bda,enhancer
rs1795061	1:214409280	T C	1q32.3	5.62x10 ⁻¹¹	rs1795061	8.80x10 ⁻¹¹	1	td,bda,enhancer,self
rs629301	1:109818306	G T	<i>CELSR2</i>	7.32x10 ⁻¹¹	rs602633	6.58x10 ⁻⁰⁹	0.90	td,bda,enhancer,chromhmm,gerp
rs10985349	9:124425243	C T	<i>DAB2IP</i>	7.46x10 ⁻¹¹	rs10985349	2.40x10 ⁻¹¹	1	td,bda,enhancer,self
rs10985350	9:124429196	A C	<i>DAB2IP</i>	1.67x10 ⁻¹⁰	rs10985349	2.40x10 ⁻¹¹	0.81	td,bda,enhancer
rs660240	1:109817838	T C	<i>CELSR2</i>	1.88x10 ⁻¹⁰	rs602633	6.58x10 ⁻⁰⁹	0.96	td,bda,enhancer,chromhmm,gerp
rs7528419	1:109817192	A G	<i>CELSR2</i>	4.03x10 ⁻¹⁰	rs602633	6.58x10 ⁻⁰⁹	0.90	td,bda,enhancer,chromhmm,gerp
rs1795064	1:214406272	C T	1q32.3	5.07x10 ⁻¹⁰	rs1795061	8.80x10 ⁻¹¹	0.97	td,bda,enhancer
rs1795062	1:214406721	T C	1q32.3	5.73x10 ⁻¹⁰	rs1795061	8.80x10 ⁻¹¹	0.97	td,bda,enhancer
rs1660371	1:214409248	T A	1q32.3	9.29x10 ⁻¹⁰	rs1795061	8.80x10 ⁻¹¹	0.97	td,bda,enhancer
rs1795063	1:214406508	G A	1q32.3	9.72x10 ⁻¹⁰	rs1795061	8.80x10 ⁻¹¹	0.97	td,bda,enhancer
rs9316871	13:22861921	A G	13q12.11	1.26x10 ⁻⁰⁹	rs9316871	4.80x10 ⁻¹⁰	1	td,bda,enhancer,self
rs9506822	13:22862220	A G	13q12.11	1.89x10 ⁻⁰⁹	rs9316871	4.80x10 ⁻¹⁰	0.87	td,bda,enhancer
rs2836411	21:39819830	C T	<i>ERG</i>	4.72x10 ⁻⁰⁹	rs2836411	5.80x10 ⁻⁰⁹	1	bda,enhancer,self

107

BIOINFORMATIC IDENTIFICATION OF CANDIDATE AAA GENES AND PATHWAYS USING DEPICT

An integrated gene function analysis was performed using the DEPICT version 1.1 tool¹⁰⁸. DEPICT was installed, tested and run using meta-GWAS summary statistics following the recommended procedure outlined at <https://github.com/perslab/depict>. Two separate runs were performed using either all independent SNPs with discovery metaGWAS $P < 5 \times 10^{-6}$ or just those 10 SNPs which reached $P < 1 \times 10^{-6}$ in the combined analysis. Results are shown in **Online Table XVIII** and the full dataset is available in the online data supplement.

Online Table XVIII, DEPICT gene enrichment sets (nominal $P < 0.05$) based on the top 10 validated loci.

There is a notable presence of descriptions associated with transforming growth factor beta regulation, lipoprotein metabolism, inflammation induced extracellular matrix remodelling (eg. RFX1), vascular smooth muscle cell function, vascular injury (including haemorrhage), immune cell function (particularly T & B cells), acute phase response (including IL6 secretion), apoptosis, hyperglycemia and the PIK3K, JNK and MAPK cascades. In addition, there are several descriptions associated with long bone size, an observation which may be consistent with previous reports linking height with cardiovascular disease risk. All gene sets had a false discovery rate > 0.2 with the exception of the most significant gene set, MP:0006396 (decreased long bone epiphyseal plate size), where the FDR was < 0.2 . This table spans 11 pages.

Original gene set ID	Original gene set description	DEPICT Nominal P-value
MP:0006396	decreased long bone epiphyseal plate size	1.14×10^{-9}
GO:0034381	plasma lipoprotein particle clearance	5.22×10^{-7}
ENSG00000205250	E2F4 PPI subnetwork	1.27×10^{-6}
ENSG00000132005	RFX1 PPI subnetwork	2.28×10^{-6}
MP:0000708	thymus hyperplasia	6.32×10^{-6}
ENSG00000167553	TUBA1C PPI subnetwork	3.18×10^{-5}
ENSG00000170421	KRT8 PPI subnetwork	9.59×10^{-5}
MP:0003645	increased pancreatic beta cell number	1.12×10^{-4}
ENSG00000166866	MYO1A PPI subnetwork	2.32×10^{-4}
REACTOME	REACTOME_apoptotic_execution__phase	2.92×10^{-4}
MP:0008182	decreased marginal zone B cell number	3.06×10^{-4}
GO:0008375	acetylglucosaminyltransferase activity	3.62×10^{-4}
ENSG00000131941	RHPN2 PPI subnetwork	3.75×10^{-4}
ENSG00000169710	FASN PPI subnetwork	4.55×10^{-4}
REACTOME	Reactome_apoptotic_cleavage_of_cellular_proteins	5.46×10^{-4}
ENSG0000013297	CLDN11 PPI subnetwork	6.28×10^{-4}
ENSG00000070159	PTPN3 PPI subnetwork	6.56×10^{-4}
ENSG00000091409	ITGA6 PPI subnetwork	7.26×10^{-4}
ENSG00000178209	PLEC PPI subnetwork	8.57×10^{-4}
REACTOME	Reactome_p75_ntr_receptor:mediated_signalling	1.07×10^{-3}
GO:0001890	placenta development	1.08×10^{-3}
ENSG00000164344	KLKB1 PPI subnetwork	1.09×10^{-3}
MP:0002136	abnormal kidney physiology	1.17×10^{-3}
MP:0002655	abnormal keratinocyte morphology	1.45×10^{-3}

Original gene set ID	Original gene set description	DEPICT Nominal P-value
ENSG00000143375	CGN PPI subnetwork	1.48x10 ⁻³
MP:0005595	abnormal vascular smooth muscle physiology	1.55x10 ⁻³
ENSG00000122641	INHBA PPI subnetwork	1.79x10 ⁻³
MP:0002764	short tibia	1.79x10 ⁻³
MP:0003662	abnormal long bone epiphyseal plate proliferative zone	2.01x10 ⁻³
ENSG00000169047	IRS1 PPI subnetwork	2.21x10 ⁻³
ENSG00000125503	PPP1R12C PPI subnetwork	2.23x10 ⁻³
MP:0001179	thick pulmonary interalveolar septum	2.30x10 ⁻³
GO:0043256	laminin complex	2.33x10 ⁻³
ENSG00000116809	ZBTB17 PPI subnetwork	2.46x10 ⁻³
GO:0050431	transforming growth factor beta binding	2.47x10 ⁻³
ENSG00000039560	RAI14 PPI subnetwork	2.60x10 ⁻³
ENSG00000164733	CTSB PPI subnetwork	2.64x10 ⁻³
ENSG00000139567	ACVRL1 PPI subnetwork	2.75x10 ⁻³
MP:0005590	increased vasodilation	3.45x10 ⁻³
GO:0071813	lipoprotein particle binding	3.51x10 ⁻³
GO:0071814	protein-lipid complex binding	3.51x10 ⁻³
MP:0002082	postnatal lethality	3.53x10 ⁻³
GO:0071902	positive regulation of protein serine/threonine kinase activity	3.87x10 ⁻³
ENSG00000130147	SH3BP4 PPI subnetwork	3.91x10 ⁻³
GO:0005178	integrin binding	4.08x10 ⁻³
ENSG00000133056	PIK3C2B PPI subnetwork	4.40x10 ⁻³
ENSG00000172725	CORO1B PPI subnetwork	4.45x10 ⁻³
ENSG00000136286	MYO1G PPI subnetwork	4.65x10 ⁻³
ENSG00000078142	PIK3C3 PPI subnetwork	4.72x10 ⁻³
MP:0005095	decreased T cell proliferation	4.84x10 ⁻³
ENSG00000145715	RASA1 PPI subnetwork	4.96x10 ⁻³
ENSG00000104725	ENSG00000104725 PPI subnetwork	5.08x10 ⁻³
KEGG_PATHWAYS	KEGG_PATHWAYS_IN_CANCER	5.17x10 ⁻³
GO:0008194	UDP-glycosyltransferase activity	5.46x10 ⁻³
ENSG00000078747	ITCH PPI subnetwork	5.48x10 ⁻³
ENSG00000149257	SERPINH1 PPI subnetwork	5.79x10 ⁻³
ENSG00000114062	UBE3A PPI subnetwork	5.85x10 ⁻³
ENSG00000139144	PIK3C2G PPI subnetwork	5.85x10 ⁻³
ENSG00000143393	PI4KB PPI subnetwork	5.87x10 ⁻³
ENSG00000148498	PARD3 PPI subnetwork	6.00x10 ⁻³
ENSG00000196455	PIK3R4 PPI subnetwork	6.19x10 ⁻³
ENSG00000148660	CAMK2G PPI subnetwork	6.48x10 ⁻³
ENSG00000034152	MAP2K3 PPI subnetwork	6.58x10 ⁻³
ENSG00000123124	WWP1 PPI subnetwork	6.95x10 ⁻³
MP:0008813	decreased common myeloid progenitor cell number	7.37x10 ⁻³
ENSG00000204175	GPRIN2 PPI subnetwork	7.39x10 ⁻³
GO:0001772	immunological synapse	7.40x10 ⁻³
REACTOME	Reactome_caspase:mediated_cleavage_of_cytoskeletal_proteins	7.46x10 ⁻³
ENSG00000017427	IGF1 PPI subnetwork	7.51x10 ⁻³
MP:0001954	respiratory distress	7.56x10 ⁻³
GO:0016051	carbohydrate biosynthetic process	7.65x10 ⁻³

Original gene set ID	Original gene set description	DEPICT Nominal P-value
GO:0043406	positive regulation of MAP kinase activity	7.65x10 ⁻³
REACTOME	Reactome_cell_death_signalling_via_nrage_nrif_and_nade	7.67x10 ⁻³
MP:0000180	abnormal circulating cholesterol level	7.71x10 ⁻³
ENSG00000170759	KIF5B PPI subnetwork	7.79x10 ⁻³
ENSG00000180530	NRIP1 PPI subnetwork	7.86x10 ⁻³
ENSG00000138771	SHROOM3 PPI subnetwork	7.89x10 ⁻³
ENSG00000065882	TBC1D1 PPI subnetwork	7.97x10 ⁻³
ENSG00000138592	USP8 PPI subnetwork	7.99x10 ⁻³
MP:0001915	intracranial hemorrhage	8.00x10 ⁻³
ENSG00000131746	TNS4 PPI subnetwork	8.01x10 ⁻³
MP:0004883	abnormal vascular wound healing	8.15x10 ⁻³
ENSG00000091073	ENSG00000091073 PPI subnetwork	8.22x10 ⁻³
ENSG00000081189	MEF2C PPI subnetwork	8.24x10 ⁻³
ENSG00000154415	PPP1R3A PPI subnetwork	8.33x10 ⁻³
ENSG00000188313	PLSCR1 PPI subnetwork	8.55x10 ⁻³
MP:0004933	abnormal epididymis epithelium morphology	8.61x10 ⁻³
ENSG00000147065	MSN PPI subnetwork	8.64x10 ⁻³
ENSG00000165409	TSHR PPI subnetwork	8.64x10 ⁻³
ENSG00000106992	AK1 PPI subnetwork	8.69x10 ⁻³
GO:0007292	female gamete generation	8.93x10 ⁻³
ENSG00000144061	NPHP1 PPI subnetwork	8.95x10 ⁻³
MP:0003419	delayed endochondral bone ossification	8.98x10 ⁻³
ENSG00000110880	CORO1C PPI subnetwork	9.04x10 ⁻³
ENSG00000197879	MYO1C PPI subnetwork	9.22x10 ⁻³
ENSG00000176476	CCDC101 PPI subnetwork	9.31x10 ⁻³
ENSG00000176108	CHMP6 PPI subnetwork	9.44x10 ⁻³
REACTOME	Reactome_integrin_cell_surface_interactions	9.47x10 ⁻³
GO:0016758	transferase activity, transferring hexosyl groups	9.49x10 ⁻³
ENSG00000103197	TSC2 PPI subnetwork	9.49x10 ⁻³
MP:0003909	increased eating behavior	9.57x10 ⁻³
MP:0000716	abnormal immune system cell morphology	9.63x10 ⁻³
MP:0008803	abnormal placental labyrinth vasculature morphology	9.67x10 ⁻³
ENSG00000137801	THBS1 PPI subnetwork	9.71x10 ⁻³
ENSG00000130522	JUND PPI subnetwork	9.72x10 ⁻³
GO:0005088	Ras guanyl-nucleotide exchange factor activity	9.78x10 ⁻³
ENSG00000170581	STAT2 PPI subnetwork	9.79x10 ⁻³
ENSG00000173757	STAT5B PPI subnetwork	9.84x10 ⁻³
GO:0043277	apoptotic cell clearance	9.98x10 ⁻³
GO:0006917	induction of apoptosis	0.01
MP:0001828	abnormal T cell activation	0.01
ENSG00000171241	SHCBP1 PPI subnetwork	0.01
REACTOME	REACTOME_apoptosis	0.01
MP:0011106	partial embryonic lethality before somite formation	0.01
GO:0030169	low-density lipoprotein particle binding	0.01
MP:0003731	abnormal retinal outer nuclear layer morphology	0.01
MP:0009400	decreased skeletal muscle fiber size	0.01
ENSG00000137693	YAP1 PPI subnetwork	0.01

Original gene set ID	Original gene set description	DEPICT Nominal P-value
REACTOME	Reactome_nrage_signals_death_through_jnk	0.01
ENSG00000145794	MEGF10 PPI subnetwork	0.01
MP:0008478	increased spleen white pulp amount	0.01
MP:0005079	defective cytotoxic T cell cytolysis	0.01
ENSG00000141506	PIK3R5 PPI subnetwork	0.01
GO:0000989	transcription factor binding transcription factor activity	0.01
MP:0002161	abnormal fertility/fecundity	0.01
GO:0040029	regulation of gene expression, epigenetic	0.01
ENSG00000115963	RND3 PPI subnetwork	0.01
GO:0043236	laminin binding	0.01
ENSG00000211660	ENSG00000211660 PPI subnetwork	0.01
ENSG00000211653	ENSG00000211653 PPI subnetwork	0.01
ENSG00000160310	PRMT2 PPI subnetwork	0.01
ENSG00000127688	GAN PPI subnetwork	0.01
ENSG00000167711	SERPINF2 PPI subnetwork	0.01
GO:0043491	protein kinase B signaling cascade	0.01
ENSG00000136068	FLNB PPI subnetwork	0.01
GO:0002020	protease binding	0.01
ENSG00000198053	SIRPA PPI subnetwork	0.01
ENSG00000182319	SGK223 PPI subnetwork	0.01
ENSG00000174292	TNK1 PPI subnetwork	0.01
ENSG00000132825	PPP1R3D PPI subnetwork	0.01
GO:0051015	actin filament binding	0.01
ENSG00000140443	IGF1R PPI subnetwork	0.01
MP:0000281	abnormal interventricular septum morphology	0.01
ENSG000000067560	RHOA PPI subnetwork	0.01
MP:0006094	increased fat cell size	0.01
ENSG00000197555	SIPA1L1 PPI subnetwork	0.01
ENSG00000183386	FHL3 PPI subnetwork	0.01
MP:0003229	abnormal vitelline vasculature morphology	0.01
MP:0001231	abnormal epidermis stratum basale morphology	0.01
MP:0000511	abnormal intestinal mucosa morphology	0.01
KEGG	KEGG_ACUTE_MYELOID_LEUKEMIA	0.01
GO:0007254	JNK cascade	0.01
GO:0008624	induction of apoptosis by extracellular signals	0.01
GO:0000988	protein binding transcription factor activity	0.02
MP:0002452	abnormal antigen presenting cell physiology	0.02
ENSG00000185950	IRS2 PPI subnetwork	0.02
KEGG	KEGG_leukocyte_transendothelial_migration	0.02
GO:0051568	histone H3-K4 methylation	0.02
ENSG00000165516	KLHDC2 PPI subnetwork	0.02
REACTOME	Reactome_cell_surface_interactions_at_the_vascular_wall	0.02
ENSG00000198838	RYR3 PPI subnetwork	0.02
MP:0001711	abnormal placenta morphology	0.02
GO:0014910	regulation of smooth muscle cell migration	0.02
ENSG00000104960	PTOV1 PPI subnetwork	0.02
GO:0001968	fibronectin binding	0.02

Original gene set ID	Original gene set description	DEPICT Nominal P-value
GO:0012502	induction of programmed cell death	0.02
ENSG00000100364	KIAA0930 PPI subnetwork	0.02
ENSG00000165410	CFL2 PPI subnetwork	0.02
MP:0004994	abnormal brain wave pattern	0.02
MP:0001552	increased circulating triglyceride level	0.02
ENSG00000116141	MARK1 PPI subnetwork	0.02
GO:0032403	protein complex binding	0.02
ENSG00000179364	PACS2 PPI subnetwork	0.02
MP:0001559	hyperglycemia	0.02
ENSG00000105851	PIK3CG PPI subnetwork	0.02
MP:0004031	insulinitis	0.02
MP:0010124	decreased bone mineral content	0.02
ENSG00000165197	FIGF PPI subnetwork	0.02
ENSG00000126561	STAT5A PPI subnetwork	0.02
ENSG00000136156	ITM2B PPI subnetwork	0.02
ENSG00000164327	RICTOR PPI subnetwork	0.02
ENSG00000159166	LAD1 PPI subnetwork	0.02
MP:0001716	abnormal placenta labyrinth morphology	0.02
MP:0002427	disproportionate dwarf	0.02
ENSG00000105371	ICAM4 PPI subnetwork	0.02
ENSG00000165476	REEP3 PPI subnetwork	0.02
GO:0046625	sphingolipid binding	0.02
MP:0000585	kinked tail	0.02
MP:0000889	abnormal cerebellar molecular layer	0.02
ENSG00000105699	LSR PPI subnetwork	0.02
GO:0005545	1-phosphatidylinositol binding	0.02
MP:0001134	absent corpus luteum	0.02
ENSG00000100097	LGALS1 PPI subnetwork	0.02
MP:0002079	increased circulating insulin level	0.02
ENSG00000150093	ITGB1 PPI subnetwork	0.02
GO:0001871	pattern binding	0.02
GO:0030247	polysaccharide binding	0.02
ENSG00000126934	MAP2K2 PPI subnetwork	0.02
ENSG00000110395	CBL PPI subnetwork	0.02
ENSG00000179151	EDC3 PPI subnetwork	0.02
ENSG00000154162	CDH12 PPI subnetwork	0.02
ENSG00000184363	PKP3 PPI subnetwork	0.02
ENSG00000020577	SAMD4A PPI subnetwork	0.02
MP:0004139	abnormal gastric parietal cell morphology	0.02
ENSG00000168476	REEP4 PPI subnetwork	0.02
ENSG00000110651	CD81 PPI subnetwork	0.02
ENSG00000134184	GSTM1 PPI subnetwork	0.02
ENSG00000105376	ICAM5 PPI subnetwork	0.02
ENSG00000196954	CASP4 PPI subnetwork	0.02
MP:0003704	abnormal hair follicle development	0.02
ENSG00000050820	BCAR1 PPI subnetwork	0.02
ENSG00000151748	SAV1 PPI subnetwork	0.02

Original gene set ID	Original gene set description	DEPICT Nominal P-value
GO:0003714	transcription corepressor activity	0.02
ENSG00000115904	SOS1 PPI subnetwork	0.02
ENSG00000175793	SFN PPI subnetwork	0.02
ENSG00000100345	MYH9 PPI subnetwork	0.02
GO:0035091	phosphatidylinositol binding	0.02
ENSG00000149930	TAOK2 PPI subnetwork	0.02
GO:0042054	histone methyltransferase activity	0.02
MP:0000689	abnormal spleen morphology	0.02
GO:0001892	embryonic placenta development	0.02
ENSG00000130294	KIF1A PPI subnetwork	0.02
ENSG00000148965	SAA4 PPI subnetwork	0.02
GO:0034774	secretory granule lumen	0.02
ENSG00000166483	WEE1 PPI subnetwork	0.02
ENSG00000110237	ARHGEF17 PPI subnetwork	0.02
GO:0032608	interferon-beta production	0.02
ENSG00000152518	ZFP36L2 PPI subnetwork	0.02
MP:0010792	abnormal stomach mucosa morphology	0.02
ENSG00000189319	FAM53B PPI subnetwork	0.02
ENSG00000117461	PIK3R3 PPI subnetwork	0.02
GO:0034362	low-density lipoprotein particle	0.02
ENSG00000134072	CAMK1 PPI subnetwork	0.02
ENSG00000163362	C1orf106 PPI subnetwork	0.02
MP:0002816	colitis	0.02
GO:0050900	leukocyte migration	0.03
GO:0044304	main axon	0.03
ENSG00000071909	MYO3B PPI subnetwork	0.03
ENSG00000100714	MTHFD1 PPI subnetwork	0.03
ENSG00000198836	OPA1 PPI subnetwork	0.03
ENSG00000197442	MAP3K5 PPI subnetwork	0.03
ENSG00000206306	HLA-DRB1 PPI subnetwork	0.03
ENSG00000206240	HLA-DRB1 PPI subnetwork	0.03
GO:0031983	vesicle lumen	0.03
KEGG	KEGG_regulation_of_actin_cytoskeleton	0.03
GO:0004713	protein tyrosine kinase activity	0.03
GO:0006953	acute-phase response	0.03
GO:0003712	transcription cofactor activity	0.03
MP:0000295	trabecula carnea hypoplasia	0.03
ENSG00000105647	PIK3R2 PPI subnetwork	0.03
GO:0060205	cytoplasmic membrane-bounded vesicle lumen	0.03
ENSG00000107566	ERLIN1 PPI subnetwork	0.03
ENSG00000114270	COL7A1 PPI subnetwork	0.03
ENSG00000135930	EIF4E2 PPI subnetwork	0.03
MP:0006413	increased T cell apoptosis	0.03
ENSG00000211949	ENSG00000211949 PPI subnetwork	0.03
ENSG00000125731	SH2D3A PPI subnetwork	0.03
MP:0000414	alopecia	0.03
ENSG00000160691	SHC1 PPI subnetwork	0.03

Original gene set ID	Original gene set description	DEPICT Nominal P-value
MP:0001282	short vibrissae	0.03
MP:0003996	clonic seizures	0.03
ENSG00000019991	HGF PPI subnetwork	0.03
MP:0010025	decreased total body fat amount	0.03
GO:0007568	aging	0.03
GO:0042809	vitamin D receptor binding	0.03
MP:0005331	insulin resistance	0.03
GO:0045682	regulation of epidermis development	0.03
MP:0001923	reduced female fertility	0.03
MP:0001219	thick epidermis	0.03
ENSG00000068615	REEP1 PPI subnetwork	0.03
ENSG000000171219	CDC42BPG PPI subnetwork	0.03
MP:0009583	increased keratinocyte proliferation	0.03
ENSG000000105810	CDK6 PPI subnetwork	0.03
ENSG000000105662	CRTC1 PPI subnetwork	0.03
MP:0003957	abnormal nitric oxide homeostasis	0.03
KEGG	KEGG_small_cell_lung_cancer	0.03
GO:0030669	clathrin-coated endocytic vesicle membrane	0.03
ENSG000000100030	MAPK1 PPI subnetwork	0.03
GO:0046328	regulation of JNK cascade	0.03
GO:0014070	response to organic cyclic compound	0.03
GO:0033500	carbohydrate homeostasis	0.03
GO:0042593	glucose homeostasis	0.03
REACTOME	Reactome_ptm_gamma_carboxylation_hypusine_formation_and_arylsulfatase_activation	0.03
REACTOME	Reactome_regulation_of_signaling_by_cbl	0.03
MP:0002418	increased susceptibility to viral infection	0.03
MP:0003721	increased tumor growth/size	0.03
GO:0071845	cellular component disassembly at cellular level	0.03
GO:0030518	intracellular steroid hormone receptor signaling pathway	0.03
ENSG000000116824	CD2 PPI subnetwork	0.03
MP:0003566	abnormal cell adhesion	0.03
GO:0034061	DNA polymerase activity	0.03
ENSG000000141968	VAV1 PPI subnetwork	0.03
GO:0001701	in utero embryonic development	0.03
MP:0000166	abnormal chondrocyte morphology	0.03
MP:0003400	kinked neural tube	0.03
GO:0000790	nuclear chromatin	0.03
ENSG000000197102	DYNC1H1 PPI subnetwork	0.03
GO:0043566	structure-specific DNA binding	0.03
ENSG000000075413	MARK3 PPI subnetwork	0.03
GO:0000271	polysaccharide biosynthetic process	0.03
REACTOME	Reactome_cell:cell_communication	0.03
MP:0000410	waved hair	0.03
ENSG000000154556	SORBS2 PPI subnetwork	0.03
ENSG000000104368	PLAT PPI subnetwork	0.03
GO:0043123	positive regulation of I-kappaB kinase/NF-kappaB cascade	0.03
ENSG000000156127	BATF PPI subnetwork	0.03

Original gene set ID	Original gene set description	DEPICT Nominal P-value
ENSG00000132470	ITGB4 PPI subnetwork	0.03
GO:0038024	cargo receptor activity	0.03
ENSG00000100014	SPECC1L PPI subnetwork	0.03
ENSG00000163083	INHBB PPI subnetwork	0.03
ENSG00000110931	CAMKK2 PPI subnetwork	0.03
MP:0002088	abnormal embryonic growth/weight/body size	0.03
GO:0016571	histone methylation	0.03
GO:0033559	unsaturated fatty acid metabolic process	0.03
MP:0005350	increased susceptibility to autoimmune disorder	0.03
ENSG00000136111	TBC1D4 PPI subnetwork	0.03
REACTOME	Reactome_nephrin_interactions	0.03
ENSG00000182195	LDOC1 PPI subnetwork	0.03
ENSG00000123685	BATF3 PPI subnetwork	0.03
ENSG00000215699	ENSG00000215699 PPI subnetwork	0.03
GO:0005720	nuclear heterochromatin	0.03
ENSG00000092969	TGFB2 PPI subnetwork	0.03
KEGG	KEGG_ECM_receptor_interaction	0.03
MP:0001201	translucent skin	0.03
GO:0016278	lysine N-methyltransferase activity	0.03
GO:0016279	protein-lysine N-methyltransferase activity	0.03
ENSG00000196586	MYO6 PPI subnetwork	0.03
GO:0004702	receptor signaling protein serine/threonine kinase activity	0.03
ENSG00000072518	MARK2 PPI subnetwork	0.03
ENSG00000165025	SYK PPI subnetwork	0.03
MP:0002109	abnormal limb morphology	0.03
ENSG00000157764	BRAF PPI subnetwork	0.03
ENSG00000152256	PDK1 PPI subnetwork	0.03
ENSG00000065618	COL17A1 PPI subnetwork	0.04
ENSG00000169220	RGS14 PPI subnetwork	0.04
ENSG00000100311	PDGFB PPI subnetwork	0.04
ENSG00000134202	GSTM3 PPI subnetwork	0.04
ENSG00000142515	KLK3 PPI subnetwork	0.04
MP:0002619	abnormal lymphocyte morphology	0.04
ENSG00000161395	PGAP3 PPI subnetwork	0.04
ENSG00000145431	PDGFC PPI subnetwork	0.04
ENSG00000170962	PDGFD PPI subnetwork	0.04
ENSG00000153879	CEBPG PPI subnetwork	0.04
ENSG00000077380	DYNC1I2 PPI subnetwork	0.04
ENSG00000197122	SRC PPI subnetwork	0.04
MP:0004399	abnormal cochlear outer hair cell morphology	0.04
ENSG00000174996	KLC2 PPI subnetwork	0.04
MP:0002376	abnormal dendritic cell physiology	0.04
MP:0000709	enlarged thymus	0.04
MP:0008706	decreased interleukin-6 secretion	0.04
MP:0004686	decreased length of long bones	0.04
GO:0050810	regulation of steroid biosynthetic process	0.04
ENSG00000138396	ENSG00000138396 PPI subnetwork	0.04

Original gene set ID	Original gene set description	DEPICT Nominal P-value
ENSG00000148400	NOTCH1 PPI subnetwork	0.04
ENSG00000137171	KLC4 PPI subnetwork	0.04
ENSG00000196396	PTPN1 PPI subnetwork	0.04
ENSG00000148672	GLUD1 PPI subnetwork	0.04
GO:0000975	regulatory region DNA binding	0.04
GO:0001067	regulatory region nucleic acid binding	0.04
GO:0022411	cellular component disassembly	0.04
ENSG00000026025	VIM PPI subnetwork	0.04
ENSG00000061273	HDAC7 PPI subnetwork	0.04
ENSG00000104067	TJP1 PPI subnetwork	0.04
MP:0004813	absent linear vestibular evoked potential	0.04
ENSG00000091136	LAMB1 PPI subnetwork	0.04
KEGG	KEGG_renal_cell_carcinoma	0.04
KEGG	KEGG_focal_adhesion	0.04
GO:0031581	hemidesmosome assembly	0.04
ENSG00000141068	KSR1 PPI subnetwork	0.04
MP:0004214	abnormal long bone diaphysis morphology	0.04
ENSG00000123836	PFKFB2 PPI subnetwork	0.04
ENSG00000168090	COPS6 PPI subnetwork	0.04
ENSG00000132356	PRKAA1 PPI subnetwork	0.04
GO:0031093	platelet alpha granule lumen	0.04
GO:0048545	response to steroid hormone stimulus	0.04
MP:0003109	short femur	0.04
ENSG00000113758	DBN1 PPI subnetwork	0.04
GO:0008276	protein methyltransferase activity	0.04
MP:0003383	abnormal gluconeogenesis	0.04
ENSG00000162614	NEXN PPI subnetwork	0.04
ENSG00000162614	NEXN PPI subnetwork	0.04
ENSG00000169641	LUZP1 PPI subnetwork	0.04
MP:0002152	abnormal brain morphology	0.04
ENSG00000204257	HLA-DMA PPI subnetwork	0.04
ENSG00000206229	ENSG00000206229 PPI subnetwork	0.04
ENSG00000206293	ENSG00000206293 PPI subnetwork	0.04
ENSG00000138439	FAM117B PPI subnetwork	0.04
GO:0006636	unsaturated fatty acid biosynthetic process	0.04
ENSG00000176444	CLK2 PPI subnetwork	0.04
MP:0000703	abnormal thymus morphology	0.04
REACTOME	Reactome_zinc_transporters	0.04
ENSG00000125952	MAX PPI subnetwork	0.04
GO:0046456	icosanoid biosynthetic process	0.04
ENSG00000132964	CDK8 PPI subnetwork	0.04
MP:0008688	decreased interleukin-2 secretion	0.04
ENSG00000196218	RYR1 PPI subnetwork	0.04
MP:0004770	abnormal synaptic vesicle recycling	0.04
ENSG00000121879	PIK3CA PPI subnetwork	0.04
ENSG00000196735	HLA-DQA1 PPI subnetwork	0.04
MP:0009355	increased liver triglyceride level	0.04

Original gene set ID	Original gene set description	DEPICT Nominal P-value
MP:0009399	increased skeletal muscle fiber size	0.04
ENSG00000160678	S100A1 PPI subnetwork	0.04
ENSG00000064999	ANKS1A PPI subnetwork	0.04
ENSG00000173327	MAP3K11 PPI subnetwork	0.04
GO:0051183	vitamin transporter activity	0.04
GO:0006690	icosanoid metabolic process	0.04
ENSG00000134363	FST PPI subnetwork	0.04
GO:0060053	neurofilament cytoskeleton	0.04
ENSG00000151914	DST PPI subnetwork	0.04
ENSG00000189079	ARID2 PPI subnetwork	0.04
ENSG00000065559	MAP2K4 PPI subnetwork	0.05
ENSG00000120709	FAM53C PPI subnetwork	0.05
MP:0002110	abnormal digit morphology	0.05
GO:0005976	polysaccharide metabolic process	0.05
ENSG00000054523	KIF1B PPI subnetwork	0.05
ENSG00000100906	NFKBIA PPI subnetwork	0.05
ENSG00000136518	ACTL6A PPI subnetwork	0.05
GO:0004709	MAP kinase kinase kinase activity	0.05
GO:0060711	labyrinthine layer development	0.05
KEGG_	KEGG_circadian_rhythm_mammal	0.05
REACTOME	Reactome_classical_antibody:mediated_complement_activation	0.05
ENSG00000211979	ENSG00000211979 PPI subnetwork	0.05
ENSG00000211973	ENSG00000211973 PPI subnetwork	0.05
ENSG00000172534	HCFC1 PPI subnetwork	0.05
ENSG00000136270	TBRG4 PPI subnetwork	0.05
GO:0032648	regulation of interferon-beta production	0.05
GO:0034375	high-density lipoprotein particle remodeling	0.05
ENSG00000185811	IKZF1 PPI subnetwork	0.05
ENSG00000198802	ENSG00000198802 PPI subnetwork	0.05
MP:0006262	testis tumor	0.05
ENSG00000171992	SYNPO PPI subnetwork	0.05
ENSG00000213341	CHUK PPI subnetwork	0.05
ENSG00000175197	DDIT3 PPI subnetwork	0.05
MP:0005150	cachexia	0.05
GO:0043122	regulation of I-kappaB kinase/NF-kappaB cascade	0.05
GO:0097006	regulation of plasma lipoprotein particle levels	0.05
ENSG00000162772	ATF3 PPI subnetwork	0.05
GO:0000122	negative regulation of transcription from RNA polymerase II promoter	0.05
GO:0005858	axonemal dynein complex	0.05
ENSG00000051382	PIK3CB PPI subnetwork	0.05
GO:0043405	regulation of MAP kinase activity	0.05
MP:0008722	abnormal chemokine secretion	0.05
KEGG	KEGG_chronic_myeloid_leukemia	0.05
REACTOME	Reactome_regulated_PROTEOLYSIS_OF_P75NTR	0.05
GO:0043588	skin development	0.05
GO:0010627	regulation of intracellular protein kinase cascade	0.05
GO:0044212	transcription regulatory region DNA binding	0.05

Original gene set ID	Original gene set description	DEPICT Nominal P-value
GO:0030027	lamellipodium	0.05
ENSG00000105976	MET PPI subnetwork	0.05
MP:0002792	abnormal retinal vasculature morphology	0.05
MP:0000069	kyphoscoliosis	0.05
GO:0034339	regulation of transcription from RNA polymerase II promoter by nuclear hormone receptor	0.05
ENSG00000141551	CSNK1D PPI subnetwork	0.05
MP:0005108	abnormal ulna morphology	0.05
MP:0002419	abnormal innate immunity	0.05
GO:0016757	transferase activity, transferring glycosyl groups	0.05
ENSG00000161800	RACGAP1 PPI subnetwork	0.05
MP:0006387	abnormal T cell number	0.05
GO:0005089	Rho guanyl-nucleotide exchange factor activity	0.05
ENSG00000117984	CTSD PPI subnetwork	0.05
ENSG00000105971	CAV2 PPI subnetwork	0.05
ENSG00000115085	ZAP70 PPI subnetwork	0.05
MP:0004609	vertebral fusion	0.05
ENSG00000135862	LAMC1 PPI subnetwork	0.05
MP:0003449	abnormal intestinal goblet cell morphology	0.05
MP:0002687	oligozoospermia	0.05
MP:0000714	increased thymocyte number	0.05
ENSG00000133030	MPRIIP PPI subnetwork	0.05
ENSG00000079841	RIMS1 PPI subnetwork	0.05
ENSG00000130638	ATXN10 PPI subnetwork	0.05
MP:0002656	abnormal keratinocyte differentiation	0.05
ENSG00000129691	ASH2L PPI subnetwork	0.05
MP:0002650	abnormal ameloblast morphology	0.05
ENSG00000135503	ACVR1B PPI subnetwork	0.05
GO:0004715	non-membrane spanning protein tyrosine kinase activity	0.05
ENSG00000001497	LAS1L PPI subnetwork	0.05
GO:0018024	histone-lysine N-methyltransferase activity	0.05
GO:0000792	heterochromatin	0.05
ENSG00000111961	SASH1 PPI subnetwork	0.05
MP:0008840	abnormal spike wave discharge	0.05
ENSG00000139514	SLC7A1 PPI subnetwork	0.05
GO:0007249	I-kappaB kinase/NF-kappaB cascade	0.05

Functional effects of SNPs at AAA loci

1: Expression SNP database lookup (Online Table XIX)

Evidence for functional effects of AAA associated SNPs/loci was sought in two eQTL datasets curated by Andrew Johnson at the NIH National Heart Lung and Blood Institute, Framingham, USA. Firstly, index and proxy SNPs were queried in a collected database of expression SNP (eSNP) results. The collected eSNP results met criteria for statistical thresholds for association with gene transcript levels as described in the original papers. A general overview of a subset of >50 eQTL studies has been published¹⁰⁹, with specific citations for >100 studies included in the current query following here:

Blood cell related eQTL studies included fresh lymphocytes¹¹⁰, fresh leukocytes¹¹¹, leukocyte samples in individuals with Celiac disease¹¹², whole blood samples¹¹³⁻¹²⁶, lymphoblastoid cell lines (LCL) derived from asthmatic children^{127, 128}, HapMap LCL from 3 populations¹²⁹, a separate study on HapMap CEU LCL¹³⁰, additional LCL population samples¹³¹⁻¹³⁶, CD19⁺ B cells¹³⁷, primary PHA-stimulated T cells^{133, 135}, CD4⁺ T cells¹³⁸, peripheral blood monocytes^{137, 139, 140} and CD14⁺ monocytes before and after stimulation with LPS or interferon-gamma¹⁴¹, CD11⁺ dendritic cells before and after *Mycobacterium tuberculosis* infection¹⁴² and a separate study of dendritic cells before or after stimulation with LPS, influenza or interferon-beta¹⁴³. Micro-RNA QTLs¹⁴⁴ and DNase-I QTLs¹⁴⁵ were also queried for LCL.

Non-blood cell tissue eQTLs searched included omental and subcutaneous adipose^{115, 134, 146, 147}, stomach¹⁴⁷, endometrial carcinomas¹⁴⁸, ER+ and ER- breast cancer tumor cells¹⁴⁹, liver^{147, 150-153}, osteoblasts¹⁵⁴, intestine¹⁵⁵ and normal and cancerous colon¹⁵⁶, skeletal muscle¹⁵⁷, breast tissue (normal and cancer)^{158, 159}, lung^{146, 160, 161}, skin^{134, 146, 162}, primary fibroblasts^{133, 135, 163}, sputum¹⁶⁴, pancreatic islet cells¹⁶⁵ and heart tissue from left ventricles^{146, 166} and left and right atria¹⁶⁷. Micro-RNA QTLs were also queried for gluteal and abdominal adipose¹⁶⁸ and liver¹⁶⁹. Further mRNA and micro-RNA QTLs were queried from ER+ invasive breast cancer samples, colon-, kidney renal clear-, lung- and prostate-adenocarcinoma samples¹⁷⁰.

Brain eQTL studies included brain cortex^{139, 171, 172}, cerebellar cortex¹⁷³, cerebellum^{172, 174-177}, frontal cortex^{173, 175, 176}, gliomas¹⁷⁸, hippocampus^{173, 176}, inferior olivary nucleus (from medulla)¹⁷³, intralobular white matter¹⁷³, occipital cortex¹⁷³, parietal lobe¹⁷⁴, pons¹⁷⁵, pre-frontal cortex^{176, 177, 179, 180}, putamen (at the level of anterior commissure)¹⁷³, substantia nigra¹⁷³, temporal cortex^{172, 173, 175, 176}, thalamus¹⁷⁶ and visual cortex¹⁷⁷.

Secondly, additional eQTL data were integrated from online sources including ScanDB, the Broad Institute GTex browser, and the Pritchard Lab (eqtl.uchicago.edu). Cerebellum, parietal lobe and liver eQTL data was downloaded from ScanDB and cis-eQTLs were limited to those with $P < 1.0 \times 10^{-6}$ and trans-eQTLs with $P < 5.0 \times 10^{-8}$. The top 1000 eQTL results were downloaded from the GTex Browser at the Broad Institute for 9 tissues on 11/26/2013: thyroid, leg skin (sun exposed), tibial nerve, tibial artery, skeletal muscle, lung, heart (left ventricle), whole blood, and subcutaneous adipose¹⁴⁶. All GTex results had associations with $P < 8.4 \times 10^{-7}$.

2: eQTL lookup in the Advanced Study of Aortic Pathology (Online Table XX and Online Figure III)

eQTL data were obtained from the Advanced Study of Aortic Pathology (ASAP) dataset which has previously been described¹⁸¹. Tissue samples were selected from individuals undergoing aortic valve surgery. Five tissue types were collected from each patient: mammary artery, liver, aorta intima-media, aorta adventitia, and heart. RNA was extracted from tissues and hybridised to Affymetrix ST 1.0 exon arrays (Santa Clara, CA, USA) and data were robust multiarray average normalised before log₂ transformation. DNA extracted from whole blood was genotyped on the Illumina 610w-Quad

bead array (San Diego, CA, USA) platform. SNPs with >95% call rate were used for imputation, and imputed SNPs with quality scores of MACH <0.3 were excluded from analysis. An additive model for associations between SNPs and gene expression was assumed. Genotypes for 5 of the 10 lead SNPs at AAA risk loci were directly genotyped on Illumina 610wQuad arrays.

3: RNA-seq (Online Table XXI)

RNA-seq data were obtained from the Stockholm-Tartu Atherosclerosis Reverse Network Engineering Task (STARNET) database¹⁸² (<http://www.mountsinai.org/profiles/johan-bjorkegren>). These consist of RNA-seq data from 9 cardiovascular tissues from up to 600 CAD patients obtained during coronary artery by-pass grafting surgery. Gene expression was measured with a standard RNA-seq protocol, followed by normalization of raw read counts to adjust for library size and batch effects. Adjusted read counts were subsequently log₂-transformed, and the association between genotype and expression was tested using a linear model. Permutation was used to assess the statistical significance. Significant results for the lead SNPs at each AAA risk locus are shown in **Online Table XX**.

4: Peripheral blood monocyte eQTL analysis (Online Table XXII)

Data from an eQTL analysis of peripheral blood monocytes was obtained from the Cardiogenics Consortium^{183, 184}. The description of the cohort sample collection and processing and the eQTL analysis have previously been described in detail. Briefly, genome-wide expression and genotype data were obtained from peripheral blood monocytes from 363 patients with CAD or myocardial infarction and 395 healthy individuals. Expression profiling was performed using the Illumina HumanRef-8 v3 beadchip array (Illumina Inc., San Diego, CA) containing 24,516 probes corresponding to 18,311 distinct genes and 21,793 Ref Seq annotated transcripts. Genome-wide genotyping was carried out using two Illumina arrays, the Sentrix Human Custom 1.2M array and the Human 610 Quad Custom array. SNP analysis was restricted to autosomal SNPs with MAF >0.01, call rate >0.95 and HWE testing $P > 1 \times 10^{-5}$. After quality control, 522,603 SNPs were used for association analyses with expression. All replicated AAA associated SNPs were tested for association with regional gene expression. Significant results are shown in **Online Table XXII**.

Online Table XIX: eQTL data (1). This table spans 2 pages.

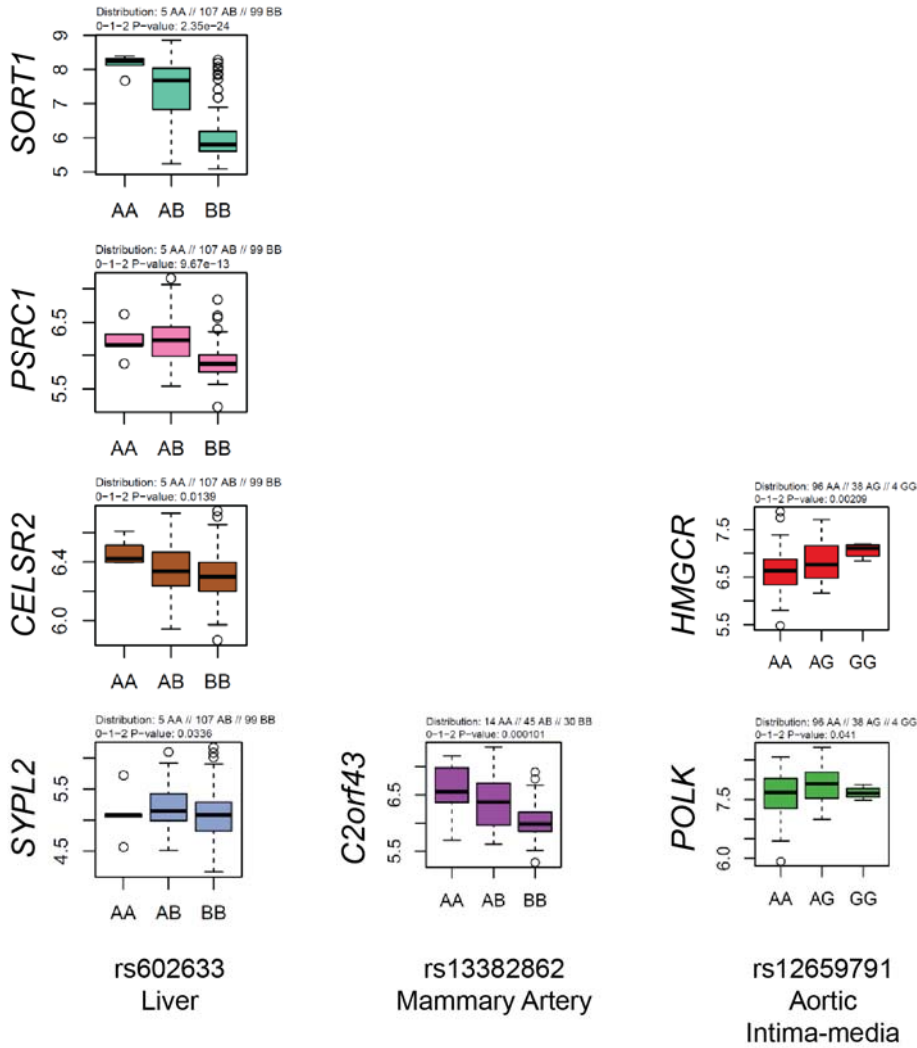
Locus	Lead AAA SNP	Gene	Tissue	Transcript	Proxy SNP looked up in eQTL database			Peak regional SNP in eQTL database					
					Proxy SNP	r2 to AAA SNP	eQTL P-Value for lead AAA SNP or proxy	Peak SNP	r2 (Peak SNP to AAA SNP)	eQTL P-Value for peak SNP			
1q21.3	rs4129267	IL6R	Average in 10 brain regions [PMID 25174004]	INTS3	rs4576655	1	5.59x10 ⁻⁰⁶	rs12068901	NA	3.32x10 ⁻⁴²			
			Average in 10 brain regions [PMID 25174004]	SLC39A1	rs4845372	0.965	4.75x10 ⁻⁰⁶	rs4845372	0.965	4.75x10 ⁻⁰⁶			
			Average in 10 brain regions [PMID 25174004]	PYGO2	rs6684439	0.839	2.96x10 ⁻⁰⁶	rs6684439	0.839	2.96x10 ⁻⁰⁶			
			CD14+ monocytes (untreated) [PMID 24604202]	IL6R			6.64x10 ⁻⁰⁴	rs7518199	0.965	5.27x10 ⁻⁰⁴			
			Intestine (normal ileum) [PMID 23474282]	IL6R			8.81x10 ⁻⁰⁶	rs7553796	0.49	8.20x10 ⁻¹¹			
			Lymph [PMID 17873875]	IL6R	rs4537545	1	2.63x10 ⁻⁰³	rs4845623	0.965	1.88x10 ⁻⁰³			
			Prefrontal cortex (all samples) [PMID 23622250]	MUC1	rs8192284	0.982	6.33x10 ⁻⁰⁵	rs8192284	0.982	6.33x10 ⁻⁰⁵			
			Whole blood (Battle) [PMID 24092820]	IL6R	rs4537545	1	2.62x10 ⁻²⁰	rs4537545	1	2.62x10 ⁻²⁰			
			Whole blood (CHARGE) [PMID 24013639]	IL6R			3.15x10 ⁻²⁷	rs4537545	1	2.02x10 ⁻²⁹			
			Whole blood (CHARGE) [PMID 24013639]	UBE2Q1			9.75x10 ⁻⁰⁸	rs6660775	0.058	3.93x10 ⁻²¹			
			1p13.3	rs602633	CELSR2/SORT1	CD14+ monocytes (24h LPS stimulated) [PMID 24604202]	PSRC1	rs599839	1	9.50x10 ⁻⁰⁵	rs646776	0.895	3.53x10 ⁻⁰⁵
						CD14+ monocytes (IFNg stimulated) [PMID 24604202]	PSRC1	rs599839	1	4.25x10 ⁻¹³	rs646776	0.895	7.40x10 ⁻¹⁴
						CD14+ monocytes (untreated) [PMID 24604202]	PSRC1	rs599839	1	7.31x10 ⁻⁴⁴	rs599839	1	7.31x10 ⁻⁴⁴
						Cerebellum (all samples) [PMID 23622250]	PSRC1			9.12x10 ⁻⁰⁶	rs602633	Same SNP	9.12x10 ⁻⁰⁶
Cerebellum (Huntington's) [PMID 23622250]	PSRC1	rs646776				0.895	5.19x10 ⁻⁰⁵	rs646776	0.895	5.19x10 ⁻⁰⁵			
Liver (ScanDB)	SORT1	rs646776				0.895	3.18x10 ⁻⁴³	rs646776	0.895	3.18x10 ⁻⁴³			
Liver (ScanDB)	PSRC1	rs646776				0.895	2.92x10 ⁻³⁷	rs646776	0.895	2.92x10 ⁻³⁷			
Liver (ScanDB)	CELSR2	rs646776				0.895	4.48x10 ⁻²⁴	rs646776	0.895	4.48x10 ⁻²⁴			
Liver (Greenawalt) [PMID 21602305]	SORT1	rs646776				0.895	5.20x10 ⁻⁸⁸	rs646776	0.895	5.20x10 ⁻⁸⁸			
Liver (Greenawalt) [PMID 21602305]	PSRC1	rs646776				0.895	3.05x10 ⁻⁸⁶	rs646776	0.895	3.05x10 ⁻⁸⁶			
Liver (Greenawalt) [PMID 21602305]	CELSR2	rs646776				0.895	6.27x10 ⁻⁶⁸	rs646776	0.895	6.27x10 ⁻⁶⁸			
Liver (Schroder) [PMID 22006096]	SORT1	rs646776				0.895	2.14x10 ⁻²⁷	rs646776	0.895	2.14x10 ⁻²⁷			
Liver (Schroder) [PMID 22006096]	CELSR2	rs646776				0.895	3.66x10 ⁻²²	rs646776	0.895	3.66x10 ⁻²²			
Liver (Schroder) [PMID 22006096]	PSRC1	rs646776				0.895	8.72x10 ⁻¹⁷	rs646776	0.895	8.72x10 ⁻¹⁷			
Liver (UChicago) [PMID 21637794]	CELSR2	rs12740374				0.895	<1x10 ⁻¹⁶	rs12740374	0.895	<1e ⁻¹⁶			
Liver (UChicago) [PMID 21637794]	SORT1	rs12740374				0.895	<1x10 ⁻¹⁶	rs12740374	0.895	<1e ⁻¹⁶			
Liver (UWash) [PMID 21637794]	SORT1	rs12740374				0.895	2.86x10 ⁻²²	rs12740374	0.895	2.86x10 ⁻²²			
Liver (UWash) [PMID 21637794]	CELSR2	rs12740374				0.895	5.31x10 ⁻¹¹	rs12740374	0.895	5.31x10 ⁻¹¹			
Lymph [PMID 17873875]	PSRC1	rs646776				0.895	2.10x10 ⁻⁰⁸	rs646776	0.895	2.10x10 ⁻⁰⁸			
Monocytes (CD14+) [PMID 22446964]	PSRC1	rs599839				1	6.65x10 ⁻¹⁸	rs599839	1	6.65x10 ⁻¹⁸			
Monocytes [PMID 20502693]	PSRC1	rs599839				1	5.30x10 ⁻⁵⁵	rs629301	0.895	2.34x10 ⁻⁵⁶			
Muscle_Skeletal [PMID 23715323]	CELSR2	rs12740374				0.895	1.40x10 ⁻⁰⁸	rs12740374	0.895	1.40x10 ⁻⁰⁸			
Prefrontal cortex (all samples) [PMID 23622250]	CELSR2	rs646776				0.895	4.10x10 ⁻¹⁰	rs646776	0.895	4.10x10 ⁻¹⁰			
Prefrontal cortex (all samples) [PMID 23622250]	PSRC1	rs646776				0.895	1.67x10 ⁻⁰⁹	rs646776	0.895	1.67x10 ⁻⁰⁹			
Prefrontal cortex (Alzheimer's) [PMID 23622250]	PSRC1	rs646776				0.895	7.93x10 ⁻⁰⁸	rs646776	0.895	7.93x10 ⁻⁰⁸			
Prefrontal cortex (Alzheimer's) [PMID 23622250]	CELSR2	rs646776				0.895	3.24x10 ⁻⁰⁵	rs646776	0.895	3.24x10 ⁻⁰⁵			
Prefrontal cortex (Huntington's) [PMID 23622250]	CELSR2						1.52x10 ⁻⁰⁶	rs602633	Same SNP	1.52x10 ⁻⁰⁶			
PrefrontalCortex [PMID 20351726]	PSRC1	rs599839				1	2.62x10 ⁻⁰⁶	rs599839	1	2.62x10 ⁻⁰⁶			
SchadtLiver [PMID 18462017]	SORT1	rs599839	1	1.52x10 ⁻⁵⁶	rs599839	1	1.52x10 ⁻⁵⁶						
SchadtLiver [PMID 18462017]	CELSR2	rs646776	0.895	3.09x10 ⁻²⁴	rs646776	0.895	3.09x10 ⁻²⁴						
SubCutAdipose (Greenawalt) [PMID 21602305]	CELSR2			2.93x10 ⁻⁰⁸	rs602633	Same SNP	2.93x10 ⁻⁰⁸						

			Visual cortex (all samples) [PMID 23622250]	<i>PSRC1</i>	rs646776	0.895	7.66x10 ⁻¹¹	rs646776	0.895	7.66x10 ⁻¹¹
			Visual cortex (Alzheimer's) [PMID 23622250]	<i>PSRC1</i>	rs646776	0.895	1.44x10 ⁻⁰⁹	rs646776	0.895	1.44x10 ⁻⁰⁹
			Whole blood (Battle) [PMID 24092820]	<i>PSRC1</i>	rs599839	1	4.93x10 ⁻⁸⁷	rs599839	1	4.93x10 ⁻⁸⁷
			Whole blood (Schramm et al.) [PMID 24740359]	<i>PSRC1</i>	rs599839	1	1.23x10 ⁻²⁴	rs599839	1	1.23x10 ⁻²⁴
			Whole blood (Wright, n=4,647) [PMID 24728292]	<i>CELSR2</i>	rs629301	0.895	6.73x10 ⁻¹⁸	rs629301	0.895	6.73x10 ⁻¹⁸
9p21	rs10757274	<i>ANRIL</i>	SubCutAdipose(Greenawalt) [PMID 21602305]	<i>CDKN2B</i>	rs1537370	0.901	1.48x10 ⁻⁰⁴	rs1537370	Same SNP	1.48x10 ⁻⁰⁴
			Omental adipose [PMID 21602305]	<i>CDKN2B</i>	rs2383207	0.846	3.10x10 ⁻⁰⁷	rs2383207	Same SNP	3.10x10 ⁻⁰⁷
9q33.2	rs10985349	<i>DAB2IP</i>	CD14+ monocytes (2h LPS stimulated) [PMID 24604202]	<i>GGTA1</i>			6.64x10 ⁻⁰⁴	rs10985349	Same SNP	6.64x10 ⁻⁰⁴
20q13.12	rs3827066	Near <i>PCIF1/MMP9/ZNF335</i>	Bcells (CD19+) [PMID 22446964]	<i>PLTP</i>			2.98x10 ⁻⁰⁹	rs394643	0.229	9.89x10 ⁻⁴⁰
			CD14+ monocytes (24h LPS stimulated) [PMID 24604202]	<i>PLTP</i>			2.46x10 ⁻¹¹	rs3827066	Same SNP	2.46x10 ⁻¹¹
			CD14+ monocytes (24h LPS stimulated) [PMID 24604202]	<i>DNTTIP1</i>			8.41x10 ⁻⁰⁹	rs2664529	0.108	1.02x10 ⁻⁶³
			CD14+ monocytes (2h LPS stimulated) [PMID 24604202]	<i>PLTP</i>			3.89x10 ⁻¹¹	rs3843763	0.506	2.46x10 ⁻¹³
			CD14+ monocytes (2h LPS stimulated) [PMID 24604202]	<i>DNTTIP1</i>			9.56x10 ⁻¹⁰	rs2664529	0.108	1.60x10 ⁻⁶³
			CD14+ monocytes (IFNg stimulated) [PMID 24604202]	<i>PLTP</i>			2.20x10 ⁻⁴³	rs3827066	Same SNP	2.20x10 ⁻⁴³
			CD14+ monocytes (IFNg stimulated) [PMID 24604202]	<i>DNTTIP1</i>			2.68x10 ⁻¹⁰	rs6032531	0.148	8.85x10 ⁻⁷⁶
			CD14+ monocytes (IFNg stimulated) [PMID 24604202]	<i>PLTP</i>			8.25x10 ⁻⁰⁷	rs3827066	Same SNP	2.20x10 ⁻⁴³
			CD14+ monocytes (untreated) [PMID 24604202]	<i>DNTTIP1</i>			3.69x10 ⁻⁰⁹	rs6032531	0.148	1.11x10 ⁻⁴⁹
			CD14+ monocytes (untreated) [PMID 24604202]	<i>CD40</i>			4.03x10 ⁻⁰⁴	rs745307	0.086	4.24x10 ⁻⁸⁸
			LCL (MuTHER) [PMID 22941192]	<i>PLTP</i>			1.20x10 ⁻⁰⁶	rs441346	0.214	1.64x10 ⁻³⁷
			Liver(UChicago) [PMID 21637794]	<i>NEURL2</i>			2.29x10 ⁻⁰⁶	rs3827066	Same SNP	2.29x10 ⁻⁰⁶
			Liver(UChicago) [PMID 21637794]	<i>C20orf165</i>	rs7270354	1	1.22x10 ⁻⁰³	rs7270354	1	1.22x10 ⁻⁰³
			Liver(UWash) [PMID 21637794]	<i>NEURL2</i>			1.02x10 ⁻⁰³	rs3827066	Same SNP	1.02x10 ⁻⁰³
			Peripheral artery plaque [PMID 24973796]	<i>NEURL2</i>	rs7270354	1	2.51x10 ⁻⁰⁸	rs7270354	1	2.51x10 ⁻⁰⁸
			Skin (MuTHER) [PMID 22941192]	<i>WFDC3</i>			2.60x10 ⁻¹²	rs2664529	0.108	5.47x10 ⁻⁷⁴
			Subc adipose (MuTHER) [PMID 22941192]	<i>PLTP</i>			6.67x10 ⁻¹¹	rs6104410	0.486	2.62x10 ⁻¹¹
			Subc adipose (MuTHER) [PMID 22941192]	<i>NEURL2</i>			9.51x10 ⁻⁰⁹	rs3827066	Same SNP	9.51x10 ⁻⁰⁹
			Subc adipose (MuTHER) [PMID 22941192]	<i>WFDC3</i>			1.26x10 ⁻⁰⁵	rs6032544	0.11	5.99x10 ⁻³⁶
			Whole blood (CHARGE) [PMID 24013639]	<i>TNNC2</i>			3.98x10 ⁻¹⁹	rs6104350	0.11	3.33x10 ⁻⁶³
			Whole blood (CHARGE) [PMID 24013639]	<i>DNTTIP1</i>			2.52x10 ⁻¹⁴	rs6104350	0.11	7.89x10 ⁻⁷¹

Online Table XX: eQTL from the Advanced Study of Aortic Pathology¹⁸¹.

Chr	SNP	Position	Imputed (quality score)	Genes	Aortic Adventitia (Effect, P, Quartile)	Aortic Media (Effect, P, Quartile)	Heart (Effect, P, Quartile)	Liver (Effect, P, Quartile)	LIMA (Effect, P, Quartile)
1	rs1795061	214409280	Yes (0.7908)	<i>PROX1</i>	0.0264, 0.764, 2	-0.008, 0.82, 1	-0.0534, 0.449, 4	0.0132, 0.801, 4	0.0565, 0.234, 1
				<i>SMYD2</i>	0.0597, 0.237, 2	-0.0871, 0.0694, 2	0.0254, 0.643, 4	-0.0408, 0.285, 3	-0.0632, 0.302, 2
				<i>PTPN14</i>	-0.071, 0.116, 4	-0.0158, 0.736, 4	0.024, 0.663, 3	0.0299, 0.251, 2	0.00447, 0.933, 4
1	rs4129267	154426264		<i>UBAP2L</i>	0.00819, 0.814, 4	-0.000356, 0.993, 4	0.0361, 0.579, 4	0.0467, 0.106, 4	0.046, 0.3, 4
				<i>HAX1</i>	0.115, 0.0484, 3	-0.0725, 0.223, 4	0.0377, 0.547, 4	0.0398, 0.291, 4	-0.0667, 0.253, 4
				<i>RNU6-239P</i>	nd	nd	nd	nd	nd
				<i>RNU6-121P</i>	nd	nd	nd	nd	nd
				<i>AQP10</i>	-0.00947, 0.769, 1	-0.0213, 0.494, 1	-0.00645, 0.832, 2	-0.00193, 0.931, 1	0.0217, 0.579, 1
				<i>ATP8B2</i>	0.0769, 0.161, 4	0.0443, 0.32, 4	-0.0216, 0.588, 3	0.0223, 0.446, 3	0.08, 0.161, 4
				<i>IL6R</i>	-0.0261, 0.55, 2	-0.0277, 0.45, 2	-0.028, 0.294, 2	0.0292, 0.49, 4	-0.0128, 0.698, 2
				<i>PSMD8P1</i>	nd	nd	nd	nd	nd
				<i>SHE</i>	nd	nd	nd	nd	nd
				<i>TDRD10</i>	-0.0646, 0.146, 2	-0.0249, 0.465, 2	-0.0246, 0.49, 2	-0.00838, 0.779, 2	0.0332, 0.429, 2
				<i>UBE2Q1</i>	0.0798, 0.0377, 4	-0.0194, 0.636, 4	-0.0343, 0.483, 4	0.0769, 0.0323, 4	0.0562, 0.198, 4
				<i>UBE2Q1-AS1</i>	nd	nd	nd	nd	nd
				<i>CHRN2B</i>	0.0103, 0.758, 2	0.0322, 0.367, 2	-0.0525, 0.17, 2	0.00361, 0.898, 2	0.00785, 0.856, 2
				<i>ADAR</i>	0.0195, 0.674, 4	0.000942, 0.986, 4	0.0382, 0.559, 4	0.055, 0.107, 4	0.0846, 0.146, 4
1	rs602633	109821511	Yes (0.51863)	<i>TMEM167B</i>	nd	nd	nd	nd	nd
				<i>SCARNA2</i>	nd	nd	nd	nd	nd
				<i>C1orf194</i>	nd	nd	nd	nd	nd
				<i>KIAA1324</i>	0.0254, 0.3, 1	0.00596, 0.762, 1	0.0279, 0.189, 1	-0.0172, 0.26, 1	-0.00434, 0.868, 1
				<i>SARS</i>	-0.0594, 0.2, 4	-0.0245, 0.546, 4	-0.0825, 0.2, 4	0.0736, 0.0725, 4	0.0937, 0.087, 4
				<i>CELSR2</i>	0.00668, 0.806, 3	-0.0101, 0.643, 3	0.0198, 0.46, 3	0.0522, 0.0139, 3	-0.0384, 0.208, 3
				<i>PSRC1</i>	0.00324, 0.91, 2	-0.0272, 0.36, 2	0.0288, 0.343, 2	0.281, 9.67x10⁻¹³, 2	0.0057, 0.877, 2
				<i>MYBPHL</i>	nd	nd	nd	nd	nd
				<i>SORT1</i>	-0.145, 0.135, 4	-0.0409, 0.532, 4	-0.203, 0.009, 4	1.25, 2.35x10⁻²⁴, 3	0.0304, 0.648, 4
				<i>PSMA5</i>	-0.137, 0.0753, 3	-0.0474, 0.489, 3	-0.145, 0.0884, 4	0.102, 0.0705, 4	0.131, 0.191, 3
				<i>SYPL2</i>	-0.0904, 0.0412, 1	-0.0385, 0.461, 2	-0.211, 0.0312, 2	0.0977, 0.0336, 2	-0.0657, 0.28, 2
9	rs10757274	22096055	Yes (0.78299)	<i>MTAP</i>	0.0276, 0.416, 3	0.0231, 0.403, 3	0.0554, 0.142, 3	-0.0111, 0.668, 3	0.0137, 0.702, 3
				<i>ERVFRD-3</i>	nd	nd	nd	nd	nd
				<i>CDKN2A-AS1</i>	nd	nd	nd	nd	nd
				<i>CDKN2A</i>	0.0379, 0.215, 2	0.0337, 0.296, 2	-0.0227, 0.449, 2	-0.00872, 0.68, 2	0.022, 0.515, 2
				<i>ANRIL</i>	nd	nd	nd	nd	nd
				<i>CDKN2B</i>	0.0101, 0.728, 3	-0.0237, 0.405, 3	0.000812, 0.979, 3	0.0047, 0.82, 3	0.0369, 0.325, 3
				<i>UBA52P6</i>	nd	nd	nd	nd	nd
9	rs10985349	124425243	Yes (0.58069)	<i>GGTA1P</i>	nd	nd	nd	nd	nd
				<i>RN7SL187P</i>	nd	nd	nd	nd	nd
				<i>HMG1P37</i>	nd	nd	nd	nd	nd
				<i>DAB2IP</i>	0.0586, 0.13, 3	0.0653, 0.11, 3	-0.0288, 0.571, 3	-0.0159, 0.547, 3	-0.0644, 0.0833, 3
				<i>TLLL1</i>	0.0213, 0.64, 3	0.0515, 0.163, 3	-0.0772, 0.0168, 3	0.0161, 0.445, 3	-0.0992, 0.00289, 4
13	rs9316871	22861921		<i>LINC00540</i>	nd	nd	nd	nd	nd
				<i>NME1P1</i>	nd	nd	nd	nd	nd
				<i>MTND3P1</i>	nd	nd	nd	nd	nd
19	rs6511720	11202306		<i>CARM1</i>	0.00983, 0.861, 3	-0.0297, 0.577, 3	-0.00125, 0.987, 3	-0.0163, 0.662, 3	0.0162, 0.744, 3
				<i>YIPF2</i>	0.00883, 0.881, 3	-0.00788, 0.863, 3	-0.0105, 0.871, 3	-0.0461, 0.237, 3	0.0308, 0.624, 3
				<i>C19orf52</i>	-0.0462, 0.458, 3	0.0269, 0.58, 3	-0.023, 0.717, 3	-0.0214, 0.559, 3	-0.0201, 0.772, 3
				<i>SMARCA4</i>	0.0288, 0.569, 3	-0.105, 0.0407, 3	-0.018, 0.787, 3	-0.0268, 0.393, 3	-0.0647, 0.323, 3
				<i>LDLR</i>	0.164, 0.118, 3	0.19, 0.112, 3	-0.0297, 0.634, 3	0.0024, 0.982, 4	0.221, 0.177, 3
				<i>MIR6886</i>	nd	nd	nd	nd	nd
				<i>SPC24</i>	-0.0229, 0.651, 1	0.0159, 0.721, 2	0.0378, 0.507, 2	-0.0246, 0.459, 1	0.0153, 0.781, 2
				<i>KANK2</i>	-0.0233, 0.851, 4	-0.00958, 0.911, 4	0.0425, 0.71, 4	-0.0695, 0.141, 3	-0.0716, 0.395, 4
				<i>DOCK6</i>	-0.018, 0.749, 3	-0.0289, 0.469, 3	-0.0386, 0.526, 3	-0.0229, 0.523, 3	-0.0288, 0.513, 3
				<i>C19orf80</i>	nd	nd	nd	nd	nd
20	rs3827066	44586023	Yes (0.6275)	<i>WFDC3</i>	0.0626, 0.15, 2	0.0772, 0.0433, 2	-0.00286, 0.961, 2	-0.0196, 0.542, 2	0.0407, 0.375, 2
				<i>RNU6ATAC38P</i>	nd	nd	nd	nd	nd
				<i>DNTTIP1</i>	-0.0666, 0.132, 3	-0.0711, 0.0606, 3	-0.0573, 0.316, 3	-0.0781, 0.00627, 3	-0.0715, 0.0459, 3
				<i>UBE2C</i>	0.0147, 0.729, 2	0.0206, 0.616, 2	-0.0565, 0.219, 2	0.0164, 0.538, 2	0.0859, 0.025, 2
				<i>TNNC2</i>	-0.0322, 0.621, 2	0.059, 0.304, 2	0.0675, 0.431, 2	0.007, 0.872, 2	0.121, 0.082, 2
				<i>SNX21</i>	-0.0545, 0.228, 3	0.00543, 0.875, 3	-0.0359, 0.544, 3	-0.00772, 0.773, 3	0.0266, 0.539, 3
				<i>ACOT8</i>	-0.00969, 0.816, 3	0.0458, 0.17, 3	-0.1, 0.277, 3	0.0303, 0.313, 3	-0.024, 0.53, 3
				<i>ZSWIM3</i>	0.0582, 0.209, 1	0.0493, 0.187, 1	-0.0382, 0.563, 1	0.0258, 0.402, 1	-0.00447, 0.922, 1
				<i>ZSWIM1</i>	-0.0458, 0.427, 2	-0.0743, 0.123, 2	-0.0861, 0.374, 2	-0.0159, 0.655, 2	0.0164, 0.78, 2
				<i>SPATA25</i>	nd	nd	nd	nd	nd
				<i>NEURL2</i>	nd	nd	nd	nd	nd
				<i>CTSA</i>	0.0231, 0.616, 4	-0.0716, 0.321, 4	0.0481, 0.487, 4	0.105, 0.0111, 4	-0.141, 0.101, 4
				<i>PLTP</i>	0.513, 0.0118, 4	-0.00838, 0.958, 4	0.0306, 0.832, 4	0.0375, 0.587, 4	-0.0865, 0.561, 3
				<i>PCIF1</i>	-0.0435, 0.361, 3	-0.0633, 0.0975, 3	-0.000238, 0.998, 3	-0.0277, 0.278, 3	-0.042, 0.389, 3
				<i>ZNF335</i>	-0.0467, 0.107, 3	0.0401, 0.123, 3	0.0213, 0.631, 3	0.0105, 0.608, 3	-0.0174, 0.579, 3
				<i>FTLP1</i>	nd	nd	nd	nd	nd
				<i>MMP9</i>	0.107, 0.333, 2	0.168, 0.0796, 2	0.0236, 0.623, 2	0.0107, 0.79, 2	0.0262, 0.566, 2
				<i>SLC12A5</i>	-0.0409, 0.175, 2	-0.00016, 0.995, 2	0.0189, 0.654, 2	-0.00367, 0.866, 1	-0.0206, 0.544, 2
				<i>NCOA5</i>	-0.00203, 0.962, 3	-0.0311, 0.449, 4	-0.0941, 0.29, 3	-0.0339, 0.424, 3	-0.0258, 0.597, 4
				<i>RPL13P2</i>	nd	nd	nd	nd	nd
				<i>CD40</i>	-0.0309, 0.531, 2	-0.0095, 0.813, 2	-0.0416, 0.391, 2	0.0104, 0.681, 2	0.0118, 0.755, 2
21	rs2836411	39819830		<i>KCNJ15</i>	-0.00282, 0.958, 2	-0.0161, 0.634, 1	-0.00692, 0.809, 1	-0.0181, 0.635, 2	-0.0407, 0.236, 1
				<i>LINC01423</i>	nd	nd	nd	nd	nd
				<i>ERG</i>	-0.0351, 0.636, 4	-0.0324, 0.573, 4	0.0247, 0.648, 3	0.0276, 0.309, 3	-0.106, 0.0762, 4
				<i>SNRPGP13</i>	nd	nd	nd	nd	nd

Online Figure III: Significant eQTL plots for data from ASAP study. Each column of plots represents data for the SNP and tissue stated at the bottom of each column. The gene for which expression has been assessed in each plot is shown to the left of each plot.



Online Table XXI: eQTL results based on RNA seq data

Chr	Position	SNP	Locus	Gene(s)	Tissue	gene for RNA-Seq	index SNP	index SNP beta	index SNP P	Lead SNP in region	Lead SNP beta	Lead SNP P	index SNP effect independent
1	109821511	rs602633	1p13.3	CELSR2/SORT1	Blood	PSRC1	rs602633	0.640465606	4.49x10 ⁻¹⁷	rs629301	0.61412198	1.03x10 ⁻¹⁵	Yes
					LIV	PSRC1	rs602633	-1.292449889	9.43x10 ⁻¹⁰	rs7528419	1.26797503	4.33x10 ⁻¹⁰³	Yes
					LIV	SARS	rs602633	0.495537791	2.37x10 ⁻¹²	rs1277930	0.49333558	2.97x10 ⁻¹²	Yes
					LIV	SORT1	rs602633	-1.365654087	2.98x10 ⁻¹³	rs7528419	1.33525433	1.79x10 ⁻¹²²	Yes
					LIV	CELSR2	rs602633	1.298741331	1.79x10 ⁻¹⁰	rs629301	1.27447629	8.75x10 ⁻¹⁰⁵	Yes
1	154426264	rs4129267	1q21.3	IL6R	MAM	IL6R	rs4129267	0.652344491	1.97x10 ⁻²⁶	rs7518199	0.63498045	3.78x10 ⁻²⁴	Yes
13	22861921	rs9316871	13q12.11	LINC00540	MAM	FGF9	rs9316871	-0.699526462	1.76x10 ⁻²³	rs9506822	-0.7027035	2.44x10 ⁻²³	Yes
20	44586023	rs3827066	20q13.12	Near PCIF1/MMP9/ZNF335	AOR	PLTP	rs3827066	-0.756619944	1.65x10 ⁻²¹	rs7267295	-0.7193854	5.40x10 ⁻¹⁸	Yes
					SF	PLTP	rs3827066	-0.905646216	4.93x10 ⁻²⁹	rs7270354	-0.8474133	2.10x10 ⁻²⁶	Yes
					SKLM	PLTP	rs3827066	-0.484882963	2.76x10 ⁻²⁹	rs7267295	-0.4860579	1.40x10 ⁻⁰⁸	Yes
					VAF	PLTP	rs3827066	-0.610415837	1.39x10 ⁻¹²	rs8124182	-0.5513566	1.48x10 ⁻¹⁰	Yes
					MAM	ERG	rs386574671	0.271607451	1.88x10 ⁻⁰⁵	rs386574671	0.27160745	1.88x10 ⁻⁰⁵	Yes

Online Table XXII: Peripheral blood monocyte eQTLs

Chr	Position	SNP	Locus	Gene(s)	Probe_ID	ILMN_Gene	beta	beta_se	P	FDR	Cell type					
1	109821511	rs602633	1p13.3	CELSR2/SORT1	ILMN_1671843	PSRC1	-0.2202	0.0195	7.91x10 ⁻²⁷	1.08x10 ⁻²³	Macrophage					
					ILMN_2315964	PSRC1	-0.0763	0.0168	6.32x10 ⁻⁰⁶	8.65x10 ⁻⁰⁴	Macrophage					
					ILMN_1671843	PSRC1	-0.1512	0.0121	1.96x10 ⁻³²	2.33x10 ⁻²⁹	Monocyte					
					ILMN_2315964	PSRC1	-0.1261	0.0158	4.72x10 ⁻¹⁵	1.83x10 ⁻¹²	Monocyte					
					ILMN_1711208	CELSR2	-0.0696	0.0139	7.41x10 ⁻⁰⁷	1.23x10 ⁻⁰⁴	Macrophage					
					ILMN_1707077	SORT1	-0.0752	0.0183	4.38x10 ⁻⁰⁵	4.95x10 ⁻⁰³	Macrophage					
					ILMN_1671843	PSRC1	-0.2202	0.0195	7.91x10 ⁻²⁷	1.08x10 ⁻²³	Macrophage					
					ILMN_1711208	CELSR2	-0.0696	0.0139	7.41x10 ⁻⁰⁷	1.23x10 ⁻⁰⁴	Macrophage					
					ILMN_2315964	PSRC1	-0.0763	0.0168	6.32x10 ⁻⁰⁶	8.65x10 ⁻⁰⁴	Macrophage					
					ILMN_1707077	SORT1	-0.0752	0.0183	4.38x10 ⁻⁰⁵	4.95x10 ⁻⁰³	Macrophage					
					ILMN_1671843	PSRC1	-0.1512	0.0121	1.96x10 ⁻³²	2.33x10 ⁻²⁹	Monocyte					
					ILMN_2315964	PSRC1	-0.1261	0.0158	4.72x10 ⁻¹⁵	1.83x10 ⁻¹²	Monocyte					
					20	44586023	rs3827066	20q13.12	Near PCIF1/MMP9/ZNF335	ILMN_1777113	NEURL2	-0.1058	0.0255	3.86x10 ⁻⁰⁵	3.11x10 ⁻⁰³	Macrophage
										ILMN_1773389	PLTP	-0.3127	0.0796	9.57x10 ⁻⁰⁵	6.86x10 ⁻⁰³	Macrophage
ILMN_1711748	PLTP	-0.2266	0.0587	1.27x10 ⁻⁰⁴						8.82x10 ⁻⁰³	Macrophage					
ILMN_2367818	CD40	0.0828	0.0245	7.75x10 ⁻⁰⁴						4.08x10 ⁻⁰²	Macrophage					
ILMN_1691117	DNTTIP1	0.0741	0.0109	1.95x10 ⁻¹¹						3.13x10 ⁻⁰⁹	Monocyte					
ILMN_2367818	CD40	0.0752	0.0176	2.20x10 ⁻⁰⁵						1.45x10 ⁻⁰³	Monocyte					
ILMN_1779257	CD40	0.1136	0.0317	3.63x10 ⁻⁰⁴						1.74x10 ⁻⁰²	Monocyte					
21	39819830	rs2836411	21q22.2	ERG	ILMN_1757074	GNG10	-0.0626	0.0138	6.84x10 ⁻⁰⁶	5.28x10 ⁻⁰¹	Monocyte					

VALIDATION OF GWAS3D RESULTS USING mRNA EXPRESSION DATA FOR AAA AND CONTROL AORTA

To determine the potential utility of the GWAS3D chromatin state analysis to identify trans interactions, a validation analysis was performed comparing mRNA expression of putative genes in abdominal aortic tissue. Relative mRNA expression profiles of candidate genes, indicated by either SNP proximity (cis-acting regulatory variant) or GWAS3D predicted distal interaction, was derived using the Biros *et al* 2015 (GSE57691) dataset (**Online Table XXIII**). The composition and analysis of this dataset has been previously described¹⁰⁷. All genes at AAA loci (Table 1) were included in this analysis. Case (49 AAA, including 29 large and 20 small) and control (10 organ donor) abdominal aortic samples were compared using data generated from the Illumina HumanHT-12 V4.0 expression beadchip (GPL10558).

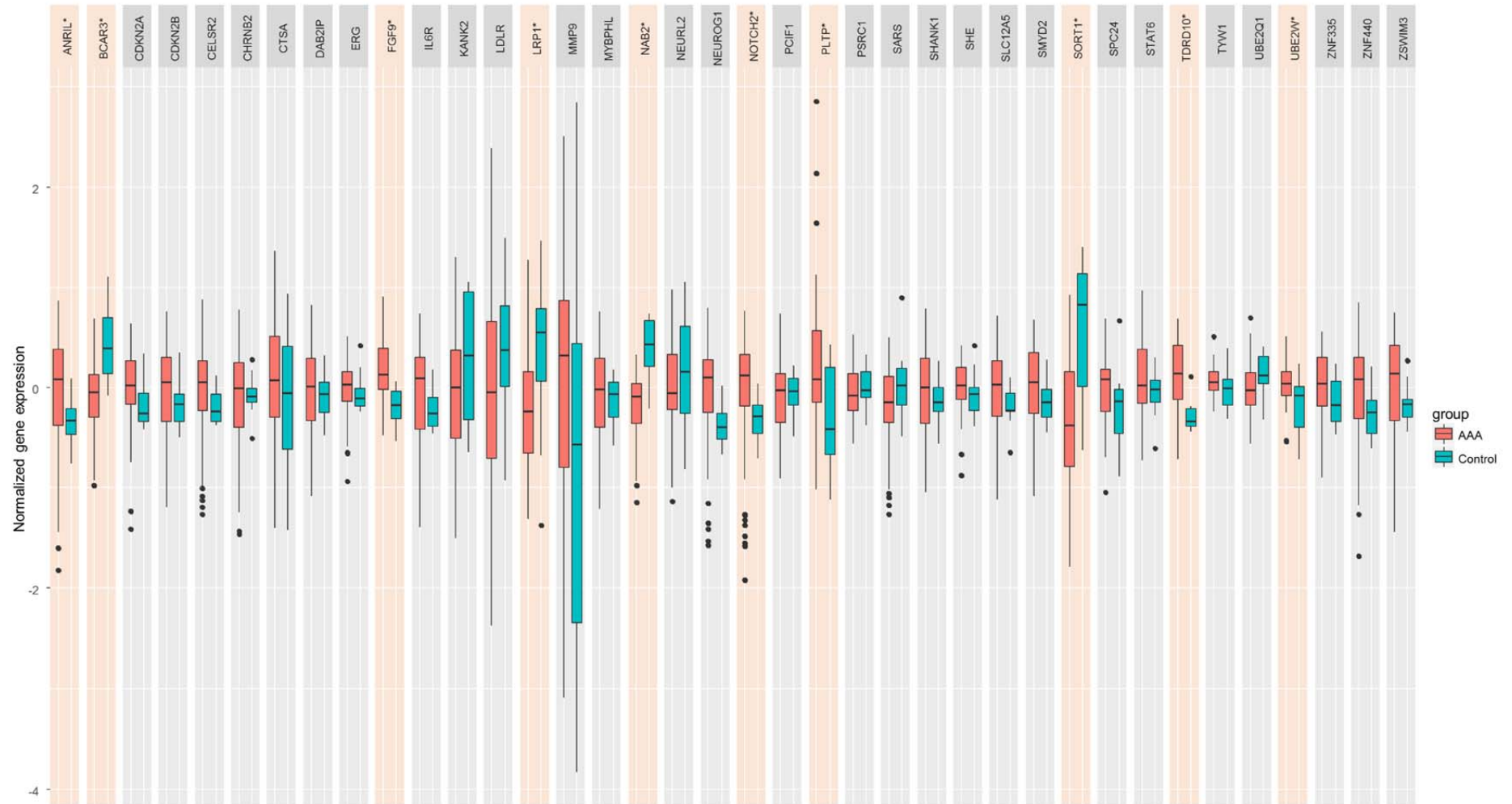
Several of the GWAS3D predicted distal gene interactions appeared to have differential case/ control gene expression (**Online Table XXIII and Online Figure IV**). For example, not only was the mRNA expression of *SORT1* (which is within the locus suggested by rs602633) significantly different between cases and controls, but predicted distal interactions in *BCAR3* and *NOTCH2* also had altered expression. The predicted distal interaction between rs4129267 (*IL6R* locus) and *TDRD10* also appeared concordant with an observed differential gene expression profile. The intergenic SNP rs9316871 (closest gene *LINC0540*) had a predicted interaction with *FGF9* which also had increased expression in AAA versus control aortic tissue.

It should be noted that absence of differential gene expression in this analysis does not specifically preclude a role in AAA pathogenesis. Many genes will have temporal expression and may, for example, only be differentially expressed in specific phases of the pathology. In addition, other genes may have significantly altered expression in other tissues (such as the liver, kidney or circulating leukocytes) the results of which may have indirect effects on the aortic wall. Nevertheless, these results appear to, at least in part, validate the potential utility of chromatin state-based analysis to identify functional mechanisms underlying SNP associations.

Online Table XXIII: AAA tissue mRNA expression for genes in close proximity to validated SNPs or having predicted distal gene interactions based on GWAS3D analysis.

Gene selection criteria	Gene	Locus	Entrez Gene ID	mRNA p-value	AAA mRNA expression
metaGWAS SNP proximity	ANRIL	9p21.3	1030	0.0025	increased
GWAS3D predicted distal interaction (SORT1)	BCAR3	1p22.1	8412	1.8x10⁻⁴	decreased
metaGWAS SNP proximity	CDKN2A	9p21.3	1029	0.217	
metaGWAS SNP proximity	CDKN2BAS1	9p21.3	100048912	0.266	
metaGWAS SNP proximity	CELSR2	1p13.3	1952	0.479	
metaGWAS SNP proximity	CHRN2	1q21.3	1141	0.829	
metaGWAS SNP proximity	CTSA	20q13.12	5476	0.174	
metaGWAS SNP proximity	DAB2IP	9q33.1	153090	0.213	
metaGWAS SNP proximity	ERG	21q21.3	2078	0.095	
GWAS3D predicted distal interaction (LINC00540)	FGF9	13q11	2254	0.002	increased
metaGWAS SNP proximity	IL6R	1q21	3570	0.087	
metaGWAS SNP proximity	KANK2	19p13.2	25959	0.132	
metaGWAS SNP proximity	LDLR	19p13.2	3949	0.197	
metaGWAS SNP proximity	LRP1	12q13.3	4035	0.0084	decreased
metaGWAS SNP proximity	MMP9	20q13.12	4318	0.132	
metaGWAS SNP proximity	MYBPHL	1p13.3	343263	0.897	
metaGWAS SNP proximity	NAB2	12q13.3	4665	1.1x10⁻⁵	decreased
metaGWAS SNP proximity	NEURL2	20q13.12	140825	0.576	
GWAS3D predicted distal interaction (LDLR)	NEUROG1	5q23	4762	0.138	
GWAS3D predicted distal interaction (SORT1)	NOTCH2	1p12	4853	4.6x10⁻⁷	increased
metaGWAS SNP proximity	PCIF1	20q13.12	63935	0.968	
metaGWAS SNP proximity	PLTP	20q13.12	5360	0.011	increased
metaGWAS SNP proximity	PSRC1	1p13.3	84722	0.440	
metaGWAS SNP proximity	SARS	1p13.3	6301	0.095	
GWAS3D predicted distal interaction (LDLR)	SHANK1	19p13.3	50944	0.567	
metaGWAS SNP proximity	SHE	1q21.3	126669	0.396	
metaGWAS SNP proximity	SLC12A5	20q13.12	57468	0.329	
metaGWAS SNP proximity	SMYD2	1q41	56950	0.317	
metaGWAS SNP proximity	SORT1	1p13.3	6272	1.1x10⁻⁴	decreased
metaGWAS SNP proximity	SPC24	19p13.2	147841	0.211	
metaGWAS SNP proximity	STAT6	12q13.3	6778	0.423	
GWAS3D predicted distal interaction (IL6R)	TDRD10	1q21.3	126668	0.006	increased
GWAS3D predicted distal interaction (IL6R)	TYW1	7q11.21	55253	0.320	
metaGWAS SNP proximity	UBE2Q1	1q21.3	55585	0.157	
GWAS3D predicted distal interaction (CDKN2B-AS1)	UBE2W	8q21.11	55284	0.0292	increased
metaGWAS SNP proximity	ZNF335	20q13.12	63925	0.205	
GWAS3D predicted distal interaction (LDLR)	ZNF440	19p13.2	126070	0.406	
metaGWAS SNP proximity	ZSWIM3	20q13.12	140831	0.235	

Online Figure IV: Box and whiskers plots of gene expression in AAA tissue and control tissue for genes in close proximity to validated SNPs or having predicted distal gene interactions based on GWAS3D analysis. Significant differences between AAA and controls are highlighted. Gene expression is log base 2, normalized to the 75th percentile.



LOOK-UP FOR TRANSCRIPTION FACTOR BINDING SITES IN GENES HARBORING AAA-ASSOCIATED VARIANTS

We previously performed a chromatin-immunoprecipitation (ChIP) study using AAA and control aorta tissue for the TFs ELF1, ETS2, RUNX1 and STAT5¹⁸⁵. These TFs were chosen because they were enriched in genes differentially expressed between AAA and control aorta; ELF1, ETS2, and RUNX1 were identified as relevant to most upregulated genes¹⁸⁶ and STAT5 was a driver for genes in the complement cascade¹⁸⁷.

The TF binding data were obtained from tables published in a paper by Pahl et al.¹⁸⁵, which describes ChIP-chip for TFs ELF1, ETS2, RUNX1 and STAT5 using human aortic tissue (AAA and control aorta). We performed a lookup in these data for evidence supporting that the genes near the SNPs identified by the meta-GWAS are relevant to AAA pathobiology. Lack of evidence in these data does not preclude involvement in AAA, but presence of evidence is a useful indicator that the gene is likely involved. This is especially useful for genes with little or no annotation in the major databases such as *SMYD2* and *ERG*. The results are summarized in **Online Table XXIV**. Chromatin enriched regions (cher) with binding sites for the TF ETS2 were found in *SMYD2* and *SORT1*. TF STAT5 had binding sites with chers in *CDKN2B-AS1ANRIL*, *ERG* and *DAB2IP*, and TF ELF1 had multiple binding sites in *ERG*. None of the TF binding sites in these genes contained the lead SNPs identified at the AAA risk loci.

Online Table XXIV: ChIP-chip data on human aortic tissue for the genes harbouring AAA-associated SNPs. Genome-wide ChIP-chip data were available on 4 transcription factors: ETS2, ELF1, STAT5 and RUNX1. For details, see Pahl et al. 2015¹⁸⁵. AAA, aortic tissue from abdominal aortic aneurysm; cher, chromatin enriched region; CTL, control abdominal aorta; TFBS, transcription factor binding site as defined by Transfac®.

SNP	Chr	Position	Gene(s)	Gene Symbol	Cher for TF (tissue source)	TFBS in cher
rs602633	1	109821511	PSRC1-CELSR2-SORT1	<i>CELSR2</i>	None	
				<i>SORT1</i>	ETS2 (CTL)	ETS2 (1 site)
				<i>PSRC</i>	None	
rs4129267	1	154426264	IL6R	<i>IL6R</i>	None	
rs1795061	1	214409280	SMYD2	<i>SMYD2</i>	ETS2 (AAA)	ETS2 (4 sites)
rs10757274	9	22096055	ANRIL	<i>ANRIL</i>	STAT5 (CTL)	STAT5 (1 site)
rs10985349	9	124425243	DAB2IP	<i>DAB2IP</i>	STAT5 (CTL)	STAT5 (1 site)
rs9316871	13	22861921	LINC00540	<i>LINC00540</i>	None	
rs6511720	19	11202306	LDLR	<i>LDLR</i>	None	
rs3827066	20	44586023	PCIF1-ZNF335-MMP9	<i>PCIF1</i>	None	
				<i>MMP9</i>	None	
				<i>ZNF335</i>	None	
rs2836411	21	39819830	ERG	<i>ERG</i>	STAT5 (AAA)	STAT5 (1 site)
					ELF1 (AAA)	ELF1 (4 sites)
					ELF1 (CTL)	

NETWORK ANALYSIS

We investigated whether most of the loci could be connected into a single network through intermediate nodes and interactions. A network integrating most of the loci would suggest mechanisms by which the loci could act in concert, whether synergistically or antagonistically, to affect the phenotype. The network(s) would also provide hypotheses for future investigation. Potential interactions between molecules encoded by genes harboring AAA-associated SNPs were analyzed using two independent analysis tools: Ingenuity Pathway Analysis® (IPA) tool version 9.0 (Qiagen's Ingenuity Systems, Redwood City, CA, USA; www.ingenuity.com) and ConsensusPathDB (<http://cpdb.molgen.mpg.de/CPDB>)¹⁸⁸⁻¹⁹¹. The analyzed gene set had 14 genes: 2 loci identified by the 9 AAA-associated SNPs included clusters of 3 genes (see **Online Table XIV** for SNP annotations), we also included TNF since recent literature indicated that SMYD2 suppresses IL6 and TNF production^{192, 193} and this had been published since the latest database update for each pathway analysis tool used. The gene symbols included in the network analyses were: *CDKN2BAS1*, *CELSR2*, *DAB2IP*, *ERG*, *IL6R*, *LDLR*, *LINC00540*, *MMP9*, *PCIF1*, *PSRC1*, *SMYD2*, *SORT1*, *ZNF335*, and *TNF*.

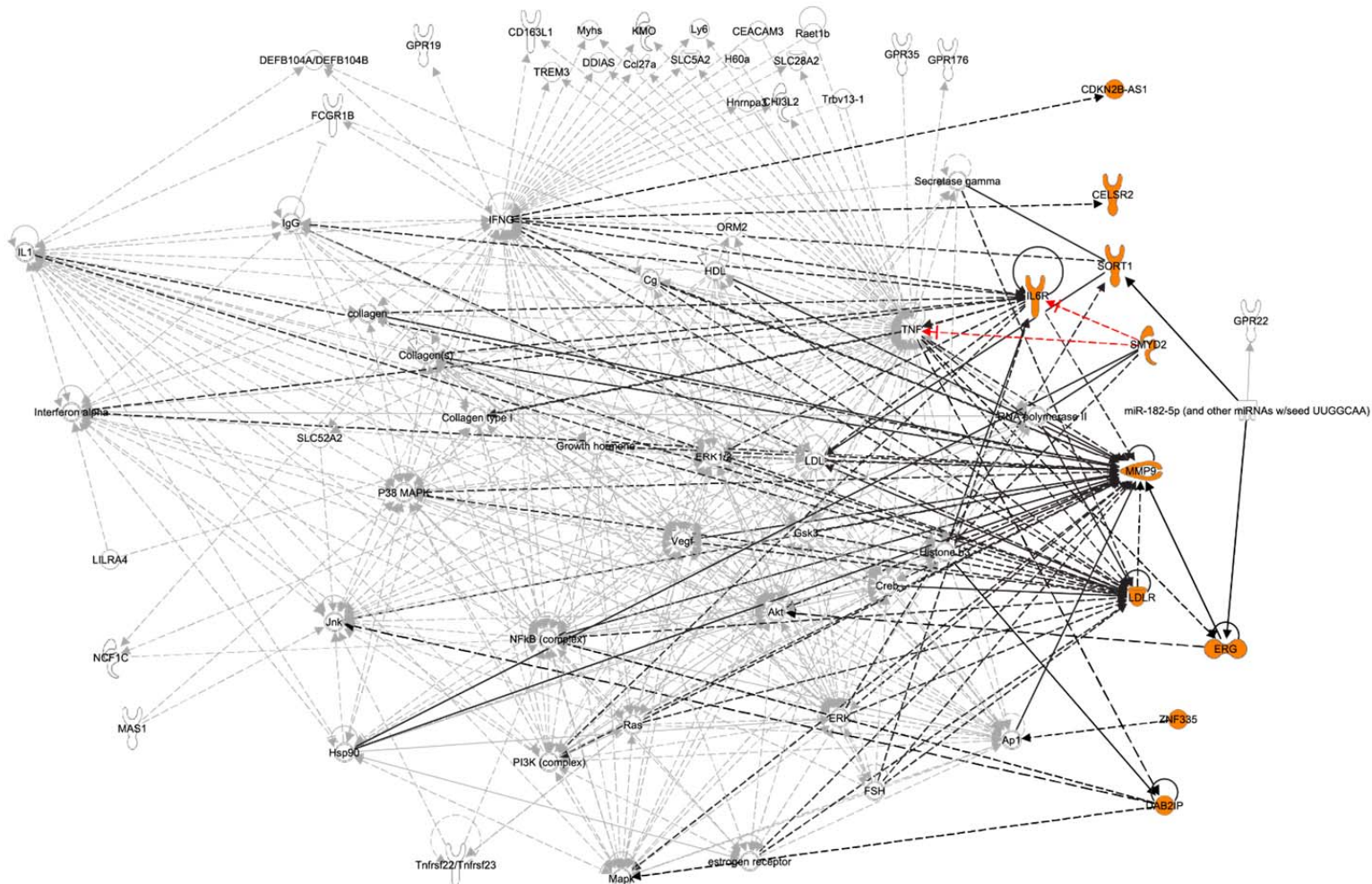
The parameters for the IPA were: 1. the Ingenuity Knowledge Base was used as a reference set; 2. both direct and indirect relationships were considered; and 3. only relationships that were either experimentally observed or had predictions with high confidence were considered. The relationships displayed as direct interactions mean that the two molecules make physical contact with each other such as binding or phosphorylation, and those displayed as indirect interactions do not require physical contact between the two molecules, such as signaling events. The IPA network generation algorithm has been described previously¹⁹⁴. The IPA's Core Analysis generated 2 networks, (1) "cardiovascular disease, cellular movement, developmental disorders" ($P=1 \times 10^{-21}$; 8/12 molecules), and (2) "cell signalling, nucleic acid metabolism, small molecular biochemistry" ($P=1 \times 10^{-7}$; 3/12 molecules). We merged the two networks into an interaction figure (**Online Figure V**). This identified that *ERG*, *IL6R* and *LDLR* were predicted modifiers of *MMP9*, with a direct interaction between *ERG* and *MMP9*. *SORT* and *LDLR* appear coupled via *ERK* and *LDL*. *IL6R* affects *DAB2IP* which in turn regulates *NFKB*. Several gene products, such as *ANRIL*, *CELSR2*, *ZNF335* and *SMYD2* have poorly defined functions at present, and *LINC00540*, a long non-coding RNA expressed in the hippocampus and lacking annotation information, did not belong to either of the 2 networks. The long non-coding RNA *ANRIL*, our strongest hit in the genome (**Figure 1**), has been reported in numerous studies as a GWAS hotspot and a candidate gene for CAD, intracranial aneurysms, and diverse cardiometabolic disorders¹⁹⁵.

The same gene list was submitted to the ConsensusPathDB web-based tool for generating an inferred network. ConsensusPathDB-human integrates interaction networks in *Homo sapiens* including binary and complex protein-protein, genetic, metabolic, signaling, gene regulatory and drug-target interactions, as well as biochemical pathways. Data currently originate from 32 public resources for interactions and interactions that have been curated from the literature. The interaction data are integrated in a manner to avoid redundancies, resulting in an interaction network containing different types of interactions. When the analysis was carried out, the database contained the following annotations: 158,523 unique physical entities; 458,570 unique interactions (17,098 gene regulation, 261,085 protein interaction, 443 genetic, 21,070 biochemical reactions, and 158,874 drug-target interactions), and 4,593 pathways. ConsensusPathDB infers a network to include proteins or metabolites that are not in the user-supplied input list, but associate two or more nodes (gene/protein/metabolite) on the input list with each other. These nodes are termed intermediate nodes and are ranked according to the significance of association with the input nodes given their overall connectivity in the background network. This is quantified by a z-score calculated for each intermediate node with the binomial

proportions test. The default z-score was used. The network was visualized using Cytoscape (version 3.4.0).

Four genes from the input list did not map to known entities in ConsensusPathDB: ANRIL and LINC00540 are long non-coding RNAs and not represented; similarly PCIF1 and ZNF335 are poorly annotated and not currently represented in source databases (**Online Figure VI**). The inferred network generated by ConsensusPathDB is largely similar to that produced by IPA, although it lacks the interaction between SMYD2 and IL6R, and SMYD2 and TNF. The absence of these interactions could be due to the recent elucidation as well as the unknown mechanism by which the SMYD2 suppression of TNF and IL6 occurs. The number of interactions of a node is a function of the true number of interactions as well as how well studied the protein or gene is. In the network (**Online Figure VI**) MMP9 and TNF have a large number of interactions. Interestingly LDLR and SMYD2 both have indirect interactions with MMP9 and TNF through CREBP, and could have synergistic effects on the AAA phenotype. Additionally CREBP has an interaction with NFKB complex and ETS1. Inhibition of NFKB and ETS1 was shown to reduce AAA in a rat model¹⁹⁶ and their promoter binding sites were enriched in the promoters of genes upregulated in human AAA¹⁹⁷.

Online Figure V. Potential interactions between gene products of AAA related genes. This figure shows IPA networks 1 and 2 merged together. Molecules are represented as nodes, and the biological relationship between two nodes as a line. Solid lines represent direct and dashed lines indirect interactions. All lines are supported by at least one literature citation or are from canonical information stored in the Ingenuity Pathways Knowledge Base (Qiagen's Ingenuity Systems). Nodes are displayed using various shapes that represent the functional class of the gene product. Molecules in orange are encoded by genes harboring AAA-associated variants. Red dashed lines indicate new information on SMYD2, IL6 and TNF found in recent literature^{192, 193}



CONSORTIA CONTRIBUTING DATA

List of members of the Cardiogenics consortium

Tony Attwood¹, Stephanie Belz², Peter Braund³, Jessy Brocheton⁴, François Cambien⁴, Jason Cooper⁵, Abi Crisp-Hihn¹, Patrick Diemert (formerly Linsel-Nitschke)², Panos Deloukas⁶, Jeanette Eardman², Nicola Foad¹, Tiphaine Godefroy⁴, Alison H Goodall^{3,11}, Jay Gracey³, Emma Gray⁶, Rhian Gwilliams⁶, Susanne Heimerl⁷, Christian Hengstenberg⁷, Jennifer Jolley¹, Unni Krishnan³, Heather Lloyd-Jones¹, Ulrika Liljedahl⁸, Ingrid Lugauer⁷, Per Lundmark⁸, Seraya Maouche^{2,4}, Jasbir S Moore³, Gilles Montalescot⁴, David Muir¹, Elizabeth Murray¹, Chris P Nelson³, Jessica Neudert⁹, David Niblett⁶, Karen O'Leary¹, Willem H Ouwehand^{1,6}, Helen Pollard³, Carole Proust⁴, Angela Rankin¹, Augusto Rendon¹², Catherine M Rice⁶, Hendrik B Sager², Nilesh J Samani^{3,11}, Jennifer Sambrook¹, Gerd Schmitz¹⁰, Michael Scholz⁹, Laura Schroeder², Heribert Schunkert², Jonathan Stephens¹, Ann-Christine Syvannen⁸, Stefanie Tennstedt (formerly Gulde)², Chris Wallace⁵.

¹Department of Haematology, University of Cambridge, Long Road, Cambridge, CB2 2PT, UK and National Health Service Blood and Transplant, Cambridge Centre, Long Road, Cambridge, CB2 2PT, UK;

²Medizinische Klinik 2, Universität zu Lübeck, Lübeck Germany

³Department of Cardiovascular Sciences, University of Leicester, Glenfield Hospital, Groby Road, Leicester, LE3 9QP, UK

⁴INSERM UMRS 937, Pierre and Marie Curie University (UPMC, Paris 6) and Medical School, 91 Bd de l'Hôpital 75013, Paris, France

⁵Juvenile Diabetes Research Foundation/Wellcome Trust Diabetes and Inflammation Laboratory, Department of Medical Genetics, Cambridge Institute for Medical Research, University of Cambridge, Wellcome Trust/MRC Building, Cambridge, CB2 0XY, UK

⁶The Wellcome Trust Sanger Institute, Wellcome Trust Genome Campus, Hinxton, Cambridge CB10 1SA, UK

⁷Klinik und Poliklinik für Innere Medizin II, Universität Regensburg, Germany

⁸Molecular Medicine, Department of Medical Sciences, Uppsala University, Uppsala, Sweden

⁹Trium, Analysis Online GmbH, Hohenlindenerstr. 1, 81677, München, Germany

¹⁰Institut für Klinische Chemie und Laboratoriumsmedizin, Universität, Regensburg, D-93053 Regensburg, Germany

¹¹Leicester NIHR Biomedical Research Unit in Cardiovascular Disease, Glenfield Hospital, Leicester, LE3 9QP, UK

¹²European Bioinformatics Institute, Wellcome Trust Genome Campus, Hinxton, Cambridge, CB10 1SD, UK

List of members of ICBP: The International Consortium for Blood Pressure Genome-Wide Association Studies¹⁹⁸

Georg B. Ehret, Patricia B. Munroe, Kenneth M. Rice, Murielle Bochud, Andrew D. Johnson, Daniel I. Chasman, Albert V. Smith, Martin D. Tobin, Germaine C. Verwoert, Shih-Jen Hwang, Vasyl Pihur, Peter Vollenweider, Paul F. O'Reilly, Najaf Amin, Jennifer L. Bragg-Gresham, Alexander Teumer, Nicole L. Glazer, Lenore Launer, Jing Hua Zhao, Yurii Aulchenko, Simon Heath, Siim Söber, Afshin Parsa, Jian'an Luan, Pankaj Arora, Abbas Dehghan, Feng Zhang, Gavin Lucas, Andrew A. Hicks, Anne U. Jackson, John F Peden, Toshiko Tanaka, Sarah H. Wild, Igor Rudan, Wilmar Igl, Yuri Milaneschi, Alex N. Parker, Cristiano Fava, John C. Chambers, Ervin R. Fox, Meena Kumari, Min Jin Go, Pim van der Harst, Wen Hong Linda Kao, Marketa Sjögren, D. G. Vinay, Myriam Alexander, Yasuharu Tabara, Sue Shaw-Hawkins, Peter H. Whincup, Yongmei Liu, Gang Shi, Johanna Kuusisto, Bamidele Tayo, Mark Seielstad, Xueling Sim, Khanh-Dung Hoang Nguyen, Terho Lehtimäki, Giuseppe Matullo, Ying Wu, Tom R. Gaunt, N. Charlotte Onland-

Moret, Matthew N. Cooper, Carl G. P. Platou, Elin Org, Rebecca Hardy, Santosh Dahgam, Jutta Palmen, Veronique Vitart, Peter S. Braund, Tatiana Kuznetsova, Cuno S. P. M. Uiterwaal, Adebowale Adeyemo, Walter Palmas, Harry Campbell, Barbara Ludwig, Maciej Tomaszewski, Ioanna Tzoulaki, Nicholette D. Palmer, CARDIoGRAM consortium, CKDGen Consortium, KidneyGen Consortium, EchoGen consortium, CHARGE-HF consortium, Thor Aspelund, Melissa Garcia, Yen-Pei C. Chang, Jeffrey R. O'Connell, Nanette I. Steinle, Diederick E. Grobbee, Dan E. Arking, Sharon L. Kardia, Alanna C. Morrison, Dena Hernandez, Samer Najjar, Wendy L. McArdle, David Hadley, Morris J. Brown, John M. Connell, Aroon D. Hingorani, Ian N.M. Day, Debbie A. Lawlor, John P. Beilby, Robert W. Lawrence, Robert Clarke, Jemma C. Hopewell, Halit Ongen, Albert W. Dreisbach, Yali Li, J. Hunter Young, Joshua C. Bis, Mika Kähönen, Jorma Viikari, Linda S. Adair, Nanette R. Lee, Ming-Huei Chen, Matthias Olden, Cristian Pattaro, Judith A. Hoffman Bolton, Anna Köttgen, Sven Bergmann, Vincent Mooser, Nish Chaturvedi, Timothy M. Frayling, Muhammad Islam, Tazeen H. Jafar, Jeanette Erdmann, Smita R. Kulkarni, Stefan R. Bornstein, Jürgen Grässler, Leif Groop, Benjamin F. Voight, Johannes Kettunen, Philip Howard, Andrew Taylor, Simonetta Guarrera, Fulvio Ricceri, Valur Emilsson, Andrew Plump, Inês Barroso, Kay-Tee Khaw, Alan B. Weder, Steven C. Hunt, Yan V. Sun, Richard N. Bergman, Francis S. Collins, Lori L. Bonnycastle, Laura J. Scott, Heather M. Stringham, Leena Peltonen, Markus Perola, Erkki Vartiainen, Stefan-Martin Brand, Jan A. Staessen, Thomas J. Wang, Paul R. Burton, Maria Soler Artigas, Yanbin Dong, Harold Snieder, Xiaoling Wang, Haidong Zhu, Kurt K. Lohman, Megan E. Rudock, Susan R. Heckbert, Nicholas L. Smith, Kerri L. Wiggins, Ayo Doumatey, Daniel Shriener, Gudrun Veldre, Margus Viigimaa, Sanjay Kinra, Dorairaj Prabhakaran, Vikal Tripathy, Carl D. Langefeld, Annika Rosengren, Dag S. Thelle, Anna Maria Corsi, Andrew Singleton, Terrence Forrester, Gina Hilton, Colin A. McKenzie, Tunde Salako, Naoharu Iwai, Yoshikuni Kita, Toshio Ogihara, Takayoshi Ohkubo, Tomonori Okamura, Hirotsugu Ueshima, Satoshi Umemura, Susana Eyheramendy, Thomas Meitinger, H.-Erich Wichmann, Yoon Shin Cho, Hyung-Lae Kim, Jong-Young Lee, James Scott, Joban S. Sehmi, Weihua Zhang, Bo Hedblad, Peter Nilsson, George Davey Smith, Andrew Wong, Narisu Narisu, Alena Stančáková, Leslie J. Raffel, Jie Yao, Sekar Kathiresan, Christopher J. O'Donnell, Stephen M. Schwartz, M. Arfan Ikram, W. T. Longstreth Jr, Thomas H. Mosley, Sudha Seshadri, Nick R.G. Shrine, Louise V. Wain, Mario A. Morken, Amy J. Swift, Jaana Laitinen, Inga Prokopenko, Paavo Zitting, Jackie A. Cooper, Steve E. Humphries, John Danesh, Asif Rasheed, Anuj Goel, Anders Hamsten, Hugh Watkins, Stephan J. L. Bakker, Wiek H. van Gilst, Charles S. Janipalli, K. Radha Mani, Chittaranjan S. Yajnik, Albert Hofman, Francesco U. S. Mattace-Raso, Ben A. Oostra, Ayse Demirkan, Aaron Isaacs, Fernando Rivadeneira, Edward G. Lakatta, Marco Orzu, Angelo Scuteri, Mika Ala-Korpela, Antti J. Kangas, Leo-Pekka Lytykäinen, Pasi Soininen, Taru Tukiainen, Peter Würtz, Rick Twee-Hee Ong, Marcus Dörr, Heyo K. Kroemer, Uwe Völker, Henry Völzke, Pilar Galan, Serge Herberg, Mark Lathrop, Diana Zelenika, Panos Deloukas, Massimo Mangino, Tim D. Spector, Guangju Zhai, James F. Meschia, Michael A. Nalls, Pankaj Sharma, Janos Terzic, M. V. Kranthi Kumar, Matthew Denniff, Ewa Zukowska-Szczechowska, Lynne E. Wagenknecht, F. Gerald R. Fowkes, Fadi J. Charchar, Peter E. H. Schwarz, Caroline Hayward, Xiuqing Guo, Charles Rotimi, Michiel L. Bots, Eva Brand, Nilesh J. Samani, Ozren Polasek, Philippa J. Talmud, Fredrik Nyberg, Diana Kuh, Maris Laan, Kristian Hveem, Lyle J. Palmer, Yvonne T. van der Schouw, Juan P. Casas, Karen L. Mohlke, Paolo Vineis, Olli Raitakari, Santhi K. Ganesh, Tien Y. Wong, E Shyong Tai, Richard S. Cooper, Markku Laakso, Dabeeru C. Rao, Tamara B. Harris, Richard W. Morris, Anna F. Dominiczak, Mika Kivimäki, Michael G. Marmot, Tetsuro Miki, Danish Saleheen, Giriraj R. Chandak, Josef Coresh, Gerjan Navis, Veikko Salomaa, Bok-Ghee Han, Xiaofeng Zhu, Jaspal S. Kooner, Olle Melander, Paul M Ridker, Stefania Bandinelli, Ulf B. Gyllensten, Alan F. Wright, James F. Wilson, Luigi Ferrucci, Martin Farrall, Jaakko Tuomilehto, Peter P. Pramstaller, Roberto Elosua, Nicole Soranzo, Eric J. G. Sijbrands, David Altshuler, Ruth J. F. Loos, Alan R. Shuldiner, Christian Gieger, Pierre Meneton, Andre G. Uitterlinden, Nicholas J. Wareham, Vilmundur Gudnason, Jerome I. Rotter, Rainer Rettig, Manuela Uda, David P. Strachan, Jacqueline C. M. Witteman, Anna-Liisa Hartikainen, Jacques S. Beckmann, Eric Boerwinkle, Ramachandran S. Vasan, Michael Boehnke, Martin G. Larson,

Marjo-Riitta Järvelin, Bruce M. Psaty, Gonçalo R. Abecasis, Aravinda Chakravarti, Paul Elliott, Cornelia M. van Duijn, Christopher Newton-Cheh, Daniel Levy, Mark J. Caulfield & Toby Johnson.

REFERENCES

1. Bown MJ, Jones GT, Harrison SC, et al. Abdominal aortic aneurysm is associated with a variant in low-density lipoprotein receptor-related protein 1. *Am J Hum Genet.* 2011;89:619-627
2. Gretarsdottir S, Baas AF, Thorleifsson G, et al. Genome-wide association study identifies a sequence variant within the *dab2ip* gene conferring susceptibility to abdominal aortic aneurysm. *Nature Genet.* 2010;42:692-U671
3. Jones GT, Bown MJ, Gretarsdottir S, et al. A sequence variant associated with sortilin-1 (*sort1*) on 1p13.3 is independently associated with abdominal aortic aneurysm. *Hum Mol Genet.* 2013
4. Harrison SC, Zabaneh D, Asselbergs FW, et al. A gene-centric study of common carotid artery remodelling. *Atherosclerosis.* 2013;226:440-446
5. Teo YY. Genotype calling for the illumina platform. *Methods Mol Biol.* 2012;850:525-538
6. Purcell S, Neale B, Todd-Brown K, Thomas L, Ferreira MA, Bender D, Maller J, Sklar P, de Bakker PI, Daly MJ, Sham PC. Plink: A tool set for whole-genome association and population-based linkage analyses. *Am J Hum Genet.* 2007;81:559-575
7. Elmore JR, Obmann MA, Kuivaniemi H, Tromp G, Gerhard GS, Franklin DP, Boddy AM, Carey DJ. Identification of a genetic variant associated with abdominal aortic aneurysms on chromosome 3p12.3 by genome wide association. *J Vasc Surg.* 2009;49:1525-1531
8. Borthwick KM, Smelser DT, Bock JA, et al. Ephenotyping for abdominal aortic aneurysm in the electronic medical records and genomics (emerge) network: Algorithm development and konstanz information miner workflow. *Int J Biomed Data Mining.* 2015;4
9. Verma SS, de Andrade M, Tromp G, et al. Imputation and quality control steps for combining multiple genome-wide datasets. *Front Genet.* 2014;5:370
10. Delaneau O, Marchini J, Zagury JF. A linear complexity phasing method for thousands of genomes. *Nat Methods.* 2012;9:179-181
11. Howie B, Fuchsberger C, Stephens M, Marchini J, Abecasis GR. Fast and accurate genotype imputation in genome-wide association studies through pre-phasing. *Nat Genet.* 2012;44:955-959
12. Gretarsdottir S, Thorleifsson G, Reynisdottir ST, et al. The gene encoding phosphodiesterase 4d confers risk of ischemic stroke. *Nat Genet.* 2003;35:131-138
13. Rice JA. Generalized likelihood ratio tests. In: Rice ja, editor. *Mathematical statistics and data analysis.* Vol. 1. International thomson publishing; 1995. P. 308–310.
14. Rafnar T, Sulem P, Stacey SN, et al. Sequence variants at the *tert-clptm1l* locus associate with many cancer types. *Nat Genet.* 2009;41:221-227
15. Kiemeny LA, Thorlacius S, Sulem P, et al. Sequence variant on 8q24 confers susceptibility to urinary bladder cancer. *Nat Genet.* 2008;40:1307-1312
16. Wetzels JF, Kiemeny LA, Swinkels DW, Willems HL, den Heijer M. Age- and gender-specific reference values of estimated gfr in caucasians: The nijmegen biomedical study. *Kidney Int.* 2007;72:632-637

17. Bown MJ, Braund PS, Thompson J, London NJ, Samani NJ, Sayers RD. Association between the coronary artery disease risk locus on chromosome 9p21.3 and abdominal aortic aneurysm. *Circ Cardiovasc Genet*. 2008;1:39-42
18. Howie B, Marchini J, Stephens M. Genotype imputation with thousands of genomes. *G3 (Bethesda)*. 2011;1:457-470
19. Devlin B, Roeder K. Genomic control for association studies. *Biometrics*. 1999;55:997-1004
20. Shi YY, He L. Shesis, a powerful software platform for analyses of linkage disequilibrium, haplotype construction, and genetic association at polymorphism loci. *Cell Res*. 2005;15:97-98
21. Helgadóttir A, Thorleifsson G, Magnusson KP, et al. The same sequence variant on 9p21 associates with myocardial infarction, abdominal aortic aneurysm and intracranial aneurysm. *Nat Genet*. 2008;40:217-224
22. Ogata T, Shibamura H, Tromp G, Sinha M, Goddard KA, Sakalihan N, Limet R, MacKean GL, Arthur C, Sueda T, Land S, Kuivaniemi H. Genetic analysis of polymorphisms in biologically relevant candidate genes in patients with abdominal aortic aneurysms. *J Vasc Surg*. 2005;41:1036-1042
23. Gottesman O, Kuivaniemi H, Tromp G, et al. The electronic medical records and genomics (emerge) network: Past, present, and future. *Genet Med*. 2013;15:761-771
24. Ye Z, Kalloo FS, Dalenberg AK, Kullo IJ. An electronic medical record-linked biorepository to identify novel biomarkers for atherosclerotic cardiovascular disease. *Glob Cardiol Sci Pract*. 2013;2013:82-90
25. St Jean PL, Zhang XC, Hart BK, Lamlum H, Webster MW, Steed DL, Henney AM, Ferrell RE. Characterization of a dinucleotide repeat in the 92 kda type iv collagenase gene (clg4b), localization of clg4b to chromosome 20 and the role of clg4b in aortic aneurysmal disease. *Ann Hum Genet*. 1995;59:17-24
26. Pulley J, Clayton E, Bernard GR, Roden DM, Masys DR. Principles of human subjects protections applied in an opt-out, de-identified biobank. *Clin Transl Sci*. 2010;3:42-48
27. McCarty CA, Wilke RA, Giampietro PF, Wesbrook SD, Caldwell MD. Marshfield clinic personalized medicine research project (pmrp): Design, methods and recruitment for a large population-based biobank. *Personalized Medicine*. 2005;2:49-79
28. Tayo BO, Teil M, Tong L, Qin H, Khitrov G, Zhang W, Song Q, Gottesman O, Zhu X, Pereira AC, Cooper RS, Bottinger EP. Genetic background of patients from a university medical center in manhattan: Implications for personalized medicine. *PLoS One*. 2011;6:e19166
29. Kho AN, Hayes MG, Rasmussen-Torvik L, et al. Use of diverse electronic medical record systems to identify genetic risk for type 2 diabetes within a genome-wide association study. *J Am Med Inform Assoc*. 2012;19:212-218
30. Galora S, Saracini C, Pratesi G, Sticchi E, Pulli R, Pratesi C, Abbate R, Giusti B. Association of rs1466535 lrp1 but not rs3019885 slc30a8 and rs6674171 tdrd10 gene polymorphisms with abdominal aortic aneurysm in italian patients. *J Vasc Surg*. 2014
31. Strauss E, Waliszewski K, Oszkinis G, Staniszewski R. Polymorphisms of genes involved in the hypoxia signaling pathway and the development of abdominal aortic aneurysms or large-artery atherosclerosis. *J Vasc Surg*. 2015;61:1105-1113.e1103

32. Willer CJ, Li Y, Abecasis GR. Metal: Fast and efficient meta-analysis of genomewide association scans. *Bioinformatics*. 2010;26:2190-2191
33. Han B, Eskin E. Random-effects model aimed at discovering associations in meta-analysis of genome-wide association studies. *Am J Hum Genet*. 2011;88:586-598
34. Morris AP, Voight BF, Teslovich TM, et al. Large-scale association analysis provides insights into the genetic architecture and pathophysiology of type 2 diabetes. *Nat Genet*. 2012;44:981-990
35. Schunkert H, König IR, Kathiresan S, et al. Large-scale association analysis identifies 13 new susceptibility loci for coronary artery disease. *Nat Genet*. 2011;43:333-338
36. Willer CJ, Schmidt EM, Sengupta S, et al. Discovery and refinement of loci associated with lipid levels. *Nat Genet*. 2013;45:1274-1283
37. Wain LV, Verwoert GC, O'Reilly PF, et al. Genome-wide association study identifies six new loci influencing pulse pressure and mean arterial pressure. *Nat Genet*. 2011;43:1005-1011
38. Ramos EM, Hoffman D, Junkins HA, Maglott D, Phan L, Sherry ST, Feolo M, Hindorff LA. Phenotype-genotype integrator (phegeni): Synthesizing genome-wide association study (gwas) data with existing genomic resources. *Eur J Hum Genet*. 2014;22:144-147
39. Eicher JD, Landowski C, Stackhouse B, Sloan A, Chen W, Jensen N, Lien JP, Leslie R, Johnson AD. Grasp v2.0: An update on the genome-wide repository of associations between snps and phenotypes. *Nucleic Acids Res*. 2015;43:D799-804
40. Leslie R, O'Donnell CJ, Johnson AD. Grasp: Analysis of genotype-phenotype results from 1390 genome-wide association studies and corresponding open access database. *Bioinformatics*. 2014;30:i185-194
41. Willer CJ, Sanna S, Jackson AU, et al. Newly identified loci that influence lipid concentrations and risk of coronary artery disease. *Nat Genet*. 2008;40:161-169
42. Sandhu MS, Waterworth DM, Debenham SL, et al. Ldl-cholesterol concentrations: A genome-wide association study. *Lancet*. 2008;371:483-491
43. Kathiresan S, Willer CJ, Peloso GM, et al. Common variants at 30 loci contribute to polygenic dyslipidemia. *Nat Genet*. 2009;41:56-65
44. Talmud PJ, Drenos F, Shah S, et al. Gene-centric association signals for lipids and apolipoproteins identified via the human cvd beadchip. *Am J Hum Genet*. 2009;85:628-642
45. Clarke R, Peden JF, Hopewell JC, et al. Genetic variants associated with lp(a) lipoprotein level and coronary disease. *N Engl J Med*. 2009;361:2518-2528
46. Barber MJ, Mangravite LM, Hyde CL, et al. Genome-wide association of lipid-lowering response to statins in combined study populations. *PLoS One*. 2010;5:e9763
47. Teslovich TM, Musunuru K, Smith AV, et al. Biological, clinical and population relevance of 95 loci for blood lipids. *Nature*. 2010;466:707-713
48. Lango Allen H, Estrada K, Lettre G, et al. Hundreds of variants clustered in genomic loci and biological pathways affect human height. *Nature*. 2010;467:832-838
49. Lettre G, Palmer CD, Young T, et al. Genome-wide association study of coronary heart disease and its risk factors in 8,090 african americans: The nhlbi care project. *PLoS Genet*. 2011;7:e1001300

50. Middelberg RP, Ferreira MA, Henders AK, Heath AC, Madden PA, Montgomery GW, Martin NG, Whitfield JB. Genetic variants in *lpl*, *oasl* and *tomm40/apoe-c1-c2-c4* genes are associated with multiple cardiovascular-related traits. *BMC Med Genet.* 2011;12:123
51. Trompet S, de Craen AJ, Postmus I, Ford I, Sattar N, Caslake M, Stott DJ, Buckley BM, Sacks F, Devlin JJ, Slagboom PE, Westendorp RG, Jukema JW. Replication of *ldl* gwas hits in *prosper/phase* as validation for future (pharmaco)genetic analyses. *BMC Med Genet.* 2011;12:131
52. Grallert H, Dupuis J, Bis JC, et al. Eight genetic loci associated with variation in lipoprotein-associated phospholipase a2 mass and activity and coronary heart disease: Meta-analysis of genome-wide association studies from five community-based studies. *Eur Heart J.* 2012;33:238-251
53. Asselbergs FW, Guo Y, van Iperen EP, et al. Large-scale gene-centric meta-analysis across 32 studies identifies multiple lipid loci. *Am J Hum Genet.* 2012;91:823-838
54. Deloukas P, Kanoni S, Willenborg C, et al. Large-scale association analysis identifies new risk loci for coronary artery disease. *Nat Genet.* 2013;45:25-33
55. Wilk JB, Walter RE, Laramie JM, Gottlieb DJ, O'Connor GT. Framingham heart study genome-wide association: Results for pulmonary function measures. *BMC Med Genet.* 2007;8 Suppl 1:S8
56. Ridker PM, Pare G, Parker A, Zee RY, Danik JS, Buring JE, Kwiatkowski D, Cook NR, Miletich JP, Chasman DI. Loci related to metabolic-syndrome pathways including *lepr*, *hnf1a*, *il6r*, and *gckr* associate with plasma c-reactive protein: The women's genome health study. *Am J Hum Genet.* 2008;82:1185-1192
57. Melzer D, Perry JR, Hernandez D, et al. A genome-wide association study identifies protein quantitative trait loci (pqtls). *PLoS Genet.* 2008;4:e1000072
58. Sabatti C, Service SK, Hartikainen AL, et al. Genome-wide association analysis of metabolic traits in a birth cohort from a founder population. *Nat Genet.* 2009;41:35-46
59. Danik JS, Pare G, Chasman DI, Zee RY, Kwiatkowski DJ, Parker A, Miletich JP, Ridker PM. Novel loci, including those related to crohn disease, psoriasis, and inflammation, identified in a genome-wide association study of fibrinogen in 17 686 women: The women's genome health study. *Circ Cardiovasc Genet.* 2009;2:134-141
60. Ferreira MA, Matheson MC, Duffy DL, et al. Identification of *il6r* and chromosome 11q13.5 as risk loci for asthma. *Lancet.* 2011;378:1006-1014
61. Wassel CL, Lange LA, Keating BJ, et al. Association of genomic loci from a cardiovascular gene snp array with fibrinogen levels in european americans and african-americans from six cohort studies: The candidate gene association resource (care). *Blood.* 2011;117:268-275
62. Dehghan A, Dupuis J, Barbalic M, et al. Meta-analysis of genome-wide association studies in >80 000 subjects identifies multiple loci for c-reactive protein levels. *Circulation.* 2011;123:731-738
63. Naitza S, Porcu E, Steri M, et al. A genome-wide association scan on the levels of markers of inflammation in sardinians reveals associations that underpin its complex regulation. *PLoS Genet.* 2012;8:e1002480

64. Reiner AP, Beleza S, Franceschini N, Auer PL, Robinson JG, Kooperberg C, Peters U, Tang H. Genome-wide association and population genetic analysis of c-reactive protein in african american and hispanic american women. *Am J Hum Genet.* 2012;91:502-512
65. Shah T, Zabaneh D, Gaunt T, et al. Gene-centric analysis identifies variants associated with interleukin-6 levels and shared pathways with other inflammation markers. *Circ Cardiovasc Genet.* 2013;6:163-170
66. McPherson R, Pertsemlidis A, Kavaslar N, Stewart A, Roberts R, Cox DR, Hinds DA, Pennacchio LA, Tybjaerg-Hansen A, Folsom AR, Boerwinkle E, Hobbs HH, Cohen JC. A common allele on chromosome 9 associated with coronary heart disease. *Science.* 2007;316:1488-1491
67. Lu X, Wang L, Chen S, et al. Genome-wide association study in han chinese identifies four new susceptibility loci for coronary artery disease. *Nat Genet.* 2012;44:890-894
68. Pechlivanis S, Muhleisen TW, Mohlenkamp S, Schadendorf D, Erbel R, Jockel KH, Hoffmann P, Nothen MM, Scherag A, Moebus S. Risk loci for coronary artery calcification replicated at 9p21 and 6q24 in the heinz nixdorf recall study. *BMC Med Genet.* 2013;14:23
69. Ferguson JF, Matthews GJ, Townsend RR, et al. Candidate gene association study of coronary artery calcification in chronic kidney disease: Findings from the cric study (chronic renal insufficiency cohort). *J Am Coll Cardiol.* 2013;62:789-798
70. Saxena R, Voight BF, Lyssenko V, et al. Genome-wide association analysis identifies loci for type 2 diabetes and triglyceride levels. *Science.* 2007;316:1331-1336
71. Stefansson H, Ophoff RA, Steinberg S, et al. Common variants conferring risk of schizophrenia. *Nature.* 2009;460:744-747
72. Kathiresan S, Melander O, Guiducci C, et al. Six new loci associated with blood low-density lipoprotein cholesterol, high-density lipoprotein cholesterol or triglycerides in humans. *Nat Genet.* 2008;40:189-197
73. Aulchenko YS, Ripatti S, Lindqvist I, et al. Loci influencing lipid levels and coronary heart disease risk in 16 european population cohorts. *Nat Genet.* 2009;41:47-55
74. Chasman DI, Pare G, Zee RY, et al. Genetic loci associated with plasma concentration of low-density lipoprotein cholesterol, high-density lipoprotein cholesterol, triglycerides, apolipoprotein a1, and apolipoprotein b among 6382 white women in genome-wide analysis with replication. *Circ Cardiovasc Genet.* 2008;1:21-30
75. Chasman DI, Pare G, Mora S, et al. Forty-three loci associated with plasma lipoprotein size, concentration, and cholesterol content in genome-wide analysis. *PLoS Genet.* 2009;5:e1000730
76. Bis JC, Kavousi M, Franceschini N, et al. Meta-analysis of genome-wide association studies from the charge consortium identifies common variants associated with carotid intima media thickness and plaque. *Nat Genet.* 2011;43:940-947
77. Large-scale gene-centric analysis identifies novel variants for coronary artery disease. *PLoS Genet.* 2011;7:e1002260
78. Avery CL, He Q, North KE, et al. A phenomics-based strategy identifies loci on apoc1, brap, and plcg1 associated with metabolic syndrome phenotype domains. *PLoS Genet.* 2011;7:e1002322

79. Musunuru K, Romaine SP, Lettre G, et al. Multi-ethnic analysis of lipid-associated loci: The nhlbi care project. *PLoS One*. 2012;7:e36473
80. Hopewell JC, Parish S, Offer A, Link E, Clarke R, Lathrop M, Armitage J, Collins R. Impact of common genetic variation on response to simvastatin therapy among 18 705 participants in the heart protection study. *Eur Heart J*. 2013;34:982-992
81. Elbers CC, Guo Y, Tragante V, et al. Gene-centric meta-analysis of lipid traits in african, east asian and hispanic populations. *PLoS One*. 2012;7:e50198
82. Weissglas-Volkov D, Aguilar-Salinas CA, Nikkola E, et al. Genomic study in mexicans identifies a new locus for triglycerides and refines european lipid loci. *J Med Genet*. 2013;50:298-308
83. Denny JC, Ritchie MD, Basford MA, Pulley JM, Bastarache L, Brown-Gentry K, Wang D, Masys DR, Roden DM, Crawford DC. Phewas: Demonstrating the feasibility of a phenome-wide scan to discover gene-disease associations. *Bioinformatics*. 2010;26:1205-1210
84. Pendergrass SA, Brown-Gentry K, Dudek S, et al. Phenome-wide association study (phewas) for detection of pleiotropy within the population architecture using genomics and epidemiology (page) network. *PLoS Genet*. 2013;9:e1003087
85. Hsu F, Kent WJ, Clawson H, Kuhn RM, Diekhans M, Haussler D. The ucsc known genes. *Bioinformatics*. 2006;22:1036-1046
86. Benson DA, Karsch-Mizrachi I, Lipman DJ, Ostell J, Wheeler DL. Genbank: Update. *Nucleic Acids Res*. 2004;32:D23-26
87. Kent WJ. Blat--the blast-like alignment tool. *Genome Res*. 2002;12:656-664
88. Pruitt KD, Tatusova T, Maglott DR. Ncbi reference sequence (refseq): A curated non-redundant sequence database of genomes, transcripts and proteins. *Nucleic Acids Res*. 2005;33:D501-504
89. Gardner PP, Daub J, Tate J, Moore BL, Osuch IH, Griffiths-Jones S, Finn RD, Nawrocki EP, Kolbe DL, Eddy SR, Bateman A. Rfam: Wikipedia, clans and the "decimal" release. *Nucleic Acids Res*. 2011;39:D141-145
90. Lowe TM, Eddy SR. Trnascan-se: A program for improved detection of transfer rna genes in genomic sequence. *Nucleic Acids Res*. 1997;25:955-964
91. Reorganizing the protein space at the universal protein resource (uniprot). *Nucleic Acids Res*. 2012;40:D71-75
92. Harrow J, Frankish A, Gonzalez JM, et al. Gencode: The reference human genome annotation for the encode project. *Genome Res*. 2012;22:1760-1774
93. Cabili MN, Trapnell C, Goff L, Koziol M, Tazon-Vega B, Regev A, Rinn JL. Integrative annotation of human large intergenic noncoding rnas reveals global properties and specific subclasses. *Genes Dev*. 2011;25:1915-1927
94. Trapnell C, Williams BA, Pertea G, Mortazavi A, Kwan G, van Baren MJ, Salzberg SL, Wold BJ, Pachter L. Transcript assembly and quantification by rna-seq reveals unannotated transcripts and isoform switching during cell differentiation. *Nat Biotechnol*. 2010;28:511-515
95. Kent WJ, Sugnet CW, Furey TS, Roskin KM, Pringle TH, Zahler AM, Haussler D. The human genome browser at ucsc. *Genome Res*. 2002;12:996-1006

96. Friedman RC, Farh KK, Burge CB, Bartel DP. Most mammalian mRNAs are conserved targets of miRNAs. *Genome Res.* 2009;19:92-105
97. Grimson A, Farh KK, Johnston WK, Garrett-Engle P, Lim LP, Bartel DP. miRNA targeting specificity in mammals: Determinants beyond seed pairing. *Mol Cell.* 2007;27:91-105
98. Mortazavi A, Williams BA, McCue K, Schaeffer L, Wold B. Mapping and quantifying mammalian transcriptomes by RNA-seq. *Nat Methods.* 2008;5:621-628
99. Ernst J, Kheradpour P, Mikkelson TS, Shores N, Ward LD, Epstein CB, Zhang X, Wang L, Issner R, Coyne M, Ku M, Durham T, Kellis M, Bernstein BE. Mapping and analysis of chromatin state dynamics in nine human cell types. *Nature.* 2011;473:43-49
100. An integrated encyclopedia of DNA elements in the human genome. *Nature.* 2012;489:57-74
101. Wang J, Zhuang J, Iyer S, et al. Sequence features and chromatin structure around the genomic regions bound by 119 human transcription factors. *Genome Res.* 2012;22:1798-1812
102. Wang J, Zhuang J, Iyer S, Lin XY, Greven MC, Kim BH, Moore J, Pierce BG, Dong X, Virgil D, Birney E, Hung JH, Weng Z. Factorbook.org: A wiki-based database for transcription factor-binding data generated by the ENCODE Consortium. *Nucleic Acids Res.* 2013;41:D171-176
103. Hubisz MJ, Pollard KS, Siepel A. Phast and rPhast: Phylogenetic analysis with space/time models. *Brief Bioinform.* 2011;12:41-51
104. Jurka J. Repbase update: A database and an electronic journal of repetitive elements. *Trends Genet.* 2000;16:418-420
105. Reumers J, Conde L, Medina I, Maurer-Stroh S, Van Durme J, Dopazo J, Rousseau F, Schymkowitz J. Joint annotation of coding and non-coding single nucleotide polymorphisms and mutations in the SNPeff and PupaSuite databases. *Nucleic Acids Res.* 2008;36:D825-829
106. Li MJ, Wang LY, Xia Z, Sham PC, Wang J. Gwas3d: Detecting human regulatory variants by integrative analysis of genome-wide associations, chromosome interactions and histone modifications. *Nucleic Acids Res.* 2013;41:W150-158
107. Biro E, Gabel G, Moran CS, Schreurs C, Lindeman JH, Walker PJ, Nataatmadja M, West M, Holdt LM, Hinterseher I, Pilarsky C, Golledge J. Differential gene expression in human abdominal aortic aneurysm and aortic occlusive disease. *Oncotarget.* 2015;6:12984-12996
108. Pers TH, Karjalainen JM, Chan Y, et al. Biological interpretation of genome-wide association studies using predicted gene functions. *Nat Commun.* 2015;6:5890
109. Zhang X, Gierman HJ, Levy D, Plump A, Dobrin R, Goring HH, Curran JE, Johnson MP, Blangero J, Kim SK, O'Donnell CJ, Emilsson V, Johnson AD. Synthesis of 53 tissue and cell line expression QTL datasets reveals master eQTLs. *BMC Genomics.* 2014;15:532
110. Goring HH, Curran JE, Johnson MP, et al. Discovery of expression QTLs using large-scale transcriptional profiling in human lymphocytes. *Nat Genet.* 2007;39:1208-1216
111. Idaghdour Y, Czika W, Shianna KV, Lee SH, Visscher PM, Martin HC, Miclaus K, Jadallah SJ, Goldstein DB, Wolfinger RD, Gibson G. Geographical genomics of human leukocyte gene expression variation in southern Morocco. *Nat Genet.* 2010;42:62-67

112. Heap GA, Trynka G, Jansen RC, Bruinenberg M, Swertz MA, Dinesen LC, Hunt KA, Wijmenga C, Vanheel DA, Franke L. Complex nature of snp genotype effects on gene expression in primary human leucocytes. *BMC Med Genomics*. 2009;2:1
113. Battle A, Mostafavi S, Zhu X, Potash JB, Weissman MM, McCormick C, Haudenschild CD, Beckman KB, Shi J, Mei R, Urban AE, Montgomery SB, Levinson DF, Koller D. Characterizing the genetic basis of transcriptome diversity through rna-sequencing of 922 individuals. *Genome Res*. 2014;24:14-24
114. Benton MC, Lea RA, Macartney-Coxson D, Carless MA, Goring HH, Bellis C, Hanna M, Eccles D, Chambers GK, Curran JE, Harper JL, Blangero J, Griffiths LR. Mapping eqtls in the norfolk island genetic isolate identifies candidate genes for cvd risk traits. *Am J Hum Genet*. 2013;93:1087-1099
115. Emilsson V, Thorleifsson G, Zhang B, et al. Genetics of gene expression and its effect on disease. *Nature*. 2008;452:423-428
116. Fehrmann RS, Jansen RC, Veldink JH, et al. Trans-eqtls reveal that independent genetic variants associated with a complex phenotype converge on intermediate genes, with a major role for the hla. *PLoS Genet*. 2011;7:e1002197
117. Landmark-Hoyvik H, Dumeaux V, Nebdal D, Lund E, Tost J, Kamatani Y, Renault V, Borresen-Dale AL, Kristensen V, Edvardsen H. Genome-wide association study in breast cancer survivors reveals snps associated with gene expression of genes belonging to mhc class i and ii. *Genomics*. 2013;102:278-287
118. Mehta D, Heim K, Herder C, Carstensen M, Eckstein G, Schurmann C, Homuth G, Nauck M, Volker U, Roden M, Illig T, Gieger C, Meitinger T, Prokisch H. Impact of common regulatory single-nucleotide variants on gene expression profiles in whole blood. *Eur J Hum Genet*. 2013;21:48-54
119. Narahara M, Higasa K, Nakamura S, Tabara Y, Kawaguchi T, Ishii M, Matsubara K, Matsuda F, Yamada R. Large-scale east-asian eqtl mapping reveals novel candidate genes for ld mapping and the genomic landscape of transcriptional effects of sequence variants. *PLoS One*. 2014;9:e100924
120. Quinlan J, Idaghdour Y, Goulet JP, Gbeha E, de Malliard T, Bruat V, Grenier JC, Gomez S, Sanni A, Rahimy MC, Awadalla P. Genomic architecture of sickle cell disease in west african children. *Front Genet*. 2014;5:26
121. Sasayama D, Hori H, Nakamura S, Miyata R, Teraishi T, Hattori K, Ota M, Yamamoto N, Higuchi T, Amano N, Kunugi H. Identification of single nucleotide polymorphisms regulating peripheral blood mrna expression with genome-wide significance: An eqtl study in the japanese population. *PLoS One*. 2013;8:e54967
122. Schramm K, Marzi C, Schurmann C, et al. Mapping the genetic architecture of gene regulation in whole blood. *PLoS One*. 2014;9:e93844
123. van Eijk KR, de Jong S, Boks MP, Langeveld T, Colas F, Veldink JH, de Kovel CG, Janson E, Strengman E, Langfelder P, Kahn RS, van den Berg LH, Horvath S, Ophoff RA. Genetic analysis of DNA methylation and gene expression levels in whole blood of healthy human subjects. *BMC Genomics*. 2012;13:636
124. Westra HJ, Peters MJ, Esko T, et al. Systematic identification of trans eqtls as putative drivers of known disease associations. *Nat Genet*. 2013;45:1238-1243

125. Wright FA, Sullivan PF. Heritability and genomics of gene expression in peripheral blood. *2014*;46:430-437
126. Zhernakova DV, de Klerk E, Westra HJ, et al. Deepsage reveals genetic variants associated with alternative polyadenylation and expression of coding and non-coding transcripts. *PLoS Genet.* 2013;9:e1003594
127. Dixon AL, Liang L, Moffatt MF, Chen W, Heath S, Wong KC, Taylor J, Burnett E, Gut I, Farrall M, Lathrop GM, Abecasis GR, Cookson WO. A genome-wide association study of global gene expression. *Nat Genet.* 2007;39:1202-1207
128. Liang L, Morar N, Dixon AL, Lathrop GM, Abecasis GR, Moffatt MF, Cookson WO. A cross-platform analysis of 14,177 expression quantitative trait loci derived from lymphoblastoid cell lines. *Genome Res.* 2013;23:716-726
129. Stranger BE, Nica AC, Forrest MS, Dimas A, Bird CP, Beazley C, Ingle CE, Dunning M, Flicek P, Koller D, Montgomery S, Tavares S, Deloukas P, Dermitzakis ET. Population genomics of human gene expression. *Nat Genet.* 2007;39:1217-1224
130. Kwan T, Benovoy D, Dias C, Gurd S, Provencher C, Beaulieu P, Hudson TJ, Sladek R, Majewski J. Genome-wide analysis of transcript isoform variation in humans. *Nat Genet.* 2008;40:225-231
131. Bryois J, Buil A, Evans DM, Kemp JP, Montgomery SB, Conrad DF, Ho KM, Ring S, Hurles M, Deloukas P, Davey Smith G, Dermitzakis ET. Cis and trans effects of human genomic variants on gene expression. *PLoS Genet.* 2014;10:e1004461
132. Cusanovich DA, Billstrand C, Zhou X, Chavarria C, De Leon S, Michelini K, Pai AA, Ober C, Gilad Y. The combination of a genome-wide association study of lymphocyte count and analysis of gene expression data reveals novel asthma candidate genes. *Hum Mol Genet.* 2012;21:2111-2123
133. Dimas AS, Deutsch S, Stranger BE, et al. Common regulatory variation impacts gene expression in a cell type-dependent manner. *Science.* 2009;325:1246-1250
134. Grundberg E, Small KS, Hedman AK, et al. Mapping cis- and trans-regulatory effects across multiple tissues in twins. *Nat Genet.* 2012;44:1084-1089
135. Gutierrez-Arcelus M, Lappalainen T, Montgomery SB, et al. Passive and active DNA methylation and the interplay with genetic variation in gene regulation. *Elife.* 2013;2:e00523
136. Mangravite LM, Engelhardt BE, Medina MW, et al. A statin-dependent qtl for gatm expression is associated with statin-induced myopathy. *Nature.* 2013;502:377-380
137. Fairfax BP, Makino S, Radhakrishnan J, Plant K, Leslie S, Dilthey A, Ellis P, Langford C, Vannberg FO, Knight JC. Genetics of gene expression in primary immune cells identifies cell type-specific master regulators and roles of hla alleles. *Nat Genet.* 2012;44:502-510
138. Murphy A, Chu JH, Xu M, et al. Mapping of numerous disease-associated expression polymorphisms in primary peripheral blood cd4+ lymphocytes. *Hum Mol Genet.* 2010;19:4745-4757
139. Heinzen EL, Ge D, Cronin KD, Maia JM, Shianna KV, Gabriel WN, Welsh-Bohmer KA, Hulet CM, Denny TN, Goldstein DB. Tissue-specific genetic control of splicing: Implications for the study of complex traits. *PLoS Biol.* 2008;6:e1
140. Zeller T, Wild P, Szymczak S, et al. Genetics and beyond--the transcriptome of human monocytes and disease susceptibility. *PLoS One.* 2010;5:e10693

141. Fairfax BP, Humburg P, Makino S, Naranbhai V, Wong D, Lau E, Jostins L, Plant K, Andrews R, McGee C, Knight JC. Innate immune activity conditions the effect of regulatory variants upon monocyte gene expression. *Science*. 2014;343:1246949
142. Barreiro LB, Tailleux L, Pai AA, Gicquel B, Marioni JC, Gilad Y. Deciphering the genetic architecture of variation in the immune response to mycobacterium tuberculosis infection. *Proc Natl Acad Sci U S A*. 2012;109:1204-1209
143. Lee MN, Ye C, Villani AC, et al. Common genetic variants modulate pathogen-sensing responses in human dendritic cells. *Science*. 2014;343:1246980
144. Huang RS, Gamazon ER, Ziliak D, Wen Y, Im HK, Zhang W, Wing C, Duan S, Bleibel WK, Cox NJ, Dolan ME. Population differences in microRNA expression and biological implications. *RNA Biol*. 2011;8:692-701
145. Degner JF, Pai AA, Pique-Regi R, Veyrieras JB, Gaffney DJ, Pickrell JK, De Leon S, Michelini K, Lewellen N, Crawford GE, Stephens M, Gilad Y, Pritchard JK. DNase I sensitivity QTLs are a major determinant of human expression variation. *Nature*. 2012;482:390-394
146. The genotype-tissue expression (GTEx) project. *Nat Genet*. 2013;45:580-585
147. Greenawald DM, Dobrin R, Chudin E, et al. A survey of the genetics of stomach, liver, and adipose gene expression from a morbidly obese cohort. *Genome Res*. 2011;21:1008-1016
148. Kompass KS, Witte JS. Co-regulatory expression quantitative trait loci mapping: Method and application to endometrial cancer. *BMC Med Genomics*. 2011;4:6
149. Li Q, Seo JH, Stranger B, McKenna A, Pe'er I, Laframboise T, Brown M, Tyekuceva S, Freedman ML. Integrative eQTL-based analyses reveal the biology of breast cancer risk loci. *Cell*. 2013;152:633-641
150. Chen TH, D'Ambrosio D, Gallins P, et al. Mapping of hepatic expression quantitative trait loci (eQTLs) in a Han Chinese population. *Nat Genet*. 2014;51:319-326
151. Innocenti F, Cooper GM, Stanaway IB, et al. Identification, replication, and functional fine-mapping of expression quantitative trait loci in primary human liver tissue. *PLoS Genet*. 2011;7:e1002078
152. Schadt EE, Molony C, Chudin E, et al. Mapping the genetic architecture of gene expression in human liver. *PLoS Biol*. 2008;6:e107
153. Schroder A, Klein K, Winter S, Schwab M, Bonin M, Zell A, Zanger UM. Genomics of ADME gene expression: Mapping expression quantitative trait loci relevant for absorption, distribution, metabolism and excretion of drugs in human liver. *Pharmacogenomics J*. 2013;13:12-20
154. Grundberg E, Kwan T, Ge B, et al. Population genomics in a disease targeted primary cell model. *Genome Res*. 2009;19:1942-1952
155. Kabakchiev B, Silverberg MS. Expression quantitative trait loci analysis identifies associations between genotype and gene expression in human intestine. *Gastroenterology*. 2013;144:1488-1496, 1496.e1481-1483
156. Ongen H, Andersen CL, Bramsen JB, et al. Putative cis-regulatory drivers in colorectal cancer. *Nature*. 2014;512:87-90
157. Keildson S, Fadista J, Ladenvall C, et al. Expression of phosphofructokinase in skeletal muscle is influenced by genetic variation and associated with insulin sensitivity. *Diabetes*. 2014;63:1154-1165

158. Curtis C, Shah SP, Chin SF, et al. The genomic and transcriptomic architecture of 2,000 breast tumours reveals novel subgroups. *Nature*. 2012;486:346-352
159. Quigley DA, Fiorito E, Nord S, et al. The 5p12 breast cancer susceptibility locus affects mrps30 expression in estrogen-receptor positive tumors. *Mol Oncol*. 2014;8:273-284
160. Gao C, Tignor NL, Salit J, Strulovici-Barel Y, Hackett NR, Crystal RG, Mezey JG. Heft: Eqtl analysis of many thousands of expressed genes while simultaneously controlling for hidden factors. *Bioinformatics*. 2014;30:369-376
161. Hao K, Bosse Y, Nickle DC, et al. Lung eqtls to help reveal the molecular underpinnings of asthma. *PLoS Genet*. 2012;8:e1003029
162. Ding J, Gudjonsson JE, Liang L, Stuart PE, Li Y, Chen W, Weichenthal M, Ellinghaus E, Franke A, Cookson W, Nair RP, Elder JT, Abecasis GR. Gene expression in skin and lymphoblastoid cells: Refined statistical method reveals extensive overlap in cis-eqtl signals. *Am J Hum Genet*. 2010;87:779-789
163. Wagner JR, Busche S, Ge B, Kwan T, Pastinen T, Blanchette M. The relationship between DNA methylation, genetic and expression inter-individual variation in untransformed human fibroblasts. *Genome Biol*. 2014;15:R37
164. Qiu W, Cho MH, Riley JH, et al. Genetics of sputum gene expression in chronic obstructive pulmonary disease. *PLoS One*. 2011;6:e24395
165. Fadista J, Vikman P, Laakso EO, et al. Global genomic and transcriptomic analysis of human pancreatic islets reveals novel genes influencing glucose metabolism. *Proc Natl Acad Sci U S A*. 2014;111:13924-13929
166. Koopmann TT, Adriaens ME, Moerland PD, et al. Genome-wide identification of expression quantitative trait loci (eqtls) in human heart. *PLoS One*. 2014;9:e97380
167. Lin H, Dolmatova EV, Morley MP, Lunetta KL, McManus DD, Magnani JW, Margulies KB, Hakonarson H, del Monte F, Benjamin EJ, Cappola TP, Ellinor PT. Gene expression and genetic variation in human atria. *Heart Rhythm*. 2014;11:266-271
168. Rantalainen M, Herrera BM, Nicholson G, et al. MicroRNA expression in abdominal and gluteal adipose tissue is associated with mrna expression levels and partly genetically driven. *PLoS One*. 2011;6:e27338
169. Gamazon ER, Innocenti F, Wei R, Wang L, Zhang M, Mirkov S, Ramirez J, Huang RS, Cox NJ, Ratain MJ, Liu W. A genome-wide integrative study of micrnas in human liver. *BMC Genomics*. 2013;14:395
170. Li Q, Stram A, Chen C, Kar S, Gayther S, Pharoah P, Haiman C, Stranger B, Kraft P, Freedman ML. Expression qtl-based analyses reveal candidate causal genes and loci across five tumor types. *Hum Mol Genet*. 2014;23:5294-5302
171. Webster JA, Gibbs JR, Clarke J, et al. Genetic control of human brain transcript expression in alzheimer disease. *Am J Hum Genet*. 2009;84:445-458
172. Zou F, Chai HS, Younkin CS, et al. Brain expression genome-wide association study (egwas) identifies human disease-associated variants. *PLoS Genet*. 2012;8:e1002707
173. Ramasamy A, Trabzuni D, Guelfi S, Varghese V, Smith C, Walker R, De T, Coin L, de Silva R, Cookson MR, Singleton AB, Hardy J, Ryten M, Weale ME. Genetic variability in the regulation of gene expression in ten regions of the human brain. *Nat Neurosci*. 2014;17:1418-1428

174. Gamazon ER, Badner JA, Cheng L, et al. Enrichment of cis-regulatory gene expression snps and methylation quantitative trait loci among bipolar disorder susceptibility variants. *Mol Psychiatry*. 2013;18:340-346
175. Gibbs JR, van der Brug MP, Hernandez DG, et al. Abundant quantitative trait loci exist for DNA methylation and gene expression in human brain. *PLoS Genet*. 2010;6:e1000952
176. Kim S, Cho H, Lee D, Webster MJ. Association between snps and gene expression in multiple regions of the human brain. *Transl Psychiatry*. 2012;2:e113
177. Zhang B, Gaiteri C, Bodea LG, et al. Integrated systems approach identifies genetic nodes and networks in late-onset alzheimer's disease. *Cell*. 2013;153:707-720
178. Shpak M, Hall AW, Goldberg MM, Derryberry DZ, Ni Y, Iyer VR, Cowperthwaite MC. An eqtl analysis of the human glioblastoma multiforme genome. *Genomics*. 2014;103:252-263
179. Colantuoni C, Lipska BK, Ye T, Hyde TM, Tao R, Leek JT, Colantuoni EA, Elkahloun AG, Herman MM, Weinberger DR, Kleinman JE. Temporal dynamics and genetic control of transcription in the human prefrontal cortex. *Nature*. 2011;478:519-523
180. Liu C, Cheng L, Badner JA, Zhang D, Craig DW, Redman M, Gershon ES. Whole-genome association mapping of gene expression in the human prefrontal cortex. *Mol Psychiatry*. 2010;15:779-784
181. Folkersen L, van't Hooft F, Chernogubova E, Agardh HE, Hansson GK, Hedin U, Liska J, Syvanen AC, Paulsson-Berne G, Franco-Cereceda A, Hamsten A, Gabrielsen A, Eriksson P. Association of genetic risk variants with expression of proximal genes identifies novel susceptibility genes for cardiovascular disease. *Circ Cardiovasc Genet*. 2010;3:365-373
182. Björkegren JLM, Kovacic JC, Dudley JT, Schadt EE. Genome-wide significant loci: How important are they?: Systems genetics to understand heritability of coronary artery disease and other common complex disorders. *J Am Coll Cardiol*. 2015;65:830-845
183. Garnier S, Truong V, Brocheton J, et al. Genome-wide haplotype analysis of cis expression quantitative trait loci in monocytes. *PLoS Genet*. 2013;9:e1003240
184. Heinig M, Petretto E, Wallace C, et al. A trans-acting locus regulates an anti-viral expression network and type 1 diabetes risk. *Nature*. 2010;467:460-464
185. Pahl MC, Erdman R, Kuivaniemi H, Lillvis JH, Elmore JR, Tromp G. Transcriptional (chip-chip) analysis of elf1, ets2, runx1 and stat5 in human abdominal aortic aneurysm. *Int J Mol Sci*. 2015;16:11229-11258
186. Lenk GM, Tromp G, Weinsheimer S, Gatalica Z, Berguer R, Kuivaniemi H. Whole genome expression profiling reveals a significant role for immune function in human abdominal aortic aneurysms. *BMC Genomics*. 2007;8:237
187. Hinterseher I, Erdman R, Donoso LA, et al. Role of complement cascade in abdominal aortic aneurysms. *ATVB*. 2011;31:1653-1660
188. Kamburov A, Pentchev K, Galicka H, Wierling C, Lehrach H, Herwig R. Consensuspathdb: Toward a more complete picture of cell biology. *Nucleic Acids Res*. 2011;39:D712-717
189. Kamburov A, Stelzl U, Lehrach H, Herwig R. The consensuspathdb interaction database: 2013 update. *Nucleic Acids Res*. 2013;41:D793-800

190. Kamburov A, Wierling C, Lehrach H, Herwig R. Consensuspathdb--a database for integrating human functional interaction networks. *Nucleic Acids Res.* 2009;37:D623-628
191. Pentchev K, Ono K, Herwig R, Ideker T, Kamburov A. Evidence mining and novelty assessment of protein-protein interactions with the consensuspathdb plugin for cytoscape. *Bioinformatics.* 2010;26:2796-2797
192. Nguyen H, Allali-Hassani A, Antonysamy S, et al. Lly-507, a cell-active, potent, and selective inhibitor of protein-lysine methyltransferase smyd2. *J Biol Chem.* 2015;290:13641-13653
193. Xu G, Liu G, Xiong S, Liu H, Chen X, Zheng B. The histone methyltransferase smyd2 is a negative regulator of macrophage activation by suppressing interleukin 6 (il-6) and tumor necrosis factor alpha (tnf-alpha) production. *J Biol Chem.* 2015;290:5414-5423
194. Calvano SE, Xiao W, Richards DR, et al. A network-based analysis of systemic inflammation in humans. *Nature.* 2005;437:1032-1037
195. Hannou SA, Wouters K, Paumelle R, Staels B. Functional genomics of the cdkn2a/b locus in cardiovascular and metabolic disease: What have we learned from gwass? *Trends Endocrinol Metab.* 2015;26:176-184
196. Nakashima H, Aoki M, Miyake T, Kawasaki T, Iwai M, Jo N, Oishi M, Kataoka K, Ohgi S, Ogihara T, Kaneda Y, Morishita R. Inhibition of experimental abdominal aortic aneurysm in the rat by use of decoy oligodeoxynucleotides suppressing activity of nuclear factor kappaB and ets transcription factors. *Circulation.* 2004;109:132-138
197. Nischan J, Gatalica Z, Curtis M, Lenk GM, Tromp G, Kuivaniemi H. Binding sites for ets family of transcription factors dominate the promoter regions of differentially expressed genes in abdominal aortic aneurysms. *Circ Cardiovasc Genet.* 2009;2:565-572
198. Genetic variants in novel pathways influence blood pressure and cardiovascular disease risk. *Nature.* 2011;478:103-109